Development and Strategic Application of Metal-mediated Methods in the Synthesis Towards Agariblazeispirol C

Thesis submitted to the University of Strathclyde in fulfilment of the requirements for the degree of Doctor of Philosophy

By

Raymond W M Chung

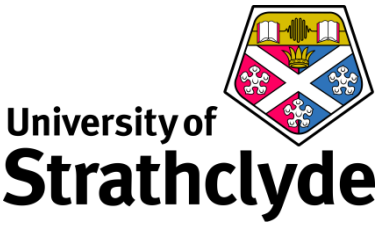

Department of Pure and Applied Chemistry
University of Strathclyde
Thomas Graham Building
295 Cathedral Street
Glasgow
G1 1XL

July 2020

Declaration of Copyright

This thesis is the result of the author's original research. It has been composed by the author and has not been previously submitted for examination which has led to the award of a degree.

Signed: 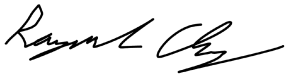 Date: 05/07/20

Acknowledgements

First, I'd like to thank Prof. Billy Kerr for giving me the opportunity to join his group as a PhD student. Thank you for all your encouragement and believing in my abilities as a chemist and overall as a person, I have learned so much over the 3.5 years working within your group. I will miss all the (interesting) stories you tell, especially at our meetings!

I'd also like to extend my deepest gratitude to Dr. David Lindsay and Dr. Laura Paterson, for all their knowledge and support since starting my PhD, and the continued guidance in my project. Words cannot express how grateful I am for helping me through my whole PhD, through positive moments such from obtaining excellent results and helping me with poster and conference presentations, to more difficult times when I needed someone to talk/rant to (mostly ranting), or when I was struggling with my chemistry/life in general!

I must thank the Kerr group for making my PhD experience as enjoyable as possible. I have had a great time working alongside every single one of you, and I will miss being part of the Kerr family. It is difficult to summarise the best moments with all of you, but it has been an experience and a half. Philippa, even though our time was short I will still remember you were the reason for the Pasha's incident, giving me all that rum at cheese and wine! Renan, I enjoyed our general discussions and that one time you decided to become a lawyer, shame you forgot the party poppers! Peter, our talk of music while you worked next to me was good fun, but I will always remember your hatred for Pizza Hut, salted caramel anything and golf!

Special thanks to both Gary and Liam, you guys helped me from the start, and I can't thank you two enough. Gary, even though you are an egg you'll always be more Asian than me. I'll remember our late night chinese takeaways in the office, when you got lost in Glasgow after karaoke and our love for rice. Liam, there are too many things I need to thank you for and not enough words. From practical and theoretical chemistry to DIY, you really taught me it all. I am extremely thankful to have tackled natural product synthesis together, and its been an absolute pleasure learning from you. I really do miss working alongside my total synthesis brother. I will remember our weekends working hard in the lab together in

your last year, our conversations about food and how you got me to go to the gym! Thanks for watching over me during your time.

Special thanks to everyone in my year group for sharing the PhD journey – Adele, Giorgia and Paul S. Adele, so much has happened since I met you as an undergrad, and it's hard to summarise our time together! There have been many ups and downs during our friendship, but I'm glad we went through it all – the last 3.5 years working with you have been phenomenal, and we've come out as close friends. We have worked so hard, so much blood, sweat and tears! You have always been there for me, during the good, the bad and ugly. I'm so grateful we've had many experiences together, from our personal conversations and sanity checks, to exploring California! Falling into a hot tub, getting body slammed into a lampshade, Katy Perry's Firework – too many memories, and now I'm rambling…Thanks for looking after me! Giorgia, it has been interesting working with you and sharing both my undergrad and PhD years with you! From Stevenage, to Glasgow, we really have had an experience! I will always remember GHOGH, our Taylor Swift moments and that time you helped me in Pasha's…

Conor, (or John, pick a name!) I will always regard you as one of my closest friends within the group. I may have been hardest on you, but it's character building! (or maybe because we are just acquaintances?) We both have been on many ups and downs during our PhD but I'm glad to have shared this experience with you. In my mind, you'll be successful in your PhD and as a chemist. From our love of Buck's, Chinese food and our constant moaning of things, the one thing we can't decide on is how crap Tennent's is! Nathan, I will never forget your 'Posh' mannerisms, from 'Cheers' to 'a pinch of DCM in my compound' – I'm hoping one day you won't get anaemic chips from Metro!

Paul M, Megan and Andrew – WestCHEM ball will always be the highlight! Paul M stung by love, Megan waking up from the dead, Andrew being sick everywhere, what an experience for our short time together! Megan, I will miss our chats, if you know what I mean… Paul M, you are a character and a half and we have so much in common for being completely different people, it's a shame you joined the group during my final year – remember you are my favourite 1st year! (sorry Megan and Andrew!).

I'd like to thank honorary members Laura Bain, Jack, Blake, James, Luke and Gillian for our time together.

I'd also like to thank Jemma, even though we only worked together for about year I feel like we had grown close in that short time! You always made sure I was ok and you were always there for me! From all our nights out, pig on a stool, eighth floor meetings and your Christmas lunch seating arrangement, I hope we continue to build good memories, looking forward to continuing our dinner clubs! Special thanks to Keith, for giving me someone else to rant to outside the group, the mate-dates after work and joining me in the gym, I hope we continue to have these once we finish our PhDs. Being able to do a PhD alongside you (even though in different groups) has been a pleasure.

I'd like to extend my thanks to GSK for their support, particularly my industrial supervisor Tom. Thank you for all your insightful discussions and all your help while I was at GSK. You made me feel welcome and always made sure I was doing well while on placement. Since then I have never stopped using post-it notes and always crave Kitchen Fudge. Sorry for all the chiral HPLC samples!

Finally, I'd like to thank my parents and brother for their continued support and love throughout my PhD studies, hopefully I will be able to repay you back to show you how much you guys have helped me through all of my academic studies. I am forever grateful.

Abstract

Within our research team, significant efforts towards the total synthesis of the natural product agariblazeispirol C (**1**) has been conducted. In our synthetic programme, and as aligned with the broader interests of our team, we proposed that the key core skeleton of the target could be constructed through a combination of two effective metal-mediated cyclisation processes. More specifically, intramolecular Heck and Pauson-Khand annulation techniques have been employed to construct the core structure of the desired natural product, leaving the installation of an oxygenated five carbon side-chain as the final requirement to complete the target. Througout this overall programme of work, each individual reaction sequence has been fully explored and strategic synthetic steps have been established, and optimised, to provide access to advanced intermediates.

Disclosed in this thesis is an extensive exploration of the asymmetric intramolecular Heck cyclisation reaction to deliver an enantioenriched 6,6-bicyclic system (rings B and C). This established the first quaternary stereocentre within the natural product, ultimately, dictating the overall diastereoselectivity in the downstream synthesis. Indeed, high enantioselectivity of the asymmetric Heck reaction was achieved *via* substantial optimisation processes, including a comprehensive chiral ligand screen – allowing the cobalt-mediated Pauson-Khand cyclisation to be studied next in our programme of work. This demanding cyclisation required the formation of the two cyclopentyl rings (rings D and E), constructing the overall polycyclic network containing a further quaternary centre within the congested system. In this regard, efficient cyclisation of two distinct Pauson-Khand precursors has delivered the overall core of the natural product as a single diastereomer, confirmed by X-ray crystallography. Exploration of the final synthetic manipulations to allow for the installation of the required oxygenated side-chain has been initiated, with promising methodology having emerged to allow the final target to be accessed.

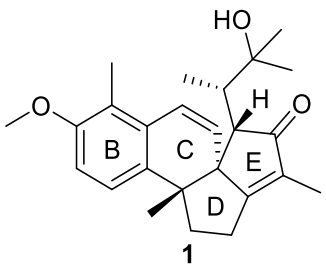

1

List of Abbreviations

Abbreviation	Definition
Ac	Acetyl
AIBN	Azobisisobutyronitrile
Ar	Aromatic
atm	Atmosphere
BBN	9-Borabicyclo(3.3.1)nonane
BINAP	2,2’-Bis(diphenylphosphino)-1,1’-binaphthyl
BIPHEP	Biphenylphosphine
Bu	Butyl
CAN	Cerium ammonium nitrate
CHIRAPHOS	2,3-Bis(diphenylphosphino)butane
COD	Cyclooctadiene
Conv.	Conversion
Cy	Cyclohexyl
DABCO	1,4-diazabicyclo[2.2.2]octane
dba	Dibenzylideneacetone
DBU	Diazabicyclo[5.4.0]undec-7-ene
DCE	Dichloroethane
DCM	Dichloromethane
DDQ	2,3-Dichloro-5,6-dicyano-1,4-benzoquinone
DIOP	4,5-bis(diphenylphosphinomethyl)-2,2-
DIPEA	*N*,*N*-Diisopropylethylamine
DM	Dimethyl
DMA	Dimethylacetamide
DME	Dimethoxymethane
DMF	Dimethylformamide
DMPU	1,3-Dimethyl-3,4,5,6-tetrahydro-2-(1*H*)-pyrimidinone
DMSO	Dimethylsulfoxide

Dod	Dodecyl
dppe	1,2-Bis(diphenylphosphino)ethane
dr	Diastereomeric ratio
D-S	Dean-Stark
DTBM	Di(3,5-di-*tert*-butyl-4-methoxyphenyl
ee	Enantiomeric excess
equiv.	Equivalents
Et	Ethyl
g	Grammes
h	Hours
HMDS	Hexamethyldisilazane
HMPA	Hexamethylphosphoramide
HPLC	High-performance liquid chromatography
HRMS	High resolution mass spectrometry
HWE	Horner-Wadsworth-Emmons
Hz	Hertz
IPA	Isopropyl alcohol
IR	Infrared
LCMS	Liquid chromatography mass spectrometry
LDA	Lithium di-*iso*-propylamide
LUMO	Lowest unoccupied molecular orbital
M	Molar
MDAP	Mass Directed Autopurification
Me	Methyl
MeCN	Acetonitrile
mg	Milligrammes
MHz	Megahertz
Min	Minutes
ml	Millilitres
mmol	Millimoles

mol	Moles
MS	Molecular sieves
MWI	Microwave irradiation
NBS	*N*-Bromosuccinimide
n.d.	Not determined
NIS	*N*-iodosuccinimide
NMO	*N*-methylmorpholine *N*-oxide
NMP	*N*-methylpyrrolidone
NMR	Nuclear magnetic resonance spectra; s – singlet d – doublet dd – double doublets dt – doublet of triplets ddd – double doublet of doublets t – triplet td – triplet of doublets tq – triplet of quartets q – quartet m – multiplet appp – apparent pentet
o	Ortho
O-TMEDA	Bis[2-(*N*,*N*-dimethylamino)ethyl] ether
p	Para
Ph	Phenyl
PHOX	Phosphinooxazolines
PK	Pauson-Khand
PKR	Pauson-Khand reaction
PMP	Pentamethyl piperidine
ppm	Parts per million

PPTS	Pyridinium *p*-toluenesulfonate
Pr	Propyl
Py	Pyridine
rt	Room temperature
s	seconds
SEGPHOS	Bis(diphenylphosphino)-4,4′-bi-1,3-benzodioxole
SM	Starting material
SYNPHOS	6,6'-Bis(diphenylphosphino)-2,2',3,3'-tetrahydro-5,5'-bi-1,4-benzodioxin
TBAF	Tetra-*n*-butylammonium fluoride
TBDPS	*tert*-Butyldiphenylsilyl
TBHP	*tert*-butyl hydroperoxide
TBS	*tert*-Butyldimethylsilyl
Temp.	Temperature
TES	Triethylsilyl
Tf	Trifluoromethanesulfonate
THF	Tetrahydrofuran
TIPS	Triisopropylsilyl
TLC	Thin layer chromatography
TMANO	Trimethylamine *N*-oxide
TMEDA	Tetramethylethylenediamine
TMS	Trimethylsilyl
TMTU	Tetramethylthiourea
Ts	*p*-Toluenesulfonyl

Table of Contents

Chapter 1

Introduction

1. Introduction

1.1 Agariblazeispirol C

1.1.1 Agaricus Blazei

Agaricus blazei is a fungus which produces several bioactive natural products.[1,2] Many of these species have been extracted and isolated from the fruiting bodies of *Agaricus blazei*, where agariblazeispirol C **1** was isolated from cultured mycelia (**Figure 1.1**).[3,4] The biological activity of compounds extracted from *Agaricus blazei* has been investigated, where studies show their ability to stimulate the immune system, increasing the production of, for example, cytotoxic T-cells.[2] This reduces tumour growth, thus can be considered as a prophylaxis against cancer. Whilst the biological effects of agariblazeispirol C have yet to be studied, its unique steroidal skeleton is similar to ergosterol derivatives, which display biological activity. As depicted in **Figure 1.1**, the conventional steroidal framework **2** consists of three six-membered rings (A, B and C) and one five-membered ring (D). However, with the A-ring omitted, and having an additional five-membered ring (E), agariblazeispirol C **1** is referred to as exhibiting the des-A-ergostane structure **3**, which is a known framework in the literature. More specifically, these structures have been isolated as sedimentary compounds from the Cretaceous black shale, originating from Italy.[5] However, these unconventional steroid skeletons have not been isolated from living organisms until the discovery of agariblazeispirol C **1** and other natural products from *Agaricus blazei*.

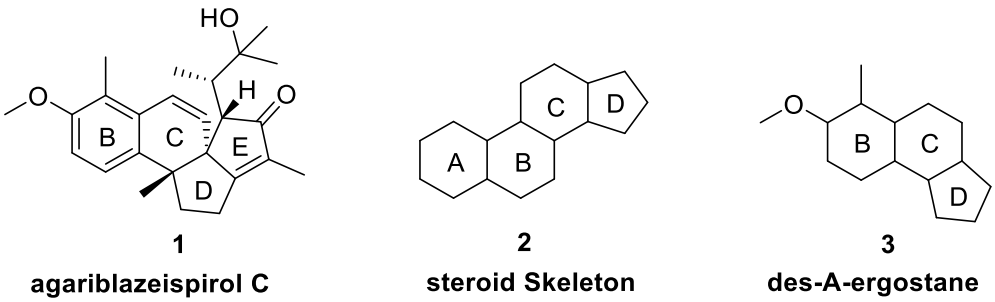

Figure 1.1

1.1.2 Proposed Biosynthesis and Origin of Agariblazeispirol C

The biomimetic synthesis of agariblazeispirol C **1** was reported by Hirotani *et al*. in their initial isolation paper and is detailed below in **Scheme 1.1**.[4] Their investigation showed that agariblazeispirol C **1** could be synthesised by placing blazeispirol A **4** (*vide infra*) under Lewis acidic conditions with boron trifluoride diethyl etherate (BF_3•OEt_2).

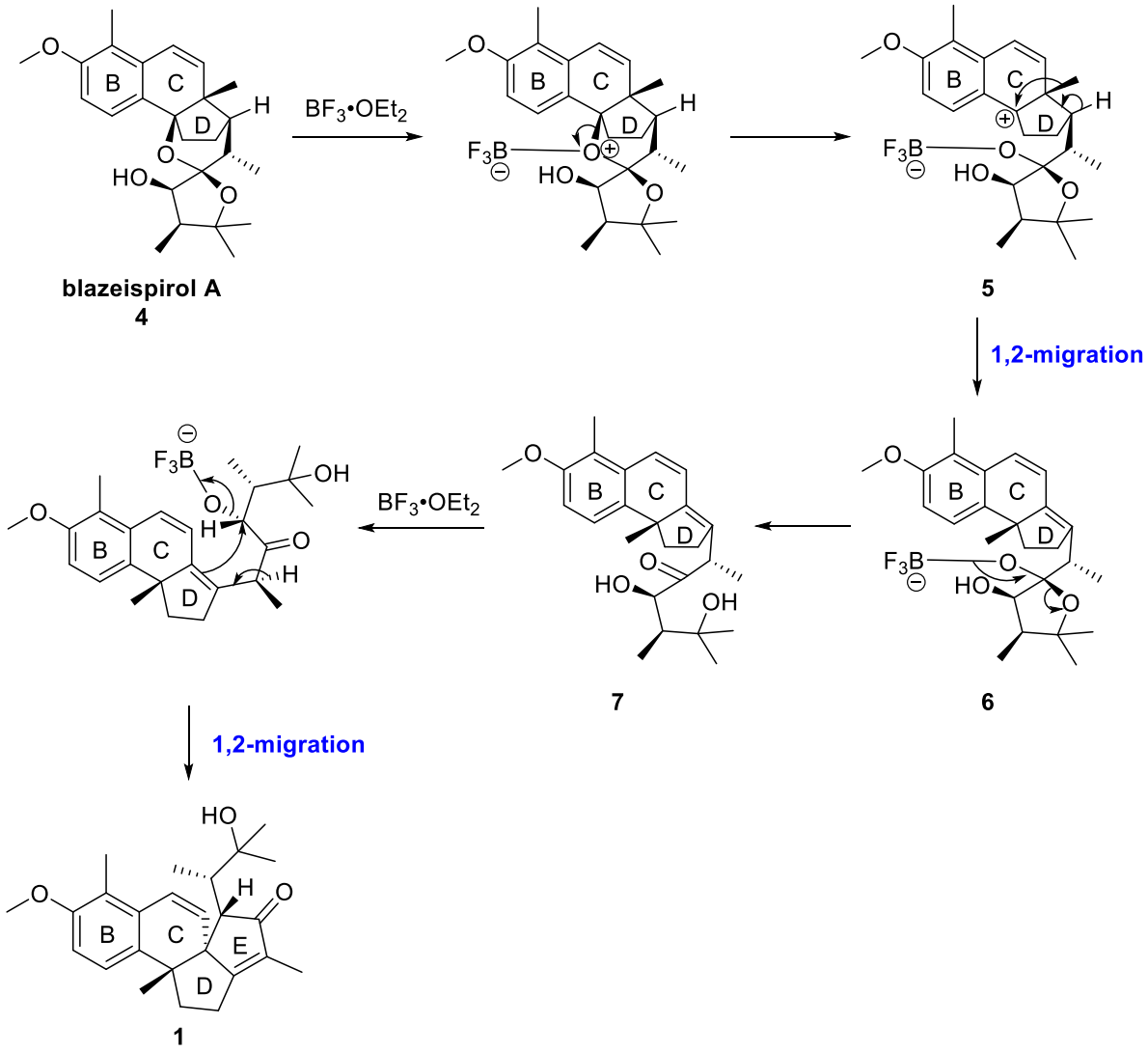

Scheme 1.1

Initial coordination of BF_3•OEt_2 onto blazeispirol A **4** results in the formation of the benzylic cationic species **5**. With this intermediate, 1,2-migration of the allylic methyl group to the benzylic cationic centre occurs, producing **6**. Here, it is proposed that

tetrahydrofuran ring opening gives **7**, constructing the overall oxygenated side-chain of agariblazeispirol C **1**. The final steps of coordination of BF_3•OEt_2 onto **7** and subsequent 1,2-migration produces the tetracyclic core (ring E), delivering the final natural target **1**.

In relation to the above, the biosynthetic route of blazeispirol A **4** has already been extensively investigated by the same authors.[6,7] In their initial studies involving ^{13}C-labelling experiments,[6] they proposed the biosynthetic pathway shown within **Scheme 1.2**. Beginning with steroidal skeleton ergostol **9** (generated from mevalonic acid **8**), oxidation of the framework provides **10**, which undergoes intramolecular acetalisation to provide **11**. Here, a three-step sequence of epoxidation, oxidation, and elimination produces **12**, which further reacts by crucially losing the A-ring, and ultimately forming blazeispirol A **4**. Deconstruction of the A-ring begins with a retro-Aldol reaction of **12** to form blazeispirol Z **13**, with a subsequent retro-Michael addition process resulting in blazeispirol D **14**. The final methylation transformation provides blazeispirol A **4**. Further evidence supporting the formation of blazeispirol Z **13** and D **14** was obtained after independently isolating these derivatives from *Agaricus blazei*,[7] providing rationale for the deconstruction of the A-ring for agariblazeispirol C **1**, blazeispirol A **4** and its derivatives.

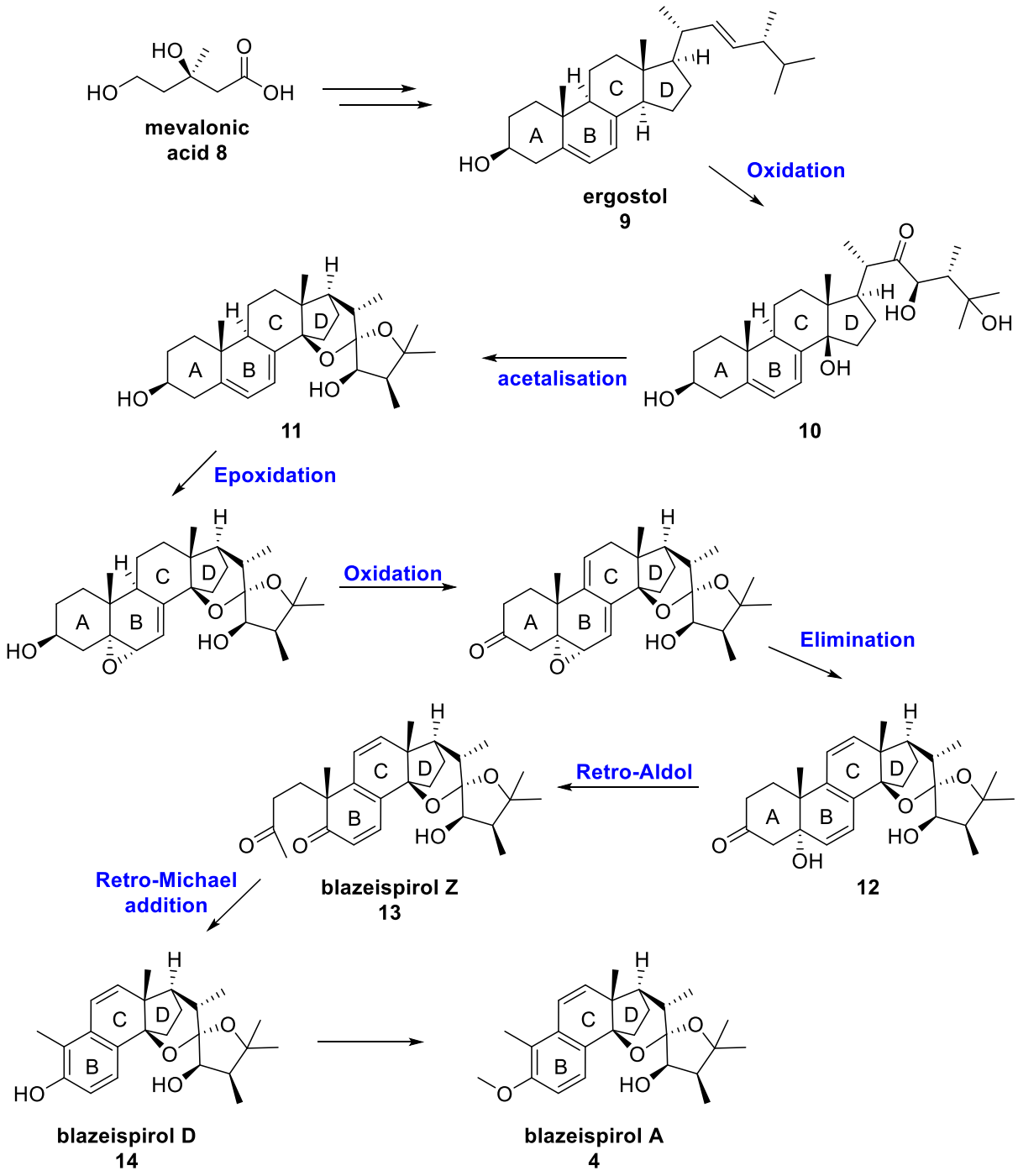

Scheme 1.2

Overall, these findings provide strong support for the proposed biosynthetic pathway of agariblazeispirol C **1** from blazeispirol A **4**, and illustrate the origins for the unusual des-A-ergostane motif present within the natural products isolated from *Agaricus blazei*.

1.1.3 Retrosynthesis of Agariblazeispirol C[8–12]

Within our group, research interests have focused primarily on the advancement of metal-mediated cyclisation methodology for application by the preparative chemistry community to generate molecular complexity in a highly efficient manner. More specifically, our research group has centred efforts on advancing the cobalt-mediated Pauson-Khand (PK) cyclisation. To this end, in addition to applying the reaction within a spectrum of natural products, we have contributed significantly to the elevation of the synthetic utility of the reaction (*vide infra*). Thus, from our thorough knowledge of the Pauson-Khand reaction (PKR), we have selected the total synthesis of agariblazeispirol C **1** as a further, and adventurous, synthetic challenge to showcase our developing PK methodology. Structurally, agariblazeispirol C **1** consists of a tetracyclic core with four contiguous chiral centres, along with an oxygenated side-chain, all of which displays a demanding synthetic campaign to integrate such stereodefined and congested centres within a complex carboskeleton. To date, no known routes have been described, providing the opportunity to present its first synthesis within the literature, and to confirm the structure of the overall natural product. To gain access to the unique des-A-ergostane framework within this natural target, we envisaged that key transition-metal mediated cyclisation transformations would provide the C, D and E ring systems, building two contingent quaternary centres within the complex tetracyclic core. More specifically, a cobalt-mediated PKR would give the D and E ring systems, and an asymmetric intramolecular Heck reaction would provide the C-ring. Hence, this proposed total synthesis presents us the opportunity to not only embellish the application of the PKR within our research group, but also to advance another metal-mediated cyclisation process – a challenging asymmetric Heck reaction. The proposed retrosynthetic analysis of agariblazeispirol C **1** is shown in **Scheme 1.3** below.

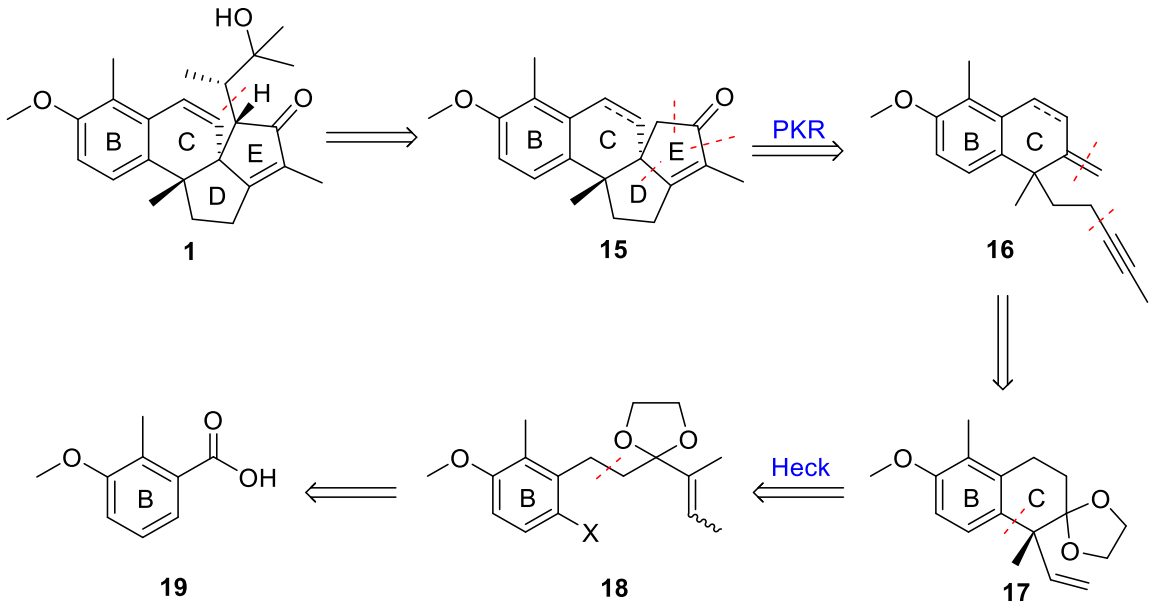

Scheme 1.3

The first disconnection involves removal the oxygenated side-chain, leaving system **15**. From this, a demanding PK disconnection can be made to give enyne **16**, constructing the 5,5-cyclic system and the overall core of the natural product. Additionally, this step would install a key quaternary carbon centre within the congested polycyclic network. To note, at this stage, the PK reaction can be exploited with or without the internal alkene being present within ring C. Enyne **16** is ultimately produced from the 6,6-fused system **17**, where an intramolecular Heck disconnection can be made to take us to **18**. More specifically, a challenging asymmetric intramolecular Heck reaction would establish the essential quaternary (*R*) stereocentre present within agariblazeispirol C, which is the key centre anticipated to dictate the overall diastereoselectivity of the downstream synthesis towards the natural product. Finally, the Heck precursor **18** can be accessed from commercially available acid **19**.

In summary, agariblazeispirol C presents a unique, unconventional steroidal framework and poses difficult synthetic challenges for its overall construction. As the asymmetric intramolecular Heck and Pauson-Khand reactions represent the key strategic transformations within this overall synthetic programme, a review of each of these processes will be detailed in the following sections.

1.2 The Mizoroki-Heck Reaction[13,14]

1.2.1 Introduction

Studied independently by Mizoroki and Heck, the Mizoroki-Heck reaction, or as more commonly known, the Heck reaction, is a metal-mediated C–C bond forming process traditionally between two sp^2 centres (**Scheme 1.4**). This palladium catalysed cross-coupling reaction has become a highly effective method to construct a C–C bond between an aryl or alkenyl halide (or pseudohalide) and an alkene. As a result of its important synthetic utility in organic synthesis, alongside other imperative Pd cross-coupling methods such as the Suzuki–Miyaura and Negishi reactions, the Nobel Prize in Chemistry was awarded to Richard Heck, Akira Suzuki, and Ei-ichi Negishi in 2010 for their investigative efforts into Pd-catalysed cross-coupling reactions.[15]

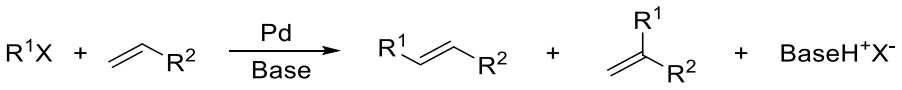

Scheme 1.4

Initial reports of the Heck reaction in the late 1960s involved the arylation of various alkenes through a metalation process with aryl mercury compounds.[16] In 1971, Mizoroki illustrated Pd cross-coupling of alkenes and iodobenzene in the presence of potassium acetate,[17] however, it was not until the 1980s that the Heck reaction was recognised as an important protocol in synthetic chemistry.[18] During this period, the efficiency and control of the Heck reaction were investigated such that control of the reaction outcomes became reliable when using certain conditions. From these rapid developments, it became facile for quaternary carbon centres to be incorporated into molecules using the Heck method.[18,19] Furthermore, an approach to an asymmetric intramolecular Heck cyclisation reaction was quickly established using chiral ligands, providing an effective tool to access natural products.[20]

1.2.2 General Mechanism

It is widely accepted that the Heck reaction proceeds through a Pd(0/II) mechanistic cycle (**Scheme 1.5**).[18,21,22] If required, a precatalyst activation step occurs to generate the Pd(0) active catalyst **20**. Oxidative addition of an electrophilic species to Pd(0) generates complex **21**. Subsequent alkene coordination displaces one ligand to **22**, allowing *syn*-carbopalladation (or migratory insertion) to proceed, producing **23**. *Syn*-β-hydride elimination generates the desired product **24** and hydridopalladium complex **25**. Reductive elimination of **25**, accelerated in the presence of base, regenerates the active catalyst **20** and thus completing the catalytic cycle.

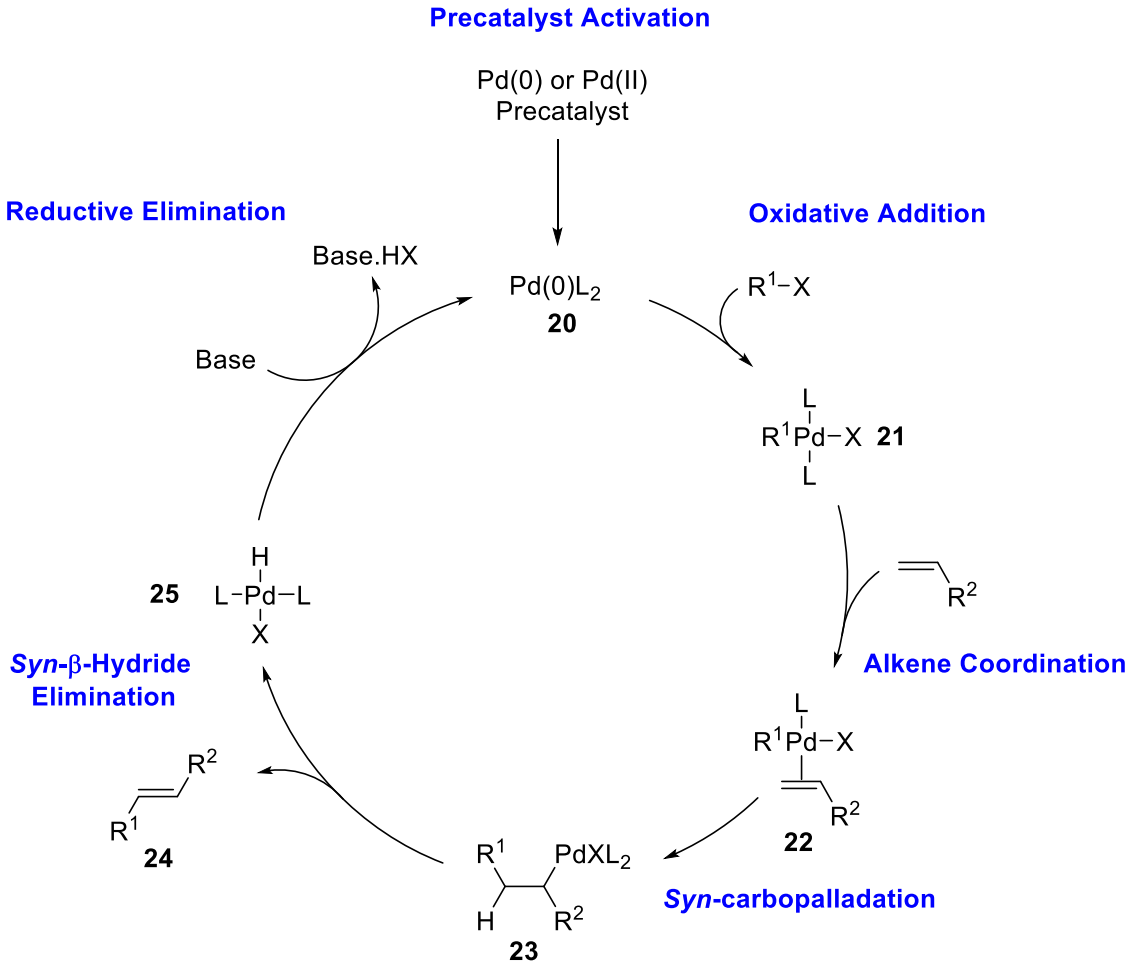

Scheme 1.5

Precatalyst Activation

Studies have shown that 14-electron di-coordinated Pd(0) complexes, such as **20**, are the active species that trigger the catalytic cycle of the Heck reaction.[21] Pd(0) catalysts can be directly employed, or these active species can be generated from Pd(II) precatalysts as Pd(0) precursors. A wide variety of Pd(0) catalysts are available, including isolated Pd(0) complexes such as $Pd(PPh_3)_4$, or complexes generated *in situ*, for example $Pd(0)dba_2$ mixed with ligands. Alternatively, Pd(II) precatalysts such as $Pd(OAc)_2$ and $PdCl_2$ are effective in these Heck reactions. For such precatalysts, first the Pd(II) complex is reduced into the Pd(0) species, and the active complex $[Pd(0)L_2]$ is formed through ligand exchange. Predominantly, phosphine ligands including PPh_3, P(*o*-tolyl)$_3$, and BINAP are employed in Heck reactions, however, nitrogen, sulfur, and carbene containing ligands are also utilised.[23] Importantly, the nature of the ligand can also have an effect on the product-determining step of the reaction, as well as play a role in defining the stereochemical outcome within the asymmetric variant of the process (*vide infra*).

Oxidative Addition

Oxidative addition of the aryl/alkenyl halide or pseudo halide into the active Pd(0) species is a concerted process where breaking of the C–X bond and formation of the Pd–C and Pd–X bonds occur simultaneously. The rate of oxidative addition is dependent on the strength of the C–X bond, therefore, the order of reactivity is generally: I > OTf > Br >> Cl,[18,21,22] and can influence chemoselectivity in Heck reactions. Demonstration of this order of chemoselectivity was shown by Hegedus in 1984 who illustrated that the Heck reaction proceeded only on the iodide position of **26**, solely furnishing **27** (**Scheme 1.6**).[24] Note here that ligand-free conditions were employed, where the active catalyst was generated through reduction of $Pd(OAc)_2$ by triethylamine (Et_3N) or the olefin.

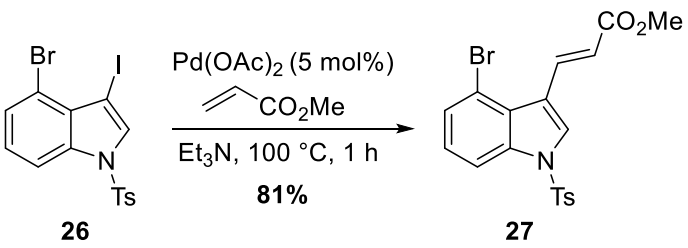

Scheme 1.6

Investigations into the effect of substituents on the aryl/alkenyl halide have also been shown to influence the rate of oxidative addition. In a relative sense, electron-withdrawing substituents enhances this process whereas electron-donating substituents hinders the oxidative addition step.[25]

Syn-carbopalladation

Following alkene coordination, *syn*-carbopalladation generates the new C–C bond (**Scheme 1.7**). The product formed could, ultimately, be either the linear or branched alkene, and it is this step that governs the regioselectivity of the product furnished. Control at this key step in the catalytic cycle will be discussed in a further section. After the resulting *syn*-carbopalladation process, C–C bond rotation must occur to allow a *syn* conformation between the Pd species and a hydrogen atom for the subsequent *syn*-β-hydride elimination step.

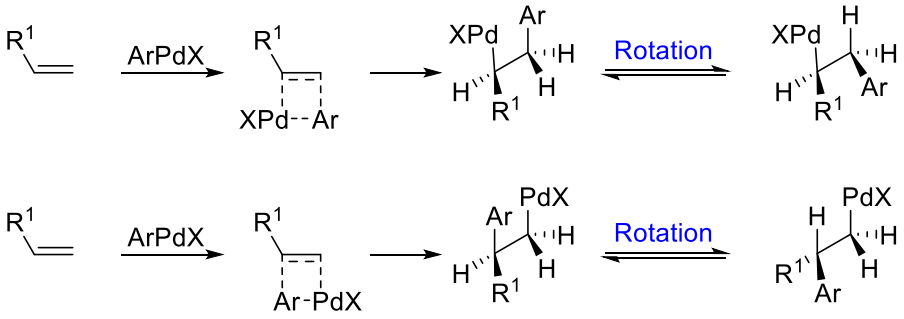

Scheme 1.7

Syn-β-hydride Elimination

Once the new C–C bond is formed, a Pd hydride species is eliminated to release the desired olefin product, and reductive elimination of the hydridopalladium complex by base regenerates the active catalyst.[18] *Syn*-β-hydride elimination predominantly affords the *E*-isomer, following the Curtin-Hammett kinetic control principle.[26] The transition state forming the *E*-alkene is favourable in energy due to the minimisation of steric clash between substituents. This effect is negligible only if the substituent is very small, such as a nitrile group (**Scheme 1.6**).

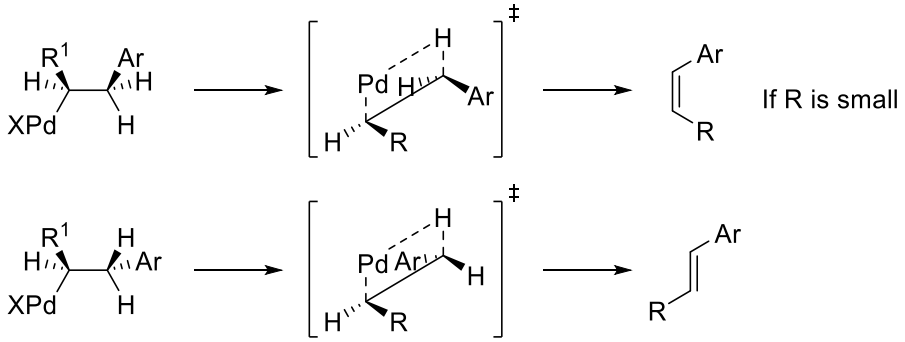

Scheme 1.8

In relation to the above, depending on the olefin partner employed, further isomerisation in the product can be observed. Indeed, if β′ hydrogen atoms are present, competing β-hydride and β′-hydride elimination occurs, leading to isomerised products (**Scheme 1.9**). To circumvent this, substrates with no β′ hydrogen atoms present are commonly used in Heck reactions.

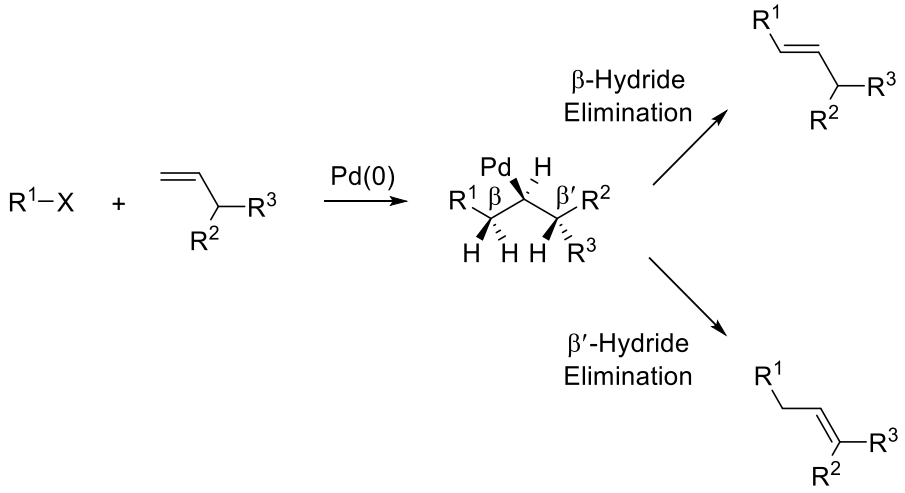

Scheme 1.9

Another pathway to isomerised products arises when there is slow reductive elimination of the hydridopalladium species by the base. The hydridopalladium complex can coordinate onto the starting alkene substrate, and, in turn, isomerise the substrate which then proceeds through the Heck reaction, affording the olefin with opposite stereochemistry. As illustrated in **Scheme 1.10**, the proposed Heck reaction with alkene **28** and ArPdX affords **29**. However, the hydridopalladium species **30** generated from the catalytic cycle could insert into **28**, giving complex **31**. β-Hydride elimination of **32** affords **33**, an overall isomerisation of alkene **28** into **33**. The Heck reaction with **33** affords **34**, inverting the stereochemistry initially observed with the reaction between **28** and ArPdX. The example displayed in **Scheme 1.10** additionally highlights the stereochemical control of each Heck reaction (**28→29** and **33→34**). Due to the *syn*-carbopalladation and *syn-β*-hydride elimination transformation requirements in the catalytic cycle, the Heck reaction of 1,2-disubstitued alkenes affords products with reversal of stereochemistry.

Example of Possible Isomerisation:

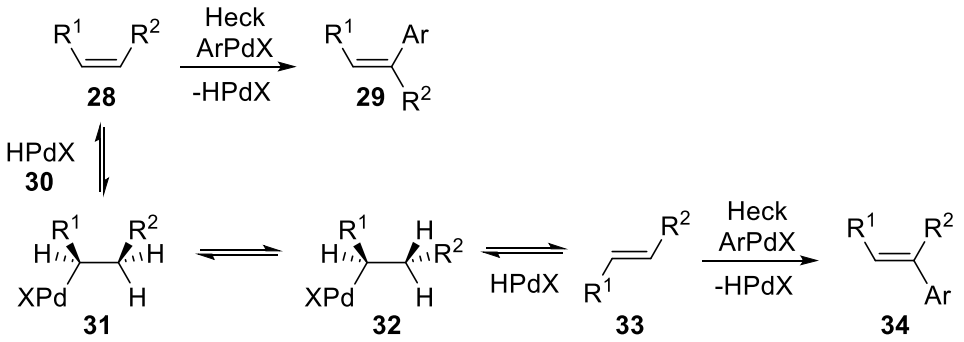

1,2-Disubstitued Olelfins:

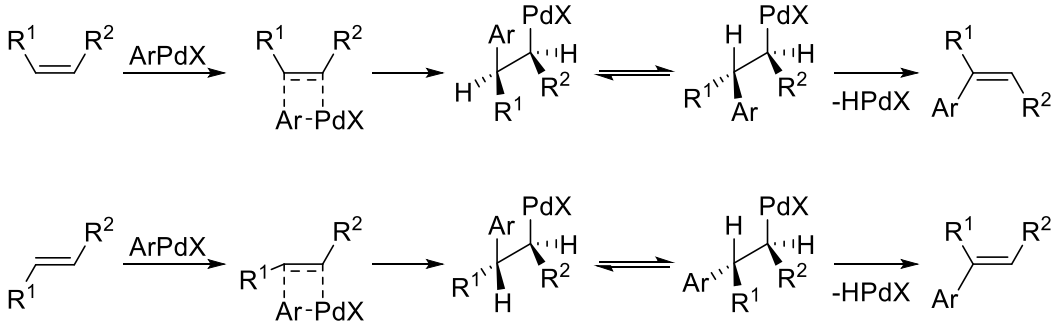

Scheme 1.10

1.2.3 Mechanistic Studies

Extensive mechanistic studies have been conducted on the catalytic cycle of the Heck reaction. Indeed, the general catalytic cycle shown in **Scheme 1.5** is a simplified overview of the Heck reaction, and does not detail the selectivity and reactivity associated with the observed outcomes of the Heck reaction. Three pathways (cationic, neutral and anionic) for the Heck reaction have been postulated through mechanistic investigations.

Cationic Pathway

In 1990, Cabri[27] and Hayashi[28] both independently reported the cationic Heck pathway for reactions between an alkene, aryl triflate (OTf), and a diphosphine-Pd(0) complex (**Scheme 1.11**). Following oxidative addition, the cationic pathway is promoted by spontaneous triflate dissociation of the weak Pd–OTf bond, forming cationic Pd complex **35**. Due to the chelate effect of bidentate ligands, ligand dissociation to complex **36** is disfavoured,

promoting triflate dissociation instead. As shown in **Scheme 1.11**, 1,3-bis(diphenylphosphino)propane (dppp) remains bound onto the Pd centre, hence dissociation of OTf allows alkene coordination to form **37**, and subsequent *syn*-carbopalladation follows to **38**. Indeed, the cationic mechanism can proceed with aryl halides using halide abstractors (commonly Ag(I) or Tl(I) salts) to assist Pd-X cleavage. The cationic pathway can favour the formation of the branched alkene **39**, as the cationic Pd complex adds into the carbon on the olefin with greatest electron density, highlighting the regiochemical control by the *syn*-carbopalladation step. However, in general, the overall regioselective outcome of the Heck reaction is influenced by both the mechanism followed and the electronics of the olefin partner, as discussed later in detail.

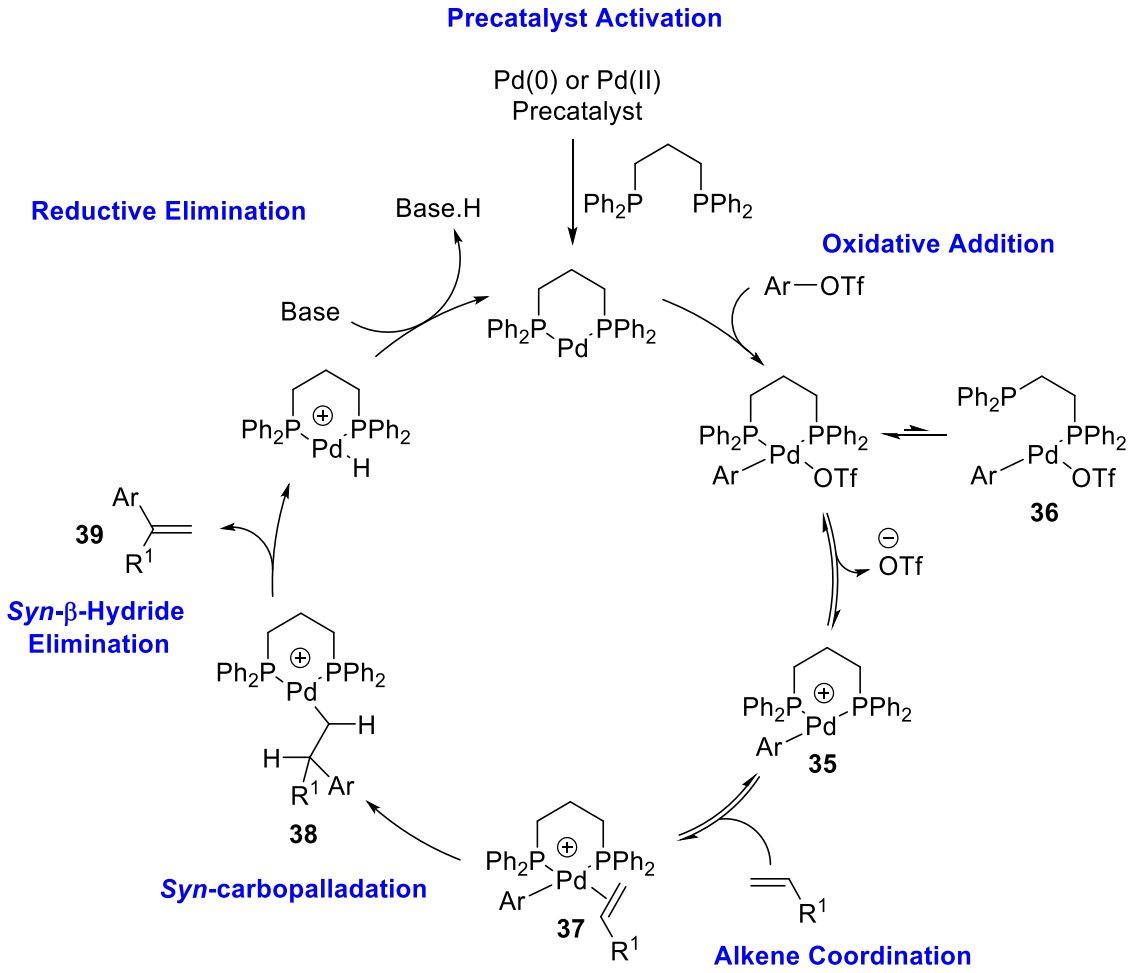

Scheme 1.11

Neutral Pathway

The neutral pathway follows the general catalytic cycle shown in **Scheme 1.5**, whereby, following oxidative addition, the ligand dissociates to allow alkene coordination and *syn*-carbopalladation. In the absence of halide abstractors and bidentate ligands, it is accepted that the standard Heck reaction favours the neutral pathway, preferentially generating linear alkene products due to steric effects as discussed earlier.

Anionic Pathway

A third mechanism was proposed by Amatore and Jutand[22] involving an anionic pathway with precatalyst $Pd(OAc)_2$ and monophosphine ligands (**Scheme 1.12**). A mixture of these components generates the anionic species $[Pd(PPh_3)_2(OAc)]^-$ **40**, which undergoes oxidative addition with the aryl halide. An anionic pentacoordinated complex $[PhPdI(OAc)(PPh_3)_2]^-$ **41** is formed, where both halide and acetate ions remain ligated onto the Pd centre, which subsequently releases the halide affording **42**. *Syn*-carbopalladation and *syn-β*-hydride elimination generates the coupled product, and reductive elimination with base regenerates the catalyst.

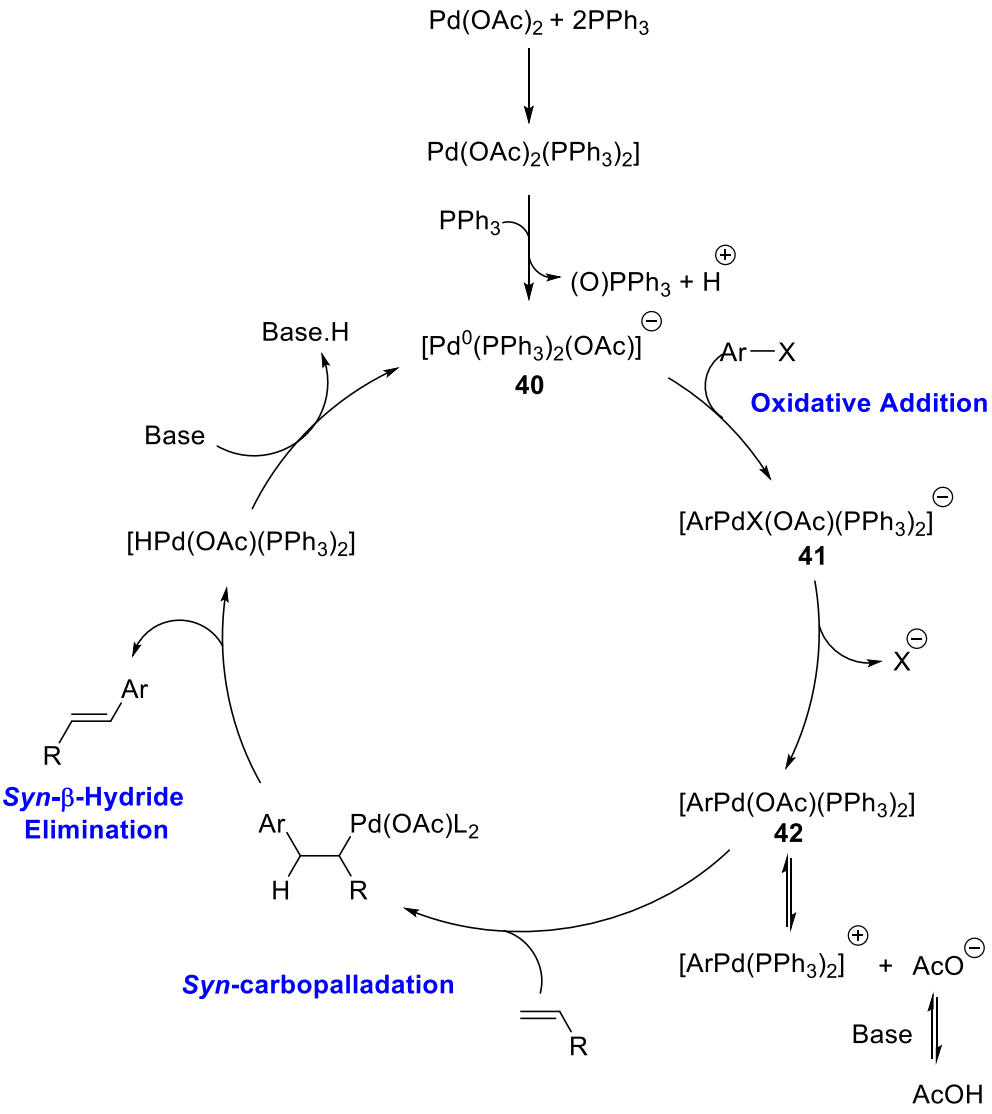

Scheme 1.12

1.2.4 Regioselectivity

As previously described, the branched or linear alkene products are preferentially favoured depending on the mechanistic pathway followed throughout the Heck reaction and the nature of the olefin. During the C–C bond forming step, preferential reactivity occurs at the most electron-deficient carbon of the alkene. In this regard, the selectivity is determined through the *syn*-carbopalladation step of the Heck reaction. In general, with the cationic pathway, electronic factors govern the preferred selectivity of the branched Heck product due to the cationic Pd complex formed, whereas steric effects favour the linear product in the neutral pathway. However, the electronics of the olefin partner is also important in

determining the regioselectivity of the Heck reaction. Cooperative regioselectivity factors are encapsulated in **Scheme 1.13**. Electron-rich olefins favour branched selectivity, and using cationic conditions, excellent branched selectivity is observed as the cationic Pd forms a Pd–C bond on the most electron-rich carbon of the olefin, further promoting α attack by R^2. The linear product is favoured through electron-poor olefins, and steric effects accelerates this selectivity under neutral conditions. Examples of excellent selectivity are shown in **Schemes 1.14**[29] and **1.15**.[30]

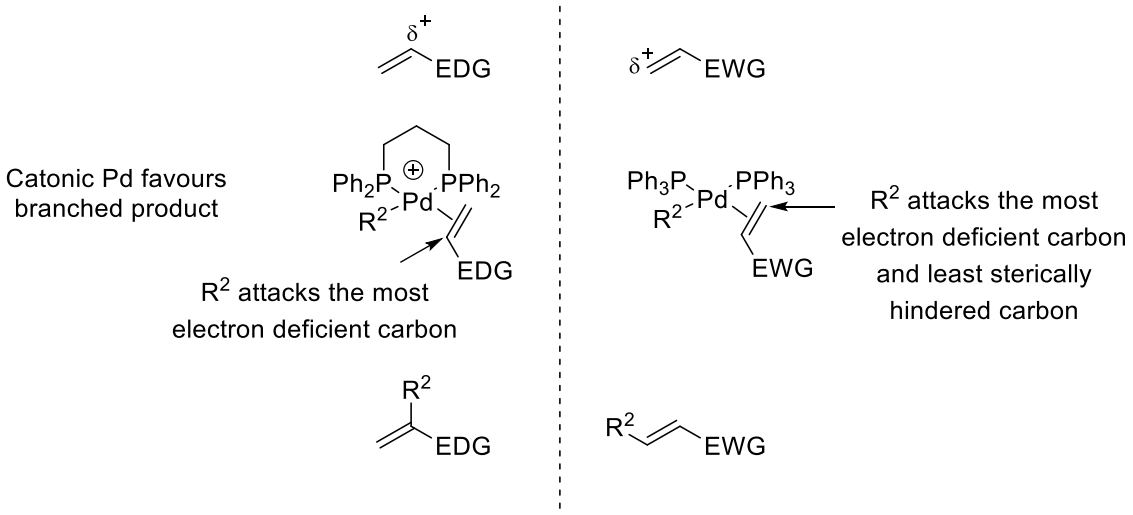

Scheme 1.13

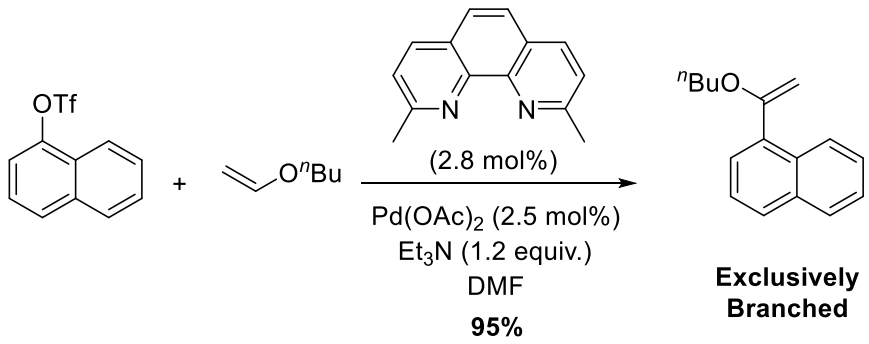

Scheme 1.14

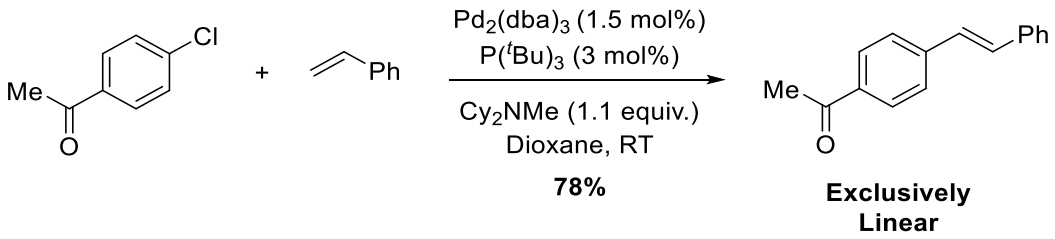

Scheme 1.15

Having stated that above, the regioselectivity is greatly influenced when there is a clash in electronic and steric preferences. For example, under neutral conditions shown in **Scheme 1.16**, the expected product would be linear.[31] However, since an electron-rich olefin is used in this Heck reaction, a mixture of both branched and linear products are obtained. The olefin does not tolerate neutral conditions with high regioselectivity due to opposing steric and electronic effects during *syn*-carbopalladation.

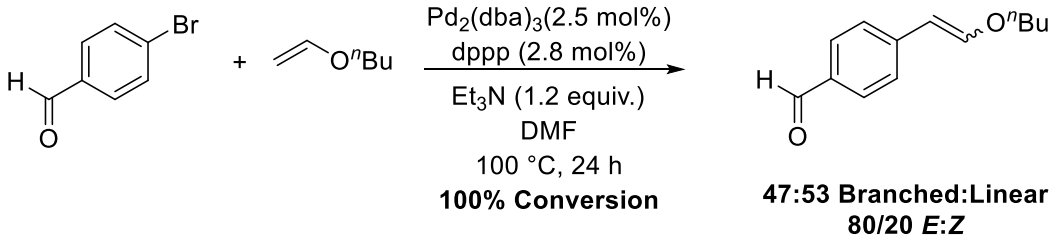

Scheme 1.16

Additionally, the regioselectivity of the intramolecular Heck cyclisation reaction can be governed by the stereospecificity of the *β*-hydride elimination step. *Syn*-elimination must occur, and, as illustrated in **Scheme 1.17**, only one isomer, **43**, can be produced from the starting cyclic alkene. Following addition across the double bond, the elimination of H_b cannot arise, and only β-hydride elimination of H_a can take place.[20]

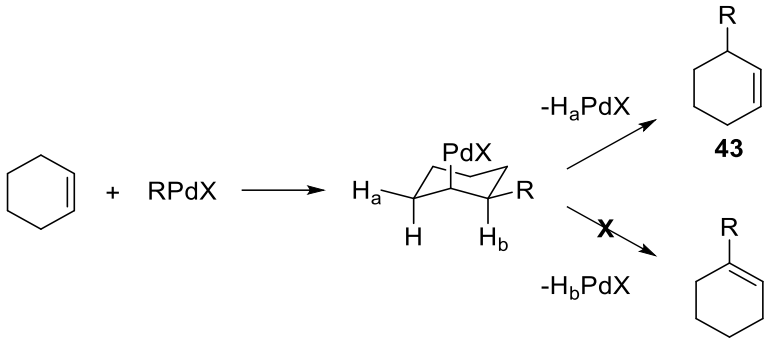

Scheme 1.17

1.2.5 The Intramolecular Heck Reaction

Intramolecular Heck cyclisation reactions can be used to construct a wide array of complex cyclic structures, varying in size. Many functional groups can be tolerated, allowing the synthesis of highly functionalised, congested systems including tertiary and quaternary carbon centres. Possible control of regio- and stereoselectivity additionally highlights its capability as a synthetic tool in natural product synthesis. Moreover, an asymmetric intramolecular Heck reaction can be employed to install chirality into the cyclic structures generated. Indeed, understanding the mechanism is important with regards to the asymmetric intramolecular Heck cyclisation reaction, and this will be discussed in a further section.

The first intramolecular Heck reaction was explored by Mori in 1971 through the reaction of an aryl bromide containing an α,β-unsaturated ester (**Scheme 1.18**).[32] Neat conditions were employed, which resulted in the synthesis of the corresponding indole in a moderate 43% yield. Note here that the 5-*exo*-trig mode of cyclisation initially generates the exocyclic alkene product, however, isomerisation leads to the formation of the more stable indole product. It has been shown that the addition of silver salts inhibits this isomerisation step, resulting in the exocyclic system.[19]

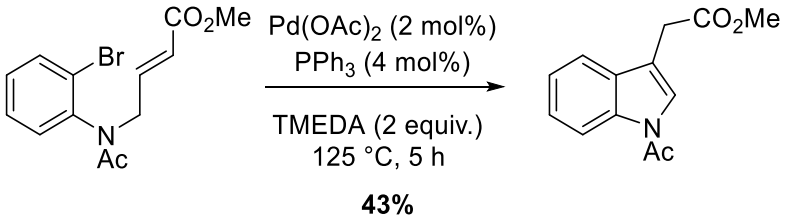

Scheme 1.18

Exo vs Endo Mode of Cyclisation

The mode of cyclisation in the intramolecular Heck reaction is an important factor in the ring size that is ultimately formed. Due to entropic factors, the *exo*-trig mode is dominant in these Heck cyclisation reactions, forming the less sterically demanding C–C bond. This concept is illustrated in **Scheme 1.19**, emphasising the preference for the *exo*-trig mode of cyclisation. For the *endo*-trig event to occur, the double bond must distort such that there is a correct alignment for *syn*-carbopalladation to take place, where the olefin moves to the inside of the loop between the olefin and the C–Pd bond. Reaching this conformation is difficult if the tether is short, therefore requiring a flexible tether in the molecule to allow the alignment to proceed. In the *exo*-mode of cyclisation, this distortion is not required for *syn*-carbopalladation to progress thus more favourable.

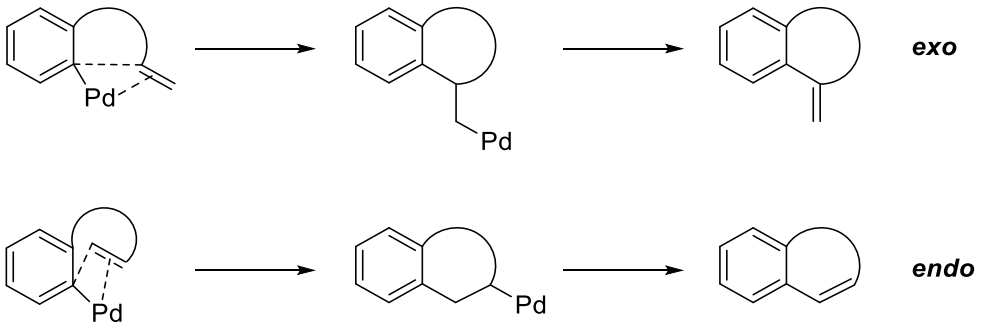

Scheme 1.19

Common examples show intramolecular Heck reactions where the olefin is activated by a carbonyl group (*c.f.* **Scheme 1.17**). However, Overman, in 1989, showed successful cyclisation of a vinyl triflate to the 6-*exo*-trig product exclusively using an isolated, and thus relatively unreactive, olefin (**Scheme 1.20**).[33]

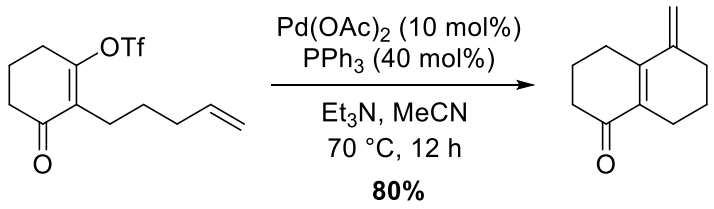

Scheme 1.20

In relation to the above, if the tether is long enough to allow flexibility in the Heck substrate, the *endo* mode of cyclisation can compete. Indeed, *endo* products can also become favoured due to electronics of the olefin used in the intramolecular Heck reaction, generating large rings.[34] This effect is explored in **Scheme 1.21, Table 1.1**, highlighting that the yield of cyclised products generated through the *endo* mode of cyclisation increases as the tether chain length increases in size. In this example, the *endo* mode of cyclisation is particularly favoured due steric and electronic factors being aligned. The example also illustrates the utility of the intramolecular Heck in the synthesis of 7, 8 and 9-membered rings.

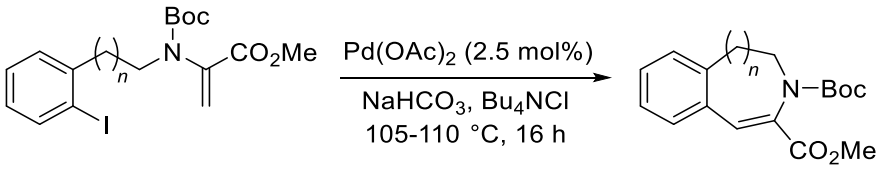

Scheme 1.21

n	**Yield (%)**
1	41
2	63
3	89

Table 1.1

Tandem Intramolecular Heck Reactions

Further complex systems can be produced from tandem intramolecular Heck cyclisation reactions, where the synthesis of spirocycles and fused-ring systems have been reported in the literature.[35] For a system to undergo a tandem intramolecular Heck reaction, various functional groups must be present for the multi-cyclisation process to occur. First, a 'starter species' such as an aryl halide must be present to begin the Heck reaction. A 'relay species' such as another olefin, where more than one can be present, facilitates further cyclisation reactions through *syn*-carbopalladation. The resulting carbopalladated complex can participate in further cyclisation reactions, or terminate such that Pd returns to the catalytic cycle through *syn*-β-hydride elimination or anion capture. **Scheme 1.22** illustrates an example of a tandem cyclisation studied by Grigg in 1992.[35]

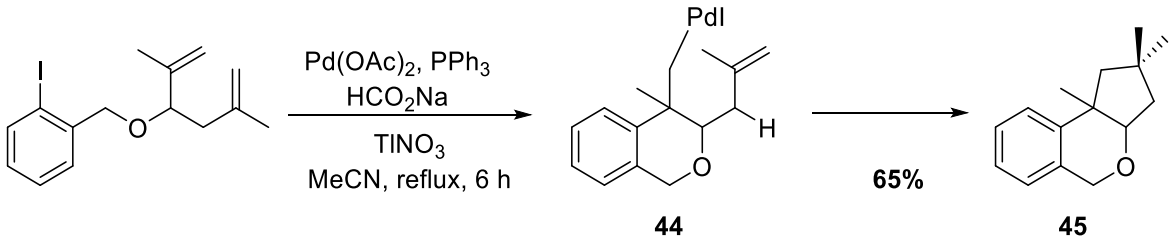

Scheme 1.22

The reaction of the initial substrate gives rise to the first cyclised product **44**, where there is no possibility for β-hydride elimination. Since an olefin (relay species) is present within the system, with no β-protons to eliminate after the initial Heck cyclisation, **44** undergoes subsequent cyclisation and hydride capture to produce **45** in a high yield of 65%.

As described thus far, the Heck reaction has quickly developed into a vital C-C bond forming transformation. Its potential to facilitate the construction of enantioenriched products, *via* manipulation of the reacting reagents and conditions, was naturally realised, which led to a significant body of further research. The following section highlights the key aspects and particularly significant developments regarding the asymmetric variant of Heck reaction.

1.2.6 The Asymmetric Intramolecular Heck Reaction

The asymmetric intramolecular Heck reaction is used to install tertiary or quaternary carbon chiral centres. The selectivity of the asymmetric intramolecular Heck reaction can be rationalised by two mechanistic pathways.[20] Cationic and neutral mechanisms have been proposed, with explanations as to why high enantioselectivity is imparted into the final product with each mechanism (*vide infra*). Generally, excellent enantioselectivity is determined by the extent of the attachment of the chiral ligand to the Pd centre throughout the Heck mechanistic cycle. If the chiral ligand partially dissociates from the Pd centre, deterioration of enantioselectivity would be observed. As such, bidentate chiral ligands are typically used in this process, examples of which are shown in **Figure 1.1**.

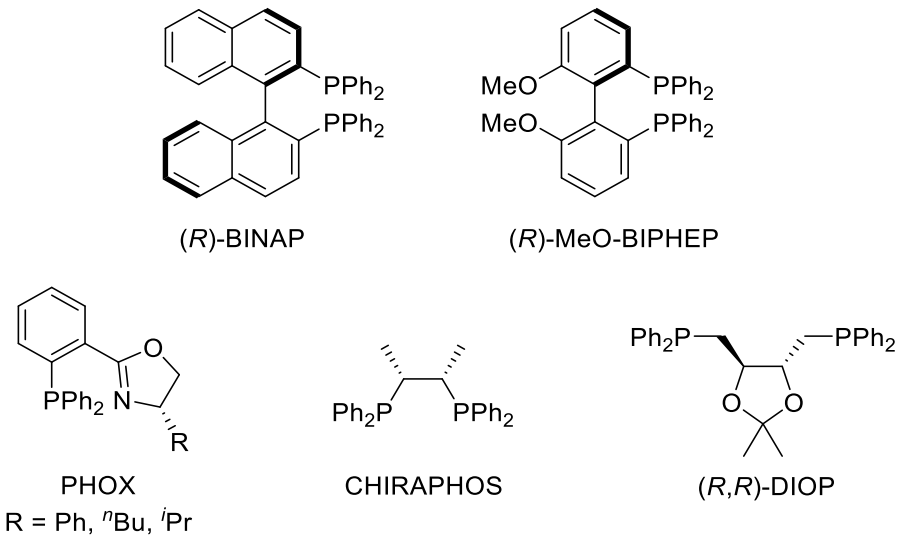

Figure 1.1

One of the first examples of a direct asymmetric Heck cyclisation forming a quaternary chiral carbon centre was demonstrated by Overman in 1989 (**Scheme 1.23**).[33] This impressive asymmetric transformation proceeded *via* a tandem cyclisation reaction, yielding the spirocyclic structure in high yields and modest enantioselectivity. This showcased the ability of the asymmetric Heck reaction to build highly congested carbon centres and complex carbon skeletons enantioselectively.

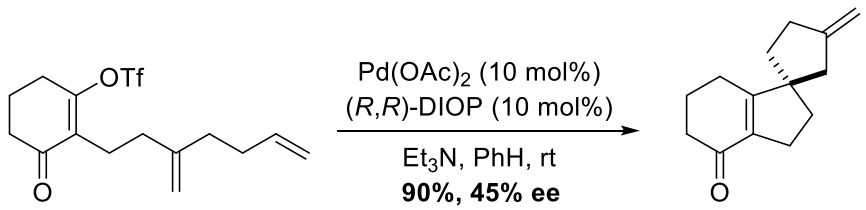

Scheme 1.23

In the same year, Shibasaki employed (*R*)-BINAP in the asymmetric Heck cyclisation process (**Scheme 1.24**),[36] furnishing the bicyclic product containing 2 quaternary centres in a high yield (74%) and with a similarly moderate enantiomeric excess (46% ee) to Overman's example.

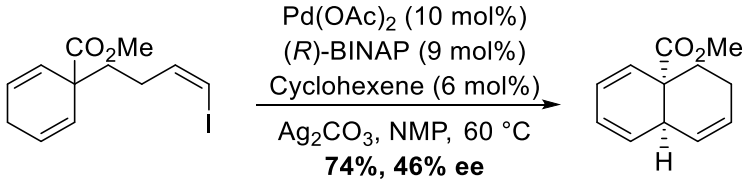

Scheme 1.24

The asymmetric Heck transformation was soon to be improved, as shown in **Scheme 1.25, Table 1.2**. Overman investigated the use of 1,2,2,6,6-pentamethylpiperidine (PMP) as the base in the asymmetric intramolecular Heck reaction under neutral conditions, and compared the result to silver promoted cationic conditions.[37] It was reported that the neutral conditions generated both excellent conversion to product and enantioselectivity compared to the cationic conditions. This raised questions about the mechanism of the asymmetric intramolecular Heck reaction, since it was somewhat surprising that neutral conditions were superior.

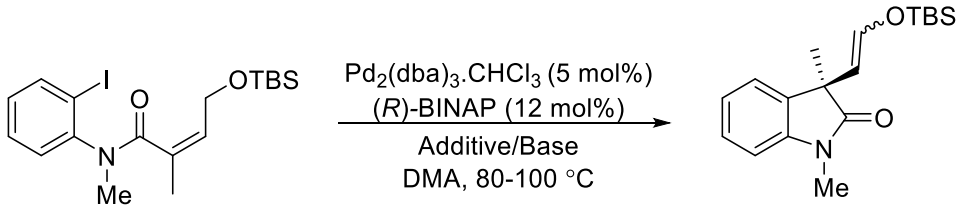

Scheme 1.25

Additive/Base	Yield (%)	ee (%)
Ag_3PO_4	78	53
PMP	92	80

Table 1.2

Mechanisms for the Intramolecular Pathway

The cationic pathway has, generally, been noted as more efficient in asymmetric Heck reactions over neutral conditions, since the bidentate chiral ligand remains attached to the Pd centre throughout the proposed mechanism (**Scheme 1.26**).[20,38] When X = I or Br, halide scavengers such Ag(I) or Tl(I) salts are required to leave a vacant coordinate site for alkene coordination and subsequent migratory insertion to take place with retention of the chiral diphosphine ligand throughout the process. As discussed before, utilising aryl triflates results in spontaneous dissociation of the OTf group, hence halide abstractors are not required for these intramolecular Heck transformations. This mechanism highlights the enantioselective determining step is most likely to be *syn*-carbopalladation.

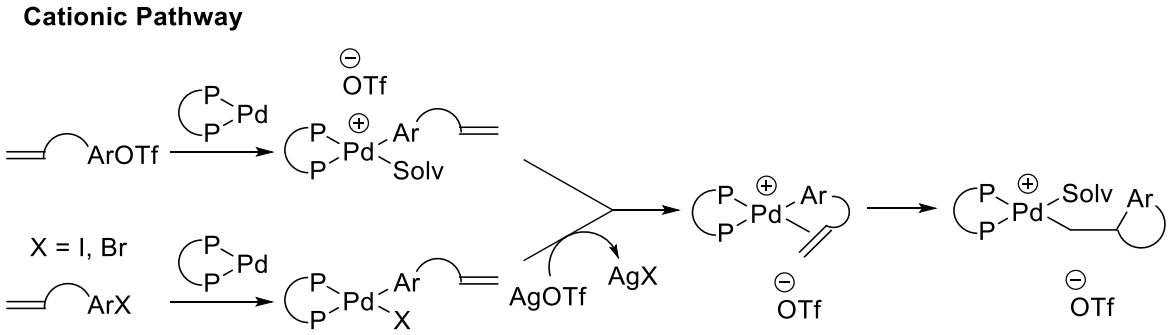

Scheme 1.26

Neutral conditions were originally thought to have resulted in low enantioselectivity due to the partial dissociation of the chiral bidentate ligand to free a vacant coordination site for alkene coordination and insertion (*c.f.* **Scheme 1.5**).[20,38] Indeed, in the absence of halide scavengers, early reports of neutral conditions illustrated low enantioselectivity with this pathway. However, in 1992, Overman studied asymmetric intramolecular Heck reactions using the bulky base 1,2,2,6,6-pentamethylpiperidine without halide scavengers present, and high enantioselectivity was obtained.[39] This resulted in mechanistic studies into the

neutral pathway, highlighted in **Scheme 1.27**.[40] In their study, they quickly ruled out pathway **46** to **48** *via* **47** with investigations involving the use of monophosphine BINAP derivatives, which undoubtedly formed intermediates of type **47**. In this case, erosion in enantioselectivity was observed in relation to diphosphine BINAP systems, therefore this route was disregarded. Additionally, the authors suggested that since neutral and cationic conditions can produce opposite enantiomers in the asymmetric Heck reaction (*vide infra*), each set of conditions must operate by two different mechanisms. Hence, the direct route from **46** to **48** *via* **49** was dismissed, due to the mechanistic similarity to the proposed cationic pathway. As pentacoordinate Pd(II) complexes have been isolated and characterised,[41] intermediate **50** has been suggested. This proposal is reinforced by the fact that associative processes can occur to allow substitution on square planar Pd(II) complexes. Hence, it is suggested that the initial axial coordination of the olefin generates pentacoordinate species **50**, and subsequent associative halide displacement occurs to form the cationic intermediate **49**, finally resulting in *syn*-carbopalladation to **48**. Theoretical and experimental investigations illustrate direct *syn*-carbopalladation to **50** from **48** is disfavoured due to high energy barriers.[42,43] Thus, they suggest the neutral mechanistic pathway is **46→50→49→48**. In this scenario, the enantioselective determining step is therefore said to be the formation of the cationic intermediate **49** by associative halide displacement.[40]

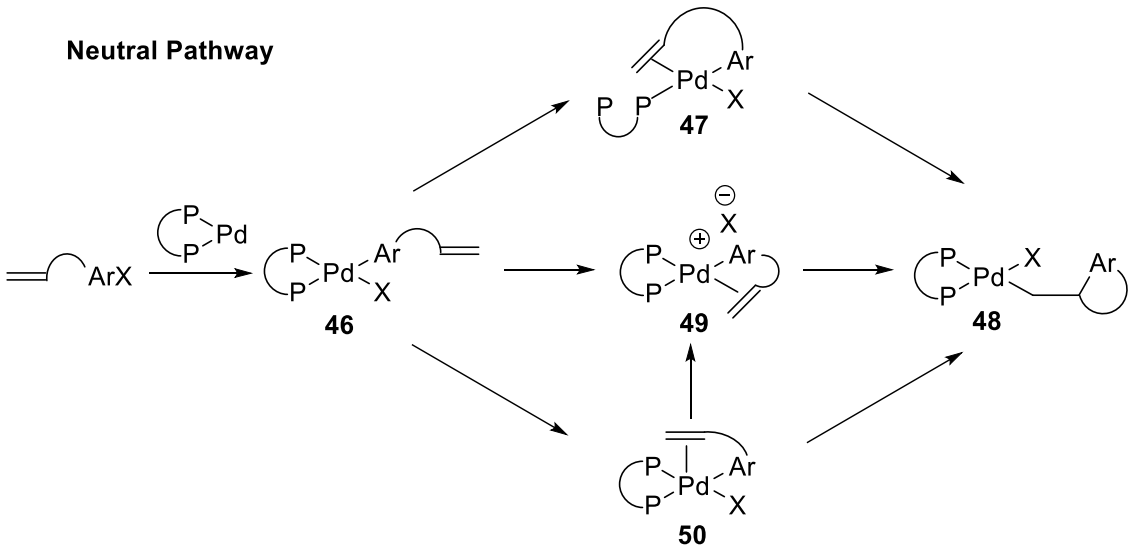

Scheme 1.27

Factors Controlling Enantioselectivity

The most common method of controlling enantioselectivity is to change the chiral ligand used in the asymmetric Heck reaction. A large library of different chiral ligands is available to screen asymmetric Heck processes, some of which were shown previously within **Figure 1.1**. However, the reaction conditions used (cationic or neutral), and the geometry of the olefin in the starting material have a substantial contribution to the enantioselectivity observed in Heck reactions.

As already stated above, using cationic or neutral conditions in the asymmetric Heck reaction can afford different enantiomers of the desired product, which is highlighted in **Scheme 1.28**.[39] In this case, a 5-*exo*-trig cyclisation of **51** under cationic conditions with Ag_3PO_4 generated the cyclised product (*S*)-(+)-**52**, in a slightly higher yield and enantioselectivity compared to the opposite enantiomer (*R*)-(-)-**52** generated under neutral conditions with PMP. In general, these results indicate that either enantiomer can be synthesised selectively by selecting the appropriate conditions, albeit in moderate enantioselectivity.

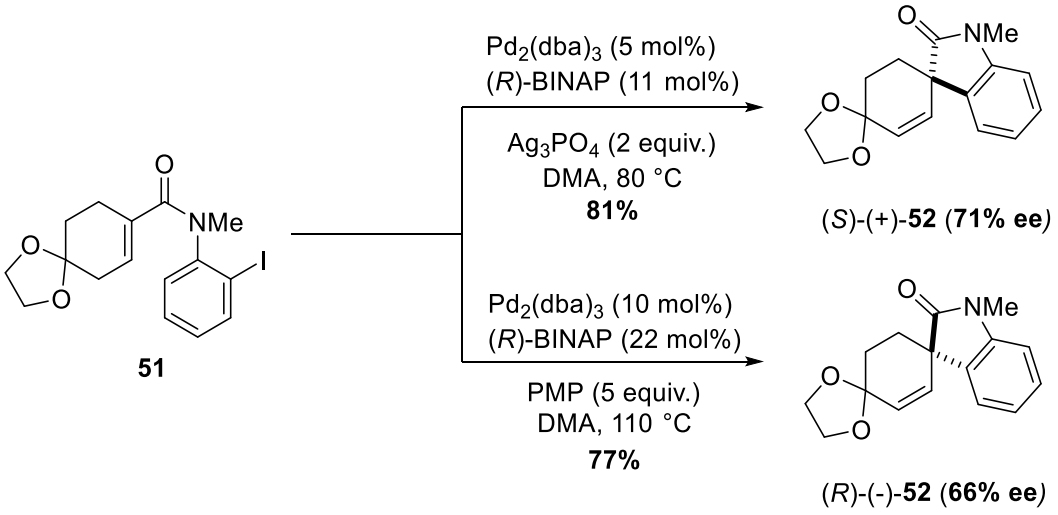

Scheme 1.28

The geometric isomer of the olefin in the initial starting material can also have an impact on the enantioselectivity of the desired product, illustrated with the asymmetric Heck comparative study of both *E* and *Z*- isomers as shown in **Scheme 1.29, Table 1.3**.[44]

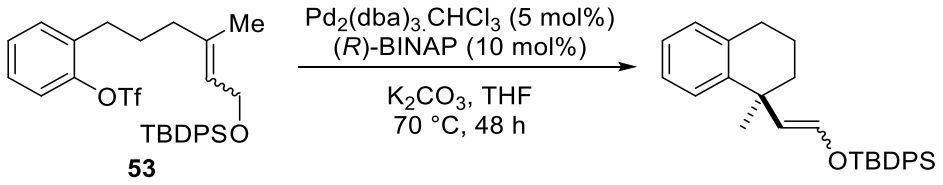

Scheme 1.29

Substrate	Yield (%)	ee (%)	*E*: *Z*
(*E*)-**53**	95	51 (*R*)	84:11
(*Z*)-**53**	97	80 (*S*)	92:5

Table 1.3

Through a 6-*exo*-trig mode of cyclisation under the same cationic reaction conditions, similar yields of the cyclised products were attained from both isomers of the starting material, however, greater enantioselectivity was exhibited with the starting *Z*-isomer (80 vs 51% ee). Moreover, opposite enantiomers were generated with each geometric isomer, where (*E*)-**53** afforded the (*R*) enantiomer and (*Z*)-**53** provided the (*S*) enantiomer. This study quickly demonstrates the complexity in the optimisation of the asymmetric Heck reaction, adding further complications with substrate synthesis prior to the Heck reaction. However, by varying the conditions (cationic or neutral) used and by careful choice of the chiral ligand employed in the reaction, the asymmetric Heck cyclisation reaction can be controlled to give the desired product.

Overall, the expansion of the intramolecular Heck reaction into an asymmetric protocol has enabled the widespread application of this key transformation in organic synthesis, and is continuing to be further developed through emerging research.

1.2.7 Recent Developments in the Asymmetric Intramolecular Heck Reaction

The advancement of the asymmetric intramolecular Heck reaction over the last three decades has enabled adaptations of the synthetically useful cyclisation procedure. More recently, this asymmetric protocol has been expanded into interesting multi-functionalisation processes, as demonstrated in the ensuing examples. This strategy centres around the capture of the alkylpalladium intermediate generated from the Heck process, allowing complex molecules to be constructed as a key quaternary stereocentre is formed with extended reactivity.

As conducted by Jia *et al*. in 2015, the asymmetric intramolecular Heck cyclisation has been utilised in the enantioselective dearomatisation of indoles *via* a Pd-catalysed reductive Heck process.[45] In their work, the authors demonstrated a facile transformation of a wide variety of indoles to tetracyclic indolines bearing a quaternary stereocentre at the C2 position with high yields and excellent enantioselectivity. As highlighted in **Scheme 1.30**, (*R*)-BINAP was employed for the enantioselective Heck process, constructing the tetracyclic ring system and the key quaternary carbon centre through a 5-*exo*-trig mode of cyclisation. Sodium formate was used as the hydride source to trap the alkylpalladium species resulting from the initial cyclisation, overall reducing the indole system. Thus, an efficient arylative and subsequent dearomatisation process of the indole unit was developed.

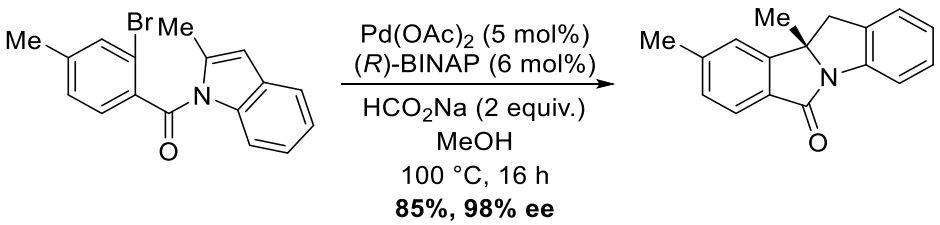

Scheme 1.30

The concept of enantioselective di-functionalisation in a single step was further expanded in 2019 by Zhang *et al.*,[46] where the group demonstrated an impressive di-carbofunctionalisation of unactivated alkenes through a Pd-catalysed tandem

enantioselective Heck/Suzuki cross-coupling procedure. Here, devising a general asymmetric domino approach with various boronic acids was extremely challenging due to potential side-reactivity. However, as illustrated in **Scheme 1.31**, this has shown success in constructing heterocyclic systems such as dihydrobenzofurans, indolines, and chromanes, depending on the heteroatom tether on the unactivated alkene. In the enantioselective Heck component with *N*-Me-Xu3 as the ligand, the 5-*exo*-trig mode of cyclisation generated the 5-membered rings with excellent % ee at the newly formed quaternary carbon centre. The resulting alkylpalladium intermediate subsequently undergoes a Suzuki cross-coupling reaction with corresponding boronic acids to construct complex scaffolds with exceptional yields and optical purity. This development was a remarkable endeavour, providing the first general protocol to facilitate a highly enantioselective intramolecular cyclisation/cross-coupling of unactivated olefin-tethered aryl halides with alkyl, alkenyl or aryl boronic acids, with >100 examples in their work.

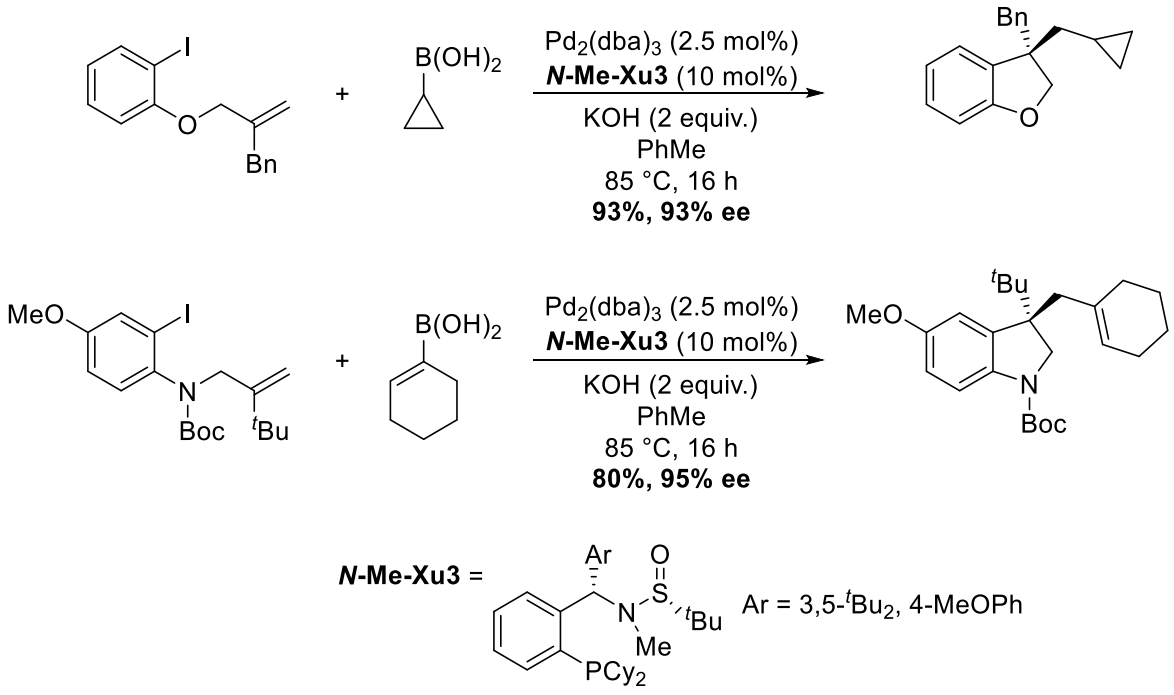

Scheme 1.31

Earlier this year in 2020, similar reports from Lu *et al*. demonstrated a general one-pot palladium and copper co-catalysed enantioselective Heck cyclisation/Sonogashira approach to efficiently generate chiral oxindoles from a trifluoromethyl-substituted *o*-

iodoacrylanilide and an alkyne (**Scheme 1.32**).[47] In their work, the initial enantioselective Heck of the activated alkene provides the quaternary centre of the oxindole through a 5-*exo*-trig mode of cyclisation. The resulting alkylpalladium species undergoes a subsequent Sonogashira coupling with the alkyne, extending the functionality of the final oxindole in good yields and excellent % ee (75%, 97% ee). The second cross-coupling component of this overall sequence provides a suitable functional handle which could be valuable in any diversity orientated synthesis.

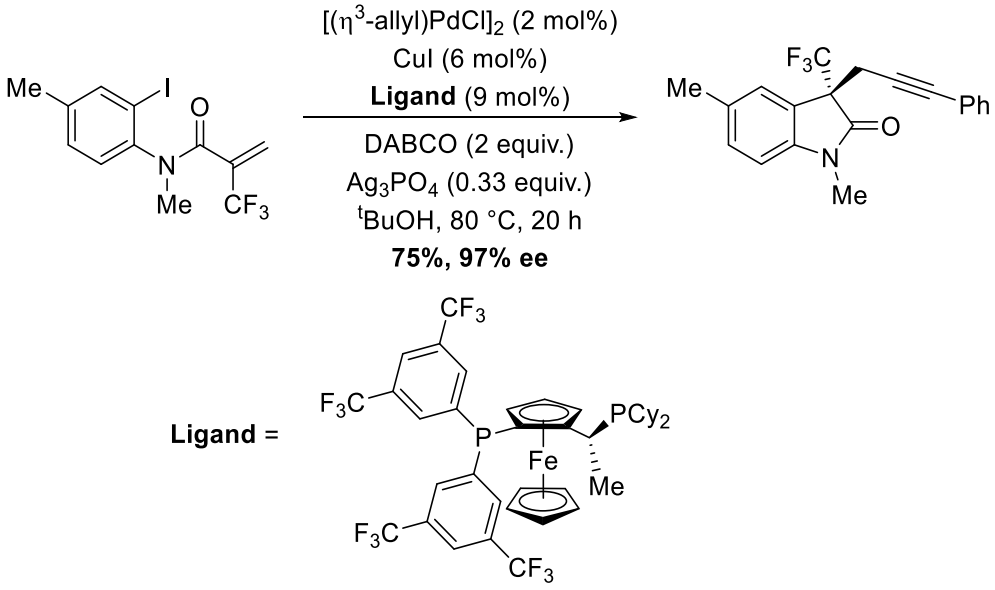

Scheme 1.32

These recent developments illustrate the ongoing progression in the application of the asymmetric intramolecular Heck reaction in tandem methodology. Undoubtedly, such emerging methods continue to represent the Heck reaction overall as one of the most impressive, and diverse, transformations within modern organic synthesis.

1.2.8 Application in Natural Product Synthesis

Based on the ability of the asymmetric intramolecular Heck reaction to generate complex structures selectively from accessible starting materials, it has unsurprisingly been used as a synthetic strategy towards the synthesis of natural products. Indeed, some of the Heck

examples shown thus far have been transformations embedded within total synthesis programmes. A further example below exemplifies the total synthesis of xestoquinone **54** *via* a tandem asymmetric intramolecular Heck cyclisation, which builds the polycyclic skeleton of the natural product in one step (**Scheme 1.33**).[48] This elegant synthesis involves the use of the cheap and readily available (*S*)-BINAP ligand to build a key quaternary centre and finalise the desired pentacyclic ring structure from a vastly more simple tricyclic framework.

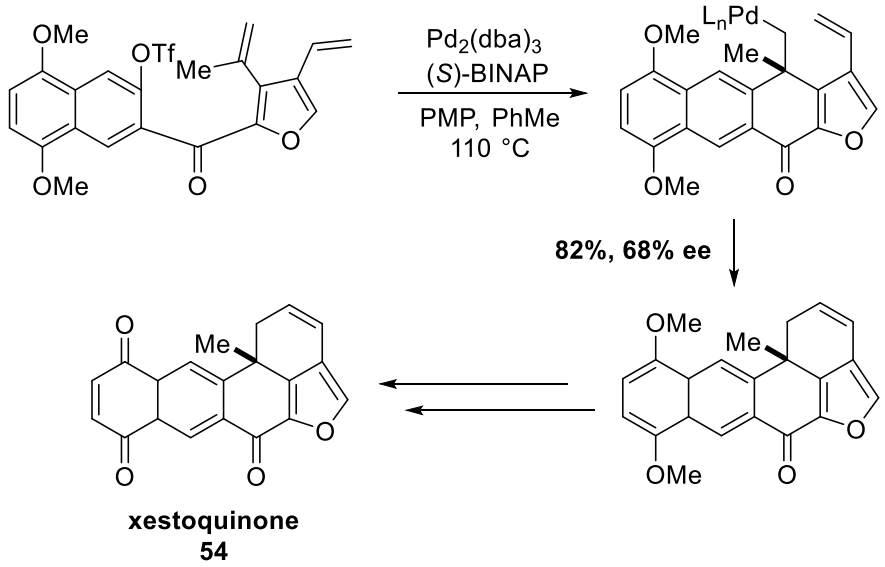

Scheme 1.33

In 2008, Overman *et al.* demonstrated the effectiveness of the chiral (phosphinoaryl)oxazoline (PHOX) ligand system in their total synthesis of the natural product (+)-minfiensine **55**.[49] In their initial synthesis, Overman *et al.* employed BINAP as the ligand within the intramolecular Heck reaction, however, the desired product **57** was not achieved and instead the isomerised target **56** was isolated (**Scheme 1.34**). Presumably, **56** was generated through the double bond migration of Pd intermediate **58**.

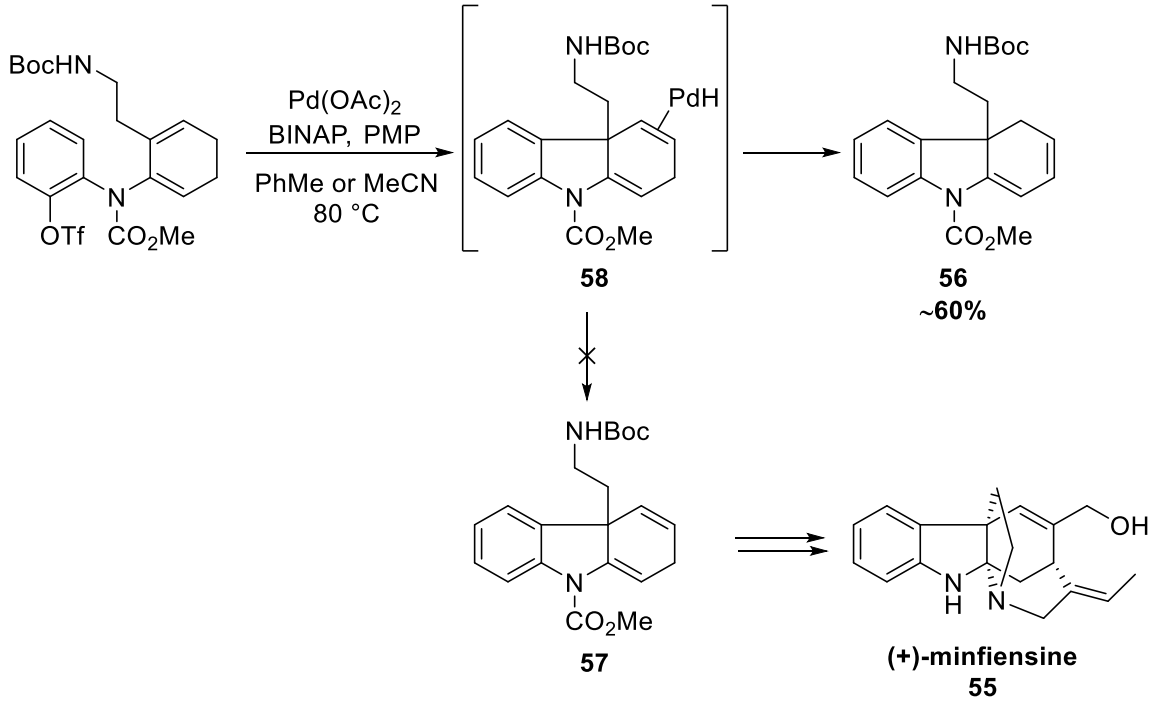

Scheme 1.34

However, when Overman *et al.* utilised commercially available PHOX ligands in their key asymmetric Heck reaction, the desired product was obtained with excellent isolated yields and enantioselectivity (**Scheme 1.35**, **Table 1.4**). Overman *et al.* reported that, under thermal conditions, they obtained excellent yields and % ee towards their desired target **57**, with no isomerisation observed (**Entries 1** and **2**). Despite achieving a remarkable 99% ee using ^{t}BuPHOX (**Entry 2**), the methodology required long reaction times of 70 h. However, after further optimisation, they were extremely delighted to have accomplished comparable yields and % ee when microwave conditions were employed, reducing the overall reaction time to just 45 min (**Entry 3**). Notably, no erosion in enantioselectivity was observed at a higher temperature of 170 °C.

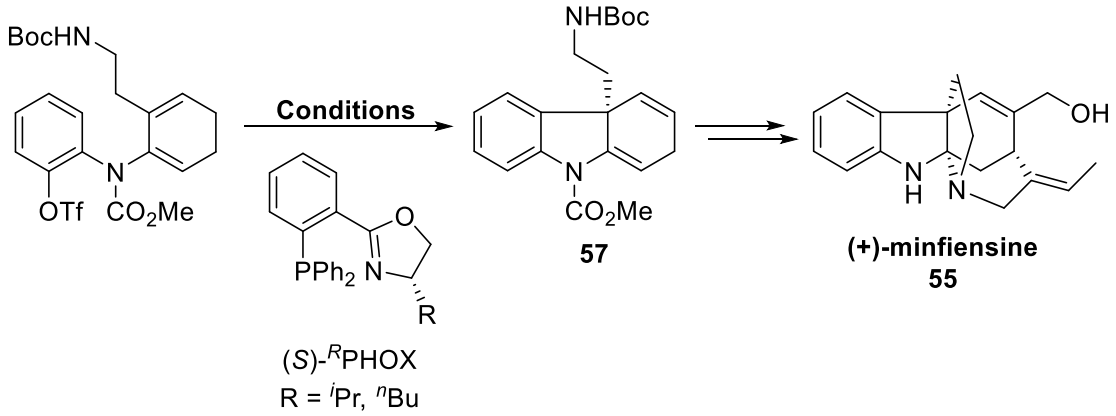

Scheme 1.35

Entry	Heating	Conditions	Yield of 57 (%)	% ee of 57 (%)
1	Thermal	$Pd(OAc)_2$ (20 mol%), (*S*)-^{i}PrPHOX (30 mol%) PMP, PhMe, 100 °C, 70 h	79	88
2	Thermal	$Pd(OAc)_2$ (20 mol%), (*S*)-^{t}BuPHOX (30 mol%) PMP, PhMe, 100 °C, 70 h	75-85	99
3	Microwave	$Pd(OAc)_2$ (20 mol%), (*S*)-^{t}BuPHOX (30 mol%) PMP, PhMe, 170 °C, 45 min	87	99

Scheme 1.4

More recently, in 2017, this particular microwave-assisted enantioselective Heck methodology was utilised as a key transformation to generate the core skeleton of the natural product (-)-viridin **59** (**Scheme 1.36**).[50] Here, Guerrero *et al*. showed that after just 80 minutes exceptional enantioselectivity was achieved in the synthesis of **60**, which represented the key pentacyclic core of the natural product.

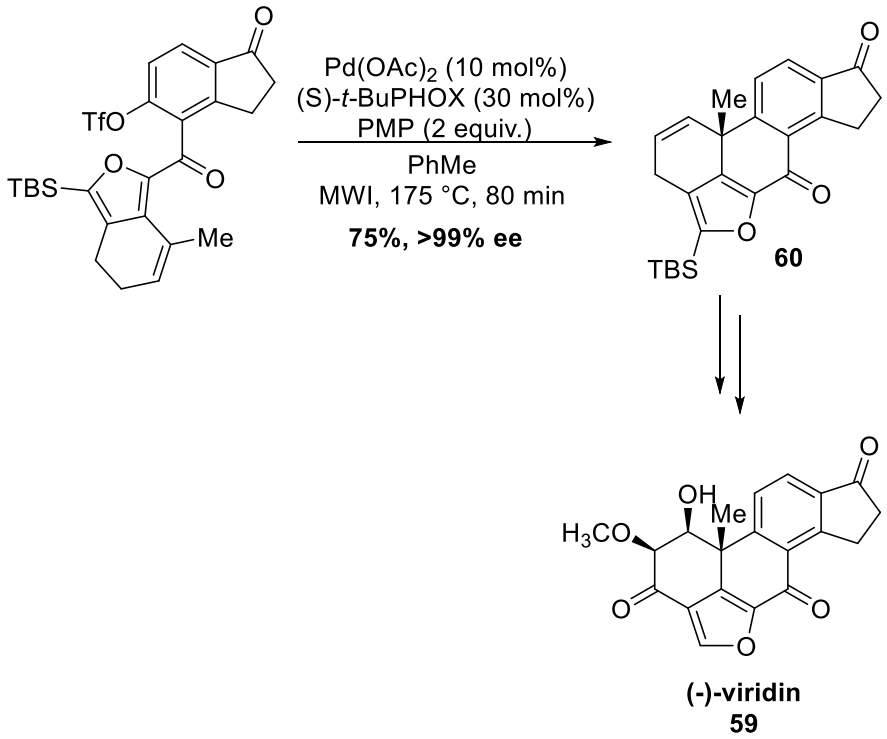

Scheme 1.36

In relation to our proposed synthesis of agariblazeispirol C, we envisage a 6-*exo*-trig mode of cyclisation using an asymmetric intramolecular Heck reaction protocol. This approach would form a C–C bond at the α position of the enone and build the bicyclic system towards the synthesis of the natural product (**Scheme 1.37**). The transformation of **61** to **62** is challenging due to a potential clash in electronics during the C-C bond forming process in the Heck reaction, not to mention the formation of a quaternary carbon centre. More specifically, whilst we desire the more favourable 6-*exo*-mode of cyclisation, the electron-poor nature of the alkene within **61** may also facilitate the undesired 7-*endo*-cyclisation. With this in mind, ketal **18**, which has the advantage of altering the electronics of the Heck cyclisation process, would also be a targeted intermediate within our synthetic programme. Regardless, in both cases, the asymmetric Heck of each precursor is novel and has no literature precedent.

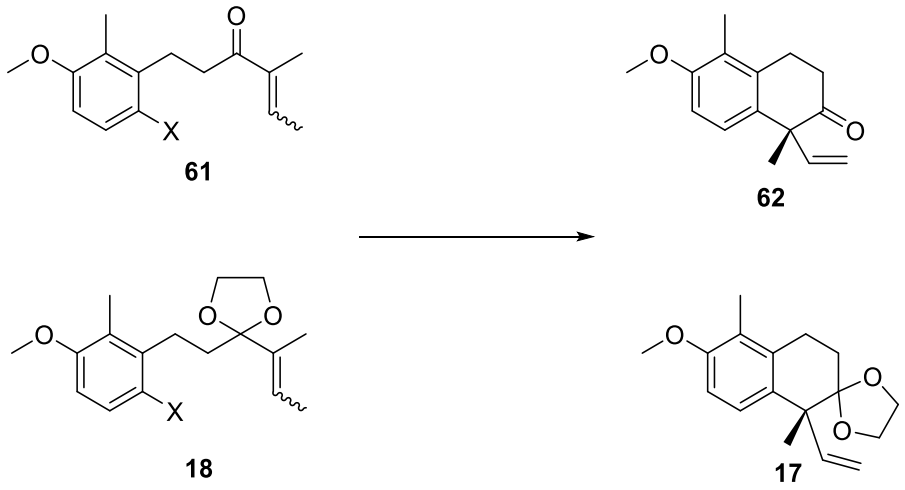

Scheme 1.37

Previous examples described in this review so far have illustrated the effectiveness of the asymmetric Heck reaction on similar systems to the one of interest, i.e. where a *exo*-trig mode takes place with an α,β-unsaturated system, obtaining high yields and enantiomeric excess. **Scheme 1.38** highlights an additional example by Overman, where a similar but-2-ene olefin is used in the asymmetric Heck reaction, and a high yield of the 5-*exo*-cyclised product was obtained but with modest enantiomeric excess.[51] However, there exists no literature examples of a 6-*exo*-trig mode of cyclisation involving an α,β-unsaturated system to compare with our key transformation.

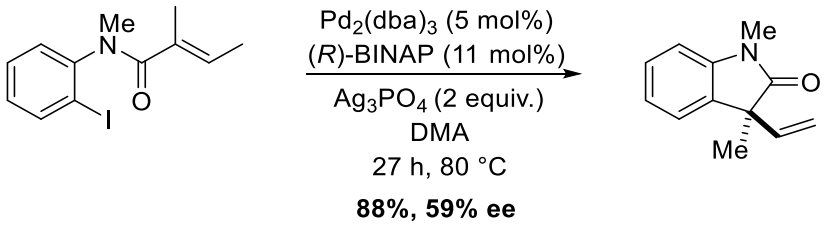

Scheme 1.38

In conclusion, the Heck reaction has become an essential synthetic technique for organic chemists to construct organic frameworks. Since the 1970s, the development of the Heck reaction has expanded into a wide array of variants, including an incredibly effective intramolecular process. As a result, the Heck reaction flourished further through the advancement of the asymmetric protocol, which has been applied to the synthesis of natural products. The exponential progression of the Heck reaction over the last few decades has been recognised, and was awarded a Nobel Prize in chemistry in 2010. Despite the success of the Heck protocol, further investigations are required to further expand the general applicability of the transformation. Indeed, there is often a requirement for substantial and specific reaction optimisation based on the varied ligands, bases, and reaction conditions that can be used in the Heck reaction.

1.3 Pauson-Khand Reaction[52–54]

1.3.1 Introduction

As previously discussed, in our research group we have focused on the development and application of the Pauson-Khand reaction. This transformation was first reported in 1971 by Ihsan U. Khand and Peter L. Pauson at the University of Strathclyde.[55] The PKR is a [2+2+1] one-pot annulation technique involving an alkyne, present as its hexacarbonyldicobalt complex, an alkene, and a molecule of carbon monoxide to form functionalised cyclopentenones (**Scheme 1.39**).[56]

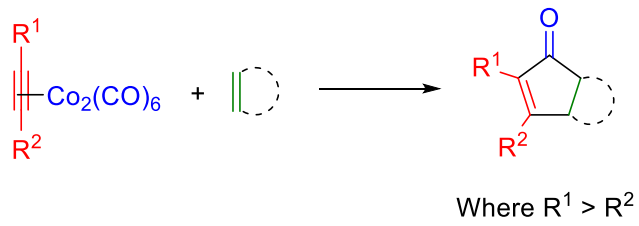

Scheme 1.39

To generate the hexacarbonyldicobalt complex required in the PKR, the alkyne **63** and octacarbonyldicobalt **64** are stirred at room temperature in an inert solvent, and the cobalt complex **65** is furnished, generally, in excellent yields (**Scheme 1.40**). This involves the displacement of two bridging carbon monoxide ligands in octacarbonyldicobalt.

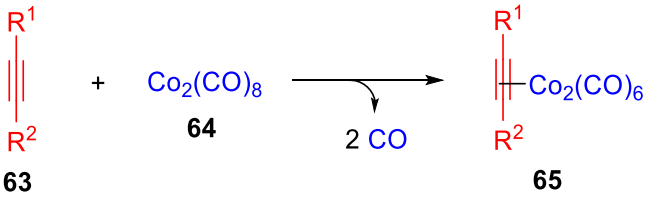

Scheme 1.40

1.3.2 General Mechanism

The generally accepted mechanism for the PKR was proposed by Magnus in 1985 (**Scheme 1.41**),[57] with many continuing mechanistic investigations presented in the literature each year (*vide infra*).

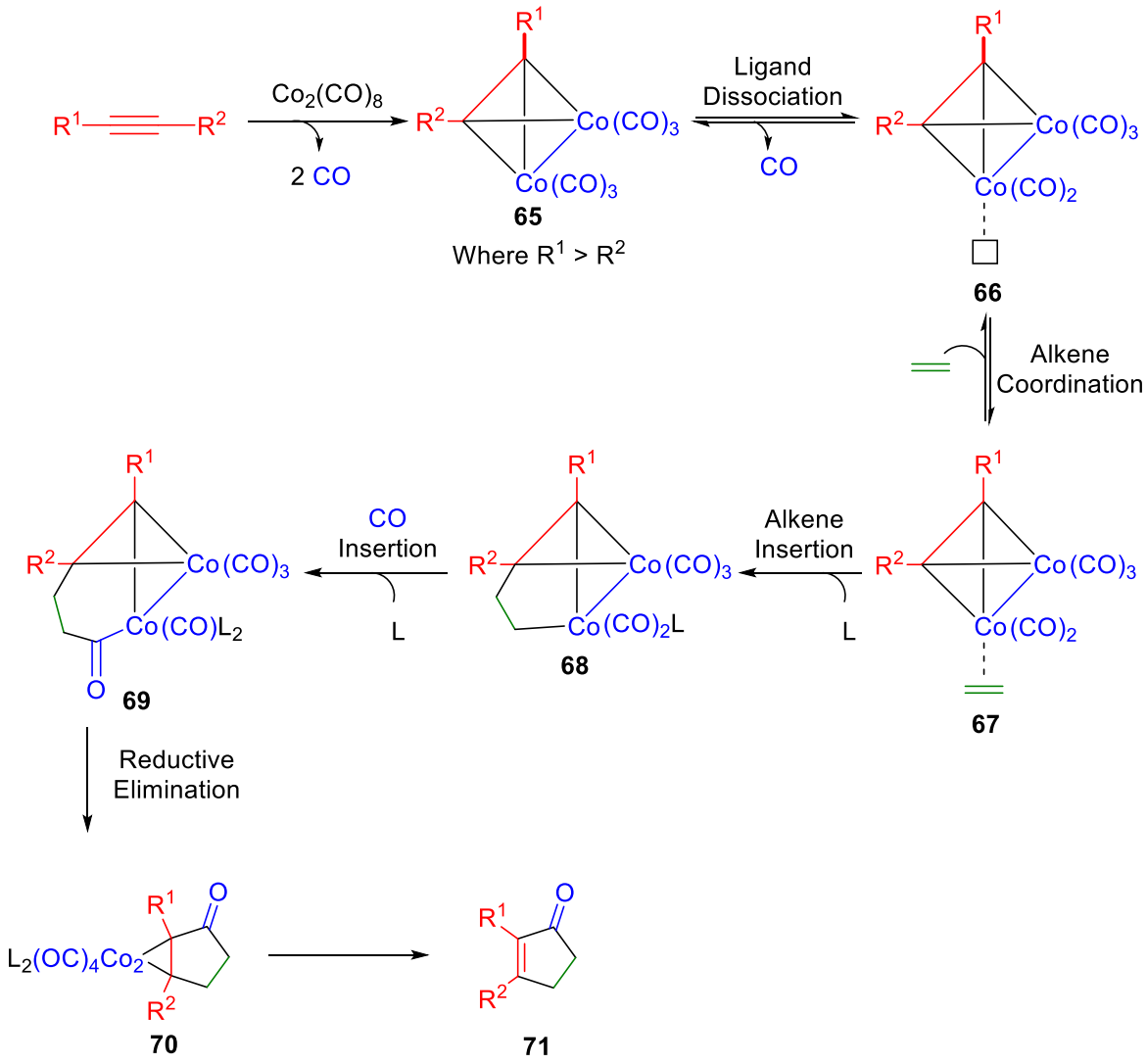

Scheme 1.41

As discussed previously, the first step involves the formation of the hexacarbonylalkynedicobalt complex **65**. Next, reversible dissociation of a carbon monoxide ligand occurs, which generates a coordinatively unsaturated dicobalt complex **66**. The alkene partner can then reversibly coordinate onto the vacant site of the dicobalt

species, sitting in a *trans* fashion to the alkyne carbon holding the sterically larger $\mathbf{R^1}$ substituent (**67**). Irreversible alkene insertion into the least hindered Co–C bond follows to provide cobaltacycle **68**. It is considered that this step is the rate determining step of the reaction,[52] in addition to controlling the regioselectivity of the final cyclopentenone product. Subsequent carbon monoxide insertion into the newly formed Co–C bond occurs to generate complex **69**, and two reductive elimination steps ensue, the first generating **70**, and the second furnishing the desired cyclopentenone **71**.

1.3.3 Regioselectivity in the Intermolecular Pauson-Khand Reaction

Regioselectivity with the Alkyne Partner

In many examples, alkyne regioselectivity is determined by steric factors whereby the larger substituent of the alkyne resides on the 2-position of the generated cyclopentenone product due to steric effects as depicted in the above mechanism. Research conducted by Pauson[58] showcases the regiochemical control of alkynes, and is highlighted in **Scheme 1.42** where **72** was formed exclusively.

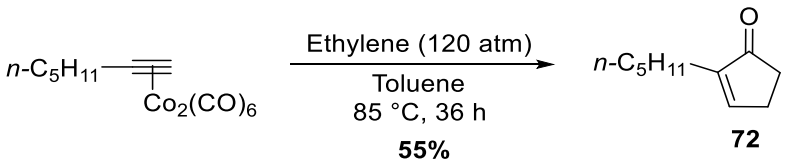

Scheme 1.42

Having stated that above, exceptions of this rule are observed, especially when unsymmetrical internal alkynes are used in the PKR. Indeed, shown through the studies conducted by Pauson,[59] using an internal alkyne with similar sized substituents resulted in a mixture of both regioisomers (**Scheme 1.43**). Although the predicted regioisomer was preferentially formed in **24%**, a small amount (**3%**) of the other regioisomer was obtained.

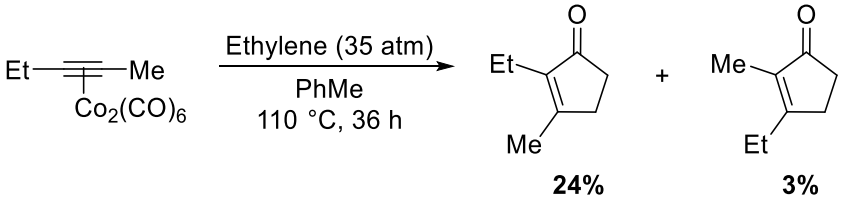

Scheme 1.43

Gimbert and Greene[60] illustrated another exception where the regioselectivity cannot be interpreted through steric effects (**Scheme 1.44**). When unsymmetrical alkynes bear substituents with electronic bias, but are sterically similar, the annulation process affords the cyclopentenone where the electron-withdrawing group resides on the 3-position as the exclusive product. Here, regioselectivity is governed through electronic factors, where alkyne polarisation effects dictate the 3-position selectivity.

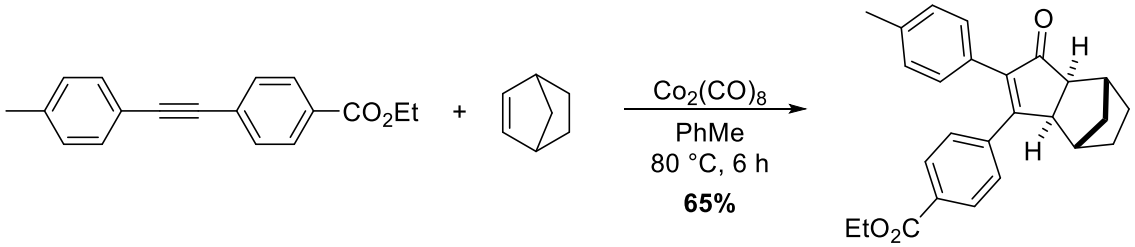

Scheme 1.44

Regioselectivity and Reactivity with the Alkene Partner

Predicting the regioselectivity in the PKR with regards to the alkene component is much more difficult. Poor regioselectivity was observed in the investigation conducted by Pauson (**Scheme 1.45**),[61] where a terminal alkene was reacted with a terminal alkyne. Although the selectivity associated with the alkyne component was maintained in the cyclopentenone formed (where the large substituent occupies the 2-position), no regioselectivity in terms of the alkene partner was observed since a 1:1 mixture of each regioisomer was obtained.

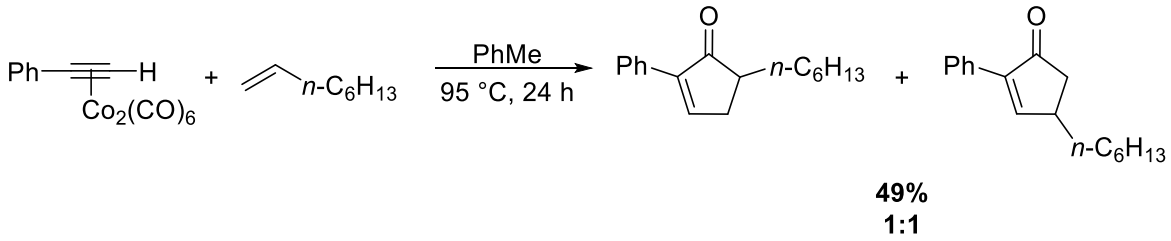

Scheme 1.45

In contrast, using the same alkene partner as above, Krafft highlighted that regioselectivity associated with the alkene can be controlled and predicted when an internal alkyne is used in the PKR (**Scheme 1.46**).[62] In this regard, steric factors control the regioselectivity such that the large substituent on the alkene resides on the 5-position of the final cyclopentenone with excellent preference (**19:1**), albeit with low chemical yields observed overall.

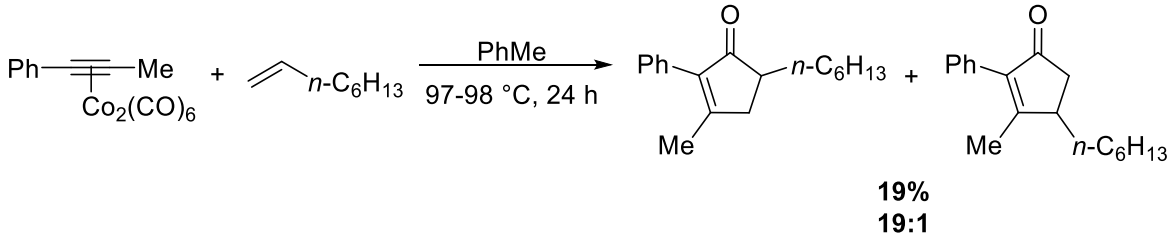

Scheme 1.46

In an attempt to have more control over alkene regioselectivity, Krafft explored the concept of a directed PKR (**Scheme 1.47**).[62] This involves a heteroatom linked to the reacting alkene whereby the heteroatom can behave as a soft donor ligand, controlling regioselectivity by chelating onto the cobalt atom. This chelating ability conformationally locks the complexed alkene, favouring the production of the 5-substitued cyclopentenone.

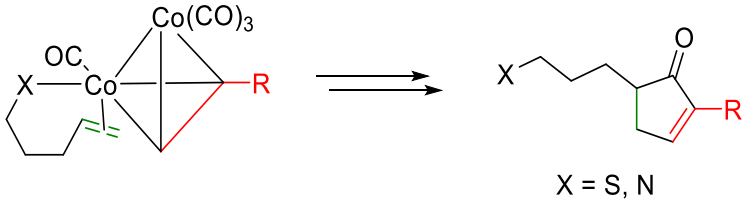

Scheme 1.47

Indeed, homoallylic or bishomoallylic sulfides and amines can act as directing ligands, not only to enhance the regioselectivity of the PKR, but also accelerating the yield of the annulation process overall (**Scheme 1.48**).

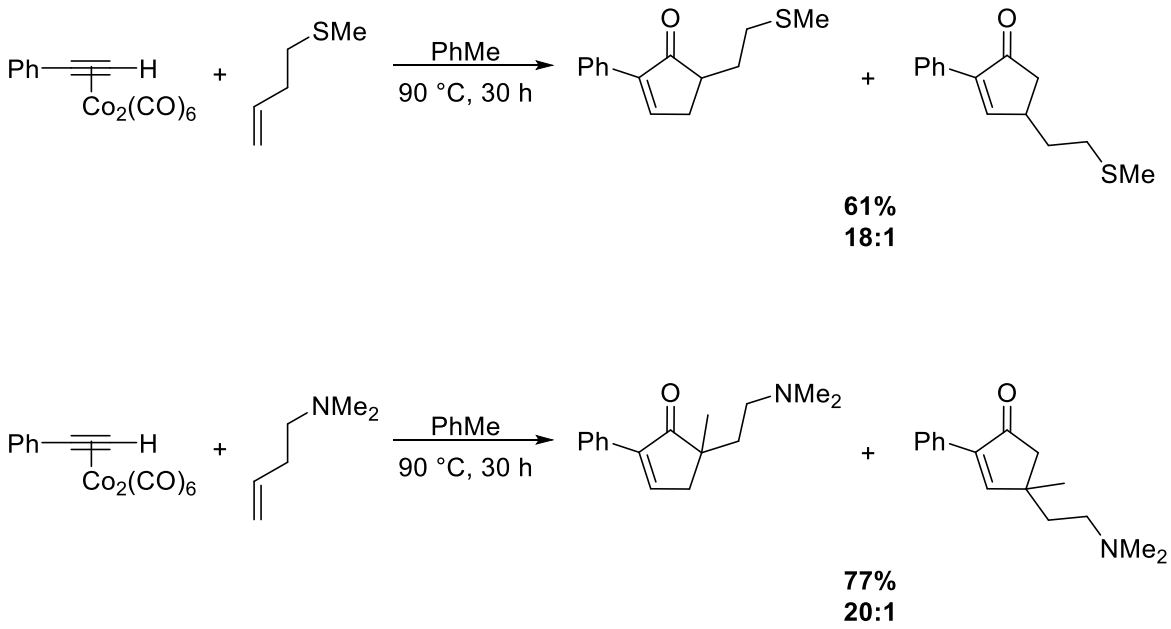

Scheme 1.48

To explore the reactivity of alkenes in intermolecular PKRs, extensive studies have been conducted, and have shown that strained cyclic alkene partners give better yields of the desired cyclopentenone products. Milet, Gimbert, and co-workers rationalised the relationship between back-donation of electrons from the cobalt metal centre to the π* orbital of the olefin (LUMO).[63] In their efforts, they established a correlation between the energy of the LUMO and the angle of the C=C-C bond. It was determined that the smaller the bond angle, the lower the LUMO energy. This correlation aligns with experimental observations in the PKR with strained alkenes (**Scheme 1.49, Table 1.5**).[64] The PKR of the highly strained norbornene (**Table 1.5, Entry 1**) proceeded under mild conditions, achieving moderate yields. Employing less strained alkenes in the PKR (**Entries 2** and **3**) requires harsher reaction conditions, although only moderate to low yields are obtained.

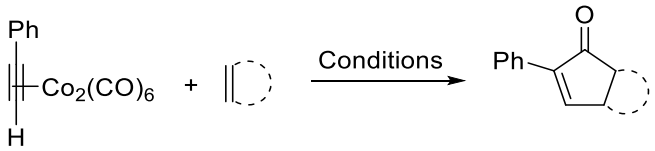

Scheme 1.49

Entry	Alkene	C=C-C Bond Angle (°)	$LUMO_{Coord}$ of Olefin (eV)	Reaction Conditions	Yield (%)
1	Norbornene	107	- 0.087	Mesitylene, 60-70 °C, 4 h	59
2	Cyclopentene	112	+0.203	Toluene, 160 °C, 80 atm, 7 h	47
3	Cyclohexene	128	+0.336	Toluene, reflux, 6 h	3

Table 1.5

Conjugated Alkenes

The PKR of conjugated alkene systems has demonstrated to be a difficult annulation process in the literature. In the intermolecular sense, the primary issue with these systems is their propensity to engage in a side reaction, which inhibits the formation of the desired cyclopentenone. Pauson reported this competing observation during the reaction between hexacarbonylalkynedicobalt complex **73** and styrene (**Scheme 1.50**).[65] Under these traditional reaction conditions, the desired cyclopentenone **74** was not the major product, and instead the formation of conjugated diene **75** was favoured.

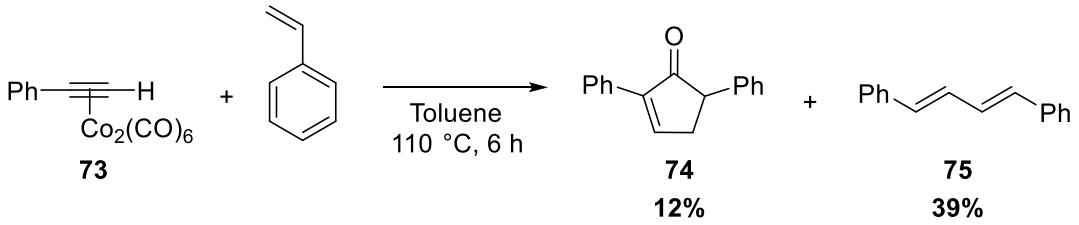

Scheme 1.50

The alternative route to the unwanted coupled product is proposed to be through a β-hydride elimination pathway, which competes against the insertion of carbon monoxide in the

Pauson-Khand process to form the cyclopentenone (**Scheme 1.51**). Preferential formation of the by-product suggests that the insertion of carbon monoxide is significantly slower than the a β-hydride elimination, highlighting the strenuous nature of the insertion of carbon monoxide in the PKR of conjugated alkene systems.

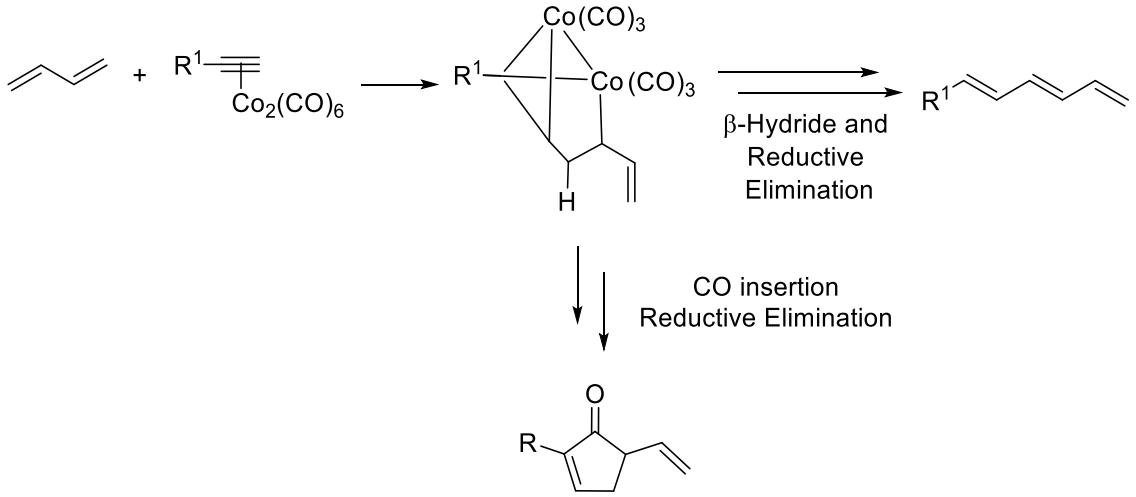

Scheme 1.51

Since conjugated alkenes are challenging systems in Pauson-Khand processes, Wender *et al.* turned their attention to these systems to improve product selectivity.[66] Indeed, they developed rhodium-catalysed conditions, where, under an atmosphere of carbon monoxide, the desired cyclopentenone product was afforded exclusively and in exceptional yields (**Scheme 1.52**). In their work, they provided nine other examples to highlight the applicability of their transformation for this difficult process. However, 10 equivalents of the initial conjugated alkene were required. Nevertheless, this example highlights the use of other transition-metals in the PKR, and, indeed, in a catalytic sense.

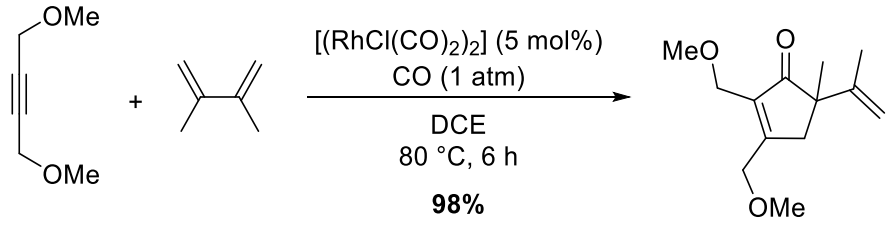

Scheme 1.52

1.3.4 Intramolecular Pauson-Khand Reactions

Control and prediction of regioselectivity in the intermolecular PKR can be challenging, however, these issues are removed with the intramolecular variation. By tethering the alkyne unit onto the alkene component, intramolecular PKRs can be used to furnish cyclised cyclopentenones as one regioisomer with respect to both the alkyne and alkene components. The intramolecular PKR was first developed by Schore in 1981,[67] where bicyclic enones were generated from tethered enynes, although the initial results were low yielding and the reaction conditions were somewhat harsh (**Scheme 1.53, Table 1.6**).

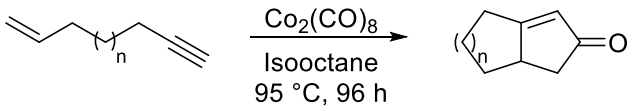

Scheme 1.53

n	**Yield (%)**
1	31
2	35

Table 1.6

The intramolecular PKR eventually expanded into using nitrogen[68] and oxygen-tethered[69] enynes to deliver similar bicyclic enones (**Scheme 1.54**). Moderate to low yields were also obtained with these cyclisation reactions, particularly with the latter example where harsher (atmosphere of CO) and prolonged (96 h) reaction conditions were required.

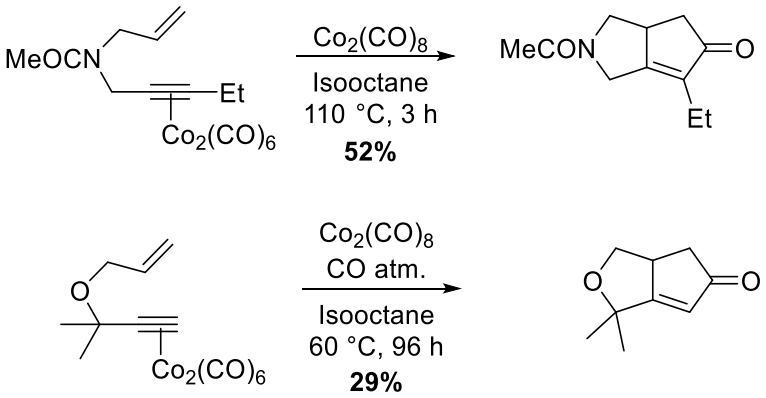

Scheme 1.54

1.3.5 Advances in the Pauson-Khand Reaction

Traditional PK cyclisations required harsh conditions, typically employing high temperatures and sometimes pressures. Consequently, the overall yield of these annulation processes was generally low to moderate, with various organic and organometallic by-products being formed. Challenging purification is therefore required to extract the cyclopentenone from the complex mixture. Due to these problematic issues of the initial PKR, the reaction conditions have since been enhanced to allow milder conditions for the cyclisation reaction. Beginning in the 1980s, modifications of the PKR by various groups allowed the development of the PKR into a robust synthetic tool. Initially, dry state absorption,[70] ultrasound,[58] and developments in microwave techniques[71] were investigated, which significantly increased the efficiency of the PKR compared to the original thermal reaction conditions. The most effective, and widely used, methods of enhancing the PKR is to use amine-*N*-oxide, amine or sulfide promoters. Additionally, a drive to develop an efficient catalytic PKR has been explored, as traditional methods employ stoichiometric amounts of $Co_2(CO)_8$ to pre-form the desired cobalt alkyne complex for the subsequent cyclisation.

Amine-N-Oxides

In 1990, Schreiber first introduced the addition of an amine-*N*-oxide to accelerate the PKR.[72] Excellent yields were achieved from this advancement, which made amine-*N*-oxides the most popular additives to enhance the efficiency of the PKR. The role of amine-*N*-oxide in the PKR is to remove carbon monoxide from the metal centre, thus the first step in the PKR becomes irreversible and promotes the annulation process to progress faster (**Scheme 1.55**).[73]

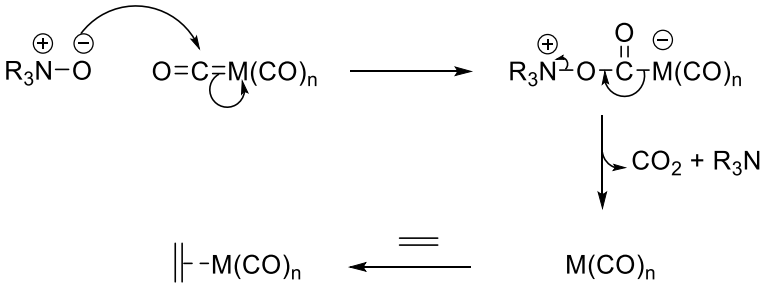

Scheme 1.55

Comparing the use of this additive with the dry state absorption technique illustrated that much milder PKR conditions can be used with amine-*N*-oxides to achieve superior reaction efficiency (**Scheme 1.56, Table 1.7**).[72] Here, the dry state absorption conditions require elevated temperatures to achieve 59% yield, whereas when using the amine-*N*-oxide, *N*-methylmorpholine *N*-oxide (NMO), the PKR can be performed at room temperature to achieve 92% yield, albeit at a longer reaction time.

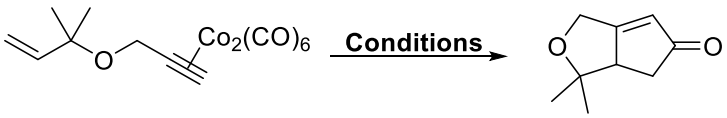

Scheme 1.56

Entry	Enhancement Technique	Conditions	Yield
1	Dry State Absorption	SiO_2, O_2, 55 °C, 1.5 h	59
2	Amine-*N*-Oxide	NMO, CH_2Cl_2, rt, 12 h	92

Table 1.7

Shortly after, Jeong reported trimethylamine *N*-oxide (TMANO) as another impressive amine-*N*-oxide.[73] It was demonstrated that TMANO could be used to enhance both intramolecular and intermolecular PKRs effectively (**Scheme 1.57**).

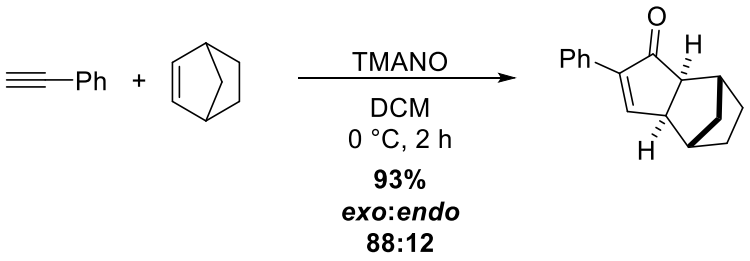

Scheme 1.57

Amines

In 1997, Yamaguchi and co-workers investigated the use of various primary amines in promoting the PKR.[74] Initially, it was suggested that Lewis bases would improve the cyclisation since nitrogen or oxygen atom containing ligands could accelerate the dissocation of carbon monoxide, creating an unsaturated vacant site for olefin insertion to proceed. However, in 2005, Milet, Gimbert, and co-workers conducted computational studies, and from their findings they proposed that a Lewis base can coordinate onto the metal and promote olefin insertion through irreversibility of the process, stabilising any coordinatively unsaturated intermediates in the PKR.[75] Nevertheless, Yamaguchi illustrated that a wide range of amines could promote the PKR, with cyclohexylamine giving the best results (**Scheme 1.58, Table 1.8**).[74] Interestingly, ammonia, produced from ammonium hydroxide in 1,4-dioxane, was also shown to be an additive to enhance the annulation process.

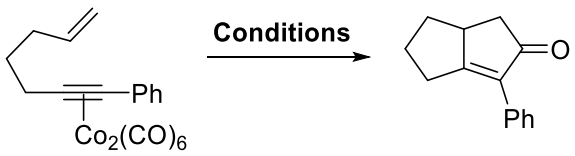

Scheme 1.58

Entry	Conditions	Yield
1	3.5 equiv. $CyNH_2$, DCE, reflux, 5 min	99
2	1 M NH_4OH/1,4-dioxane (3:1), 100 °C, 45 min	96

Table 1.8

Although amine additives promote the PKR effectively, slightly more forcing conditions are required with these conditions compared to amine-*N*-oxides.

Sulfide Promoters

Not only did Yamaguchi and co-workers discover the use of amines to accelerate the PKR, they also reported sulfides as another class of now popular promoters.[76] Alkyl methyl sulfides were described to be the better promoters, particularly *n*-butyl methyl sulfide (^{n}BuSMe). The advantage of using this promoter compared to cyclohexylamine is illustrated in **Scheme 1.59**, where the desired cyclopentenone product **76** was obtained with ^{n}BuSMe but not with cyclohexylamine. With the amine, it was seen that the alkyne containing fragment of the starting material was cleaved, isolating **77** instead.

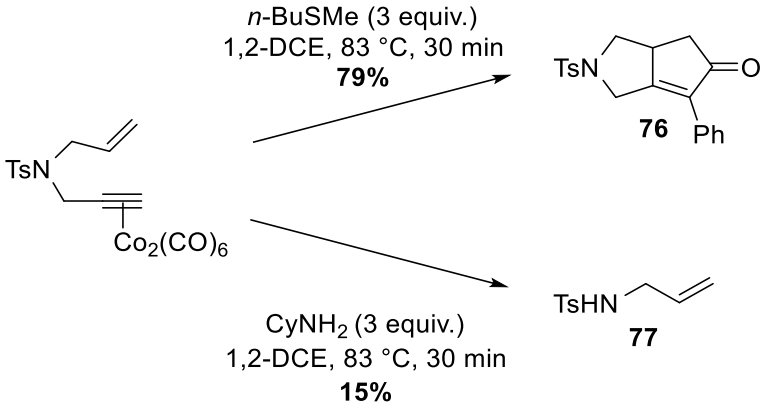

Scheme 1.59

Excellent yields can be achieved using ^{n}BuSMe, however, higher temperatures are required to match the efficiency of PKR promoted by amine-*N*-oxides. Other issues with ^{n}BuSMe is the lachrymatory effects and its unpleasant smell. Research from within our own laboratories has developed a polymer-supported sulfide, which removes the unwanted attributes associated with ^{n}BuSMe (**Scheme 1.60**).[77] The polymer-supported sulfide has shown comparable efficiencies to ^{n}BuSMe, with additional advantages in that the promoter can now be reused with excellent retention in activity over many cycles and simplified purification since both additive and cobalt complex can be removed *via* filtration.

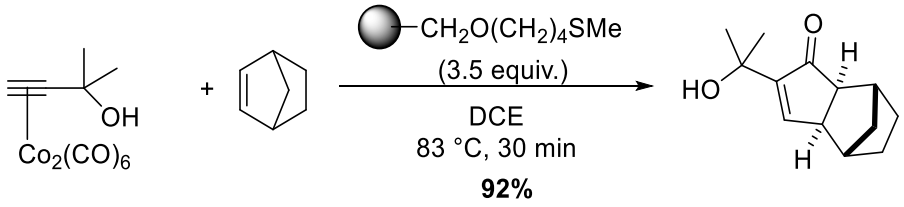

Scheme 1.60

In addition to the above, we have further enhanced PK methodology through the use of another solution phase sulfide promoter, dodecyl methyl sulfide (DodSMe).[78] This odour free promoter has been shown to enhance many Pauson-Khand processes, generating comparable yields to the less practical ^{n}BuSMe (**Scheme 1.61**).

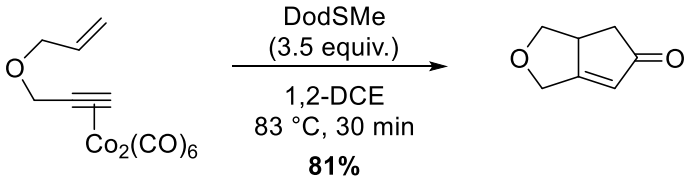

Scheme 1.61

Catalytic PKR

Up until this point, bar Wender's rhodium catalysed method,[66] examples of the PKR involved a purified, pre-formed cobalt alkyne complex, generated from stoichiometric amounts of $Co_2(CO)_8$, which was subsequently subjected into the annulation conditions. Hence, developing an efficient catalytic variant would reduce the amount of cobalt metal used and remove the need to isolate and purify the cobalt complex, increasing its applicability within organic research and industry. The initial development of a catalytic PKR required harsh reaction conditions, such as high temperatures and pressures of CO.[52,79,80] Researchers had noted one of the key issues in developing a robust catalytic PKR was to avoid the formation of inactive metal clusters, due to the unstable, coordinately unsaturated $CO_2(CO)_6$ complex formed in the catalytic system.

One method to circumvent this issue in catalytic PKR protocols was to stabilise the $CO_2(CO)_6$ complex formed within the PKR. Jeong *et al*.[81] demonstrated this through the application of triphenylphosphite additives, as these stabilise the cobalt complex through displacement of a CO ligand. Thus, this development provided one of the first methods of a practical catalytic PK cyclisation. As highlighted in **Scheme 1.62**, despite requiring 3 atm of CO and high temperatures of 120 °C, a low catalyst and ligand loading was employed to achieve the desired cyclopentenone product in an 82% yield.

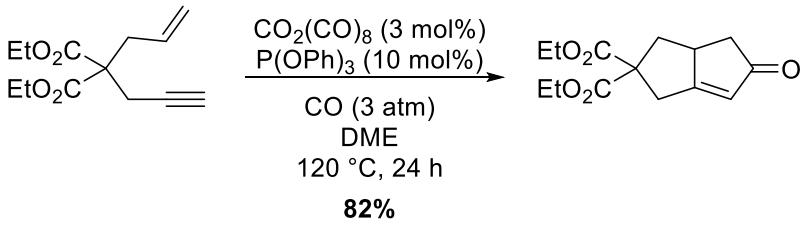

Scheme 1.62

Further advancements in the catalytic PKR has resulted in efficient methodology, as reported by Yang *et al*. in 2005.[82] In their work, the authors illustrated that thiourea additives could be employed for an efficient catalytic PKR, where tetramethylthiourea (TMTU) was also employed in catalytic amounts (**Scheme 1.63**). Here, mild reaction conditions with only 1 atm of external CO was required to furnish the desired cyclised product in an excellent 95% yield.

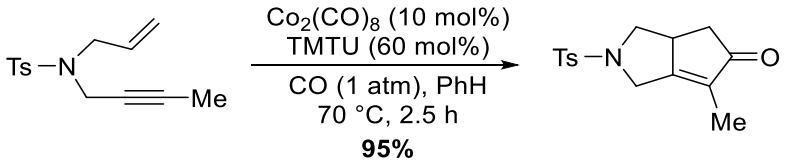

Scheme 1.63

In general, the PKR has developed into a practical synthetic tool in organic synthesis. Despite the associated complications of the intermolecular PKR with regards reactivity and regioselectivity, the intramolecular variant has become an extremely effective

transformation in synthesis through the advancements of PK promoters and catalytic protocols.

1.3.6 Recent Developments in the Intramolecular Pauson-Khand Reaction

As detailed in this report thus far, the intramolecular PKR is commonly employed to generate 5,5-bicyclic systems – indeed whilst the synthesis of 5,6- and 5,7-bicyclic systems are also possible, such annulations are often more difficult. Notably, one of the key limitations of the intramolecular PKR is the absence of any substantial functionality on the reacting alkene and alkyne components. Indeed, current PKR methodology is somewhat limited to furnishing relatively unfunctionalised cyclopentenones bearing simple alkyl/aryl substituents around the ring, as illustrated in the many examples above. This key drawback prevents the generation of more diverse, and synthetically intriguing, functionalised products. The construction of functionally rich polycyclic motifs is, of course, of significant interest within synthetic methodology, and it is only very recently that emerging PK methods seem to be venturing into this untapped area.

Recently in 2019, Barrio *et al*. pursued to address this key limitation through the intramolecular PKR of enynes containing a vinyl fluoride moiety.[83] This served as the first example of such in the literature (**Scheme 1.64**).

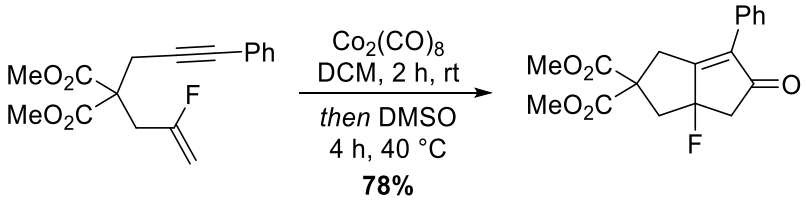

Scheme 1.64

In their work, they demonstrated the ability to generate a variety of cyclopentenone products containing a synthetically useful tertiary fluoride centre. A one-pot PKR process was applied, where the initial hexacarbonyldicobalt alkyne complex was formed *in-situ* which subsequently underwent the cyclisation, with DMSO as the promoter. However, the

key drawback of their methodology, which resulted in lower yields, was the elimination of hydrogen fluoride, destroying the important heteroatom functionality installed in the fluoro-PKR.

The same authors further embellished their work in this area through the application of enantioriched enynes containing a vinyl fluoride into their established protocol (**Scheme 1.65**).[84] Here, a diastereoselective PKR delivered the desired enantioriched 5,6-bicyclic system featuring the tertiary fluoride substituent in good yields and excellent diastereoselectivities. Overall, the recent work conducted by Barrio *et al*. has established emerging PK methodology to generate more functionally diverse bicyclic systems, enhancing the overall annulation technique.

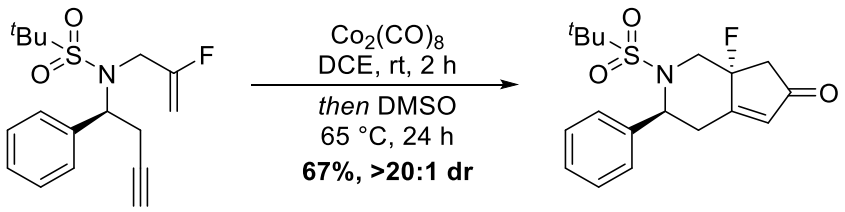

Scheme 1.65

Within our own research group, current efforts have been devoted into developing PKR protocols which deliver more functionalised scaffolds through probing the functionality around the reacting centres. More specifically, we have recently probed the olefin component of the reaction, establishing the first intramolecular PK cyclisation of silyl enol ether substrates, examples of which are shown in **Scheme 1.66**.[85] We have demonstrated that this emerging methodology can furnish either synthetically challenging quaternary centres containing a C-O bond, or α-oxygenated cyclopentenone products depending on the nature of the starting silyl enol ether selected. Hence, our PK methodology provides access to intriguing cyclopentenone scaffolds containing an additional oxygen atom, further increasing the diversity of the PK substrate scope.

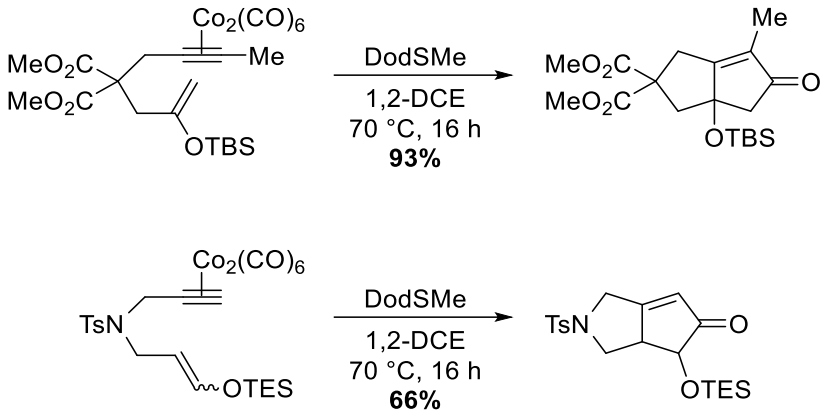

Scheme 1.66

In summary, although one of the key drawbacks of the intramolecular PKR is the lack of functional diversity in the substrate scope (where emerging methodology is beginning to improve the overall scope), developments in the PKR has enabled the facile synthesis of cyclopentenone motifs. Henceforth, the intramolecular PKR has been highly utilised in the construction of complex scaffolds in organic synthesis, as showcased in a variety of challenging natural product syntheses.

.

1.3.7 Application in Natural Product Synthesis

Through the enhancement of the PKR as described previously, it comes as no surprise that the reaction has become a robust synthetic tool in the synthesis of natural products. Cyclopentenone cores are present within many natural products, therefore, the PK annulation, with its ability to build structural complexity in just one step, has become an effective method in building impressive polycyclic frameworks.

Scheme 1.67 shows the synthesis of 2-epi-α-cedren-3-one **78** from our own research laboratories, where the PKR delivers the cyclic core of the natural product.[78] Using the DodSMe promoter, and after a short reaction time of only 40 minutes at 83 °C, the desired product **80** was obtained in an excellent yield of 92%.

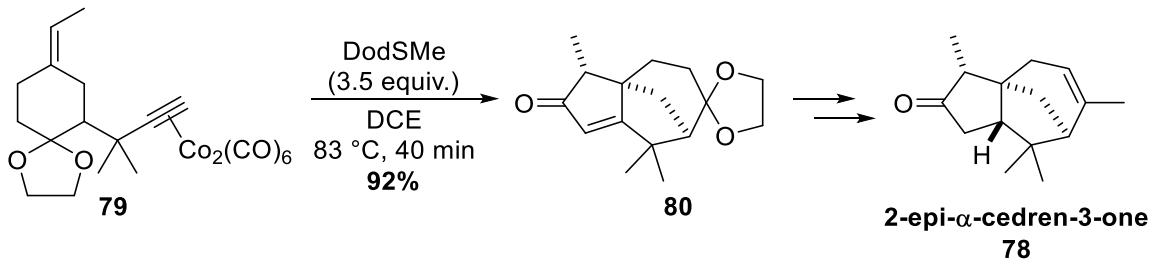

Scheme 1.67

More recently, the PKR has been used in the asymmetric total synthesis of lancifodilactone G acetate **81** by Yang and co-workers (**Scheme 1.68**).[86] Here, the authors use their own developed PKR conditions, where additive TMTU promoted the cyclisation reaction of **82** under catalytic conditions, employing an atmosphere of carbon monoxide. The PKR proceeded in an appreciably high yield of 73%, generating the congested cyclic core **83** as one isomer.

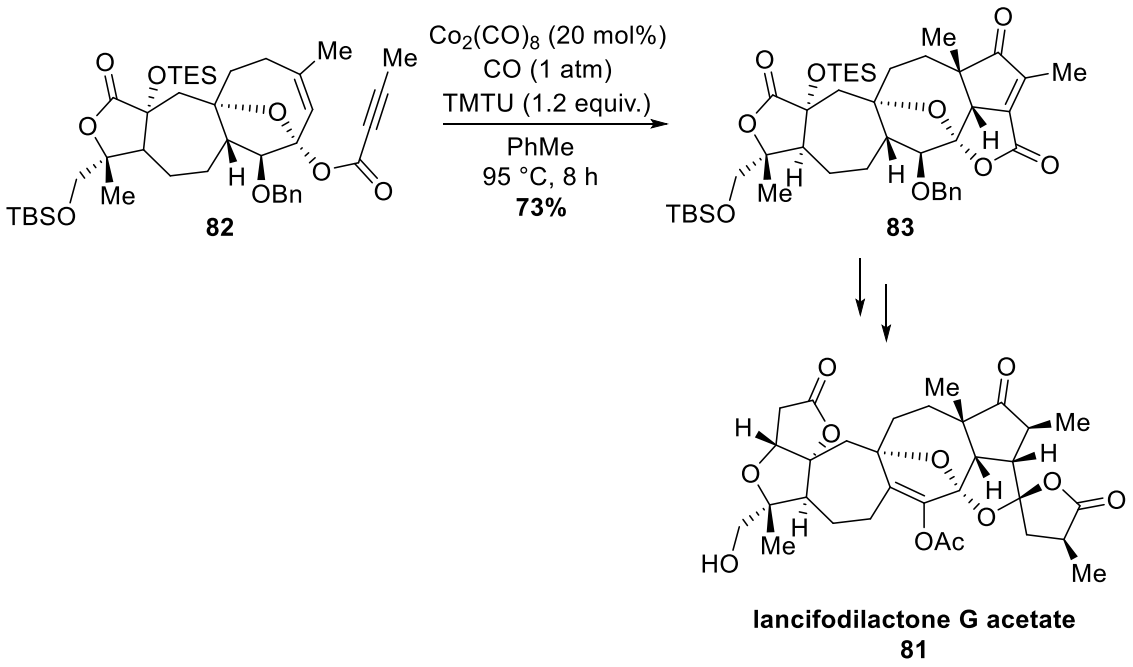

Scheme 1.68

In a total synthesis conducted by the same group, the PKR was utilised to construct the core of (±)-5-*epi*-cyanthiwigin I **84**.[87] In this synthesis, super-stoichiometric amounts of Co_2CO_8 and a large excess of additive NMO (5 equivalents) were used in the diastereoselective one-

pot PK cyclisation of **85** to **86** (**Scheme 1.69**). This example illustrates a synthetic strategy where a, traditionally more difficult, 5,6-bicyclic system is constructed through the PKR. Pleasingly, the desired product was obtained in a 70% isolated yield, and as a single diastereomer. It was interesting to note that, when performing the PKR without NMO, the cyclisation proceeded in a comparable yield of 70%, however as a 10:1 ratio of diastereomers at the C9 position.

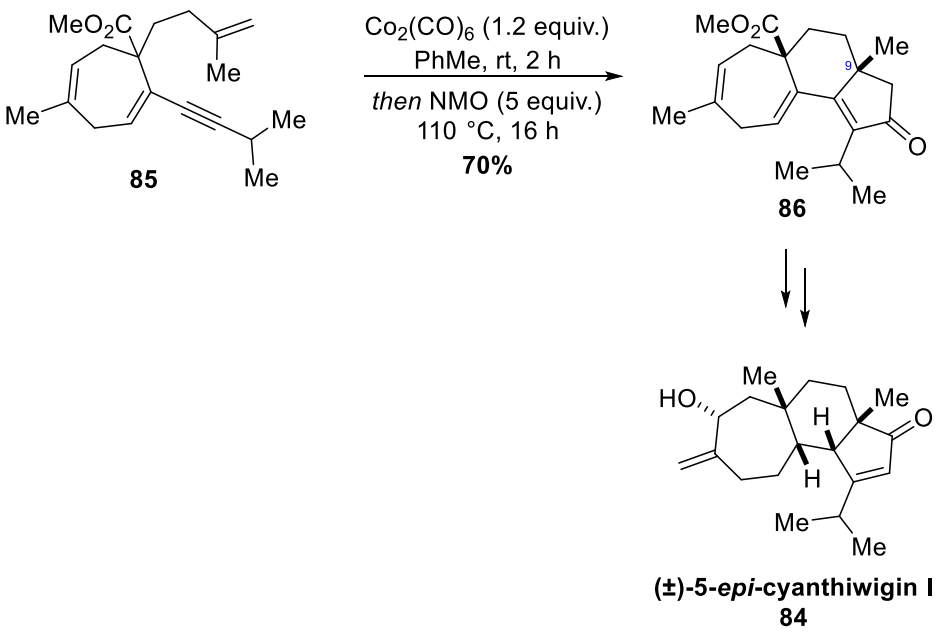

Scheme 1.69

As discussed earlier, our proposed synthesis of agariblazeispirol C relies on the PKR of substrate type **16** to build the two five-membered rings in the final natural product, an overall demanding cyclisation procedure (**Scheme 1.70**).

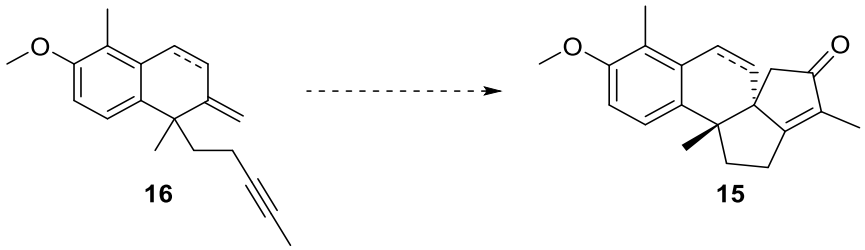

Scheme 1.70

Two possible pathways can be explored: the first being the cobalt-mediated intramolecular PKR of the terminal alkene precursor, the cyclisation of which is anticipated to be more facile due to literature evidence. This route would leave the final internal olefin to be subsequently introduced into the core. Ishizaki and Hoshino[88] have demonstrated that the PKR can be used to generate a similar, yet tricyclic, congested system (**Scheme 1.71**). Here, they applied thermal PK conditions to enyne **87**, affording tricylic product **88** in a modest 63% yield as a single diastereomer. It was interesting to note that the *anti*-stereochemistry of the tricyclic system was obtained – the arrangement desired for agariblazeispirol C.

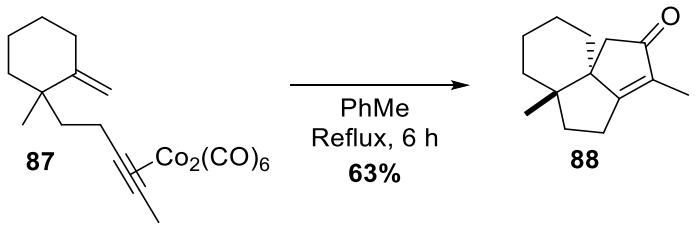

Scheme 1.71

The alternative PK precursor which could be utilised within our synthetic programme involves the more difficult conjugated alkene system to directly furnish the desired polycyclic core. Indeed, there is no literature precedence available for such a cobalt-mediated intramolecular process. However, as mentioned previously, success has been shown by Wender,[89] whereby a rhodium-mediated intramolecular PKR facilitates the required cyclisation of diene-yne substrates to furnish bicyclic systems. With their conditions, involving catalytic amounts of $RhCl(CO)(PPh_3)_2$ and an atmosphere of CO, conjugated diene PK precursor **89** was converted to bicyclic product **90** in an excellent 86% yield as one diastereomer (**Scheme 1.72**). However, our system is considerably more demanding, as the conjugated diene is fixed within a 6-membered ring, thus an overall more complex PK precursor. Regardless of our approach, substrate **16** represents a challenge in that an internal alkyne and a terminal alkene (or diene) embedded within a bicyclic system are required to cyclise, forming two new rings, whilst generating a chiral quaternary centre in one cyclisation.

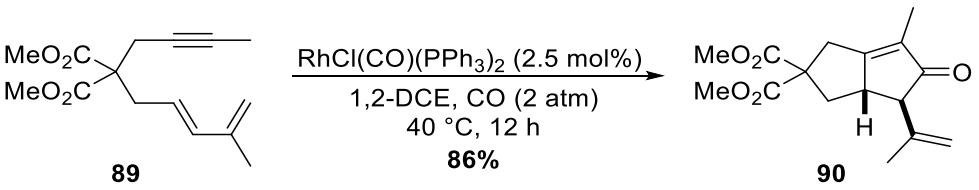

89 90

Scheme 1.72

In summary, the PKR has been developed into an effective cyclisation technique to furnish complicated and challenging frameworks. Since its discovery in the 1970s, advances in the practicality of PKR unlocked its efficient and diverse utility in organic synthesis. As a result, the intramolecular PKR protocol has been strategically applied to the synthesis of many natural products to date, with varing levels of difficulty apparent within individually applied transformations. However, the PKR still suffers from many drawbacks such as the lack of functionality around the reacting centres to generate diverse structural motifs, and the intermolecular PKR is somewhat limited to strained olefin partners. Despite this, methodologies are continuing to emerge to address these issues, further enhancing the overall utility of the PK cyclisation.

Chapter 2

Previous and Proposed Work

2. Previous and Proposed Work

2.1 Previous Work

The synthesis towards the natural product agariblazeispirol C has been explored within our research team, but has yet to be completed.[8–12] Thus far, work has mainly focused on the racemic synthesis of the natural target, where the preparation of advanced key intermediates has been achieved. Most recently, and as part of a more demanding extension to this research, preliminary work towards the establishment of an asymmetric synthesis of agariblazeispirol C has centred on an asymmetric Heck reaction to generate the bicyclic core of the natural target in an enantiomeric pure form.[12] In this work, Heck precursor **91** was targeted, as it was anticipated that the cyclised product **92** would provide an oxygenated functional handle, enabling easier derivatisation in the downstream synthesis (**Scheme 2.1**).[10,12] Unfortunately, only a racemic mixture was obtained in this original study. Again, with work still in its infancy, applying simplified Heck precursor **93** to asymmetric Heck conditions was problematic. Disappointingly, and unexpectedly, an indene side-product **94** was observed, compromising the overall yield to **62**. Even with the desired Heck product **62** isolated, it was found to exist as a racemic mixture. As a result, and also due to many avenues still left unexplored in this expanse area, the asymmetric Heck reaction must be extensively examined further to enable the asymmetric synthesis of our natural product.

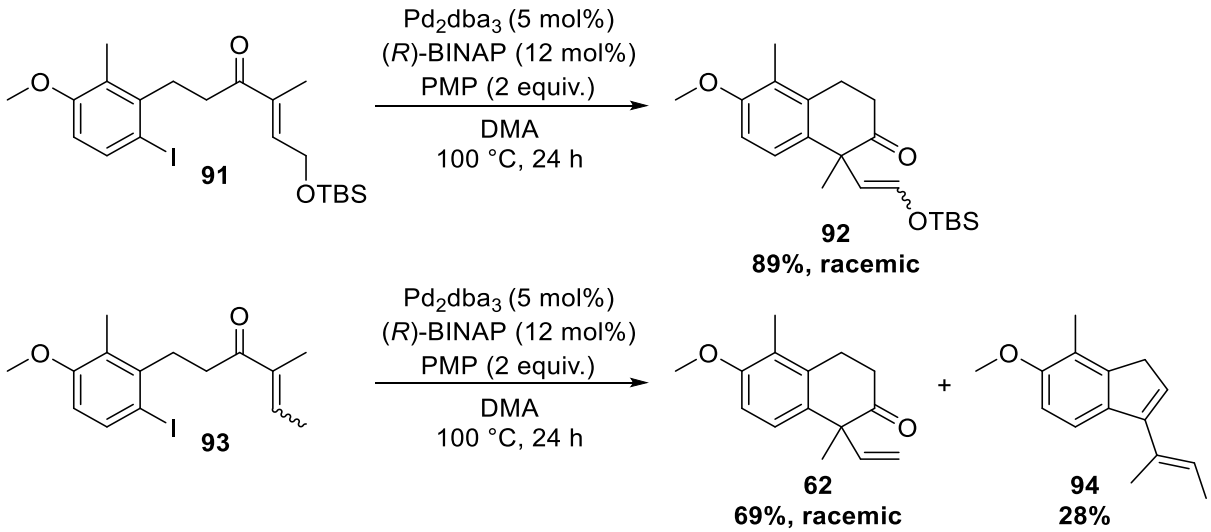

Scheme 2.1

In relation to the second key transition-metal mediated process, the PKR of precursors **95** and **96** have been previously attempted within the group (**Scheme 2.2**).[8–10] The PK cyclisation of enyne precursor **95** generated the tetracyclic core **97** in an excellent yield of 86% from the cobalt complex, and was isolated as a single diastereomer.[10] The *anti*-arrangement within the core was demonstrated through X-ray crystallography, also providing evidence for the formation of the polycyclic network. The PKR of diene-yne precursor **96** required longer reaction times of 60 h to achieve **98** in a moderate yield of 61%, again as one diastereomer.[9] However, the annulation of **96** was extremely capricious, where the 61% yield was irreproducible, therefore, the current PKR protocol is somewhat unreliable.

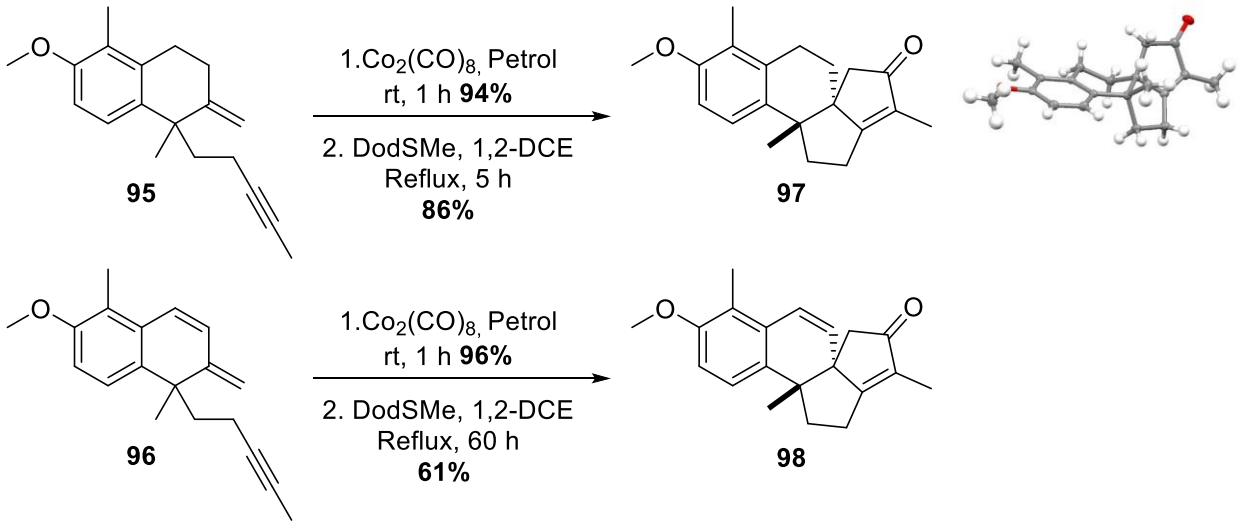

Scheme 2.2

Despite some initial preliminary investigations, an effective pathway to generate the final target from the Pauson-Khand products (**97** or **98**) has yet to be realised. From tetracyclic core **97**, initial efforts to transform this to the unsaturated core **98** have been fruitless (**Scheme 2.3**).[10] Thus, access to the overall core of agariblazeispirol C from PK product **97** is currently uknown from this key tetracyclic intermediate.

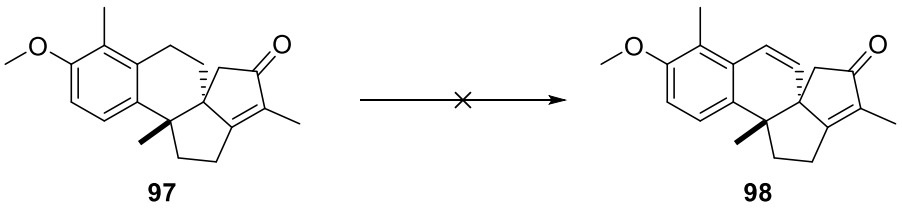

97 **98**

Scheme 2.3

Despite failed efforts to convert **97** to **98**, previous work has allowed access to **98** through the PKR of **96** albeit in a lower (and unreliable) yield and on milligram scale.[8] Within this work, attempts at completing the overall synthesis of agariblazeispirol C through an alkylation approach was undertaken to no avail (**Scheme 2.4**). Having said this, these initial experiments were performed on milligram scale, and internal quenching through adventitious water was posed as a potential issue within the synthesis.

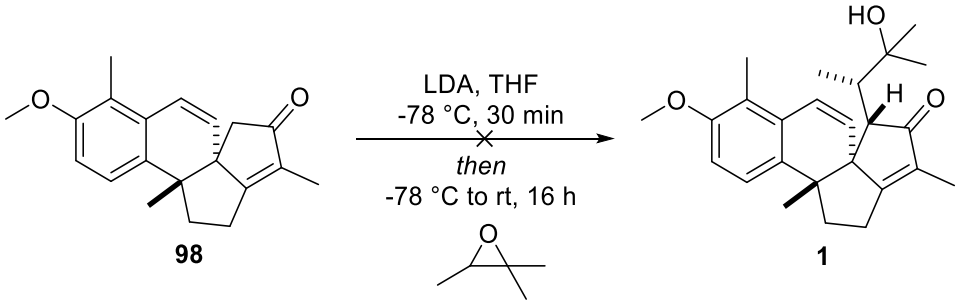

98 **1**

Scheme 2.4

2.2 Proposed Work

Despite the research performed within our group towards agariblazeispirol C, many areas within this total synthesis programme have yet to be fully explored, specifically an asymmetric route, and further investigation and optimisation of key transformations are required. This includes the asymmetric intramolecular Heck reaction, a new synthetic route towards each PK precursor from the novel enantiomerically pure Heck product, and the addition of the key oxygenated side-chain for the completion of the total synthesis.

As mentioned previously, recent efforts towards the development of an effective asymmetric Heck cyclisation had been met with a number of challenges. Specifically, only racemic products have been obtained with preliminary methodology, and certain Heck cyclisation protocols led to an unwanted by-product **94**, which was assumed to be due to the presence of the carbonyl functionality in the starting substrate. To address these issues in this body of work, it is anticipated that protection of enone **93** as the corresponding ketal **18** could prevent the formation of the undesired by-product (**Scheme 2.5**). Indeed, one must be cautious that the change in electronics of this newly proposed system may affect the performance of the reaction. Additionally, in previous studies, enone **93** was present as a mixture of *E/Z* isomers – ultimately, this may be the reason for lack of enantioselectivity observed to date, as it has been reported in the literature that different geometric isomers can furnish opposite enantiomers (*vide supra*). In this regard, it is perhaps unsurprising that the outcomes so far with enone **62** have only been racemic mixtures. Henceforth, the first goal is to synthesise both Heck precursors **(*E*)-18** and **(*Z*)-18**, then subsequently establish whether these exclusively (*E)*- or (*Z)*- Heck precursors can undergo the asymmetric intramolecular Heck reaction with high enantioselectivity. Furthermore, and to fully explore the capability of the system, it is our intention to synthesise each respective iodide and triflate Heck precursors, thus in total we can explore the Heck reaction of four Heck precursors: iodide precursors **(*E*)-100** and **(*Z*)-100**; and triflate precursors **(*E*)-101** and **(*Z*)-101**.

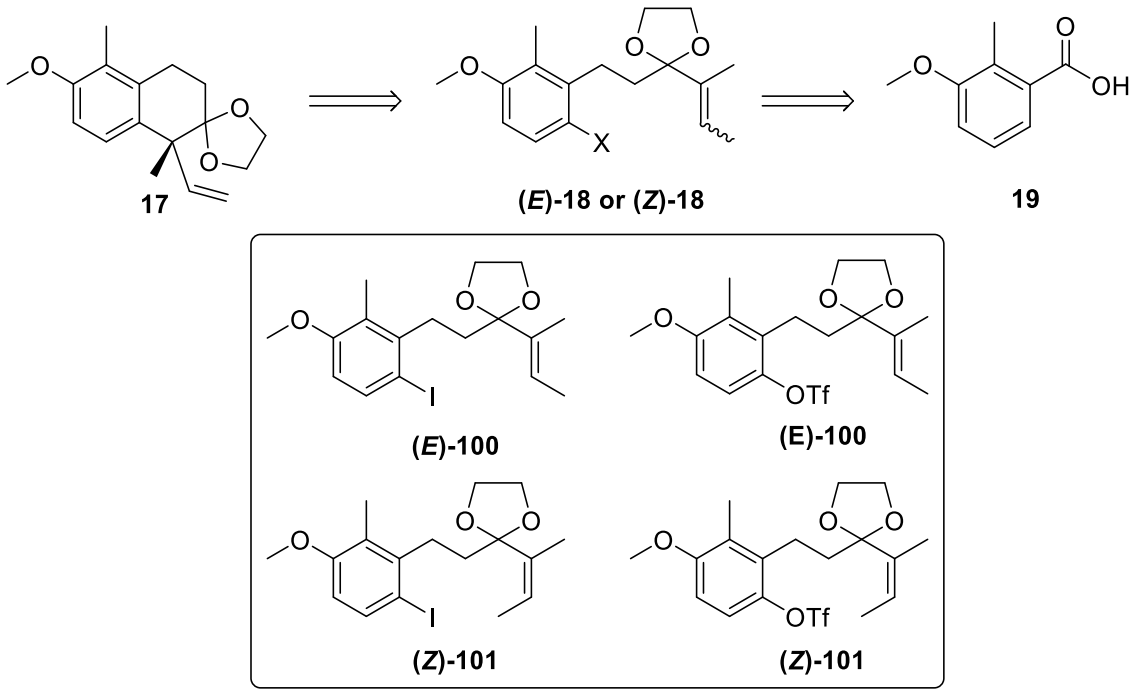

Scheme 2.5

With these new Heck precursors in hand, the asymmetric intramolecular Heck reaction will be explored under various reaction conditions, and a series of chiral ligands will be probed as part of the optimisation efforts (**Scheme 2.6**). A successful outcome at this stage will incorporate the stereocentre on the bicyclic system for the final target, which has yet to be fulfilled in the synthesis of this challenging natural product.

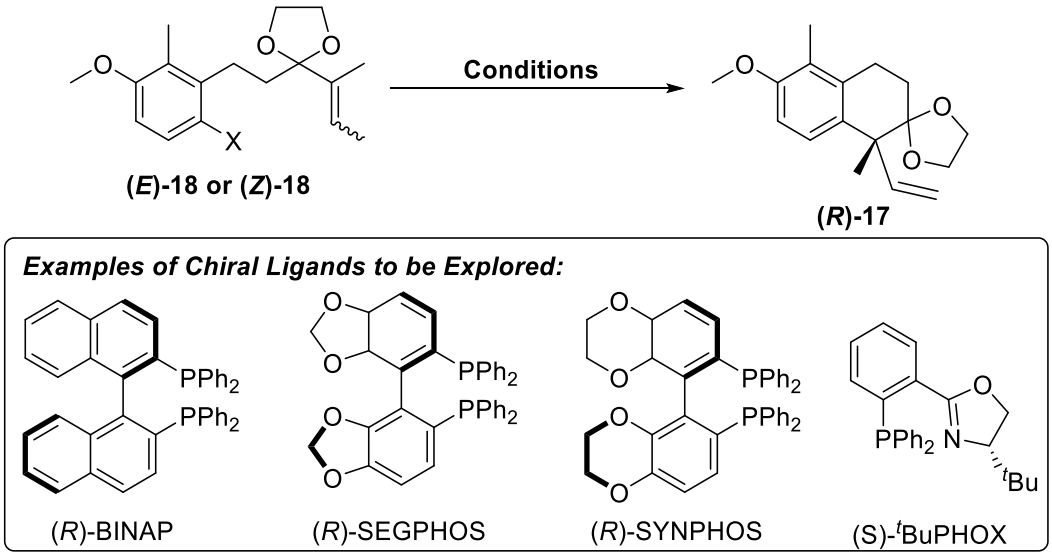

Scheme 2.6

Once the asymmetric Heck reaction has been established, the next goal would focus on the development of a new and robust synthetic pathway towards the PK precursor(s) **16** from **17**, as previous synthetic routes devised within the group will not translate across to the newly proposed Heck intermediate **17** (**Scheme 2.7**). We propose to concentrate our efforts towards two separate precursors, as they individually present key advantages in the overall synthesis: the terminal alkene species (enyne) already works well under cyclisation conditions but requires late-stage oxidation to complete the core of the natural product; whilst, in contrast, the conjugated diene (diene-yne) demands a challenging annulation, but the product of such directly represents the full core of agariblazeispirol C. Once constructed, the PKR of both precursors can be explored, with the view to optimise the process further in each case. In particular, efforts will focus on improving the efficiency (and reproducibility) of the conjugated diene PKR as this currently requires long reaction times and the resulting product has only been synthesised in milligram quantities.

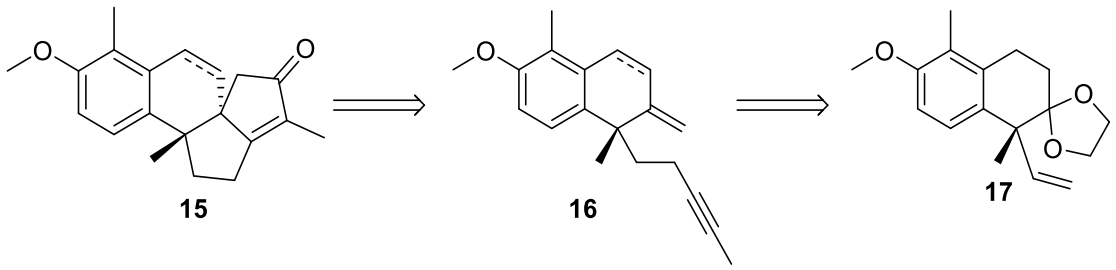

Scheme 2.7

Finally, it is anticipated that the completion of agariblazeispirol C **1** will be fully investigated (**Scheme 2.8**). Depending on the substrate employed, late-stage oxidation to introduce the internal alkene into the tetracyclic system may be necessary. With the core of the natural target in hand, the crucial addition of the oxygenated side-chain can be performed through alkylation strategies. Addition of various electrophiles onto the tetracyclic core can be extensively explored, and on larger scales than previously performed before, ruling out the issue of adventitious water within the reaction system.

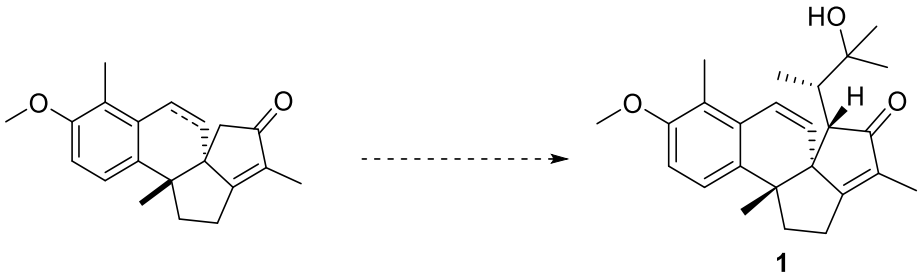

Scheme 2.8

Chapter 3

Asymmetric Intramolecular Heck Reaction

3. Asymmetric Intramolecular Heck Reaction

3.1 Syntheses Towards the Heck Precursors

3.1.1 Preparation of Weinreb Amide Intermediates

To begin the total synthesis programme, the preparation of various Heck precursors was pursued. It was envisioned that varying the aryl halide component of the Heck substrate would allow for full exploration of the system, and that each derivative could be synthesised from a common Weinreb amide intermediate **102** (**Scheme 3.1**). **102** could be generated from the corresponding α,β-unsaturated amide **103** through a reduction process**,** ultimately prepared *via* an oxidation and Horner-Wadworth-Emmons (HWE) sequence from benzyl alcohol **104**. The iodide, from which other halides (or pseudo halides) could be derived, would be installed from compound **105**, which, ultimately, can be prepared from the reduction of acid **19**. The specifically targeted Weinreb amide compounds were iodide **106** and triflate **107**.

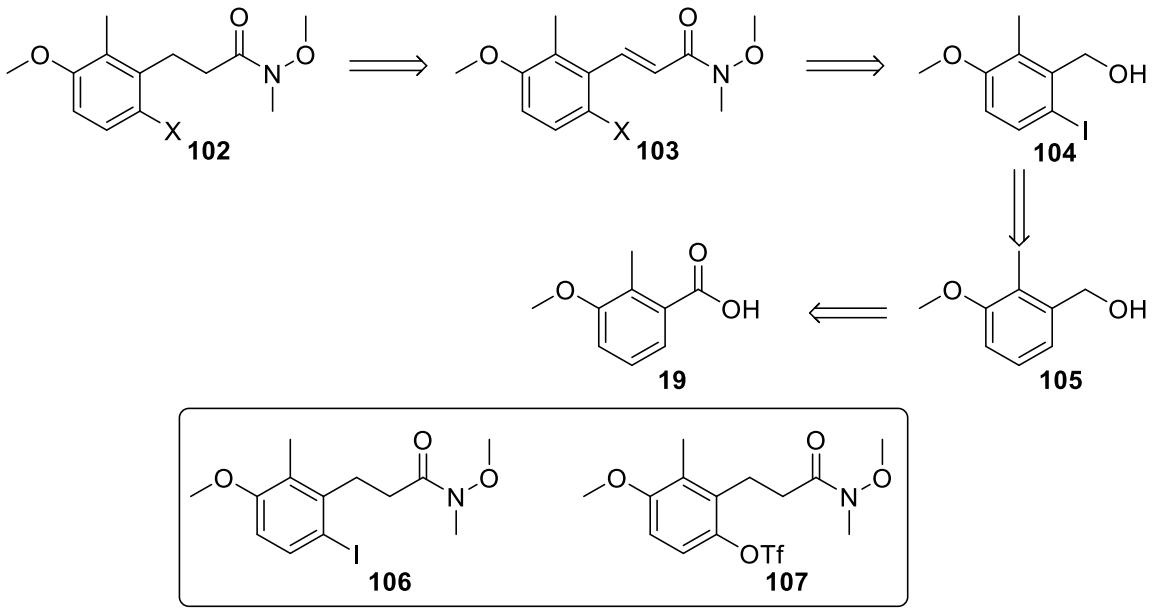

Scheme 3.1

The first step in the synthesis towards **106** and **107** involved the reduction of the commercially available acid **19** using lithium aluminium hydride ($LiAlH_4$). This furnished alcohol **105** in an exceptional 95% yield (**Scheme 3.2**). Following this, iodination of **105** generated the desired product **104** in a high 81% yield.

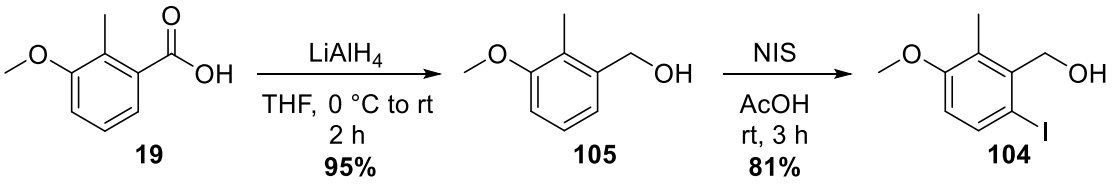

Scheme 3.2

Next, the required phosphonate ester **110** for the ensuing HWE reaction was synthesised following a known literature procedure, involving formation of the Weinreb amide **109** from chloroacetyl chloride **108** and *N*,*O*-dimethylhydroxylamine hydrochloride.[90] Through the Arbuzov reaction, **110** was delivered in 73% yield over the two steps (**Scheme 3.3**).

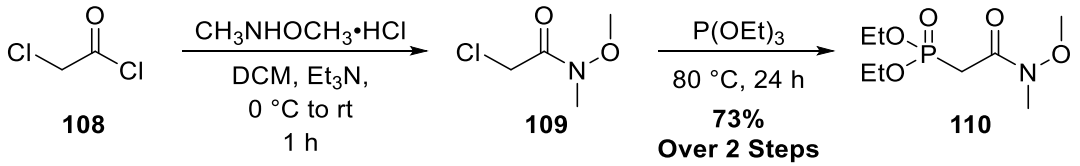

Scheme 3.3

From previously prepared alcohol **104**, we sought to prepare the α,β-unsaturated amide *via* a tandem oxidation and HWE sequence.[91] Once the Swern oxidation was complete, aldehyde **111** was progressed through the HWE reaction with phosphonate ester **110** under Masamune-Roush conditions.[92] Pleasingly, a high yield of **112** (74% over 2 steps) was obtained from this process (**Scheme 3.4**).

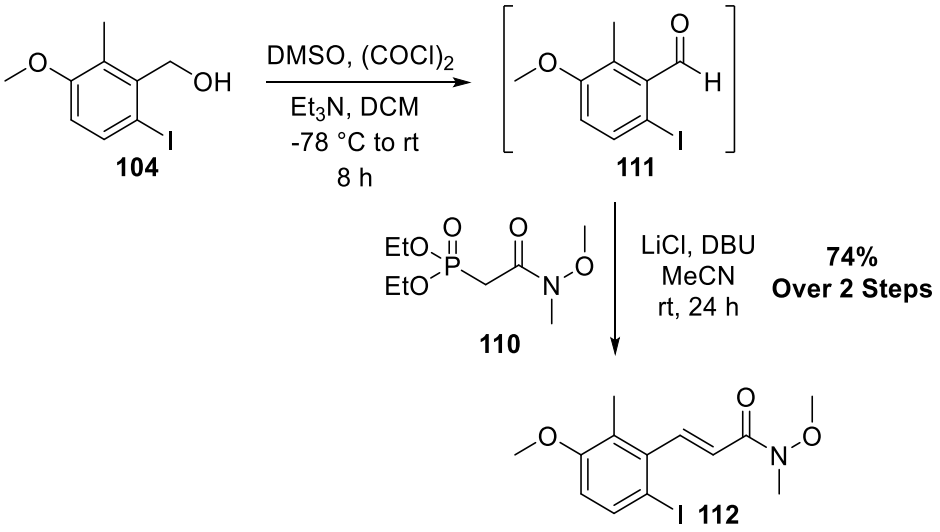

Scheme 3.4

The success of the tandem Swern oxidation-HWE reaction allowed the investigation of the ensuing hydrogenation reaction. It has been reported by our research group that iridium catalysts, developed within our laboratories, can efficiently hydrogenate various unsaturated systems with pendant directing groups. Indeed, it had been previously shown that the bromo derivative **113** could be effectively reduced using our developed iridium catalyst **115** (**Scheme 3.5**).[93] Notably, using traditional reducing methods, such as palladium on carbon, both de-halogenation and hydrogenation of the substrate was observed.

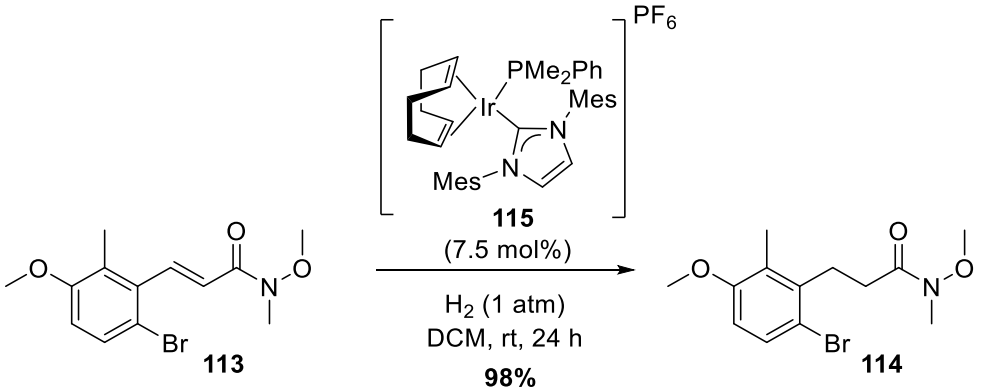

Scheme 3.5

More recently, our research in iridium catalysis has shown that employing the BAr^F counter anion within our complex results in an extremely effective reduction protocol to fully reduce **116** to **117** (**Scheme 3.6**).[94] Indeed, a catalyst loading of only 0.5 mol% was sufficient to reduce the substrate, and a short reaction time of just 2 hours emphasises the efficiency and reacitivy of this developed system.

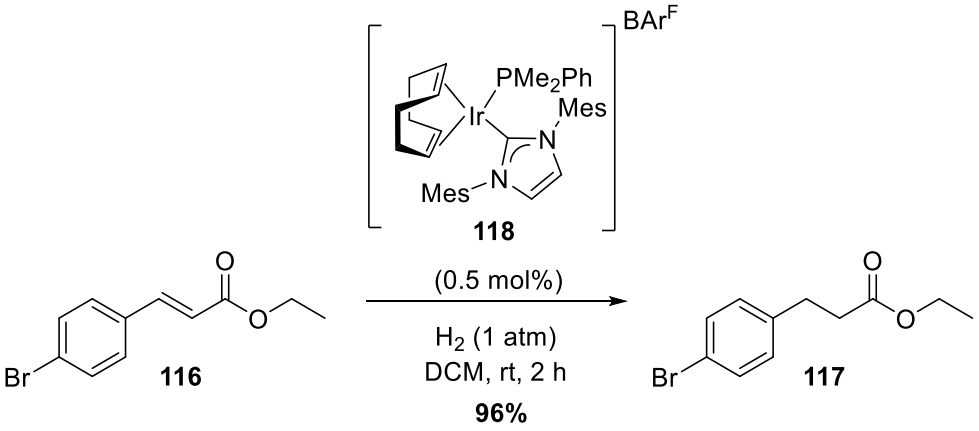

Scheme 3.6

As such, we focused on employing our active iridium catalysts in the reduction of compound **112** to deliver our targeted iodide Weinreb amide **106**. Unfortunately, the hydrogenation of **112** was more strenuous than initially perceived, even with a range of developed iridium catalysts available (**Scheme 3.7, Table 3.1**).

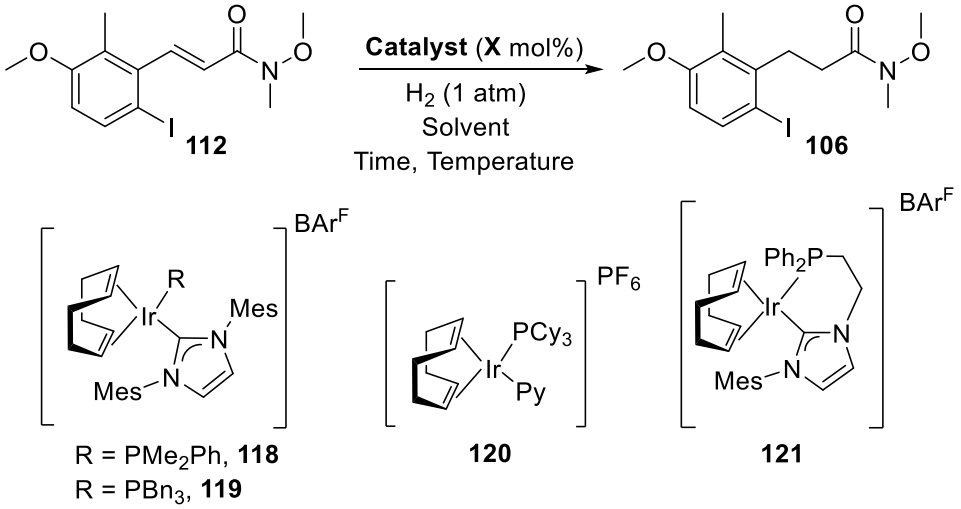

Scheme 3.7

Entry	Catalyst	Solvent	Time (h)	Temperature (° C)	Conversion (%)
1	**118** (1 mol%)	DCM	16	RT	0
2	**118** (5 mol%)	DCM	16	RT	2
3	**119** (5 mol%)	DCM	16	RT	11
4	**119** (5 mol%)	DCM	40	35	23
5	**120** (7.5 mol%)	DCM	24	RT	21
6	**119** (5 mol%)	PhMe	16	RT	16
7	**121** (5 mol%)	PhMe	16	RT	4

Table 3.1

Using one of our most active catalysts, **118**, no conversion to the desired product was observed at the low loading level of 1 mol% (**Entry 1**). Unfortunately, very little effect was obtained when increasing the catalyst loading to 5 mol% (**Entry 2**). Discouraged by the initial results, further reading into our previous work suggested that catalyst **119** would be most optimal for the hydrogenation of **112**. Indeed, it had been previously shown that when an iodide group is *ortho* to the unsaturated system, only catalysts containing phosphine ligand PBn_3 were effective in the hydrogenation reaction.[93] Despite having this knowledge in hand, only a slight improvement in conversions were achieved (**Entries 3** and **4**), even at slightly harsher reaction conditions (**Entry 4**). Disappointed with these outcomes, hydrogenation conditions using Crabtree's catalyst **120** was explored (**Entry 5**). However, again, poor conversions to the desired saturated material were obtained. One of the advantages of our iridium catalysts is that it is soluble in a plethora of solvents. Indeed, PhMe had previously been favourable in a competition study with catalyst **119**,[94] however, our case, no improvement was achieved (**Entry 6**). The failure of the hydrogenation reaction suggested that perhaps the α,β-unsaturated system within **112** was too hindered by the iodo- substituent present on the aromatic ring. In a last effort to hydrogenate the olefin, our chelating catalyst **121**, a species shown to be most accepting of sterics when comparing our range of iridium complexes**,** was employed, but, again, very little conversion was observed (**Entry 7**).

Dismayed with these findings, at this point, it was accepted that the substrate was incompatible with our iridium species for hydrogenation. Despite the success towards the synthesis of **112**, the last hydrogenation step to **106** failed to proceed in high conversions.

Hence, it was clear that this route was not suitable for the multi-gram scale synthesis required and an alternative sequence was considered.

The alternative strategy involved rearranging the previous synthetic sequence such that iodination is performed at the final step, i.e. the hydrogenation of the α,β-unsaturated amide would take place on the unsubsituted aryl species (**Scheme 3.8**). Henceforth, the synthetic steps were altered such that intermediate **106** could be generated through iodination of **123**. It was expected that reduction of **122** to **123** would be facile, and that α,β-unsaturated amide **122** could be prepared through similar Swern oxidation-HWE methodology from the previously synthesised alcohol **105** (*c.f.* **Scheme 3.1**).

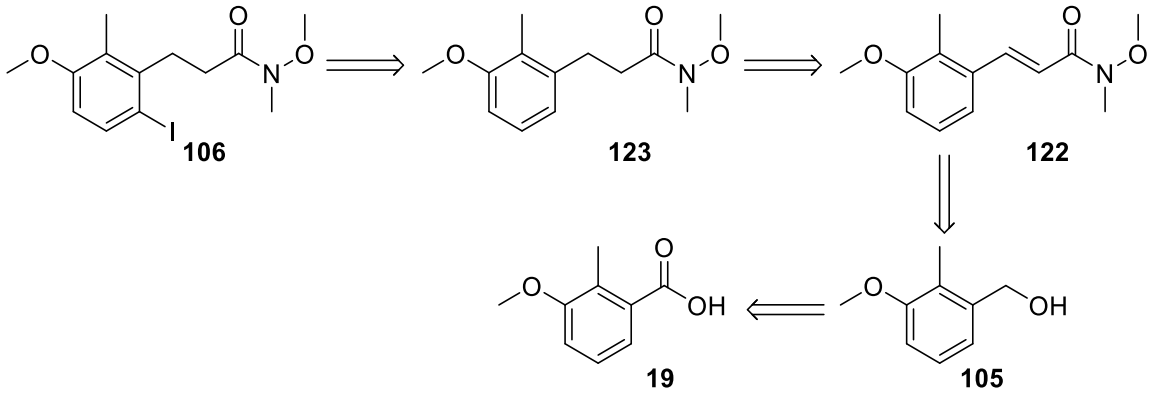

Scheme 3.8

To begin this alternative route, the Swern oxidation-HWE sequence with **105** and the previously synthesised phosphonate ester **110** was conducted, delivering **122** in large quantities in an excellent yield of 88% across two steps (**Scheme 3.9**).

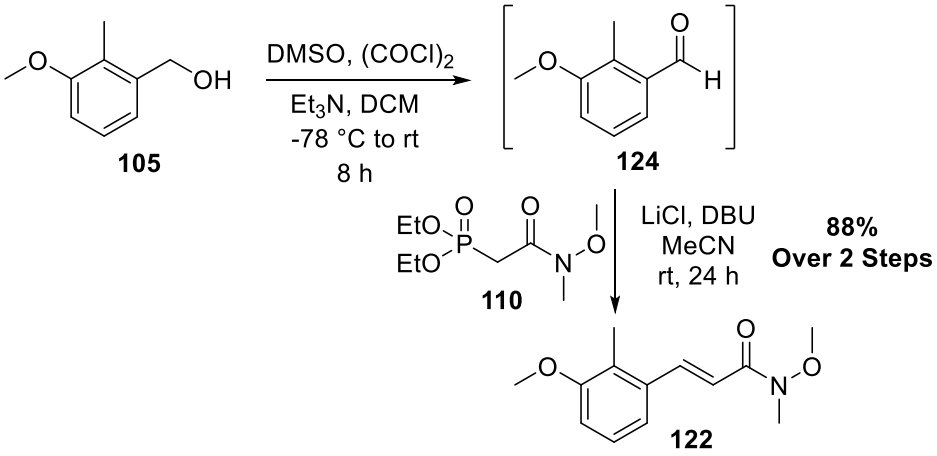

Scheme 3.9

Pleasingly, hydrogenation of intermediate **122** to **123** was now facile, further supporting the suspected hinderance of the iodide group in the previous substrate (**Scheme 3.10, Table 3.2**). Both our in-house developed iridium-based catalyst **119** and the more traditional Pd/C method allowed the hydrogenation to proceed with full conversion and high isolated yields (**Table 3.2**, **Entries 1** and **2**), despite higher pressures of H_2 (5 atm) being required when performing the Pd/C protocol on a large scale (**Entry 3**).

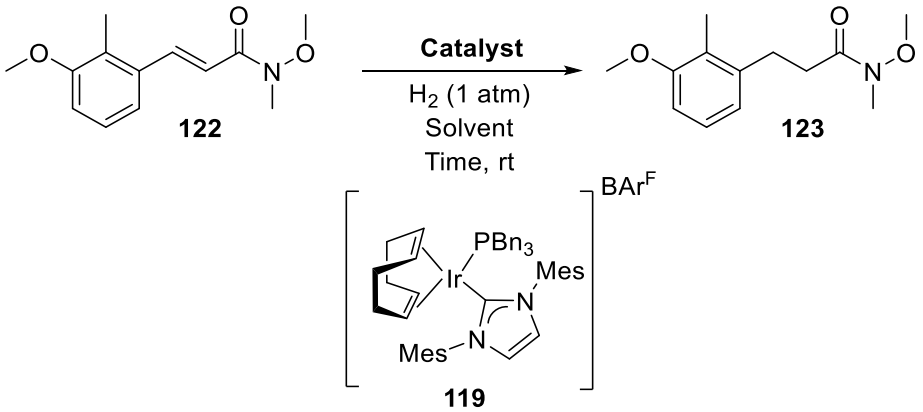

Scheme 3.10

Entry	Scale (mmol)	Catalyst	Solvent	Time (h)	Yield (%)
1	0.41	**119** (1 mol%)	DCM	16	97
2	0.41	Pd/C (10 mol%)	MeOH	16	96
3[a]	25.50	Pd/C (10 mol%)	MeOH	24	91

[a]5 atm H_2 used

Table 3.2

The last step to synthesise Weinreb amide intermediate **106** was iodination of **123** using NIS, which furnished the desired key product **106** in an excellent yield of 96% (**Scheme 3.11**).

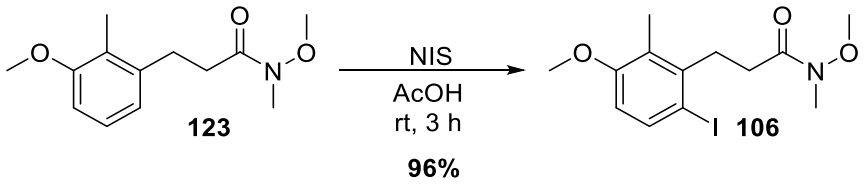

Scheme 3.11

By altering the specific order of the synthetic steps such that iodination was performed after hydrogenation, the desired key intermediate **106** was obtained in excellent yields over five steps.

To further expand our asymmetric Heck investigation, the synthesis of various Heck precursors will be explored, and, as such, the triflate Weinreb amide intermediate **107** was targeted to make the corresponding triflate Heck precursor. This could be generated directly from the previously prepared iodide Weinreb amide intermediate **106** (**Scheme 3.12**).

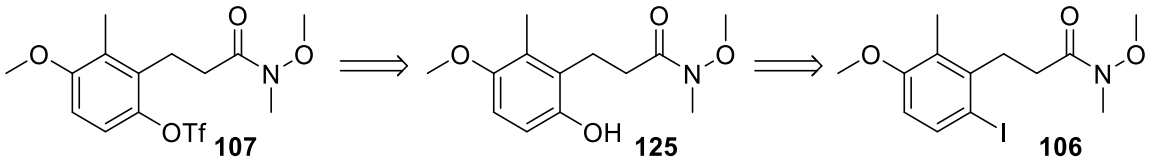

Scheme 3.12

It was envisaged that phenol **125** could be constructed through a borylation/oxidation sequence from **106** (**Scheme 3.13, Table 3.3**). In practice, it was found that the oxidation component, when using K_2CO_3 with H_2O_2, produced inconsistent results, particularly on larger scale (**Table 3.3**, **Entries 1** and **2**). Despite this, changing the oxidant to Oxone®[95] improved the overall reaction yield, and reliable outcomes were consistently obtained on multiple scales, achieving a pleasing 74% yield across the two steps (**Entries 3** and **4**).

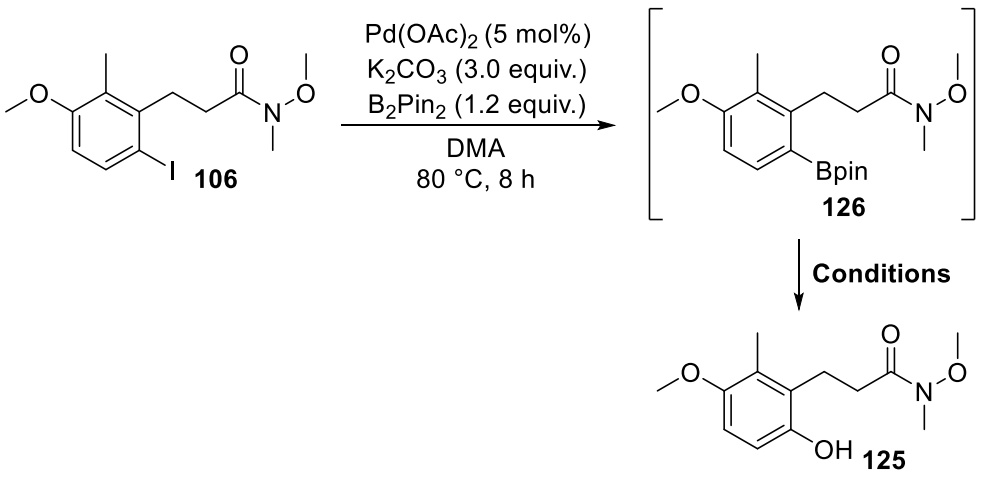

Scheme 3.13

Entry	Scale (mmol)	Conditions	Yield of 125 over 2 Steps (%)
1	0.55	K_2CO_3 (3 equiv.), H_2O_2 (10 equiv.), dioxane, rt, 16 h	56
2	3.0	K_2CO_3 (3 equiv.), H_2O_2 (10 equiv.), dioxane, rt, 16 h	40
3	0.55	Oxone® (1 equiv.), acetone:water, rt, 16 h	72
4	5.8	Oxone® (1 equiv.), acetone:water, rt, 16 h	74

Table 3.3

With phenol **125** in hand, the triflate Weinreb amide **107** was synthesised from the reaction of **125** with triflic anhydride, providing an excellent yield of 92% (**Scheme 3.14**).

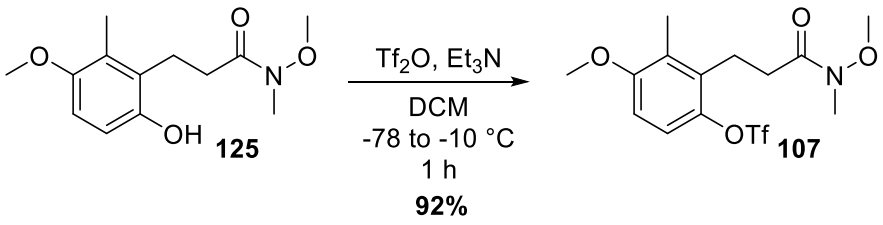

Scheme 3.14

3.1.2 Preparation of Heck Precursors

With both iodide **106** and triflate **107** Weinreb amide intermediates now in hand, the next step involved converting these into various Heck precursors for the exploration of the key asymmetric Heck reaction. It was anticipated that such species could be formed through a Grignard and ketalisation process from the corresponding Weinreb amide intermediates (**Scheme 3.15**). In this case, from our intermediates, four precursors can be targeted – the iodide variants **(*E*)-100** and **(*Z*)-100**, and the triflate variants **(*E*)-101** and **(*Z*)-101**.

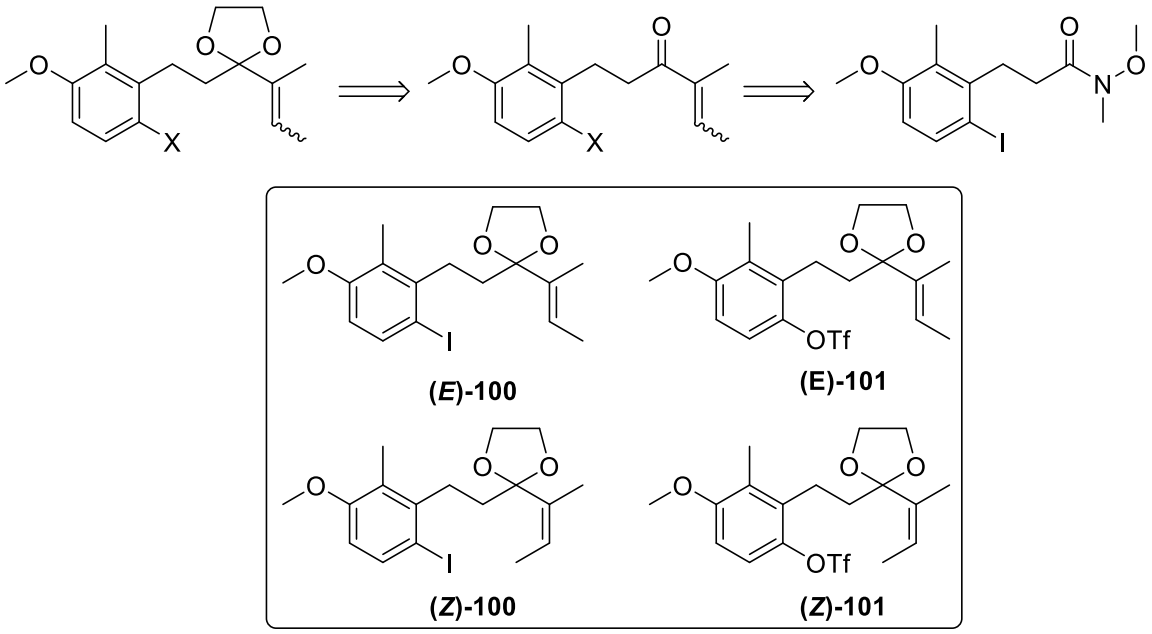

Scheme 3.15

First, the (*E*)-Heck precursors were targeted, which required vinyl bromide **(*E*)-127** for the proposed Grignard reaction. Following a literature procedure,[96] **(*E*)-127** can be generated in moderate yields as the single (*E)*-isomer through an elimination reaction of *meso*-2,3-dibromobutane **126** (**Scheme 3.16**). Whilst the literature indicated a 45-minute reaction time, in our hands, an overnight protocol was necessary. Indeed, good quantities of the desired vinyl bromide **(*E*)-127** were obtained.

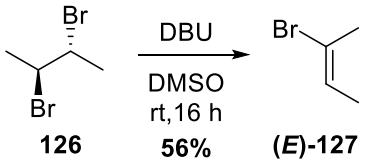

Scheme 3.16

Next, both iodide and triflate Heck precursors **(*E*)-100** and **(*E*)-101** were constructed in excellent yields following a Grignard addition of **(*E*)-128** (generated from **(*E*)-127**) into each corresponding Weinreb amide, then ketalisation of the resulting enone moiety with ethylene glycol (**Scheme 3.17**).

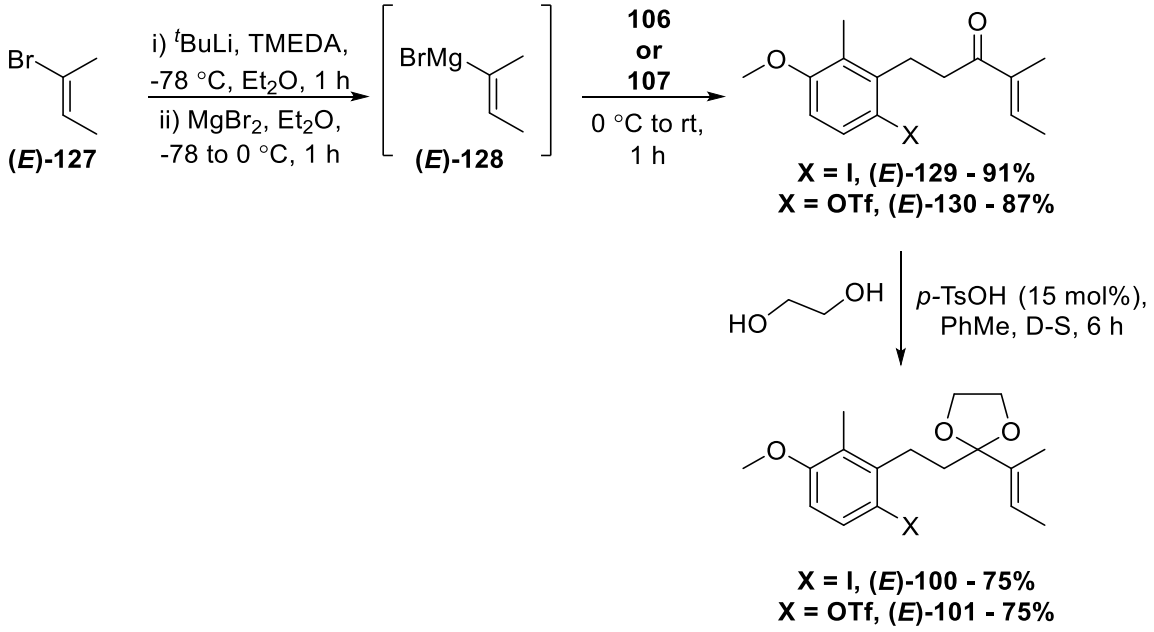

Scheme 3.17

Overall, very good yields were obtained for this sequence of reactions for both the iodide and triflate derivatives. The Grignard reaction of iodide Weinreb amide intermediate **106** with **(*E*)-128** furnished **(*E*)-129** in an excellent yield of 91%, delivering Heck precursor **(*E*)-100** after ketalisation in 75% yield. Pleasingly, following the same procedures, **(*E*)-130** was obtained in a high yield of 87%, which, ultimately, produced Heck precursor **(*E*)-101** in a good 75% yield after ketalisation.

With the (*E*)-Heck precursors in hand, focus turned to the synthesis of (*Z*)-Heck starting substrates for the asymmetric Heck reaction. Following the same synthetic procedure with commercially available (*Z*)-vinyl bromide **(*Z*)-127**, enones **(*Z*)-129** and **(*Z*)-130** were constructed in sufficient (yet unoptimised) yields (**Scheme 3.18**). Frustratingly, initial ketalisation conditions employed with enone **(*Z*)-129** resulted in full isomerisation into **(*E*)-100**.

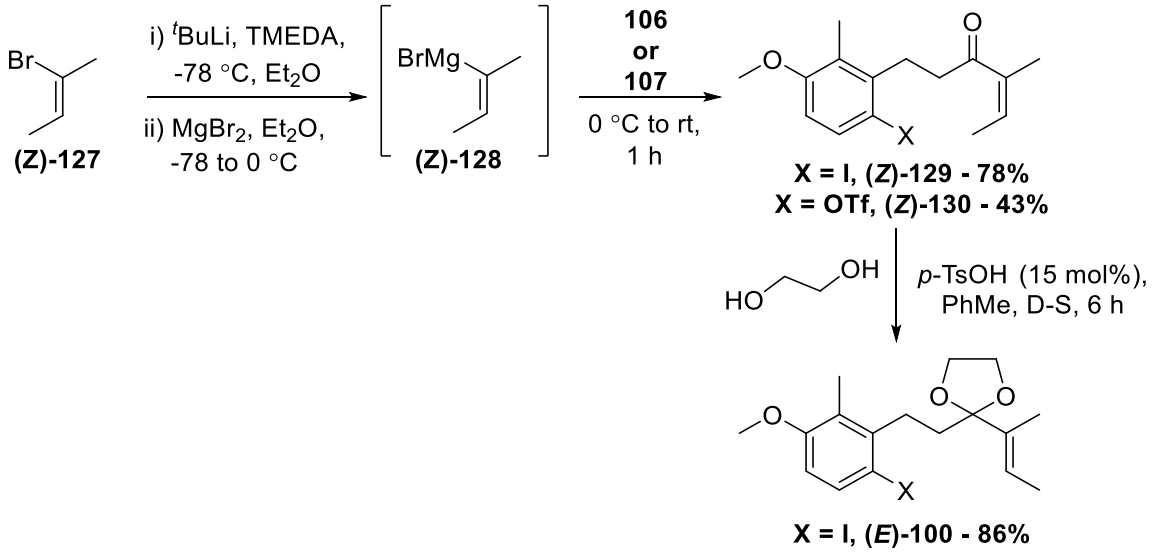

Scheme 3.18

Undeterred, alternative protecting strategies were explored in an attempt to overcome the issue with isomerisation, concentrating on the use of more mild conditions as it was thought that the presence of an acid catalyst with heat had promoted isomerisation to occur (**Scheme 3.19, Table 3.4**). Applying $ZrCl_4$[97] as a Lewis acid with triethylorthoformate unfortunately also afforded the *E*-Heck precursor **(*E*)-100** (**Table 3.4**, **Entry 1**). Whilst it had been shown in the literature that BF_3•OEt_2 can be used as a Lewis acid in the protection of carbonyl moieties at -78 °C,[98,99] no reactivity was observed in our case, despite increasing the equivalents of BF_3•OEt_2 **(Entries 2** and **3**). Conducting a temperature screen (**Entries 4** to **9**) showed that at temperatures between -50 to -30 °C (**Entries 5** to **7**), the protection was slow, providing an inseparable mixture of the desired sole (*Z*)-product **(*Z*)-100** with starting material. Disappointingly, increasing the temperature above -20 °C (**Entries 8** and **9**) resulted in an inseparable mixture of both isomeric products.

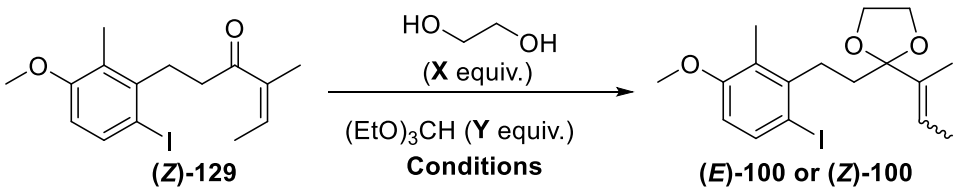

Scheme 3.19

Entry	X	Y	Conditions	Conversion (%)	*E*:*Z*
1	2	1.2	$ZrCl_4$ (3 mol%), DCM, rt, 20 h	100 (72)[a]	100:0
2	3	2	BF_3•OEt_2 (10 mol%), DCM, -78 °C, 2 h	No reaction	-
3	3	2	BF_3•OEt_2 (1 equiv.), DCM, -78 °C, 2 h	No reaction	-
4	3	2	BF_3•OEt_2 (1 equiv.), DCM, -60 °C, 16 h	No reaction	-
5	3	2	BF_3•OEt_2 (1 equiv.), DCM, -50 °C, 16 h	15	0:100
6	3	2	BF_3•OEt_2 (1 equiv.), DCM, -40 °C, 16 h	26	0:100
7	3	2	BF_3•OEt_2 (1 equiv.), DCM, -30 °C, 16 h	32	0:100
8	3	2	BF_3•OEt_2 (1 equiv.), DCM, -20 °C, 16 h	43	1:3
9	3	2	BF_3•OEt_2 (1 equiv.), DCM, -10 °C, 16 h	100 (67)[a]	1:9

[a]Isolated yield

Table 3.4

With the triflate enone **(*Z*)-130**, the developed ketalisation conditions in **Table 3.4**, **Entry 9** were utilised, however, the resulting **(*Z*)-101** could not be obtained as a single geometric isomer (**Scheme 3.20**).

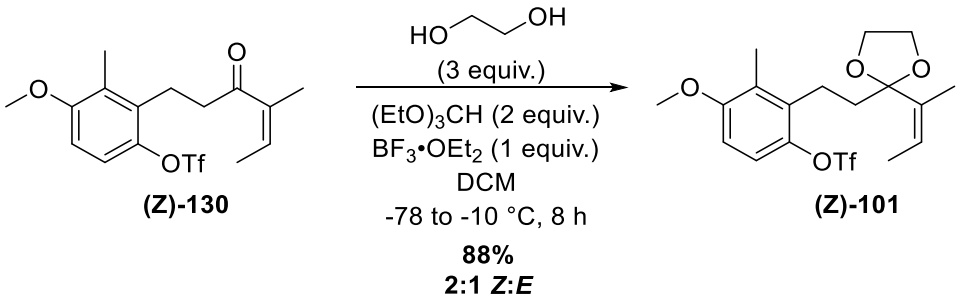

Scheme 3.20

Despite our lack of success with solely generating the (*Z*)-Heck precursors, returning to the ketalisation of **(*E*)-129**, it was pleasing to observe that the established alternative ketalisation conditions furnished the iodide Heck precursor **(*E*)-100** in quantitative yield,

furnishing large quantities of our desired intermediate for our overall synthesis (**Scheme 3.21**).

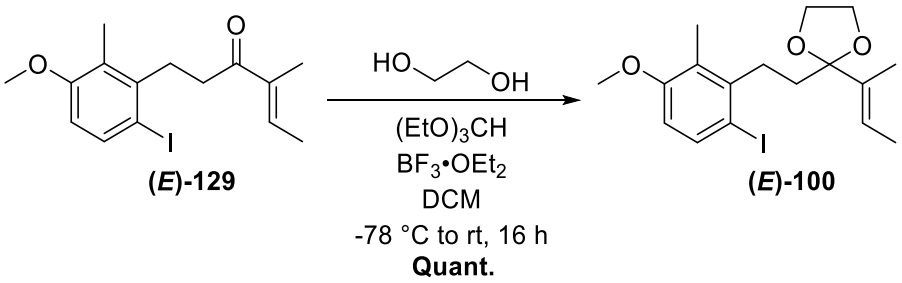

Scheme 3.21

In summary, unfortunately exclusive access to the (*Z)*-Heck precursors had not been viable *via* the methods attempted above. Nonetheless, preparation of **(*E*)-100** and **(*E*)-101** allowed the subsequent exploration the asymmetric Heck reaction.

3.2 Initial Investigations into the Asymmetric Heck Reaction

With synthetic routes established for the synthesis of **(*E*)-100** and **(*E*)-101** Heck precursors, the next crucial objective was to establish an asymmetric intramolecular Heck cyclisation to construct the C ring of the natural product, as well as the vital quaternary centre with high enantioselectivtity. Indeed, this centre dictates the overall diastereoselectivity downstream in the natural product synthesis.

3.2.1 Initial Preparations and Screening of Additives and Solvents

To start, the racemic mixture of **62** was synthesised through the previously established intramolecular Heck reaction developed within our group,[8] providing a racemic sample of this product for future analysis of asymmetric variants. Using the developed conditions with **(*E*)-129**, the racemic mixture of **62** was obtained in an excellent 93% yield. (**Scheme 3.22**). It must be noted that the undesired indene by-product **94** (*vide supra*) was not formed under achiral reaction conditions, highlighting that the bidentate ligand choice within our previously attempted asymmetric protocols may be the cause for its formation.

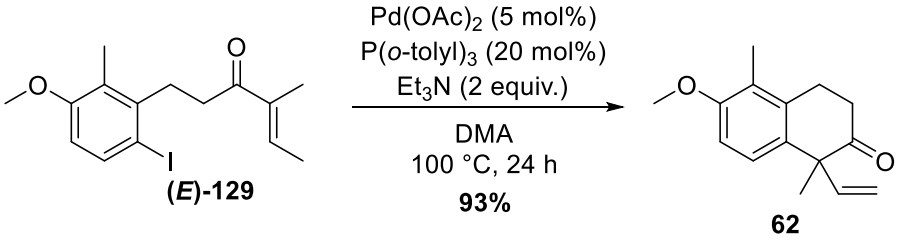

Scheme 3.22

In the preliminary investigations towards an asymmetric Heck protocol, deprotection of the Heck product was necessary to determine the enantiomeric excess by chiral HPLC, as it was reported that the two enantiomers of the protected variant could not be separated for analysis.[12] To confirm this observation, the racemic mixture of **17** was synthesised in a high yield of 79% under achiral conditions as shown in **Scheme 3.23**. Indeed, the enantiomers of **17** could not be separated, therefore (at this stage) **62** must be prepared for chiral HPLC

analysis. An exceptional conversion of **17** to **62** was accomplished, providing a 98% yield of **62**.

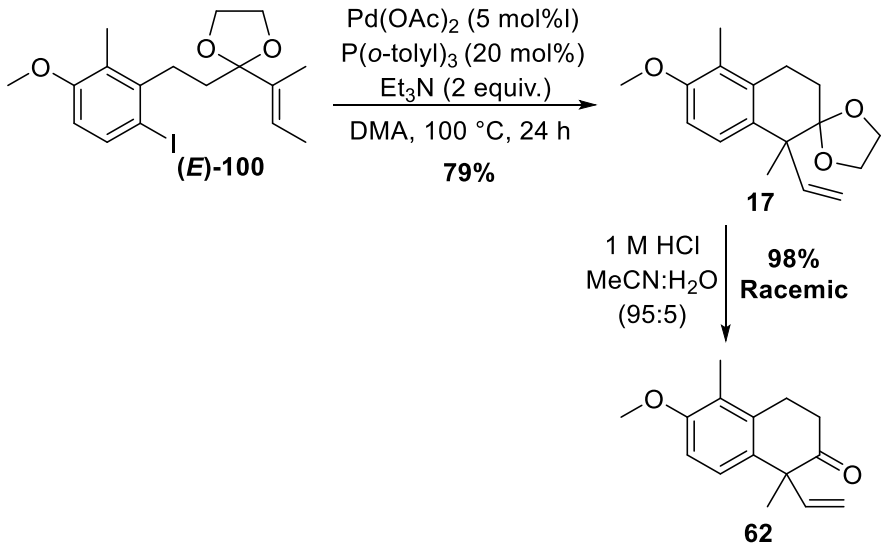

Scheme 3.23

Having established the analysis method required for the asymmetric Heck reaction studies, optimisation of the procedure was the next key focus. First, a solvent screen of cationic conditions, using silver phosphate (Ag_3PO_4) and (*R*)-BINAP, was investigated. Ag_3PO_4 was chosen as it was previously observed to be the most optimal silver additive.[12] In the initial optimisation studies, the solvent screen investigation with Ag_3PO_4 demonstrated promising results for our asymmetric Heck process (**Scheme 3.24, Table 3.5**).

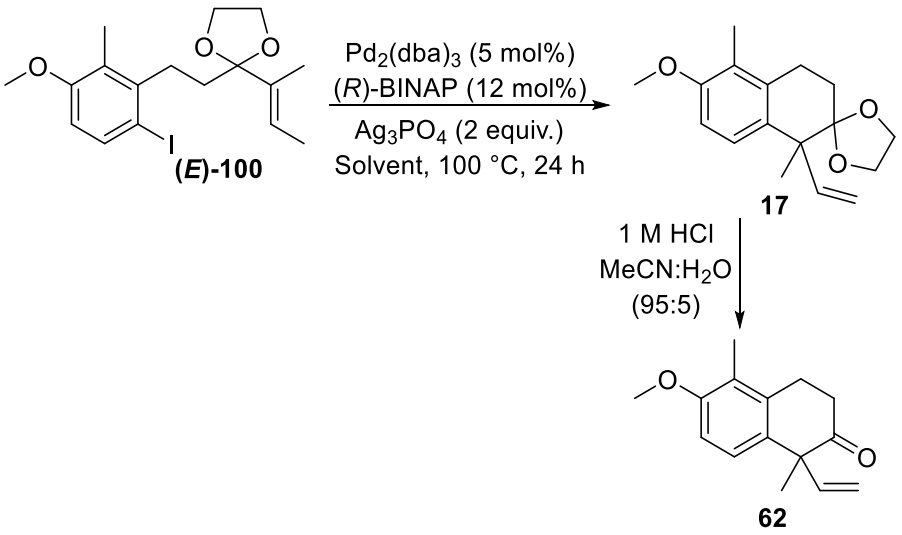

Scheme 3.24

Entry	Solvent	Yield of 17 (%)	ee of 62 (%)
1	DMA	82	0
2	PhMe	67	0
3	NMP	75	0
4	MeCN	80	26
5	1,2-DCE	66	40
6	PhCl	69	8
7	THF	76	10
8	DMF	77	8

Table 3.5

Commonly used solvents for the asymmetric Heck reaction were investigated in this screen. Focusing on the enantioselectivity of the reaction, initially discouraging results were obtained with solvents DMA, PhMe and NMP, as racemic mixtures of the Heck product were being produced in these reaction media (**Table 3.5**, **Entries 1-3**). However, expanding the solvent scope further uncovered the potential for an enantioselective process for the Heck reaction. More specifically, employing MeCN as the reaction solvent revealed enantioselectivity within this process for the first time, whereby a 26% ee with 80% isolated yield of the cyclised product was observed (**Entry 4**). Extremely pleased with this initial result, moving to 1,2-DCE as the solvent saw an increase to 40% ee (**Entry 5**). Switching to PhCl, THF, and DMF as the solvent did not improve the enantioselectivity of the reaction beyond that with 1,2-DCE (**Entries 6-8**).

With fairly promising results, our next focus was to explore the use of an organic base in the asymmetric Heck reaction in place of the silver additive utilised above. Commonly used organic bases in this reaction are PMP and Et_3N, and both were studied using a range of solvents. (**Scheme 3.25, Table 3.6**).

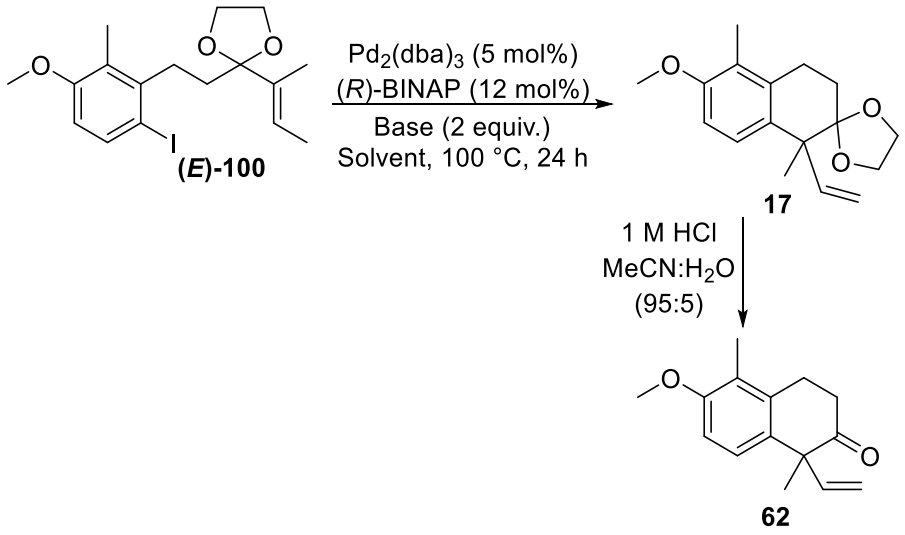

Scheme 3.25

Entry	Solvent	Additive	Yield of 17 (%)	ee of 62 (%)
1	DMA	PMP	91	6
2	1,2-DCE	PMP	39	46
3	1,2-DCE	Et_3N	45	60
4	MeCN	PMP	64	62
5	MeCN	Et_3N	60	64
6	THF	Et_3N	42	32
7	PhMe	Et_3N	52	40
8	NMP	Et_3N	41	18
9	DMF	Et_3N	62	60

Table 3.6

First, DMA was chosen as the solvent since, under silver promoted conditions, this provided the most optimal yield. Our initial reaction explored the use of PMP, which is notably the most commonly used base for asymmetric Heck reactions. Using this combination, again, an excellent yield of 91% was obtained with DMA as the solvent, but, unfortunately, the reaction displayed a very low ee (**Table 3.6, Entry 1**). As 1,2-DCE gave the best enantioselectivity in the Ag_3PO_4 study, this was investigated next, and a similar

enantioselectivity of 46% ee was observed (**Entry 2**). Alternatively, employing Et_3N as the organic base significantly increased the enantioselectivity to 60% ee (**Entry 3**). Pleased with this outcome, a comparison of both PMP and Et_3N was examined with MeCN as the solvent (**Entries 4** and **5**). Here, it was observed that the enantioselectivities using both bases were high and comparable (62 and 64% ee, using PMP and Et_3N, respectively). At this stage, due to substrate limitation, it was decided that Et_3N would be used in further investigations as it was seen to either be comparable or better than PMP in these intitial experiments. THF, NMP, and PhMe as reaction media gave lower entantiomeric excesses, however, DMF gave comparable enantioselectivity to the most optimal solvents studied so far (**Entries 6-9**). This solvent screen highlighted that using MeCN as the solvent with $E_{t3}N$ as the base generated the best overall outcome. It must be noted that whilst cationic and neutral conditions can favour opposite enantiomers in the asymmetric Heck reaction, in these investigations, the same enantiomer was favoured in all cases as part of this optimisation process.

Pleased with these results, the next parameter to investigate was the temperature of the reaction, as it was envisaged that improved enantioselectivity would be obtained at lower temperatures. Indeed, we anticipated that a reduction in temperature would, in turn, decrease the rate of the reaction. Therefore, to circumvent this, we allowed the reaction to run for a prolonged time (**Scheme 3.26, Table 3.7**).

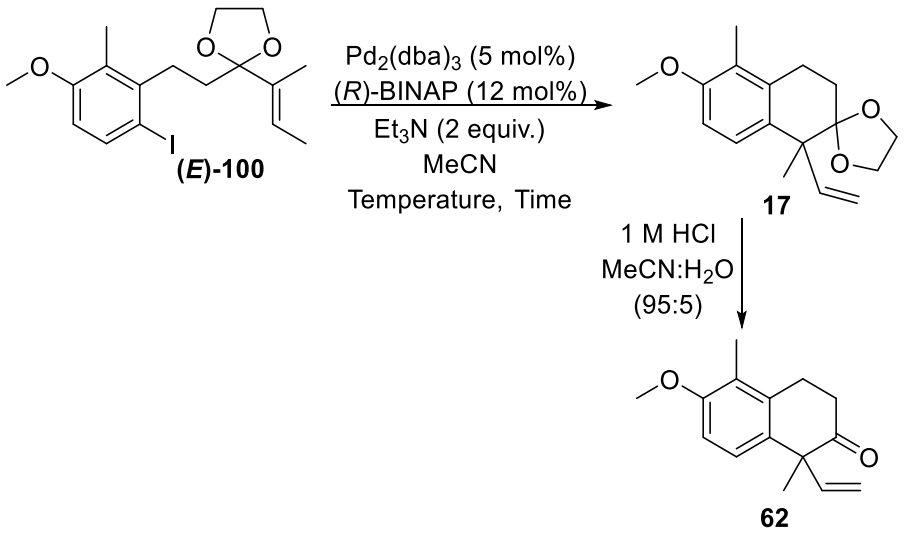

Scheme 3.26

Entry	Temperature (°C)	Time (h)	Yield of 17 (%)	ee of 62 (%)
1	80	69	90	70
2	60	72	56	68

Table 3.7

Using the previously optimised conditions, we were delighted to see that a 70 % ee was obtained, alongside an excellent yield of 90% when the temperature was decreased to 80 °C (**Table 3.7, Entry 1**). Unfortunately, whilst decreasing the temperature further resulted in comparable enantioselectively, this was concomitant with significantly reduced yield (**Entry 2**). With these results, we did not believe that a further reduction in reaction temperature would improve the overall efficiency of the asymmetric Heck reaction. Nevertheless, **Entry 1** above represented our best conditions yet with an excellent yield and very good enantiomeric excess. At this stage, investigations into the additive employed and the reaction temperature, as well as a significant solvent screen, provided a good initial understanding of our key Heck transformation. Ultimately, this resulted in an excellent yield and good enantiomeric excess of the desired bicyclic intermediate, with many optimisation areas yet to be explored.

*3.2.2 Initial Investigations with Triflate Precursor **(E)-101***

Continuing efforts to improve our key cyclisation process, application of triflate Heck precursor **(*E*)-101** was examined to determine its effectiveness in the asymmetric intramolecular Heck reaction, and if the overall reactivity and enantioselectivity with this precursor is superior over the iodide precursor **(*E*)-100**. (**Scheme 3.27, Table 3.8**). Using the conditions initially employed with **(*E*)-100**, it was encouraging to observe, at 100 °C for 24 hours, a significant improvement in yield on applying the triflate derivative, with an increase in enantioselectivity to 68% ee (**Table 3.8**, **Entry 1** vs **Entry 2**). This is comparable to the enantioselectivity observed when performing the reaction at a lower temperature of 80 °C with the iodide precursor (**Entry 3**) albeit with a reduced yield. Disappointingly, whilst another increase in yield (to 85%) was obtained when reducing the reaction temperature further with triflate precursor **(*E*)-101,** no improvement in the overall enantioselectivity of the reaction was gained (**Entry 4**).

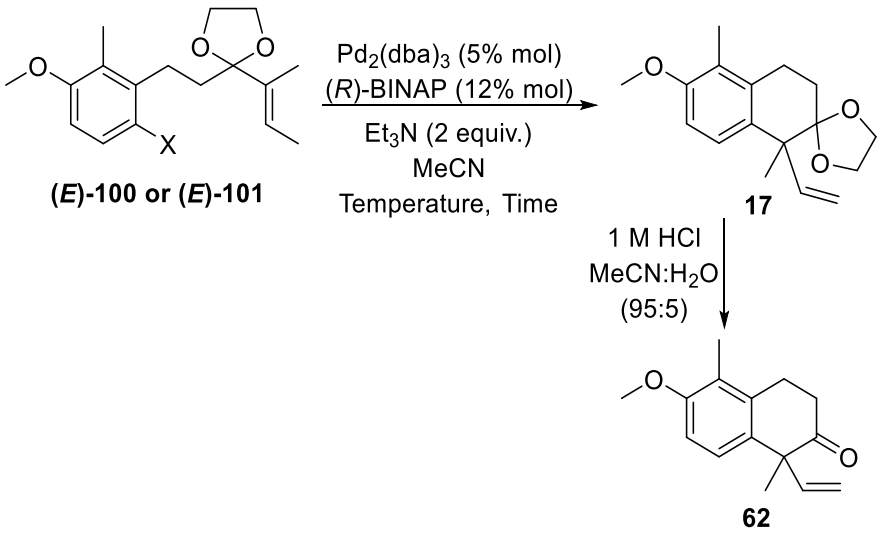

Scheme 3.27

Entry	X	Solvent	Temperature (° C)	Time (h)	Yield of 17 (%)	ee of 87 (%)
1[a]	I	MeCN	100	24	60	64
2	OTf	MeCN	100	24	79	68
3[a]	I	MeCN	80	69	90	70
4	OTf	MeCN	80	69	85	68

[a]Reactions previously performed and shown for comparison (*vide supra)*

Table 3.8

Although no improvement in the enantioselectivity of the reaction was observed when comparing the triflate precursor **(*E*)-101** with the iodide Heck precursor **(*E*)-100** (**Scheme 3.27, Table 3.8, Entry 3** vs **4**), the triflate precursor **(*E*)-101** notably provided improved reactivity (**Entry 1** vs **2**), which could be important when exploring further parameters within the overall system. Furthermore, the results obtained above could suggest a maximum limit of around 70% ee with the current conditions, indicating that investigations into the chiral ligand employed could be explored to facilitate greater enantioselectivity. Additionally, long reaction times were necessary for our current asymmetric Heck reaction, therefore we next focused our efforts into reducing the overall time.

3.2.3 Microwave Conditions Screen

To improve the overall reaction time and to investigate the effect on the enantioselectivity of the asymmetric Heck reaction, studies using microwave conditions were conducted with **(*E*)-100** (**Scheme 3.28, Table 3.9**).

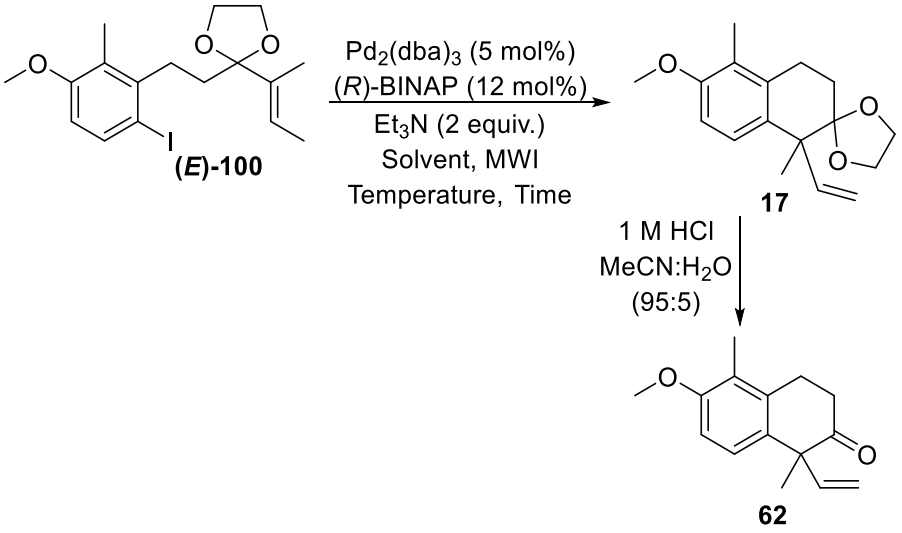

Scheme 3.28

Entry	Solvent	Temperature (° C)	Time (min)	Yield of 17 (%)	ee of 62 (%)
1	PhMe	100	50	29	0
2	1,2-DCE	100	50	32	45
3	MeCN	100	50	91	54
4	MeCN	80	50	60	56
5	MeCN	60	50	39	54
6	MeCN	100	20	61	58
7	MeCN	130	8	92	58

Table 3.9

A small solvent screen was first performed (**Table 3.9**, **Entries 1-3**), with the selection of solvents based on preliminary work (*vide supra*). Pleasingly, it was shown that using MeCN as the solvent could afford an excellent yield of 91% under microwave conditions for 50 minutes, a remarkable enhancement in reactivity compared to thermal conditions – which required 69 hours at 80 °C. Unfortunately, erosion of ee was observed (54% ee compared to 64% ee under thermal conditions) and decreasing the reaction temperature did

not improve the enantioselectivity of the reaction (**Entries 4** and **5**). In contrast with the results observed under thermal conditions, where a 70% ee was observed at 80 °C, only 56% ee was obtained using microwave conditions (**Entry 4**). Reducing the overall reaction time did not improve the ee significantly (**Entry 6**), however, it was pleasing to observe full conversion to desired product in just 8 minutes at 130 °C under harsher conditions, with retention of the 58% ee (**Entry 7**).

Despite the loss in enantioselectivity when using microwave conditions, it was shown that this technique could be used to significantly improve the overall reaction time of the cyclisation reaction. Having explored many parameters, information from the investigations thus far indicated that a change in chiral ligand should become a priority within this optimisation.

3.3 Chiral Ligands in the Asymmetric Heck Reaction

From the study of the asymmetric intramolecular Heck reaction thus far, it was clear that in order to enhance the enantioselectivity of the process, a screen, and subsequent optimisation, of various chiral ligands was required.

3.3.1 PHOX ligand Optimisation

It has been shown in the literature that (phosphinoaryl)oxazoline (PHOX) ligand systems have been utilised, with notable effect, within asymmetric intramolecular Heck reactions, particularly in natural product synthesis by Overman and Guerrero (*vide supra*).[49,50] Our objective was to capitalise on such conditions to enhance the asymmetric intramolecular Heck reaction as part of our synthesis towards agariblazeispirol C. To explore the application of the PHOX ligand in our system of interest, a number of conditions, using either microwave irradiation or thermal methods, were applied (**Scheme 3.29, Table 3.10**). Previous work by Overman and Guerrero[49,50] employed triflate Heck precursors, therefore initial screens with PHOX ligands featured **(*E*)-101**. Furthermore, the authors utlilised $Pd(OAc)_2$ as the catalyst and PMP as the base, therefore we also mirrored this usage in our own system.

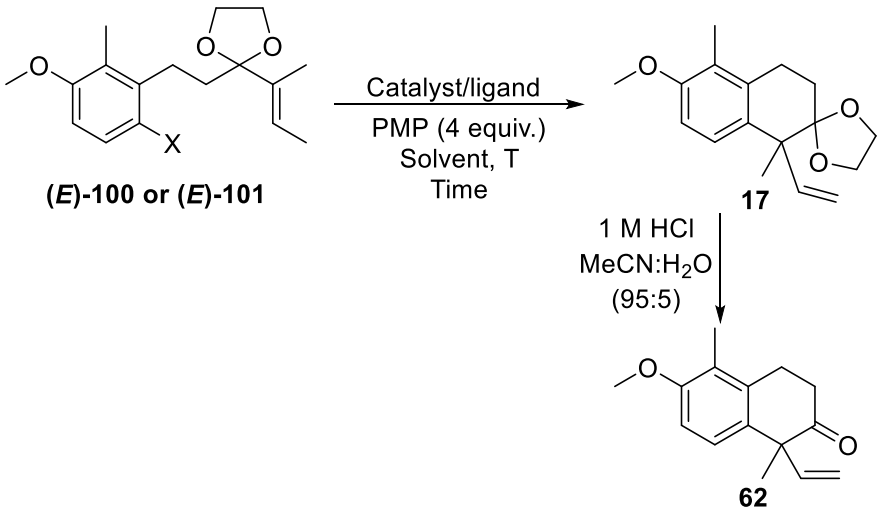

Scheme 3.29

Entry	X	Solvent	Catalyst/Ligand	T (° C)	Time	Yield of 17 (%)	ee of 62 (%)
1[a]	OTf	PhMe	$Pd(OAc)_2$ (10 mol%), (*S*)-^{t}BuPHOX (30 mol%)	170	50 min	18	54
2[a]	OTf	MeCN	$Pd(OAc)_2$ (10 mol%), (*S*)-^{t}BuPHOX (30 mol%)	130	20 min	14[c]	72
3[b]	OTf	MeCN	$Pd(OAc)_2$ (10 mol%), (*S*)-^{t}BuPHOX (30 mol%)	80	69 h	13	86
4[b]	I	MeCN	$Pd(OAc)_2$ (10 mol%), (*S*)-^{t}BuPHOX (30 mol%)	80	69 h	32	6
5[b,d]	OTf	MeCN	$Pd_2(dba)_3$ (5 mol%) (*S*)-^{t}BuPHOX (12 mol%)	80	69 h	31	74
6[b]	OTf	MeCN	$Pd(OAc)_2$ (10 mol%), (*S*)-^{i}PrPHOX (30 mol%)	80	69 h	11[c]	80

[a]microwave conditions; [b]thermal conditions; [c]contains starting material; [d]Et_3N (2 equiv.) used

Table 3.10

Employing literature conditions provided significantly lower yields and enantioselectivity towards our desired Heck product, as compared to previous conditions employed in our current optimisation with (*R*)-BINAP as the chiral ligand (**Table 3.10**, **Entry 1**). Moreover, **(*E*)-101** was difficult to separate from compound **17** by silica chromatography, which often resulted in residual quantities of **(*E*)-101** being detected during the isolation of **17**, particularly when poorer yields were observed (**Entries 2** and **6**). With the knowledge thus far indicating that, for our system, MeCN was the optimal solvent, the literature conditions were tuned to incorporate this solvent, and our following attempt employed microwave irradiation at 130 °C for 20 minutes. In doing so, a boost in enantioselectivity to 72% ee was obtained, albeit with a poor product yield. (**Entry 2**). As microwave conditions had provided reduced enantioselectivities thus far, modified thermal conditions with the (*S*)-^{t}BuPHOX ligand were explored instead. Pleasingly, heating thermally to 80 °C provided an excellent 86% ee, representing the highest enantioselectivity seen for our system to this stage, although with a very poor isolated yield (**Entry 3**). Applying iodide **(*E*)-100** as the Heck precursor, unfortunately, resulted in an almost completely diminished ee, but with a surprisingly higher yield of 32% (**Entry 4**), indicating that the trends observed previously with (*R*)-BINAP do not apply with the PHOX ligand system. Additionally, whilst reverting to use of Pd_2dba_3 as the catalyst species provided a good 74% ee (**Entry 5**), this was not an improvement on the optimal 86%. (**Entry 5**). Futhermore, despite obtaining an 80% ee,

using the (*S*)-^{i}PrPHOX variant did not enhance the overall yield (**Entry 6**). It was apparent that the balance between reaction conversion and enantioselectivity represented a challenge within these PHOX-based systems, and further examination of the reaction conditions was required.

In an effort to obtain higher yields with the (*S*)-^{t}BuPHOX ligand, a palladium catalyst screen was performed using triflate substrate **(*E*)-101** to investigate the effect of the catalyst employed on both conversion and enantioselectivity (**Scheme 3.30, Table 3.11**).

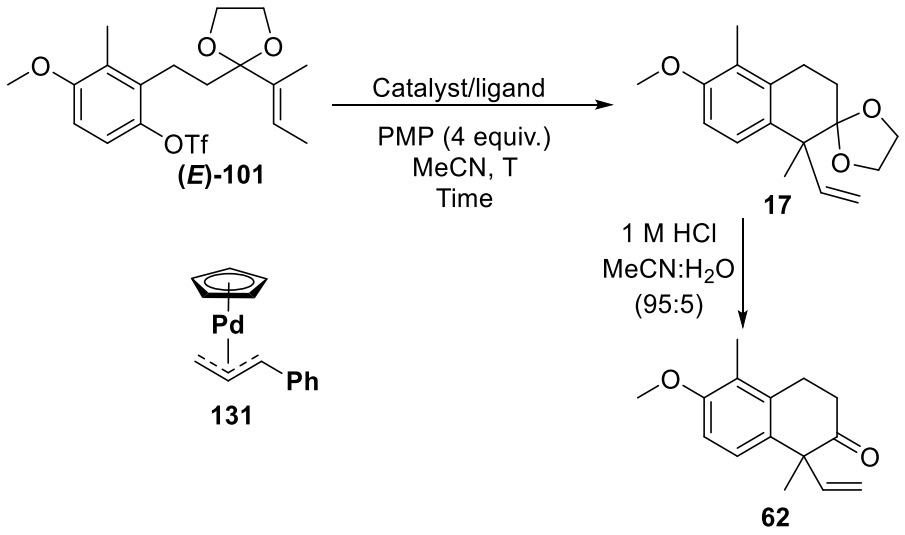

Scheme 3.30

Entry	Conditions	Catalyst/Ligand	T (° C)	Time (h)	Yield of 17 (%)	ee of 62 (%)
1	Thermal	$Pd(dba)_2$ (5 mol%) (*S*)-^{t}BuPHOX (12 mol%)	80	69	Trace	-
2	Thermal	$PdCl_2$ (10 mol%) (*S*)-^{t}BuPHOX (10 mol%)	80	69	Trace	-
3	Thermal	**131** (10 mol%) (*S*)-^{t}BuPHOX (30 mol%)	80	69	28	86
4	Microwave	**131** (10 mol%) (*S*)-^{t}BuPHOX (30 mol%)	130	1	40	82
5	Microwave	**131** (10 mol%) (*S*)-^{t}BuPHOX (30 mol%)	130	4	49	76

Table 3.11

The initial palladium screen with $Pd(dba)_2$ and $PdCl_2$ provided only trace amounts of the desired product (**Table 3.11**, **Entries 1** and **2**), illustrating that the choice of palladium catalyst is crucial to the overall conversion. However, when **131** was employed, which has been shown in the literature to be an effective Pd(0) precursor,[100] an improved 28% yield was observed with retention of the enantioselectivity at an impressive 86% ee **(Entry 3)**. Applying microwave conditions did improve the overall yield to **17**, however, erosion of enantioselectivity was observed, particularly when longer irradiation periods were employed (**Entries 4** and **5**).

With these encouraging results, a base screen was conducted in efforts to, again, boost the overall yield to **17** (**Scheme 3.31, Table 3.12**). Various organic and inorganic bases were applied into our Heck transformation.

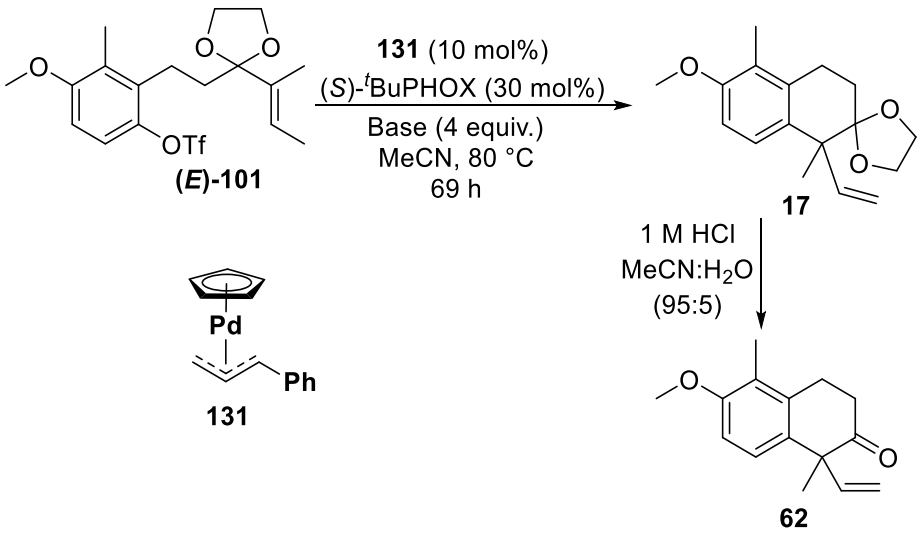

Scheme 3.31

Entry	Base	Yield of 17 (%)	ee of 62 (%)
1	Et_3N	24	86
2	DIPEA	22	88
3	Proton Sponge®	28[a]	90
4	DABCO	42[a]	90
5	K_2CO_3	34[a]	90

[a]contains starting material

Table 3.12

Despite Et_3N and DIPEA providing comparable enantioselectivity (**Table 3.12**, **Entries 1 and 2**), promising outcomes were seen with the other bases screened. Employing the proton sponge®, DABCO, and inorganic base K_2CO_3 furnished the desired product **17** with an excellent 90% ee (**Entries 3-5**). It was also promising to see an enhancement in overall yield with DABCO (**Entry 4**) as the base, which was carried through into further optimisation studies that explored solvent, temperature, and reaction time (**Scheme 3.32, Table 3.13**).

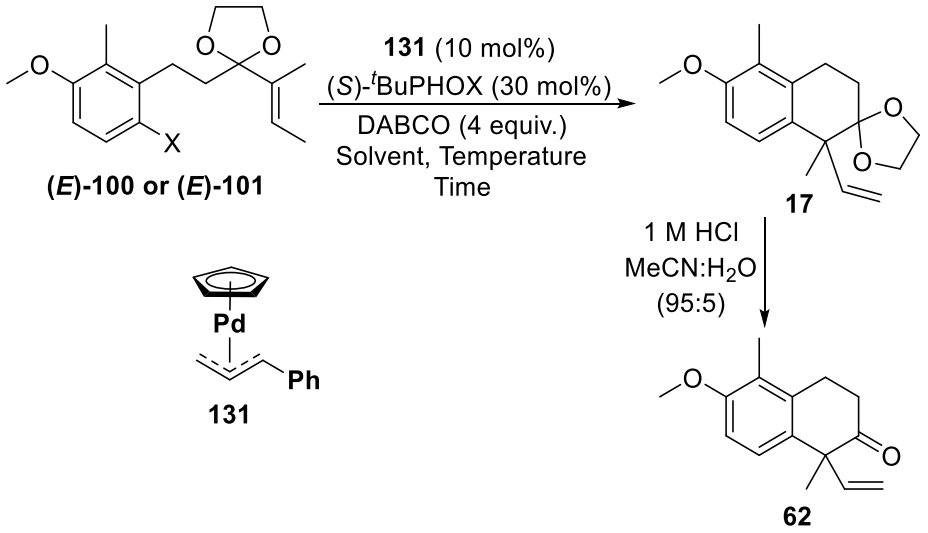

Scheme 3.32

Entry	X	Conditions	Solvent	T (° C)	Time (h)	Yield of 17 (%)	ee of 62 (%)
1	OTf	Thermal	1,2-DCE	80	69	Trace	-
2	OTf	Thermal	DMF	80	69	Trace	-
3	OTf	Thermal	THF	80	69	20[a]	84
4	OTf	Thermal	MeCN	90	69	11[a]	88
5	OTf	Thermal	MeCN	100	69	19[a]	86
6[b]	OTf	Thermal	MeCN	80	69	42	89
7	OTf	Microwave	MeCN	130	1	32	83
8	OTf	Microwave	MeCN	130	4	44	82
9[b]	OTf	Microwave	MeCN	130	4	62	84
10	I	Thermal	MeCN	80	69	34	56

[a]contains starting material; [b]**131** (20 mol%), (*S*)-^{t}BuPHOX (60 mol%)

Table 3.13

With DABCO selected as the base for the asymmetric intramolecular Heck reaction, a short solvent screen was completed (**Table 3.13**, **Entries 1-3**), however, no improvement in either the isolated yield or enantioselectivity was obtained in 1,2-DCE, DMF, or THF, as compared to MeCN. A temperature screen was also conducted, probing reaction temperatures of 90 and 100 °C (**Entries 4** and **5**), with the results highlighting that significantly lower yields of **17** were obtained in both cases, as compared to the same reaction at 80 °C (*c.f.* **Scheme 3.31, Table 3.12, Entry 4**). Furthermore, the enantioselectivity also dropped moving from 80°C, where a 90% ee was obtained, through 90 °C (88% ee), to 100 °C, where an 86% ee was obtained. In an attempt to increase the overall yield to **17**, increased quantities of catalyst (20 mol%) and ligand (60 mol%) were applied, as detailed in **Entry 6**. Pleasingly, a significantly higher isolated yield to the desired product was observed, with retention of the enantioselectivity (89% ee), however, it should be noted that the 42% isolated yield is unrepresentative of the reaction conversion, with the lower value due to the challenging separation of the product from the starting substrate. Again, exploration of microwave irradiation was considered to enhance the yield to **17** (**Entries 7-9**). Indeed, moderate isolated yields at shorter reaction times were obtained on moving to microwave irradiation, with only a small loss in enantioselectivity. Pleasingly, an improvment in the yield to 62% was observed when using the higher quantities of catalyst and ligand (**Entry 9**). In a final attempt, iodide **(*E*)-100** was employed using the optimised thermal conditions with triflate **(*E*)-101** until this stage. Unfortunately, this resulted in only 34% isolated yield and a significantly reduced 56% ee (**Entry 10**).

Despite extensive optimisation using the (*S*)-^{t}BuPHOX ligand system, whereby an appreciable 62% overall yield and excellent enantioselectivity of 84% ee was achieved, to fully scope our system, further investigations with other chiral ligands were required. The current conditions with the (*S*)-^{t}BuPHOX ligand system demanded high Pd catalyst and ligand loading, and onerous purification, which resulted in reduced overall efficiency of the asymmetric intramolecular Heck reaction, particularly on larger scale. Based on these findings, and in order to maintain both a high isolated yield and excellent enantioselectivity for our desired transformation, alternative chiral ligands were considered.

3.3.2 Diphosphine ligand Screen and Optimisation

It should be noted that the PhD research contained within this thesis was supported collaboratively through an EPSRC industrial CASE Award with leading pharmaceutical company GlaxoSmithKline (GSK). During a three-month secondment period to GSK, further advancement of our current asymmetric Heck system was possible. More specifically, a comprehensive ligand screen, particularly focusing on diphosphine ligands due to the successful reactivty of our system with (*R*)-BINAP, was carried out. Asymmetric Heck conditions previously optimised with Pd_2dba_3, (*R*)-BINAP, Et_3N and iodide precursor **(*E*)-100** were explored in this chiral ligand screen. **(*E*)-100** was chosen due to easier accessibility of this substrate, and, to this stage, we had observed similar levels of enantioselectivity with both iodide and triflate Heck precursors with (*R*)-BINAP (*vide supra*). The availability of state-of-the-art purification instruments allowed a rapid turnaround of results, and the ability to separate the enantiomers of the protected Heck bicyclic product **17** removed the need to deprotect the system to **62** before chiral analysis, as previously was required. The experimental procedure was also simplified, removing the freeze-pump-thaw protocol with liquid nitrogen for the reaction which was previously required (see the *Experimental Section* for more details). As shown in **Scheme 3.33**, **Table 3.14**, 14 additional chiral ligands were screened for our asymmetric intramolecular Heck transformation. The chemical structures of these chiral ligands can be found in *Appendix 9.1*.

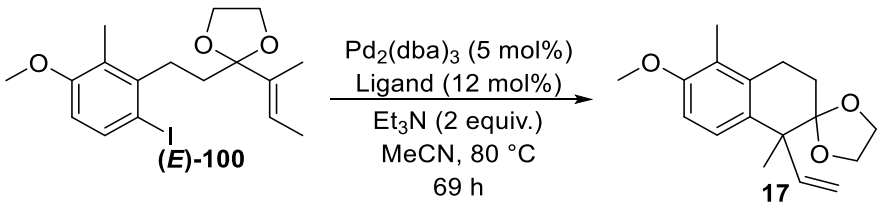

Scheme 3.33

Entry	Ligand	Conversion by LCMS (%)	% ee
1	(*R*)-BINAP	100	70
2	(*R*)-Tol-BINAP	95	77
3	(*R*)-DM-BINAP	100	17
4	(*R*)-SEGPHOS	100	71
5	(*S*)-DM-SEGPHOS	100	83
6	(*S*)-DTBM-SEGPHOS	15	29
7	(*R*)-SYNPHOS	100	86
8	(*R*)-H_8-BINAP	100	67
9	*(S)*-MeO-BIPHEP	100	61
10	(*R*)-P-Phos	50	70
11	(*S*)-Phanephos	100	4
12	(-)-DIOP	100	6
13	Josiphos (SL-J001-1)	100	3
14	Walphos (SL-W001-1)	100	4
15	Taniaphos (SL-T001-1)	100	8

Table 3.14

For rapid turnover of results, each reaction was purified by mass-directed autopurification (MDAP), a purification technique known to lose mass of product during purification. Thus, only the conversion to **17**, estimated by LCMS, and the % ee induced by each chiral ligand was reported. To probe the reproducibility of the asymmetric Heck protocol while on secondment, an initial test reaction with (*R*)-BINAP was conducted and, to our delight, comparable conversion and enantioselectivity was obtained with respect to the previous findings (**Table 3.14**, **Entry 1**). To begin the screen, chiral ligands structurally close to BINAP were chosen (**Entries 2-8**). Pleasingly, in this series, high conversion to the product was achieved, with the exception of (*S*)-DTBM-SEGPHOS (**Entry 6**). With respect to enantioselectivity, applying the more sterically encumbered (*R*)-tol-BINAP (**Entry 2**) furnished the product with an increased 77% ee. Increasing the bulk of the phosphine further in (*R*)-DM-BINAP decreased the enantiomeric excess dramatically to 17% (**Entry 3**). A similar trend was observed with the SEGPHOS family, whereby (*R*)-SEGPHOS (**Entry 4**) provided similar enantioselectivity to (*R*)-BINAP (71% ee), which could be

subsequently improved by increasing the bulk of the phosphine; (*S*)-DM-SEGPHOS delivered the desired compound with an excellent 83% ee (**Entry 5**). As with the BINAP series, there existed a limitation with regards to sterics and further increasing the bulk by employing (*S*)-DTBM-SEGPHOS (**Entry 6**) revealed both poorer conversion (15%) and enantioselectivity (29% ee). Results from the screening of these families indicated a trend whereby increasing the steric bulk of the phosphine appeared to augment enantioselectivity, however, if the substituents become too large, a detrimental effect on conversion and % ee was observed. In continuing efforts to enhance the enantioselectivity of our Heck transformation, gratifyingly, (*R*)-SYNPHOS provided the best overall outcome, not only for the chiral ligand screen, but for the entire asymmetric Heck optimisation thus far with full conversion and 86% ee being achieved (**Entry 7**). This result represented a significant improvement to the PHOX ligand systems presented previously, where similar enantioselectivities could be achieved but with poorer isolated yields, which, in turn, led to difficult purifications. To extend the depth of this study, a variety of other chiral ligands were investigated (**Entries 9-15**), however, despite observing full conversion for the majority of these ligands, no improvement on enantioselectivity was observed.

In summary, 14 different chiral ligands were rapidly screened and revealed (*R*)-SYNPHOS as an improved chiral ligand for our asymmetric intramolecular Heck protocol. To our delight, through simplified experimental, purification, and analysis procedures, we accomplished the synthesis of the desired product with a high 86% ee and with 100% conversion using (*R*)-SYNPHOS with iodide **(*E*)-100**.

*3.3.3 X-ray Crystallography and Assignment of **(R)-17***

While performing the chiral ligand screen described above, compound **17** collected from the asymmetric Heck reaction with (*S*)-DM-SEGPHOS as the ligand yielded an off-white solid, which was recrystallised from petroleum ether (40–60 °C). X-ray crystallography provided the structure shown in **Figure 3.1**. Pleasingly, the crystal structure not only confirmed product **17** had been synthesised, but additionally highlighted the absolute stereochemistry of the key quaternary carbon centre generated from the asymmetric intramolecular Heck reaction. Analysis of the crystal structure showed the formation of the

(*R*)-17 enantiomer when performing the reaction with (*S*)-DM-SEGPHOS; indeed, this is the correct enantiomer as targeted for the synthesis of agariblazeispirol C **1**. This provided an aid for chiral analysis work, as each peak in the chromatogram could now be identified as either the (*R*) or (*S*) enantiomer (**Figure 3.2**).

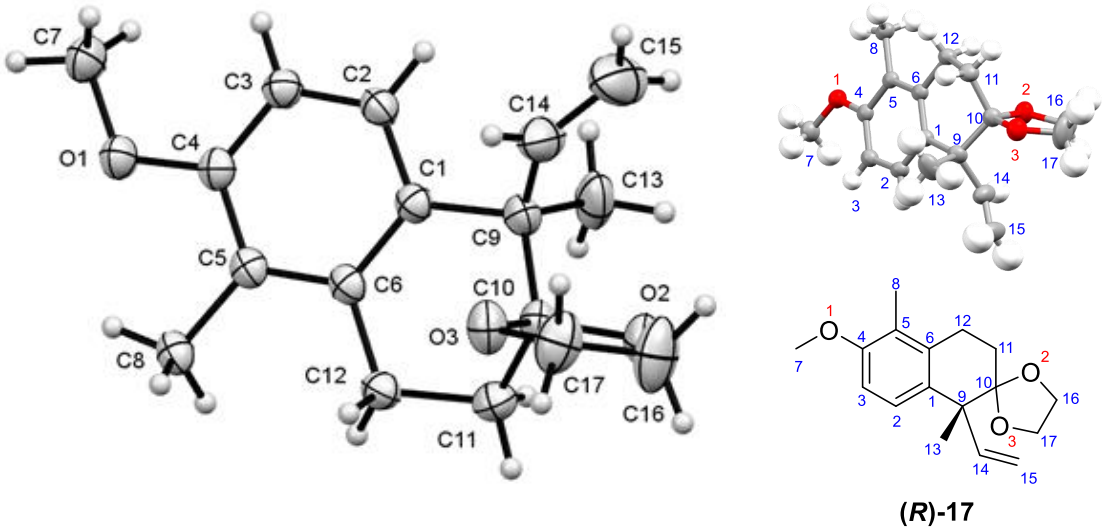

Figure 3.1

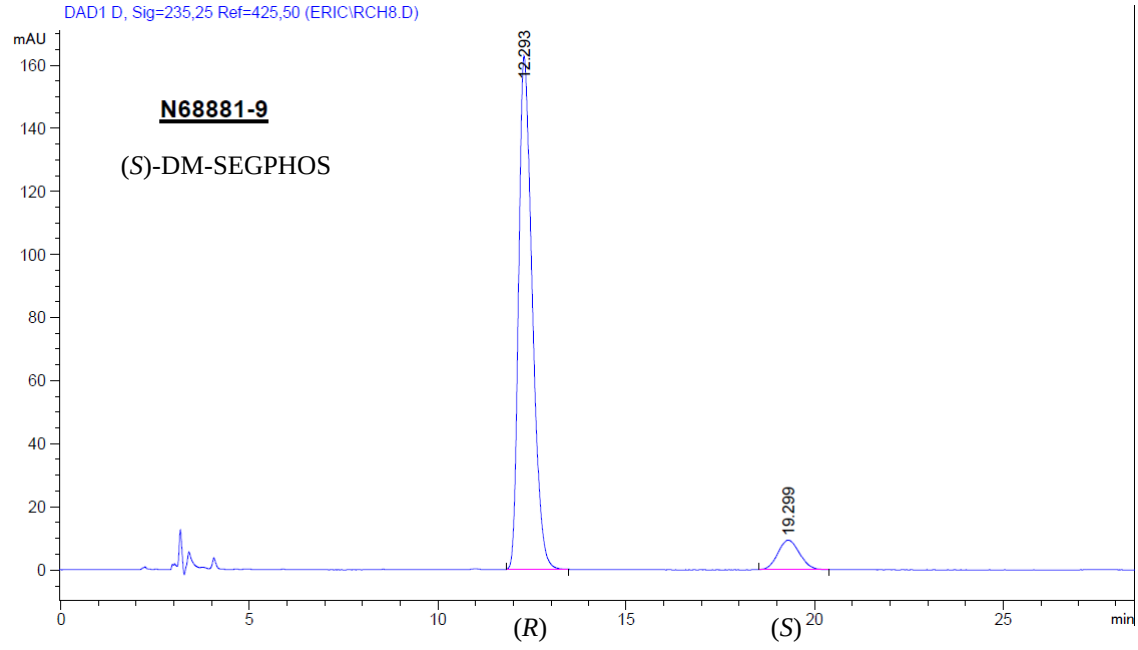

Figure 3.2

3.3.4 Final Optimisations of the Asymmetric Intramolecular Heck Reaction

To improve upon the excellent result obtained with (*R*)-SYNPHOS, a base screen was investigated (**Scheme 3.34**, **Table 3.15**). This work was conducted without prior knowledge of the stereochemical assignment of **17** (*vide supra*), however, it was later determined through chiral HPLC analysis that **(*S*)-17** was synthesised in these reactions.

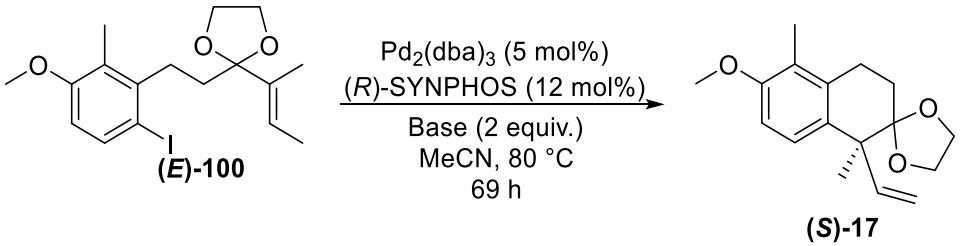

Scheme 3.34

Entry	Base	Conversion by LCMS (%)	% ee
1	DIPEA	100	86
2	PMP	100	86
3	DABCO	80	40

Table 3.15

Applications of bases DIPEA and PMP both furnished the desired compound **17** with full conversion and a comparable 86% ee was obtained when considering the previous result with Et_3N as the base (**Table 3.15, Entries 1** and **2**). Despite showing no improvement in enantioselectivity, reproducibility of high conversions and % ee were highlighted in these studies. When DABCO was used as the base, a lower conversion and erosion of enantioselectivity to 40% ee was observed (**Entry 3**).

Considering all of the above, the final optimisations of our key asymmetric intramolecular Heck reaction were completed (**Scheme 3.35**, **Table 3.16**).

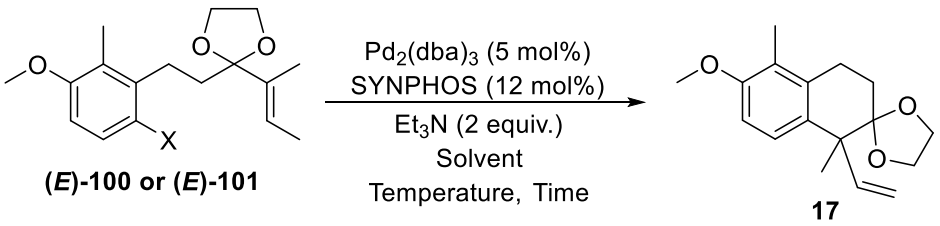

Scheme 3.35

Entry	X	Ligand	Solvent	Temperature (°C)	Time	Yield (%)	% ee
1	I	(*R*)	MeCN	80	69 h	84	86 (*S*)
2	OTf	(*R*)	MeCN	80	69 h	88	86 (*S*)
3[a]	I	(*R*)	MeCN	130	8 min	42	76 (*S*)
4	I	(*R*)	MeCN	100	24 h	84	86 (*S*)
5	I	(*S*)	MeCN	100	24 h	85	86 (*R*)
6	I	(*S*)	DMF	100	24 h	90	68 (*R*)
7	I	(*S*)	1,2-DCE	100	24 h	29	72 (*R*)

[a]reaction performed under MWI

Table 3.16

First, and now back within the laboratories at the University of Strathclyde, the optimised conditions developed whilst at GSK were repeated to allow full isolation of the product and establishment of the true the chemical yield of the reaction. It was pleasing to see that the results were reproducible, generating an 84% isolated yield of our desired bicyclic system **17** and maintaining the high levels of enantioselectivity at 86% ee (**Table 3.16, Entry 1**). Next, triflate Heck precursor **(*E*)-101** was employed, producing the desired product with comparable yields and % ee to the iodide Heck precursor **(*E*)-100** (**Entry 2**). As mentioned before, access to substrate **(*E*)-100** is easier, hence optimisation studies continued to employ this substrate. Microwave irridation was revisited in an attempt to reduce the overall reaction time, however, both isolated yield and % ee diminished to 42%, and 76%, respectively (**Entry 3**). Undeterred, and returning to thermal conditions, the temperature of the reaction was increased to 100 °C, with the overall time reduced to 24 hours. Gratifyingly, no erosion of either the conversion to **17** or enantioselectivity was observed, instead maintaining an excellent 84% isolated yield and 86% ee at this higher temperature and a shorter reaction time (**Entry 4**). Changing the ligand from (*R*)-SYNPHOS to (*S*)-SYNPHOS had no effect on the reaction yield or % ee, with now our desired enantiomer **(*R*)-17** being isolated within our key transformation (**Entry 5**). Finally, a short screen of

solvents was conducted using DMF and 1,2-DCE (choices based on previous studies), however, no improvement in reaction efficiency or selectivity was observed. (**Entries 6** and **7**).

At this stage, we were delighted to have completed our extensive optimisation of our key asymmetric Heck cyclisation procedure – through establishing (*S*)-SYNPHOS as the most optimal chiral ligand for our system, we arrived at our final conditions, as shown on **Table 3.16, Entry 5**, which generated an 85% isolated yield and an 86% ee of **(*R*)-17**.

3.4 Summary

As demonstrated in this chapter, various routes were undertaken to synthesise a variety of Heck precursors, and a comprehensive optimisation campaign of our key asymmetric intramolecular Heck cyclisation has been fully performed. Gratefully, we are delighted to have established a synthetic strategy towards the essential bicyclic system, with the critical quaternary stereocentre set within the total synthesis of agriblazeispirol C.

Despite facing initial difficulties towards the synthesis of iodide Weinreb amide intermediate **106**, this compound can be made in large quantities, with an excellent 75% yield over 5 steps from the starting acid **19** (**Scheme 3.36**). **106** can be converted into the triflate variant **107** in 3 further steps with a 68% overall yield. With both Weinreb amide intermediates in hand, both the iodo and the triflate variant of the direct Heck precursor can be synthesised in high yields; 91% over 2 steps for **(*E*)-100**; and 65% over 2 steps for **(*E*)-101**.

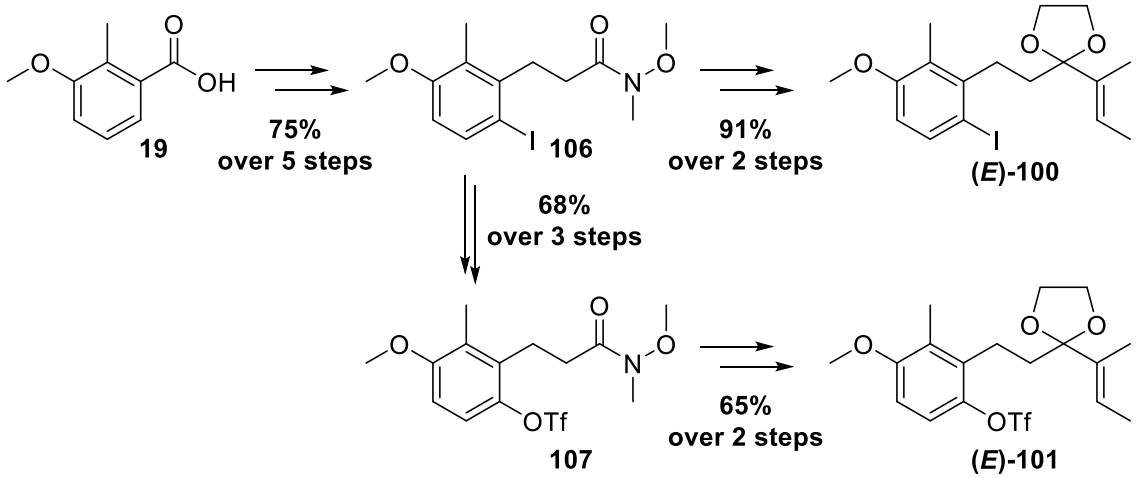

Scheme 3.36

With regards the exploration of the key asymmetric Heck reaction, an expansive investigation into this transformation was executed to generate the bicyclic intermediate **17** in high yields and enantioselectivity. From the initial additive screen (Ag_3PO_4, Et_3N and PMP) with 8 different solvents, and looking at a range of reaction temperatures and times,

we were encouraged with the excellent yield of 90% and good level of enantioselectivity (70% ee) at such an early stage of the overall investigation, with (*R*)-BINAP as the chiral ligand (**Scheme 3.37**). In these studies, it was found that employing the triflate precusor **(*E*)-101** was not benficial, and while microwave irridation reduced the overall reaction time to 8 minutes, this was concomitant with an erosion in enantioselectivity.

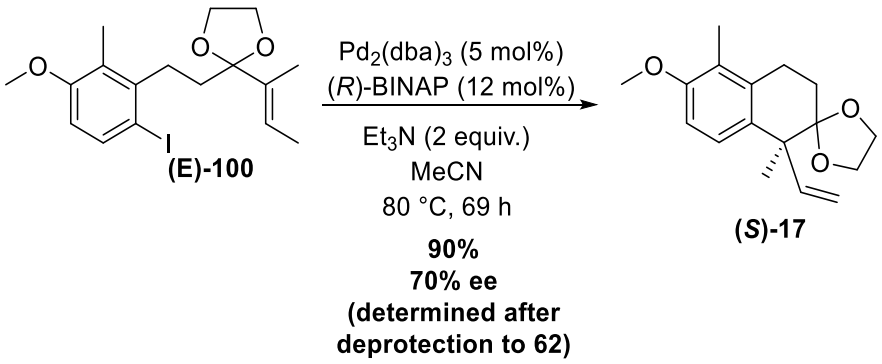

Scheme 3.37

Next in our optimisation campaign was to further elevate the overall enantioselectivity of the Heck process through an investigation of chiral ligands. Studied extensively first was the PHOX ligand system, where intial conditions applied from the literature was fruitless. This resulted in an arduous examination of various bases and reaction conditions with both **(*E*)-100** and **(*E*)-101** to enhance the overall yield and % ee. From these studies, it was concluded that high levels of enantioselectivity could be achieved (up to 90% ee) as a consequence of poor yields and high catalyst and ligand loadings, both of which are undesirable. Hence, developing conditions which balanced both yield and enantioselectivty was sought after. To do this, a screen of a wide array of commercially available chiral ligands was implemented, which identified more suitable chiral diphosphine ligands for our Heck transformation, as summarised in **Figure 3.3**. From this, (*S*)-SYNPHOS was established as our best chiral ligand, which furnished our desired (*R*)-stereocentre, and, after further optimisations, completed our overall Heck study. **Scheme 3.38** highlights our final reaction conditions – critical to the high yields and enantioselectivity are the use of MeCN as the solvent, Et_3N as the additive, and (*S*)-SYNPHOS as the chiral ligand.

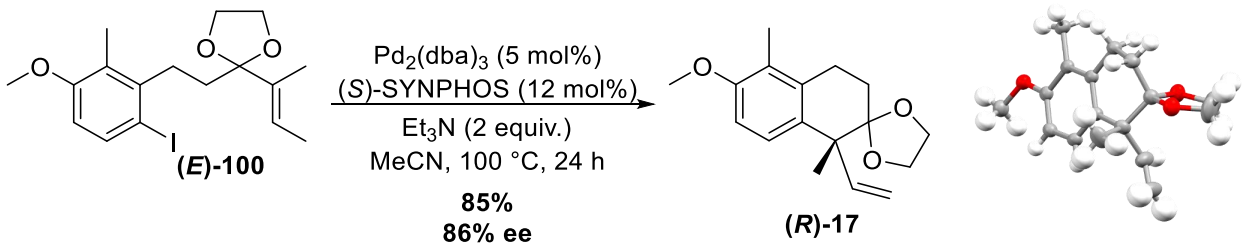

Scheme 3.38

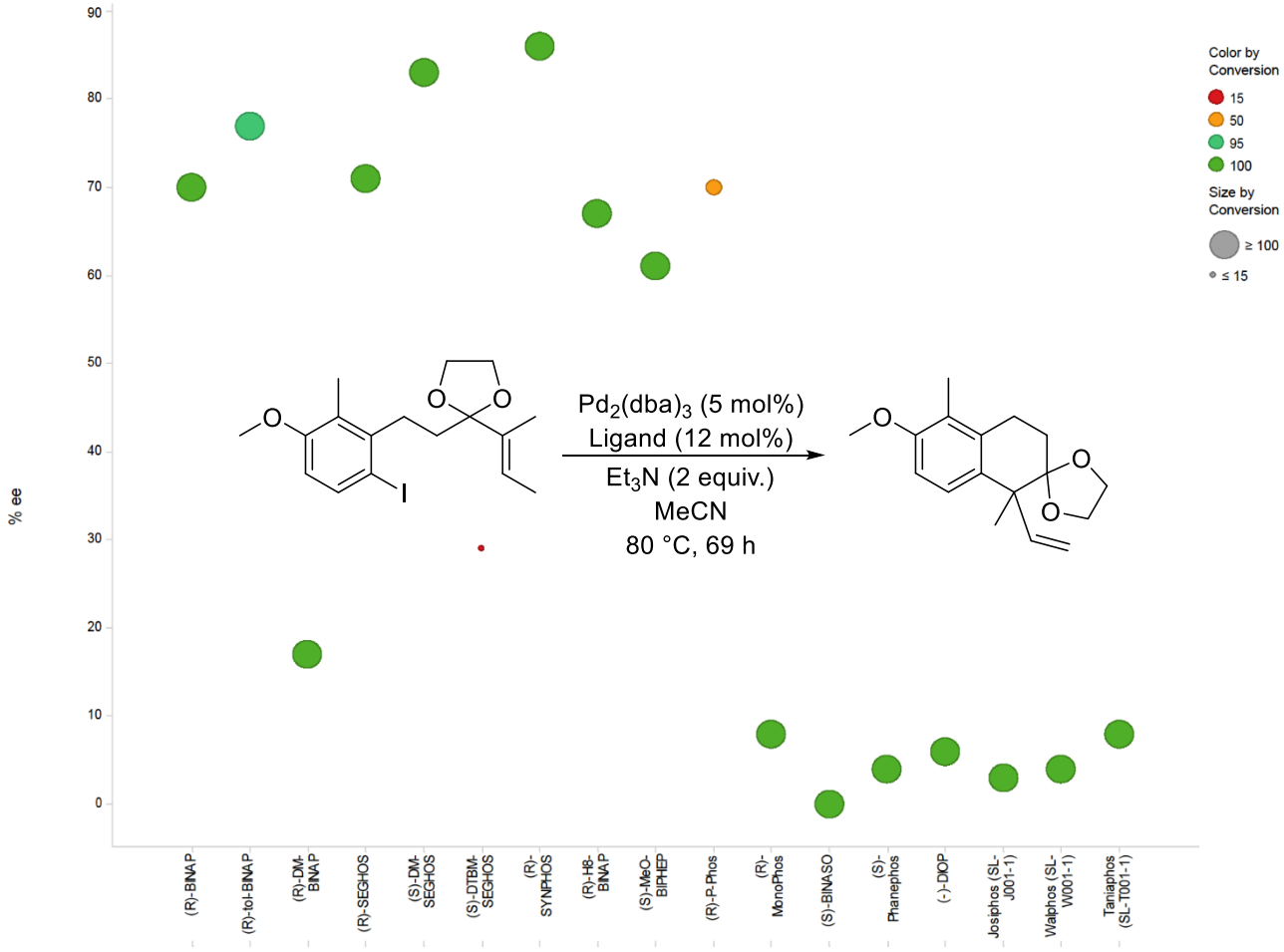

Figure 3.3

Chapter 4

Intramolecular Pauson-Khand Reaction

4. Intramolecular Pauson-Khand Reaction

4.1 Synthesis Towards the Enyne PK Precursor

In our proposed total synthesis programme, we wished to synthesise two distinct Pauson-Khand precursors – the first to be targeted was the enyne PK precursor **95** (**Scheme 4.1**). The key advantage of using this precursor is its known excellent reactivity within the PK cyclisation to generate the tetracyclic core **97**.[10] However, a challenging late-stage oxidation of **97** to deliver the true polycyclic framework of the natural product has yet to be realised. Even though enyne **95** has been previously synthesised within the group, in a racemic sense, the methodology could not be directly translated from the novel Heck product **17**, hence, a new strategy was devised, optimising each step. For these studies, and to avoid the use of precious enantiopure material, racemic **17** was used to first establish routes towards the final target.

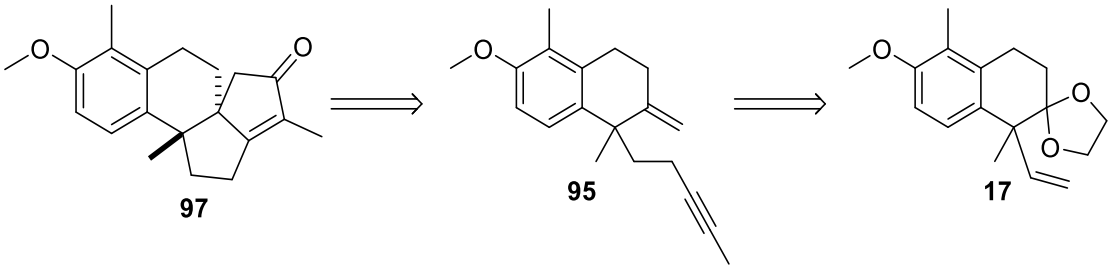

Scheme 4.1

*4.1.1 Preparation of Enyne PK Precursor **95***

We anticipated that the enyne PK precursor **95** could be generated from the key Heck product **17**, through a variety of synthetic transformations (**Scheme 4.2**). PK precursor **95** could be produced from TMS protected enyne **132**, which, in turn, can be made from ketone **133** through olefination and alkynylation strategies. Overall, this approach involves a late-stage carbon homologation to synthesise our desired PK precursor.

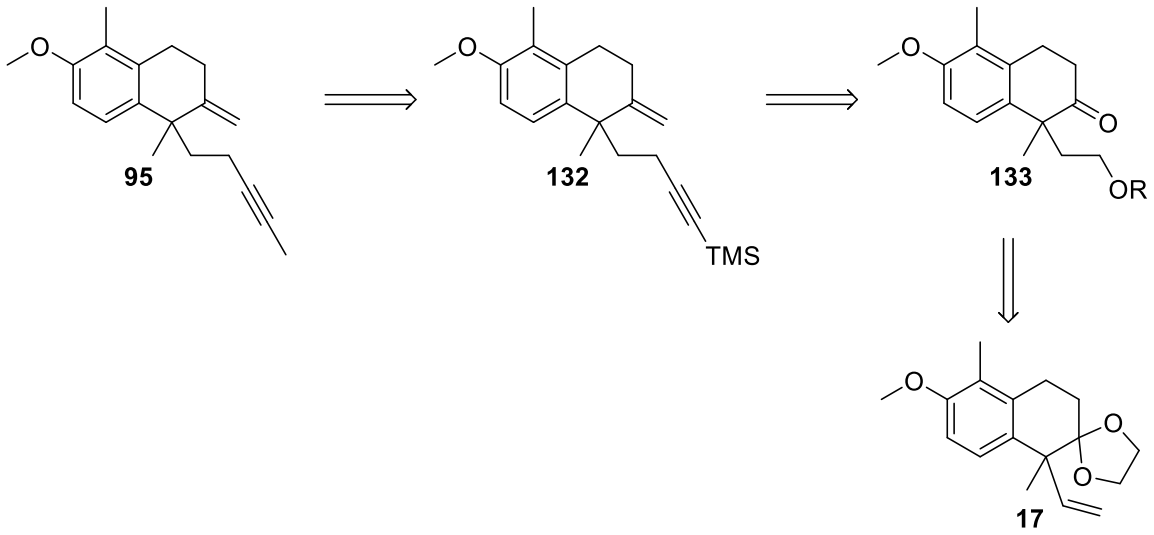

Scheme 4.2

To begin this novel sequence, attention turned towards the synthesis of ketone **133**. Installing the oxygen functionality onto the alkene in **17** was essential in this proposed route, and a hydroboration/oxidation process was applied (**Scheme 4.3**). Pleasingly, the desired alcohol **134** was furnished in an excellent yield of 93%.

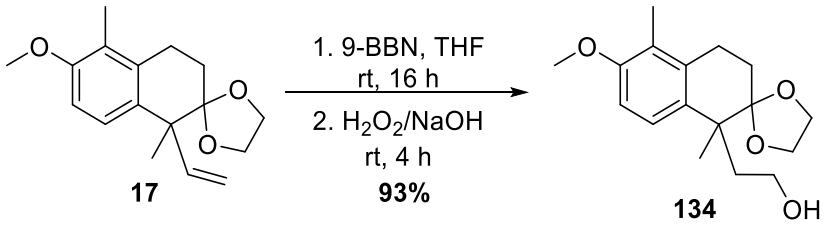

Scheme 4.3

Next, alcohol **134** was protected in preparation for the ensuing selective ketal deprotection later in the synthesis. Accordingly, a range of silyl protecting groups were added onto our alcohol intermediate **134** (**Scheme 4.4, Table 4.1**). Three protected alcohols were generated in high yields, with the synthesis of TBDPS protected alcohol **137** being possible on a large scale in quantitative yield (**Table 4.1, Entry 3**). Constructing of a range of protected intermediates was essential in our selective ketal deprotection study (*vide infra*).

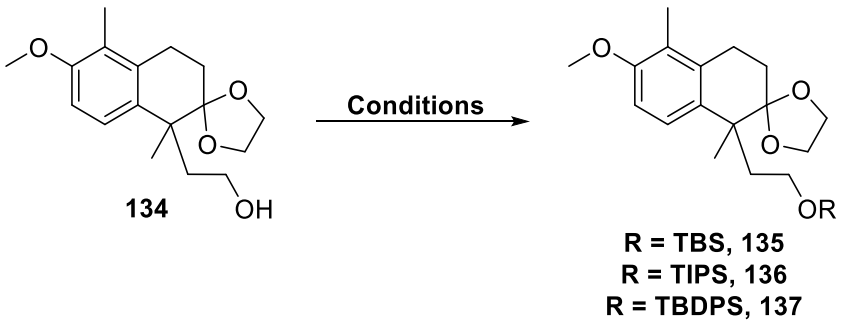

Scheme 4.4

Entry	Conditions	R	Yield (%)
1	TBSCl, imidazole, DCM, 3 h, rt	TBS, **135**	86
2	TIPSCl, imidazole, THF, 3 h, rt	TIPS, **136**	83
3	TBDPSCl, imidazole, THF, 16 h, rt	TBDPS, **137**	Quant.

Table 4.1

Each protected alcohol was then examined, in turn, within the following selective ketal deprotection step. First, TBS protected alcohol **135** was extensively investigated under various ketal deprotection conditions to afford the desired ketone **138** (**Scheme 4.5, Table 4.2**). Initial conditions using the mild acid pyridinium *p*-toluenesulfonate (PPTS) at moderate temperatures disappointingly afforded tricyclic system **139**, where conversions were determined by ^{1}H NMR analysis (**Table 4.2, Entry 1)**. This undesired intermediate was proposed to have formed through the deprotection of both alcohol and ketal moieties present in **135**, forming **140**, whereby the pendant alkyl alcohol in **140** can then attack the embedded cyclohexanone to generate the tricyclic product **139** (**Scheme 4.6**). Surprisingly, performing the PPTS deprotection reaction at room temperature only resulted in the deprotection of the TBS protected alcohol to **134**, leaving the ketal intact (**Entry 2**). Using Lewis acids $CeCl_3 \bullet 7H_2O$ and $Ce(OTf)_3 \bullet 7H_2O$, known within the literature to selectively reduce ketals,[101,102] produced a mixture of products and returned starting material despite a range of reaction times and temperatures being probed (**Entries 3-5**). Examining the results in **Entries 2** and **4** revealed that the TBS protecting group within our molecule is removed preferably over the ketal moiety under mild acidic conditions, contrary to literature reports.[101,102] Methods using I_2[103] were also fruitless, giving only tricyclic product **139** (**Entry 6**). In summary, these results were unexpected, as it is well recognised that ketals can be selectively removed with appropriate conditions when within the presence of other

functinonality. Undeterred, we continued this study with more resistant protecting groups **136** and **137**.

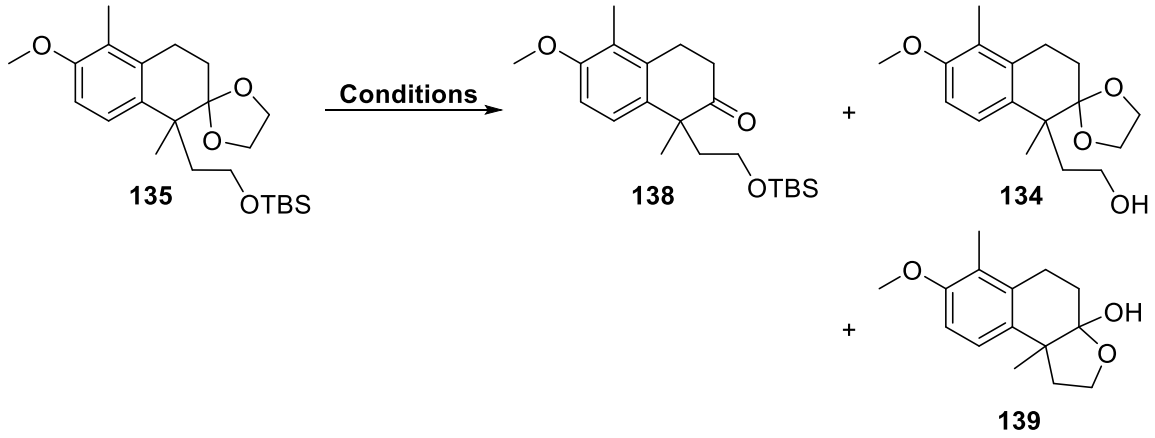

Scheme 4.5

Entry	Conditions	138 (%)[a]	139 (%)[a]	134 (%)[a]	135 (%)[a]
1	PPTS (10 mol%) acetone:H_2O (4:1), 60 °C, 5 h	0	83	0	17
2	PPTS (10 mol%), acetone:H_2O (4:1), rt, 16 h	0	0	>99	0
3	$CeCl_3$•$7H_2O$ (1.5 equiv.), NaI (15 mol%), MeCN, rt, 16 h	0	0	0	>99
4	$CeCl_3$•$7H_2O$ (1.5 equiv.), NaI (15 mol%), MeCN, reflux, 1 h	0	33	33	33
5	$Ce(OTf)_3$•$7H_2O$ (5 mol%) $MeNO_2$, rt, 1 h	0	28	0	72
6	I_2 (10 mol%) acetone, rt, 1 h	0	>99	0	0

[a]conversion determined *via* ^{1}H NMR analysis

Table 4.2

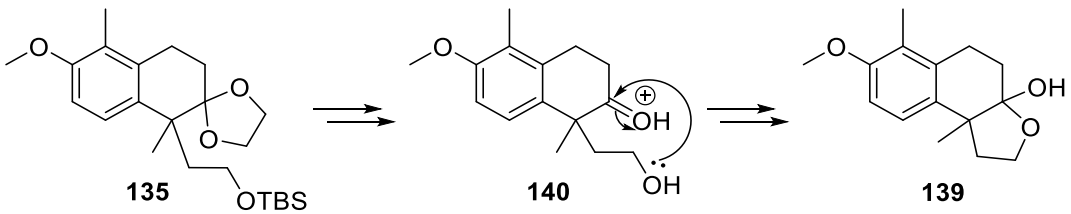

Scheme 4.6

Efforts shifted to the selective deprotection of the ketal within TIPS containing compound **136**. A selected set of conditions were applied, which had previously resulted in the, albeit unselective, deprotection of the ketal above (**Scheme 4.7, Table 4.3**).

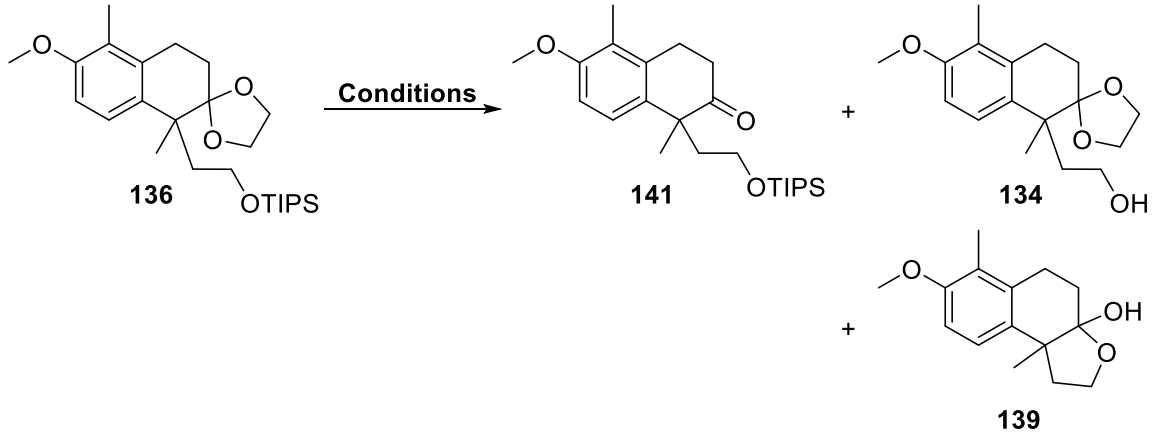

Scheme 4.7

Entry	Conditions	141 (%)[a]	139 (%)[a]	134 (%)[a]	136 (%)[a]
1	PPTS (10 mol%) acetone:H_2O (4:1), 60 °C, 5 h	Undetermined mixture of **134**, **139** and **136**			
2	$Ce(OTf)_3$•$7H_2O$ (5 mol%) $MeNO_2$, reflux, 1 h	0	63	0	37
3	I_2 (10 mol%) acetone, rt, 1 h	0	>99	0	0

[a]conversion determined *via* ^{1}H NMR analysis

Table 4.3

We were disappointed to observe that the bulkier, and robust, TIPS protecting group did not survive the mild acidic conditions employed, and that, again, selective ketal deprotection could not be achieved with varying conditions (**Table 4.3, Entries 1-3**). Again, it was surprising to see that the TIPS protecting group willingly deprotects faster than the removal of the relatively weaker ketal group, with mixtures being obtained with PPTS (**Entry 1**), and tricyclic product **139** being predominantly formed with $Ce(OTf)_3$•$7H_2O$ and I_2 methods (**Entries 2** and **3**).

Determined to develop selective ketal deprotection conditions, which ultimately would allow the installation of the requiste exocyclic alkene component for the PKR, focus moved next to the application of the TBDPS protected alcohol **137** into our study (**Scheme 4.8, Table 4.3**).

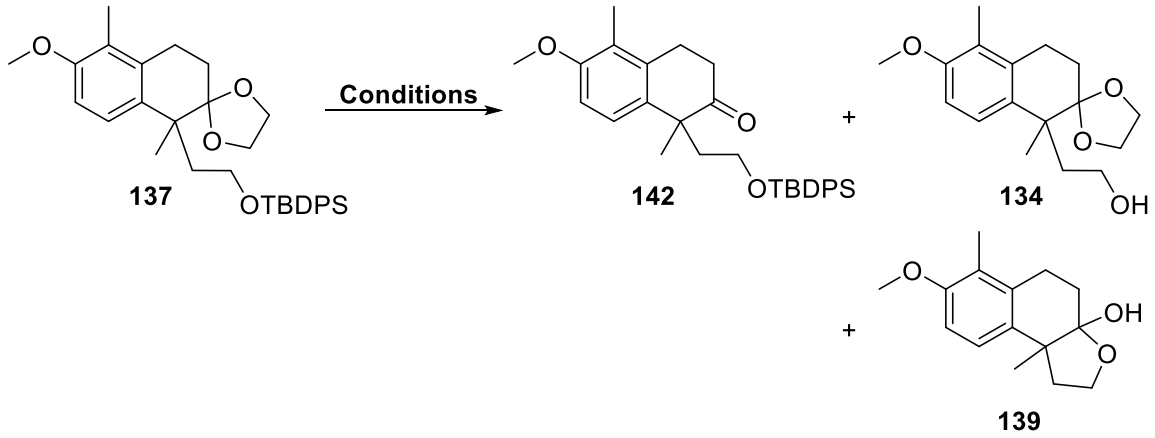

Scheme 4.8

Entry	Conditions	142 (%)[a]	139 (%)[a]	134 (%)[a]	137 (%)[a]
1	PPTS (10 mol%) acetone:H_2O (4:1), 60 °C, 5 h	0	0	0	100
2	$Ce(OTf)_3$•$7H_2O$ (5 mol%) $MeNO_2$, reflux, 1 h	0	0	0	100
3	1 M HCl acetone:H_2O (4:1), 60 °C, 5 h	0	0	0	100
4	I_2 (10 mol%) acetone, rt, 1 h	80	20	0	0
5	I_2 (10 mol%) acetone, rt, 30 min	83	9	0	8
6	I_2 (10 mol%) acetone, 0 °C, 1 h	0	0	0	100

[a]conversion determined *via* ^{1}H NMR analysis

Table 4.4

It was interesting to note that there was no reactivity at either of the TBDPS and ketal protecting groups in **137** during initial attempts using PPTS and $Ce(OTf)_3$•$7H_2O$ (**Table 4.3, Entries 1** and **2**). Utilising stronger acidic conditions with 1 M HCl at elevated temperatures also rendered the starting substrate untouched (**Entry 3**) – it was surprising to observe high resiliency of the ketal under all of these conditions. Pleasingly, using

conditions involving I_2 resulted in a favourable deprotection of the ketal to **142**, with only a small amount of TBDPS removal and subsequent formation of the tricyclic system **139** (**Entries 4** and **5**). Using **137**, we were pleased to see that the ketal moiety was removed far easier than the more resistant TBDPS group, obtaining an 80% conversion towards our desired ketone **142**, and just 20% of the unwanted tricyclic product **139** (**Entry 4**). Performing the deprotection over a shorter reaction time also generated the desired ketone **142** in comparable yields, with small amounts of **139** and starting material **137** obtained. In an attempt to boost selectivity to **142** further, the deprotection was performed at a lower temperature of 0 °C (**Entry 6**), however, no reaction was observed. Overall, we were pleased to have arrived at conditions for selective deprotection of the ketal group within **137**, and we explored further optimisation of this procedure through increasing the quantity of iodine, as well as now fully isolating the desired product (**Scheme 4.9, Table 4.4**).

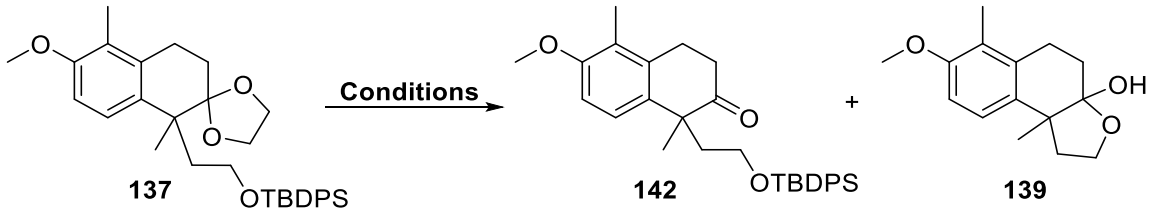

Scheme 4.9

Entry	Conditions	Yield of 142 (%)[a]	Yield of 139 (%)[a]
1	I_2 (10 mol%) acetone, rt, 40 min	81	Trace
2	I_2 (20 mol%) acetone, rt, 20 min	85	Trace

Table 4.4

In relation to the above, excellent isolated yields were achieved using deprotection conditions with I_2 (**Table 4.4**). Performing the reaction with 10 mol% iodine over 40 minutes resulted in an 81% yield of our desired ketone **142** (**Entry 1**), while, to our delight, increasing the catalyst loading of I_2 to 20 mol% (and reducing the reaction time to just 20 minutes) improved the isolated yield further to 85%, (**Entry 2**). In both cases, only trace quantities of the tricyclic product **139** were obtained, highlighting our ability to now selectively remove the ketal moiety through this transformation.

After challenging synthetic endeavours, despite observing facile removal of the TBS and TIPS protecting groups on the alcohol (with the ketal group relatively untouched in some cases), we were pleased to have developed methodology using catalytic amounts of I_2 and TBDPS protected **137**.

Next in this synthetic sequence was the olefination of ketone **142** to prepare alkene **143** *via* a Wittig reaction (**Scheme 4.10**). Employing standard conditions, the desired alkene was isolated in a high 83% yield.

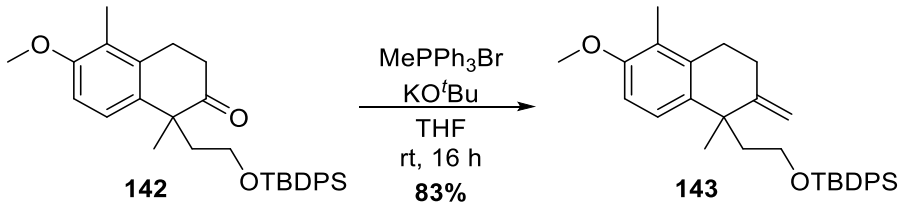

Scheme 4.10

From alkene **143**, the TBDPS silyl protecting group was removed to reveal the alcohol **144** in an excellent yield of 93%, through reaction with tetrabutylammonium fluoride (TBAF) (**Scheme 4.11**). Previously within the group, alcohol **144** has been employed, as a racemic product, for the preparation of PK precursor **95**, therefore this common intermediate could be utilised to complete the current route towards our target enyne.

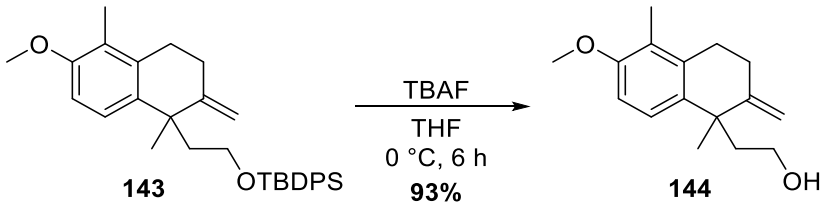

Scheme 4.11

Based on previous methodology, the next crucial transformation involved the appendage of the alkyne onto our intermediate, which would culminate the two key reacting components for the PK reaction.[10] Alkynylation was performed through a capricious

displacement reaction involving alkyl triflate **145** (converted from alcohol **144**, and used without purification) and lithium TMS acetylide **146** (**Scheme 4.12**). Here, the desired TMS protected enyne **132** was furnished in a good yield of 77% across two steps (**Scheme 4.12**). Key to this demanding sequence is using freshly distilled Tf_2O for the formation of alkyl triflate **145**.

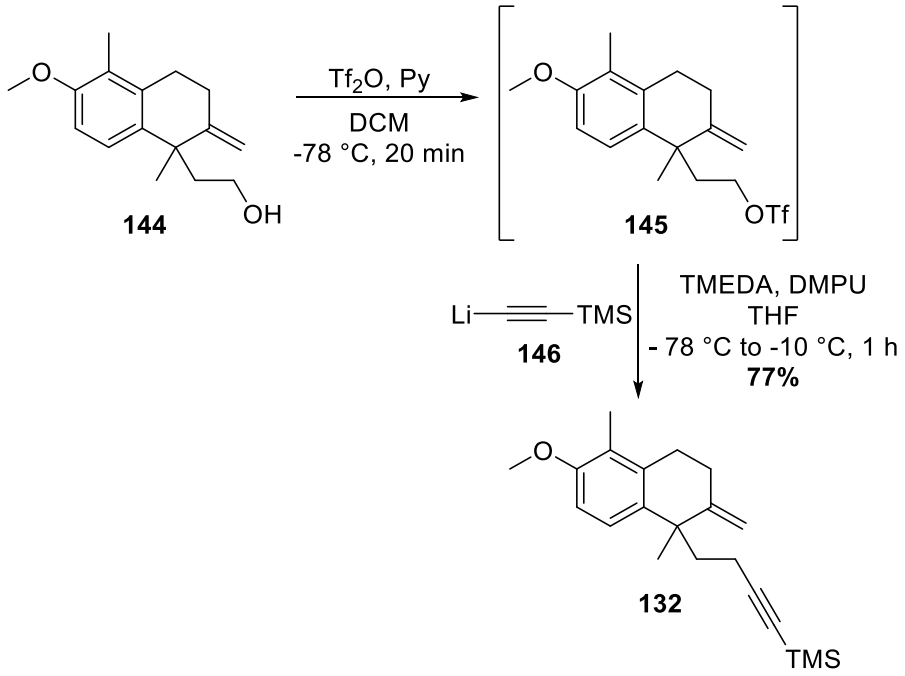

Scheme 4.12

Finally, the desired terminal alkene PK precursor **95** was constructed in exceptional yields over two steps from protected enyne **132** (**Scheme 4.13**). Pleasingly, TMS deprotection afforded alkyne **147** in a 96% yield, then subsequent deprotonation and methylation generated the desired PK precursor **95** in 99% yield.

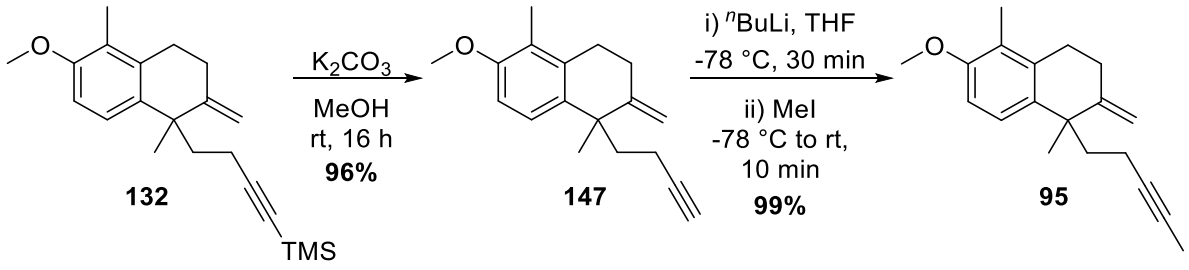

Scheme 4.13

Attempts at devising a more concise synthetic route by employing alternative alkynylation strategies to the target enyne PK precursor **95** were also explored (**Scheme 4.14**). Specifically, we considered alkyl iodide **148** as a potential intermediate where various transformations could be examined.

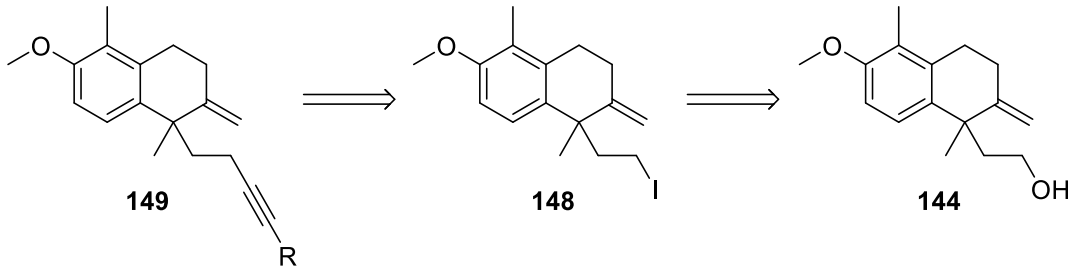

Scheme 4.14

With this new approach in mind, using alcohol **144**, the corresponding alkyl iodide **148** was synthesised in an unoptimised 67% yield under Appel conditions with I_2 (**Scheme 4.15**).

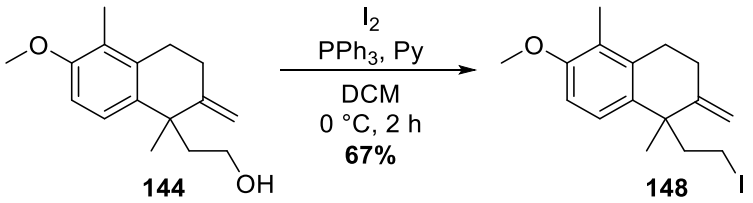

Scheme 4.15

Various alkynylation strategies could now be explored with alkyl iodide **148** in hand. First tested was an sp–sp^3 Kumada type iron cross-coupling reaction[104] of iodide **148** and 1-propynylmagnesium bromide **150**, with bis[2-(*N*,*N*-dimethylamino)ethyl] ether (*o*-TMEDA) as an additive. However, our attempt was unsuccessful, only observing degradation of starting material (**Scheme 4.16**).

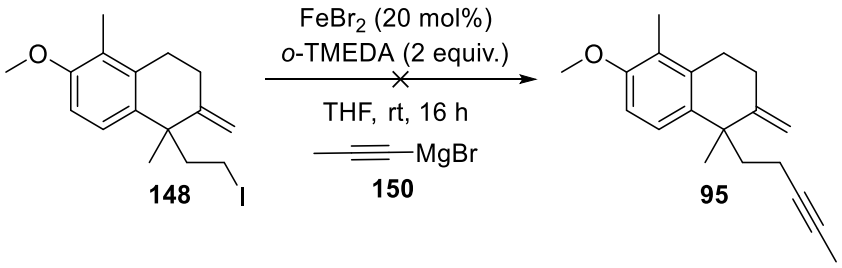

Scheme 4.16

In a similar vein, direct displacement of iodide **148** using 1-propynylmagnesium bromide **150** was also not successful and starting material was returned. (**Scheme 4.17**).

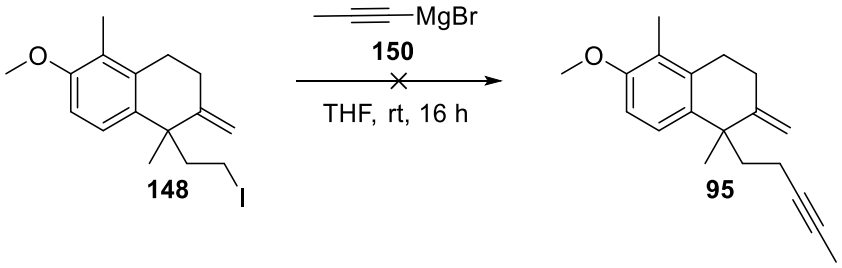

Scheme 4.17

Displacement of **148** using lithium acetylide ethylenediamine complex **151** was pursued,[88] however, this proved ineffective towards the synthesis of **147** and only degradation of starting material was obtained (**Scheme 4.18**).

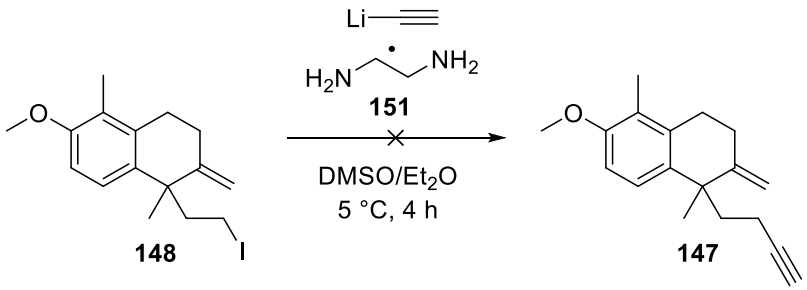

Scheme 4.18

Although attempts to streamline this particular set of transformations were not successful, a solid route has been established towards the desired PK precursor **95**. Overall, and from the newly established Heck product, our desired target was prepared in excellent yields and sufficient quantities for the central intramolecular PK cyclisation, and subsequent transformations towards the synthesis of agariblazeispirol C. However, we were not fully satisfied with the length of the synthetic pathway, and we envisaged that the route towards **95** could be shortened to enable a more efficient synthesis, therefore this was explored next.

4.1.2 Attempts at an Early Stage Alkynylation

An alternative, and novel, synthetic approach to our desired enyne PK precursor **95** was to target a route whereby the alkyne portion of the PK precursor is introduced earlier in the sequence. As highlighted above in our successful route, it was designed such that the formation of the requisite exocyclic alkene component of the PK was prioritised first, and prior to the alkynylation step. On the other hand, designing the synthesis whereby alkynylation proceeds first could present a more concise route towards our desired PK precursor (**Scheme 4.19**). As such, it was conceptualised that alkyne **152** could be generated from intermediate **153** *via* displacement or cross-coupling methodology as before, overall starting from our key Heck product **17**.

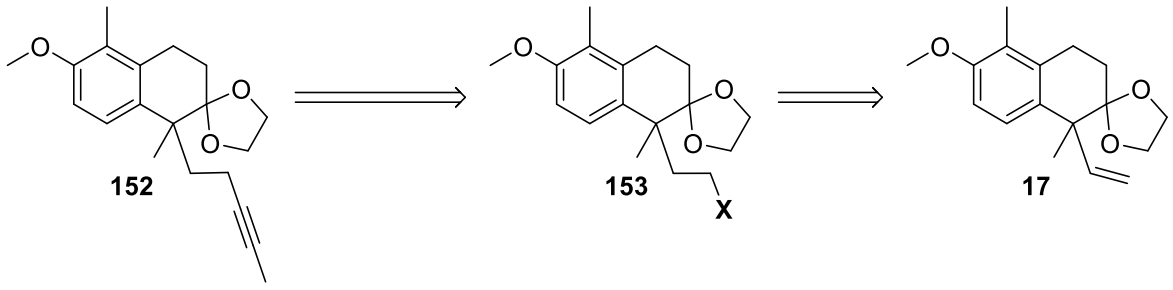

Scheme 4.19

The initial task was to access alkyl iodide **154** directly from **17**, and it was anticipated that hydrozirconation using Schwartz's reagent ($(C_5H_5)_2ZrHCl$), followed by a quench with a source of iodine, would furnish the desired system in one step (**Scheme 4.20**, **Table 4.5**).

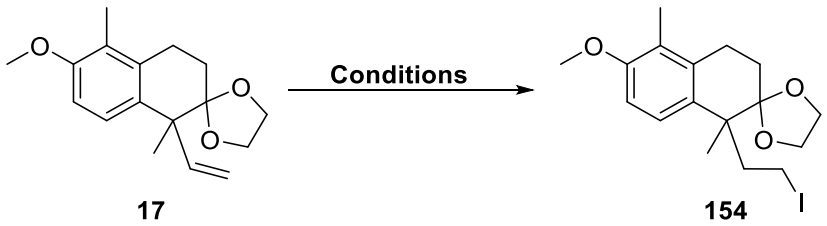

Scheme 4.20

Entry	Conditions	Outcome
1	i) $(C_5H_5)_2ZrHCl$, DCM, 0° C to rt, 2 h; ii) NIS, rt, 1 h	No reaction; return of SM
2	i) $(C_5H_5)_2ZrHCl$, THF, 0° C to 40 °C, 5 h; ii) NIS, rt, 3 h	No reaction; return of SM

Table 4.5

Disappointingly, the conditions applied to alkene **17** did not generate the desired alkyl iodide **154** in our hands (**Table 4.5**, **Entries 1** and **2**). Both mild (**Entry 1**) and harsher (**Entry 2**) conditions using Schwartz's reagent only yielded starting material, with no side-products formed or decomposition observed. This suggested that the initial hydrozirconation of the alkene failed to occur, and that **17** is unreactive to the reaction conditions. Indeed, we realised that this could possibly be attributed to the large ketal group sterically hindering the addition of Schwartz's reagent across the alkene.

Alternatively, previously synthesised alcohol **134** could be used to construct the corresponding alkyl halide. It was thought that bromination of alcohol **134** could afford alkyl bromide **155** using freshly distilled PBr_3 (**Scheme 4.21**). However, no desired product was obtained, and decomposition of the starting material was observed.

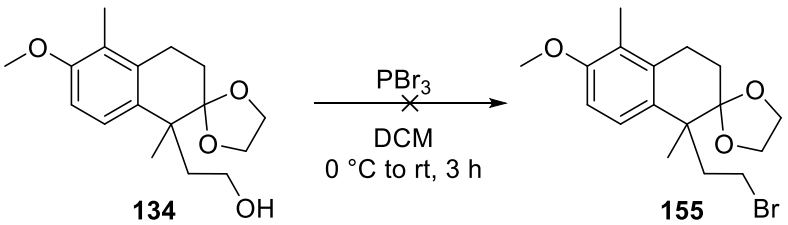

Scheme 4.21

In a similar vein, alcohol **134** was treated with freshly distilled Tf_2O in an attempt to prepare the corresponding alkyl triflate **156** (**Scheme 4.22**), however, again, complete decomposition of the starting material occured.

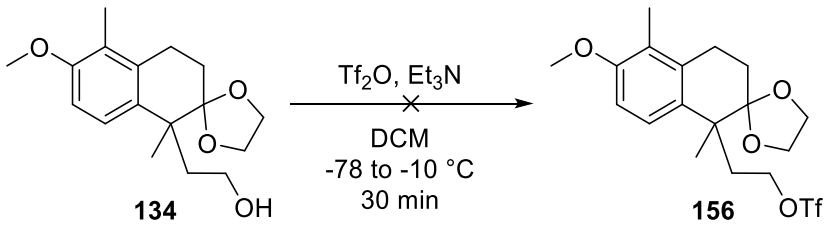

Scheme 4.22

The final tactic employed to furnish the desired alkyl halide was to form alkyl iodide **154** through a mesylation/Finkelstein transformation from **134** (**Scheme 4.23** and **4.24**).[105,106] Initially, a one-pot methodology was conducted to generate the corresponding mesylate intermediate *in situ*, and NaI was subsequently added to convert to the desired alkyl iodide **154** (**Scheme 4.23**). LCMS analysis showed conversion to the mesylate intermediate, however, only a trace quantity of the desired product **154** was produced.

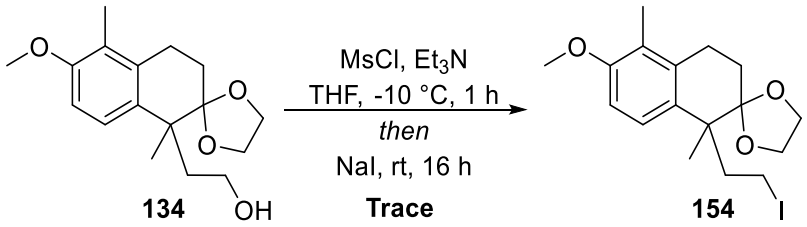

Scheme 4.23

Next, a telescoped method was investigated, which allowed a solvent switch to the more common acetone for the Finkelstein reaction (**Scheme 4.24**). As before, LCMS analysis showed full conversion to the desired mesylate intermediate, however, the Finkelstein conditions resulted in both the formation of the alkyl iodide and deprotection of the ketal to give **157**, with no starting material or mesylate intermediate present.

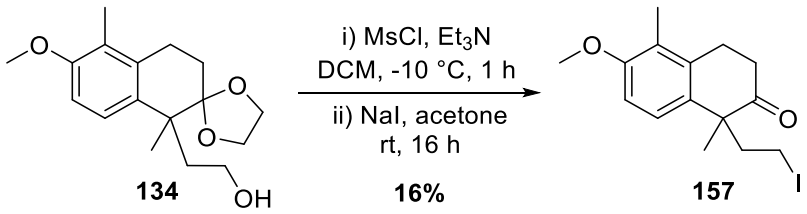

Scheme 4.24

In summary, from the novel Heck product, our target terminal alkene PK precursor **95** was generated in excellent yields through a late-stage carbon homologation strategy, utilising information based on previous work. Hence, large scale synthesis of the enantiomerically pure enyne **95** can be conducted with this work. In terms of a more concise route, at this stage, it was evident that an early stage alkynylation of our Heck product was particularly demanding, and it was decided that efforts should be instead focused on the construction of the diene-yne PK precursor and the key intramolecular PK annulations themselves.

4.2 Synthesis Towards Diene-yne PK Precursor

The next target within our total synthesis programme was the diene-yne PK precursor **96** (**Scheme 4.25**). Despite inherently representing as a particularly challenging PK cyclisation substrate, due to the conjugated diene system, we believed it was beneficial to seek precursor **96** as it directly, and fully, constructs the tetracyclic core of agariblazeispirol C, with no late-stage introduction of the internal olefin within the C ring required. Again, despite previous work into the synthesis of precursor **96** through a racemic route, furnishing **96** from the novel Heck product **17** required the establishment of an entirely new strategy.

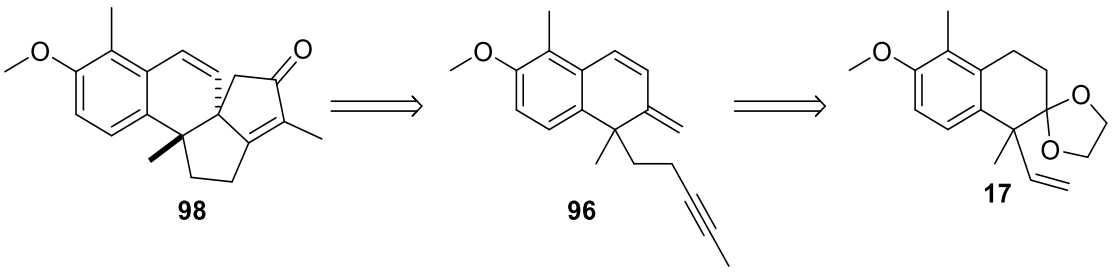

Scheme 4.25

*4.2.1 Attempts at Late-Stage Homologation to Diene-yne PK Precursor **96***

Implementing a similar approach to the construction of enyne PK precursor **95** through late-stage homologation, as demonstrated in the previous section, common intermediate ketone **142** could be employed to synthesise our diene-yne PK precursor **96**. Our desired target **96** could be made from alcohol **158** through alkynylation, which, in turn, can be generated from ketone **142** through an oxidation and olefination approach (**Scheme 4.26**).

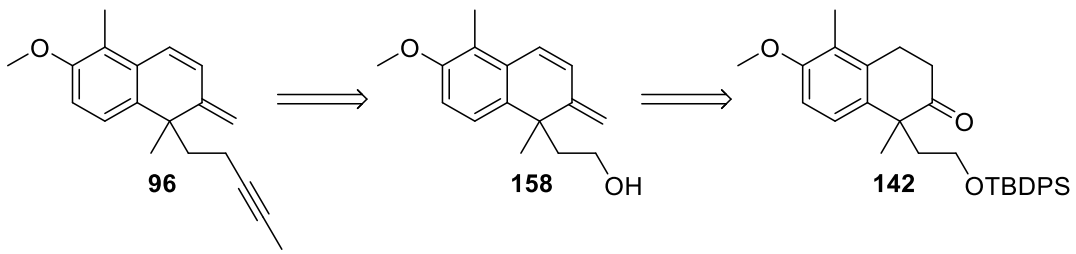

Scheme 4.26

In relation to the above, we proposed to utilise Saegusa oxidation conditions to construct the corresponding enone, from which an olefination procedure could then be performed. As such, the corresponding silyl enol ether **159** was synthesised in an excellent yield of 86% (**Scheme 4.27**).

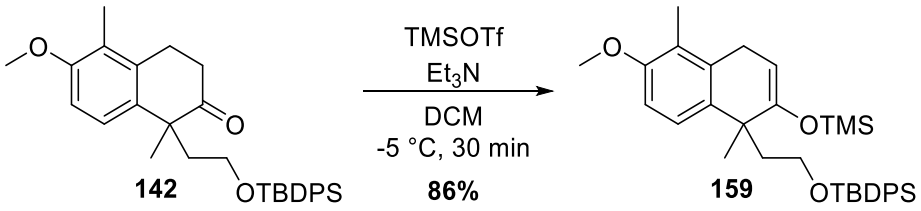

Scheme 4.27

With silyl enol ether **159** in hand, the Saegusa oxidation was conducted to afford our desired enone **160** (**Scheme 4.28, Table 4.6**).

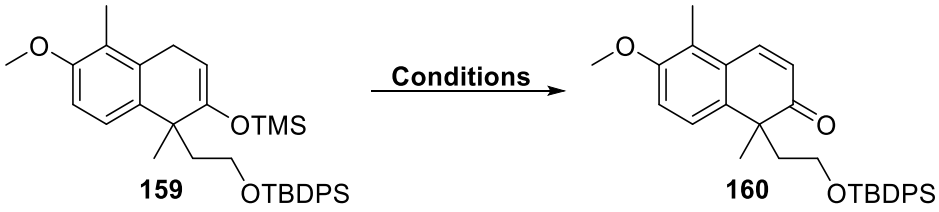

Scheme 4.28

Entry	Conditions	Yield (%)
1	$Pd(OAc)_2$ (1.1 equiv.), MeCN, 40 °C, 16 h	85
2	$Pd(OAc)_2$ (10 mol%), O_2 (1 atm), DMSO, 80 °C, 16 h	34

Table 4.6

Pleasingly, the target enone **160** was furnished in a good 85% yield (**Table 4.6, Entry 1**). As this procedure uses super-stoichiometric amounts of $Pd(OAc)_2$, hence a relatively expensive transformation, we explored the possibility of a catalytic protocol instead (**Entry 2**). Using O_2 within the catalytic variant, we were disheartened that a lower yield of 34% was achieved under these conditions, with no recovery of starting material. In order to further progress our goal towards diene-yne **96**, we decided that super-stoichiometric Saegusa oxidation conditions were acceptable for our synthetic work.

In a similar vein to previous methods towards the terminal alkene PK precursor, alcohol **158** could be constructed following olefination of **160** to **161**, and subsequent deprotection of the TBPDS protecting group (**Scheme 4.29**). Pleasingly, with enone **160**, both the Wittig reaction to install the conjugated diene moiety and the TBAF deprotection to reveal the alcohol generated **158** in exquisite yields across two steps, 93% and 94%, respectively.

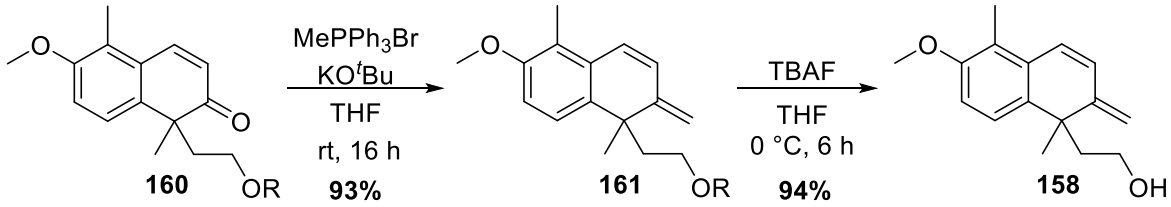

Scheme 4.29

Next, the key alkynylation sequence was investigated to produce our desired, protected, diene-yne **163**. As before, the strategy involved the formation of an alkyl triflate species, **162**, which was then proposed to undergo a displacement reaction with lithium TMS acetylide **146** (**Scheme 4.30, Table 4.7**).

Frustratingly, it was found that this alkynylation sequence was extremely troublesome. It was first noted that alkyl triflate **162** with the conjugated diene moiety was relatively unstable, despite meticulous handling of this intermediate and using freshly distilled reagents and solvents. As soon as the crude mixture of **162** was isolated, it was immediately employed in the displacement step. Unfortunately, the initial attempts using short reaction times, and subsequent warming after the addition of reagents, resulted in complete degradation of triflate **162**, with no identifiable products observed *via* ^{1}H NMR analysis or isolated by silica chromatography (**Table 4.7, Entry 1**). In defiance of this result, lower temperatures were explored in the displacement process, warming to only -10 °C for 1 hour (**Entry 2**). It was found that the alkyl triflate remained present with no formation of product, therefore, the reaction was repeated and left instead for 16 hours at -10 °C, monitored by silica TLC and ^{1}H NMR analysis (**Entry 3)**. Despite these, not insignificant, efforts into investigating this procedure, the desired product **163** could not be obtained. Performing and repeating the reaction multiple times at -10 °C over 16 h showed consumption of the alkyl

triflate **162**, with various related intermediates produced from the reaction inferred on analysis of the ^{1}H NMR spectra. However, no isolable products were obtained after silica column chromatography on any occasion. It was postulated that the protected diene-yne **163** was unstable within a Lewis acidic silica environment, therefore, the crude mixture was purified on alumina, however to no avail (**Entry 4**). Considering that the previous alkynylation transformation with alcohol **144** produced a relatively clean reaction profile when proceeding through its corresponding alkyl triflate derivative (*vide supra*), it was concluded that either TMS protected diene-yne **163** was remarkably unstable, or that alkyl triflate **162** displays undesired reactivity due to the presence of the conjugated diene system.

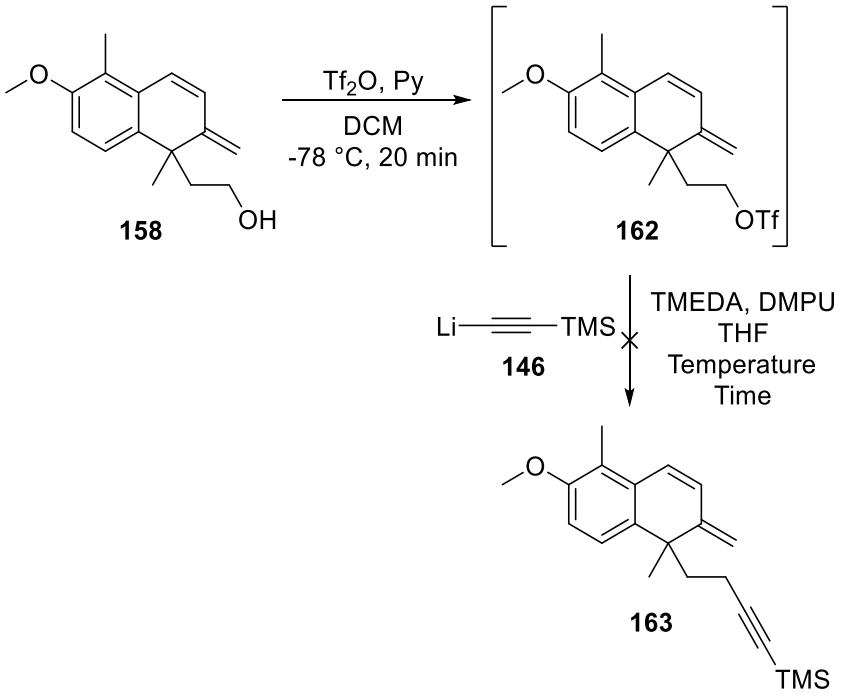

Scheme 4.30

Entry	Temperature (°C)	Time (h)	Outcome
1	-78 °C to rt	1	Consumption of **162**, no products isolated
2	-78 to -10 °C	1	**162** shown by TLC
3	-78 to -10 °C	16	Consumption of **162**, no products isolated
4	-78 to -10 °C	16	Consumption of **162**, no products isolated[a]

[a]purified by alumina chromatography

Table 4.7

With the possibility of TMS protected enyne **163** being unstable, we sought to synthesise the corresponding TIPS protected diene-yne **164** as an alternative intermediate (**Scheme 4.31**). Regrettably, performing the displacement reaction using lithium TIPS acetylide **165** with alkyl triflate **162** did not furnish our desired diene-yne **164**, with no discernable intermediates produced.

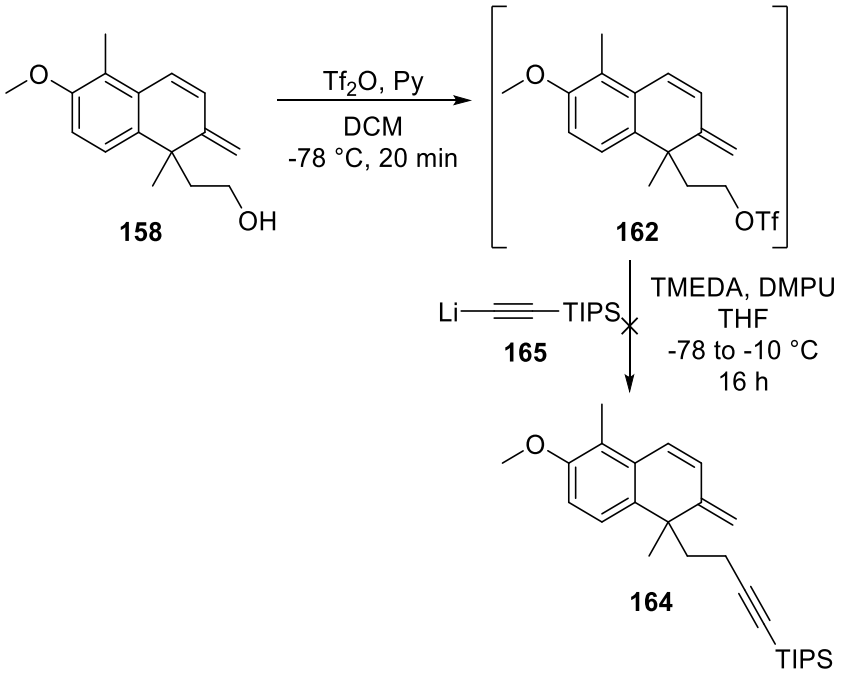

Scheme 4.31

Despite these failures thus far, we wanted to establish whether the alkyl triflate **162** was unstable itself under reaction conditions, preventing the alkynylation reaction from occurring. To this end, we wanted to investigate the reactivity alkyl iodide **166**, which can be synthesised from the iodination of alcohol **158** in a good 80% yield under Appel conditions (**Scheme 4.32**).

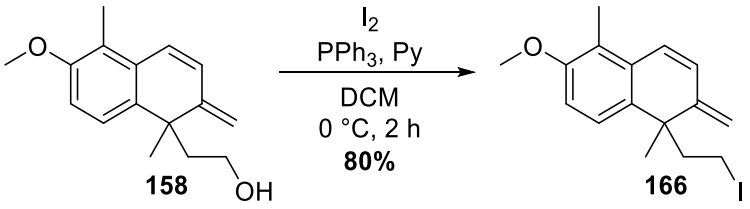

Scheme 4.32

With this in hand, we could explore the displacement conditions as before to generate protected diene-yne **163** with alkyl iodide **166** instead (**Scheme 4.33, Table 4.8**).

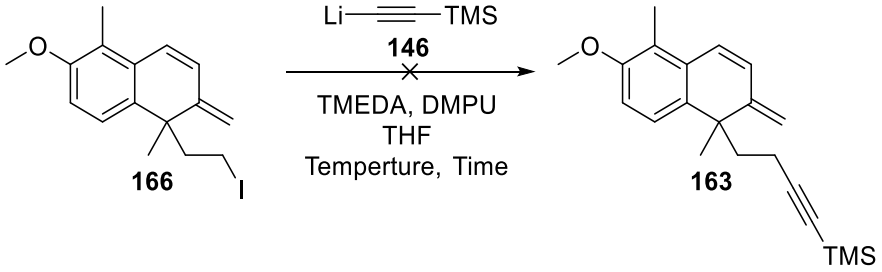

Scheme 4.33

Entry	Temperature (°C)	Time (h)	Outcome
1	-78 °C to rt	16	100% SM returned
2	-78 to 50 °C	5	80% SM returned

Table 4.8

Whilst the desired target **163** was not obtained from this study (**Table 4.8**), it was interesting to note that utilising these conditions with alkyl iodide **166** exhibited different reactivity compared to alkyl triflate **162**. Under initial displacement conditions at room temperature for 16 hours (**Entry 1**), no reactivity was observed and starting material was left unscathed. This was a stark contrast to the result obtained with alkyl triflate **162** (**Table 4.7**), where degradation was observed instead, highlighting the instability of the alkyl triflate under these reaction conditions. Indeed, at a higher temperature of 50 °C (**Entry 2**), which was employed in an attempt to drive the alkynylation process, it was interesting to note again that the starting material was recovered, with little degradation observed. These findings emphasise that the presence, and potential reactivity of the conjugated diene itself, is not the sole reason for the failure of the displacement step with alkyl triflate **162**.

An alternative approach to access TMS protected enyne **163** was to employ a Pd catalysed Kumada cross-coupling reaction,[107] again with lithium TMS acetylide **146** (**Scheme 4.34**). Discouragingly, no desired product was isolated, with degradation of starting material observed.

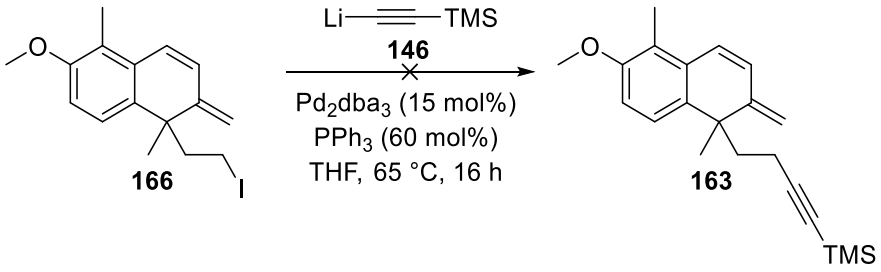

Scheme 4.34

Dismayed with these findings so far and the failure to construct protected diene-yne **163**, we turned to alternative alkynylation procedures to append our alkyne functionality using alkyl iodide **166**. We explored conditions previously tested (yet unsuccessful) in the synthesis towards the enyne PK precursor, however, we were hopeful that the reactivity of the overall system could change with this intermediate.

A direct alkynylation approach to our desired diene-yne PK precursor **96** was undertaken with reaction of alkyl iodide **166** and 1-propynylmagnesium bromide **150** (**Scheme 4.35, Table 4.9**). An attempt at direct displacement of **166** using **150** was unsuccessful (**Entry 1**), with sp–sp^3 Kumada type iron cross-coupling conditions resulting in degradation of starting material (**Entry 2**).

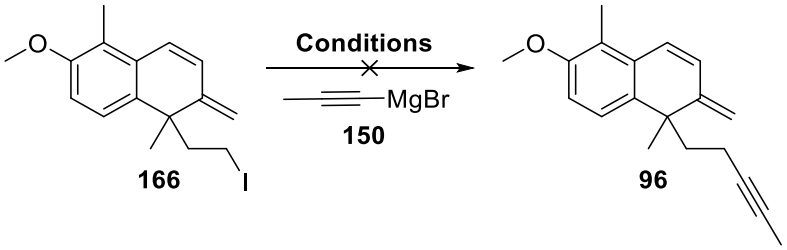

Scheme 4.35

Entry	Conditions	Outcome
1	THF, 0 °C to rt, 16 h	100% SM returned
2	$FeBr_2$ (20 mol%), *o*-TMEDA (2 equiv.), THF, rt, 16 h	0% SM returned

Table 4.9

Furthermore, displacement of alkyl iodide **166** using lithium acetylide ethylenediamine complex **151** was conducted, though, fruitlessly, **167** was not isolated, and only degradation of starting material was observed (**Scheme 4.36**).

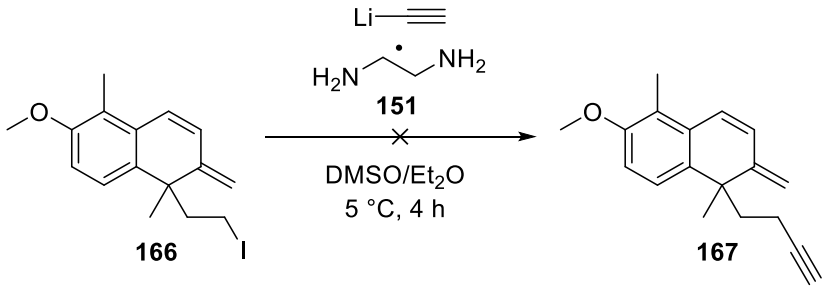

Scheme 4.36

In summary, after comprehensive synthetic endeavours towards the desired diene-yne PK precursor **96** through a late-stage carbon homologation pathway, introduction of the alkyne was immensely problematic. The key alkynylation process of alkyl triflate **162** resulted in only mass deterioration, whereas the corresponding alkyl iodide **166** was unreactive to the methods explored. Henceforth, a new strategy was devised to construct the conjugated diene-yne target.

*4.2.2 Synthesis of Diene-yne Precursor **96** via Early-stage Homologation*

With issues associated with late-stage carbon homologation in our studies thus far (*via* alkynylation on a diene species), we decided to change tact and focus efforts towards an early-stage carbon homologation within our synthetic route towards diene-yne PK precursor **96**. Here, we conceptualised hydroformylation whereby, in a single step, we could potentially reduce the corresponding alkene from within the Heck product and introduce carbonyl functionality, a useful handle for further derivatisation. With this in mind, we proposed that precursor **96** could be prepared from dibromolefin intermediate **168**, through the remainder of the Ramirez-Corey-Fuchs reaction[9] to generate the alkyne, and olefination chemistry to gain the conjugated diene (**Scheme 4.37**). Enone **168** can be generated from oxidation of **169**, where the dibromolefin can be installed from aldehyde **170**. Thus, **170** can be synthesised through our proposed hydroformylation reaction from

62, the product formed ultimately from deprotetion of the ketal moiety in our key Heck product **17**.

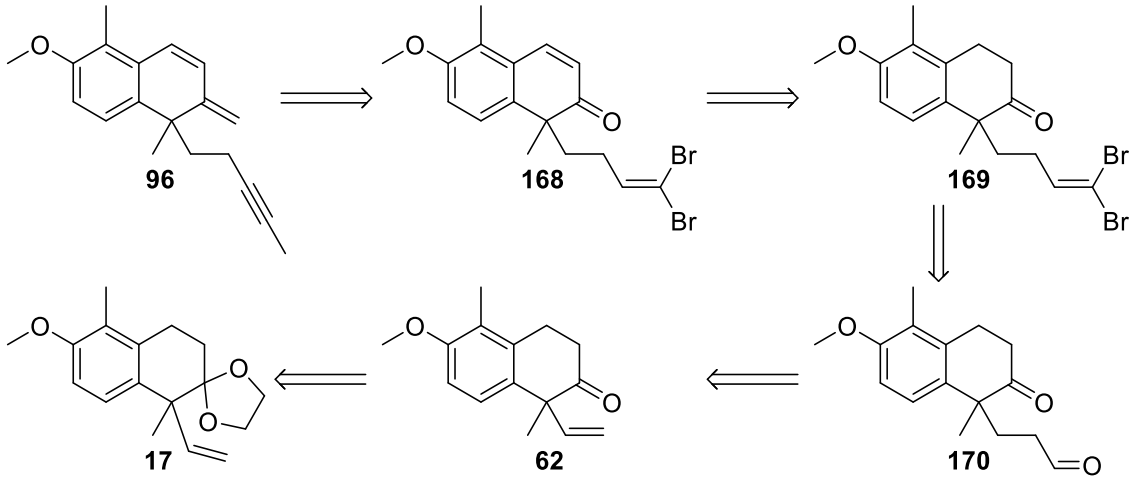

Scheme 4.37

To embark on this synthetic route, the key hydroformylation transformation of **62** to **170** was investigated. First, acid-mediated deprotection of **17** furnished ketone **62** in a quantitative yield (**Scheme 4.38**).

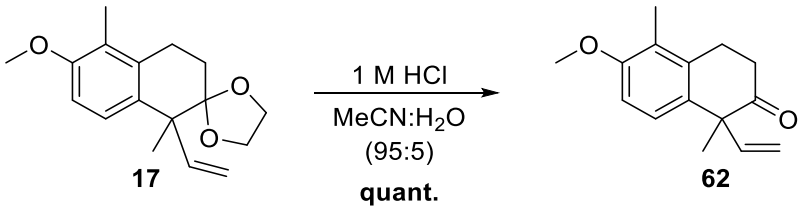

Scheme 4.38

With **62** in hand, and in appreciable quantities, the key hydroformylation procedure was explored. Initially, a syngas-free protocol was targeted, with formaldehyde as the source of CO and H_2, which has been studied by Morimoto *et al.*[108] and shown to exhibit high productivity and regioselectivity. In their optimised procedure, they utilised 1 mol% $[RhCl(COD)]_2$, commercially available BINAP and xantphos as ligands, and formaldehyde as a syngas substitute. Under thermal conditions at 90 °C in PhMe, the hydroformylation reaction of 1-decene **171** was highly regioselective (**Scheme 4.39, Table 4.9**).

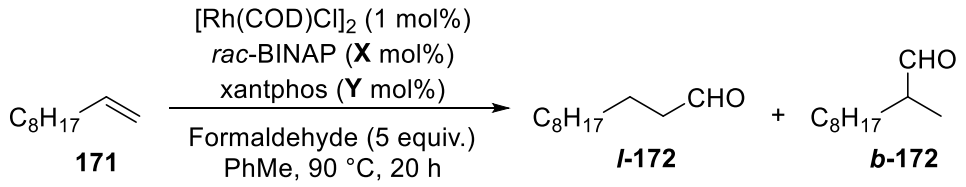

Scheme 4.39

Entry	X (mol%)	Y (mol%)	Overall Conversion (%)	Overall Yield of 172 (%) (*l*-172/*b*-172)
1	2	2	98	80 (97:3)
2	4	0	85	85 (64/36)
3	0	4	77	8 (88/12)

Table 4.10

Employing 2 mol% of each ligand, they were delighted to achieve excellent isolated yields of 80%, predominantly forming the linear aldehyde *l*-**172** in a 97:3 ratio (**Table 4.9, Entry 1**). The application of two ligands was shown to be imperative, with poor regioselectivity obtained when using only BINAP as the ligand (**Entry 2**), and poor isolated yield when xantphos is solely used (**Entry 3**). These results indicated an essential combination of two individual bidentate ligands to achieve high yields and selectivity, as each ligand operates two separate catalytic systems. It is proposed that BINAP controls the decarbonylation process of formaldehyde to generate CO and H_2 gas, and xantphos mediates the hydroformylation catalytic cycle more efficiently with these gases and the corresponding alkene.

With these hydroformylation conditions developed, Taddei *et al.*[109] advanced these conditions further, such that the hydroformylation can be performed using a microwave protocol (**Scheme 4.40**). Here, exceptional yields and regioselectivity towards *l*-**172** were achieved with significantly reduced reaction times of 30 minutes. This highlights that the hydroformylation reaction can be performed rapidly, and with more forcing conditions (under microwave irradiation) if required. From these findings by both Morimoto[108] and Taddei,[109] we looked to apply the developed hydroformylation protocols within our own system for the construction of conjugated diene PK precursor **96**.

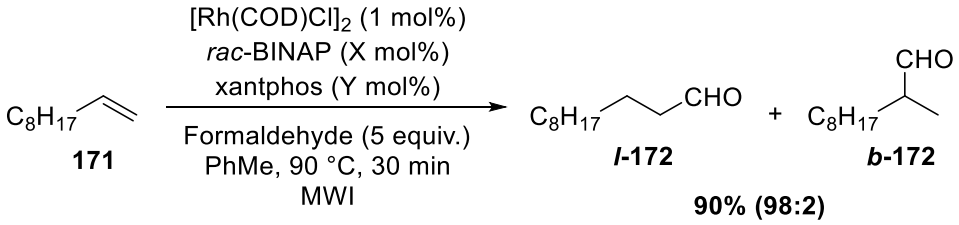

Scheme 4.40

Applying this methodology into our complex system to synthesise aldehyde **170**, it was found that an extensive examination into the hydroformylation transformation was necessary in order to develop a successful procedure (**Scheme 4.41, Table 4.10**).

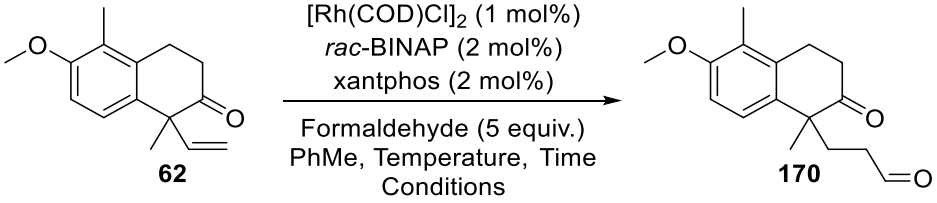

Scheme 4.41

Entry	Conditions	Temperature (°C)	Time (h)	Yield (%)	Recovery of 62 (%)
1	Thermal	90	24	0	76
2	Thermal	110	24	0	71
3	Microwave	90	1	Trace	82
4	Microwave	90	5	Trace	78
5	Microwave	110	5	38	15

Table 4.11

The original protocol reported by Morimoto *et al.*[108] involving thermal conditions at 90 °C was employed into our hydroformylation investigation, however, no reactivity was observed (**Table 4.10, Entry 1**), and increasing the temperature to 110 °C provided no improvment (**Entry 2**). Not discouraged, microwave conditions were explored next, and to our delight, initial (albeit low) conversion to our desired aldehyde **170** was observed at 90 °C for 1 and 5 hours (**Entries 3** and **4**). At the higher temperature of 110 °C, improved conversion towards our desired aldehyde **170** was achieved, with an isolated yield of 38% being obtained (**Entry 5**). We were extremely pleased to have prepared our target aldehyde

with this transformation under microwave conditions, with the linear aldehyde as the sole product from the hydroformylation reaction.

With these promising results, we sought to enhance the overall yield towards aldehyde **170** through the exploration of reaction parameters of the key hydroformylation procedure (**Scheme 4.42, Table 4.11**).

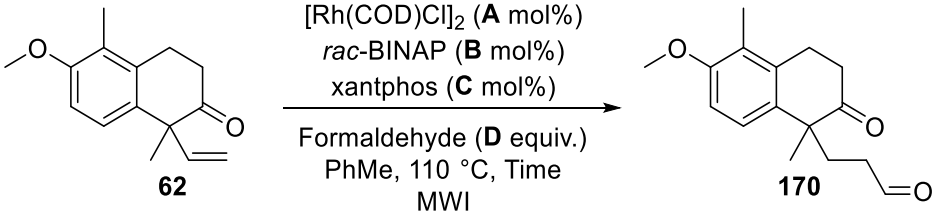

Scheme 4.42

Entry	A	B	C	D	Time (h)	Yield (%)	Recovery of 62 (%)
1	2	4	4	5	5	47	14
2	2	4	4	5	18	0	11
3	2	4	4	10	5	43	17
4	2	4	4	2	5	29	26
5	5	10	10	5	5	60	Trace
6	5	10	0	5	5	Trace	73
7	5	0	10	5	5	Trace	79

Table 4.12

First, the catalyst and ligand loadings were increased to 2 mol% and 4 mol%, respectively, where an improvement in isolated yield of aldehyde **170** was obtained at 47% (**Table 4.11, Entry 1**). Unfortunately, prolonged reaction times of 18 hours resulted in loss of starting material and no isolated product (**Entry 2**). It was thought that aldehyde **170** was degrading when exposed to longer microwave irradiation times. Next, the amount of syngas surrogate formaldehyde used was investigated, where it was found that increasing the equivalents to 10 (**Entry 3**) and decreasing to 2 (**Entry 4**) did not lift the overall yield towards **170**. We were pleased to see when increasing the catalyst and ligand loadings further to 5 mol% and 10 mol%, respectively, we could boost our isolated yield to a good 60% (**Entry 5**). During the investigation, it was also found that reproducible results could be achieved at these loadings compared to at 2 mol% and 4 mol% catalyst and ligand, respectively. The need

for a combination of ligands was justified as highlighted in **Entries 6** and **7**, where only 10 mol% of each sole ligand was employed but did not afford aldehyde **170**, corroborating with the published work of Morimoto *et al*.[108]

In our final attempts to optimise the key hydroformylation transformation, we seeked to lower the reaction temperature to 90 °C to improve reaction efficiency, and investigated the microwave apparatus utilised to potentially enable an automated proceedure (**Scheme 4.43, Table 4.12**).

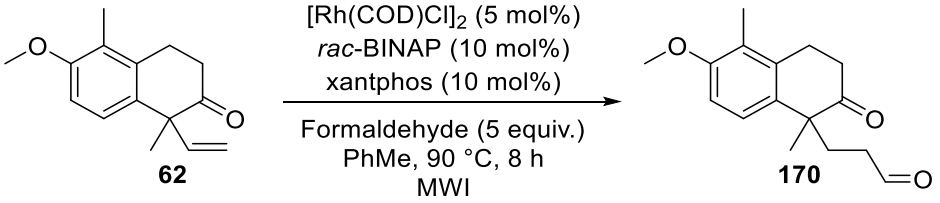

Scheme 4.43

Entry	Scale (mmol)	Microwave Model	Yield (%)	Recovery of 62 (%)
1	0.18	CEM	80	Trace
2	0.18	CEM	65	9
3	0.18	CEM	63	8
4	0.18	Biotage	59	12
5	0.78	Biotage	60	10
6	1.8	Biotage	53	20
7	1.8 (x 6)	Biotage	50	24

Table 4.13

Initially, we were extremely pleased to have accomplished an 80% isolated yield of our desired aldehyde **170** when the hydroformylation was performed at a lower temperature of 90 °C for 8 hours (**Scheme 4.43, Table 4.12, Entry 1**). It was thought that at the higher temperature previously studied (110 °C), degradation of starting materials and product occurred. Despite this early success, it was disheartening to report that achieving this exceptional yield was a rare phenomenon, with reproducible yields sitting only at 65% and 63% (**Entries 2** and **3**). Even though this was disappointing, the desired aldehyde **170** can still be isolated in good yields, which is more than sufficient for our challenging targeted route. Until this point, this methodology suffered from the reaction scale, as, in our hands, we could only perform this procedure on a small scale due to our CEM microwave reactor.

This was not suitable for our natural product synthesis, as large quantities of the aldehyde **170** were required for further synthetic steps. To rectify this, we sought to utilise an automated Biotage system, which would allow us to rapidly perform these hydroformylation reactions, albeit only on a moderately larger scale (1.8 mmol scale). Despite this, having an automated system would enable more efficient access to aldehyde **170**. Applying our conditions into the Biotage microwave, only a minor decrease in yield was achieved (**Entry 4**). As we increased the scale of the reaction, initially, no erosion in isolated yield was observed (**Entry 5**, 0.78 mmol, 60%), however, as we increase the scale to 1.80 mmol, a reduced yield of 53% was obtained (**Entry 6**). In spite of these eroded yields, the Biotage enabled faster production of aldehyde **170** for our synthetic route, as demonstrated in **Entry 7** where multiple reactions were performed sequentially, then pooled together for purification to achieve a 50% yield overall. In all of these cases, the remaining starting material was recovered and re-subjected into the hydroformylation protocol.

In summary, following a broad optimisation process, a synthetically efficient hydroformylation protocol was enabled for the construction towards diene-yne PK precursor **96**, where a synthetically useful handle was furnished for further derivatisation. This hydroformylation process uses relatively cheap, commercially available ligands and formaldehyde as a syngas substitute for a more practical experimental procedure. Despite requiring the use of an automated Biotage microwave system to facilitate large scale production of our target, this is a satisfying outcome for our demanding synthetic route towards PK precursor **96**.

With aldehyde **170** in hand, progression towards the target precursor could now be conducted. It was thought that aldehyde **170** could be transformed into the desired alkyne directly using in-house prepared Ohira-Bestmann reagent **174** (**Scheme 4.44**).[110] Discouragingly, alkyne **173** was not obtained, with no starting material recovered from the process.

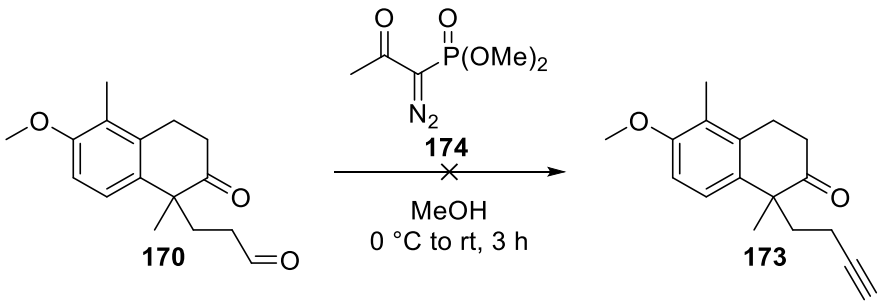

Scheme 4.44

Returning to our proposed synthesis of the targeted PK precursor, we anticipated that performing the Ramirez-Corey-Fuchs sequence would ultimately deliver our alkyne funtionality. Hence, dibromo olefin **169** was synthesised in an excellent yield of 92%, from aldehyde **170** treated with CBr_4 and PPh_3 (**Scheme 4.45**).

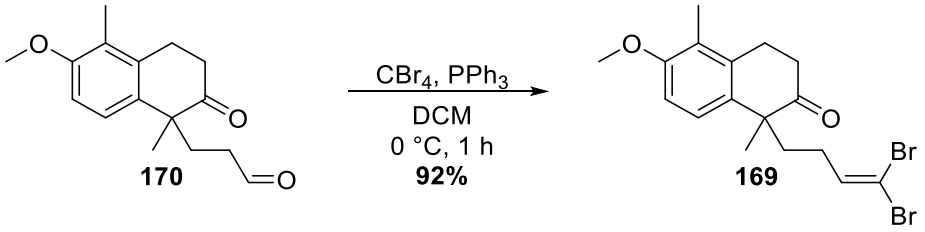

Scheme 4.45

From here, the next step involved the formation of enone **168**, leaving the dibromo olefin moiety intact. Previous work conducted within the group involved enone **168**,[9] therefore it was anticipitated that targetting this common intermediate in this overall route would grant access to our desired diene-yne PK precursor **96**. Proceeding with a familiar strategy as before, the enone could be generated through Saegusa oxidation of **169**. For this sequence, silyl enol ether **175** must be prepared, which is then subjected to Saegusa oxidation conditions (**Scheme 4.46, Table 4.14**). It was found that silyl enol ether **175** was particularly sensitive and, therefore, it was immediately used after purification.

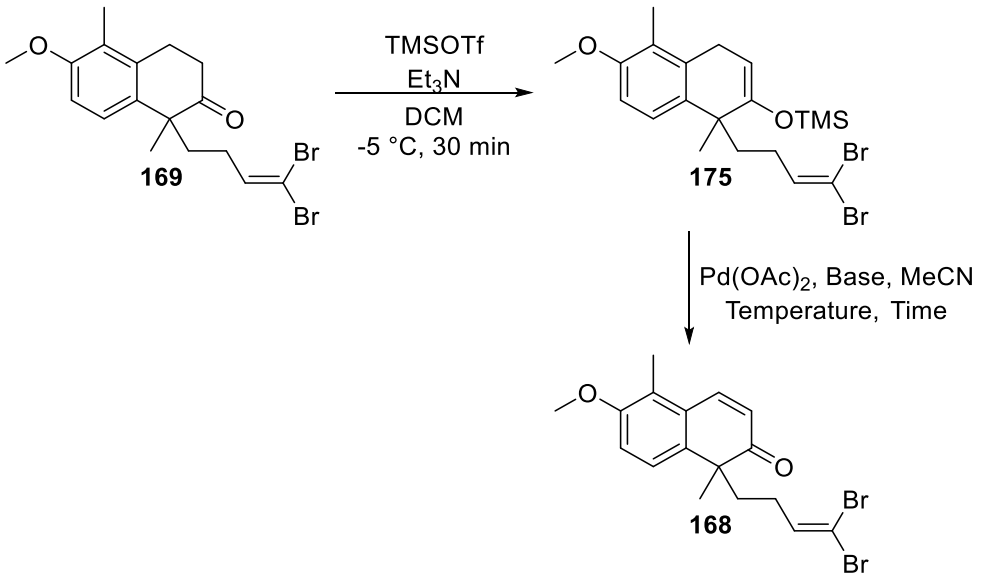

Scheme 4.46

Entry	Base (1.3 equiv.)	Temperature (°C)	Time (h)	Yield over 2 Steps (%)
1	-	40	16	53
2	-	30	16	51
3	-	25	16	47
4	Na_2CO_3	40	16	33
5	Na_2CO_3	40	65	51
6	Na_2CO_3	60	16	27
7	Et_3N	40	16	0

Table 4.14

In our initial attempt at the Saegusa oxidation of silyl enol ether **175**, similar conditions previously employed furnished the desired enone **168** in a 53% yield over 2 steps, which, ultimately, became our optimised conditions (**Table 4.14, Entry 1**). During the study of this oxidation procedure, ketone **169** was often re-isolated, therefore, it was thought that under the reaction conditions, hydrolysis of silyl enol ether **175** was simultaneously occurring. This evaluation corroborates with the sensitive nature of silyl enol ether **175** during its synthesis and isolation. To combat this, the Saegusa oxidation was performed at lower temperatures, however, no improvement in yield was reported (**Entries 2** and **3**). In this Saegusa oxidation, acetic acid is a key by-product, which drives the overall oxidation process. Hence, the accumulation of acetic acid within the reaction medium would aid hydrolysis of the unstable silyl enol ether **175**. To alleviate this potential determinantal effect, bases were added into the reaction mixture (**Entries 4-8**). The addition of Na_2CO_3

into the Saegusa oxidation procedure is known,[111] however, in our hands, no enhancement in the overall transformation was observed (**Entry 4**). Performing the reaction at longer times (**Entry 5**) and higher temperatures (**Entries 6**) did not improve upon the initial yield of 53%. Here, it was interesting to note that the levels of hydrolysis were reduced through both recovery of silyl enol ether **175** and dibromo olefin **169**, but to no advantage for the overall oxidation process. Finally, treating our transformation with Et_3N inhibited the reaction, re-isolating only **175** and **169** (**Entry 7**).

Still not quite content, an attempt to reduce hydrolysis of the silyl enol ether in the Saegusa oxidation was carried out *via* the use of the more stable TES enol ether **176**. Although **176** was isolated in an excellent yield of 83%, no improvement in the subsequent oxidation was observed (**Scheme 4.47**).

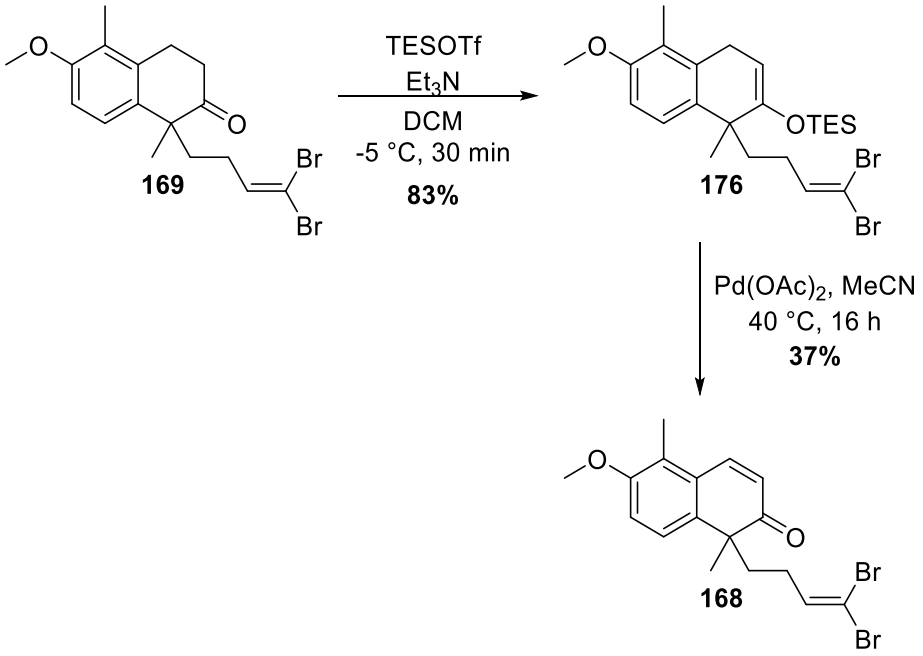

Scheme 4.47

Despite failed efforts to improve this particular Saegusa oxidation protocol through mediation of hydrolysis by the addition of bases, performing the reaction at lower temperatures, or by using the more stable TES intermediate **176**, we could still access enone **168** in a moderate yield of 53% over a 2-step sequence with TMS enol ether **175**.

Alternative oxidation strategies to generate enone **168** were screened as part of the overall investigation. First, direct introduction of the enone could be conducted through the use of lithium *di*-isopropylamide (LDA) and sulfinimidoyl chloride **177** (prepared in two steps, see *experimental section* for full details),[112] however, to no avail (**Scheme 4.48**).

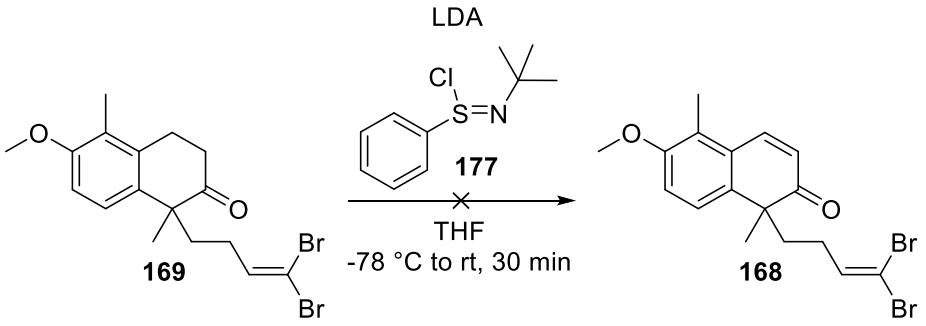

Scheme 4.48

Direct construction of the enone involving copper-catalysed desaturation conditions, recently developed by Dong *et al.*,[113] was also utilised. Here, the desired enone **168** was furnished in a poor 11% yield, with no starting material re-isolated. (**Scheme 4.49**).

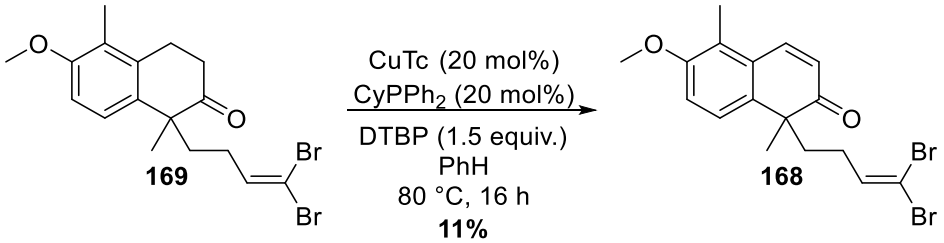

Scheme 4.49

Furthermore, it was envisaged that enone **168** could be generated *via* oxidation and elimination from selenide **178**, however, its initial formation using LDA and PhSeBr was not successful (**Scheme 4.50**).

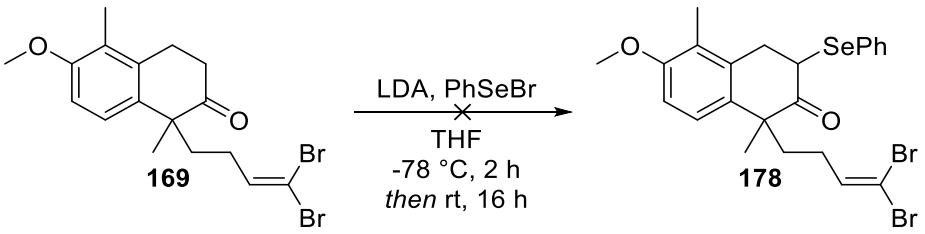

Scheme 4.50

Despite these failures, and with the Saegusa oxidation established with moderate efficiency, it was decided to progress through to the synthesis of the diene-yne PK precursor **96** using previously developed methodology.[9] With enone **168** in hand, **96** can be synthesised through an olefination protocol, forming the conjugated diene moiety. Depending on the olefination conditions used, rearrangement from the remainder of the Ramirez-Corey-Fuchs can also occur, generating various intermediates **179**, **180** and **167**. Regardless, under methylation conditions, all intermediates convert into our desired diene-yne PK precursor **96** (**Scheme 4.51, Table 4.15**).

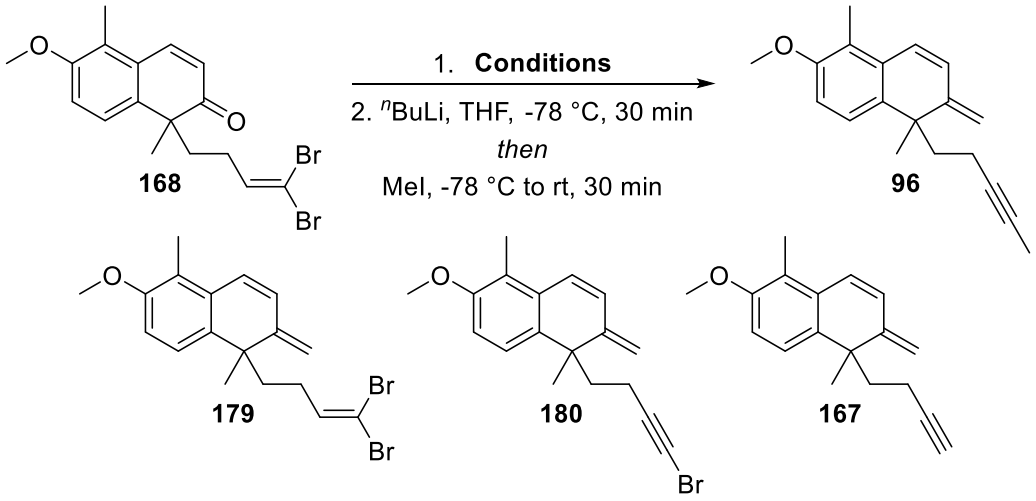

Scheme 4.51

Entry	Conditions (Step 1)	Estimated Ratio and Yield of Step 1 (%)	Yield of 96 over 2 Steps (%)
1	Ph_3PMeBr, KO^{t}Bu (6 equiv.) THF, 0 °C, 2 h	1:1 **179:180** ~52%	37
2	i) Ph_3PMeBr, KO^{t}Bu (3 equiv.), THF, 0 °C, 1 h ii) KO^{t}Bu (3 equiv.), 0 °C, 30 min	19:1 **167:179** ~70%	71

Table 4.15

Initially, it was thought that a large excess amount of KO^{t}Bu as the base could facilitate both the formation of the conjugated diene and perform the rearrangement of the dibromo olefin to the target alkyne (**Entry 1**). Using these conditions, an approximate 1:1 ratio of **179** and bromo alkyne **180** was achieved, in an estimated total yield of 52%. **180** was thought to have been produced *via* an HBr elimination process. Applying this mixture into the methylation step resulted in a low 37% yield overall towards **96**. Interestingly, if the first step is modified such that extra base is added one hour after the initial olefination procedure, **167** can be formed in an approximately 70% yield, with a small amount of **179** present (**Entry 2**). To our delight, implementing this mixture into the methylation protocol furnished the desired conjugated diene PK precursor **96** in a very good 71% over 2 steps.

At this juncture, and following an extensive study towards the synthesis of diene-yne PK precursor **96**, we have refined the synthetic strategy to construct our second key PK precursor. In defiance of all challenges faced within our intended synthetic routes, early-stage carbon homologation *via* hydroformylation was pivotal, and granted a synthetic pathway to construct PK precursor **96** in good yields overall. A concise route of 7 steps from the Heck product was developed, despite involving the introduction of the additional conjugated diene moiety, compared to the longer synthesis (albeit in a higher overall yield) of terminal alkene PK precursor **95**. Additionally, previous research conducted (in the racemic sense) within the group required a longer and more capricious route towards **96**, whereas the robust methodology reported here can be utilised in the synthesis towards the enantiomeric diene-yne **96**.

4.3 PK Cyclisation of Enyne 95

*4.3.1 One-pot PK Cyclisation of Enyne **95***

With a significant amount of enyne PK precursor **95** in hand, the key cobalt-mediated Pauson-Khand annulation could be investigated. In a single process, three new carbon bonds can be generated, forming the two cyclopentyl units in agariblazeispirol C. Additionally, the PKR establishes the second quaternary carbon centre within the natural target's core carbon skeleton. As mentioned before, previous methodology developed within the group involved a two-step PK process,[10] where the corresponding cobalt complex **181** was first generated in a 94% yield (**Scheme 4.52**). Once isolated, **181** was then subjected into the PK cyclisation reaction. Applying DodSMe as the overall promoter for the PKR and heating the reaction to reflux, the desired tetracyclic core **97** was synthesised in an exceptional yield of 86% as a single diastereomer. X-ray analysis of **97** indicated the *anti*-relationship present within the polycyclic network, the stereochemistry we require for the overall natural product synthesis.

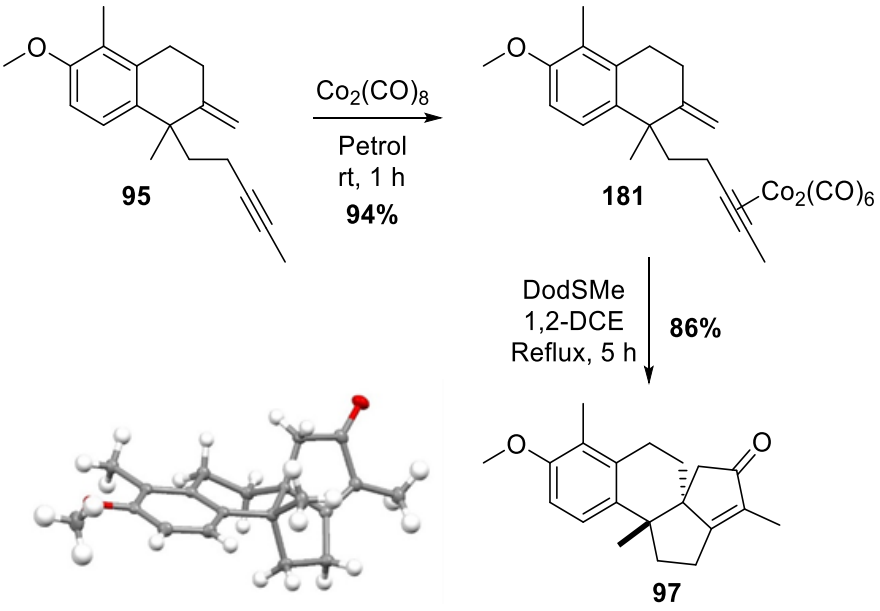

Scheme 4.52

Prominent to this cyclisation protocol is the formation of the second quaternary carbon centre adjacent to the existing one already present in enyne **95** In general, this is a synthetically challenging PKR of an internal alkyne to form a fused ploycyclic system, however, our PKR conditions accommodate this challenge well, producing the desired tetracycle containing the two contiguous quaternary carbon centres in an excellent overall yield. Despite this success, we wanted to further elevate our impressive annulation technique. To improve the efficiency of our PKR of terminal alkene precursor **95**, and thus the overall synthesis towards agariblazeispirol C as part of this programme of work, we aspired to develop a one-pot PK cyclisation process to generate the target tetracyclic core **97**. This would remove the need to isolate cobalt complex **181**, thus reducing a step in our synthesis towards the natural product.

To this end, our goal was to establish conditions for a one-pot process to enhance our overall PKR protocol. In our approach, the initial formation of the requisite cobalt complex took place in our cyclisation solvent, 1,2-DCE (**Scheme 4.53, Table 4.16**). Monitored by TLC, once the cobalt complex was completely formed *in-situ*, the reaction mixture was treated with DodSMe and heated to reflux for 5 hours to furnish our desired tetracyclic core **95**.

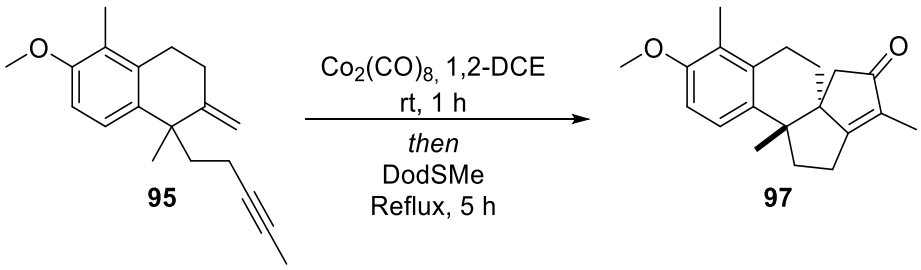

Scheme 4.53

Entry	Scale (mmol)	Yield (%)
1	0.48	77
2	1.6	76

Table 4.16

Delightfully, cyclised PK product **97** was accessed in excellent yields through a one-pot procedure, and as a single diastereomer (**Table 4.16**). This annulation performs well on a larger scale at 76%, obtaining comparable yields with the initial test reaction at 77% (**Entries 1** and **2**). These results highlight the viability of a one-pot PK annulation protocol, eliminating the isolation of the cobalt complex, and reducing the overall number of steps towards the targeted tetracyclic product, overall facilitating a more efficient process. The cyclic system can now be implemented within investigations to complete the natural product synthesis of agariblazeispirol C.

4.4 PK Cyclisation of Diene-yne 96

*4.4.1 Two-step PK Cyclisation of Diene-yne **96***

With synthetic access to diene-yne PK precursor **96** now established, the Pauson-Khand cyclisation could be explored. As described before, the intramolecular PKR in the synthesis towards agariblazeispirol C is a synthetically arduous transformation, as we require the formation of the two 5-membered rings, establishing the second quaternary carbon centre within the congested network. To further add to this complexity, the PKR of precursor **96** is even more cumbersome due to the presence of the conjugated diene moiety. It is known within the literature, with intermolecular examples, that the cobalt-mediated PKR of conjugated dienes are sluggish, due to the lower rate of carbon monoxide insertion in the PK mechanism. In addition to this, there are no examples within the literature of a cobalt-mediated intramolecular PK annulation of conjugated diene systems. Considering all of this, the PKR of diene-yne **96** to directly generate the core of the natural product **98** poses a challenging system to optimise overall.

Previously within our group, the best yield reported for the PKR of **96** involved a two-step process, where the cobalt complex was purified prior to the cyclisation (**Scheme 4.54**).[9] The PK annulation utilised DodSMe as the promoter, requiring a prolonged reaction time of 60 h. Tetracycle **98** was isolated as a single diastereomer, but the exact stereochemistry was not conclusively confirmed – however, analogous to the crystal structure obtained with tetracyclic core **96**, it was thought that the *anti*-arrangement was present. Despite attaining a 61% yield of **98**, it was reported that the protocol was highly capricious, therefore the results were not reproducible. Additionally, a similar one-pot strategy has been investigated using the same solvent and additive, however early attempts were fruitless – yielding only 11% of **98**.[8] Hence, the PK cyclisation of diene-yne **96** must be augmented further for the overall programme of work. To complete the total synthesis of agariblazeispirol C, tetracyclic core **98** must be generated in large quantities to investigate the final step of introducing the oxygenated side-chain. Whilst the previous efforts provided encouraging results, as part of this study, we aimed to deveop a more practically accessible system

capable of providing the quantities needed to complete the total synthesis. This will involve establishing a robust PKR protocol with an overall reduced cyclisation time.

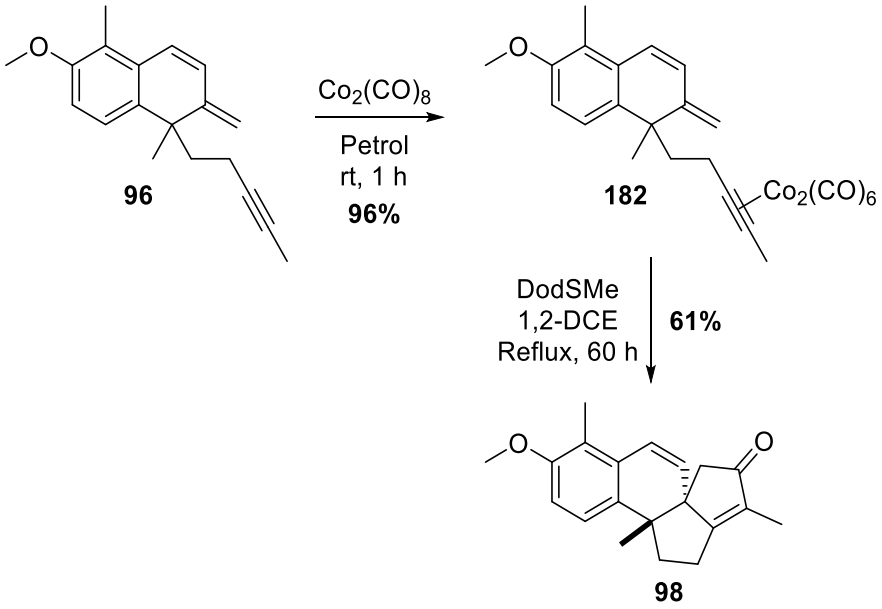

Scheme 4.54

To begin the vital optimisation of the ensuing two-step PKR, first, cobalt complex **182** was generated in an excellent 97% yield for our PKR investigation, providing sufficient quantities for the key PKR transformation (**Scheme 4.55**).

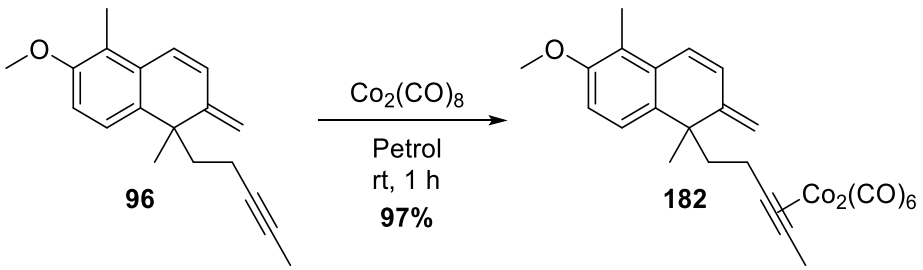

Scheme 4.55

As shown in **Scheme 4.56, Table 4.17**, the initial attempt to prepare tetracyclic core **98** utilised previously reported conditions – this furnished the desired product in a 32% yield, and as a single diastereomer (**Entry 1**). Indeed, this result was unsurprising as the yields

were never reproducible and often decomplexation and degradation occurred due to the prolonged reaction times. Unable to replicate the results previously reported, we sought to optimise this overall procedure to develop a robust, and reliable, protocol. As decomplexation of **182** to precursor **96** was observed by TLC, additional equivalents of $Co_2(CO)_8$ and DodSMe were added at various stages during the course of the reaction. With this modification, only a slight increase in yield to 39% was obtained (**Entry 2**). Undeterred, the reaction temperature was increased in an effort to accelerate the process – in order to do this with 1,2-DCE, the reaction was performed in a sealed tube. Under these conditions, while a slight drop in yield to 27% was obtained, it was pleasing to see that the overall reaction time could be significiantly reduced to 24 h (**Entry 3**). Again, decomplexation was observed through TLC analysis, hence, in an effort to increase conversion, once more, the cyclisation was performed at a longer reaction time of 70 hours, adding additional reagents at certain time points (**Entry 4**). Unfortunately, a further diminished yield of 16% was achieved, suggesting decomposition of cobalt complex **182** or our desired product at these longer reaction times and higher temperatures. Reconsidering the system, PhMe was studied as the solvent medium. At refluxing temperatures, the tetracyclic core was formed in 38% yield (**Entry 5**), comparable to when 1,2-DCE was used (*c.f.* **Entry 2**). Furthermore, the overall reaction time can be reduced to 24 hours with only one extra addition of reagents. Gratifyingly, the reaction time was shortened further to 16 hours to achieve the same yield (**Entry 6**). Elevating the temperature further to 130 °C, by performing the reaction in a sealed tube, resulted in a slightly reduced yield of 31% towards core **98** (**Entry 7**).

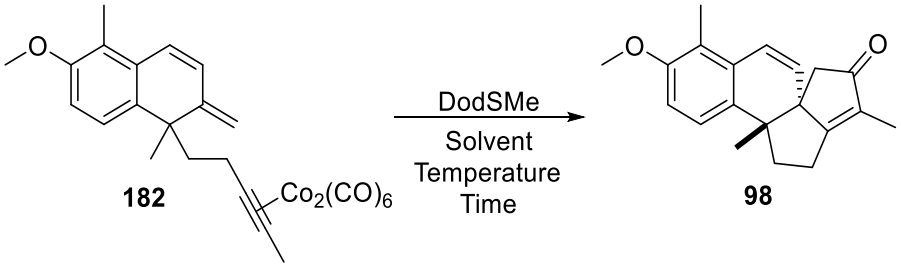

Scheme 4.56

Entry	Solvent	Temperature (°C)	Time (h)	Yield (%)	Comment
1	1,2-DCE	Reflux	60	32	-
2	1,2-DCE	Reflux	70	39	Added an additional equiv. Co and DodSMe at 16 h *then* at 40 h
3	1,2-DCE	100	24	27	Sealed tube
4	1,2-DCE	100	70	16	Sealed tube, added an additional equiv. Co and DodSMe at 16 h *then* at 40 h
5	PhMe	Reflux	24	38	Added an additional equiv. Co and DodSMe at 16 h
6	PhMe	Reflux	10	38	Added an additional equiv. Co and DodSMe at 5 h
7	PhMe	130	10	31	Sealed tube, added an additional equiv. Co and DodSMe at 5 h

Table 4.17

At this moment, we were content to have developed a more time efficient and robust procedure for the construction of core **98**, achieving a moderate yield of 38% in only 10 hours for a remarkably demanding PKR. This surpasses previous methodology reported within the group, which required extremely long reaction times and was overall irreproducible.

*4.4.2 One-pot PK Cyclisation of Diene-yne **96***

At this stage, we revisited the one-pot PKR methodology as it was highlighted that changing the solvent could provide enhanced reactivity, as emphasised with PhMe in our two-step process. Additionally, this would reduce the overall number of steps towards the natural product by one. Henceforth, the effect of solvent in the one-pot process was examined, where previously an 11% isolated yield of **98** was achieved in this annulation process. In this study, we reviewed the solvent effects of PhMe and xylenes (**Scheme 4.57, Table 4.18**).

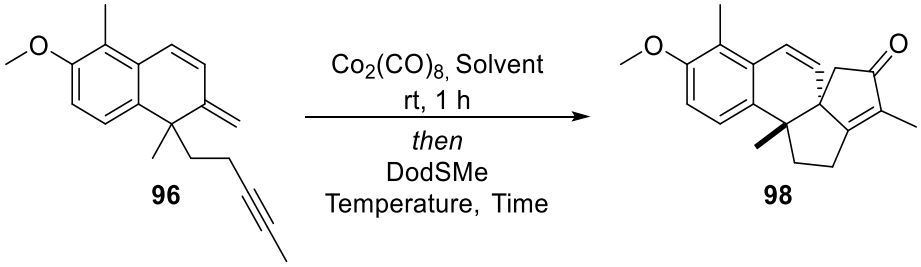

Scheme 4.57

Entry	Solvent	Temperature (°C)	Time (h)	Yield (%)	Comment
1	PhMe	Reflux	10	45	Added an additional equiv. of Co and DodSMe after 4 h
2	PhMe	130	8	50	Sealed tube, added an additional equiv. of Co and DodSMe after 4 h
3	Xylenes	160	6	38	Sealed tube, added an additional equiv. of Co and DodSMe after 3 h

Table 4.18

We were extremely pleased to have improved the overall reactivity and isolated yield towards tetracycle **98** to an appreciable yield of 45% in just 10 hours through a one-pot PK cyclisation using PhMe as the solvent (**Table 4.18, Entry 1**). Indeed, the product was again isolated as a single diastereomer. TLC analysis during the process exhibited decomplexation of the *in-situ* formed cobalt complex to **96**, therefore, after 4 hours reaction time, further equivalents of $Co_2(CO)_8$ and DodSMe were added to re-instate the required cobalt complex. Delightfully, performing the same annulation in a sealed vessel, thus allowing an increase in the overall reaction temperature, enhanced the yield further to a good 50%, where the reaction time was only 8 hours (**Entry 2**). We sought to further elevate the temperature of the transformation by utilising xylenes as the reaction medium (**Entry 3**), however, a diminished yield of 38% was obtained. From this study, we were pleased to have generated core **98** in a rapid one-pot fashion, using PhMe as the solvent.

Final optimisations to further boost the efficiency of our developed one-pot PKR involved investigating the amounts of $Co_2(CO)_8$ and sulfide promoter DodSMe used within the transformation. In the reactions described above, 1.2 equivalents of $Co_2(CO)_8$ and 3.5 equivalents of DodSMe were used in our protocol, with the need for supplementary additions of these reagents to increase the overall yield of our PKR. Hence, we wanted to

remove this necessity through increasing the initial equivalents used in the annulation process (**Scheme 4.58, Table 4.19**).

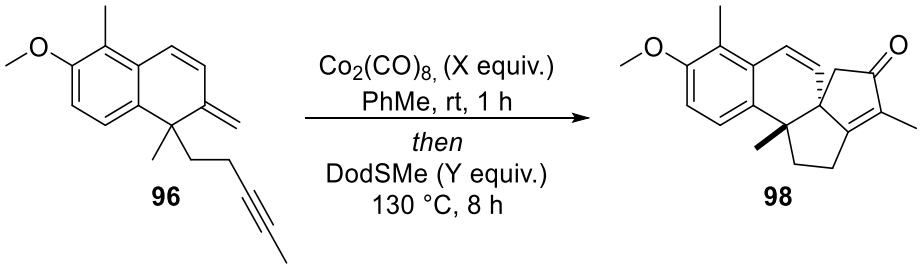

Scheme 4.58

Entry	X	Y	Yield (%)
1	2.2	3.5	36
2	1.2	6	23

Table 4.19

First, as it was shown through reaction monitoring that decomplexation of the *in-situ* formed cobalt complex to **182** occurred readily in the process, the amount of $Co_2(CO)_8$ initially used was explored. Thus, 2.2 equivalents of $Co_2(CO)_8$ was employed in the reaction, however, a decrease in yield towards core **98** was observed (**Table 4.19**, **Entry 1**). With these conditions, neither starting material **96** or its corresponding cobalt complex were re-isolated. Unfortunately, applying 6 equivalents of the sulfide promoter DodSMe also showed an erosion in yield towards the desired product **98**, again, with no starting material or cobalt complex isolated at the end of the reaction (**Entry 2**).

In defiance of all adversities faced during the development of this challenging intramolecular Pauson-Khand cyclisation, we established a robust one-pot protocol where the desired tetracyclic core of agariblazeispirol C can be formed directly in modest yields, and at faster reaction times than previously reported within the group. We are extremely pleased with our PK transformation, as this demanding cyclisation involves the formation of three new carbon bonds in a single process from an enyne embedded with a conjugated diene moiety, constructing two five-membered rings and the second quaternary carbon centre within the congested core.

*4.4.3 X-ray Analysis of Tetracyclic Core **98***

As noted above, a single diastereomer is furnished from our developed intramolecular PKR of precursor **98**. However, up until this point, the stereochemistry had not been confirmed with absolute certainty. Pleasingly, during these investigations, crystallisation through slow diffusion with petrol resulted in the formation of yellow crystals, and X-ray analysis could be conducted. This is shown in **Figure 4.2**, where the *anti*-arrangement within the core is highlighted – the methyl group C10 on the quaternary carbon centre C9 sits *trans* to the C4–C11 backbone of the C-ring. Thus, from this PKR, our desired stereochemistry is generated for our natural product synthesis of agariblazeispirol C.

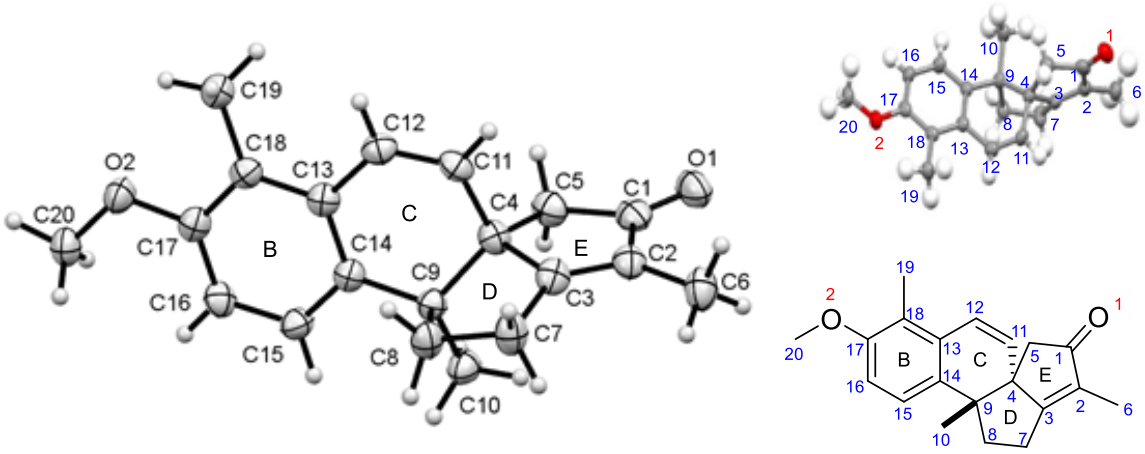

Figure 4.1

4.5 Summary

As illustrated in this chapter, numerous synthetic strategies were embarked upon to synthesise our two distinct Pauson-Khand precursors, which, in turn, were explored within a demanding annulation procedure. Despite facing many synthetically challenging endeavours, we were pleased to have established synthetic routes to generate the tetracyclic core required within the synthesis of agariblazeispirol C.

First, the enyne PK precursor **95** was generated in an excellent 40% yield over 9 steps from Heck product **17** (**Scheme 4.59**). This strategy involved the key optimisation of a selective ketal deprotection protocol of **134** to **142**, and a capricious alkynylation of alcohol **144**. Further chemical transformations delivered the desired PK precursor **95**.

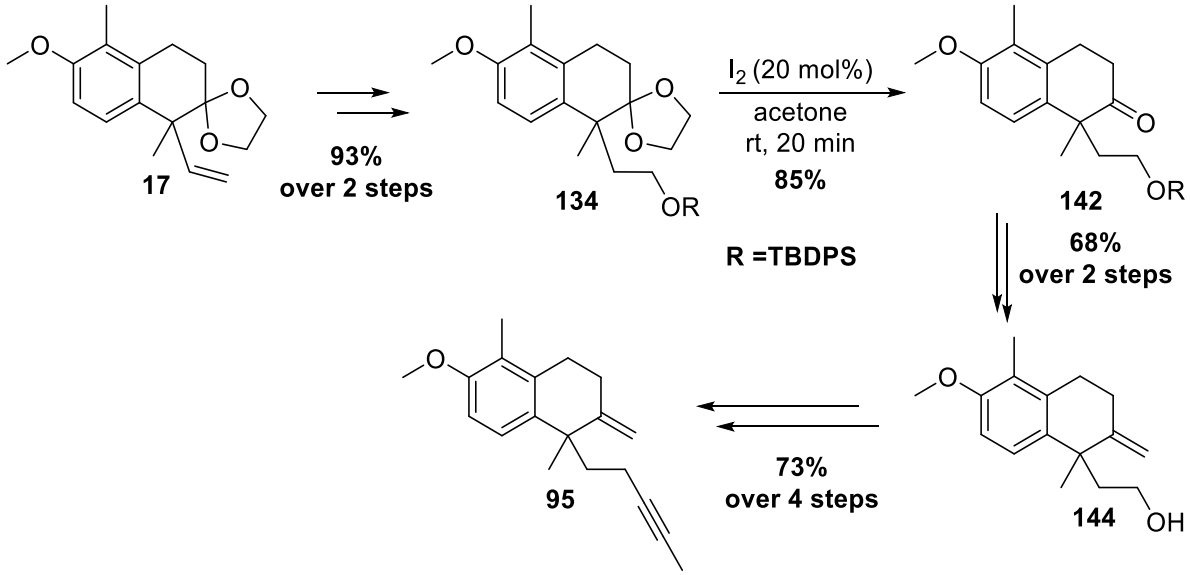

Scheme 4.59

An entirely different approach was optimised fully to construct the diene-yne PK precursor **96** (**Scheme 4.60**). Here, an imperative rhodium-catalysed hydroformylation reaction under microwave irradiation was examined thoroughly to provide aldehyde **170**. Olefination and rearrangement of the dibromo olefin in **168** furnished the desired PK precursor in a 22% yield over 7 steps. In theory, this synthetic pathway could also be implemented to generate enyne PK precursor **95** in a more efficient manner.

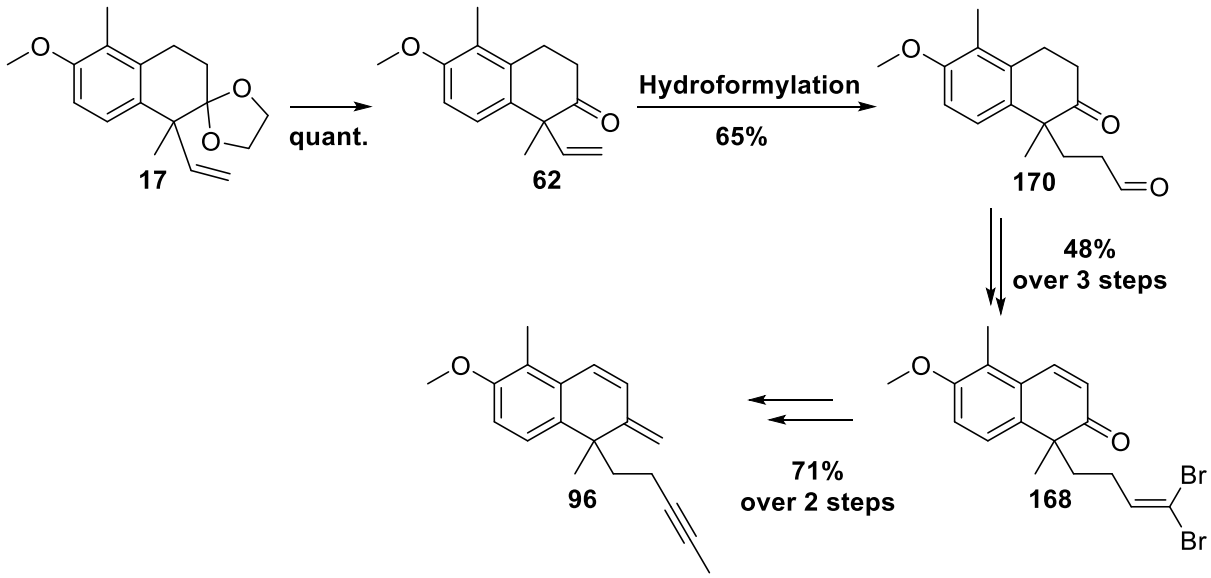

Scheme 4.60

With each PKR precursor in hand, these were examined for the construction of the core of the natural product. Initial investigations with enyne PK precursor **95** resulted in the development of a one-pot PK annulation technique, generating the desired tetracycle **97** in a 77% overall as one single diastereomer (**Scheme 4.61**).

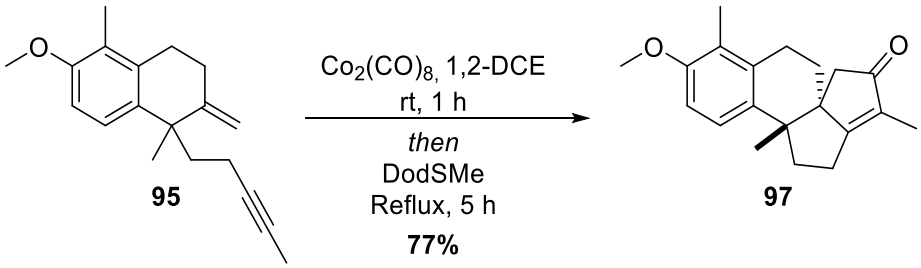

Scheme 4.61

Optimisation of the PKR with diene-yne precursor **96** was more troublesome, where initial investigations first focused on a two-step annulation process, isolating the corresponding cobalt complex (**Scheme 4.62**). It was found that after modifying the experimental procedure to include supplementary additions of reagents, and performing the reaction in PhMe for 10 h, the desired core **98** was generated in a moderate 38% yield. Indeed, this reaction time is notable given that previous attempts required up to 60 h.

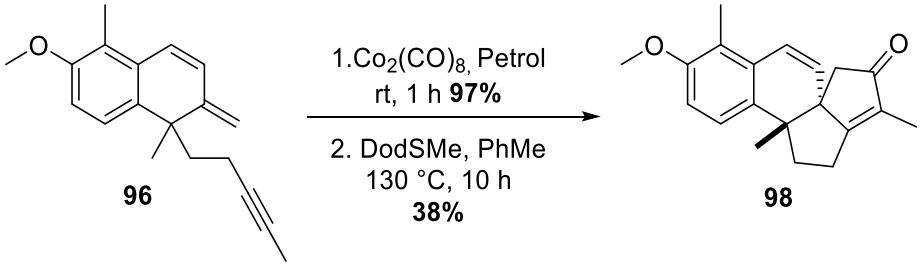

Scheme 4.62

Further improvements were made when developing a robust one-pot protocol (**Scheme 4.63**). We were delighted to have obtained a much improved 50% yield towards tetracyclic core **98** after just 8 hours reaction time. As exemplified by the crystal structure obtained, the single diastereomer produced from the PKR contains the desired *anti*-arrangement within our desired core.

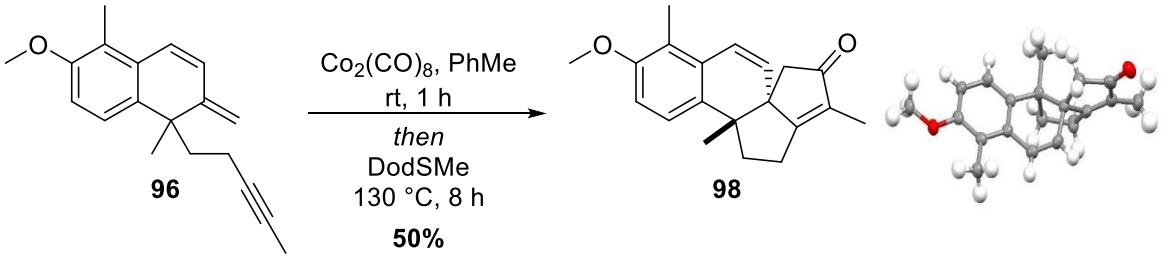

Scheme 4.63

Thus, overall, we were extremely pleased to showcase the Pauson-Khand reaction's capabilities within complex molecule synthesis. Indeed, the formation of the congested tetracyclic core, containing two contiguous chiral quaternary carbon centres, now allowed final efforts to be focused on the completion of the natural target agariblazeispirol C.

Chapter 5

Towards the Completion of Agariblazeispirol C

5. Towards the Completion of Agariblazeispirol C

Having achieved the generation of both polycyclic networks **97** and **98**, despite encountering synthetically challenging obstacles during our overall total synthesis campaign, the final steps towards the completion of agariblazeispirol C could now be explored.

5.1 Late-Stage Benzylic Oxidation of Tetracycle 97

5.1.1 Attempts at Direct Oxidation to Introduce Unsaturation

To manipulate tetracyclic system **97** into our natural product, late-stage benzylic oxidation must be achieved to produce our target core **98**, where the olefin is introduced into the polycyclic carboskeleton (**Scheme 5.1**).

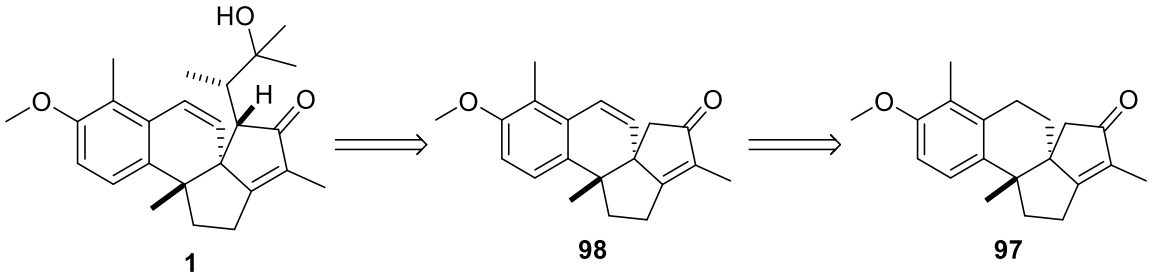

Scheme 5.1

Preliminary investigations into direct late-stage benzylic oxidation from **97** to **98** have been previously performed.[10] These initial attempts displayed encouraging results, where an *in-situ* bromination and elimination approach was utilised with **97**. In this sequence, benzyl bromide **183** could be formed initially with *N*-bromosuccinimide (NBS), which can then undergo the elimination process to **98** after the addition of base DBU (**Scheme 5.2**). Disparagingly, early findings reported poor mass recovery and an inseparable mixture of product **98** and starting material **97**.

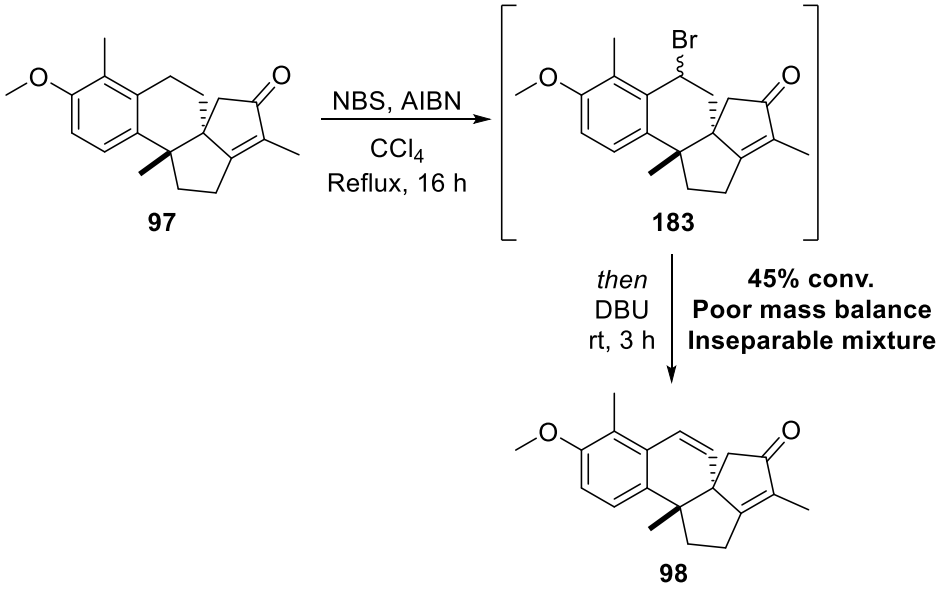

Scheme 5.2

In this thesis, we wanted to examine this transformation further, as it was thought that by isolating and purifying the bromide intermediate **183** prior to the elimination step, this could, ultimately, provide us with tetracycle **98** as a single, pure product. Hence, the intial benzylic bromination of **97** was first probed in our desired sequence (**Scheme 5.3, Table 5.1**).

The initial examination utilised NBS and dibenzoyl peroxide as the radical initiator in the benzylic bromination procedure (**Table 5.1, Entries 1-4**). Disappointingly, in all cases, the bromide intermediate **183** formed could not be purified and separated from the complex mixture, which was analysed by ^{1}H NMR. From these techniques, analysis was difficult, and ratios of starting material **97**, bromide **183** and oxidised product **98** could not be reported with accuracy. Frustratingly, elimination of bromide **183** to **98** proceeded under the bromination conditions used, complicating the overall process. Efforts to achieve full consumption of **97** were fruitless, where increasing the reaction time (**Entry 2**) and amounts of reagents used (**Entries 3** and **4**) always returned starting material.

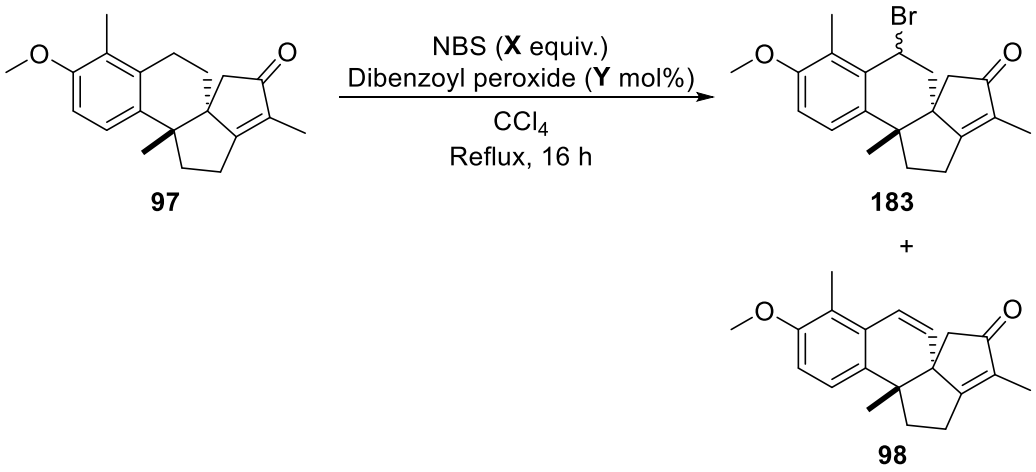

Scheme 5.3

Entry	X	Y	Time (h)	Outcome
1	5	1	5	Mixture of **183**, **98** and **97**
2	5	1	16	Mixture of **183**, **98** and **97**
3	10	1	5	Mixture of **183**, **98** and **97**
4	5	2	5	Mixture of **183**, **98** and **97**

Table 5.1

Undeterred from the failure to purify and isolate bromide **183** as a single compound, it was decided that the purified mixture from the bromination step could be subjected into the elimination procedure. Impurities from the first step in the corresponding one-pot approach could affect the subsequent elimination reaction and result in mass degradation previously observed. If successful, it was thought that **97** and **98** could be separated through chromatography with silver nitrate.[114] Indeed, elimination using DBU as the base was next investigated, however to no avail. (**Scheme 5.4**). In this sequence, the initial mixture of **183**, **97** and **98** produced from the bromination step was purified, as before, and subjected immediately into the elimination conditions. Dispairingly, substantial mass degradation was reported, only recovering trace quantities of desired tetracyclic core **98** containing impurities.

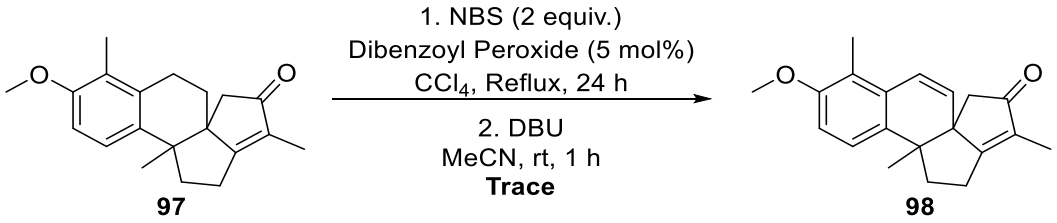

Scheme 5.4

As things stand, direct late-stage oxidation to afford our desired core of the natural product has been difficult thus far. However, simultaneous to these experiments, an alternative strategy was investigated which involved the preparation of a benzylic ketone derivative, which, in turn, could be reduced into tetracycle **97**.

5.1.2 Attempts at Benzylic Oxidation to Install Carbonyl Functionality

An approach anticpitated to generate core **98** from **97** involved the formation of the ketone functionality through benzylic oxidation strategies. It was proposed that ketone **99** could be utilised in a Shaprio reaction, or participate in a sequence involving reduction to the alcohol and subsequent elimination to introduce unsaturation to the core (**Scheme 5.5**). A short screen of various oxidants has been studied to achieve the desired benzylic oxidation, however, these preliminary attempts were ineffective.[10]

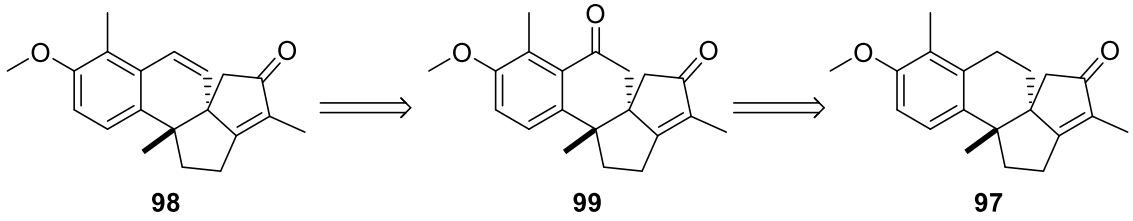

Scheme 5.5

Regardless, selective benzylic oxidation is an attractive transformation to synthetic chemists, with additional literature procedures emerging for such a transformation in recent years.[115–118] Accordingly, these were utilised in our study to selectively generate ketone **98**. First attempted was methodology developed by Moriyama and Togo,[117] where they utilised

KBr and oxidant Oxone® (**Scheme 5.6, Table 5.2**). Here, they proposed the overall mechanism involves the initial formation of a bromo radical between KBr and Oxone®, generating the subsequent benzyl radical from the reacting substrate through hydrogen abstraction. This forms the desired ketone through a one-electron oxidation with Oxone®.

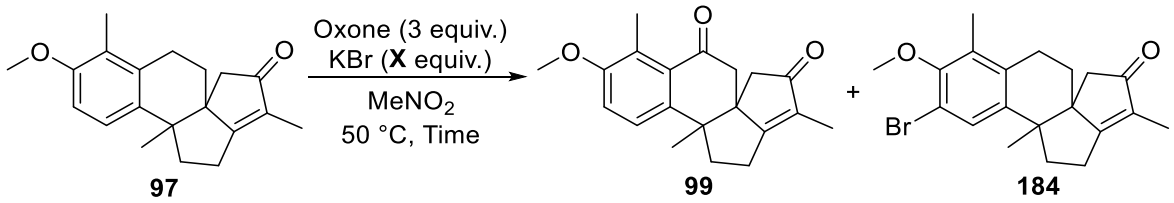

Scheme 5.6

Entry	X	Time (h)	Outcome
1	0.5	24	Inseparable mixture of **97** and **184**, 40% conversion
2	2.5	24	Decomposition
3	1.1	70	Decomposition

Table 5.2

Disappointingly, applying these benzylic oxidation conditions into our system did not furnish desired ketone **99** (**Table 5.2**). Instead, bromination of the aromatic ring *ortho* to the methoxy substituent occurred, generating a 40% conversion to **184** as an inseparable mixture (**Entry 1**). Efforts to achieve both bromination and benzylic oxidation was explored by increasing the equivalents of KBr used, however, only decomposition was observed (**Entry 2**). Performing the reaction at a longer reaction time of 70 h with 1.1 equiv. of KBr was also fruitless (**Entry 3**).

Next, a selective copper-catalysed benzylic oxidation protocol, developed by Tanaka *et al.*[119] was applied to tetracycle **97** (**Scheme 5.7**). This protocol presented as a rather mild set of reaction conditions, using open air as the oxidant in the presence of *tert*-butyl hydroperoxide (TBHP). Frustratingly, this procedure resulted in a reaction profile containing many intermediates and poor mass balance. ^{1}H NMR and LCMS analysis indicated the presence of starting material and an intermediate containing an aldehyde

signal, potentially revealing that benzylic oxidation at the methyl position of the aromatic ring had occurred to generate **185**.

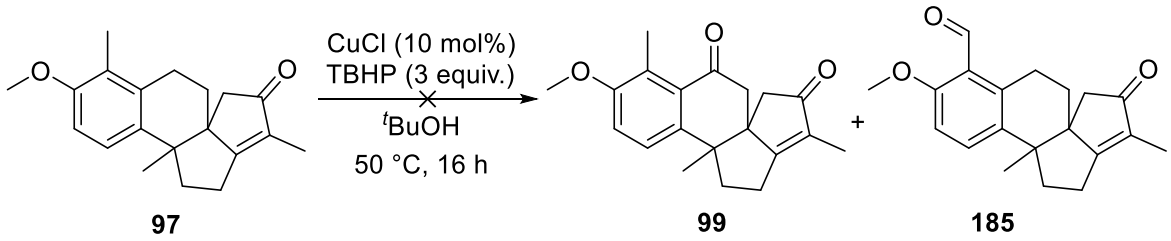

Scheme 5.7

With regards to selective benzylic oxidation of tetracycle **97**, despite many efforts conducted in the group, as shown here and in previous work, we could not overcome the issues associated with late-stage oxidation. At this stage, it was decided our focus should be devoted towards the installation of the oxygenated side-chain, completing the synthesis of the final natural product using core **98**.

5.2 Late-Stage Alkylation to Complete Agariblazeispirol C

*5.2.1 Alkylation Attempts with Epoxide **186***

The final challenge to synthesise our natural product, agariblazeispirol C **1**, involved the addition of the oxygenated side-chain onto our complex tetracyclic core **98**, at the carbon α to the enone (**Scheme 5.8**). Originally, we envisaged an alkylation procedure with various electrophiles would allow the construction of the side-chain. More specifically, direct attachment of the oxygenated chain could be achieved using epoxide **(*R*)-186** as our electrophile.

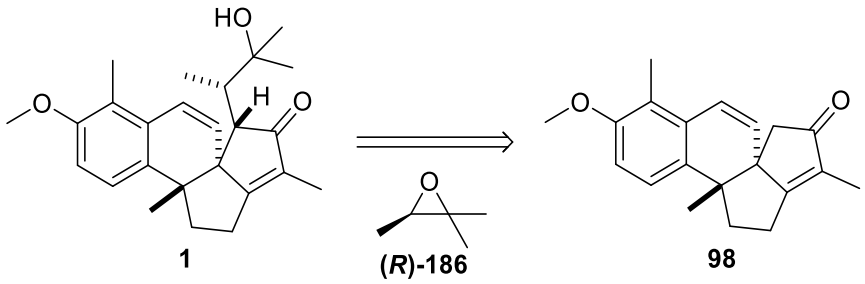

Scheme 5.8

At this time, only a small quantity of core **98** had been acquired from the challenging optimisation of the PK cyclisation. However, during our studies, tetracyclic core **97** was accumulated in large amounts, henceforth, we explored our key alkylation procedure using **97** to establish our synthetic protocol. The initial experiment conducted involved the direct generation of the corresponding enolate of **97**, and reaction with commercially available racemic epoxide **186** (**Scheme 5.9**). Regrettably, alkylated core **187** could not be produced and the starting material was left unreacted.

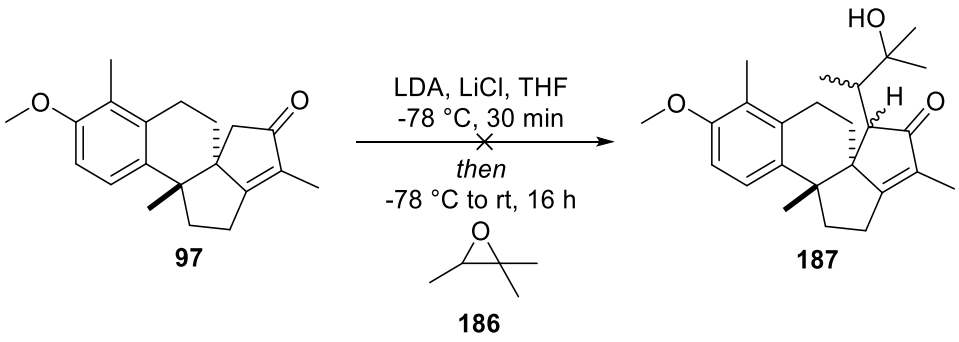

Scheme 5.9

To ensure tetracyclic core **97** was not a complication in the alkylation procedure, our desired core **98** was implemented within this transformation but no reactivity was observed towards our target natural product (**Scheme 5.10**).

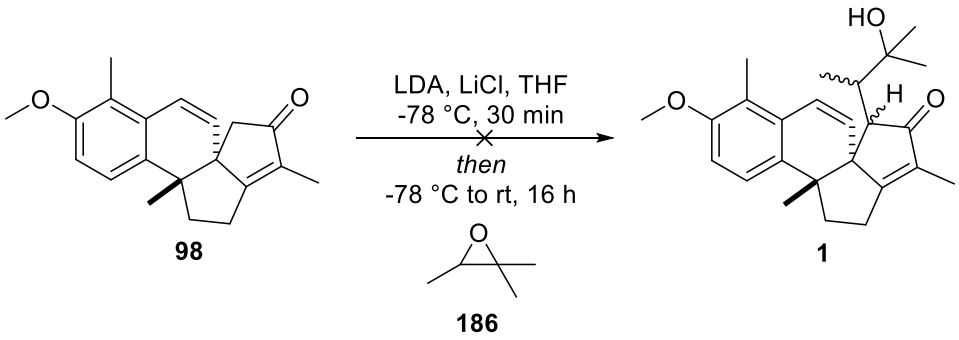

Scheme 5.10

To address the failed attempts with this alkylation procedure, we questioned whether the lithium enolate species of **97** or **98** was actually being formed with the reaction using LDA. Probing this, we performed the initial lithium enolate formation of **97** and subsequently quenched with D_2O (**Scheme 5.11**). This experiment highlighted no incorporation of deuterium at the carbon α to the enone, **d-97**, concluding that the lithium enolate was not being generated under our reaction conditions. Thus, an alternative method to furnish our lithium enolate species needed to be investigated.

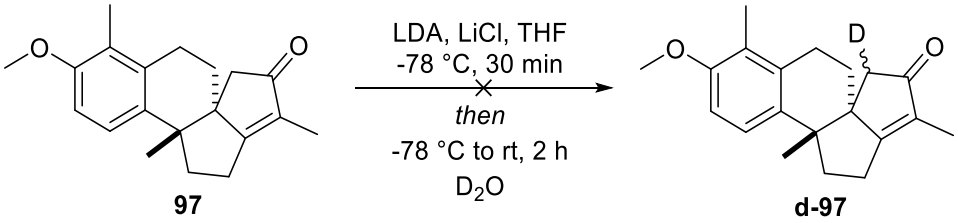

Scheme 5.11

It is known within the literature that a silyl enol ether can be converted into the reactive lithium enolate intermediate through the application of methyl lithium (MeLi).[120] Hence, the corresponding silyl enol ether **188** was generated from tetracycle **97**, and subjected directly into the alkylation conditions (**Scheme 5.12**). In our investigations, it was found that the silyl enol ether **188** could not be purified and characterised fully due to facile hydrolysis, therefore, our studies have involved the direct application of **188** as a crude mixture. We were extremely delighted to isolate deuterated **d-97** through this particular sequence, observing >98% deuterium incorporation at the carbon α to the enone and some diastereoselectivity of 7:3 dr.

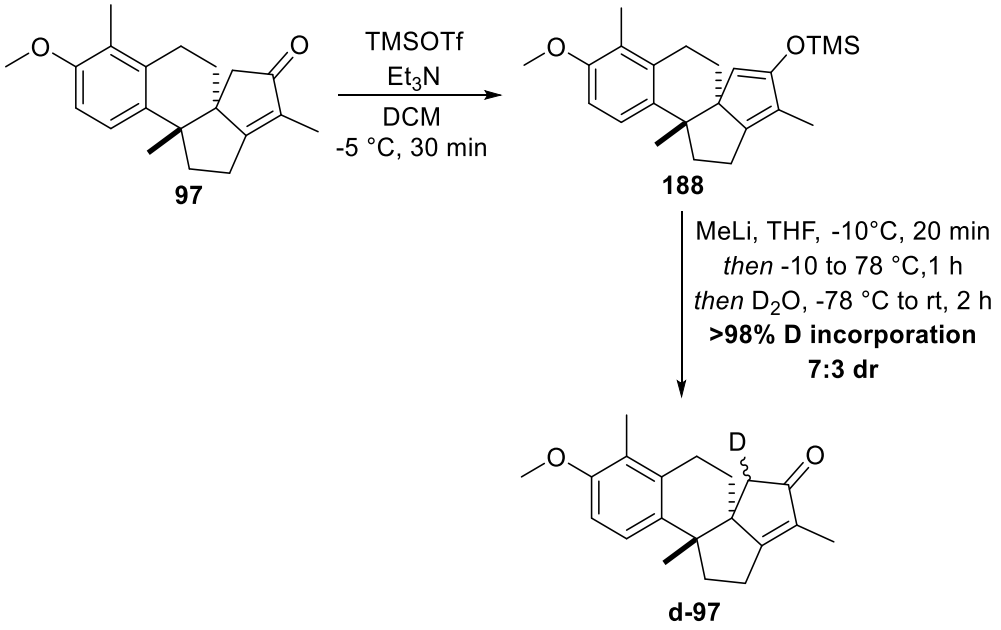

Scheme 5.12

With methodology to generate our reactive lithium enolate in hand, we explored the alkylation procedure with epoxide **186** treated with different additives/Lewis acids in an attempt to enhance the overall reactivity of epoxide (**Scheme 5.13, Table 5.3**).

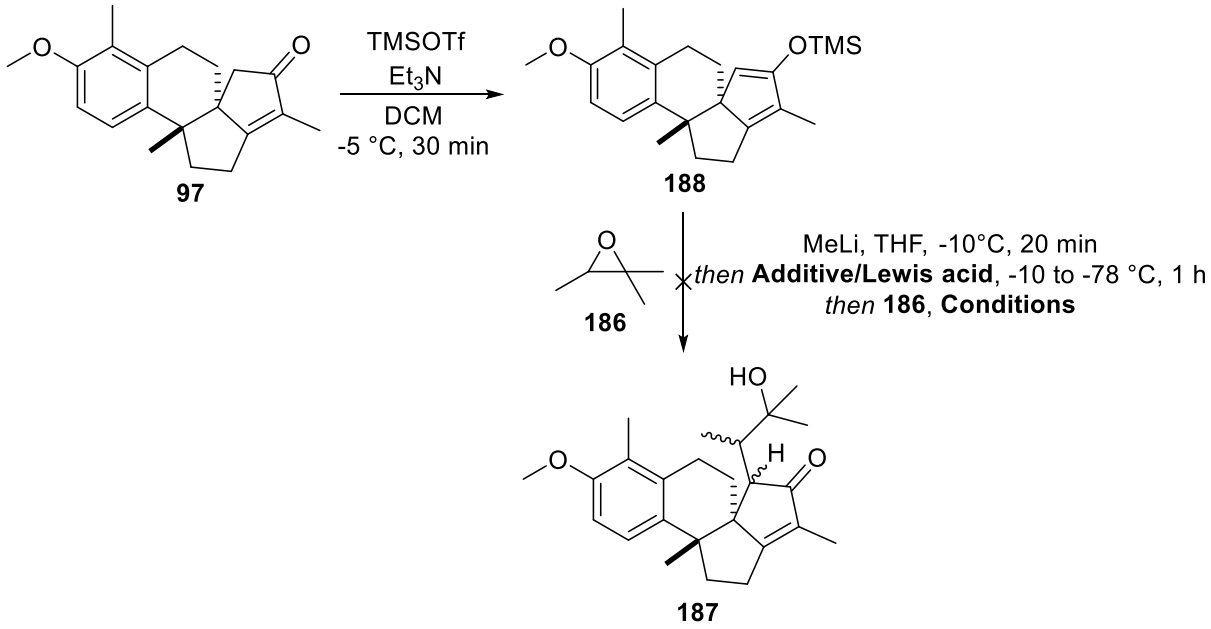

Scheme 5.13

Entry	Additive/Lewis acid	Conditions	Outcome
1	HMPA	-78 °C to rt, 16 h, THF	86% of **97**
2	BF_3•OEt_2	-78 °C to -30 °C, 16 h, THF	70% of **97**
3	$TiCl_4$	-78 °C to -30 °C, 16 h, THF	55% of **97**

Table 5.3

Disappointingly, employing this reaction sequence did not afford our desired product **187** (**Table 5.3**). Application of HMPA as an additive resulted in only starting material **97** isolated (**Entry 1**). Conditions involving Lewis acids BF_3•OEt_2 and $TiCl_4$ led to some decomposition, returning only tetracycle **97** and no other identifiable intermediates.

To confirm that the failure of this alkylation sequence with epoxide **186** was not due to the substrate, core **98** was utilised in our developing process, whereby the desired natural product was not isolated from the reaction mixture (**Scheme 5.14**).

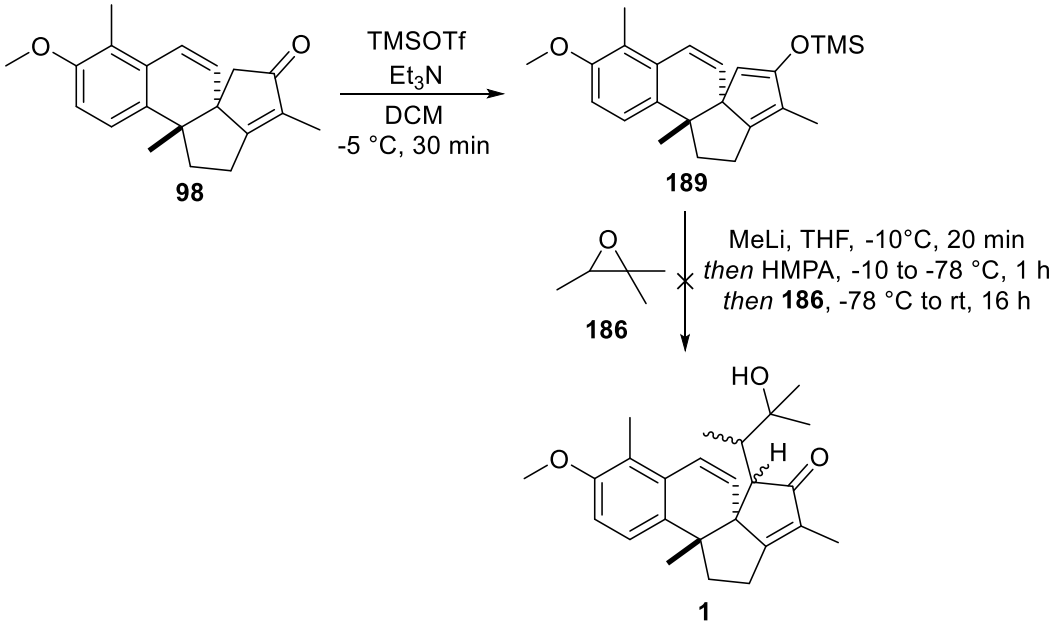

Scheme 5.14

We speculated whether the silyl enol ether intermediate **189** itself could undergo the alkylation process, therefore the sequence was repeated with no formation of the lithium enolate species (**Scheme 5.15**). Dismally, the desired alkylation transformation did not proceed.

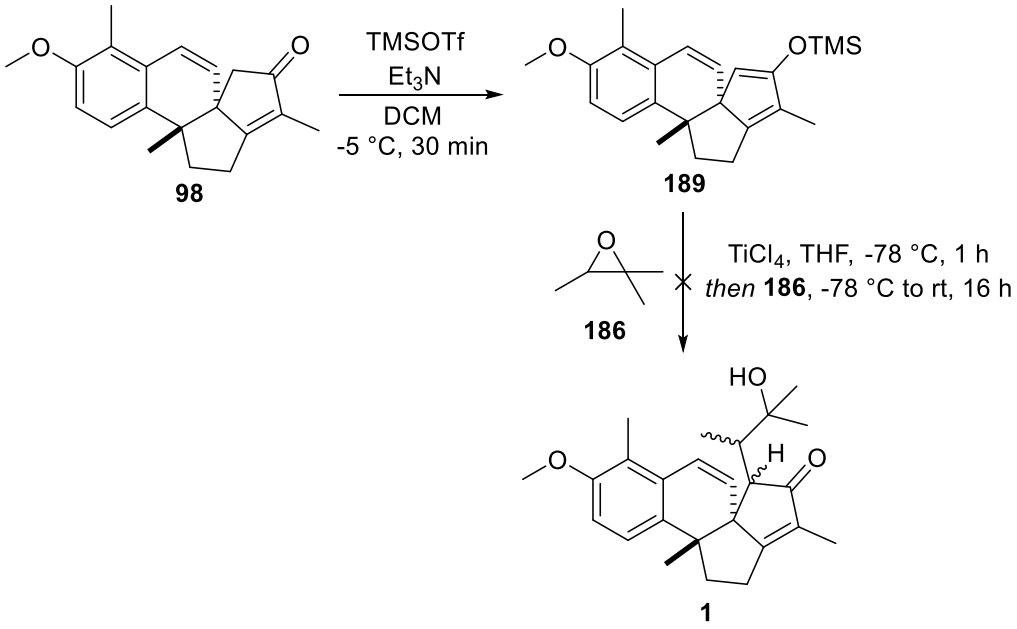

Scheme 5.15

In these studies, we were unable to successfully perform the alkylation procedure with epoxide **186** as the electrophile to furnish agariblazeispirol C directly. With the generation of the desired lithium enolate species achievable, as indicated by the deuterium experiment, we concluded that epoxide **186** was inactive within our system, and that the exploration of more reactive electrophiles was necessary for the addition of the oxygenated side-chain.

5.2.2 Alkylation Attempts with Various Electrophiles

Undeterred by the previous alkylation results with epoxide **186**, we sought to examine various electrophiles for the introduction of our desired side-chain. We conceptualised that the addition of a carbonyl handle in **190** would provide us closer access towards agariblazeispirol C **1**, whilst also providing the potential to employ more reactive electrophiles (**Scheme 5.16**). Here, selective methylation would yield the target oxygenated side-chain for the overall total synthesis.

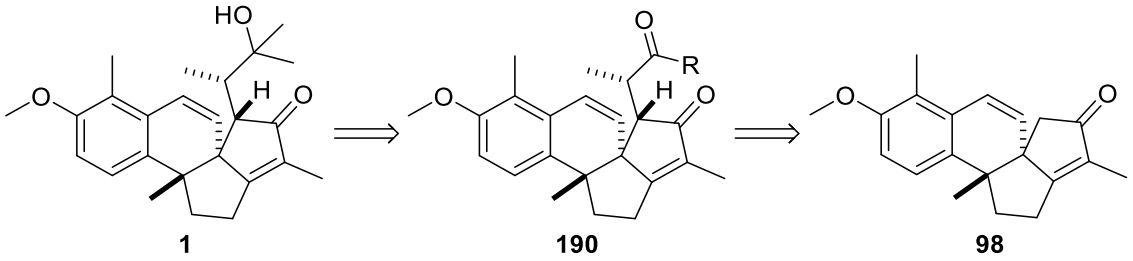

Scheme 5.16

First investigated with core **97,** using our developed silyl enol ether formation/alkylation sequence, was the application of commercially available (racemic) chloroketone **191** to ultimately deliver diketone **192** (**Scheme 5.17**). Fruitlessly, under the reaction conditions, no alkylation was observed and only starting material **97** remained.

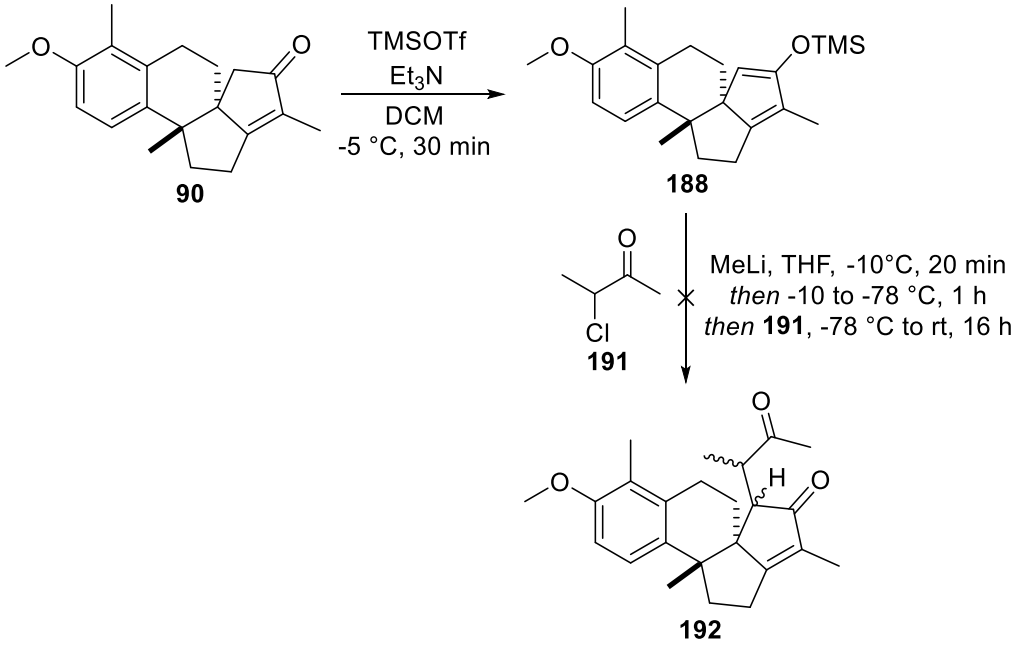

Scheme 5.17

Increasing the overall reactivity of the electrophile employed, alkylation using triflate ester **(*S*)-194** was studied (**Scheme 5.18**). Although converting the corresponding dicarbonyl product into our target would be a potentially arduous task, this would provide us with a first proof of concept of an alkylation procedure. First, triflate ester **(*S*)-194** was synthesised in an excellent 80% yield by treating (*S*)-2-hydroxypropanoate **(*S*)-193** with Tf_2O and Et_3N.

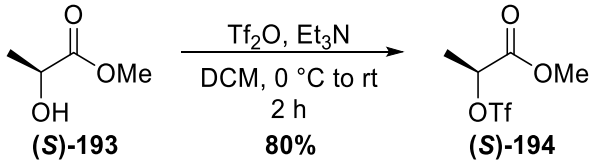

Scheme 5.18

With triflate ester **(*S*)-194** in hand, the key alkylation procedure to synthesise dicarbonyl species **195** could be studied (**Scheme 5.19**).

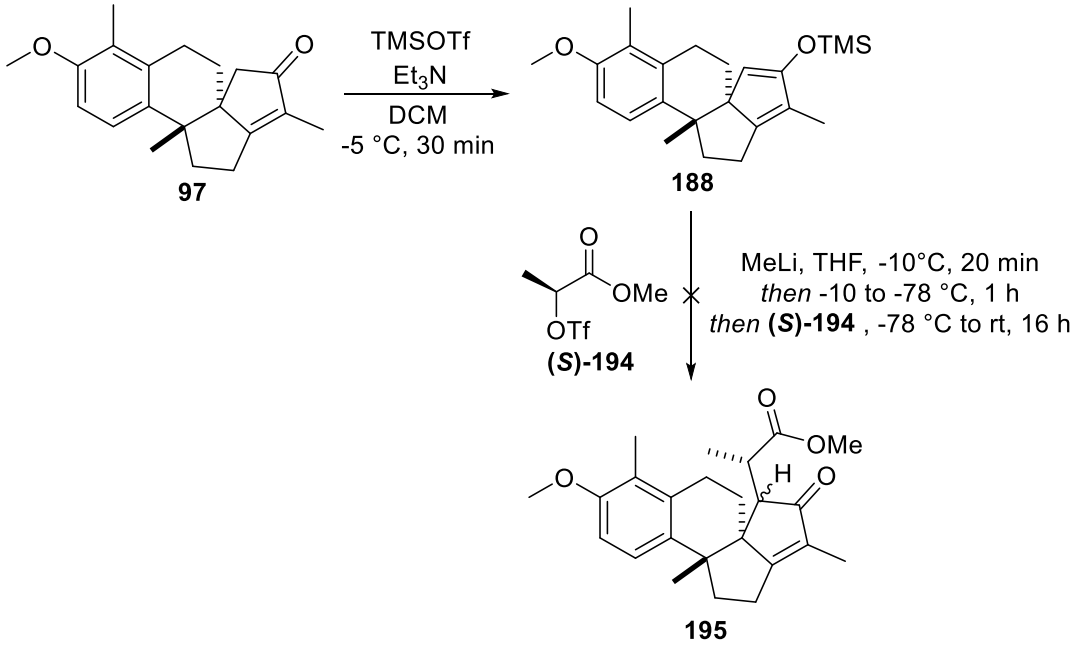

Scheme 5.19

Unfortunately, again, no desired alkylation was achieved using triflate ester **(*S*)-194**. In this case, consumption of starting material was detected, however, the potential by-product(s) formed could not be fully identified. ^{19}F NMR analysis of the mixture collected indicated the presence of a singlet at -75.2 ppm, possibly revealing the existence of an intermediate containing a vinyl triflate moiety. From this, a viable pathway could involve the oxygen position of the lithium enolate species attacking the triflate in **(*S*)-194** – however, this could not be confirmed during our studies.

At this point in our investigation, it was suggested that the carbon α to the enone of our core was sterically hindered, rendering alkylation at this position challenging. To explore this prospect, for proof of concept, we considered the use of the more reactive primary allylic bromide **196** to construct alkylated product **197** (**Scheme 5.20**). So far in our alkylation studies, only secondary electrophiles, which are more sterically demanding, have been implemented. However, if alkylation at our desired position is not a feasible route, **196** could be employed for an *o*-alkylation instead to furnish **198**, which could undergo Claisen rearrangement to, ultimately, generate our natural product following a final manipulation (*vide infra*).

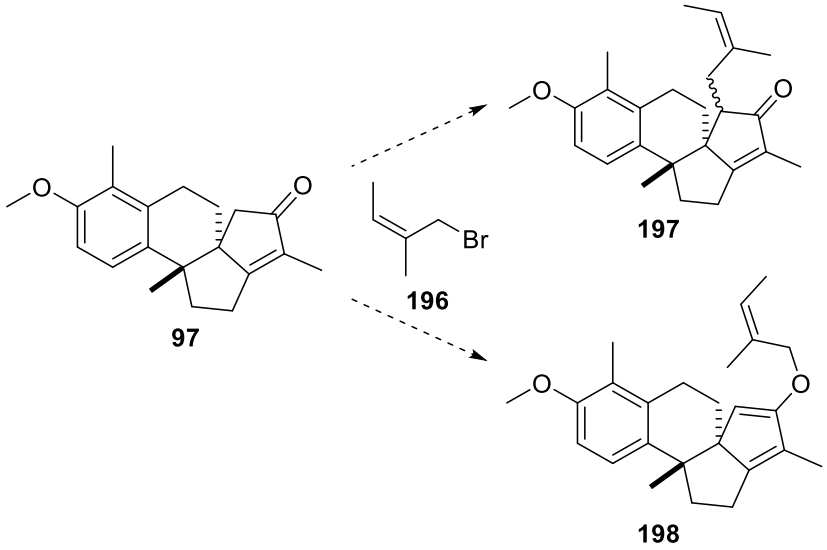

Scheme 5.20

To commence this study, primary allylic bromide **196** was synthesised (**Scheme 5.21**). Methyl angelate **199** was first reduced using $LiAlH_4$, affording allylic alcohol **200** in an exceptional yield of 96%.[121] From here, bromination involving PBr_3 generated our desired allylic bromide **196** in an unoptimised yield of 33%.

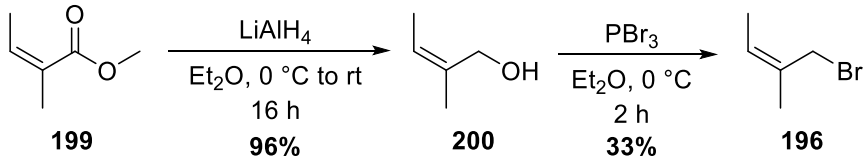

Scheme 5.21

Primary allylic bromide **196** was then employed into our alkylation procedure with tetracylic system **97** (**Scheme 5.22**). With this electrophile, we were extremely pleased to have shown our first example of alkylation at the carbon α to the enone, furnishing **197** in a low, yet unoptimised yield of 14% over 2 steps. Delightfully, this overall process generated **197** with an exemplary diastereoselectivity of 95:5 dr, albeit, at this stage, it was not possible to establish exactly which diastereomer that we had in hand. The achievement of this alkylation could be due to the application of the less sterically demanding primary electrophile, or the presence of a more suitable leaving group, the bromide. Hence, this finding emphasises the potential success of our key alkylation procedure for the synthesis

towards agariblazeispirol C, whereby the selection of an appropriate electrophile is essential.

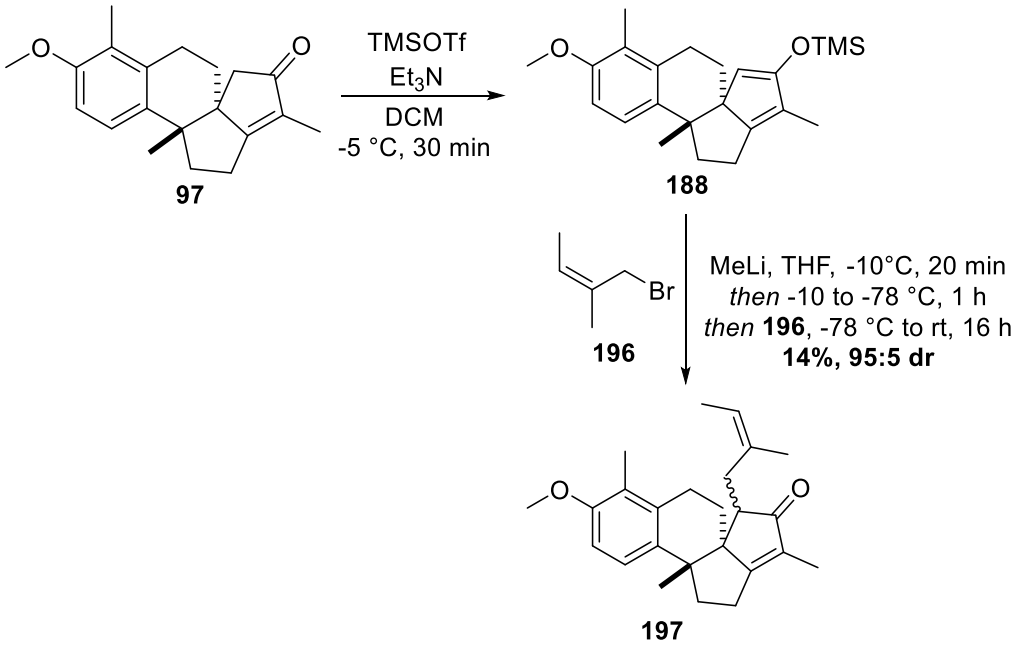

Scheme 5.22

From these studies so far, it was apparent that the choice of electrophile was imperative for the overall process. Alkylation utilising primary allylic bromide **196** was successful, with the product isolated in high diastereoselectivity. For secondary electrophiles, chloroketone **191** was too inert for the alkylation procedure, while triflate ester **(*S*)-194** was too reactive, undergoing unwanted reactions. Accordingly, commercially available bromoketone **201** was explored next as our key electrophile with core **98**, in our ongoing efforts to generate our natural target (**Scheme 5.23, Table 5.4**).

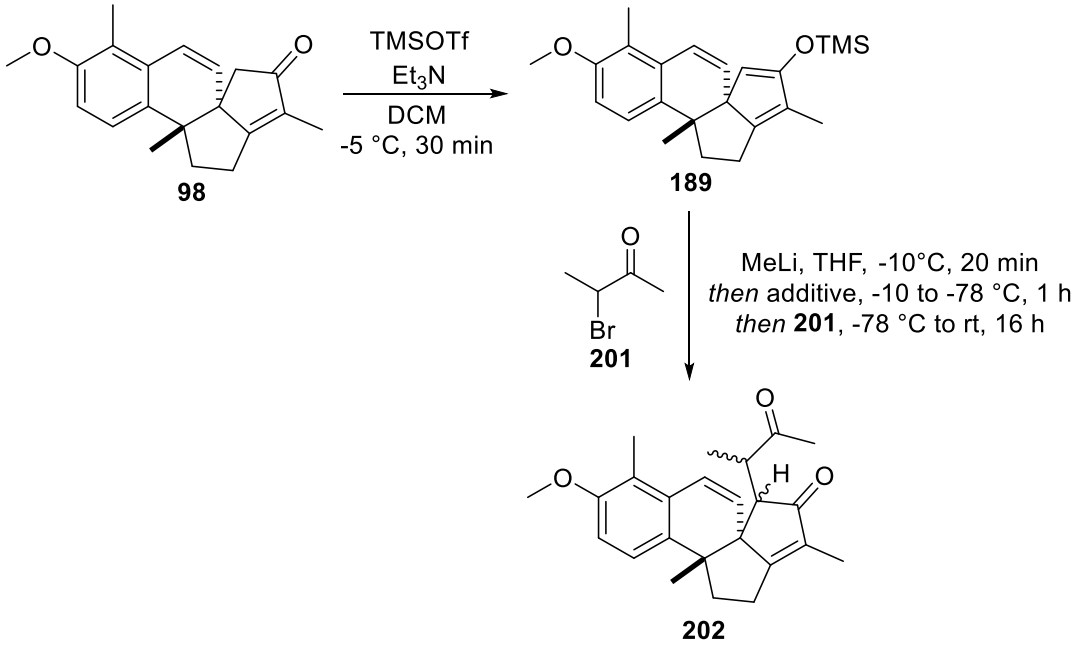

Scheme 5.23

Entry	Additive	Outcome
1	None	**202** identified by NMR and LCMS
2	HMPA	**202** identified by NMR and LCMS

Table 5.4

Performing the alkylation protocol with bromoketone **201**, we were delighted to have observed our desired product **202** within the mixture isolated *via* NMR and LCMS analysis (**Table 5.4, Entry 1**). LCMS analysis indicated the corresponding mass associated with diketone **202**, while NMR data highlighted that the appropriate signals were present within the mixture isolated. However, at this time, we have been unable to purify diketone **202** for full analysis and confirmation of structure. We suspect the diastereomers of **202** cannot be separated, and contained other impurities, resulting in complex NMR data and multiple peaks on the LCMS spectrum. The addition of HMPA was also studied, however the same mixture containing diketone **202** was isolated after column chromatography (**Entry 2**). Despite our failed attempts in purifying **202**, we were extremely pleased to have shown the potential success of our alkylation process to generate agariblazeispirol C.

*5.2.3 Synthesis and Application of bromoketone **(S)-201***

At this juncture, it was proposed that the diastereomers generated from the alkylation reaction with racemic bromoketone **201** could be hindering the overall analysis and confirmation of our desired compound. In theory, four different diastereomers can be produced from our developed protocol, and the presence of all four in an NMR spectrum would severely interfere with interpretation. With this in mind, it was crucial to employ the bromoketone as a single enantiomer, halving the theoretical number of potential diastereomers produced to two in the alkylation step. Thus, the overall analysis could be potentially simplified.

To begin this investigation, the single enantiomer of bromoketone **(*S*)-201** was targetted for our alkylation sequence, which would deliver our desired stereocentre within the final product. First, bromination of commercially available methyl (*R*)-2-hydroxypropanoate **(*R*)-203** was performed under Appel conditions, generating a moderate 46% yield of the bromo ester **(*S*)-204** (**Scheme 5.24**).

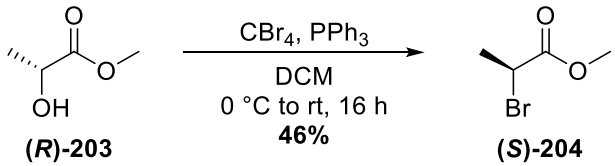

Scheme 5.24

Next, bromo ketone **(*S*)-201** can be synthesised from bromo ester **(*S*)-204** through a Grignard addition with MeMgBr (**Scheme 5.25**).[122] In this reaction sequence, *N*,*O*-dimethylhydroxylamine hydrochloride is quickly deprotonated under the presence of MeMgBr, which immediately attacks bromo ester **(*S*)-204** to form the corresponding Weinreb amide intermediate. Here, again through slow introduction of MeMgBr, the Weinreb amide is converted into our targeted bromoketone **(*S*)-201**. Even though full conversion towards bromoketone (***S*)-201** was recorded, a poor yield of 16% was obtained. This is entirely due to the volatility of bromoketone (***S*)-201**, where precious material was lost during purification. Overall, after overcoming these practical complications of

handling and purifying bromoketone **(*S*)-201**, acceptable quantities were collected for the exploration of our key alkylation reaction.

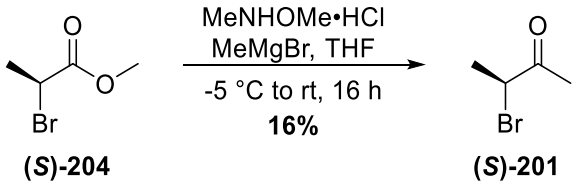

Scheme 5.25

With bromoketone **(*S*)-201** now in hand, this was applied to our crucial alkylation sequence with core **98** in the hope to achieve a better overall reaction profile, as, theoretically, less diastereomers associated with **202** would be formed (**Scheme 5.26**). Regrettably, no improvement towards alkylated product **202** was accomplished when using a single enantiomer of the electrophile. NMR and LCMS analysis conducted with the mixture isolated was comparable to previous results using the racemic electrophile, suggesting the presence of multiple diastereomers could not be the main reason for difficult analytical interpretation. On the other hand, perhaps bromoketone **(*S*)-201** underwent racemisation under the reaction conditions, generating racemic **201** for the alkylation procedure. Regardless, this study highlights our inability to isolate **202** in pure form at this current moment in time. Further investigations are required to facilitate the utility of **202** for the completion of agariblazeispirol C.

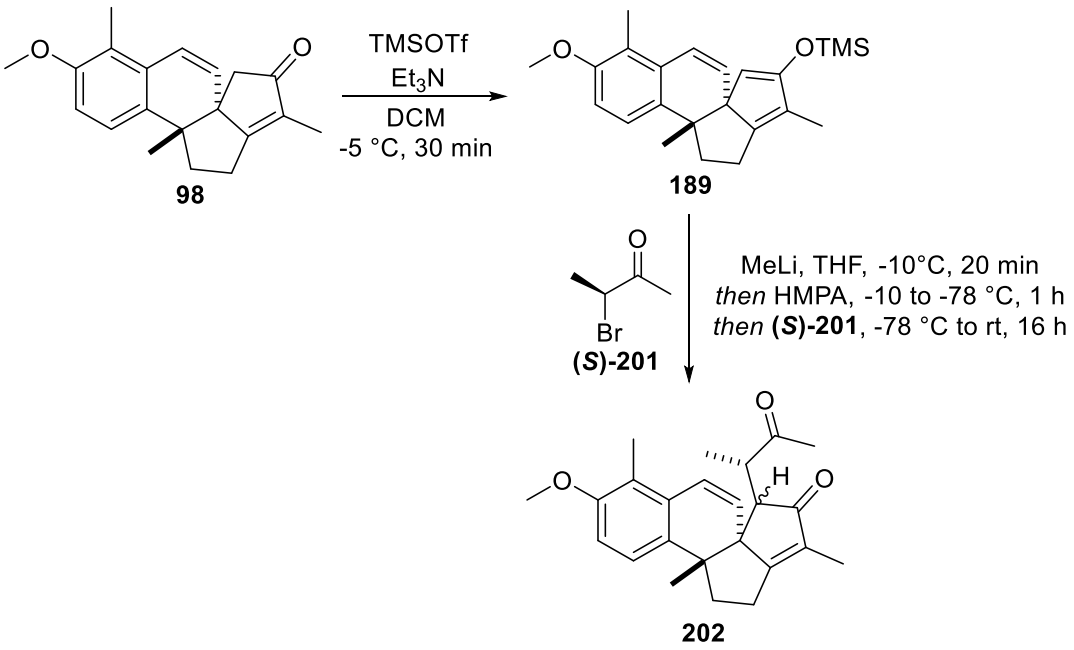

Scheme 5.26

Despite developing an alkylation procedure which generates the desired lithium enolate species within our core, and performing a comprehensive examination of suitable electrophiles, the target natural product has yet to be synthesised. Further investigations involving alkylation procedures, or alternative synthetic approaches, can still be explored to construct agariblazeispirol C.

5.3 Summary

As highlighted in this chapter, numerous synthetic endeavours have been performed to construct our natural product agariblazeispirol C. Initial investigations involved the oxidation of tetracycle **97** into our desired core **98**, and despite exploring many benzylic bromination and oxidation procedures, conversion of tetracycle **97** to **98** has been fruitless thus far (**Scheme 5.27**). Hence, in our synthetic programme towards agariblazeispirol C, it is currently necessary to furnish core **98** directly from the intramolecular Pauson-Khand cyclisation of diene-yne **96**.

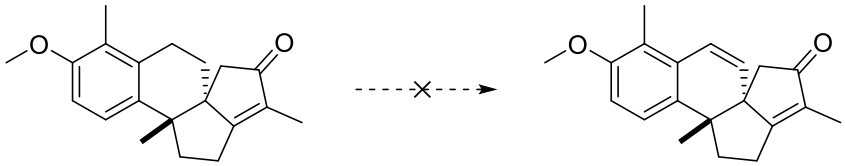

90 **92**

Scheme 5.27

With both **97** and **98** in our hands, the ultimate step of introducing the oxygenated side-chain could be explored to synthesise agariblazeispirol C. We envisaged an alkylation reaction with our polycyclic core would furnish the natural target directly. In order for the alkylation process to proceed, the lithium enolate species of the core must be generated through the corresponding silyl enol ether. Employing the developed silyl enol ether formation/alkylation sequence, generally promising results were achieved when certain electrophiles were used (**Scheme 5.28**). To begin, the formation of the reactive lithium enolate intermediate was illustrated through our deuterium incorporation experiment with D_2O, producing **d-97**. Our first example of successful alkylation was illustrated with primary allylic bromide **196** as the key electrophile, where **197** was generated in a low, yet unoptimised yield of 14% over 2 steps with high diastereoselectivity of 95:5 dr. This crucial finding suggested the importance of the electrophile used, as secondary electrophiles had proven to be troublesome. Chloroketone **191** showed no reactivity, whilst over reactivity was indicated with triflate ester **(*S*)-194**, perhaps also illustrating the importance of the leaving group of the electrophile. This was emphasised with the application of bromoketone **201**, where the crude mixture isolated showed the presence of our desired

product **202** by NMR and LCMS analysis, a contrary result compared to the analogous chloroketone **191**. Regrettably, using the corresponding enantiomer of bromoketone **(*S*)-201** did not improve the overall reaction profile, and further examination is required.

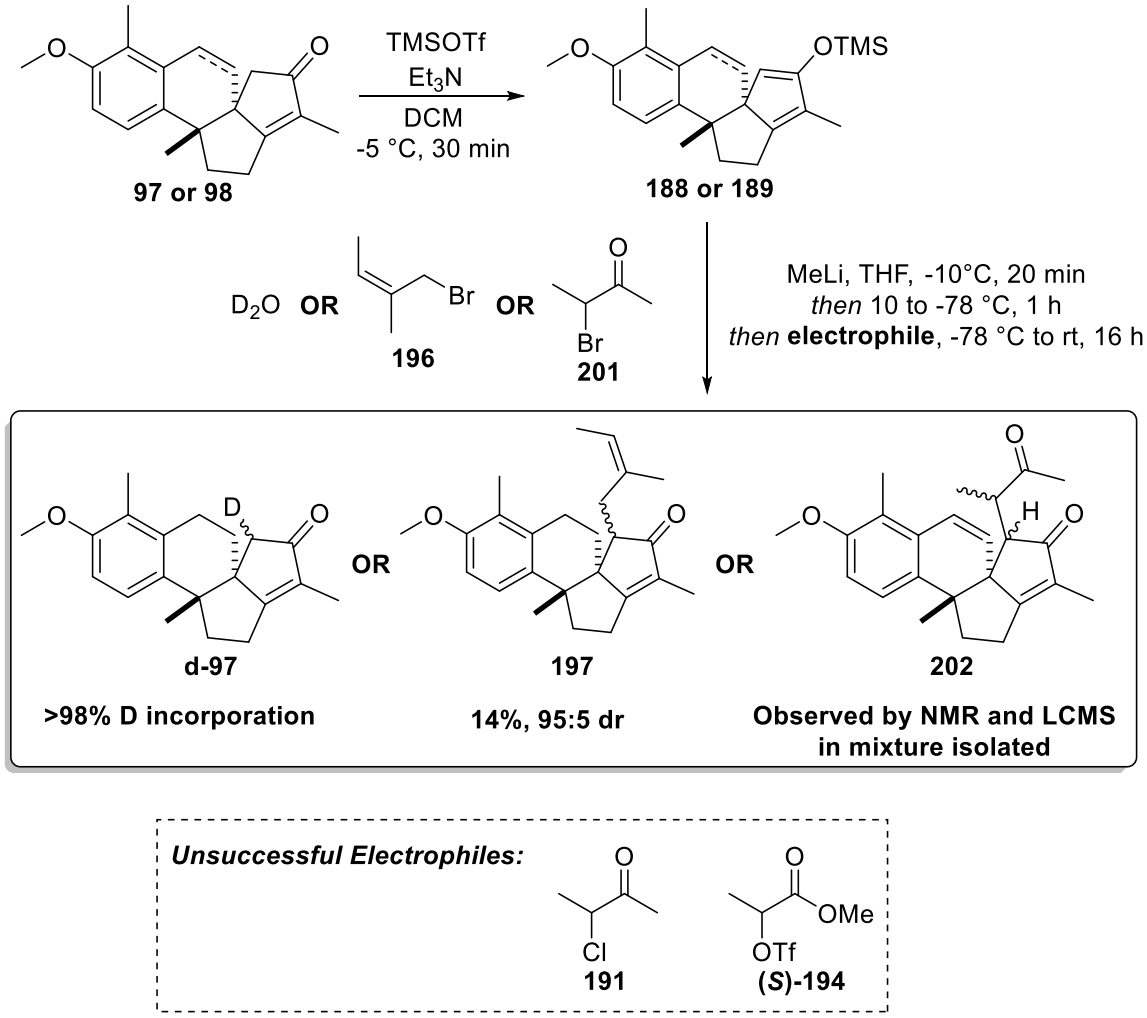

Scheme 5.28

Further work in this overall alkylation sequence must be investigated to complete our formidable synthesis towards agariblazeispirol C, to present its first preparation within the literature, and to confirm the overall structure of the unique natural product. A full summary of the research performed as part of this PhD Thesis, alongside possible future research avenues, are discussed within the following chapter.

Chapter 6

Overall Summary and Future Work

6. Overall Summary and Future Work

6.1 Overall Summary

Within this programme of work, a comprehensive investigation towards the synthesis of agariblazeispirol C has been performed. The preparation of advanced intermediates embedded within each devised synthetic route was achieved and fully optimised, and the examination of the two-key transition-metal mediated cyclisation processes were successful in generating the overall core of the natural target.

The development of the novel asymmetric intramolecular Heck cyclisation was first explored, where the synthesis of various Heck precursors was pursued. The construction of *E*-iodide Heck precursor **(*E*)-100** was achieved in exceptional yields of 68% over 7 steps, requiring non-trivial reaction procedures on multigram scale. Following a similar strategy, the triflate *E*- Heck precursor **(*E*)-101** was generated in 33% over 9 steps. Unfortunately, the preparations of each corresponding *Z*- Heck precursor were unsuccessful in our studies, due to alkene isomerisation during their construction. Despite this, Heck precursors **(*E*)-100** and **(*E*)-101** were employed in the optimisation of our key asymmetric Heck reaction, where initial studies focused on a solvent and additive screen with **(*E*)-100**. Primary screening of conditions highlighted Et_3N as the optimal organic base, and MeCN as the preferred solvent, producing good enantioselectivity towards the desired bicyclic system **62**. From here, application of microwave irradiation and Heck precursor **(*E*)-101** did not uplift the overall % ee of our system, hence the exploration of various chiral ligands was conducted. It was discovered, after extensive optimisation, that (S)-^{t}BuPHOX was capable of reaching exceptional enantioselectivity, however at a cost of poor reaction yield, high catalyst and ligand loading, and difficult purification. This procedure would be extremely inefficient in our synthetic programme, especially during reaction scale-up. As a result, a screen of commercially available diphosphine chiral ligands was performed with **(*E*)-100**, where we were extremely pleased to have identified (*S*)-SYNPHOS as best chiral ligand. Through further optimisation work, we established our key asymmetric intramolecular Heck cyclisation, providing an 85% yield of **17** with excellent enantioselectivity of 86% ee, creating the first stereocentre within our natural product synthesis (**Scheme 6.1**).

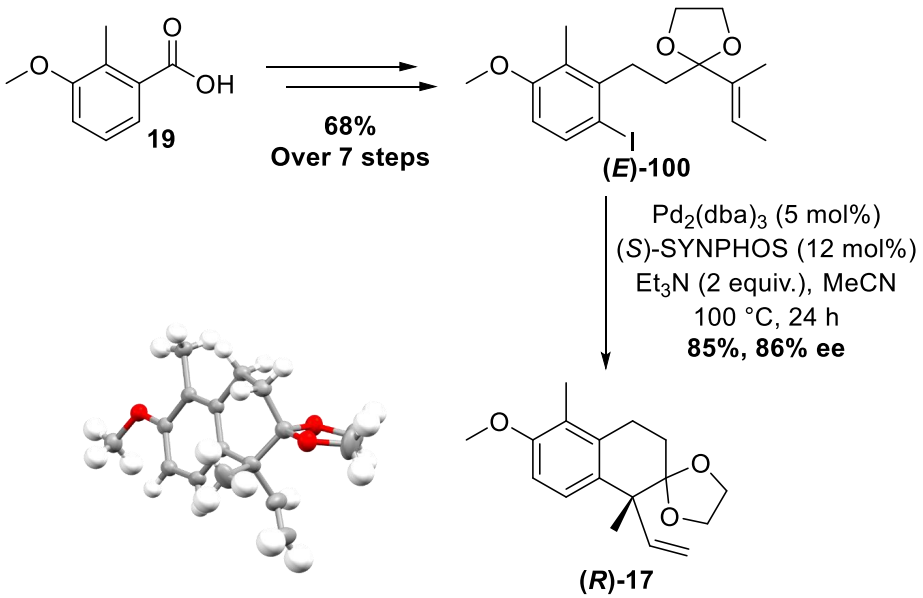

Scheme 6.1

With the first challenging transition-metal mediated cyclisation secured, focus shifted towards the demanding intramolecular Pauson-Khand annulation to construct the congested polycyclic core of agariblazeispirol C (**Scheme 6.2**). This involved the establishment of two individual PK precursors, enyne **95** and diene-yne **96**, both having their own advantages. Separate synthetic paths were necessary, each involving challenging optimisations of various advanced intermediates. Overall, the construction of terminal alkene PK precursor **95** was obtained in a good yield of 40% over 9 steps. Even though this involved a longer, and initially troublesome protection/deprotection strategy, **95** was produced in favourable amounts for the subsequent PKR. The preparation of conjugated diene PK precursor **96** was more strenuous, as this involved the optimisation of a key hydroformylation process. Pleasingly, the conjugated diene precursor **96** can be generated in a concise 7 steps, despite requiring the installation of additional functionality compared to the synthesis of precursor **95**. However, the intermediates within this synthetic pathway were sensitive, resulting in an overall reduced yield of 22% across the 7 steps. With tenacious efforts performed thus far in generating PK precursors **95** and **96**, the PK annulation of both was explored. The challenging PKR was able to construct the two cyclopentyl rings within agariblazeispirol C, furnishing the congested core including two contiguous, and chiral, quaternary carbon centres. A one-pot PK cyclisation of enyne **95** furnished tetracycle **97** in a very good yield of 77% as one single diastereomer, by

employing DodSMe as the promoter. PKR of conjugated diene **96** was more demanding, requiring elevated temperatures for the annulation to proceed efficiently. Delightfully, after optimisation, the complete tetracyclic core **98** of agariblazeispirol C was achieved in an appreciable 50% isolated yield, again as one single diastereomer containing our desired *anti*-stereochemistry within the core (**Figure 6.1**). Overall, from the carboxylic acid starting material **19**, tetracycle **97** was produced in an 18% yield over 18 steps, and **98** was furnished in 6% yield over 16 steps.

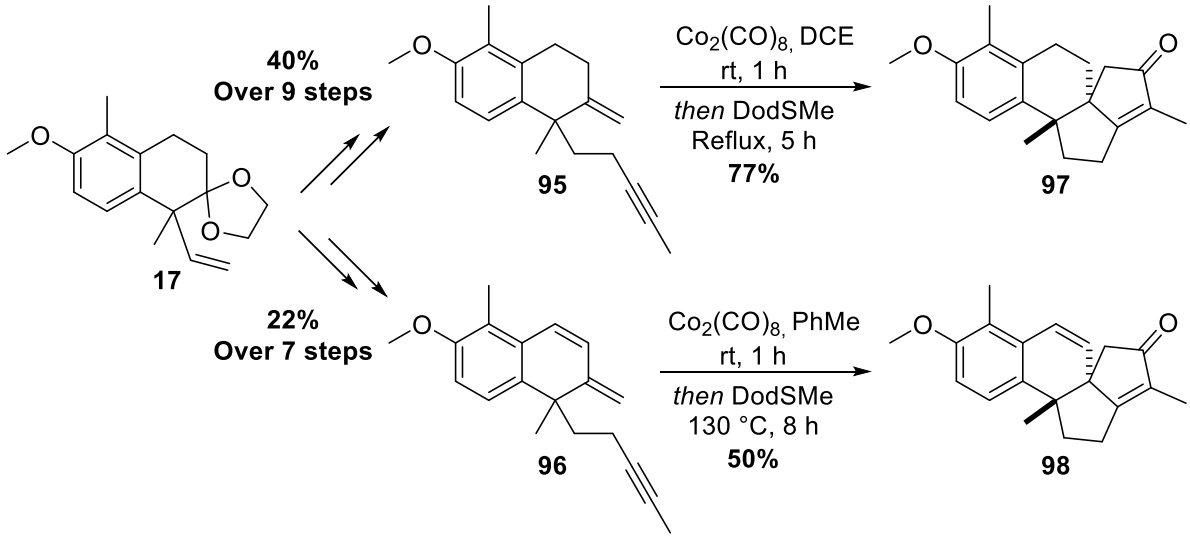

Scheme 6.2

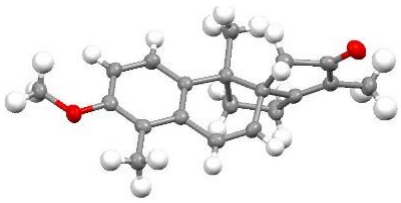

Figure 6.1

In our concluding efforts, attempts to construct agariblazeispirol C was investigated. Late-stage oxidation of tetracycle **97** to the desired core **98** was unsuccessful, therefore, the direct PKR of diene-yne **96** to **98** is vital in our synthesis. Regardless, excellent progress towards the introduction of the oxygenated side-chain *via* alkylation has been disclosed. In our current protocol, successful attack of specific electrophiles has been achieved through a silyl enol ether formation/alkylation sequence. Our work has exhibited promising potential to complete this synthesis, with various avenues yet to be explored in this final challenge.

6.2 Future Work

Assuredly, subsequent work will follow to expand upon the alkylation procedure to install the oxygenated side-chain, thus completing the synthesis of agariblazeispirol C **1**. However, prior to this extensive study, firstly the single enantiomer of core ***ent*-98** should be generated in large quantities for the concluding studies towards **1**. Following our developed synthetic route, this would involve performing the asymmetric intramolecular Heck cyclisation on large scale, then implementing the material into our established Pauson-Khand annulation. With enantiopure ***ent*-98** in hand, to enable rapid access to our target, the isolated mixture of diketone **202**, generated from our silyl enol ether formation/alkylation procedure with bromoketone **(*S*)-201**, could be further purified by advanced separation techniques. Preparative HPLC could solely isolate diketone ***ent*-202** with high purity, setting the stage for selective late-stage methylation of the diketone to provide agariblazeispirol C **1** (**Scheme 6.3**).

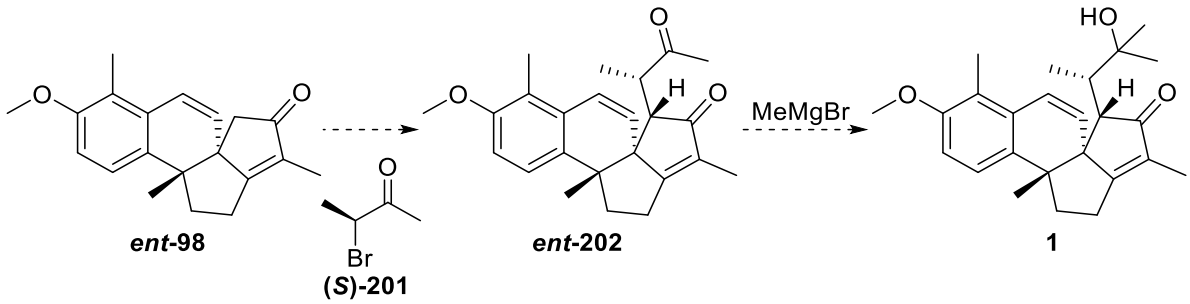

Scheme 6.3

With our previous work illustrating the success of primary allylic bromide **196** as an electrophile, an alternative alkylation procedure could involve reactive primary bromoketone **205** to produce ***ent*-206** – however, this will involve an additional methylation step towards the synthesis of our target **1** (**Scheme 6.4**). From our previous study with primary allylic bromide **196**, the alkylation proceeded with a high diastereoselectivity of 95:5. Hence, in this proposed synthesis, we hope to achieve diketone ***ent*-202** with the same selectivity and favouring our desired stereochemistry. From ***ent*-206**, the formation of the thermodynamically favoured enolate must ensue, which can then undergo the methylation procedure. The diastereoselectivity of this process is uncertain at this point, however, it

may be possible to separate and purify our desired product ***ent*-202**. Lastly, the second selective methylation step of the ketone generates agariblazeispirol C **1**. Even though this proposed route could afford our natural product through purification of diastereomers, having no control over the diastereoselective outcome could be an issue overall.

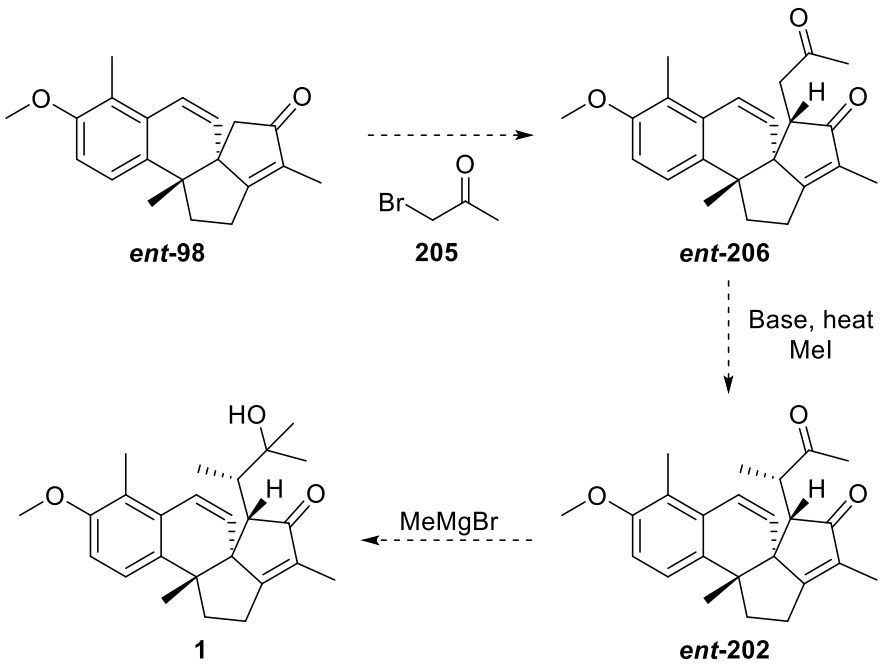

Scheme 6.4

An alternative approach to introduce our side-chain could involve the application of an asymmetric Tsuji-Trost allylation reaction (**Scheme 6.5**).[123–126] Here, using our core ***ent*-98**, we propose the formation of enol carbonate **208** through employment of carbamate **207** (which can be prepared in two steps).[124] We suggest carbamate **207** and conditions involving Lewis acid BF_3•OEt_2, as the formation of the enol carbonate within our intricate system could be challenging, and this optimised procedure was successful in the complex synthesis of the A−D fragment of gambieric acids.[124] Having said this, traditional methods could still be explored.[126] With enol carbonate **208** in hand, the key asymmetric Tsuji-Trost protocol can be investigated to deliver ***ent*-209**, utilising (*S*)-^{t}BuPHOX as the chiral ligand. The overall process could be highly diastereoselective, or if a mixture of diastereomers is formed, they could be separated by column chromatography. After isolating ***ent*-209**, selective late-stage hydration of the terminal alkene would afford agariblazeispirol C **1**.

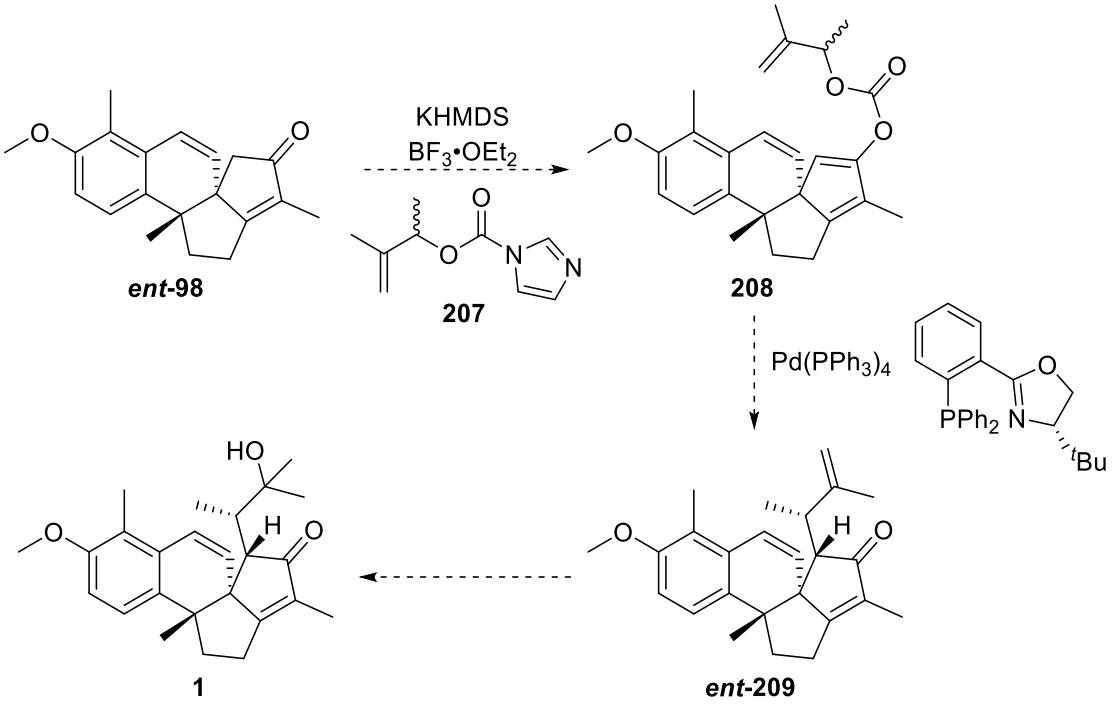

Scheme 6.5

Although the above methodologies would be useful for presenting the first synthesis of agariblazeispirol C **1** and confirming its overall structure, the proposed routes could be inefficient, requiring either a specialised separation protocol or a non-diastereoselective route, both which could result in low isolated yields of intermediates towards the natural target. Another strategy, which was briefly mentioned within the main body of this thesis, could involve the employment of a Claisen rearrangement to introduce our oxygenated side-chain in a diastereoselective fashion (**Scheme 6.6**). Here, traditional *o*-alkylation strategies could be probed to generate the target Claisen precursor ***ent*-198**. In addition to this, another interesting approach we propose is to modify and optimise a procedure developed by Buchwald.[127] This involves a domino copper-catalysed C–O cross-coupling/Claisen rearrangement with *Z*- allyl alcohol **200** and enol triflate ***ent*-210**, which would generate our Claisen product ***ent*-209** *via* precursor ***ent*-198**. This would efficiently provide ***ent*-209** in a one-step diastereoselective process, as it is anticipated the *Z*- allyl alcohol **200** would give the correct stereochemistry required for the methyl group in the desired target. The synthesis of enol triflates from silyl enol ethers are known in the literature, [128,129] where ***ent*-210** can be generated by modifying our previously developed silyl enol ether/alkylation conditions. Here, the electrophile would instead be *N*-phenyltriflimide **211**, providing triflate ***ent*-210**. Once the domino C–O cross-

coupling/Claisen rearrangement has been optimised, selective late-stage hydration of ***ent*-209** would provide us with agariblazeispirol C **1**.

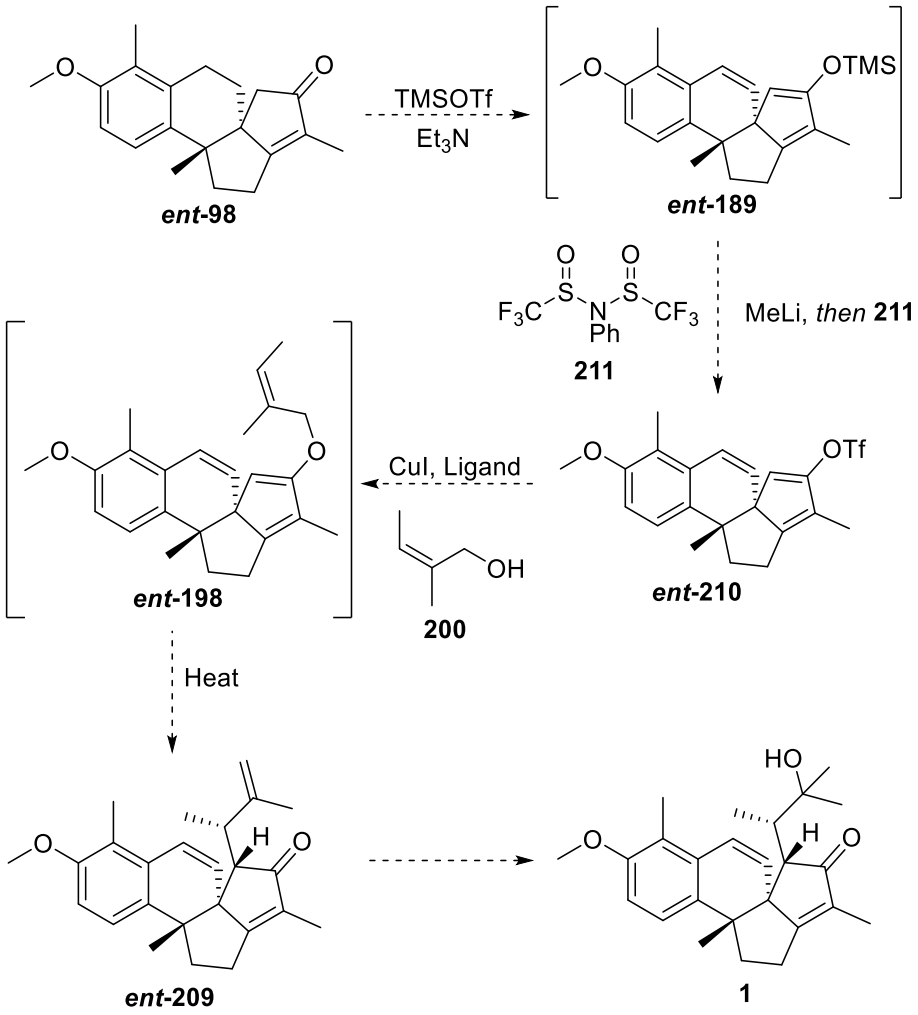

Scheme 6.6

Chapter 7

Experimental

7. Experimental

7.1 General Information for Reactions carried out at the University of Strathclyde

All experimental procedures were performed at the University of Strathclyde, Glasgow, unless otherwise stated within the procedure.

7.1.1 Reagents

All reagents used were obtained from commercial suppliers and used without further purification, unless otherwise stated. All reactions were carried out under an inert, dry nitrogen atmosphere, unless otherwise stated. Purification was carried out according to standard laboratory methods.[130]

THF was dried by heating to reflux over sodium wire, using benzophenone ketyl as an indicator, then distilled under argon. DCM, Et_2O, PhMe, and MeCN were dried by heating to reflux over calcium hydride, then distilled under argon. For large volumes (>400 mL) of dry THF and DCM, these were obtained from an Innovative Technology, Pure Solv, SPS-400-5 solvent purification system.

Petrol refers to petroleum ether in the boiling point range of 40-60 °C.

^{n}BuLi and ^{t}BuLi were obtained as solutions in hexanes and pentanes respectively, and standardised using diphenylacetic acid in THF.[131]

MeMgBr was obtained as a solution in Et_2O, and standardised using I_2 and LiCl in THF.[132]

7.1.2 Instrumentation and Data

Thin layer chromatography was carried out using TLC silica gel 60 F_{254} plates (Merck) and developed using vanillin and potassium permanganate solutions.

Flash column chromatography was carried out using Prolabo silica gel (230-400 mesh).

Melting points were obtained (uncorrected) on a Gallenkamp Griffin melting point apparatus.

IR spectra were obtained as neat samples on a Shimadzu IR Affinity-1 Spectrophotometer machine and data are reported in cm^{-1} unless stated otherwise.

^{1}H, ^{13}C, ^{19}F, and ^{31}P NMR spectra were recorded on a Bruker DPX 400 spectrometer at 400 MHz, 101 MHz, 362 MHz, and 162 MHz, respectively, or a Bruker DRX 600 spectrometer at 600 MHz. Chemical shifts are reported in ppm. Coupling constants are reported in Hz and refer to $^{3}J_{H\text{-}H}$ interactions, unless otherwise stated.

Reactions performed under microwave irradiation were carried out either in a CEM Discover or Biotage instrument, using sealed glass tubes.

Low-resolution mass spectra (LRMS) were obtained using an Agilent Technologies 1200 series LC-MS instrument with a 6130 single Quadropole, a ThermoQuest Finnigan LC duo coupled to a Razel syringe pump. LC traces were recorded at a wavelength of 254 nm.

HRMS were recorded either on a Thermo Finnigan MAT 90XLT instrument at the EPSRC Mass Spectrometry facility at the University of Wales, Swansea, or on a Thermo Finnigan MAT 900CP instrument at the University of Edinburgh.

Chiral HPLC was carried out using a CHIRALCEL® OD-H or CHIRALCEL® OJ-H column using a Gilson Model 302 pump, and a Milton Roy Spectromonitor® 3100 tuneable absorbance detector (set at 254 nm unless stated otherwise). Chromatographic data was processed using a Dionex Advanced computer interface module.

Optical rotation measurements were carried out using a Perkin Elmer Polarimeter 341 or Rudolph Research Analytical Autopol III Automatic Polarimeter. Optical rotation values are quoted in 10^{-1} deg cm^2 g^{-1} and concentrations are expressed in g ml^{-1}.

7.2 General Information for Reactions carried out at GSK, Stevenage

Experimental procedures performed at GSK, Stevenage, will be explicitly detailed within each procedure.

7.2.1 Reagents and Solvents

Solvents and reagents were purchased from commercial suppliers and used as received, unless otherwise stated. Reactions were monitored by TLC or LCMS analysis. Heating was conducted using hotplates with DrySyn adaptors.

7.2.2 Instrumental and Data

TLC was carried out using POLYGRAM®-backed 50 precoated silica plates (particle size 0.2 mm). Spots were visualised by ultraviolet (UV) light (λ_{max} = 254 nm or 365 nm) and then stained with potassium permanganate solution followed by gentle heating. Flash column chromatography was carried out using the Teledyne ISCO Combi*Flash*® *Rf+* apparatus with Redi*Sep*® or Biotage® SNAP KP-NH cartridges.

LCMS analysis was carried out on a Waters Acquity ultra performance liquid chromatography instrument equipped with an ethylene bridged hybrid column (50 mm x 2.1 mm, 1.7 µm packing diameter) and Waters micromass ZQ mass spectrometer using alternate-scan positive and negative electrospray. Analytes were detected as a summed UV wavelength of 210–350 nm.

^{1}H, and ^{13}C NMR spectra were recorded on a Bruker AV-400 spectrometer at 400 MHz and 101 MHz, respectively. Chemical shifts are reported in ppm. Coupling constants are reported in Hz and refer to $^{3}J_{H\text{-}H}$ interactions, unless otherwise stated.

Mass-directed automatic purification (MDAP) was carried out using a Waters ZQ mass spectrometer using alternate-scan positive and negative electrospray and a summed UV wavelength of 210–350 nm. One liquid phase method was used: High pH – XSelect CSH C18 column (100 mm x 19 mm, 5 µm packing diameter, 20 mL/min flow rate) or XSelect CSH C18 column (150 mm x 30 mm, 5 µm packing diameter, 40 mL/min flow rate). Gradient elution at ambient temperature with the mobile phases as (A) 10 mM aqueous ammonium bicarbonate solution, adjusted to pH 10 with 0.88 M aqueous ammonia and (B) acetonitrile.

Chiral HPLC was carried out using a CHIRALCEL® OD-H or CHIRALCEL® OJ-H column using an Agilent 1100 analytical HPLC system incorporating a G1312A binary pump, G1379A degasser unit, G1316A thermostated column compartment, G1317A autosampler and G1315B diode array UV detector (set at 235 nm unless stated otherwise). Chromatographic data was processed using Agilent Chemstation software.

7.3 General Procedures for Experiments

7.3.1 Standard General Procedures

General Procedure A – Hydrogenation

A 50 mL round-bottom flask equipped with a double oblique stopcock adaptor was flame-dried and cooled under argon. Substrate (a), catalyst (b), and solvent (c) were added into the flask. The flask was cooled to -78 °C in a dry ice/acetone bath. The flask was then evacuated and flushed with hydrogen from a balloon, and this cycle was repeated a further two times. Following the final flush, the stopcock was left open to the balloon and the flask was immersed in an oil bath set to the specified reaction temperature (d). The mixture was left under the hydrogen atmosphere for the specified time (e), before replacing the system with air. The solvent was removed, the crude mixture was analysed by NMR, and, if possible, was purified by column chromatography (eluent: 0-33% Et_2O in petrol) (f).

General Procedure B – Borylation/oxidation with H_2O_2

To a flame-dried round bottom flask, $Pd(OAc)_2$ (a), K_2CO_3 (b), B_2Pin_2 (c), and **106** (d) were added, dissolved in DMA (e), and the flask was sealed. The solution was degassed with argon for 10 min, which was subsequently heated to 80 °C for 8 h. After this time, the solution was diluted with Et_2O and filtered through a pad of celite®. The mixture was washed with brine, dried over sodium sulfate, filtered, and evaporated. The crude mixture **126** was used directly in the next step.

The crude mixture was dissolved in 1,4-dioxane (f) and charged into a round bottom flask, where K_2CO_3 (g) was then added. H_2O_2 (h) was then introduced dropwise into the reaction mixture and left to stir for 16 h at room temperature. The reaction mixture was quenched with 1 M HCl (10 mL) and extracted with Et_2O. The organic layer collected was washed with brine, dried over sodium sulfate, filtered, and evaporated. The resulting crude mixture was purified by column chromatography (eluent: 0-100% Et_2O in petrol), affording the product **125** as a white solid (i).

General Procedure C – Borylation/oxidation with Oxone®

To a flame-dried round bottom flask, $Pd(OAc)_2$ (a), K_2CO_3 (b), B_2Pin_2 (c) and **106** (d) were added, dissolved in DMA (e), and the flask was sealed. The solution was degassed with argon for 10 min, which was subsequently heated to 80 °C for 8 h. After this time, the solution was diluted with Et_2O and filtered through a pad of celite®. The mixture was washed with brine, dried over sodium sulfate, filtered, and evaporated. The crude mixture **126** was used directly in the next step.

The crude mixture was dissolved in acetone (f) and, at room temperature, a solution of Oxone® (g) in water (h) was added dropwise, which was then left to stir vigorously for 16 h. The reaction mixture was quenched with saturated sodium bisulfite solution and extracted with Et_2O. The organic layer collected was washed with brine, dried over sodium sulfate, filtered, and evaporated. The resulting crude mixture was purified by column chromatography (eluent: 0-33% Et_2O in petrol), affording the product **125** as a white solid (i).

*General Procedure D – Protection of **(Z)-129***

(*Z*)-129 (50 mg, 0.14 mmol), triethylorthoformate (47 µL, 0.28 mmol) and ethylene glycol (23 µL, 0.42 mmol) were dissolved in DCM (0.5 mL), and were charged into a microwave vial and cooled to -78 °C using a cryocooler. After this, BF_3•OEt_2 (a) was added dropwise, and left for the specified temperature (b) and time (c). The mixture was quenched with Et_3N and saturated sodium bicarbonate solution, washed with water, and then dried with sodium sulfate. The mixture was filtered, the solvent was evaporated and the crude mixture was analysed by NMR, determining conversion (d) and the **(*E*)-100:(*Z*)-100** ratio (e). If applicable, the crude mixture was purified using column chromatography (eluent: 0-33% Et_2O in petrol) to afford an *E:Z* mixture of **100** (f) as a colourless oil.

General Procedure E – Deprotection Using Mild Acidic Conditions

In an oven-dried microwave vial, substrate (a) was dissolved in acetone (b). Subsequently, water (c) and acid (d) were added, and the reaction mixture was left at the specified temperature (e) using a heat block for the specified time (f). After this time, the mixture

was quenched with saturated sodium bicarbonate solution, and extracted with DCM. The organic solution was then dried with sodium sulfate, filtered, and evaporated. The crude mixture was directly analysed by ^{1}H NMR to determine overall conversions (g).

General Procedure F – Deprotection Using $CeCl_3$•$7H_2O$

In an oven-dried microwave vial, substrate (a) was dissolved in MeCN (b). Subsequently, NaI (c) and $CeCl_3$•$7H_2O$ (d) were added, and the reaction mixture was left at the specified temperature (e) using a heat block for the specified time (f). After this time, the mixture was quenched with saturated sodium bicarbonate solution, and extracted with DCM. The organic solution was then dried with sodium sulfate, filtered, and evaporated. The crude mixture was directly analysed by ^{1}H NMR to determine overall conversions (g).

General Procedure G – Deprotection Using $Ce(OTf)_3$•$7H_2O$

In an oven-dried microwave vial, substrate (a) was dissolved in $MeNO_2$ (b). Subsequently, $Ce(OTf)_3$•$7H_2O$ (c) was added, and the reaction mixture was left at room temperature for 1 h. After this time, the mixture was quenched with saturated sodium bicarbonate solution, and extracted with DCM. The organic solution was then dried with sodium sulfate, filtered, and evaporated. The crude mixture was directly analysed by ^{1}H NMR to determine overall conversions (d).

General Procedure H – Deprotection Using I_2

In an oven-dried microwave vial, substrate (a) was dissolved in acetone (b). Subsequently, I_2 (c) was added, and the reaction mixture was left at the specified temperature (d) using a heat block for the specified time (e). After this time, the mixture was quenched with saturated sodium bisulfite solution, and extracted with DCM. The organic solution was then dried with sodium sulfate, filtered, and evaporated. The crude mixture was directly analysed by ^{1}H NMR to determine overall conversions, and if applicable, purified by silica chromatography (eluent: 0-33% Et_2O in petrol) to afford the product (f).

General Procedure I – Hydrozirconation

To a flame-dried microwave vial, $(C_5H_5)_2ZrHCl$ (57 mg, 0.22 mmol), dissolved in DCM (0.4 mL), was added before being charged with **17** (20 mg, 0.07 mmol) dissolved in the specified solvent (0.4 mL) (a). After this addition, the suspension was allowed to stir at the specified temperature (b) for the specified time (c). After this time, the mixture was cooled to 0 °C using an ice bath and NIS (84 mg, 0.37 mmol), dissolved in the specified solvent (0.2 mL) (a), was charged into the reaction mixture. The resulting solution was left to stir at this temperature for 30 min before being warmed to room temperature and left to stir for the specified time (d). After this time, the reaction mixture was cooled to 0 °C using an ice bath, quenched with saturated sodium thiosulfate solution, and extracted with Et_2O. The organic layer was dried over sodium sulfate, filtered, and evaporated. The crude mixture was purified by column chromatography (eluent: 0-33% Et_2O in petrol).

*General Procedure J – Displacement to Generate Protected Diene-yne Intermediates from **158***

To a flame-dried round bottom flask, silyl protected acetylene (a) and THF (b) were charged and cooled to -78 °C using a dry ice/acetone bath. At this temperature, ^{n}BuLi (c) was added dropwise *via* syringe. The resulting mixture was left to stir at this temperature for 1 h.

To another flame-dried round bottom flask, **158** (d) dissolved in DCM (e) and pyridine (f) was charged and cooled to -78 °C using a dry ice/acetone bath. At this temperature, Tf_2O (g) was added dropwise *via* syringe. The resulting mixture was left to stir at this temperature for 20 min before being quenched with saturated sodium bicarbonate solution, and extracted with DCM. The organic solution was washed with brine, then dried with sodium sulfate, filtered, and evaporated. The crude mixture containing triflate **162** was dissolved in THF (h), and subsequently TMEDA (i) and DMPU (j) were added. The resulting mixture was cooled to -78 °C using a dry ice/acetone bath. At this temperature, the solution was cannulated directly to the previously prepared silyl protected acetylene solution. The resulting mixture was left to stir at -78 °C for 5 min, before being warmed to the specified temperature (k), and subsequently left at the specified time (l). After this, the mixture was quenched with saturated ammonium chloride. The mixture was extracted with Et_2O,

washed with brine, then dried with sodium sulfate, filtered, and evaporated. The crude mixture was analysed by NMR and purification was attempted (m).

*General Procedure K – Displacement to Generate Protected Diene-yne Intermediates from **166***

To a flame-dried round bottom flask, silyl protected acetylene (a) and THF (b) were charged and cooled to -78 °C using a dry ice/acetone bath. At this temperature, ^{n}BuLi (c) was added dropwise *via* syringe. The resulting mixture was left to stir at this temperature for 1 h.

To another flame-dried round bottom flask, **166** (d) was dissolved in THF (e), and subsequently TMEDA (f) and DMPU (g) were added. The resulting mixture was cooled to -78 °C using a dry ice/acetone bath. At this temperature, the solution was cannulated directly to the previously prepared silyl protected acetylene solution. The resulting mixture was left to stir at -78 °C for 5 min, before being warmed to the specified temperature (h), and subsequently left at the specified time (i). After this, the mixture was quenched with saturated ammonium chloride. The mixture was extracted with Et_2O, washed with brine, then dried with sodium sulfate, filtered, and evaporated. The crude mixture was analysed by NMR and was purified by column chromatography (eluent: 0-33% Et_2O in petrol) (j).

General Procedure L – Hydroformylation

To a flame-dried microwave vial containing $[Rh(COD)Cl]_2$ (a), *rac*-BINAP (b) and xantphos (c), **62** (d), dissolved in PhMe (e), was charged. Formaldehyde (f) was subsequently added into the reaction mixture, which was then degassed by freeze-pump-thaw cycle, which was repeated 3 times. The microwave vial was then placed into either an oil bath or microwave reactor (g), and heated to the specified temperature (h) for the specified time (i). After this time, the mixture was filtered over celite® to remove the solids, and the filter cake was washed with Et_2O. The solvent was removed, and the crude mixture was purified by silica chromatography (eluent: 0-100% Et_2O in petrol) to afford **170** (j) as a colourless oil and starting material **62** (k).

General Procedure M – Saegusa Oxidation

To a flame-dried round bottom flask, **169** (a) dissolved in DCM (b) was charged, then subsequently Et_3N (c) was added. The reaction mixture was cooled to -5 °C before the dropwise addition of TMSOTf (d) *via* syringe. The resulting mixture was left to stir at this temperature for 30 min. After this time, the mixture was quenched with saturated sodium bicarbonate solution, and extracted with DCM. The organic solution was then dried with sodium sulfate, filtered, and evaporated. The crude mixture was purified by silica chromatography (eluent: 0-33% Et_2O in petrol) to afford **175** (e), which was used immediately in the next step due to its instability. To another flame-dried round bottom flask, isolated **175** (e) dissolved in MeCN (f) was charged, and, subsequently, $Pd(OAc)_2$ (g) was added, and base if necessary (h). The reaction mixture was left at the specified temperature (i) using an oil bath for the specified time (j). After this time, the mixture was filtered over celite® to remove the solids, and the filter cake was washed with Et_2O. The solvent was removed, and the crude mixture was purified by silica chromatography (eluent: 0-33% Et_2O in petrol) to afford **168** (k) as a colourless oil.

*General Procedure N– One-pot PK Using Enyne **95***

To a flame-dried round bottom flask equipped with a condenser, **95** (a) dissolved in 1,2-DCE (b) was charged, and to the resulting mixture $CO_2(CO)_8$ (c) was quickly added. The reaction mixture was stirred at room temperature for 1 h. Once the complexation was completed, monitored by TLC analysis, DodSMe (d) was added to the reaction *via* syringe, and heated to reflux using an oil bath for 5 h. After this time, the reaction mixture was filtered over celite® to remove the solids, and the filter cake was washed with Et_2O. The solvent was removed, and the crude mixture was purified by silica chromatography (eluent: 0-100% Et_2O in petrol) to afford **97** (e) as white solid.

*General Procedure O – PK Using Cobalt Complex **182***

To a flame-dried round bottom flask equipped with a condenser or a flame-dried microwave vial (a), **182** (b) dissolved in the solvent (c) was charged. To the resulting mixture, DodSMe (d) was added *via* syringe, and the solution was heated to the specified temperature (e) using an oil bath for the specified time (f). When stated, during the course of the reaction, further quantities of $Co_2(CO)_8$ and DodSMe were added to the resulting mixture at the

specified time(s) (g). After the full reaction time stated, the reaction mixture was filtered over celite® to remove the solids, and the filter cake was washed with Et_2O. The solvent was removed, and the crude mixture was purified by silica chromatography (eluent: 0-100% Et_2O in petrol) to afford **98** (h) as a yellow oil. Crystallisation was achieved by slow diffusion using petrol, affording yellow crystals.

*General Procedure P– One-pot PK Using Diene-yne **96***

To a flame-dried round bottom flask equipped with a condenser or a flame-dried microwave vial (a), **96** (b) dissolved in the solvent (c) was charged. To the resulting mixture, $Co_2(CO)_8$ (d) was added and the solution was left to stir for 1 h. After this time, DodSMe (e) was added to the reaction *via* syringe, and the solution was heated to the specified temperature (f) using an oil bath for the specified time (g). When stated, during the course of the reaction, further quantities of $Co_2(CO)_8$ and DodSMe were added to the resulting mixture at the specified time(s) (h). After the full reaction time stated, the reaction mixture was filtered over celite® to remove the solids, and the filter cake was washed with Et_2O. The solvent was removed, and the crude mixture was purified by silica chromatography (eluent: 0-100% Et_2O in petrol) to afford **98** (i) as a yellow oil. Crystallisation was achieved by slow diffusion using petrol, affording yellow crystals.

General Procedure Q – Benzylic Bromination

To a flame-dried round bottom flask equipped with a condenser, **97** (a) dissolved in the CCl_4 (b) was charged. To the resulting mixture, NBS (c) and dibenzoyl peroxide (25% in H_2O) (d) were added and the solution was heated to reflux using an oil bath for the specified time (e). After this time, the reaction mixture was diluted with DCM and passed through a small silica plug to remove the solids. The solvent was removed and the crude mixture was analysed by NMR (f).

General Procedure R – Benzylic Oxidation

To a flame-dried microwave vial, **97** (a) and Oxone® (b) were added with $MeNO_2$ (c). To the resulting mixture, KBr (d) was added and the solution was heated to the specified temperature (e) using an oil bath for the specified time (f). After this time, the reaction

mixture was diluted with DCM and passed through a small silica plug to remove the solids. The solvent was removed and the crude mixture was analysed by NMR (g).

General Procedure S – Alkylation via Silyl Enol Ether Formation

To a flame-dried round bottom flask, the specified core (a) dissolved in DCM (b) was charged, then, subsequently, Et_3N (c) was added. The reaction mixture was cooled to -5 °C using an ice bath, and, to the resulting mixture, TMSOTf (d) was added dropwise *via* syringe. The solution was left to stir for 30 min at this temperature before being quenched with saturated sodium bicarbonate solution and extracted with DCM. The organic solution was then dried with sodium sulfate, filtered, and evaporated. The crude silyl enol ether was used immediately in the next step due to its instability. To another flame-dried round bottom flask, the specified crude silyl enol ether (e) dissolved in THF (f) was charged, and subsequently cooled to -10 °C using an ice/salt bath. At this temperature, MeLi (g) was added dropwise *via* syringe, and the solution was left to stir for 20 min. After this time, the resulting mixture was cooled to -78 °C using a dry ice bath. The reaction mixture was left to stir for 1 h at this temperature, and, if specified, the additive (h) was added dropwise *via* syringe during this period. Following this, the electrophile (i) was added dropwise *via* syringe and left to stir for 1 h before being allowed to warm to room temperature overnight. The reaction mixture was quenched with saturated sodium bicarbonate solution and extracted with Et_2O. The organic solution was washed with brine, then dried with sodium sulfate, filtered, and evaporated. The crude mixture was analysed by NMR and/or LCMS, and if applicable, purified by silica chromatography (eluent: 0-100% Et_2O in petrol) (j).

General Procedure T – Alkylation via Silyl Enol Ether Formation using TiCl4 and BF_3•OEt_2

To a flame-dried round bottom flask, the specified core (a) dissolved in DCM (b) was charged, then, subsequently, Et_3N (c) was added. The reaction mixture was cooled to -5 °C using an ice bath, and, to the resulting mixture, TMSOTf (d) was added dropwise *via* syringe. The solution was left to stir for 30 min at this temperature before being quenched with saturated sodium bicarbonate solution and extracted with DCM. The organic solution was then dried with sodium sulfate, filtered, and evaporated. The crude silyl enol ether was used immediately in the next step due to its instability. To another flame-dried round

bottom flask, the specified crude silyl enol ether (e) dissolved in THF (f) was charged, and subsequently cooled to -10 °C using an ice/salt bath. At this temperature, MeLi (g) was added dropwise *via* syringe, and the solution was left to stir for 20 min. After this time, the resulting mixture was cooled to -78 °C using a dry ice bath. The reaction mixture was left to stir for 1 h at this temperature, and, if specified, the additive (h) was added dropwise *via* syringe during this period. Following this, the electrophile (i) was added dropwise *via* syringe and left to stir for 1 h before being allowed to warm to -30 °C and left to stir for 16 h. The reaction mixture was quenched with saturated sodium bicarbonate solution and extracted with Et_2O. The organic solution was washed with brine, then dried with sodium sulfate, filtered, and evaporated. The crude mixture was analysed by NMR and/or LCMS, and if applicable, purified by silica chromatography (eluent: 0-100% Et_2O in petrol) (j).

7.3.2 General Procedures for the Asymmetric Heck Optimisation

Heck General Procedure A – Initial Screening with Ag_3PO_4

To a flame-dried microwave vial, $Pd_2(dba)_3$ (9.16 mg, 0.01 mmol), (*R*)-BINAP (18.7 mg, 0.03 mmol), Ag_3PO_4 (210 mg, 0.50 mmol) and solvent (a) (1.50 mL) were added. The mixture was degassed with argon and left to stir at room temperature for 30 min. After this time, **(*E*)-100** (100 mg, 0.25 mmol) in solvent (a) (1.00 mL) was added into the mixture. Following the addition, the vial was degassed by freeze-pump-thaw cycle, which was repeated 3 times. The microwave vial was sealed, placed into a sand bath, and heated at the 100 °C for 24 h. After this time, the mixture was then diluted with Et_2O and washed with water three times. The organic layer was dried over sodium sulfate, filtered, and evaporated. The crude mixture was purified by column chromatography (eluent: 0-33% Et_2O in petroleum ether), affording product **17** as a colourless oil (b). The resulting oil was dissolved in 95% MeCN:H_2O (0.83 mL) and HCl (0.17 mL, 6.00 M in H_2O) was added. The reaction mixture was left to stir for 3 hours before being diluted with water and extracted with Et_2O. The organic layer was dried with sodium sulfate and passed through a plug of silica (eluent: Et_2O), and **62** was analysed by chiral HPLC to determine the enantiomeric excess (c).

Heck General Procedure B – Initial Screening with Organic Bases

To a flame-dried microwave vial, $Pd_2(dba)_3$ (9.16 mg, 0.01 mmol), (*R*)-BINAP (18.7 mg, 0.03 mmol) and solvent (a) (1.50 mL) were added. The mixture was degassed with argon and left to stir at room temperature for 30 min. After this time, **(*E*)-100** (100 mg, 0.25 mmol) and the organic base (0.5 mmol) (b) in solvent (a) (1.00 mL) was added into the mixture. Following the addition, the vial was degassed by freeze-pump-thaw cycle, which was repeated 3 times. The microwave vial was sealed, placed into a sand bath, and heated 100 °C for 24 h. After this time, the mixture was then diluted with Et_2O and washed with water. The organic layer was dried over sodium sulfate, filtered, and evaporated. The crude mixture was purified by column chromatography (eluent: 0-33% Et_2O in petroleum ether), affording product **17** as a colourless oil (c). The resulting oil was dissolved in 95% MeCN:H_2O (0.83 mL) and HCl (0.17 mL, 6.00 M in H_2O) was added. The reaction mixture was left to stir for 3 hours before being diluted with water and extracted with Et_2O. The organic layer was dried with sodium sulfate and passed through a plug of silica (eluent: Et_2O), and **62** was analysed by chiral HPLC to determine the enantiomeric excess (d).

Heck General Procedure C – Study of Temperature and Time

To a flame-dried microwave vial, $Pd_2(dba)_3$ (9.16 mg, 0.01 mmol), (*R*)-BINAP (18.7 mg, 0.03 mmol), additive (0.50 mmol), and MeCN (1.50 mL) were added. The mixture was degassed with argon and left to stir at room temperature for 30 min. After this time, **(*E*)-100** or **(*E*)-101** (a) (0.25 mmol) and Et_3N (69 µL, 0.50 mmol) in MeCN (1 mL) was added into the mixture. Following the addition, the vial was degassed by freeze-pump-thaw cycle, which was repeated 3 times. The microwave vial was sealed, and placed into a sand bath, and heated at the specified temperature (b) for the specified time (c). After this time, the mixture was then diluted with Et_2O and washed with water three times. The organic layer was dried over sodium sulfate, filtered, and evaporated. The crude mixture was purified by column chromatography (eluent: 0-33% Et_2O in petroleum ether), affording product **17** as a colourless oil (d). The resulting oil was dissolved in 95% MeCN:H_2O (0.83 mL) and HCl (0.17 mL, 6.00 M in H_2O) was added. The reaction mixture was left to stir for 3 hours before being diluted with water and extracted with Et_2O. The organic layer was dried with sodium sulfate and passed through a plug of silica (eluent: Et_2O), and **62** was analysed by chiral HPLC to determine the enantiomeric excess (e).

Heck General Procedure D – Initial Microwave Study

To a flame-dried microwave vial, $Pd_2(dba)_3$ (9.26 mg, 0.01 mmol), (*R*)-BINAP (18.7 mg, 0.03 mmol) and solvent (a) (1.50 mL) were added. The mixture was degassed with argon and left to stir at room temperature for 30 min. After this time, **(*E*)-100** or **(*E*)-101** (b) (0.25 mmol) and Et_3N (69 µL, 0.5 mmol) in solvent (a) (1.00 mL) was added into the mixture. Following the addition, the vial was degassed by freeze-pump-thaw cycle, which was repeated 3 times. The microwave vial was then sealed, placed into a microwave reactor, and heated at the specified temperature (d) for the specified time (e). After this time, the mixture was then diluted with Et_2O and washed with water. The organic layer was dried over sodium sulfate, filtered, and evaporated. The crude mixture was purified by column chromatography (eluent: 0-33% Et_2O in petroleum ether), affording product **17** as a colourless oil (f). The resulting oil was dissolved in 95% MeCN:H_2O (0.83 mL) and HCl (0.17 mL, 6.00 M in H_2O) was added. The reaction mixture was left to stir for 3 hours before being diluted with water and extracted with Et_2O. The organic layer was dried with sodium sulfate and passed through a plug of silica (eluent: Et_2O), and **62** was analysed by chiral HPLC to determine the enantiomeric excess (g).

Heck General Procedure E – Optimisation Using PHOX Ligands

To a flame-dried microwave vial, Pd catalyst (a), chiral ligand (b), and solvent (c) were added. The mixture was degassed with argon whilst stirring at room temperature for 10 min. After this time, **(*E*)-100** or **(*E*)-101** (d) and base (e) in solvent (f) was added into the mixture. Following the addition, the vial was further degassed with argon for 10 minutes. The microwave vial was sealed, placed into a microwave reactor or sand bath (g), and heated at the specified temperature (h) for the specified time (i). After this time, the mixture was then diluted with Et_2O and washed with water. The organic layer was dried over sodium sulfate, filtered, and evaporated. The crude mixture was purified by column chromatography (eluent: 0-33% Et_2O in petroleum ether), affording product **17** as a colourless oil (j). The resulting oil was dissolved in 95% MeCN:H_2O (0.83 mL) and HCl (0.17 mL, 6.0 M in H_2O) was added. The reaction mixture was left to stir for 3 hours before being diluted with water and extracted with Et_2O. The organic layer was dried using sodium sulfate and passed through a plug of silica (eluent: Et_2O), and **62** was analysed by chiral HPLC to determine the enantiomeric excess (k).

Heck General Procedure F – Experiments Performed at GSK, Stevenage

To a microwave vial, Pd_2dba_3 (8.0 mg, 0.01 mmol) and chiral ligand (0.02 mmol) (a) were added and MeCN (0.8 mL) was added. This mixture was degassed with argon for 10 minutes, then left to stir for 20 minutes at room temperature. After this time, **(*E*)-100** (70 mg, 0.17 mmol) and base (0.35 mmol) (b) dissolved in MeCN (0.6 mL) was added into the mixture and degassed, again with argon, for 10 minutes. The reaction mixture was then left to stir at 80° C for 69 h. After this time, the reaction mixture was diluted with Et_2O and filtered through celite®, then the solvent was evaporated to provide the crude product. The conversion of the reaction was estimated by LCMS analysis (c). The samples were dissolved in 1:1 MeOH:DMSO (1.00 mL) and purified by Open Access Mass Directed AutoPrep on an Xbridge column using acetonitrile/water with an ammonium carbonate modifier. The desired fractions were collected, combined and evaporated to give the desired product as an off-white solid, which was directly analysed by chiral HPLC (d). It should be noted that the product from this reaction was compound **17**, i.e. further deprotection of the ketal moiety to determine enantiomeric excess was now unnecessary. Chiral HPLC analysis details are provided on *page 248*.

Heck General Procedure G – Final Optimised Procedure

To a microwave vial, Pd_2dba_3 (8.00 mg, 0.01 mmol), (*R*)-SYNPHOS or (*S*)-SYNPHOS (13.3 mg, 0.02 mmol) (a), and solvent (0.80 mL) (b) were added. The resulting solution was degassed with argon for 10 minutes, then left to stir for 20 minutes at room temperature. After this time, **(*E*)-100 or (*E*)-101** (0.17 mmol) (c) and Et_3N (49 µL, 0.35 mmol) dissolved in solvent (0.60 mL) (b) was added into the mixture and degassed, again with argon, for 10 minutes. The reaction mixture was then left to stir at the specified temperature (d) for the specified time (e) in an oil bath or microwave reactor (f). After this time, the mixture was diluted with Et_2O and washed with water. The organic layer was dried with sodium sulfate, filtered, and evaporated. The crude mixture was purified by column chromatography (eluent: 0-33% Et_2O in petroleum ether), affording the product **17** as a colourless oil (g), which slowly crystallises upon storage at -4 °C, or upon recrystallisation by slow diffusion using petrol. The product was analysed by chiral HPLC to determine the enantiomeric excess (h).

7.4 Synthetic Substrates and Intermediates for Chapter 3

7.4.1 Substrates and Intermediates Towards the Asymmetric Heck Reaction

Preparation of (3-methoxy-2-methylphenyl)methanol ***105***[133]

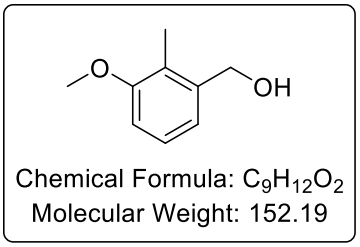

Scheme 3.2

To a flame-dried 3-neck round bottom flask, THF (240 mL) was added and cooled to 0 °C using an ice bath, then lithium aluminium hydride (5.94 g, 157 mmol) was added portion-wise. 3-Methoxy-2-methyl-benzoic acid **19** (20.0 g, 120 mmol) was dissolved in THF (80.0 mL) and was then added dropwise to the hydride solution *via* syringe pump. The mixture was allowed to stir at 0 °C for 20 min, then warmed to room temperature and left to stir for 2 h. After this, the slurry was cooled to 0 °C using an ice bath and quenched slowly with Na_2SO_4•$10H_2O$ and water, forming a white solid. The solid was filtered, the crude mixture was extracted with Et_2O, and washed with brine. The organic solution was dried with sodium sulfate, filtered, and evaporated. The crude mixture was purified by recrystallisation (hexane) to afford **105** (17.4 g, 95%) as a white solid.

Melting point: 60–61 °C.

FTIR (neat): 1470, 1587, 2835, 2859, 2911, 3282 cm^{-1}.

^{1}H NMR δ(400 MHz, $CDCl_3$): 1.62 – 1.58 (m, 1H, OH), 2.22 (s, 3H, $ArCH_3$), 3.83 (s, 3H, $ArOCH_3$), 4.70 (d, *J* = 5.9 Hz, 2H, benzylic CH_2), 6.83 (d, *J* = 8.0 Hz, 1H, ArH), 6.98 (d, *J* = 7.9 Hz, 1H, ArH), 7.18 ppm (t, *J* = 7.9 Hz, 1H, ArH).

^{13}C NMR δ(101 MHz, $CDCl_3$): 11.0, 55.8, 63.8, 110.0, 120.2, 124.9, 126.5, 140.1, 157.9 ppm.

Preparation of (6-iodo-3-methoxy-2-methylphenyl)methanol ***104***[12]

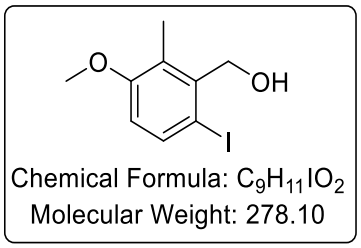

Chemical Formula: $C_9H_{11}IO_2$
Molecular Weight: 278.10

Scheme 3.2

105 (16.7 g, 110 mmol), *N*-iodosuccinimide (27.2 g, 121 mmol) and glacial acetic acid (95.0 mL) were added into a flame-dried round bottom flask wrapped in aluminium foil. The resulting mixture was stirred at room temperature for 3 h under argon. After this time, the solution was diluted with Et_2O and quenched with saturated sodium bicarbonate solution and 10% aqueous solution of sodium thiosulfate. The organic layer was collected, dried with sodium sulfate, filtered, and evaporated. The crude mixture was purified by recrystallisation (hexane) to afford **104** (24.7 g, 81%) as a white solid.

FTIR (neat): 1009, 1256, 1570, 2911, 2934, 3335 cm^{-1}.

^{1}H NMR δ(400 MHz, $CDCl_3$): 1.76 (t, *J* = 6.5 Hz, 1H, OH), 2.37 (s, 3H, $ArCH_3$), 3.81 (s, 3H, $ArOCH_3$), 4.84 (d, *J* = 6.5 Hz, 2H, benzylic CH_2), 6.58 (d, *J* = 8.7 Hz, 1H, ArH), 7.65 ppm (d, *J* = 8.7 Hz, 1H, ArH).

^{13}C NMR δ(101 MHz, $CDCl_3$): 12.6, 55.9, 67.3, 90.2, 112.4, 128.5, 137.1, 141.2, 158.5 ppm.

Preparation of diethyl (2-(methoxy(methyl)amino)-2-oxoethyl)phosphonate ***110***[90]

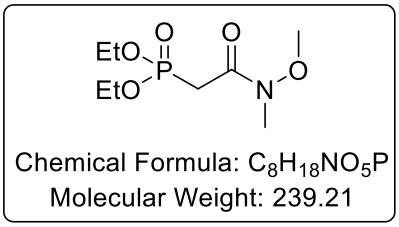

Chemical Formula: $C_8H_{18}NO_5P$
Molecular Weight: 239.21

Scheme 3.3

To a 3-neck round bottom flask fitted with an internal thermometer, *N*-methoxymethylamine hydrochloride salt (10.0 g, 103 mmol) was added and the vessel was charged with DCM (130 mL). The reaction mixture was cooled 0 °C, then triethylamine (28.6 mL, 205 mmol) was slowly added. Chloroacetyl chloride **108** (8.17 mL, 103 mmol) was then added dropwise to the solution. These additions were conducted using a syringe pump and the temperature was maintained below 4 °C throughout. The solution was then allowed to warm to room temperature and stirred for 1 h before quenching the reaction with saturated sodium bicarbonate solution. The two layers were separated, and the organic phase was collected, washed with 1 M HCl and brine, which was then dried over sodium sulfate. The solution was filtered, evaporated, and Weinreb amide **109** was collected as a yellow oil. The crude mixture was transferred to flame-dried round bottom flask equipped with a condenser, and triethylphosphite (17.6 mL, 103 mmol) was then added. The crude mixture was warmed to 80 °C and left to stir for 24 h. Following this, excess triethylphosphite was removed *in vacuo* and the crude mixture was distilled (170 °C at 0.75 mmHg) to afford the **110** (18.0 g, 73% over 2 steps) as a colourless oil.

FTIR (neat): 1022, 1246, 1379, 1655, 2901, 2970 cm^{-1}.

^{1}H NMR δ(400 MHz, $CDCl_3$): 1.26 (t, J = 7.1 Hz, 6H, 2 × CH_3), 3.02 – 3.15 (m, 5H, NCH_3, PCH_2), 3.68 (s, 3H, OCH_3), 4.06 – 4.24 ppm (m, 4H, 2 × OCH_2).

^{13}C NMR δ(101 MHz, $CDCl_3$): 16.3 (d, $^3J_{P\text{-}C}$ = 6.4 Hz), 31.4 (d, $^1J_{P\text{-}C}$ = 136.8 Hz), 32.1, 61.4, 62.5 (d, $^2J_{P\text{-}C}$ = 6.3 Hz), 166.1 ppm.

^{31}P NMR (162 MHz, $CDCl_3$): 21.1 ppm.

Preparation of (E)-3-(6-iodo-3-methoxy-2-methylphenyl)-N-methoxy-N-methylacrylamide ***112***

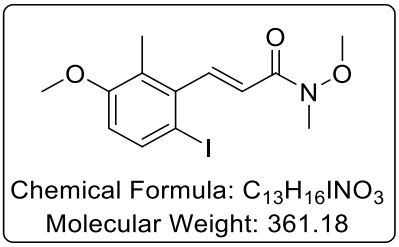

Chemical Formula: $C_{13}H_{16}INO_3$
Molecular Weight: 361.18

Scheme 3.4

A 3-neck round bottom flask was flame-dried then charged with oxalyl chloride (0.80 mL, 9.4 mmol) and DCM (20 mL). The solution was cooled to -78 °C prior to the slow addition of DMSO (1.2 mL, 17 mmol) *via* syringe. The resulting mixture was then stirred at this temperature for 10 min prior to the addition of a solution of **104** (2.0 g, 7.2 mmol) in DCM (4.0 mL). The reaction mixture was left to stir for 15 min before the addition of triethylamine (5.0 mL, 36 mmol). Upon complete addition, the mixture was allowed to warm to room temperature. During the warming process, a pale-yellow slurry formed and the reaction was monitored by TLC. After 8 h, the reaction was quenched with saturated ammonium chloride solution, washed with water and brine. The organic solution was dried over sodium sulfate, filtered, and evaporated to collect the crude mixture of **111**.

In a separate flask, the HWE solution was prepared by dissolving LiCl (0.55 g, 13 mmol) in MeCN (15 mL). The flask was then charged with the phosphonate ester **110** (2.6 g, 11 mmol) and DBU (1.6 mL, 10.8 mmol), and the resulting mixture was stirred at room temperature for 1 h. After this time, the HWE solution was then added into the crude mixture of **104** and left to stir for 24 h. The reaction was quenched with saturated ammonium chloride solution, extracted using Et_2O, dried with sodium sulfate, and evaporated. The resulting crude mixture was purified by column chromatography (eluent: 0-33% Et_2O in petrol), affording the product **112** (1.9 g, 74% over 2 steps) as a pale-yellow solid.

Melting point: 109–110 °C.

FTIR (neat): 1111, 1381, 1452, 1620, 1653, 2959, 2999 cm^{-1}.

^{1}H NMR δ(400 MHz, $CDCl_3$): 2.25 (s, 3H, $ArCH_3$), 3.32 (s, 3H, NCH_3), 3.74 (s, 3H, OCH_3), 3.82 (s, 3H, $ArOCH_3$), 6.59 – 6.64 (m, 2H, olefinic CH, ArH), 7.67 – 7.72 ppm (m, 2H, olefinic CH, ArH).

^{13}C NMR δ(101 MHz, $CDCl_3$): 14.5, 32.7, 55.9, 62.3, 87.6, 111.9, 123.7, 126.9, 136.9, 140.5, 145.8, 158.3, 166.2 ppm.

HRMS *m*/*z* (ESI): Calc. for $C_{13}H_{17}INO_3$ (M^++H): 362.0248. Found: 362.0249.

Preparation of 3-(6-iodo-3-methoxy-2-methylphenyl)-N-methoxy-N-methylpropanamide ***106***

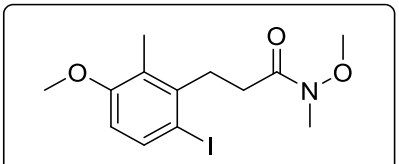

Chemical Formula: $C_{13}H_{18}INO_3$
Molecular Weight: 363.20

Scheme 3.7, Table 3.1

The following experiments were performed using *General Procedure A*. Results are reported as: (a) amount of **112**, (b) amount of catalyst, (c) volume of solvent, (d) temperature, (e) time, and (f) conversion by ^{1}H NMR analysis, comparing peaks at 3.74 ppm (**112**) and 3.68 ppm (**106**).

Entry 1: (a) 140 mg, 0.40 mmol, (b) **118**, 6.7 mg, 4.0 µmol, (c), DCM, 4.0 mL, (d) RT, (e) 16 h, and (f) No conversion.

Entry 2: (a) 140 mg, 0.40 mmol, (b) **118**, 33 mg, 20.0 µmol, (c), DCM, 4.0 mL, (d) RT, (e) 16 h, and (f) 2%.

Entry 3: (a) 140 mg, 0.40 mmol, (b) **119**, 37 mg, 20.0 µmol, (c) DCM, 4.0 mL, (d) RT, (e) 16 h, and (f) 11%.

Entry 4: (a) 140 mg, 0.40 mmol, (b) **119**, 37 mg, 20.0 µmol, (c) DCM, 4.0 mL, (d) 35 °C, (e) 40 h, and (f) 23%.

Entry 5: (a) 140 mg, 0.40 mmol, (b) **120**, 25 mg, 30.0 µmol, (c) DCM, 4.0 mL, (d) RT, (e) 24 h, and (f) 21%.

Entry 6: (a) 140 mg, 0.40 mmol, (b) **119**, 37 mg, 20.0 µmol, (c) PhMe, 4.0 mL, (d) RT, (e) 16 h, and (f) 16%.

Entry 7: (a) 140 mg, 0.40 mmol, (b) **121**, 20 mg, 20.0 µmol, (c) PhMe, 4.0 mL, (d) RT, (e) 16 h, and (f) 4%.

Melting point: 70–72 °C.

FTIR (neat): 1092, 1256, 1458, 1649, 2936, 2959 cm^{-1}.

^{1}H NMR δ(400 MHz, $CDCl_3$): 2.28 (s, 3H, $ArCH_3$), 2.54 – 2.65 (m, 2H, alkyl CH_2), 3.09 – 3.17 (m, 2H, benzylic CH_2), 3.22 (s, 3H, NCH_3), 3.68 (s, 3H, OCH_3), 3.79 (s, 3H, $ArOCH_3$), 6.50 (d, *J* = 8.7 Hz, 1H, ArH), 7.64 ppm (d, *J* = 8.7 Hz, 1H, ArH).

^{13}C NMR δ(101 MHz, $CDCl_3$): 12.9, 31.1, 33.4, 55.8, 61.5, 90.7, 107.8, 110.7, 126.8, 137.1, 142.6, 158.3, 173.5 ppm.

HRMS *m*/*z* (ESI): Calc. for $C_{13}H_{19}INO_3$ (M^++H): 364.0404. Found: 364.0399.

*Preparation of (E)-N-methoxy-3-(3-methoxy-2-methylphenyl)-N-methylacrylamide **122***

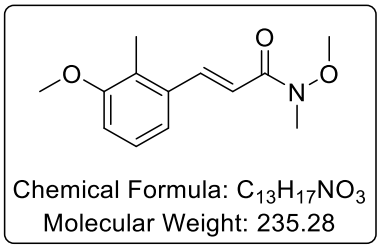

Chemical Formula: $C_{13}H_{17}NO_3$
Molecular Weight: 235.28

Scheme 3.9

A 3-neck round bottom flask equipped with a dropping funnel was flame-dried and charged with oxalyl chloride (10.7 mL, 125 mmol) and DCM (130 mL). The solution was cooled to -78°C prior to the dropwise addition of a mixture of DMSO (15.7 mL, 221 mmol) and DCM (130 mL). The resulting solution was then stirred at this temperature for 10 min prior to the addition of a solution of **105** (14.6 g, 96.2 mmol) in dry DCM (65.0 mL). The reaction mixture was left to stir for 15 min before addition of triethylamine (66.6 mL, 481 mmol). Upon complete addition, the mixture was allowed to warm to room temperature. During the warming process, a pale-yellow slurry formed and the reaction was monitored by TLC. After 8 h, the reaction was quenched with saturated ammonium chloride solution, extracted with DCM, and washed with water and brine. The organic solution was dried over sodium sulfate, filtered, and evaporated to collect the crude mixture of the aldehyde intermediate **124**.

In a separate flask, the HWE solution was prepared by dissolving LiCl (7.34 g, 173 mmol) in MeCN (195 mL). The flask was then charged with the phosphonate ester **110** (34.5 g, 144 mmol) and DBU (21.5 mL, 144 mmol), and the resulting mixture was stirred at room temperature for 1 h. After this time, the HWE solution was then added into the aldehyde crude mixture and left to stir for 24 h. The reaction was quenched with saturated ammonium chloride solution, extracted using Et_2O, dried with sodium sulfate, and evaporated. The resulting crude mixture was purified by column chromatography (eluent: 0-33% Et_2O in petrol), affording the product **122** (19.9 g, 88% over two steps) as a pale-yellow solid.

Melting point: 81–83 °C.

FTIR (neat): 1665, 2932, 2963 cm^{-1}.

^{1}H NMR δ(400 MHz, $CDCl_3$): 2.31 (s, 3H, $ArCH_3$), 3.31 (s, 3H, NCH_3), 3.76 (s, 3H, OCH_3), 3.84 (s, 3H, $ArOCH_3$), 6.86 (dd, J = 7.7, ^{4}J = 1.4 Hz, 1H, ArH), 6.92 (d, J = 15.6 Hz, 1H, olefinic CH), 7.14 – 7.23 (m, 2H, ArH), 8.05 ppm (d, J = 15.6 Hz, 1H, olefinic CH).

^{13}C NMR δ(101 MHz, $CDCl_3$): 11.8, 32.7, 55.9, 62.0, 111.2, 118.0, 119.0, 126.4, 126.9, 135.8, 141.7, 158.2, 167.2 ppm.

HRMS *m*/*z* (ESI): Calc. for $C_{13}H_{18}NO_3$ (M^++H): 236.1282. Found: 236.1281.

*Preparation of N-methoxy-3-(3-methoxy-2-methylphenyl)-N-methylpropanamide **123***

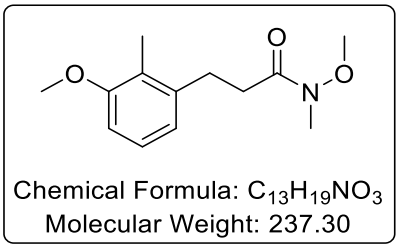

Scheme 3.10 Table 3.2

The following experiments were performed using *General Procedure A*. Results are reported as: (a) amount of **122**, (b) amount of catalyst, (c) volume of solvent, (d) temperature, (e) time, and (f) isolated yield of **123**.

Entry 1: (a) 94 mg, 0.41 mmol, (b) **119**, 6.7 mg, 4.1 µmol, (c), DCM, 4 mL, (d) RT, (e) 16 h, and (f) 92 mg, 97%.

Entry 2: (a) 94 mg, 0.41 mmol, (b) 10% Pd/C, 4.3 mg, 0.04 mmol, (c), MeOH, 13 mL, (d) RT, (e) 16 h, and (f) 91 mg, 96%.

Entry 3

122 (6.00 g, 25.5 mmol), 10% Pd/C (271 mg, 2.55 mmol) and methanol (500 mL) were added into a 1 L Parr hydrogenation apparatus equipped with a magnetic stirrer bar and placed under an atmosphere of hydrogen (5 atm) for 24 hours. After this time, the mixture was filtered over celite® to remove the solids, and the filter cake was washed with DCM. The solvent was removed, and the crude mixture was purified by column chromatography (eluent: 0-33% Et_2O in petrol), affording the product **123** (5.53 g, 91%) as a pale-yellow solid.

Melting point: 38–40 °C.

FTIR (neat): 1665, 2932, 2963 cm^{-1}.

^{1}H NMR δ(400 MHz, $CDCl_3$): 2.20 (s, 3H, $ArCH_3$), 2.63 – 2.70 (m, 2H, alkyl CH_2), 2.92 – 2.99 (m, 2H, benzylic CH_2), 3.19 (s, 3H, NCH_3), 3.62 (s, 3H, OCH_3), 3.82 (s, 3H, $ArOCH_3$), 6.73 (d, *J* = 7.9 Hz, 1H, ArH), 6.82 ppm (d, *J* = 7.9 Hz, 1H, ArH), 7.10 (t, *J* = 7.9 Hz, 1H, ArH).

^{13}C NMR δ(101 MHz, $CDCl_3$): 11.3, 28.7, 32.4, 33.0, 55.7, 61.3, 108.4, 121.5, 124.8, 126.3, 140.94, 158.0, 174.0 ppm

HRMS *m*/*z* (ESI): Calc. for $C_{13}H_{20}NO_3$ (M^++H): 238.1439. Found: 238.1438.

Preparation of 3-(6-iodo-3-methoxy-2-methylphenyl)-N-methoxy-N-methylpropanamide ***106***

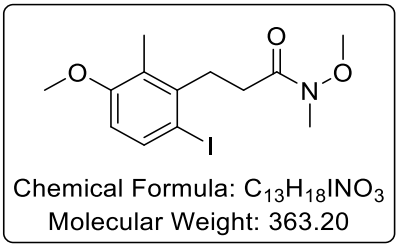

Scheme 3.11

123 (5.53 g, 23.3 mmol), *N*-iodosuccinimide (5.77 g, 25.6 mmol) and glacial acetic acid (20.0 mL) were added into a flame-dried round bottom flask wrapped in aluminium foil. The resulting mixture was stirred at room temperature for 3 h under argon. After this time, the solution was diluted with Et_2O and quenched with saturated sodium bicarbonate solution and 10% aqueous solution of sodium thiosulfate. The organic layer was collected, dried with sodium sulfate, filtered, and evaporated. The resulting crude mixture was purified by column chromatography (eluent: 0-33% Et_2O in petrol), affording the product **106** as a pale-yellow solid (8.11 g, 96%).

Data for this compound was consistent with that detailed on page 212.

*Preparation of 3-(6-hydroxy-3-methoxy-2-methylphenyl)-N-methoxy-N-methylpropanamide **125***

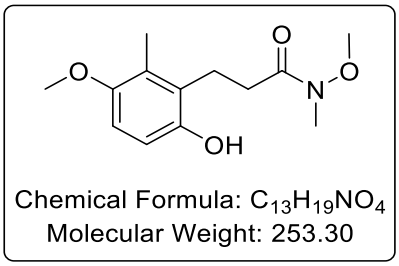

Chemical Formula: $C_{13}H_{19}NO_4$
Molecular Weight: 253.30

Scheme 3.13, Table 3.3

The following experiments were performed using *General Procedure B*. Results are reported as: (a) amount of $Pd(OAc)_2$, (b) amount of K_2CO_3, (c) amount of B_2Pin_2, (d) amount of **106**, (e) volume of DMA, (f) volume of 1,4-dioxane, (g) amount of K_2CO_3, (h) volume of H_2O_2, and (i) isolated yield of **125** over two steps.

Entry 1: (a) 6.3 mg, 0.03 mmol, (b) 230 mg, 1.7 mmol, (c) 180 mg, 0.72 mmol, (d) 200 mg, 0.55 mmol, (e) 5.0 mL, (f) 7.0 mL, (g) 230 mg, 1.7 mmol, (h) 0.56 mL, 9.8 M in H_2O, 5.5 mmol, and (i) 140 mg, 56%.

Entry 2: (a) 110 mg, 0.15 mmol, (b), 1.2 g, 8.9 mmol, (c) 0.83 g, 3.3 mmol, (d) 1.1 g, 3.0 mmol, (e) 40 mL, (f) 7.0 mL, (g) 1.2 g, 8.9 mmol, (h) 3 mL, 9.8 M in H_2O, 30 mmol, and (i) 0.30 g, 40%.

The following experiments were performed using *General Procedure C*. Results are reported as: (a) amount of $Pd(OAc)_2$, (b) amount of K_2CO_3, (c) amount of B_2Pin_2, (d) amount of **106**, (e) volume of DMA, (f) volume of acetone, (g) amount of Oxone®, (h) volume of water, and (i) isolated yield of **125** over two steps.

Entry 3: (a) 6.3 mg, 0.03 mmol, (b), 230 mg, 1.7 mmol, (c) 180 mg, 0.72 mmol, (d) 200 mg, 0.55 mmol, (e) 5.0 mL, (f) 9.6 mL, (g) 83.7 mg, 0.55 mmol, (h) 9.6 mL, and (i) 140 mg, 72%.

Entry 4: (a) 65 mg, 0.29 mmol, (b), 2.4 g, 17 mmol, (c) 1.8 g, 6.9 mmol, (d) 2.1 g, 5.8 mmol, (e) 53 mL, (f) 2.1 g, (f) 120 mL, (g) 0.88 g, 5.8 mmol, (h) 120 mL, and (i) 1.5 g, 74%.

Melting point: 113–115 °C.

FTIR (neat): 1260, 1456, 1634, 2941, 2997, 3111, 3204 cm^{-1}.

^{1}H NMR δ(400 MHz, $CDCl_3$): 2.19 (s, 3H, $ArCH_3$), 2.81 – 2.85 (m, 2H, alkyl CH_2), 2.97 (dd, *J* = 7.0, 4.4 Hz, 2H, benzylic CH_2), 3.17 (s, 3H, NCH_3), 3.63 (s, 3H, OCH_3), 3.76 (s, 3H, $ArOCH_3$), 6.68 (d, *J* = 8.8 Hz, 1H, ArH), 6.78 (d, *J* = 8.8 Hz, 1H, ArH), 8.65 ppm (s, 1H, OH).

^{13}C NMR δ(101 MHz, $CDCl_3$): 12.0, 20.5, 31.9, 32.5, 56.2, 61.2, 110.3, 115.3, 126.1, 128.3, 149.2, 151.8, 175.8 ppm.

HRMS *m*/*z* (ESI): Calc. for $C_{13}H_{20}NO_4$ (M^++H): 254.1386. Found: 254.1387.

Preparation of 4-methoxy-2-(3-(methoxy(methyl)amino)-3-oxopropyl)-3-methylphenyl trifluoromethanesulfonate ***107***

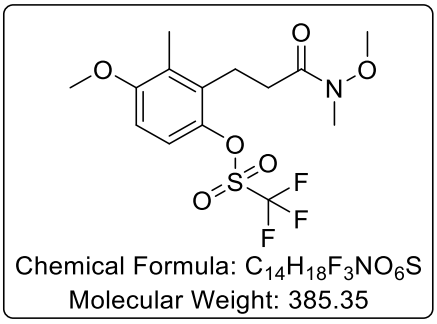

Scheme 3.14

To a flame-dried round bottom flask, **125** (1.00 g, 3.95 mmol), as a solution in DCM (10 mL), and Et_3N (1.10 mL, 7.90 mmol) were added. The resulting mixture was cooled to -78 °C then Tf_2O (0.86 mL, 5.14 mmol) was added dropwise. After this addition, the solution was warmed to -10 °C and left at this temperature for 1 h. The reaction mixture was allowed to warm to room temperature before being quenched with saturated K_2CO_3, washed with 1 M HCl and brine. The organic layer was collected, dried with sodium sulfate, filtered, and evaporated. The resulting crude mixture was purified by column chromatography (eluent: 0-33% Et_2O in petrol), affording the product **107** (1.40 g, 92%) as a pale-yellow oil.

FTIR (neat): 1136, 1207, 1416, 1663, 2941, 2968 cm^{-1}.

^{1}H NMR δ(400 MHz, $CDCl_3$): 2.24 (s, 3H, $ArCH_3$), 2.59 – 2.68 (m, 2H, alkyl CH_2), 3.14 – 2.99 (m, 2H, benzylic CH_2), 3.20 (s, 3H, NCH_3), 3.65 (s, 3H, OCH_3), 3.83 (s, 3H, $ArOCH_3$), 6.73 (d, J = 9.1 Hz, 1H, ArH), 7.10 ppm (d, J = 9.1 Hz, 1H, ArH).

^{13}C NMR δ(101 MHz, $CDCl_3$): 12.1, 22.6, 31.5, 32.3, 55.9, 61.4, 108.8, 118.8 (q, $^1J_{C\text{-}F}$ = 319 Hz, CF_3), 119.1, 128.1, 133.7, 142.0, 157.3, 173.1 ppm.

^{19}F NMR δ(362 MHz, $CDCl_3$): -73.9 ppm.

HRMS *m*/*z* (ESI): Calc. for $C_{14}H_{19}F_3NO_6S$ (M^++H): 386.0878. Found: 386.0880.

Preparation of (E)-2-bromobut-2-ene ***(E)-127***[96]

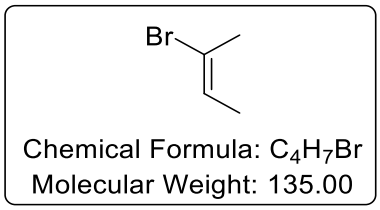

Scheme 3.16

A flame-dried round bottom flask was charged with *meso*-2,3-dibromobutene **126** (6.00 mL, 49.2 mmol), DBU (8.08 mL, 54.1 mmol), and dry DMSO (30.0 mL). The reaction was wrapped in aluminium foil and allowed to react for 16 h. The product was directly distilled (85 °C at 760 mmHg) from the reaction mixture. To ensure complete purity of **(*E*)-127**, the product was again distilled (85 °C at 760 mmHg) from calcium hydride, affording **(*E*)-127** (3.72 g, 56%) as a colourless oil.

FTIR (neat): 1121, 1381, 1429, 1655 cm^{-1}.

^{1}H NMR δ(400 MHz, $CDCl_3$): 1.61 (dq, J = 7.1, ^{5}J = 1.2 Hz, 3H, vinyl CH_3), 2.21 (app p, $^{4}J = {}^{5}J$ = 1.2 Hz, 3H, vinyl CH_3), 5.89 ppm (qq, J = 7.1, ^{4}J = 1.2 Hz, 1H, olefinic CH).

^{13}C NMR δ(101 MHz, $CDCl_3$): 15.1, 22.9, 119.6, 126.7 ppm.

HRMS *m*/*z* (ESI): Calc. for $C_4H_6{}^{76}Br$ (M^+-H): 132.9653. Found: 132.9650.

Preparation of (E)-1-(6-iodo-3-methoxy-2-methylphenyl)-4-methylhex-4-en-3-one ***(E)-129***

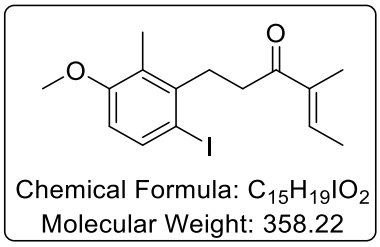

Chemical Formula: $C_{15}H_{19}IO_2$
Molecular Weight: 358.22

Scheme 3.17

Magnesium turnings (2.00 g, 82.3 mmol) were added to a 3-neck round bottom flask equipped with a condenser and were flame-dried prior to being left to stir under argon overnight. Following this, Et_2O (48.0 mL) and PhMe (12.0 mL) were charged into the flask, and stirred vigorously while 1,2-dibromoethane (5.15 mL, 59.7 mmol) was added slowly such that a gentle reflux was observed during the addition. Once complete, the mixture was left to stir at 50 °C for 1 h, then left to settle.

To a separate 3-neck round bottom flask, (*E*)-2-bromo-2-butene **127** (1.56 mL, 15.3 mmol), TMEDA (5.97 mL, 39.1 mmol) and Et_2O (58.0 mL) were added and cooled to -78 °C. ^{t}BuLi (23.0 mL, 1.70 M in pentanes, 39.1 mmol) was then added slowly and the mixture was left to stir at this temperature for 1 h. The previously prepared $MgBr_2$•Et_2O solution (15.3 mL, 1.00 M in Et_2O/PhMe, 15.3 mmol) was then added and the mixture was allowed to warm to 0 °C and left for 1 h. **106** (5.05 g, 13.9 mmol), dissolved in Et_2O (25.0 mL), was added into the mixture and the slurry was stirred at 0 °C for 1 h, then a further 1 h at room temperature. The mixture was then quenched with water and extracted with Et_2O. The organic layer was dried over sodium sulfate, filtered, and evaporated. The crude mixture was purified by column chromatography (eluent: 0-33% Et_2O in petrol), affording the product **(*E*)-129** (4.55 g, 91%) as a pale-yellow oil.

FTIR (neat): 1113, 1253, 1454, 1566, 1663, 2833, 2961 cm^{-1}.

^{1}H NMR δ(400 MHz, $CDCl_3$): 1.79 – 1.87 (m, 6H, 2 × vinyl CH_3), 2.24 (s, 3H, $ArCH_3$), 2.77 – 2.85 (m, 2H, alkyl CH_2), 3.06 – 3.13 (m, 2H, benzylic CH_2), 3.79 (s, 3H, $ArOCH_3$), 6.49 (d, J = 8.7 Hz, 1H, ArH), 6.79 (qq, J = 6.9, ^{4}J = 1.3 Hz, 1H, olefinic CH), 7.63 ppm (d, J = 8.7 Hz, 1H, ArH).

^{13}C NMR δ(101 MHz, $CDCl_3$): 11.2, 12.9, 14.9, 33.6, 36.2, 55.8, 90.7, 110.7, 126.6, 137.1, 137.8, 138.2, 142.9, 158.3, 200.5 ppm.

HRMS *m*/*z* (ESI): Calc. for $C_{15}H_{20}IO_2$ (M^++H): 359.0508. Found: 359.0509.

See the Appendix section for NOSEY data for this compound (page 352).

Preparation of (E)-4-methoxy-3-methyl-2-(4-methyl-3-oxohex-4-en-1-yl)phenyl trifluoromethanesulfonate ***(E)-130***

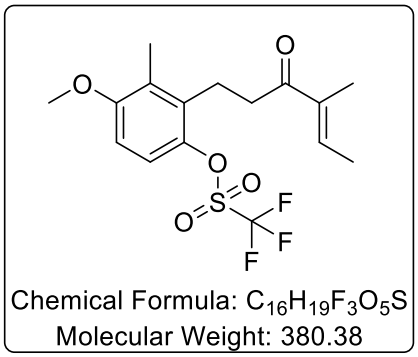

Chemical Formula: $C_{16}H_{19}F_3O_5S$
Molecular Weight: 380.38

Scheme 3.17

Magnesium turnings (0.80 g, 32.9 mmol) were added to a 3-neck round bottom flask equipped with a condenser and were flame-dried prior to being left to stir under argon overnight. Following this, Et_2O (11.0 mL) and PhMe (6.00 mL) were charged into the flask, and stirred vigorously while 1,2-dibromoethane (2.06 mL, 23.9 mmol) was added slowly such that a gentle reflux was observed during the addition. Once complete, the mixture was left to stir at 50 °C for 1 h, then left to settle.

To a separate flame-dried 3-neck round bottom flask, (*E*)-2-bromo-2-butene **127** (0.29 mL, 2.86 mmol), TMEDA (1.12 mL, 7.31 mmol) and Et_2O (11.0 mL) were added and cooled to -78 °C. ^{t}BuLi (4.30 mL, 1.70 M in pentanes, 7.31 mmol) was then added slowly and the mixture was left to stir at this temperature for 1 h. The previously prepared $MgBr_2$•Et_2O solution (2.86 mL, 1.00 M in Et_2O/PhMe, 2.86 mmol) was then added and the mixture was allowed to warm to 0 °C and left for 1 h. **107** (1.00 g, 2.60 mmol), dissolved in Et_2O (5.00 mL), was added into the mixture and the slurry was stirred at 0 °C for 1 h, then a further 1 h at room temperature. The mixture was then quenched with water and extracted with Et_2O. The organic layer was dried over sodium sulfate, filtered, and evaporated. The crude mixture was purified by column chromatography (eluent: 0-33% Et_2O in petrol), affording the product **(*E*)-130** (0.86 g, 87%) as a pale-yellow oil.

FTIR (neat): 1584, 2893, 2978 cm^{-1}.

^{1}H NMR δ(400 MHz, $CDCl_3$): 1.78 – 1.87 (m, 6H, 2 × vinyl CH_3), 2.20 (s, 3H, $ArCH_3$), 2.81 – 2.88 (m, 2H, alkyl CH_2), 2.96 – 3.05 (m, 2H, benzylic CH_2), 3.83 (s, 3H, $ArOCH_3$), 6.70 – 6.77 (m, 2H, ArH, olefinic CH), 7.09 ppm (d, J = 9.1 Hz, 1H, ArH).

^{13}C NMR δ(101 MHz, $CDCl_3$): 11.1, 12.2, 14.9, 22.9, 36.5, 56.0, 108.7, 118.8 (q, $^{1}J_{C\text{-}F}$ = 320 Hz, CF_3), 119.0, 127.9, 134.0, 137.9, 138.1, 142.0, 157.4, 200.0 ppm.

^{19}F NMR δ(362 MHz, $CDCl_3$): -73.9 ppm.

HRMS *m*/*z* (ESI): Calc. for $C_{16}H_{20}F_3O_5S$ (M^++H): 381.0984. Found: 381.0987.

See the Appendix section for NOSEY data for this compound (page 353).

Preparation of (E)-2-(but-2-en-2-yl)-2-(6-iodo-3-methoxy-2-methylphenethyl)-1,3-dioxolane ***(E)-100***

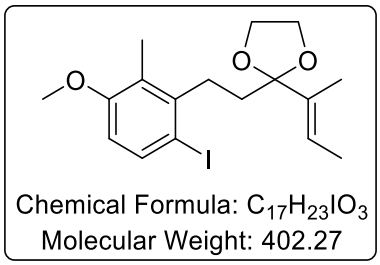

Scheme 3.17

To a round bottom flask connected to a Dean-Stark apparatus, **(*E*)-129** (0.70 g, 2.0 mmol), ethylene glycol (1.1 mL, 20 mmol), *p*-TsOH (0.05 g, 0.29 mmol) and PhMe (5.0 mL) were added. The mixture was heated to reflux for 6 h. After this time, the mixture was diluted with Et_2O, washed with saturated sodium bicarbonate solution and water. The organic solution was then dried with sodium sulfate, filtered, and evaporated. The crude mixture was purified using column chromatography (eluent: 0-33% Et_2O in petrol) to afford **(*E*)-100** (0.59 g, 75%) as a colourless oil.

FTIR (neat): 1105, 1254, 1456, 2882, 2932 cm^{-1}.

^{1}H NMR δ(400 MHz, $CDCl_3$): 1.61 – 1.70 (m, 6H, 2 × vinyl CH_3), 1.83 – 1.89 (m, 2H, alkyl CH_2), 2.25 (s, 3H, $ArCH_3$), 2.78 – 2.87 (m, 2H, benzylic CH_2), 3.78 (s, 3H, $ArOCH_3$), 3.81 – 3.87 (m, 2H, OCH_2), 3.96 – 4.01 (m, 2H, OCH_2), 5.78 (qq, J = 6.9, ^4J = 1.3 Hz, 1H, olefinic CH), 6.46 (d, J = 8.7 Hz, 1H, ArH), 7.60 (d, J = 8.7 Hz, 1H, ArH).

^{13}C NMR δ(100 MHz, $CDCl_3$): 12.4, 12.7, 13.3, 33.0, 35.0, 55.8, 64.5, 90.8, 100.1, 110.4, 111.2, 120.9, 126.6, 134.3, 136.9, 143.5, 158.2 ppm.

HRMS *m*/*z* (ESI): Calc. for $C_{17}H_{24}IO_3$ (M^++H): 403.0770. Found: 403.0770.

Preparation of (E)-2-(2-(2-(but-2-en-2-yl)-1,3-dioxolan-2-yl)ethyl)-4-methoxy-3-methylphenyl trifluoromethanesulfonate ***(E)-101***

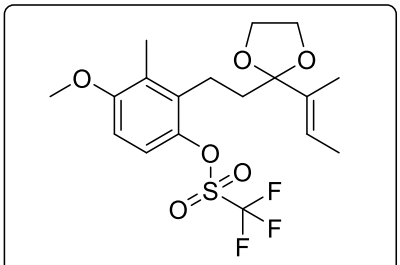

Scheme 3.17

To a round bottom flask connected to a Dean-Stark apparatus, **(*E*)-130** (0.86 g, 2.3 mmol), ethylene glycol (1.2 mL, 23 mmol), *p*-TsOH (65 mg, 0.34 mmol) and PhMe (13 mL) were added. The mixture was heated to reflux for 6 h. After this time, the mixture was diluted with Et_2O, washed with saturated sodium bicarbonate solution and water. The organic solution was then dried with sodium sulfate, filtered, and evaporated. The crude mixture was purified using column chromatography (eluent: 0-33% Et_2O in petrol) to afford **(*E*)-101** (0.72 g, 75%) as a colourless oil.

FTIR (neat): 1585, 2893, 2961 cm^{-1}.

^{1}H NMR δ(400 MHz, $CDCl_3$): 1.60 – 1.66 (m, 6H, 2 × vinyl CH_3), 1.82 – 1.88 (m, 2H, alkyl CH_2), 2.20 (s, 3H, $ArCH_3$), 2.69 – 2.76 (m, 2H, benzylic CH_2), 3.80 – 3.88 (m, 5H, OCH_3, OCH_2), 3.91 – 3.99 (m, 2H, OCH_2), 5.76 – 5.82 (m, 1H, olefinic CH), 6.46 (d, J = 9.1 Hz, 1H, ArH), 7.06 ppm (d, J = 9.1 Hz, 1H, ArH).

^{13}C NMR δ(100 MHz, $CDCl_3$): 11.9, 12.0, 132, 22.0, 35.6, 55.9, 64.5 (2 peaks), 108.3, 111.0, 118.8, 118.8 (q, $^1J_{C\text{-}F}$ = 317 Hz, CF_3), 121.2, 127.8, 134.0, 134.7, 142.1, 157.1 ppm.

^{19}F NMR δ(101 MHz, $CDCl_3$): -73.9 ppm.

HRMS *m*/*z* (ESI): Calc. for $C_{18}H_{24}F_3O_6S$ (M^++H): 425.1245. Found: 425.1242.

Preparation of (Z)-1-(6-iodo-3-methoxy-2-methylphenyl)-4-methylhex-4-en-3-one ***(Z)-129***

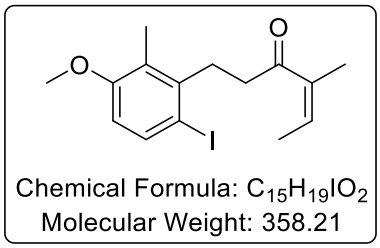

Chemical Formula: $C_{15}H_{19}IO_2$
Molecular Weight: 358.21

Scheme 3.18

Magnesium turnings (0.40 g, 17 mmol) were added to a 3-neck round bottom flask equipped with a condenser and were flame-dried prior to being left to stir under argon overnight. Following this, Et_2O (9.5 mL) and PhMe (2.5 mL) were charged into the flask, and stirred vigorously while 1,2-dibromoethane (1.0 mL, 12 mmol) was added slowly such that a gentle reflux was observed during the addition. Once complete, the mixture was left to stir at 50 °C for 1 h, then left to settle.

To a separate flame-dried 3-neck round bottom flask, (*Z*)-2-bromo-2-butene **(*Z*)-127** (0.16 mL, 1.5 mmol), TMEDA (0.59 mL, 3.9 mmol) and Et_2O (7.0 mL) were added and cooled to -78 °C. ^{t}BuLi (2.4 mL, 1.6 M in pentanes, 3.9 mmol) was then added slowly and the mixture was left to stir at this temperature for 1 h. The previously prepared $MgBr_2$•Et_2O solution (1.5 mL, 1.0 M in Et_2O/PhMe, 1.5 mmol) was then added and the mixture was allowed to warm to 0 °C and left for 1 h. **106** (0.50 g, 1.4 mmol), dissolved in Et_2O (3.0 mL), was added into the mixture and the slurry was stirred at 0 °C for 1 h, then a further 1 h at room temperature. The mixture was then quenched with water and extracted with Et_2O. The organic layer was dried over sodium sulfate, filtered, and evaporated. The crude mixture was purified by column chromatography (eluent: 0-33% Et_2O in petrol), affording the product **(*Z*)-129** as a pale-yellow oil (0.38 g, 78%).

FTIR (neat): 1252, 1454, 1566, 1686, 2833, 2938 cm^{-1}.

^{1}H NMR δ(400 MHz, $CDCl_3$): 1.88 – 1.95 (m, 6H, 2 × vinyl CH_3), 2.25 (s, 3H, $ArCH_3$), 2.67 – 2.74 (m, 2H, alkyl CH_2), 3.07 – 3.16 (m, 2H, benzylic CH_2), 3.79 (s, 3H, OCH_3), 5.83 (qq, J = 6.9, ^{4}J = 1.3 Hz, 1H, olefinic CH), 6.49 (d, J = 8.7 Hz, 1H, ArH), 7.63 ppm (d, J = 8.7 Hz, 1H, ArH).

^{13}C NMR δ(101 MHz, $CDCl_3$): 11.2, 12.9, 14.9, 33.6, 36.2, 55.8, 90.7, 110.7, 126.6, 137.1, 137.8, 138.2, 142.9, 158.3, 200.5 ppm.

HRMS *m*/*z* (ESI): Calc. for $C_{15}H_{20}IO_2$ (M^++H): 359.0508. Found: 359.0505.

See the Appendix section for NOSEY data for this compound (page 354).

Preparation of (Z)-4-methoxy-3-methyl-2-(4-methyl-3-oxohex-4-en-1-yl)phenyl trifluoromethanesulfonate ***(Z)-130***

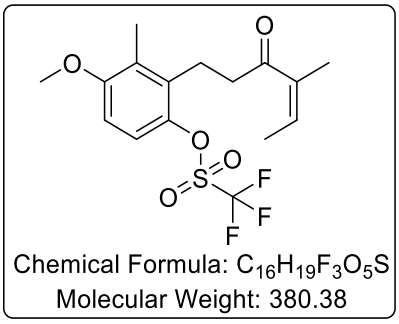

Scheme 3.18

Magnesium turnings (0.40 g, 17 mmol) were added to a 3-neck round bottom flask equipped with a condenser and were flame-dried prior to being left to stir under argon overnight. Following this, Et_2O (9.5 mL) and PhMe (2.5 mL) were charged into the flask, and stirred vigorously while 1,2-dibromoethane (1.0 mL, 12 mmol) was added slowly such that a gentle reflux was observed during the addition. Once complete, the mixture was left to stir at 50 °C for 1 h, then left to settle.

To a separate flame-dried 3-neck round bottom flask, (*Z*)-2-bromo-2-butene **(*Z*)-127** (0.12 mL, 1.4 mmol), TMEDA (0.55 mL, 3.7 mmol) and Et_2O (5.5 mL) were added and cooled to -78 °C. ^{t}BuLi (2.4 mL, 1.5 M in pentanes, 3.7 mmol) was then added slowly and the mixture was left to stir at this temperature for 1 h. The previously prepared $MgBr_2$•Et_2O solution (1.4 mL, 1.0 M in Et_2O/PhMe, 1.4 mmol) was then added and the mixture was allowed to warm to 0 °C and left for 1 h. **107** (0.50 g, 1.3 mmol), dissolved in Et_2O (5.0 mL), was added into the mixture and the slurry was stirred at 0 °C for 1 h, then a further 1 h at room temperature. The mixture was then quenched with water and extracted with Et_2O. The organic layer was dried over sodium sulfate, filtered, and evaporated. The crude mixture was purified by column chromatography (eluent: 0-33% Et_2O in petrol), affording the product **(*Z*)-130** (0.21 g, 43%) as a pale-yellow oil.

FTIR (neat): 1263, 1411, 1584, 1686, 2839, 2941 cm^{-1}.

^{1}H NMR δ(400 MHz, $CDCl_3$): 1.85 – 1.92 (m, 6H, 2 × vinyl CH_3), 2.21 (s, 3H, $ArCH_3$), 2.68 – 2.76 (m, 2H, alkyl CH_2), 2.98 – 3.05 (m, 2H, benzylic CH_2), 3.83 (s, 3H, $ArOCH_3$), 5.80 – 5.88 (m, 1H, olefinic CH), 6.73 (d, *J* = 9.1 Hz, 1H, ArH), 7.09 ppm (d, *J* = 9.1 Hz, 1H, ArH).

^{13}C NMR δ(101 MHz, $CDCl_3$): 12.1, 15.8, 20.8, 21.6, 41.0, 55.9, 108.7, 118.8 (q, $^{1}J_{C\text{-}F}$ = 320 Hz, CF_3CF_3), 119.1, 127.7, 133.8, 133.9, 135.8, 142.0, 157.2, 203.5 ppm.

^{19}F NMR δ(101 MHz, $CDCl_3$): -74.0 ppm.

HRMS *m*/*z* (ESI): Calc. for $C_{16}H_{20}F_3O_5S$ (M^++H): 381.0984. Found: 381.0982.

See the Appendix section for NOSEY data for this compound (page 355).

Attempted Preparation of (Z)-2-(but-2-en-2-yl)-2-(6-iodo-3-methoxy-2-methylphenethyl)-1,3-dioxolane ***(Z)-100***

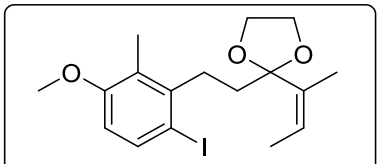

Chemical Formula: $C_{17}H_{23}IO_3$
Molecular Weight: 402.27

Scheme 3.18

To a round bottom flask connected to a Dean-Stark apparatus, **(*Z*)-129** (0.48 g, 1.3 mmol), ethylene glycol (0.73 mL, 13.4 mmol), *p*-TsOH (38 mg, 0.20 mmol) and PhMe (8.0 mL) were added. The mixture was heated to reflux for 6 h. After this time, the mixture was diluted with Et_2O, washed with saturated sodium bicarbonate solution and water. The organic solution was then dried with sodium sulfate, filtered, and evaporated. The crude mixture was purified using column chromatography (eluent: 0-33% Et_2O in petrol) to afford the fully isomerised *E*- product **(*E*)-100** (0.47 g, 86%) as a colourless oil. Data for this compound was consistent with that detailed on *page 226*.

Scheme 3.19, Table 3.4, Entry 1

(*Z*)-129 (100 mg, 0.28 mmol), triethylorthoformate (51 µL, 0.31 mmol), ethylene glycol (31 µL, 0.56 mmol), and $ZrCl_4$ (2.0 mg, 0.01 mmol) were dissolved in DCM (1.0 mL) and charged into a 10 mL microwave vial. The resulting solution was stirred at room temperature for 20 h. After this time, the mixture was quenched with cold NaOH (10%) and extracted with DCM. The organic solution was then dried with sodium sulfate, filtered, and evaporated. The crude mixture was purified using column chromatography (eluent: 0-33% Et_2O in petrol) to afford the fully isomerised *E*- product **(*E*)-100** (80 mg, 72%) as a colourless oil. Data for this compound was consistent with that shown on *page 226*.

Scheme 3.19, Table 3.4

The following experiments were performed using *General Procedure D.* Results are reported as: (a) volume of BF_3•OEt_2, (b) temperature, (c) time, (d) conversion determined by ^{1}H NMR analysis, comparing peak at 6.79 ppm (**(*Z*)-129**) with 5.78 ppm (**(*E*)-100**) and 5.45 ppm (**(*Z*)-100**), (e) *E:Z* ratio determined by NMR, comparing peaks at 5.78 ppm (**(*E*)-100**) and 5.45 ppm (**(*Z*)-100**), and (f) yield.

Entry 2: (a) 2.0 µL, 0.03 mmol, (b) -78 °C, (c) 2 h, (d) no reaction, (e) N/A, and (f) N/A.

Entry 3: (a) 17 µL, 0.28 mmol, (b) -78 °C, (c) 2 h, (d) no reaction, (e) N/A, and (f) N/A.

Entry 4: (a) 17 µL, 0.28 mmol, (b) -60 °C, (c) 16 h, d) no reaction, (e) N/A, and (f) N/A.

Entry 5: (a) 17 µL, 0.28 mmol, (b) -50 °C, (c) 16 h, (d) 15%, (e) 0:100, and (f) n.d.

Entry 6: (a) 17 µL, 0.28 mmol, (b) -40 °C, (c) 16 h, (d) 26%, (e) 0:100, and (f) n.d.

Entry 7: (a) 17 µL, 0.28 mmol, (b) -30 °C, (c) 16 h, (d) 32%, (e) 0:100, and (f) n.d.

Entry 8: (a) 17 µL, 0.28 mmol, (b) -20 °C, (c) 16 h, (d) 43%, (e) 1:3, and (f) n.d.

Entry 9: (a) 17 µL, 0.28 mmol, (b) -20 °C, (c) 16 h, (d) 100%, (e) 1:9, and (f) 56 mg, 67%.

Data for this compound was consistent with that detailed on page 226.

Attempted Preparation of (Z)-2-(but-2-en-2-yl)-2-(6-iodo-3-methoxy-2-methylphenethyl)-1,3-dioxolane ***(Z)-101***

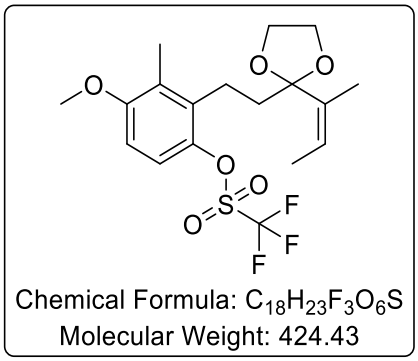

Scheme 3.20

(*Z*)-130 (100 mg, 0.26 mmol), triethylorthoformate (88 µL, 0.53 mmol) and ethylene glycol (43 µL, 0.79 mmol) were dissolved in DCM (0.75 mL), and were charged into a flame-dried round bottom flask and cooled to -78 °C using a cryocooler. After this, BF_3•OEt_2 (32 µL, 0.26 mmol) was added dropwise, and the mixture was warned slowly to -10 °C and left to stir for 8 hours. The mixture was quenched with Et_3N and saturated sodium bicarbonate solution, washed with water, and then dried with sodium sulfate. The mixture was filtered, the solvent was evaporated, and the crude mixture was purified using column chromatography (eluent: 0-33% Et_2O in petrol) to afford a 2:1 ratio of **(*Z*)-101**:**(*E*)-101** (97 mg, 88%) as a colourless oil. The isomeric ratio was determined by ^{1}H NMR analysis, comparing peaks at 5.44 ppm (**(*Z*)-101**) and 5.77 ppm (**(*E*)-101**).

Preparation of (E)-2-(but-2-en-2-yl)-2-(6-iodo-3-methoxy-2-methylphenethyl)-1,3-dioxolane ***(E)-100***

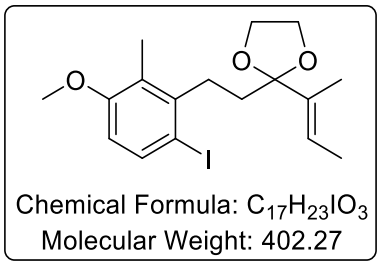

Scheme 3.21

(*E*)-129 (9.10 g, 25.4 mmol), triethylorthoformate (12.7 mL, 76.2 mmol) and ethylene glycol (5.60 mL, 102 mmol) were dissolved in DCM (81.0 mL), charged into a flame-dried round bottom flask, and cooled to -78 °C using a dry ice/acetone bath. After this, BF_3•OEt_2 (1.60 mL, 12.7 mmol) was added dropwise and the mixture was warned slowly to room temperature over 16 hours. The mixture was quenched with Et_3N and saturated sodium bicarbonate solution, washed with water, and then dried with sodium sulfate. The mixture was filtered, the solvent was evaporated, and the crude mixture was purified using column chromatography (eluent: 0-33% Et_2O in petrol) to afford **(*E*)-100** (10.2 g, quant.) as a colourless oil.

Data for this compound was consistent with that detailed on page 226.

7.4.2 Asymmetric Heck Optimisation

Preparation of 6-methoxy-1,5-dimethyl-1-vinyl-3,4-dihydronaphthalen-2(1H)-one ***62***

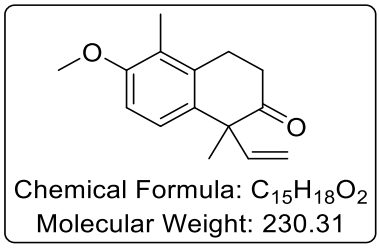

Scheme 3.22

To a flame-dried microwave vial, $Pd(OAc)_2$ (2.2 mg, 0.01 mmol), P(*o*-tolyl)$_3$ (19 mg, 0.05 mmol), and DMA (1.5 mL) were added. The mixture was degassed with argon and then left to stir at room temperature for 30 min. After this time, **(*E*)-129** (100 mg, 0.28 mmol) and Et_3N (70 µL, 0.56 mmol) in DMA (1.0 mL) was added into the mixture. Following the addition, the vial was degassed by freeze-pump-thaw cycle, which was repeated 3 times. The microwave vial was sealed and placed into a sand bath, heated at 100 °C for 24 h. After this time, the mixture was diluted with Et_2O and washed with water three times. The organic layer was dried over sodium sulfate, filtered, and evaporated. The crude mixture was purified by column chromatography (eluent: 0-33% Et_2O in petrol), affording the product **62** (64 mg, 93%) as a colourless oil.

FTIR (neat): 1099, 1258, 1481, 1584, 1707, 2889, 2978 cm^{-1}.

^{1}H NMR δ(400 MHz, $CDCl_3$): 1.54 (s, 3H, alkyl CH_3), 2.21 (s, 3H, $ArCH_3$), 2.49 – 2.57 (m, 1H, diastereotopic ring alkyl CH_2), 2.74 – 2.82 (m, 1 H, diastereotopic ring alkyl CH_2), 3.00 – 3.07 (m, 2H, benzylic CH_2), 3.84 (s, 3H, OCH_3), 4.90 (d, *J* = 17.3 Hz, 1H, terminal olefinic CH), 5.14 (d, *J* = 10.3, 1H, terminal olefinic CH), 5.86 (dd, *J* = 17.3, 10.3 Hz, 1H, olefinic CH), 6.81 (d, *J* = 8.7 Hz, 1H, ArH), 7.08 ppm (d, *J* = 8.7 Hz, 1H, ArH).

^{13}C NMR δ(101 MHz, $CDCl_3$): 11.6, 23.5, 25.2, 36.9, 55.6, 55.8, 109.1, 115.4, 123.7, 125.7, 132.9, 136.2, 142.1, 156.4, 212.1 ppm.

HRMS *m*/*z* (ESI): Calc. for $C_{15}H_{19}O_2$ (M^++H): 231.1385. Found: 231.1387.

Chiral HPLC analysis: CHIRALCEL® OD-H column, 0.5% IPA in hexane, 0.5 mL/minute flow rate, 254 nm detector, t_{R1} = 38.12 min and t_{R2} = 40.07 min.

Optical rotation details are provided on page 249.

Preparation of (R)-6-methoxy-1,5-dimethyl-1-vinyl-3,4-dihydro-1H-spiro[naphthalene-2,2'-[1,3]dioxolane]] **17**

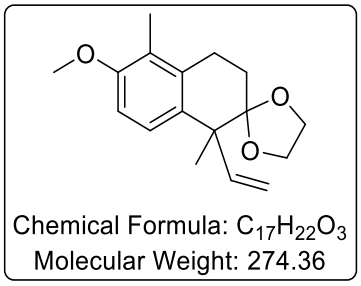

Scheme 3.23

To a flame-dried microwave vial, $Pd(OAc)_2$ (6.7 mg, 0.01 mmol), P(*o*-tolyl)$_3$ (33.5 mg, 0.05 mmol), and DMA (1.5 mL) were added. The mixture was degassed with argon and left to stir at room temperature for 30 min. After this time, **(*E*)-100** (200 mg, 0.56 mmol) and Et_3N (0.18 mL, 1.1 mmol) in DMA (1.0 mL) was added into the mixture. Following the addition, the vial was degassed by freeze-pump-thaw cycle, which was repeated 3 times. The microwave vial was sealed, placed into a sand bath, and heated at 100 °C for 24 h. After this time, the mixture was diluted with Et_2O and washed with water. The organic layer was dried with sodium sulfate, filtered, and evaporated. The crude mixture was purified by column chromatography (eluent: 0-33% Et_2O in petroleum ether), affording the product **17** (120 mg, 79%) as a colourless oil. The racemic product was analysed by chiral HPLC, however, separation of the two enantiomers was not achieved.

FTIR (neat): 1045, 1263, 1481, 2891, 2957 cm^{-1}.

^{1}H NMR δ(400 MHz, $CDCl_3$): 1.41 (s, 3H, alkyl CH_3), 2.00 (td, J = 6.9, ^2J = 3.0 Hz, 2H, ring alkyl CH_2), 2.11 (s, 3H, $ArCH_3$), 2.83 (t, J = 7.0 Hz, 2H, benzylic CH_2), 3.79 (s, 3H, $ArOCH_3$), 4.04 – 3.96 (m, 4H, 2 × OCH_2), 4.87 (dd, J = 17.4, ^2J = 1.5 Hz, 1H, terminal olefinic CH), 5.15 (dd, J = 17.4, ^2J = 1.5 Hz, 1H, terminal olefinic CH), 6.15 (dd, J = 17.5, 10.6 Hz, 1H, internal olefinic CH), 6.73 (d, J = 8.7 Hz, 1H, ArH), 7.00 (d, J = 8.7 Hz, 1H, ArH).

^{13}C NMR δ(101 MHz, $CDCl_3$): 11.4, 22.3, 26.1, 28.0, 49.4, 55.8, 65.4, 65.5, 108.8, 111.6, 115.2, 123.9, 126.3, 134.2, 134.6, 145.0, 155.8 ppm.

HRMS *m*/*z* (ESI): Calc. for $C_{17}H_{23}O_3$ (M^++H): 275.1647. Found: 275.1649.

Full chiral analysis details are provided on page 248.

Preparation of 6-methoxy-1,5-dimethyl-1-vinyl-3,4-dihydronaphthalen-2(1H)-one ***62***

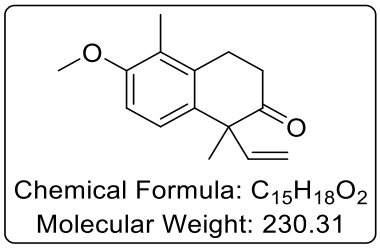

Chemical Formula: $C_{15}H_{18}O_2$
Molecular Weight: 230.31

Scheme 3.23

In a round bottom flask, **17** (100 mg, 0.36 mmol) was dissolved in 95% MeCN:H_2O (0.83 mL) and HCl (0.17 mL, 6.0 M in H_2O) was added. The reaction mixture was left to stir for 3 hours. Following this, the mixture was then diluted with water and extracted with Et_2O. The organic layer was dried with sodium sulfate, filtered, and evaporated. The crude mixture was purified by column chromatography (eluent: 0-33% Et_2O in petroleum ether), collecting **62** (81 mg, 98%, racemic) as a colourless oil.

Data for this compound was consistent with that detailed on page 236.

Initial Screening of Solvents and Additives

Scheme 3.24, Table 3.5

The following experiments were performed using *Heck General Procedure A*. Results are reported as: (a) solvent, (b) yield of **17**, and (c) % ee of **62**.

Entry 1: (a) DMA, (b) 56 mg, 82%, and (c) 0% ee.

Entry 2: (a) PhMe, (b) 46 mg, 67%, and (c) 0% ee.

Entry 3: (a) NMP, (b) 51 mg, 75%, and (c) Racemic.

Entry 4: (a) MeCN, (b) 55 mg, 80%, and (c) 26% ee.

Entry 5: (a) 1,2-DCE, (b) 45 mg, 66%, and (c) 40% ee.

Entry 6: (a) PhCl, (b) 47 mg, 69%, and (c) 8% ee.

Entry 7: (a) THF, (b) 52 mg, 76%, and (c) 10% ee.

Entry 8: (a) DMF, (b) 53 mg, 77%, and (c) 8% ee.

Scheme 3.25, Table 3.6

The following experiments were performed using *Heck General Procedure B*. Results are reported as: (a) solvent, (b) volume of organic base, (c) yield of **17**, and (d) % ee of **62**.

Entry 1: (a) DMA, (b) PMP, 90 µL, (c) 62 mg, 91%, and (d) 6% ee.

Entry 2: (a) 1,2-DCE, (b) PMP, 90 µL, (c) 27 mg, 39%, and (d) 46% ee.

Entry 3: (a) 1,2-DCE, (b) Et_3N, 69 µL, (c) 31 mg, 45%, and (d) 60% ee.

Entry 4: (a) MeCN, (b) PMP, 90 µL, (c) 44 mg, 64%, and (d) 62% ee.

Entry 5: (a) MeCN, (b) Et_3N, 69 µL, (c) 41 mg, 60%, and (d) 64% ee.

Entry 6: (a) THF, (b) Et_3N, 69 µL, (c) 29 mg, 42%, and (d) 32% ee.

Entry 7: (a) PhMe, (b) Et_3N, 69 µL, (c) 36 mg, 52%, and (d) 40% ee.

Entry 8: (a) NMP, (b) Et_3N, 69 µL, (c) 28 mg, 41%, and (d) 18% ee.

Entry 9: (a) DMF, (b) Et_3N, 69 µL, (c) 43 mg, 62%, and (d) 60% ee.

Scheme 3.26, Table 3.7

The following experiments were performed using Heck *General Procedure C*. Results are reported as: (a) **(*E*)-100**, (b) temperature, (c) time, (d) yield of **17**, (e) % ee of **62**.

Entry 1: (a) 100 mg, (b) 80 °C, (c) 69 h, (d) 62 mg, 90%, and (e) 70% ee.

Entry 2: (a) 100 mg, (b) 60 °C, (c) 72 h, (d) 38 mg, 56%, and (f) 68% ee.

Scheme 3.27, Table 3.8

The following experiments were performed using Heck *General Procedure C*. Results are reported as: (a) **(*E*)-101**, (b) temperature, (c) time, (d) yield of **17**, (e) % ee of **62**.

Entry 2: (a) 106 mg, (b) 100 °C, (c) 24 h, (d) 54 mg, 79%, and (e) 68% ee.

Entry 4: (a) 106 mg, (b) 80 °C, (c) 69 h, (d) 58 mg, 85%, and (f) 68% ee.

Microwave Study

Scheme 3.28, Table 3.9

The following experiments were performed using Heck *General Procedure D*. Results are reported as: (a) solvent, (b) **(*E*)-100**, (c) temperature, (d) time, (e) yield of **17**, and (f) % ee of **62**.

Entry 1: (a) PhMe, (b) 100 mg, (c) 100 °C, (d) 50 min, (e) 20 mg, 29%, and (f) 0% ee.

Entry 2: (a) 1,2-DCE, (b) 100 mg, (c) 100 °C, (d) 50 min, (e) 22 mg, 32%, and (f) 45% ee.

Entry 3: (a) MeCN, (b) 100 mg, (c) 100 °C, (d) 50 min, (e) 54 mg, 91%, and (f) 54% ee.

Entry 4: (a) MeCN, (b) 100 mg, (c) 80 °C, (d) 50 min, (e) 41 mg, 60%, and (f) 56% ee.

Entry 5: (a) MeCN, (b) 100 mg, (c) 60 °C, (d) 50 min, (e) 27 mg, 39%, and (f) 54% ee.

Entry 6: (a) MeCN, (b) 100 mg, (c) 100 °C, (d) 20 min, (e) 42 mg, 61%, and (f) 58% ee.

Entry 7: (a) MeCN, (b) 100 mg, (c) 130 °C, (d) 8 min, (e) 63 mg, 92%, and (f) 58% ee.

PHOX Ligands

The following experiments were performed using Heck *General Procedure E*. Results are reported as: (a) Pd catalyst, (b) chiral ligand, (c) solvent, (d) **(*E*)-100** or **(*E*)-101**, (e) base, (f) solvent, (g) microwave reactor or sand bath, (h) temperature, (i) time, (j) yield of **17**, and (k) % ee of **62**.

Scheme 3.29, Table 3.10

Entry 1: (a) $Pd(OAc)_2$, 3.8 mg, 0.02 mmol, (b) (*S*)-^{t}BuPHOX, 19 mg, 0.05 mmol, (c) PhMe, 1.0 mL, (d) **(*E*)-101**, 70 mg, 0.17 mmol, (e) PMP, 120 µL, 0.66 mmol, (f) PhMe, 1.0 mL, (g) microwave reactor, (h) 170 °C, (i) 50 min, (j) 8.4 mg, 18%, and (k) 54% ee.

Entry 2: (a) $Pd(OAc)_2$, 3.8 mg, 0.02 mmol, (b) (*S*)-^{t}BuPHOX, 19 mg, 0.05 mmol, (c) MeCN, 1.0 mL, (d) **(*E*)-101**, 70 mg, 0.17 mmol, (e) PMP, 120 µL, 0.66 mmol, (f) MeCN, 1.0 mL, (g) microwave reactor, (h) 130 °C, (i) 20 min, (j) 6.5 mg, 14% (2.5:1 **17**:**(*E*)-101**), and (k) 72% ee.

Entry 3: (a) $Pd(OAc)_2$, 3.8 mg, 0.02 mmol, (b) (*S*)-^{t}BuPHOX, 19 mg, 0.05 mmol, (c) MeCN, 1.0 mL, (d) **(*E*)-101**, 70 mg, 0.17 mmol, (e) PMP, 120 µL, 0.66 mmol, (f) MeCN, 1.0 mL, (g) sand bath, (h) 80 °C, (i) 69 h, (j) 6.1 mg, 13%, and (k) 86% ee.

Entry 4: (a) $Pd(OAc)_2$, 6.7 mg, 0.03 mmol, (b) (*S*)-^{t}BuPHOX, 30 mg, 0.08 mmol, (c) MeCN, 1.5 mL, (d) **(*E*)-100**, 100 mg, 0.25 mmol, (e) PMP, 180 µL, 1.00 mmol, (f) MeCN, 1.0 mL, (g) sand bath, (h) 80 °C, (i) 69 h, (j) 22 mg, 32%, and (k) 6% ee.

Entry 5: (a) $Pd_2(dba)_3$, 7.8 mg, 0.01 mmol, (b) (*S*)-^{t}BuPHOX, 7.7 mg, 0.02 mmol, (c) MeCN, 1.0 mL, (d) **(*E*)-101**, 70 mg, 0.17 mmol, (e) Et_3N, 180 µL, 1.00 mmol, (f) MeCN, 1.0 mL, (g) sand bath, (h) 80 °C, (i) 69 h, (j) 14 mg, 31%, and (k) 74% ee.

Entry 6: (a) $Pd(OAc)_2$, 5.4 mg, 0.02 mmol, (b) (*S*)-^{i}PrPHOX, 27 mg, 0.07 mmol, (c) MeCN, 1.5 mL, (d) **(*E*)-101**, 100 mg, 0.24 mmol, (e) PMP, 170 µL, 0.94 mmol, (f) MeCN,

1.0 mL, (g) sand bath, (h) 80 °C, (i) 69 h, (j) 7.2 mg, 11% (5:1 **17**:**(*E*)-101**), and (k) 80% ee.

Scheme 3.30, Table 3.11

Entry 1: (a) $Pd(dba)_2$, 4.0 mg, 0.01 mmol, (b) (*S*)-^{t}BuPHOX, 6.2 mg, 0.02 mmol, (c) MeCN, 0.80 mL, (d) **(*E*)-101**, 55 mg, 0.13 mmol, (e) PMP, 94 µL, 0.52 mmol, (f) MeCN, 0.60 mL, (g) sand bath, (h) 80 °C, (i) 69 h, (j) trace, and (k) n.d.

Entry 2: (a) $PdCl_2$, 2.3 mg, 0.01 mmol, (b) (*S*)-^{t}BuPHOX, 5.0 mg, 0.01 mmol, (c) MeCN, 0.80 mL, (d) **(*E*)-101**, 55 mg, 0.13 mmol, (e) PMP, 94 µL, 0.52 mmol, (f) MeCN, 0.60 mL, (g) sand bath, (h) 80 °C, (i) 69 h, (j) trace, and (k) n.d.

Entry 3: (a) **131**, 3.8 mg, 0.01 mmol, (b) (*S*)-^{t}BuPHOX, 15 mg, 0.04 mmol, (c) MeCN, 0.8 mL, (d) **(*E*)-101**, 55 mg, 0.13 mmol, (e) PMP, 94 µL, 0.52 mmol, (f) MeCN, 0.60 mL, (g) sand bath, (h) 80 °C, (i) 69 h, (j) 9.9 mg, 28%, and (k) 86% ee.

Entry 4: (a) **131**, 3.8 mg, 0.01 mmol, (b) (*S*)-^{t}BuPHOX, 15 mg, 0.04 mmol, (c) MeCN, 0.80 mL, (d) **(*E*)-101**, 55 mg, 0.13 mmol, (e) PMP, 94 µL, 0.52 mmol, (f) MeCN, 0.60 mL, (g) microwave reactor, (h) 130 °C, (i) 1 h, (j) 14 mg, 40%, and (k) 82% ee.

Entry 5: (a) **131**, 3.8 mg, 0.01 mmol, (b) (*S*)-^{t}BuPHOX, 15 mg, 0.04 mmol, (c) MeCN, 0.80 mL, (d) **(*E*)-101**, 55 mg, 0.13 mmol, (e) PMP, 94 µL, 0.52 mmol, (f) MeCN, 0.60 mL, (g) microwave reactor, (h) 130 °C, (i) 4 h, (j) 14 mg, 49%, and (k) 76% ee.

Scheme 3.31, Table 3.12

Entry 1: (a) **131**, 3.8 mg, 0.01 mmol, (b) (*S*)-^{t}BuPHOX, 15.1 mg, 0.04 mmol, (c) MeCN, 0.8 mL, (d) **(*E*)-101**, 55 mg, 0.13 mmol, (e) Et_3N, 73 µL, 0.52 mmol, (f) MeCN, 0.6 mL, (g) sand bath, (h) 80 °C, (i) 69 h, (j) 8.6 mg, 24%, and (k) 86% ee.

Entry 2: (a) **131**, 3.8 mg, 0.01 mmol, (b) (*S*)-^{t}BuPHOX, 15.1 mg, 0.04 mmol, (c) MeCN, 0.8 mL, (d) **(*E*)-101**, 55 mg, 0.13 mmol, (e) DIPEA, 91 µL, 0.52 mmol, (f) MeCN, 0.6 mL, (g) sand bath, (h) 80 °C, (i) 69 h, (j) 7.8 mg, 22%, and (k) 88% ee.

Entry 3: (a) **131**, 3.8 mg, 0.01 mmol, (b) (*S*)-^{t}BuPHOX, 15.1 mg, 0.04 mmol, (c) MeCN, 0.80 mL, (d) **(*E*)-101**, 55 mg, 0.13 mmol, (e) Proton Sponge®, 110 mg, 0.52 mmol, (f) MeCN, 0.60 mL, (g) sand bath, (h) 80 °C, (i) 69 h, (j) 10 mg, 28% (6:1 **17**:**(*E*)-101**), and (k) 90% ee.

Entry 4: (a) **131**, 3.8 mg, 0.01 mmol, (b) (*S*)-^{t}BuPHOX, 15 mg, 0.04 mmol, (c) MeCN, 0.8 mL, (d) **(*E*)-101**, 55 mg, 0.13 mmol, (e) DABCO, 58 mg, 0.52 mmol, (f) MeCN, 0.6 mL, (g) sand bath, (h) 80 °C, (i) 69 h, (j) 15.0 mg, 42% (5:1 **17**:**(*E*)-101**), and (k) 90% ee.

Entry 5: (a) **131**, 3.8 mg, 0.01 mmol, (b) (*S*)-^{t}BuPHOX, 15 mg, 0.04 mmol, (c) MeCN, 0.8 mL, (d) **(*E*)-101**, 55 mg, 0.13 mmol, (e) K_2CO_3, 72 mg, 0.52 mmol, (f) MeCN, 0.6 mL, (g) sand bath, (h) 80 °C, (i) 69 h, (j) 12.1 mg, 34% (2.5:1 **17**:**(*E*)-101**), and (k) 90% ee.

Scheme 3.32, Table 3.13

Entry 1: (a) **131**, 3.8 mg, 0.01 mmol, (b) (*S*)-^{t}BuPHOX, 15 mg, 0.04 mmol, (c) 1,2-DCE, 0.80 mL, (d) **(*E*)-101**, 55 mg, 0.13 mmol, (e) DABCO, 58 mg, 0.52 mmol, (f) 1,2-DCE, 0.60 mL, (g) sand bath, (h) 80 °C, (i) 69 h, (j) traces, and (k) n.d.

Entry 2: (a) **131**, 3.8 mg, 0.01 mmol, (b) (*S*)-^{t}BuPHOX, 15 mg, 0.04 mmol, (c) DMF, 0.80 mL, (d) **(*E*)-101**, 55 mg, 0.13 mmol, (e) DABCO, 58 mg, 0.52 mmol, (f) DMF, 0.60 mL, (g) sand bath, (h) 80 °C, (i) 69 h, (j) trace, and (k) n.d.

Entry 3: (a) **131**, 3.8 mg, 0.01 mmol, (b) (*S*)-^{t}BuPHOX, 15 mg, 0.04 mmol, (c) THF, 0.80 mL, (d) **(*E*)-101**, 55 mg, 0.13 mmol, (e) DABCO, 58 mg, 0.52 mmol, (f) THF, 0.60 mL, (g) sand bath, (h) 80 °C, (i) 69 h, (j) 7.1 mg, 20% (1.5:1 **17**:**(*E*)-101**), and (k) 84% ee.

Entry 4: (a) **131**, 3.8 mg, 0.01 mmol, (b) (*S*)-^{t}BuPHOX, 15 mg, 0.04 mmol, (c) MeCN, 0.80 mL, (d) **(*E*)-101**, 55 mg, 0.13 mmol, (e) DABCO, 58 mg, 0.52 mmol, (f) MeCN, 0.60 mL, (g) sand bath, (h) 90 °C, (i) 69 h, (j) 3.9 mg, 11% (2.5:1 **17**:**(*E*)-101**), and (k) 88% ee.

Entry 5: (a) **131**, 3.8 mg, 0.01 mmol, (b) (*S*)-^{t}BuPHOX, 15 mg, 0.04 mmol, (c) MeCN, 0.80 mL, (d) **(*E*)-101**, 55 mg, 0.13 mmol, (e) DABCO, 58 mg, 0.52 mmol, (f) MeCN, 0.60 mL, (g) sand bath, (h) 100 °C, (i) 69 h, (j) 6.8 mg, 19% (6.5:1 **17**:**(*E*)-101**), and (k) 86% ee.

Entry 6: (a) **131**, 7.5 mg, 0.03 mmol, (b) (*S*)-^{t}BuPHOX, 30 mg, 0.08 mmol, (c) MeCN, 0.80 mL, (d) **(*E*)-101**, 55 mg, 0.13 mmol, (e) DABCO, 58 mg, 0.52 mmol, (f) MeCN, 0.60 mL, (g) sand bath, (h) 80 °C, (i) 69 h, (j) 15 mg, 42%, and (k) 89% ee.

Entry 7: (a) **131**, 3.8 mg, 0.01 mmol, (b) (*S*)-^{t}BuPHOX, 15 mg, 0.04 mmol, (c) MeCN, 0.80 mL, (d) **(*E*)-101**, 55 mg, 0.13 mmol, (e) DABCO, 58 mg, 0.52 mmol, (f) MeCN, 0.60 mL, (g) microwave reactor, (h) 130 °C, (i) 1 h, (j) 11 mg, 32% and (k) 83% ee.

Entry 8: (a) **131**, 3.8 mg, 0.01 mmol, (b) (*S*)-^{t}BuPHOX, 15 mg, 0.04 mmol, (c) MeCN, 0.80 mL, (d) **(*E*)-101**, 55 mg, 0.13 mmol, (e) DABCO, 58 mg, 0.52 mmol, (f) MeCN, 0.60 mL, (g) microwave reactor, (h) 130 °C, (i) 4 h, (j) 16 mg, 44% and (k) 82% ee.

Entry 9: (a) **131**, 7.5 mg, 0.03 mmol, (b) (*S*)-^{t}BuPHOX, 30 mg, 0.08 mmol, (c) MeCN, 0.80 mL, (d) **(*E*)-101**, 55 mg, 0.13 mmol, (e) DABCO, 58 mg, 0.52 mmol, (f) MeCN, 0.60 mL, (g) microwave reactor, (h) 130 °C, (i) 4 h, (j) 22 mg, 62%, and (k) 84% ee.

Entry 10: (a) **131**, 3.8 mg, 0.01 mmol, (b) (*S*)-^{t}BuPHOX, 15 mg, 0.04 mmol, (c) MeCN, 0.80 mL, (d) **(*E*)-100**, 52 mg, 0.13 mmol, (e) DABCO, 58 mg, 0.52 mmol, (f) MeCN, 0.60 mL, (g) sand bath, (h) 80 °C, (i) 69 h, (j) 12 mg, 34%, and (k) 56% ee.

Data for this compound was consistent with that detailed on page 236.

The following reactions were carried out at GSK, Stevenage:

Chiral Ligand Screen of Commercially Available Ligands

Scheme 3.33, Table 3.14

The following experiments were performed using Heck *General Procedure F*. Results are reported as: (a) chiral ligand, (a) base, (c) estimation of conversion to **17** by LCMS, and (d) % ee of **17**.

Entry 1: (a) (*R*)-BINAP, 13 mg, (b) Et_3N, 49 µL, (c) 100%, and (d) 70% ee.

Entry 2: (a) (*R*)-Tol-BINAP, 14 mg, (b) Et_3N, 49 µL, (c) 95%, and (d) 77% ee.

Entry 3: (a) (*R*)-DM-BINAP, 15 mg, (b) Et_3N, 49 µL, (c) 100%, and (d) 17% ee.

Entry 4: (a) (*R*)-SEGPHOS, 13 mg, (b) Et_3N, 49 µL, (c) 100%, and (d) 71% ee.

Entry 5: (a) (*S*)-DM-SEGPHOS, 15 mg, (b) Et_3N, 49 µL, (c) 100%, and (d) 83% ee.

Entry 6: (a) (*S*)-DTBM-SEGPHOS, 25 mg, (b) Et_3N, 49 µL, (c) 15%, and (d) 29% ee.

Entry 7: (a) (*R*)-SYNPHOS, 13 mg, (b) Et_3N, 49 µL, (c) 100%, and (d) 86% ee.

Entry 8: (a) (*R*)-H_8-BINAP, 13 mg, (b) Et_3N, 49 µL, (c) 100%, and (d) 67% ee.

Entry 9: (a) (*S*)-MeO-BIPHEP, 8.7 mg, (b) Et_3N, 49 µL, (c) 100%, and (d) 61% ee.

Entry 10: (a) (*R*)-P-Phos, 14 mg, (b) Et_3N, 49 µL, (c) 50%, and (d) 70% ee.

Entry 11: (a) (*S*)-Phanephos, 12 mg, (b) Et_3N, 49 µL, (c) 100%, and (d) 4% ee.

Entry 12: (a) (-)-DIOP, 10 mg, (b) Et_3N, 49 µL, (c) 100%. and (d) 6% ee.

Entry 13: (a) Josiphos (SL-J001-1), 13 mg, (b) Et_3N, 49 µL, (c) 100%, and (d) 3% ee.

Entry 14: (a) Walphos (SL-W001-1), 14 mg, (b) Et_3N, 49 µL, (c) 100%, and (d) 4% ee.

Entry 15: (a) Taniaphos (SL-T001-1), 14 mg, (b) Et_3N, 49 µL, (c) 100%, and (d) 8% ee.

Final Investigations

Scheme 3.34, Table 3.15

Entry 1: (a) (*R*)-SYNPHOS, 13 mg, (b) DIPEA, 61 µL, (c) 100%, and (d) 86% ee.

Entry 2: (a) (*R*)-SYNPHOS, 13 mg, (b) PMP, 63 µL, (c) 100%, and (d) 86% ee.

Entry 3: (a) (*R*)-SYNPHOS, 13 mg, (b) DABCO, 39 mg, (c) 80%, and (d) 40% ee.

All further experiments were carried out at the University of Strathclyde.

Scheme 3.35, Table 3.16

The following experiments were performed using Heck *General Procedure G*. Results are reported as: (a) chiral ligand, (b) solvent, (c) **(*E*)-100** or **(*E*)-101**, (d) temperature, (e) time, (f) oil bath or microwave reactor, (g) yield of **17**, and (h) % ee of **17**.

Entry 1: (a) (*R*)-SYNPHOS, (b) MeCN, (c) **(*E*)-100**, 70 mg, (d) 80 °C, (e) 69 h, (f) oil bath, (g) 39 mg, 84%, and (h) 86% ee (*S*).

Entry 2: (a) (*R*)-SYNPHOS, (b) MeCN, (c) **(*E*)-101**, 72 mg, (d) 80 °C, (e) 69 h, (f) oil bath, (g) 41 mg, 88%, and (h) 86% ee (*S*).

Entry 3: (a) (*R*)-SYNPHOS, (b) MeCN, (c) **(*E*)-100**, 70 mg, (d) 130 °C, (e) 8 min, (f) microwave reactor, (g) 19 mg, 42%, and (h) 76% ee (*S*).

Entry 4: (a) (*R*)-SYNPHOS, (b) MeCN, (c) **(*E*)-100**, 70 mg, (d) 100 °C, (e) 24 h, (f) oil bath, (g) 39 mg, 84%, and (h) 86% ee (*S*).

Entry 5: (a) (*S*)-SYNPHOS, (b) MeCN, (c) **(*E*)-100**, 70 mg, (d) 100 °C, (e) 24 h, (f) oil bath, (g) 40 mg, 85%, and (h) 86% ee (*R*).

Entry 6: (a) (*S*)-SYNPHOS, (b) DMF, (c) **(*E*)-100**, 70 mg, (d) 100 °C, (e) 24 h, (f) oil bath, (g) 42 mg, 90%, and (h) 68% ee (*R*).

Entry 7: (a) (*S*)-SYNPHOS, (b) 1,2-DCE, (c) **(*E*)-100**, 70 mg, (d) 100 °C, (e) 24 h, (f) oil bath, (g) 14 mg, 29%, and (h) 72% ee (*R*).

Data for this compound was consistent with that detailed on page 238.

Additional Data for (R)-**17**

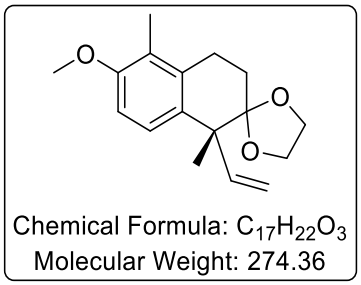

Melting point: 63–66 °C.

Chiral HPLC analysis (Strathclyde): CHIRALCEL® OJ-H column, 50% EtOH/Hexane 0.1% isopropylamine, 1.5 mL/min, 254 nm detector, t_{R1} = 17.53 min (*R*) and t_{R2} = 26.90 min (*S*).

Chiral HPLC analysis (GSK, Stevenage): CHIRALCEL® OJ-H column, 50% EtOH/heptane 0.1% isopropylamine, 1 mL/min, 235 nm detector, t_{R1} = 11.99 min (*R*) and t_{R2} = 18.22 min (*S*).

Optical Rotation: $[\alpha]_D^{20}$= -23.20° (c 1, $CHCl_3$)

See the Appendix section for X-ray crystallography data for this compound (page 356).

Additional Data for (R)-**62**

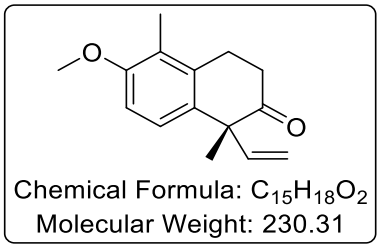

Optical Rotation: $[\alpha]_D^{20}$= -21.60° (c 1, $CHCl_3$)

7.5 Synthetic Substrates and Intermediates for Chapter 4

Preparation of 2-(6'-methoxy-1',5'-dimethyl-3',4'-dihydro-1'H-spiro[[1,3]dioxolane-2,2'-naphthalen]-1'-yl)ethanol ***134***

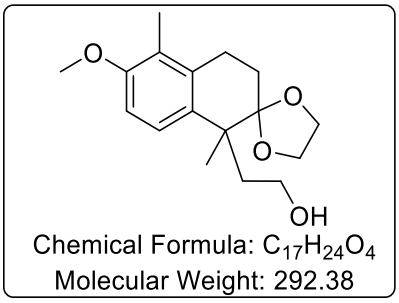

Scheme 4.3

To a flame-dried round bottom flask, **17** (2.3 g, 8.4 mmol) was dissolved in THF (70 mL) and cooled to 0°C using an ice bath, before the addition of 9-BBN (50 mL, 0.50 M in THF, 25 mmol) dropwise *via* syringe. The resulting mixture was warmed to room temperature and left to stir for 16 h. After this time, the mixture was cooled to 0°C using an ice bath and NaOH (38 mL, 2.0 M in H_2O, 76 mmol) was added dropwise. Following this addition, H_2O_2 (34 mL, 9.8 M in H_2O, 330 mmol) was added dropwise and the solution was allowed to warm to room temperature and stirred for 4 h. After this time, the mixture was quenched with water and extracted with DCM. The organic solution was then dried with sodium sulfate, filtered, and evaporated. The crude mixture was purified by silica chromatography (eluent: 0-100% Et_2O in petrol) to afford **134** (2.1 g, 93%) as a colourless oil.

FTIR (neat): 2853, 2924, 3400 cm^{-1}.

^{1}H NMR δ(400 MHz, $CDCl_3$): 1.38 (s, 3H, alkyl CH_3), 1.79 – 1.86 (m, 1H, diastereotopic alkyl CH_2), 1.96 (m, 1H, diastereotopic alkyl CH_2), 2.06 – 2.14 (m, 4H, $ArCH_3$, diastereotopic ring alkyl CH_2), 2.20 – 2.29 (m, 1H, diastereotopic ring alkyl CH_2), 2.66 (s, 1H, OH), 2.80 – 2.87 (m, 2H, benzyl CH_2), 3.56 – 3.64 (m, 1H, diastereotopic CH_2OH), 3.72 – 3.83 (m, 4H, $ArOCH_3$ and diastereotopic CH_2OH), 3.95 – 4.15 (m, 4H, 2× OCH_2), 6.74 (d, *J* = 8.7 Hz, 1H, ArH), 7.08 ppm (d, *J* = 8.7 Hz, 1H, ArH).

^{13}C NMR δ(101 MHz, $CDCl_3$): 11.5, 20.7, 26.0, 26.9, 44.8, 45.4, 55.7, 59.9, 64.9, 65.4, 108.9, 112.4, 124.3 (2 peaks), 134.2, 136.9, 155.7 ppm.

HRMS *m*/*z*: not determined due to the instability of the compound.

*Preparation of tert-butyl(2-(6-methoxy-1,5-dimethyl-3,4-dihydro-1H-spiro[naphthalene-2,2'-[1,3]dioxolan]-1-yl)ethoxy)dimethylsilane **135***

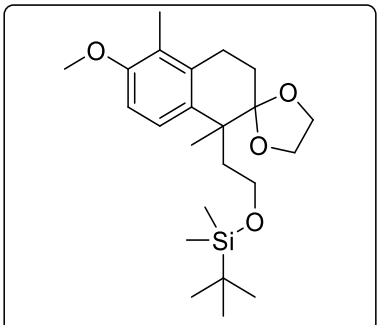

Chemical Formula: $C_{23}H_{38}O_4Si$
Molecular Weight: 406.64

Scheme 4.4, Table 4.1, Entry 1

To a flame-dried round bottom flask, **134** (130 mg, 0.45 mmol) was dissolved in DCM (6.0 mL). Imidazole (75 mg, 1.1 mmol) and TBSCl (100 mg, 0.67 mmol) were subsequently added, and the resulting mixture was left to stir for 3 h. After this time, the mixture was quenched with saturated sodium bicarbonate solution and extracted with DCM. The organic solution was then dried with sodium sulfate, filtered, and evaporated. The crude mixture was purified by silica chromatography (eluent: 0-33% Et_2O in petrol) to afford **135** (160 mg, 86%) as a colourless oil.

FTIR (neat): 1485, 1599, 2879, 2928 cm^{-1}.

^{1}H NMR δ(400 MHz, $CDCl_3$): 0.00 (s, 6H, 2 × $SiCH_3$), 0.86 (s, 9H, $SiC(CH_3)_3$), 1.33 (s, 3H, alkyl CH_3), 1.84 – 2.17 (m, 7H, $ArCH_3$, 2 × alkyl CH_2), 2.80 (t, *J* = 7.0 Hz, 2H, benzylic CH_2), 3.54 – 3.67 (m, 2H, CH_2OSi), 3.79 (s, 3H, $ArOCH_3$), 3.88 – 4.07 (m, 4H, 2 × OCH_2), 6.73 (d, *J* = 8.7 Hz, 1H, ArH), 7.11 ppm (d, *J* = 8.7 Hz, 1H, ArH).

^{13}C NMR δ(101 MHz, $CDCl_3$): -5.1, -5.0, 11.4, 18.4, 22.1, 25.9, 26.1, 26.9, 43.3, 44.6, 55.8, 60.9, 64.3, 65.2, 108.6, 112.4, 124.1, 124.8, 134.3, 135.8, 155.5 ppm.

HRMS *m*/*z* (ESI): Calc. for $C_{23}H_{39}O_4Si$ (M^++H): 407.2617. Found: 407.2616.

Preparation of triisopropyl(2-(6-methoxy-1,5-dimethyl-3,4-dihydro-1H-spiro[naphthalene-2,2'-[1,3]dioxolan]-1-yl)ethoxy)silane ***136***

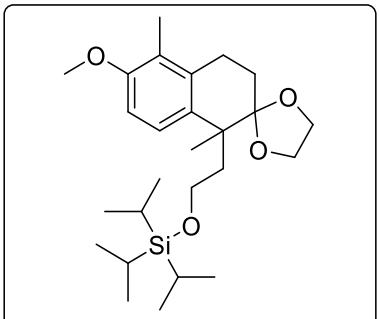

Chemical Formula: $C_{26}H_{44}O_4Si$
Molecular Weight: 448.72

Scheme 4.4, Table 4.1, Entry 2

To a flame-dried round bottom flask, **134** (130 mg, 0.43 mmol) was dissolved in THF (0.80 mL). Imidazole (32 mg, 0.47 mmol) and TIPSCl (0.10 mL, 0.47 mmol) were subsequently added, and the resulting mixture was left to stir for 16 h. After this time, the mixture was quenched with saturated sodium bicarbonate solution and extracted with Et_2O. The organic solution was then dried with sodium sulfate, filtered, and evaporated. The crude mixture was purified by silica chromatography (eluent: 0-33% Et_2O in petrol) to afford **136** (160 mg, 83%) as a colourless oil.

FTIR (neat): 1483, 1595, 2864, 2887, 2940 cm^{-1}.

^{1}H NMR δ(400 MHz, $CDCl_3$): 1.00 – 1.05 (m, 21H, 6 × SiCHC**H**$_3$, 3 × SiCH), 1.34 (s, 3H alkyl CH_3), 1.85 – 1.97 (m, 2H, alkyl CH_2), 2.00 – 2.15 (m, 5H, $ArCH_3$, ring alkyl CH_2), 2.80 (t, J = 7.1 Hz, 2H, benzylic CH_2), 3.62 – 3.76 (m, 2H, CH_2OSi), 3.79 (s, 3H, $ArOCH_3$), 3.90 – 4.07 (m, 4H, 2 × OCH_2), 6.73 (d, J = 8.7 Hz, 1H, ArH), 7.12 ppm (d, J = 8.7 Hz, 1H, ArH).

^{13}C NMR δ(101 MHz, $CDCl_3$): 11.4, 12.2, 18.2, 21.7, 25.9, 26.9, 43.5, 44.5, 55.8, 61.0, 64.9, 65.2, 108.6, 112.4, 124.1, 124.9, 134.3, 135.9, 155.5 ppm.

HRMS *m*/*z* (ESI): Calc. for $C_{26}H_{45}O_4Si$ (M^++H): 449.3087. Found: 449.3085.

*Preparation of tert-butyl(2-(6-methoxy-1,5-dimethyl-3,4-dihydro-1H-spiro[naphthalene-2,2'-[1,3]dioxolan]-1-yl)ethoxy)diphenylsilane **137***

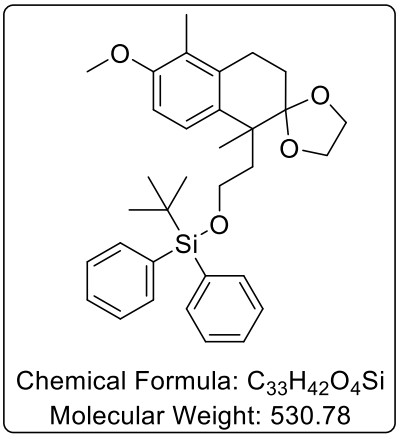

Scheme 4.4, Table 4.1, Entry 3

To a flame-dried round bottom flask, **134** (2.3 g, 7.8 mmol) was dissolved in THF (16 mL). Imidazole (1.1 g, 16 mmol) and TBDPSCl (2.2 mL, 8.1 mmol) were subsequently added, and the resulting mixture was left to stir for 16 h. After this time, the mixture was quenched with saturated sodium bicarbonate solution and extracted with Et_2O. The organic solution was then dried with sodium sulfate, filtered, and evaporated. The crude mixture was purified by silica chromatography (eluent: 0-33% $E_{t2}O$ in petrol) to afford **137** (4.2 g, quant.) as a colourless oil.

FTIR ($CHCl_3$): 1483, 2886, 2953 cm^{-1}.

^{1}H NMR δ(400 MHz, $CDCl_3$): 1.01 (s, 9H, $SiC(CH_3)_3$), 1.25 (s, 3H, alkyl CH_3), 1.82 – 1.98 (m, 3H, alkyl CH_2, 1 diastereotopic ring alkyl CH_2), 2.02 – 2.11 (m, 4H, $ArCH_3$, diastereotopic ring alkyl CH_2), 2.65 – 2.81 (m, 2H, benzylic CH_2), 3.64 – 3.84 (m, 7H, $ArOCH_3$, 2 × OCH_2), 3.96 – 3.87 (m, 2H, CH_2OSi), 6.66 (d, J = 8.7 Hz, 1H, ArH), 7.00 (d, J = 8.7 Hz, 1H, ArH), 7.42 – 7.31 (m, 6H, SiArH), 7.63 ppm (dd, J = 7.9, ^4J = 1.4 Hz, 4H, SiArH).

^{13}C NMR δ(101 MHz, $CDCl_3$): 11.4, 19.3, 22.4, 25.8, 26.8, 27.1, 42.8, 44.5, 55.7, 61.7, 64.8, 65.1, 108.6, 112.2, 124.0, 124.8, 127.6 (2 peaks), 129.5, 134.2, 134.4, 135.5, 155.5 ppm.

HRMS *m*/*z* (ESI): Calc. for $C_{33}H_{43}O_4Si$ (M^++H): 531.2931. Found: 531.2932.

*Attempted Preparation of tert-butyl(2-(6-methoxy-1,5-dimethyl-3,4-dihydro-1H-spiro[naphthalene-2,2'-[1,3]dioxolan]-1-yl)ethoxy)dimethylsilane **138***

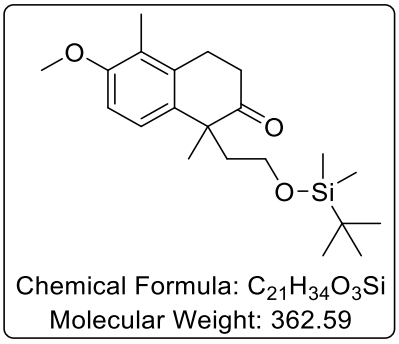

Scheme 4.5, Table 4.2

The following experiments were performed using *General Procedure E.* Results are reported as: (a) mass of **135**, (b) volume of acetone, (c) volume of water, (d) mass of PPTS (10 mol%), (e) temperature, (f) time, and (g) conversion of **135** to **139** or **134** as determined by ^{1}H NMR analysis, comparing peak at 6.73 ppm (**135**) with 6.79 ppm (**139**) or 6.75 ppm (**134**).

Entry 1: (a) 20 mg, 0.05 mmol, (b) 280 µL, (c) 70 µL, (d) 1.3 mg, 0.01 mmol, (e) 60 °C, (f) 5 h, and (g) 83% (**139**).

Entry 2: (a) 20 mg, 0.05 mmol, (b) 280 µL, (c) 70 µL, (d) 1.3 mg, 0.01 mmol, (e) room temperature, (f) 16 h, and (g) >99% (**134**).

Scheme 4.5, Table 4.2

The following experiments were performed using *General Procedure F*. Results are reported as: (a) mass of **135**, (b) volume of MeCN, (c) mass of NaI, (d) mass of $CeCl_3 \bullet 7H_2O$, (e) temperature, (f) time, and (g) conversion of **135** to **139** or **134** as determined by ^{1}H NMR analysis, comparing peak at 6.73 ppm (**135**) with 6.79 ppm (**139**) or 6.75 ppm (**134**).

Entry 3: (a) 20 mg, 0.05 mmol, (b) 490 µL, (c) 1.0 mg, 0.01 mmol, (d) 18 mg, 0.07 mmol, (e) room temperature, (f) 16 h, and (g) 0% conversion of **135**.

Entry 4: (a) 20 mg, 0.05 mmol, (b) 490 µL, (c) 1.0 mg, 0.01 mol, (d) 18 mg, 0.07 mmol (e) 60 °C, (f) 1 h, and (g) 33% (**139**) and 33% (**134**).

Scheme 4.5, Table 4.2

The following experiment was performed using *General Procedure G.* Results are reported as: (a) mass of **135**, (b) volume of $MeNO_2$, (c) mass of $Ce(OTf)_3 \bullet 7H_2O$, and (d) conversion of **135** to **139** as determined by ^1H NMR analysis, comparing peak at 6.73 ppm (**135**) with 6.79 ppm (**139**).

Entry 5: (a) 20 mg, 0.05 mmol, (b) 100 µL, (c) 5.9 mg, 0.01 mmol, and (d) 28% (**139**).

Scheme 4.5, Table 4.2

The following experiments were performed using *General Procedure H.* Results are reported as: (a) mass of **135**, (b) volume of acetone, (c) mass of I_2 (10 mol%), (d) temperature, (e) time, and (f) conversion of **135** to **139** as determined by ^1H NMR analysis, comparing peak at 6.73 ppm (**135**) with 6.79 ppm (**139**).

Entry 6: (a) 10 mg, 0.02 mmol, (b) 100 µL, (c) 0.6 mg, 2 µmol, (d) room temperature, (e) 1 h, and (f) >99% (**139**).

Data for 7-methoxy-6,9b-dimethyl-1,4,5,9b-tetrahydronaphtho[2,1-b]furan-3a(2H)-ol ***139***

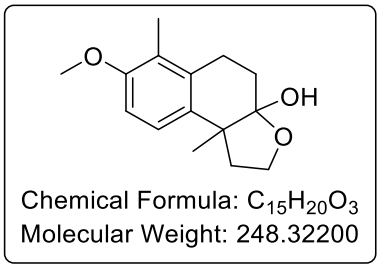

FTIR (neat): 1263, 1487, 2901, 2928, 3358 cm^{-1}.

^{1}H NMR δ(400 MHz, $CDCl_3$): 1.44 (s, 3H, alkyl CH_3), 2.00 – 2.11 (m, 6H, $ArCH_3$, alkyl CH_2, OH), 2.11 – 2.18 (m, 1H, diastereotopic ring alkyl CH_2), 2.72 – 2.77 (m, 1H, diastereotopic ring alkyl CH_2), 2.20 – 2.29 (m, 2H, benzylic CH_2), 3.35 – 3.43 (m, 1H, diastereotopic alkyl CH_2O), 3.81 (s, 3H, $ArOCH_3$), 3.92 – 3.99 (m, 1H, diastereotopic alkyl CH_2O), 6.79 (d, *J* = 8.7 Hz, 1H, ArH), 7.16 ppm (d, *J* = 8.7 Hz, 1H, ArH).

^{13}C NMR δ(101 MHz, $CDCl_3$): 11.3, 25.2 (2 peaks), 29.9, 39.6, 48.8, 55.6, 65.5, 105.0, 109.0, 123.3, 125.7, 134.8, 135.3, 155.3 ppm.

HRMS *m*/*z* (ESI): Calc. for $C_{15}H_{21}O_3$ (M^++H): 249.1491. Found: 249.1489.

*Attempted Preparation of 6-methoxy-1,5-dimethyl-1-(2-((triisopropylsilyl)oxy)ethyl)-3,4-dihydronaphthalen-2(1H)-one **141***

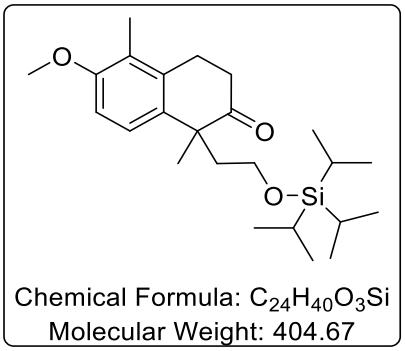

Chemical Formula: $C_{24}H_{40}O_3Si$
Molecular Weight: 404.67

Scheme 4.7, Table 4.3

The following experiment was performed using *General Procedure E.* Results are reported as: (a) mass of **136**, (b) volume of acetone, (c) volume of water, (d) mass of PPTS (10 mol%), (e) temperature, (f) time, and (g) conversion of **136** to **141** or **139** as determined by ^{1}H NMR analysis.

Entry 1: (a) 22 mg, 0.05 mmol, (b) 280 µL, (c) 70 µL, (d) 1.3 mg, 0.01 mmol, (e) 60 °C, (f) 5 h, and (g) an undetermined mixture of **136**, **141** and **139** was obtained.

Scheme 4.7, Table 4.3

The following experiment was performed using *General Procedure G.* Results are reported as: (a) mass of **136**, (b) volume of $MeNO_2$, (c) mass of $Ce(OTf)_3 \bullet 7H_2O$, and (d) conversion of **136** to **139** as determined by ^{1}H NMR analysis, comparing peak at 6.73 ppm (**136**) with 6.79 ppm (**139**).

Entry 2: (a) 22 mg, 0.05 mmol, (b) 100 µL, (c) 5.9 mg, 0.01 mmol, and (d) 63% (**139**).

Scheme 4.7, Table 4.3

The following experiment was performed using *General Procedure H.* Results are reported as: (a) mass of **136**, (b) volume of acetone, (c) mass of I_2 (10 mol%), (d) temperature, (e) time, and (f) conversion of **136** to **139** as determined by ^{1}H NMR analysis, comparing peak at 6.73 ppm (**136**) with 6.79 ppm (**139**).

Entry 3: (a) 22 mg, 0.05 mmol, (b) 200 µL, (c) 1.2 mg, 0.02 mmol, (d) room temperature, (e) 1 h, and (f) >99% (**139**).

Preparation of 1-(2-((tert-butyldiphenylsilyl)oxy)ethyl)-6-methoxy-1,5-dimethyl-3,4-dihydronaphthalen-2(1H)-one ***142***

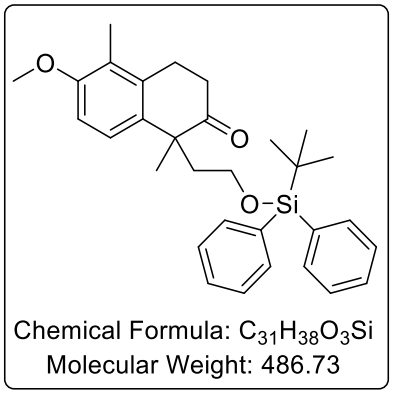

Scheme 4.8, Table 4.4

The following experiments were performed using *General Procedure E*. Results are reported as: (a) mass of **137**, (b) volume of acetone, (c) volume of water, (d) amount of acid, (e) temperature, (f) time, and (g) conversion.

Entry 1: (a) 20 mg, 0.04 mmol, (b) 280 µL, (c) 70 µL, (d) PPTS, 1.0 mg, 0.01 mmol, (e) 60 °C, (f) 5 h, and (g) 0%.

Entry 3: (a) 20 mg, 0.04 mmol, (b) 280 µL, (c) 70 µL, (d) HCl, 330 µL, 2.0 M in H_2O, 0.01 mmol, (e) 60 °C, (f) 5 h, and (g) 0%.

Scheme 4.8, Table 4.4

The following experiment was performed using *General Procedure G*. Results are reported as: (a) mass of **137**, (b) volume of $MeNO_2$, (c) mass of $Ce(OTf)_3 \bullet 7H_2O$, and (d) conversion by NMR

Entry 2: (a) 15 mg, 0.03 mmol, (b) 100 µL, (c) 3.3 mg, 0.01 mmol, and (d) 0%.

Scheme 4.8, Table 4.4

The following experiments were performed using *General Procedure H.* Results are reported as: (a) mass of **137**, (b) volume of acetone, (c) mass of I_2 (10 mol%), (d) temperature, (e) time, and (f) conversion of **137** to **142** or **139** as determined by ^{1}H NMR analysis, comparing peak at 6.66 ppm (**137**) with 6.73 ppm (**142**) or 6.79 ppm (**139**).

Entry 4: (a) 10 mg, 0.02 mmol, (b) 100 µL, (c) 0.6 mg, 2 µmol, (d) room temperature, (e) 1 h, and (f) 80% (**142**) and 20% (**139**).

Entry 5: (a) 10 mg, 0.02 mmol, (b) 100 µL, (c) 0.6 mg, 2 µmol, (d) room temperature, (e) 30 min, and (f) 83% (**142**) and 9% (**139**).

Entry 6: (a) 10 mg, 0.02 mmol, (b) 100 µL, (c) 0.6 mg, 2 µmol, (d) 0 °C, (e) 1 h, and (f) 0%.

Scheme 4.9, Table 4.4

The following experiments were performed using *General Procedure H.* Results are reported as: (a) mass of **137**, (b) volume of acetone, (c) mass of I_2, (d) temperature, (e) time, and (f) isolated yield of **142** as a colourless oil.

Entry 1: (a) 0.27 g, 0.51 mmol, (b) 2.5 mL, (c) 13 mg, 0.05 mmol, (d) room temperature, (e) 40 min, and (f) 0.20 g, 81%.

Entry 2: (a) 0.90 g, 1.7 mmol, (b) 9.5 mL, (c) 86 mg, 0.34 mmol, (d) room temperature, (e) 20 min, and (f) 0.70 g, 85%.

FTIR ($CHCl_3$): 1483, 2886, 2953 cm^{-1}.

^{1}H NMR δ(400 MHz, $CDCl_3$): 0.98 (s, 9H, $SiCH_3$), 1.38 (s, 3H, alkyl CH_3), 1.87 – 1.94 (m, 1H, diastereotopic alkyl CH_2), 2.16 (s, 3H, $ArCH_3$), 2.43 – 2.50 (m, 1H, diastereotopic alkyl CH_2), 2.54 – 2.69 (m, 2H, ring alkyl CH_2), 2.92 – 2.96 (m, 2H, benzylic CH_2), 3.35 – 3.40 (m, 2H, CH_2OSi), 3.82 (s, 3H, $ArOCH_3$), 6.73 (d, *J* = 8.7 Hz, 1H, ArH), 6.98 (d, *J* = 8.7 Hz, 1H, ArH), 7.30 – 7.42 (m, 6H, SiArH), 7.49 – 7.56 ppm (m, 4H, SiArH).

^{13}C NMR δ(101 MHz, $CDCl_3$): 11.0, 18.5, 24.7, 26.3, 27.3, 28.6, 37.0, 42.7, 48.7, 55.1, 60.3, 108.6, 122.9, 124.1, 127.1, 128.9, 129.0, 133.1, 133.3, 133.4, 134.9, 135.10, 135.11, 135.2, 155.2 ppm.

HRMS *m*/*z* (ESI): Calc. for $C_{31}H_{39}O_3Si$ (M^++H): 487.2668. Found: 487.2670.

Preparation of tert-butyl(2-(6-methoxy-1,5-dimethyl-2-methylene-1,2,3,4-tetrahydronaphthalen-1-yl)ethoxy)diphenylsilane ***143***

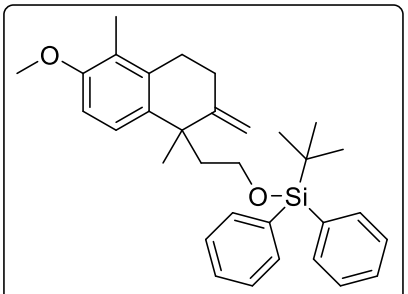

Chemical Formula: $C_{32}H_{40}O_2Si$
Molecular Weight: 484.76

Scheme 4.10

To a flame-dried round bottom flask containing $MePPh_3Br$ (6.38 g, 17.9 mmol), **142** (1.4 g, 2.88 mmol) dissolved in THF (21.0 mL) was charged. To the mixture, KO^tBu (0.82 M in THF, 21.0 mL, 17.3 mmol) was added dropwise *via* syringe. The resulting mixture was left to stir at room temperature for 16 h. After this time, the mixture was quenched with saturated sodium bicarbonate solution and extracted with Et_2O. The organic solution was then dried with sodium sulfate, filtered, and evaporated. The crude mixture was purified by silica chromatography (eluent: 0-33% Et_2O in petrol) to afford **143** (1.16 g, 83%) as a colourless oil.

FTIR ($CHCl_3$): 1483, 1589, 1645, 2973 cm^{-1}.

^{1}H NMR δ(400 MHz, $CDCl_3$): 1.00 (s, 9H, $SiC(CH_3)_3$), 1.35 (s, 3H, alkyl CH_3), 2.03 – 2.13 (m, 5H, $ArCH_3$, alkyl CH_2), 2.26 – 2.42 (m, 2H, ring alkyl CH_2), 2.62 (t, *J* = 6.6 Hz, 2H, benzylic CH_2), 3.25 – 3.36 (m, 1H, CH_2OSi), 3.26 – 3.86 (m, 1H, CH_2OSi), 3.79 (s, 3H, $ArOCH_3$), 4.70 (s, 1H, terminal olefinic CH), 4.80 (s, 1H, terminal olefinic CH), 6.70 (d, *J* = 8.7 Hz, 1H, ArH), 7.07 (d, *J* = 8.7 Hz, 1H, ArH), 7.30 – 7.44 (m, 6H, SiArH), 7.53 – 7.68 ppm (m, 4H, SiArH).

^{13}C NMR δ(101 MHz, $CDCl_3$): 11.5, 29.3, 37.0, 29.3, 30.1, 31.6, 41.7, 45.8, 55.7, 61.2, 107.7, 109.0, 123.5, 124.5, 127.7, 129.6 (2 peaks), 134.2, 134.3, 135.2, 135.8 (2 peaks), 136.8, 136.9, 152.4, 155.1 ppm.

HRMS *m*/*z* (ESI): Calc. for $C_{32}H_{41}O_2Si$ (M^++H): 485.2876. Found: 485.2909.

Preparation of 2-(1,2,3,4-tetrahydro-6-methoxy-1,5-dimethyl-2-methylenenapthalen-1-yl)ethanol ***144***[10]

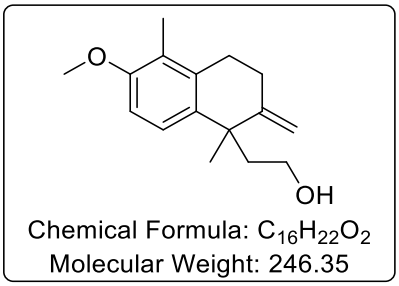

Scheme 4.11

To a flame-dried round bottom flask, **143** (1.2 g, 2.4 mmol) dissolved in THF (14 mL) was charged and then cooled to 0 °C using an ice bath. At this temperature, TBAF (1.0 M in THF, 4.8 mL, 4.8 mmol) was added dropwise *via* syringe. The resulting mixture was left to stir at this temperature for 6 h. After this time, the mixture was quenched with saturated ammonium chloride solution and extracted with Et_2O. The organic solution was washed with brine, then dried with sodium sulfate, filtered, and evaporated. The crude mixture was purified by silica chromatography (eluent: 0-100% Et_2O in petrol) to afford **144** (0.55 g, 93%) as a colourless oil.

FTIR ($CHCl_3$): 1483, 1584, 1643, 2937, 3327 cm^{-1}.

^{1}H NMR δ(400 MHz, $CDCl_3$): 1.45 (s, 3H, alkyl CH_3), 2.08 – 2.18 (m, 5H, $ArCH_3$, alkyl CH_2), 2.47 – 2.56 (m, 2H, ring alkyl CH_2), 2.67 – 2.79 (m, 2H, benzylic CH_2), 3.34 – 3.41 (m, 1H, diastereotopic CH_2OH), 3.52 – 3.58 (m, 1H, diastereotopic CH_2OH), 3.81 (s, 3H, $ArOCH_3$), 4.93 (s, 1H, olefinic CH), 4.98 (s, 1H, olefinic CH), 6.78 (d, J = 8.7 Hz, 1H, ArH), 7.19 ppm (d, J = 8.7 Hz, 1H, ArH).

^{13}C NMR δ(101 MHz, $CDCl_3$): 11.6, 29.3, 30.7, 31.9, 42.0, 46.0, 55.7, 60.4, 107.9, 109.0, 123.7, 124.7, 136.4, 137.1, 153.5, 155.3 ppm.

Preparation of (4-(6-methoxy-1,5-dimethyl-2-methylene-1,2,3,4-tetrahydronaphthalen-1-yl)but-1-yn-1-yl)trimethylsilane ***132***[10]

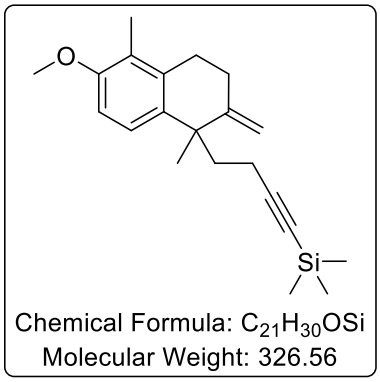

Scheme 4.12

To a flame-dried round bottom flask, trimethylsilylacetylene (1.5 mL, 11 mmol) and THF (31 mL) was charged and cooled to -78 °C using a dry ice/acetone bath. At this temperature, ^{n}BuLi (2.5 M in hexanes, 4.4 mL, 11 mmol) was added dropwise *via* syringe. The resulting mixture was left to stir at this temperature for 1 h.

To another flame-dried round bottom flask, **144** (0.54 g, 2.2 mmol) dissolved in DCM (32 mL) and pyridine (0.55 mL, 6.6 mmol) was charged and cooled to -78 °C using a dry ice/acetone bath. At this temperature, Tf_2O (1.1 mL, 6.6 mmol) was added dropwise *via* syringe. The resulting mixture was left to stir at this temperature for 20 min before being quenched with saturated sodium bicarbonate solution and extracted with DCM. The organic solution was washed with brine, then dried with sodium sulfate, filtered, and evaporated. The crude mixture containing triflate **145** was re-dissolved in THF (32 mL), and TMEDA (1.7 mL, 11 mmol) and DMPU (1.3 mL, 11 mmol) were added sequentially. The resulting mixture was cooled to -78 °C using a dry ice/acetone bath. At this temperature, the solution was cannulated directly to the previously prepared trimethylsilylacetylide solution. The resulting mixture was left to stir at -78 °C for 5 min, before being warmed to -10 °C using an ice bath, and subsequently left at this temperature for 1 h. After this time, the mixture was quenched with saturated ammonium chloride. The mixture was extracted with Et_2O, washed with brine, then dried with sodium sulfate, filtered, and evaporated. The crude

mixture was purified by silica chromatography (eluent: 0-33% Et_2O in petrol) to afford **132** (0.55 g, 77% over 2 steps) as a colourless oil.

FTIR ($CHCl_3$): 1583, 1643, 2172, 2978 cm^{-1}.

^{1}H NMR δ(400 MHz, $CDCl_3$): 0.11 (s, 9H, $Si(CH_3)_3$), 1.41 (s, 3H, alkyl CH_3), 1.67 – 1.80 (m, 1H, diastereotopic alkyl CH_2), 2.01 – 2.14 (m, 6H, diastereotopic alkyl CH_2, alkyl $CH_2C{\equiv}C$, $ArCH_3$), 2.45 (t, *J* = 6.6 Hz, 2H, ring alkyl CH_2), 2.61 – 2.78 (m, 2H, benzylic CH_2), (s, 3H, $ArOCH_3$), 4.86 (s, 1H, olefinic CH), 4.97 (s, 1H, olefinic CH), 6.77 (d, *J* = 8.7 Hz, 1H, ArH), 7.16 ppm (d, *J* = 8.7 Hz, 1H, ArH).

^{13}C NMR δ(101 MHz, $CDCl_3$): 0.3, 11.3, 15.8, 29.2, 30.1, 31.8. 42.5, 43.2, 55.7, 84.0, 108.2, 108.3, 109.0, 123.6, 124.6, 136.1, 137.3, 151.9, 155.3 ppm.

*Preparation of 1-(but-3-yn-1-yl)-6-methoxy-1,5-dimethyl-2-methylene-1,2,3,4-tetrahydronaphthalene **147** from **132***[10]

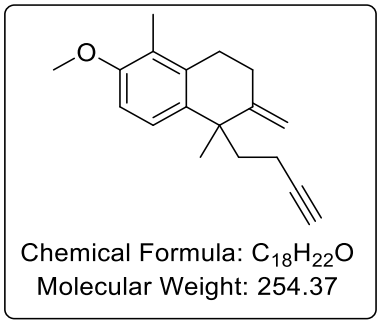

Scheme 4.13

To a flame-dried round bottom flask, **132** (0.55 g, 1.7 mmol) dissolved in MeOH (32 mL) was charged, and, subsequently, K_2CO_3 (0.23 g, 1.7 mmol) was added. The resulting mixture was left to stir at this temperature for 16 h before being diluted with EtOAc. The organic solution was washed with brine, then dried with sodium sulfate, filtered, and evaporated. The crude mixture was purified by silica chromatography (eluent: 0-33% Et_2O in petrol) to afford **147** (0.41 g, 96%) as a colourless oil.

FTIR ($CHCl_3$): 1620, 2111, 2954 cm^{-1}.

^{1}H NMR δ(400 MHz, $CDCl_3$): 1.41 (s, 3H, alkyl CH_3), 1.62 – 1.73 (m, 1H, diastereotopic alkyl CH_2), 1.83 (s, 1H, alkynyl CH), 1.99 – 2.17 (m, 6H, diastereotopic alkyl CH_2, alkyl $CH_2C{\equiv}C$, $ArCH_3$), 2.42 – 2.51 (m, 2H, ring alkyl CH_2), 2.61 – 2.79 (m, 2H, benzylic CH_2), 3.81 (s, 3H, $ArOCH_3$), 4.86 (s, 1H, olefinic CH), 4.98 (s, 1H, olefinic CH), 6.77 (d, J = 8.7 Hz, 1H, ArH), 7.15 ppm (d, J = 8.7 Hz, 1H, ArH).

^{13}C NMR δ(101 MHz, $CDCl_3$): 11.5, 14.3, 29.1, 30.6, 31.8, 42.2, 43.2, 55.7, 67.8, 85.4, 108.0, 109.1, 123.6, 124.5, 135.8, 137.4, 152.0, 155.3 ppm.

*Preparation of 6-methoxy-1,5-dimethyl-2-methylene-1-(pent-3-yn-1-yl)-1,2,3,4-tetrahydronaphthalene **95** from **147***[10]

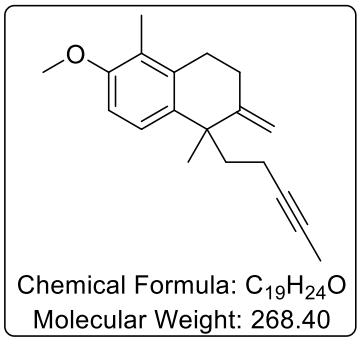

Scheme 4.13

To a flame-dried round bottom flask, **147** (0.41 g, 1.6 mmol) dissolved in THF (34 mL) was charged and cooled to -78 °C using a dry ice/acetone bath. At this temperature, ^{n}BuLi (2.5 M in hexanes, 2.6 mL, 6.4 mmol) was added into reaction mixture and left to stir for 30 min. Subsequently, MeI (0.45 mL, 7.3 mmol) was added to the solution, and, after 15 min, the reaction mixture was warmed to room temperature. The mixture was left to stir for 10 min before being quenched with saturated ammonium chloride solution and extracted with Et_2O. The organic solution was washed with brine, then dried with sodium sulfate, filtered, and evaporated. The crude mixture was purified by silica chromatography (eluent: 0-33% Et_2O in petrol) to afford **95** (0.42 g, 99%) as a colourless oil.

FTIR ($CHCl_3$): 1641, 2126, 2940 cm^{-1}.

^{1}H NMR δ(400 MHz, $CDCl_3$): 1.40 (s, 3H, alkyl CH_3), 1.57 – 1.67 (m, 1H, diastereotopic alkyl CH_2), 1.73 (t, 3H, *J* = 2.3 Hz, alkynyl CH_3), 1.92 – 2.13 (m, 6H, diastereotopic alkyl CH_2, alkyl $CH_2C{\equiv}C$, $ArCH_3$), 2.45 (t, 2H, *J* = 6.4 Hz, ring alkyl CH_2), 2.61 – 2.77 (m, 2H, benzylic CH_2), 3.81 (s, 3H, $ArOCH_3$), 4.86 (s, 1H, olefinic CH_2), 4.97 (s, 1H, olefinic CH_2), 6.76 (d, *J* = 8.7 Hz, 1H, ArH), 7.15 ppm (d, *J* = 8.7 Hz, 1H, ArH).

^{13}C NMR δ(101 MHz, $CDCl_3$): 3.6, 11.5, 14.6, 29.1, 30.6, 31.9, 42.9, 43.2, 55.7, 75.1, 79.9, 107.9, 109.0, 123.5, 124.5, 136.1, 137.4, 152.1, 155.2 ppm.

Preparation of 1-(2-iodoethyl)-6-methoxy-1,5-dimethyl-2-methylene-1,2,3,4-tetrahydronaphthalene ***148***[10]

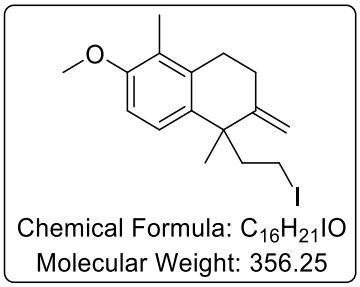

Scheme 4.15

To a flame-dried round bottom flask containing PPh_3 (64 mg, 0.24 mmol) and pyridine 32 µL, 0.39 mmol), **144** (50 mg, 0.20 mmol) dissolved in DCM (1.5 mL) was charged and cooled to 0 °C. To the mixture, I_2 (62 mg, 0.24 mmol) was added and the resulting mixture was left to stir for 2 h at this temperature. After this time, the mixture was quenched with 1 M HCl solution, then 10% sodium thiosulfate solution, and extracted with Et_2O. The organic solution was washed with brine, then dried with sodium sulfate, filtered, and evaporated. The crude mixture was purified by silica chromatography (eluent: 0-33% Et_2O in petrol) to afford **148** (50 mg, 67%) as a pale-yellow oil.

FTIR ($CHCl_3$): 1483, 1643, 2940 cm^{-1}.

^{1}H NMR δ(400 MHz, $CDCl_3$): 1.42 (s, 3H, alkyl CH_3), 2.11 (s, 3H, $ArCH_3$), 2.57 – 2.37 (m, 4H, 2 × alkyl CH_2), 2.69 – 2.59 (m, 2H, diastereotopic benzylic CH_2, CH_2I), 2.81 – 2.71 (m, 1H, diastereotopic benzylic CH_2), 3.13 – 2.92 (m, 1H, diastereotopic CH_2I), 3.81 (s, 3H, $ArOCH_3$), 4.88 (s, 1H, olefinic CH_2), 5.01 (s, 1H, olefinic CH_2), 6.78 (d, J = 8.7 Hz, 1H, ArH), 7.14 (d, J = 8.7 Hz, 1H, ArH).

^{13}C NMR δ(101 MHz, $CDCl_3$): 1.5, 11.6, 29.1, 30.8, 31.8, 45.9, 48.1, 55.7, 108.1, 109.2, 123.8, 124.4, 135.0, 137.4, 151.5, 155.4 ppm.

HRMS *m*/*z* (EI): Calc. for $C_{16}H_{21}IO$ (M^+): 356.0621. Found: 356.0632.

*Attempted Preparation of 6-methoxy-1,5-dimethyl-2-methylene-1-(pent-3-yn-1-yl)-1,2,3,4-tetrahydronaphthalene **95** from **148***

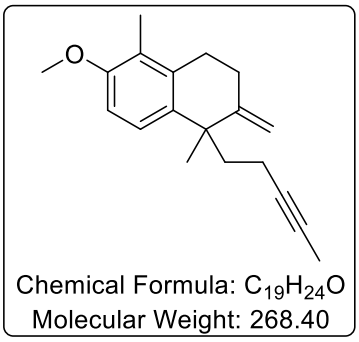

Scheme 4.16

To a flame-dried microwave vial, $FeBr_2$ (3.7 mg, 0.02 mmol) and **148** (30 mg, 0.08 mmol) dissolved in THF (340 µL) were charged. Subsequently, *o*-TMEDA (32 µL, 0.17 mmol) and 1-propynylmagnesium bromide (0.50 M in THF, 250 µL, 0.13 mmol) were added and the resulting mixture was left to stir for 16 h. After this time, the mixture was extracted with Et_2O and the organic solution was washed with brine, then dried with sodium sulfate, filtered, and evaporated. The crude mixture was purified by column chromatography (eluent: 0-33% Et_2O in petrol), unfortunately, affording none of the desired product **95** and only degradation of the starting material was observed.

Scheme 4.17

To a flame-dried round bottom flask, **148** (10 mg, 0.03 mmol) dissolved in THF (600 µL) was charged and subsequently cooled to 0 °C using an ice bath. At this temperature, 1-propynylmagnesium bromide (0.50 M in THF, 110 µL, 0.06 mmol) was added, and the resulting mixture was warmed to room temperature and left to stir for 16 h. After this time, the mixture was extracted with Et_2O and the organic solution was washed with brine, then dried with sodium sulfate, filtered, and evaporated. The crude mixture was purified by column chromatography (eluent: 0-33% Et_2O in petrol), unfortunately, affording none of the desired product **95** and only returning starting material (8 mg, 80%).

*Attempted Preparation of 1-(but-3-yn-1-yl)-6-methoxy-1,5-dimethyl-2-methylene-1,2,3,4-tetrahydronaphthalene **147** from **148***

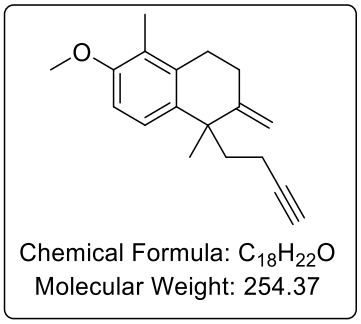

Scheme 4.18

To a flame-dried microwave vial containing lithium acetylide ethylenediamine complex **151** (22 mg, 0.14 mmol), DMSO (170 µL) and Et_2O (170 µL) were charged. The mixture was cooled to 5 °C using an ice bath before adding **148** (50 mg, 0.14 mmol) dissolved in Et_2O (50 µL). The resulting mixture was left to stir for 4 h. After this time, the solution was quenched with water and extracted with Et_2O. The organic solution was washed with brine, then dried with sodium sulfate, filtered, and evaporated. The crude mixture was purified by column chromatography (eluent: 0-33% Et_2O in petrol), unfortunately, affording none of the desired product **147** and only degradation of starting material was observed.

Attempted Preparation of 1'-(2-iodoethyl)-6'-methoxy-1',5'-dimethyl-3',4'-dihydro-1'H-spiro[[1,3]dioxolane-2,2'-naphthalene] ***154***

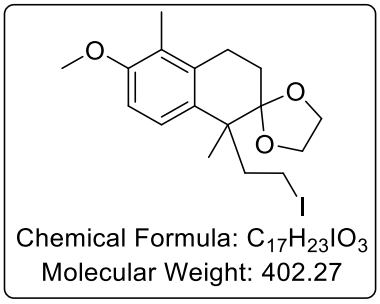

Scheme 4.20, Table 4.5

The following experiments were performed using *General Procedure I*. Results are reported as: (a) solvent, (b) temperature, (c) time (part i), (d) time (part ii), (e) yield, and (f) amount of starting material returned.

Entry 1: (a) DCM, (b) room temperature, (c) 2 h, (d) 1 h, (e) 0%, and (f) 20 mg, 100%.

Entry 2: (a) THF, (b) 40 °C, (c) 5 h, (d) 3 h, (e) 0%, and (f) 20 mg, 100%.

Attempted Preparation of 1'-(2-bromoethyl)-6'-methoxy-1',5'-dimethyl-3',4'-dihydro-1'H-spiro[[1,3]dioxolane-2,2'-naphthalene] ***155***

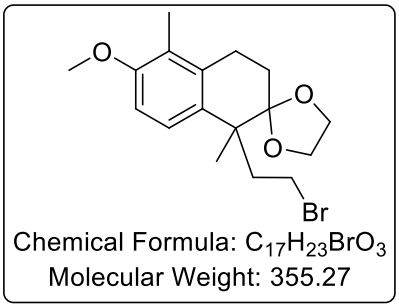

Chemical Formula: $C_{17}H_{23}BrO_3$
Molecular Weight: 355.27

Scheme 4.21

To a flame-dried round bottom flask, **134** (40 mg, 0.14 mmol), dissolved in DCM (1 mL), was added and the solution was cooled to 0 °C with an ice bath. Freshly distilled PBr_3 (9.4 µL, 0.1 mmol) was added dropwise, and the resulting solution was left to stir for 2 h at room temperature. After this time, the mixture was cooled to 0 °C using an ice bath, and was quenched with ice. The mixture was diluted with DCM and washed with brine. The organic layer was dried over sodium sulfate, filtered, and evaporated. The crude mixture was purified by column chromatography (eluent: 0-33% Et_2O in petrol), unfortunately, affording none of the desired product **155** and only degradation of starting material was observed.

Attempted Preparation of 2-(6'-methoxy-1',5'-dimethyl-3',4'-dihydro-1'H-spiro[[1,3]dioxolane-2,2'-naphthalen]-1'-yl)ethyl trifluoromethanesulfonate] ***156***

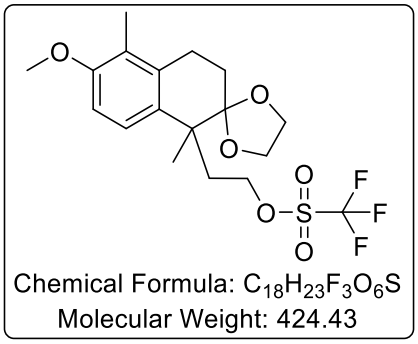

Scheme 4.22

To a flame-dried round bottom flask, **134** (85 mg, 0.14 mmol) as a solution in DCM (1 mL) and Et_3N (80 µL, 0.58 mmol) were added. The resulting mixture was cooled to -78 °C with a dry ice/acetone bath. Freshly distilled Tf_2O (60 µL, 0.38 mmol) was then added dropwise, and the resulting solution was left to stir at this temperature for 10 min. After this time, the mixture was warmed to -10 °C using a salt/ice bath, and left for 30 min. The resulting mixture was subsequently quenched with saturated K_2CO_3, and washed with brine. The organic layer was dried over sodium sulfate, filtered, and evaporated. The crude mixture was purified by column chromatography (eluent: 0-33% Et_2O in petrol), unfortunately, affording none of the desired product **136** and only degradation of starting material was observed.

Attempted Preparation of 1'-(2-iodoethyl)-6'-methoxy-1',5'-dimethyl-3',4'-dihydro-1'H-spiro[[1,3]dioxolane-2,2'-naphthalene] ***154***

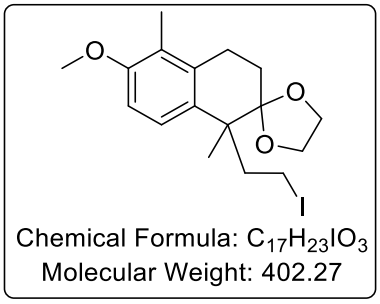

Chemical Formula: $C_{17}H_{23}IO_3$
Molecular Weight: 402.27

The following reaction was carried out at GSK, Stevenage.

Scheme 4.23

To a round bottom flask, **134** (20 mg, 0.07 mmol), dissolved in THF (3.0 mL), was added and the solution was cooled to -10°C using an ice bath. Triethylamine (11 µL, 0.08 mmol) was added, followed by the dropwise addition of MsCl (6 µL, 0.08 mmol), and the reaction mixture was allowed to stir at this temperature for 1 h. After this time, sodium iodide (41 mg, 0.27 mmol), dissolved in THF (0.3 mL), was charged into the reaction mixture and the resulting solution was warmed to room temperature and left to stir for 16 h. After this time, the reaction mixture was diluted with Et_2O, quenched with water, and extracted with DCM. The organic phase was washed with saturated sodium thiosulfate solution and saturated brine, dried using a hydrophobic frit, and evaporated to give the crude product. This material was purified using a Biotage column (eluent: 0-20% Et_2O in petroleum ether) to afford traces of **154** as a colourless oil. Unfortunately, no analytical data was obtained.

Preparation of 1-(2-iodoethyl)-6-methoxy-1,5-dimethyl-3,4-dihydronaphthalen-2(1H)-one ***157***

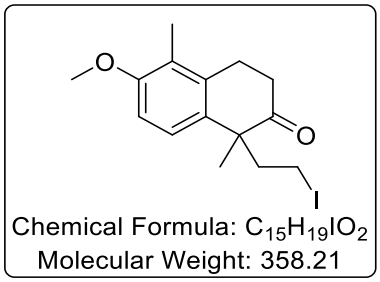

The following reaction was carried out at GSK, Stevenage.

Scheme 4.24

To a round bottom flask, **134** (61 mg, 0.21 mmol), dissolved in DCM (2.5 mL), was added and the solution was cooled to -10°C prior to the addition of Et_3N (40 µL, 0.29 mmol). MsCl (19 µL, 0.25 mmol) was then added dropwise and the reaction mixture was allowed to stir at this temperature for 1 h. The reaction was quenched with water, followed by DCM. The mixture was then washed with saturated sodium bicarbonate solution, dried using a hydrophobic frit, and evaporated *in vacuo* to give the crude material, which was analysed by LCMS and was confirmed to contain the mesylate intermediate. The crude mixture was then dissolved in acetone (2.5 mL), NaI (130 mg, 0.84 mmol) was added and the solution was left to stir for 16 h at room temperature. The reaction solvent was evaporated, and the material was diluted in water and extracted with DCM. The organic layer was washed with saturated sodium thiosulfate solution and saturated brine, dried using a hydrophobic frit, and evaporated to give the crude mixture. This material was purified using a Biotage column (eluent: 0-20% Et_2O in petroleum ether) to afford **157** (12 mg, 16%) as a colourless oil.

FTIR ($CHCl_3$): 1711, 2833, 2926, 2951 cm^{-1}.

^{1}H NMR δ(400 MHz, $CDCl_3$): δ 1.42 (s, 3H, alkyl CH_3), 2.19 (s, 3H, $ArCH_3$), 2.55 – 2.83 (m, 6H, 3 × CH_2), 2.86 – 2.95 (m, 1H, diastereotopic CH_2I), 3.09 – 3.15 (m, 1H, diastereotopic CH_2I), 3.84 (s, 3H, $ArOCH_3$), 6.84 (d, *J* = 8.7 Hz, 1H, ArH), 7.09 ppm (d, *J* = 8.7 Hz, 1H, ArH).

^{13}C NMR δ(101 MHz, $CDCl_3$): 11.7, 25.5, 25.6, 28.1, 37.8, 44.9, 53.6, 55.8, 109.7, 124.0, 124.6, 132.7, 135.8, 156.2, 213.7 ppm.

HRMS *m*/*z* (ESI): Calc. for $C_{15}H_{20}IO_2$ (M+H): 359.0508. Found: 359.0517.

Preparation of tert-butyl(2-(6-methoxy-1,5-dimethyl-2-((trimethylsilyl)oxy)-1,4-dihydronaphthalen-1-yl)ethoxy)diphenylsilane ***159***

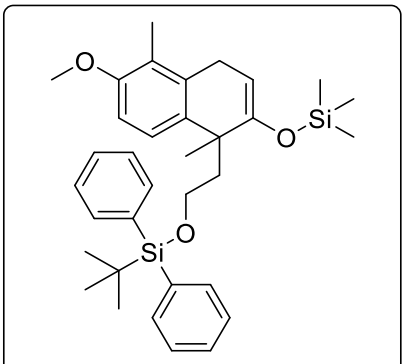

Chemical Formula: $C_{34}H_{46}O_3Si_2$
Molecular Weight: 558.91

Scheme 4.27

To a flame-dried round bottom flask, **142** (1.0 g, 2.1 mmol) dissolved in DCM (21 mL) was charged, followed by the addition of Et_3N (1.4 mL, 10 mmol). The reaction mixture was cooled to -5 °C before the dropwise addition of TMSOTf (0.55 mL, 3.1 mmol) *via* syringe. The resulting mixture was left to stir at this temperature for 30 min. After this time, the mixture was quenched with saturated sodium bicarbonate solution and extracted with DCM. The organic solution was then dried with sodium sulfate, filtered, and evaporated. The crude mixture was purified by silica chromatography (eluent: 0-33% Et_2O in petrol) to afford **159** (0.96 g, 86%) as a colourless oil.

FTIR ($CHCl_3$): 1686, 2891, 2955 cm^{-1}.

^{1}H NMR δ(400 MHz, $CDCl_3$): 0.19 (s, 9H, $Si(CH_3)_3$), 0.94 (s, 9H, $SiC(CH_3)_3$), 1.32 (s, 3H, alkyl CH_3), 1.86 – 1.96 (m, 1H, diastereotopic alkyl CH_2), 2.04 (s, 3H, $ArCH_3$), 2.32 (m, 1H, diastereotopic alkyl CH_2), 3.04 – 3.27 (m, 3H, benzylic CH_2, diastereotopic $SiOCH_2$), 3.53 (td, J = 10.1, ^2J = 5.4 Hz, 1H, diastereotopic $SiOCH_2$), 3.79 (s, 3H, $ArOCH_3$), 4.84 (t, J = 3.7 Hz, 1H, olefinic CH), 6.70 (d, J = 8.7 Hz, 1H, ArH), 7.05 (d, J = 8.7 Hz, 1H, ArH), 7.26 – 7.40 (m, 6H, SiArH), 7.40 – 7.26 ppm (m, 4H, SiArH).

^{13}C NMR δ(101 MHz, $CDCl_3$): 0.4, 11.3, 19.2, 27.0, 28.0, 29.8, 40.5, 43.3, 55.7, 61.8, 98.9, 109.2, 122.9, 124.4, 127.5, 127.6, 129.4, 129.4, 133.0, 134.2, 134.5, 134.5, 135.7, 152.0, 155.1 ppm.

HRMS *m*/*z*: unable to be obtained due to the instability of the compound.

Preparation of 1-(2-((tert-butyldiphenylsilyl)oxy)ethyl)-6-methoxy-1,5-dimethylnaphthalen-2(1H)-one ***160***

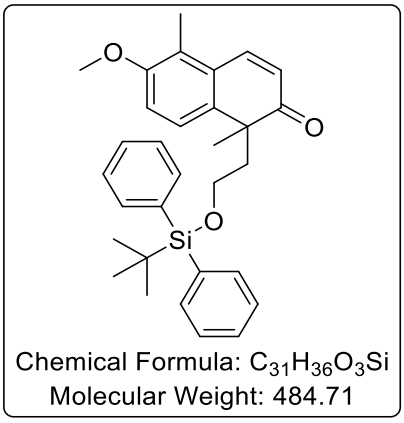

Chemical Formula: $C_{31}H_{36}O_3Si$
Molecular Weight: 484.71

Scheme 4.28, Table 4.6, Entry 1

To a round bottom flask, **159** (0.95 g, 1.7 mmol), dissolved in MeCN (7.3 mL), was charged, followed by the addition of $Pd(OAc)_2$ (0.42 g, 1.9 mmol). The reaction mixture was heated to 40 °C and was left to stir at this temperature for 16 h. After this time, the mixture was filtered over celite® to remove the solids, with the filter cake being washed with Et_2O. The solvent was removed and the crude mixture was purified by silica chromatography (eluent: 0-33% Et_2O in petrol) to afford **160** (0.71 g, 85%) as a colourless oil.

Scheme 4.28, Table 4.6, Entry 2

To a flame-dried 25 mL round bottom flask, equipped with a double oblique stopcock adaptor, **159** (68 mg, 0.12 mmol), dissolved in DMSO (2.5 mL), was charged, followed by the addition of $Pd(OAc)_2$ (2.7 mg, 0.01 mmol). The flask was then evacuated and flushed with oxygen from a balloon, and this cycle was repeated a further two times. Following the final flush, the stopcock was left open to the balloon and the flask was immersed in an oil bath set to 80 °C and stirred for 16 hours. After this time, the mixture was diluted with Et_2O and washed 3 times with water. The mixture was washed with brine, then dried with sodium sulfate and purified by silica chromatography (eluent: 0-33% Et_2O in petrol) to afford **160** (20 mg, 34%) as a colourless oil.

FTIR ($CHCl_3$): 1572, 1661, 2928, 2953 cm^{-1}.

^{1}H NMR δ(400 MHz, $CDCl_3$): δ 0.91 (s, 9H, $SiC(CH_3)_3$), 1.38 (s, 3H, alkyl CH_3), 2.04 (m, 1H, diastereotopic alkyl CH_2), 2.34 (s, 3H, $ArCH_3$), 2.71 (m, 1H, diastereotopic alkyl CH_2), 3.19 – 3.39 (m, 2H, $SiOCH_2$), 3.86 (s, 3H, $ArOCH_3$), 6.15 (d, *J* = 10.2 Hz, 1H, olefinic CH), 6.84 (d, *J* = 8.6 Hz, 1H, ArH), 7.06 (d, *J* = 8.6 Hz, 1H, ArH), 7.23 – 7.42 (m, 8H, SiArH), 7.53 (d, *J* = 8.1 Hz, 2H, SiArH), 7.72 ppm (d, *J* = 10.2 Hz, 1H, olefinic CH).

^{13}C NMR δ(101 MHz, $CDCl_3$): 10.9, 19.1, 26.8, 30.2, 43.9, 49.0, 55.9, 60.7, 112.0, 124.7, 125.1, 125.4, 127.6, 127.7, 128.9, 129.5, 129.6, 133.8, 135.0, 135.6, 135.7, 137.9, 140.3, 156.0, 203.5 ppm.

HRMS *m*/*z* (ESI): Calc. for $C_{31}H_{37}O_3Si$ (M^++H): 485.2508. Found: 485.2506.

Preparation of tert-butyl(2-(6-methoxy-1,5-dimethyl-2-methylene-1,2-dihydronaphthalen-1-yl)ethoxy)diphenylsilane ***161***

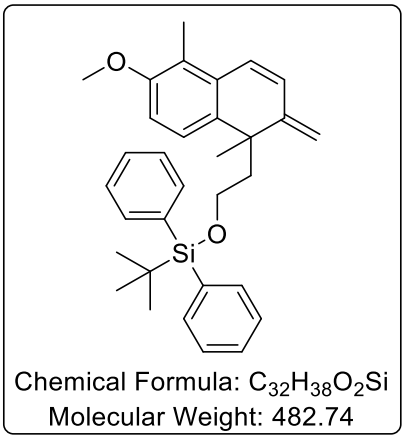

Scheme 4.29

To a flame-dried round bottom flask containing $MePPh_3Br$ (3.2 g, 8.9 mmol), **160** (0.70 g, 1.4 mmol) dissolved in THF (11 mL) was charged. To the mixture, KO^tBu dissolved in THF (0.82 M, 11 mL, 8.6 mmol) was added dropwise *via* syringe. The resulting mixture was left to stir at this temperature for 16 h. After this time, the mixture was quenched with saturated sodium bicarbonate solution and extracted with Et_2O. The organic solution was then dried with sodium sulfate, filtered, and evaporated. The crude mixture was purified by silica chromatography (eluent: 0-33% Et_2O in petrol) to afford **161** (0.65 g, 93%) as a colourless oil.

FTIR ($CHCl_3$): 1572, 1597, 2957 cm^{-1}.

^{1}H NMR δ(400 MHz, $CDCl_3$): 0.97 (s, 9H, $SiC(CH_3)_3$), 1.36 (s, 3H, alkyl CH_3), 1.97 – 2.03 (m, 1H, diastereotopic alkyl CH_2), 2.15 – 2.25 (m, 4H, $ArCH_3$, diastereotopic alkyl CH_2), 3.29 (td, J = 10.2, ^2J = 5.2 Hz, 1H, diastereotopic $SiOCH_2$), 3.51 (td, J = 10.2, ^2J = 5.2 Hz, 1H, diastereotopic $SiOCH_2$), 3.79 (s, 3H, $ArOCH_3$), 4.99 (s, 2H, terminal olefinic CH_2), 6.23 (d, J = 10.0 Hz, 1H, olefinic CH), 6.54 (d, J = 10.0 Hz, 1H, olefinic CH), 6.62 (d, J = 8.6 Hz, 1H, ArH), 7.03 (d, J = 8.6 Hz, 1H, ArH), 7.29 – 7.39 ppm (m, 6H, SiArH), 7.53 – 7.59 ppm (m, 4H, SiArH).

^{13}C NMR δ(101 MHz, $CDCl_3$): 10.8, 19.2, 27.0, 33.1, 40.8, 47.5, 55.7, 61.2, 109.5, 113.4, 122.1, 122.4, 123.4, 127.6 (3), 129.5, 129.5, 129.7, 131.4, 134.3, 135.2, 135.7 (2), 149.9, 155.8 ppm.

HRMS *m*/*z* (EI): Calc. for $C_{32}H_{38}O_2Si$ (M^+): 482.2636. Found: 482.2622.

Preparation of 2-(6-methoxy-1,5-dimethyl-2-methylene-1,2-dihydronaphthalen-1-yl)ethan-1-ol ***158***

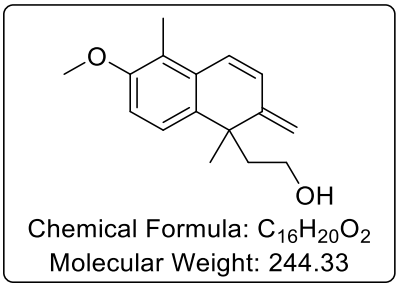

Scheme 4.29

To a flame-dried round bottom flask, **161** (0.33 g, 0.68 mmol) dissolved in THF (4.0 mL) was charged and cooled to 0 °C using an ice bath. At this temperature, TBAF (1.0 M in THF, 1.4 mL, 1.4 mmol) was added dropwise *via* syringe. The resulting mixture was left to stir at this temperature for 6 h. After this time, the mixture was quenched with saturated ammonium chloride solution and extracted with Et_2O. The organic solution was washed with brine, then dried with sodium sulfate, filtered, and evaporated. The crude mixture was purified by silica chromatography (eluent: 0-100% Et_2O in petrol) to afford **158** (0.16 g, 94%) as a colourless oil.

FTIR ($CHCl_3$): 1570, 1597, 2955, 3366 cm^{-1}.

^{1}H NMR δ(400 MHz, $CDCl_3$): 1.00 (t, *J* = 5.6 Hz, 1H, OH), 1.47 (s, 3H, alkyl CH_3), 2.08 – 1.95 (m, 1H, diastereotopic alkyl CH_2), 2.33 – 2.13 (m, 4H, $ArCH_3$, diastereotopic alkyl CH_2), 3.27 – 3.37 (m, 1H, diastereotopic CH_2OH), 3.41 – 3.51 (m, 1H, diastereotopic CH_2OH), 3.81 (s, 3H, $ArOCH_3$), 5.17 (s, 1H, terminal olefinic CH), 5.19 (s, 1H, terminal olefinic CH), 6.37 (d, *J* = 10.0 Hz, 1H, olefinic CH), 6.66 (d, *J* = 10.0 Hz, 1H, olefinic CH), 6.74 (d, *J* = 8.6 Hz, 1H, ArH), 7.21 ppm (d, *J* = 8.6 Hz, 1H, ArH).

^{13}C NMR δ(101 MHz, $CDCl_3$): 10.8, 32.7, 40.9, 49.4, 55.8, 60.5, 109.6, 113.8, 122.4, 122.7, 123.7, 129.8, 131.6, 135.0, 150.5, 156.0 ppm.

HRMS *m*/*z* (EI): Calc. for $C_{16}H_{20}O_2$ (M^+): 244.1445. Found: 244.1458.

*Attempted Preparation of (4-(6-methoxy-1,5-dimethyl-2-methylene-1,2-dihydronaphthalen-1-yl)but-1-yn-1-yl)trimethylsilane **163** from **158***

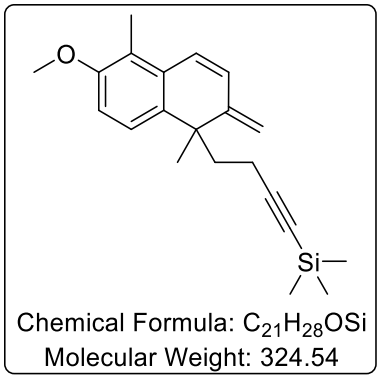

Scheme 4.30, Table 4.7

The following experiments were performed using *General Procedure J*, including the formation of triflate **162**. Results are reported as: (a) volume of trimethylsilylacetylene, (b) volume of THF, (c) volume of ^{n}BuLi, (d) mass of **158**, (e) volume of DCM, (f) volume of pyridine, (g) volume of Tf_2O, (h) volume of THF, (i) volume of TMEDA, (j) volume of DMPU, (k) temperature, (l) time, and (m) purification method and outcome.

Entry 1: (a) 40 µL, 0.37 mmol, (b) 0.6 mL, (c) 170 µL, 2.2 M in THF, 0.98 mmol, (d) 30 mg, 0.12 mmol, (e) 1.8 mL, (f) 30 µL, 0.37 mmol, (g) 62 µL, 0.37 mmol, (h) 1.2 mL, (i) 40 µL, 0.37 mmol, (j) 44 µL, 0.37 mmol, (k) room temperature, (l) 1 h, and (m) silica chromatography (eluent: 0-33% Et_2O in petrol), no products isolated.

Entry 2: (a) 0.14 mL, 0.98 mmol, (b) 1.8 mL, (c) 0.39 mL, 2.5 M in THF, 0.98 mmol, (d) 80 mg, 0.33 mmol, (e) 4.8 mL, (f) 0.08 mL, 0.98 mmol, (g) 0.17 mL, 0.98 mmol, (h) 3.2 mL, (i) 0.15 mL, 0.98 mmol, (j) 0.12 mL, 0.98 mmol, (k) -10 °C using a cryocooler, (l) 1 h, and (m) silica chromatography (eluent: 0-33% Et_2O in petrol), triflate **162** was indicated by TLC analysis.

Entry 3: (a) 0.28 mL, 2.1 mmol, (b) 6.0 mL, (c) 0.8 mL, 2.5 M in THF, 2.05 mmol, (d) 0.1 g, 0.41 mmol, (e) 6.0 mL, (f) 0.1 mL, 1.2 mmol, (g) 0.2 mL, 1.2 mmol, (h) 6.0 mL, (i) 0.3 mL, 2.1 mmol, (j) 0.15 mL, 2.1 mmol, (k) -10 °C using a cryocooler, (l) 16 h, and (m) silica chromatography, no isolated products.

Entry 4: (a) 0.28 mL, 2.1 mmol, (b) 6.0 mL, (c) 0.8 mL, 2.5 M in THF, 2.05 mmol, (d) 0.1 g, 0.41 mmol, (e) 6.0 mL, (f) 0.1 mL, 1.2 mmol, (g) 0.2 mL, 1.2 mmol, (h) 6.0 mL, (i) 0.3 mL, 2.1 mmol, (j) 0.15 mL, 2.1 mmol, (k) -10 °C using a cryocooler, (l) 16 h, and (m) neutral alumina chromatography (eluent: 0-33% Et_2O in petrol), no isolated products.

Attempted Preparation of triisopropyl(4-(6-methoxy-1,5-dimethyl-2-methylene-1,2-dihydronaphthalen-1-yl)but-1-yn-1-yl)silane ***164***

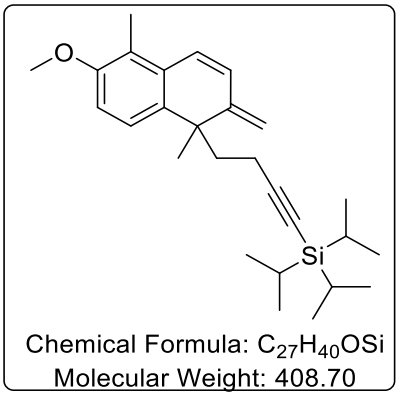

Scheme 4.31

The following experiment was performed using *General Procedure J*, including the formation of triflate **162**. Results are reported as: (a) volume of triisopropylsilylacetylene, (b) volume of THF, (c) volume of ^{n}BuLi, (d) mass of **158**, (e) volume of DCM, (f) volume of pyridine, (g) volume of Tf_2O, (h) volume of THF, (i) volume of TMEDA, (j) volume of DMPU, (k) temperature, (l) time, and (m) purification method and outcome.

Entry 1: (a) 0.28 mL, 1.0 mmol, (b) 2.0 mL, (c) 0.4 mL, 2.5 M in hexanes, 1.0 mmol, (d) 50 mg, 0.21 mmol, (e) 3.0 mL, (f) 0.05 mL, 0.21 mmol, (g) 0.1 mL, 0.21 mmol, (h) 3.0 mL, (i) 0.15 mL, 1.0 mmol, (j) 0.12 mL, 1.0 mmol, (k) -10 °C, (l) 16 h, and (m) neutral alumina chromatography (eluent: 0-33% Et_2O in petrol), no isolated products.

*Preparation of 1-(2-iodoethyl)-6-methoxy-1,5-dimethyl-2-methylene-1,2-dihydronaphthalene **166***

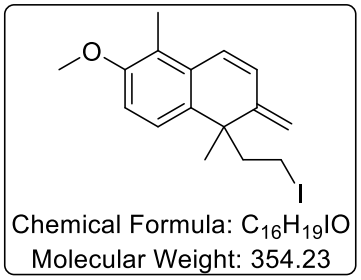

Scheme 4.32

To a flame-dried round bottom flask containing PPh_3 (77 mg, 0.3 mmol) and pyridine (38 µL, 0.47 mmol), **158** (60 mg, 0.25 mmol) dissolved in DCM (1.9 mL) was charged. The mixture was cooled to 0 °C before the addition of I_2 (75 mg, 0.30 mmol), and the resulting solution was left to stir at this temperature for 2 h. After this time, the mixture was quenched with 1 M HCl solution, then 10% sodium thiosulfate solution, and extracted with Et_2O. The organic solution was washed with brine, then dried with sodium sulfate, filtered, and evaporated. The crude mixture was purified by silica chromatography (eluent: 0-33% Et_2O in petrol) to afford **166** (71 mg, 80%) as a pale-yellow oil.

FTIR ($CHCl_3$): 1570. 1595, 2959 cm^{-1}.

^{1}H NMR δ(400 MHz, $CDCl_3$): 1.43 (s, 3H, alkyl CH_3), 2.35 – 2.22 (m, 4H, diastereotopic alkyl CH_2 and $ArCH_3$), 2.51 (td, J = 13.5, ^2J = 4.4 Hz, 1H, diastereotopic alkyl CH_2), 2.67 (td, J = 13.5, ^2J = 4.4 Hz, 1H, diastereotopic CH_2I), 2.93 (td, J = 13.5, ^2J = 4.4 Hz, 1H, diastereotopic CH_2I), 3.82 (s, 3H, $ArOCH_3$), 5.18 (s, 1H, terminal olefinic CH), 5.20 (s, 1H, terminal olefinic CH), 6.36 (d, J = 10.0 Hz, 1H, olefinic CH), 6.64 (d, J = 10.0 Hz, 1H, olefinic CH), 6.75 (d, J = 8.6 Hz, 1H, ArH), 7.16 (d, J = 8.6 Hz, 1H, ArH).

^{13}C NMR δ(101 MHz, $CDCl_3$): 1.3, 10.8, 32.1, 44.9, 51.4, 55.8, 109.7, 114.0, 122.5, 122.8, 123.4, 129.8, 131.9, 133.7, 149.2, 156.2 ppm.

HRMS *m*/*z* (EI): Calc. for $C_{16}H_{19}IO$ (M^+): 354.0464. Found: 354.0475.

*Attempted Preparation of (4-(6-methoxy-1,5-dimethyl-2-methylene-1,2-dihydronaphthalen-1-yl)but-1-yn-1-yl)trimethylsilane **163** from **166***

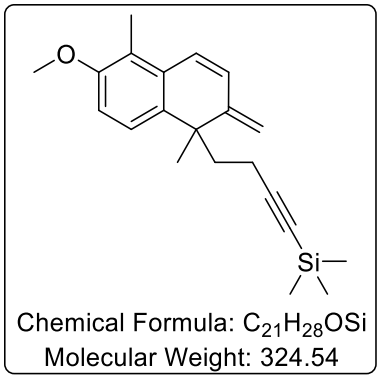

Scheme 4.33, Table 4.8

The following experiments were performed using *General Procedure K*. Results are reported as: (a) volume of trimethylsilylacetylene, (b) volume of THF, (c) volume of ^{n}BuLi, (d) mass of **166**, (e) volume of THF, (f) volume of TMEDA, (g) volume of DMPU, (h) temperature, (i) time, and (j) outcome.

Entry 1: (a) 94 µL, 0.68 mmol, (b) 1.1 mL, (c) 310 µL, 2.2 M in hexanes, 0.68 mmol, (d) 80 mg, 0.23 mmol, (h) 2.2 mL, (i) 100 µL, 0.68 mmol, (j) 80 µL, 0.68 mmol, (k) room temperature, (l) 16 h, and (m) **166** isolated, 80 mg, 100%.

Entry 2: (a) (a) 94 µL, 0.68 mmol, (b) 1.1 mL, (c) 310 µL, 2.2 M in THF, 0.68 mmol, (d) 80 mg, 0.23 mmol, (h) 2.2 mL, (i) 100 µL, 0.68 mmol, (j) 80 µL, 0.68 mmol, (k) 50 °C using an oil bath, (l) 5 h, and (m) silica chromatography, **166** isolated, 64 mg, 80%.

Scheme 4.34

To a flame-dried round bottom flask, trimethylsilylacetylene (42 µL, 0.30 mmol) and THF (0.4 mL) were charged and the resulting solution was cooled to -78 °C using a dry ice/acetone bath. At this temperature, ^{n}BuLi (140 µL, 2.2 M in hexanes, 0.30 mmol) was added dropwise *via* syringe. The resulting mixture was left to stir at this temperature for 1 h.

To another flame-dried round bottom flask containing $Pd_2(dba)_3$ (28 mg, 0.03 mmol) and PPh_3 (32 mg, 0.12 mmol), **166** (70 mg, 0.20 mmol) dissolved in THF (0.6 mL) was charged. To this reaction mixture, the previously prepared lithium trimethylsilylacetylide solution was added dropwise *via* syringe. The resulting mixture was heated to 65 °C and left to stir for 16 h before being quenched with saturated ammonium chloride. The mixture was extracted with Et_2O, washed with brine, then dried with sodium sulfate, filtered, and evaporated. The crude mixture was purified by column chromatography (eluent: 0-33% Et_2O in petrol), unfortunately, affording none of the desired product **163**.

*Attempted Preparation of 6-methoxy-1,5-dimethyl-2-methylene-1-(pent-3-yn-1-yl)-1,2-dihydronaphthalene **96** from **166***

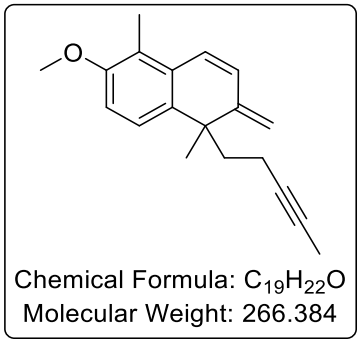

Scheme 4.35, Table 4.9, Entry 1

To a flame-dried round bottom flask, **166** (10 mg, 0.03 mmol) dissolved in THF (600 µL) was charged and subsequently cooled to 0 °C using an ice bath. At this temperature, 1-propynylmagnesium bromide (0.50 M in THF, 112 µL, 0.06 mmol) was added, and the resulting mixture was warmed to room temperature and left to stir for 16 h. After this time, the solution was Et_2O and the organic solution was washed with brine, then dried with sodium sulfate, filtered, and evaporated. The crude mixture was purified by column chromatography (eluent: 0-33% Et_2O in petrol), unfortunately, affording none of the desired product **96** and returning starting material (10 mg, 100%).

Scheme 4.35, Table 4.9, Entry 2

To a flame-dried microwave vial, $FeBr_2$ (3.7 mg, 0.02 mmol) was added and **166** (30 mg, 0.08 mmol) dissolved in THF (340 µL) was charged. Subsequently, *o*-TMEDA (32 µL, 0.17 mmol) and 1-propynylmagnesium bromide (250 µL, 0.50 M in THF, 0.13 mmol) were added and the resulting mixture was left to stir for 16 h. After this time, the solution was extracted with Et_2O and the organic solution was washed with brine, then dried with sodium sulfate, filtered, and evaporated. The crude mixture was purified by column chromatography (eluent: 0-33% Et_2O in petrol), unfortunately, affording none of the desired product **96**.

*Attempted Preparation of 1-(but-3-yn-1-yl)-6-methoxy-1,5-dimethyl-2-methylene-1,2-dihydronaphthalene **167** from **166***

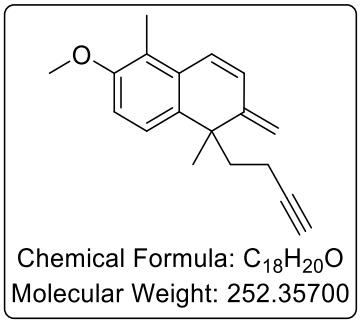

Scheme 4.36

To a flame-dried microwave vial containing lithium acetylide ethylenediamine complex **151** (22 mg, 0.14 mmol), DMSO (170 µL) and Et_2O (170 µL) were charged. The mixture was cooled to 5 °C using an ice bath before adding **166** (60 mg, 0.17 mmol) as a solution in Et_2O (50 µL). The resulting mixture was left to stir for 4 h. After this time, the solution was quenched with water and extracted with Et_2O. The organic solution was washed with brine, then dried with sodium sulfate, filtered, and evaporated. The crude mixture was purified by column chromatography (eluent: 0-33% Et_2O in petrol), unfortunately, affording none of the desired product **167**.

*Preparation of 6-methoxy-1,5-dimethyl-1-vinyl-3,4-dihydronaphthalen-2(1H)-one **62***

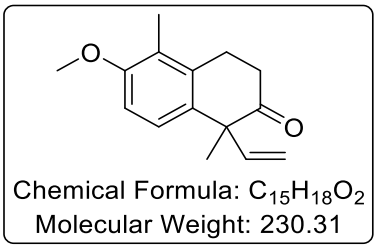

Chemical Formula: $C_{15}H_{18}O_2$
Molecular Weight: 230.31

Scheme 4.38

In a round bottom flask, **17** (2.8 g, 10 mmol) was dissolved in 95% MeCN:H_2O (18 mL) and aq. HCl (4.6 mL, 6.0 M in H_2O) was added. The reaction mixture was left to stir for 3 hours. Following this, the mixture was diluted with water and extracted with Et_2O. The organic layer was dried with sodium sulfate, filtered, and evaporated. The crude mixture was purified by column chromatography (eluent: 0-33% Et_2O in petroleum ether), collecting **62** (2.4 g, quant.) as a colourless oil.

Data for this compound was consistent with that detailed on page 236.

Preparation of 3-(6-methoxy-1,5-dimethyl-2-oxo-1,2,3,4-tetrahydronaphthalen-1-yl)propanal ***170***

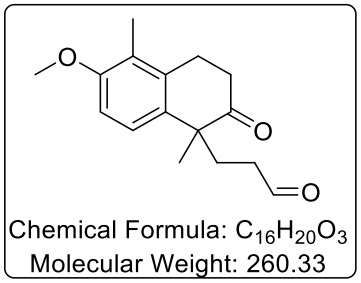

Chemical Formula: $C_{16}H_{20}O_3$
Molecular Weight: 260.33

Scheme 4.41, Table 4.11

The following experiments were performed using *General Procedure L*. Results are reported as: (a) mass of $[Rh(COD)Cl]_2$, (b) mass of *rac*-BINAP, (c) mass of xantphos, (d) mass of **62**, (e) volume of PhMe, (f) volume of formaldehyde, (g) microwave reactor or oil bath, (h) temperature, (i) time, (j) isolated yield of **170**, and (k) recovered **62**.

Entry 1: (a) 0.9 mg, 2 µmol, (b) 2.2 mg, 4 µmol, (c) 2.1 mg, 4 µmol, (d) 41 mg, 0.18 mmol, (e) 1.1 mL, (f) 25 µL, 0.90 mmol, (g) oil bath, (h) 90 °C, (i) 1 h, (j) 0%, and (k) 33 mg, 76%.

Entry 2: (a) 0.9 mg, 2 µmol, (b) 2.2 mg, 4 µmol, (c) 2.1 mg, 4 µmol, (d) 41 mg, 0.18 mmol, (e) 1.1 mL, (f) 25 µL, 0.90 mmol, (g) oil bath, (h) 110 °C, (i) 24 h, (j) 0%, and (k) 29 mg, 71%.

Entry 3: (a) 0.9 mg, 2 µmol, (b) 2.2 mg, 4 µmol, (c) 2.1 mg, 4 µmol, (d) 41 mg, 0.18 mmol, (e) 1.1 mL, (f) 25 µL, 0.90 mmol, (g) microwave, CEM, (h) 90 °C, (i) 1 h, (j) trace, and (k) 34 mg, 82%.

Entry 4: (a) 0.9 mg, 2 µmol, (b) 2.2 mg, 4 µmol, (c) 2.1 mg, 4 µmol, (d) 41 mg, 0.18 mmol, (e) 1.1 mL, (f) 25 µL, 0.90 mmol, (g) microwave, CEM, (h) 90 °C, (i) 5 h, (j) trace, and (k) 32 mg, 78%.

Entry 5: (a) 0.9 mg, 2 µmol, (b) 2.2 mg, 4 µmol, (c) 2.1 mg, 4 µmol, (d) 41 mg, 0.18 mmol, (e) 1.1 mL, (f) 25 µL, 0.90 mmol, (g) microwave, CEM, (h) 110 °C, (i) 5 h, (j) 18 mg, 38%, and (k) 6.1 mg, 15%.

Scheme 4.42, Table 4.12

The following experiments were performed using *General Procedure L*. Results are reported as: (a) mass of $[Rh(COD)Cl]_2$, (b) mass of *rac*-BINAP, (c) mass of xantphos, (d) mass of **62**, (e) volume of PhMe, (f) volume of formaldehyde, (g) microwave model, (h) temperature, (i) time, (j) isolated yield of **170**, and (k) recovered **62**.

Entry 1: (a) 1.8 mg, 3.6 µmol, (b) 4.5 mg, 7.2 µmol, (c) 4.2 mg, 7.2 µmol, (d) 41 mg, 0.18 mmol, (e) 1.1 mL, (f) 25 µL, 0.90 mmol, (g) microwave, CEM, (h) 110 °C, (i) 5 h, (j) 22 mg, 47%, and (k) 5.5 mg, 14%.

Entry 2: (a) 1.8 mg, 3.6 µmol, (b) 4.5 mg, 7.2 µmol, (c) 4.2 mg, 7.2 µmol, (d) 41 mg, 0.18 mmol, (e) 1.1 mL, (f) 25 µL, 0.90 mmol, (g) microwave, CEM, (h) 110 °C, (i) 18 h, (j) 0%, and (k) 4.2 mg, 11%.

Entry 3: (a) 1.8 mg, 4 µmol, (b) 4.5 mg, 7.2 µmol, (c) 4.2 mg, 7.2 µmol, (d) 41 mg, 0.18 mmol, (e) 1.1 mL, (f) 50 µL, 1.8 mmol, (g) microwave, CEM, (h) 110 °C, (i) 5 h, (j) 20 mg, 43%, and (k) 6.9 mg, 17%.

Entry 4: (a) 1.8 mg, 4 µmol, (b) 4.5 mg, 7.2 µmol, (c) 4.2 mg, 7.2 µmol, (d) 41 mg, 0.18 mmol, (e) 1.1 mL, (f) 10 µL, 0.36 mmol, (g) microwave, CEM, (h) 110 °C, (i) 5 h, (j) 14 mg, 29%, and (k) 11 mg, 26%.

Entry 5: (a) 4.4 mg, 9.0 µmol, (b) 11.2 mg, 18 µmol, (c) 10.4 mg, 18 µmol, (d) 41 mg, 0.18 mmol, (e) 1.1 mL, (f) 25 µL, 0.90 mmol, (g) microwave, CEM, (h) 110 °C, (i) 5 h, (j) 28 mg, 60%, and (k) trace.

Entry 6: (a) 4.4 mg, 9.0 µmol, (b) 11.2 mg, 18 µmol, (c) none, (d) 41 mg, 0.18 mmol, (e) 1.1 mL, (f) 25 µL, 0.90 mmol, (g) microwave, CEM, (h) 110 °C, (i) 5 h, (j) trace, and (k) 30 mg, 73%.

Entry 7: (a) 4.4 mg, 9.0 µmol, (b) none, (c) 10.4 mg, 18 µmol, (d) 41 mg, 0.18 mmol, (e) 1.1 mL, (f) 25 µL, 0.90 mmol, (g) microwave, CEM, (h) 110 °C, (i) 5 h, (j) trace, and (k) 33 mg, 79%.

Scheme 4.43, Table 4.13

The following experiments were performed using *General Procedure L*. Results are reported as: (a) mass of $[Rh(COD)Cl]_2$, (b) mass of *rac*-BINAP, (c) mass of xantphos, (d) mass of **62**, (e) volume of PhMe, (f) volume of formaldehyde, (g) microwave model, (h) temperature, (i) time, (j) isolated yield of **170**, and (k) recovered **62**.

Entry 1: (a) 4.4 mg, 9.0 µmol, (b) 11 mg, 18 µmol, (c) 10 mg, 18 µmol, (d) 41 mg, 0.18 mmol, (e) 1.1 mL, (f) 25 µL, 0.90 mmol, (g) microwave, CEM, (h) 90 °C, (i) 8 h, (j) 37 mg, 80%, and (k) trace.

Entry 2: (a) 4.4 mg, 9.0 µmol, (b) 11 mg, 18 µmol, (c) 10 mg, 18 µmol, (d) 41 mg, 0.18 mmol, (e) 1.1 mL, (f) 25 µL, 0.90 mmol, (g) microwave, CEM, (h) 90 °C, (i) 8 h, (j) 31 mg, 65%, and (k) 3.6 mg, 9%.

Entry 3: (a) 4.4 mg, 9.0 µmol, (b) 11 mg, 18 µmol, (c) 10 mg, 18 µmol, (d) 41 mg, 0.18 mmol, (e) 1.1 mL, (f) 25 µL, 0.90 mmol, (g) microwave, CEM, (h) 90 °C, (i) 8 h, (j) 30 mg, 63%, and (k) 3.1 mg, 8%.

Entry 4: (a) 4.4 mg, 9.0 µmol, (b) 11 mg, 18 µmol, (c) 10 mg, 18 µmol, (d) 41 mg, 0.18 mmol, (e) 1.1 mL, (f) 25 µL, 0.90 mmol, (g) microwave, Biotage, (h) 90 °C, (i) 8 h, (j) 28 mg, 59%, and (k) 4.9 mg, 12%.

Entry 5: (a) 19 mg, 0.04 mmol, (b) 49 mg, 0.08 mmol, (c) 45 mg, 0.08 mmol, (d) 180 mg, 0.78 mmol, (e) 4.7 mL, (f) 0.11 mL, 3.9 mmol, (g) microwave, Biotage, (h) 90 °C, (i) 8 h, (j) 200 mg, 60%, and (k) 18 mg, 10%.

Entry 6: (a) 44 mg, 0.09 mmol, (b) 112 mg, 0.180 mmol, (c) 104 mg, 0.180 mmol, (d) 415 mg, 1.80 mmol, (e) 10.8 mL, (f) 0.25 mL, 9.00 mmol, (g) microwave, Biotage, (h) 90 °C, (i) 8 h, (j) 250 mg, 53%, and (k) 83 mg, 20%.

Entry 7 (performed in 6 vessels, then pooled for one purification): (a) 44.3 mg, 0.09 mmol, (b) 112 mg, 0.18 mmol, (c) 104 mg, 0.18 mmol, (d) 415 mg, 1.80 mmol, (e) 10.8 mL, (f) 0.25 mL, 9.00 mmol, (g) microwave, Biotage, (h) 90 °C, (i) 8 h, (j) 1.41 g, 50%, from 6 reactions, and (k) 0.59 g, 24% from 6 reactions.

FTIR ($CHCl_3$): 1714, 2802, 2961 cm^{-1}.

^{1}H NMR δ(400 MHz, $CDCl_3$): 1.44 (s, 3H, alkyl CH_3), 1.93 – 2.03 (m, 2H, alkyl CH_2), 2.22 – 2.10 (m, 4H, $ArCH_3$, diastereotopic alkyl $CH_2C{=}O$), 2.42 – 2.48 (m, 1H, diastereotopic alkyl $CH_2C{=}O$), 2.58 – 2.64 (m, 1H, diastereotopic benzyl CH_2), 2.73 – 2.81 (m, 1H, diastereotopic ring alkyl CH_2), 2.89 – 2.97 (m, 1H, diastereotopic ring alkyl CH_2), 3.10 – 3.17 (m, 1H, diastereotopic benzyl CH_2), 3.83 (s, 3H, $ArOCH_3$), 6.81 (d, J = 8.7 Hz, 1H, ArH), 7.08 ppm (d, J = 8.7 Hz, 1H, ArH), 9.55 ppm (s, 1H, aldehyde CH).

^{13}C NMR δ(101 MHz, $CDCl_3$): 11.7, 25.6, 28.3, 32.0, 37.6, 40.2, 50.6, 55.7, 109.6, 123.8, 124.6, 133.3, 135.9, 156.2, 201.7, 214.6 ppm.

HRMS *m*/*z* (EI): Calc. for $C_{16}H_{20}O_3$ (M^+): 260.1407. Found: 260.1407.

*Attempted Preparation of 1-(but-3-yn-1-yl)-6-methoxy-1,5-dimethyl-3,4-dihydronaphthalen-2(1H)-one **173***

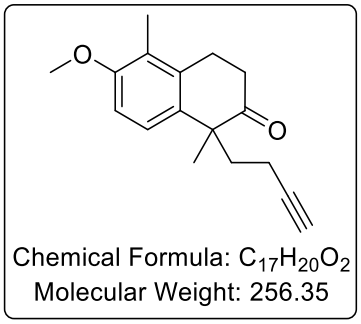

Scheme 4.44

To a flame-dried round bottom flask, **170** (50 mg, 0.19 mmol) dissolved in MeOH (1.5 mL) was charged and cooled to 0 °C using an ice bath. At this temperature, K_2CO_3 (40.0 mg, 0.29 mmol) was added, and **174** (55 mg, 0.29 mmol) dissolved in MeOH (1.5 mL) was added dropwise *via* syringe. The resulting mixture was warmed to room temperature and left to stir for 3 h. After this time, the solution was diluted with Et_2O. The organic solution was washed with saturated sodium bicarbonate solution, then dried with sodium sulfate, filtered, and evaporated. The crude mixture was purified by column chromatography (eluent: 0-33% Et_2O in petrol), unfortunately, affording none of the desired product **173**.

Preparation of 1-(4,4-dibromobut-3-en-1-yl)-6-methoxy-1,5-dimethyl-3,4-dihydronaphthalen-2(1H)-one ***169***

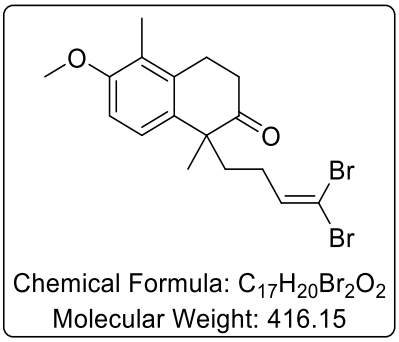

Scheme 4.45

To a flame-dried round bottom flask, CBr_4 (1.5 g, 4.6 mmol) dissolved in DCM (19 mL) was charged and cooled to 0 °C using an ice bath. At this temperature, PPh_3 (2.4 g, 9.2 mmol) was added portion wise into the reaction mixture over 10 min, and left to stir for an additional 10 min. After this time, **170** (1.0 g, 3.8 mmol) dissolved in DCM (4.3 mL) was added dropwise *via* syringe into the reaction mixture. After this, the solution was left to stir for 1 h before being diluted with hexane (15 mL). The mixture was filtered over celite® to remove the solids, with the filter cake being washed with 15% Et_2O in hexane. The solvent was removed, and the crude mixture was purified by silica chromatography (eluent: 0-33% Et_2O in petrol) to afford **169** (1.55 g, 92%) as a pale-yellow oil.

FTIR ($CHCl_3$): 1593, 1709, 2961 cm^{-1}.

^{1}H NMR δ(400 MHz, $CDCl_3$): 1.41 (s, 3H, alkyl CH_3), 1.64 – 1.78 (m, 3H, alkyl CH_2, diastereotopic alkyl CH_2), 2.16 – 2.37 (m, 4H, $ArCH_3$, diastereotopic alkyl CH_2), 2.60 (dt, ^2J = 14.6, J = 5.6 Hz, 1H, diastereotopic benzyl CH_2), 2.70 – 2.78 (m, 1H, diastereotopic ring alkyl CH_2), 2.88 – 2.98 (m, 1H, diastereotopic ring alkyl CH_2), 3.09 (dt, ^2J = 14.6, J = 5.6 Hz, 1H, diastereotopic benzyl CH_2), 3.84 (s, 3H, $ArOCH_3$), 6.17 (t, J = 7.0 Hz, 1H, vinylic CH), 6.82 (d, J = 8.7 Hz, 1H, ArH), 7.11 (d, J = 8.7 Hz, 1H, ArH) ppm.

^{13}C NMR δ(101 MHz, $CDCl_3$): 11.7, 25.6, 28.5, 29.4, 37.8, 37.9, 50.9, 55.8, 89.1, 109.5, 124.0, 124.5, 133.7, 135.9, 138.3, 156.2, 214.7 ppm.

HRMS *m*/*z* (EI): Calc. for $C_{17}H_{20}{}^{79}Br_2O_2$ (M^+): 413.9825. Found: 413.9842.

*Preparation of 1-(4,4-dibromobut-3-en-1-yl)-6-methoxy-1,5-dimethylnaphthalen-2(1H)-one **168***[9]

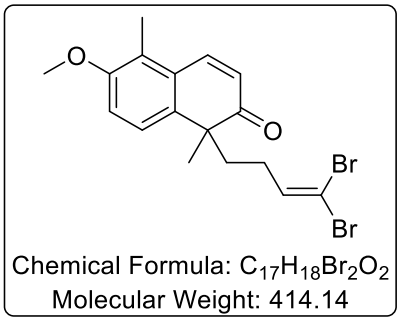

Chemical Formula: $C_{17}H_{18}Br_2O_2$
Molecular Weight: 414.14

Scheme 4.46, Table 4.14

The following experiments were performed using *General Procedure M*. Results are reported as: (a) mass of **169**, (b) volume of DCM, (c) volume of Et_3N, (d) volume of TMSOTf, (e) estimated mass of **175** isolated, (f) volume of MeCN, (g) mass of $Pd(OAc)_2$, (h) amount of base, (i) temperature (j) time, and (k) isolated yield of **168** over 2 steps.

Entry 1: (a) 1.2 g, 2.9 mmol, (b) 33 mL, (c) 2.0 mL, 15 mmol, (d) 0.8 mL, 4.4 mmol, (e) 1.4 g, ~98%, (f) 12 mL, (g) 0.7 g, 3.1 mmol, (h) none, (i) 40 °C, (j) 16 h, and (k) 0.60 g, 53% over 2 steps.

Entry 2: (a) 71 mg, 0.17 mmol, (b) 1.9 mL, (c) 0.1 mL, 0.85 mmol, (d) 47 µL, 0.26 mmol, (e) 75 mg, ~90%, (f) 0.6 mL, (g) 38 mg, 0.17 mmol, (h) none, (i) 30 °C, (j) 16 h, and (k) 36 mg, 51% over 2 steps.

Entry 3: (a) 50 mg, 0.12 mmol, (b) 1.3 mL, (c) 83 µL, 0.60 mmol, (d) 33 µL, 0.18 mmol, (e) 52 mg, ~89%, (f) 0.5 mL, (g) 26 mg, 0.12 mmol, (h) none, (i) 25 °C, (j) 16 h, and (k) 50 mg, 47% over 2 steps.

Entry 4: (a) (a) 50 mg, 0.12 mmol, (b) 1.3 mL, (c) 83 µL, 0.60 mmol, (d) 33 µL, 0.18 mmol, (e) 53 mg, ~90%, (f) 0.5 mL, (g) 26 mg, 0.12 mmol, (h) Na_2CO_3, 18 mg, 0.13 mmol, (i) 40 °C, (j) 16 h, and (k) 16 mg, 33% over 2 steps.

Entry 5: (a) 71 mg, 0.17 mmol, (b) 1.9 mL, (c) 0.1 mL, 0.85 mmol, (d) 47 µL, 0.26 mmol, (e) 80 mg, ~96%, (f) 1.4 mL, (g) 47.8 mg, 0.21 mmol, (h) Na_2CO_3, 22 mg, 0.21 mmol, (u) 40 °C, (j) 65 h, and (k) 36 mg, 51% over 2 steps.

Entry 6: (a) 80 mg, 0.19 mmol, (b) 2.1 mL, (c) 0.1 mL, 0.95 mmol, (d) 52 µL, 0.29 mmol, (e) 88 mg, ~95%, (f) 1.5 mL, (g) 44.9 mg, 0.20 mmol, (h) Na_2CO_3, 23 mg, 0.21 mmol, (i) 60 °C, (j) 16 h, and (k) 22 mg, 27% over 2 steps.

Entry 7: (a) 30 mg, 0.07 mmol, (b) 0.9 mL, (c) 49 µL, 0.35 mmol, (d) 20 µL, 0.11 mmol, (e) 31 mg, ~91%, (f) 0.3 mL, (g) 15 mg, 0.07 mmol, (h) Et_3N, 10 µL, 0.07 mmol, (i) 40 °C, (j) 16 h, and (k) 0%.

FTIR: Could not be collected due to COVID-19 lockdown.

1H NMR δ(400 MHz, $CDCl_3$): 1.40 (s, 3H, alkyl CH_3), 1.60 – 1.77 (m, 2H, alkyl CH_2), 1.90 – 1.98 (m, 1H, diastereotopic alkyl CH_2), 2.31 – 2.39 (m, 4H, $ArCH_3$, diastereotopic alkyl CH_2), 3.86 (s, 3H, $ArOCH_3$), 6.13 (t, *J* = 7.4 Hz, 1H, $CHCBr_2$), 6.21 (d, *J* = 10.2 Hz, 1H, olefinic CH), 6.95 (d, *J* = 8.6 Hz, 1H, ArH), 7.21 (d, *J* = 8.6 Hz, 1H, ArH), 7.84 ppm (d, *J* = 10.2 Hz, 1H, olefinic CH).

^{13}C NMR δ(101 MHz, $CDCl_3$): 10.9, 29.2, 29.5, 39.9, 50.8, 55.7, 89.3, 112.3, 124.6, 125.2, 125.6, 129.1, 137.6, 138.2, 141.4, 156.3, 204.2 ppm.

Preparation of ((1-(4,4-dibromobut-3-en-1-yl)-6-methoxy-1,5-dimethyl-1,4-dihydronaphthalen-2-yl)oxy)triethylsilane ***176***

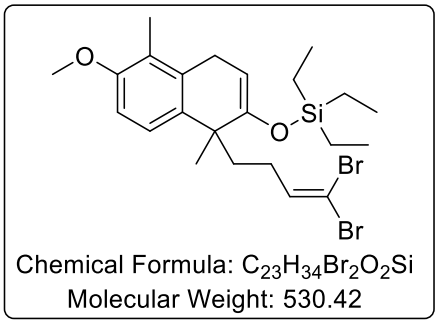

Chemical Formula: $C_{23}H_{34}Br_2O_2Si$
Molecular Weight: 530.42

Scheme 4.47

To a flame-dried round bottom flask, **169** (180 mg, 0.43 mmol) dissolved in DCM (4.8 mL) was charged, followed by the addition of Et_3N (0.30 mL, 2.2 mmol). The reaction mixture was cooled to -5 °C before the dropwise addition of TMSOTf (0.15 mL, 0.65 mmol) *via* syringe. The resulting mixture was left to stir at this temperature for 30 min. After this time, the mixture was quenched with saturated sodium bicarbonate solution and extracted with DCM. The organic solution was then dried with sodium sulfate, filtered, and evaporated. The crude mixture was purified by silica chromatography (eluent: 0-33% Et_2O in petrol) to afford **176** (190 mg, 83%) as a colourless oil.

FTIR ($CHCl_3$): 1684, 2953 cm^{-1}.

^{1}H NMR δ(400 MHz, $CDCl_3$): 0.74 (q, *J* = 7.9 Hz, 6H, 3 × $SiCH_2$), 1.02 (t, *J* = 7.9 Hz, 9H, 3 × $SiCH_2C\mathbf{H_3}$), 1.39 (s, 3H, alkyl CH_3), 1.57 – 1.63 (m, 2H, alkyl CH_2), 1.84 – 1.90 (m, 1H, diastereotopic alkyl CH_2), 2.07 – 2.13 (m, 4H, $ArCH_3$, diastereotopic alkyl CH_2), 3.29 (d, *J* = 3.6 Hz, 2H, benzyl CH_2), 3.82 (s, 3H, $ArOCH_3$), 5.00 (t, *J* = 3.6 Hz, 1H, olefinic CH), 6.13 (t, *J* = 7.2 Hz, 1H, $CHCBr_2$), 6.79 (d, *J* = 8.7 Hz, 1H, ArH), 7.12 ppm (d, *J* = 8.7 Hz, 1H, ArH).

^{13}C NMR δ(101 MHz, $CDCl_3$): 5.4, 7.1, 11.3, 28.2, 29.4, 29.6, 38.8, 42.5, 55.8, 87.6, 98.8, 101.2, 109.2, 123.2, 124.3, 133.7, 139.5, 151.4, 155.3 ppm.

HRMS *m*/*z* (EI): Calc. for $C_{23}H_{34}{}^{79}Br_2O_2Si$ (M^+): 528.0689. Found: 528.0656.

*Preparation of 1-(4,4-dibromobut-3-en-1-yl)-6-methoxy-1,5-dimethylnaphthalen-2(1H)-one **168***[9]

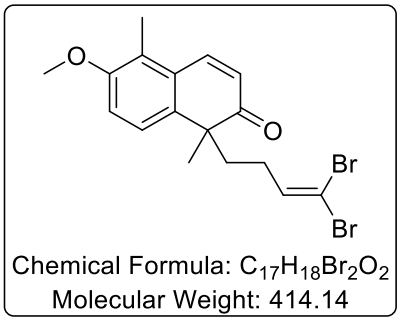

Chemical Formula: $C_{17}H_{18}Br_2O_2$
Molecular Weight: 414.14

Scheme 4.47

To a flame-dried round bottom flask, **176** (190 mg, 0.35 mmol) dissolved in MeCN (1.5 mL) was charged, followed by the addition of $Pd(OAc)_2$ (86 mg, 0.38 mmol). The reaction mixture was heated to 40 °C using an oil bath and was left to stir for 16 h. After this time, the mixture was filtered over celite® to remove the solids, with the filter cake being washed with Et_2O. The solvent was removed, and the crude mixture was purified by silica chromatography (eluent: 0-33% Et_2O in petrol) to afford **168** (53 mg, 37%) as a colourless oil.

Data for this compound was consistent with that detailed on page 303.

Scheme 4.48

To a flame-dried round bottom flask, di-*iso*-propylamine (50 µL, 0.35 mmol) and THF (3 mL) were charged and cooled to -10 °C using an ice bath. At this temperature, ^{n}BuLi (140 µL, 2.5 M in hexanes, 0.35 mmol) was added dropwise *via* syringe and the resulting solution was left to stir for 30 min. After this time, the reaction mixture was cooled to -78 °C using a dry ice/acetone bath and **169** (75 mg, 0.29 mmol) dissolved in THF (1 mL) was added. The mixture was left to stir for 1 h, prior to the addition of **177** (81 mg, 0.37 mmol; preparation described on *pages 307-308*), which was added dropwise *via* syringe. The resulting mixture was warmed to room temperature and left to stir for 30 min. After this time, the solution was quenched with saturated ammonium chloride and diluted with Et_2O.

The organic solution was washed with brine, then dried with sodium sulfate, filtered, and evaporated. The crude mixture was purified by column chromatography (eluent: 0-33% Et_2O in petrol), unfortunately, affording none of the desired product **168**.

Scheme 4.49

To a flame-dried microwave vial containing CuTc (8.2 mg, 0.04 mmol) and $CyPPh_2$ (12 mg, 0.04 mmol), **169** (90 mg, 0.22 mmol) dissolved in degassed benzene (3.0 mL) was charged. DTBP (47 mg, 0.32 mmol) was subsequently added and the reaction mixture was heated to 80 °C using an oil bath. After 16 h reaction time, the solvent was removed and the crude mixture was purified by silica chromatography (eluent: 0-33% Et_2O in petrol) to afford **168** (10 mg, 11%) as a pale-yellow oil.

Data for this compound was consistent with that detailed on page 303.

Preparation of N,N-dichloro-tert-butylamine ***212***[112]

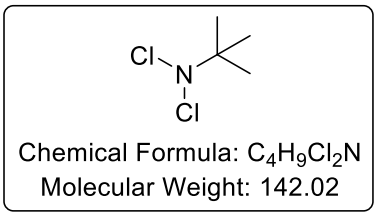

To a flame-dried 3-neck round bottom flask, calcium hypochlorite (68.4 g, 479 mmol) dissolved DCM (360 mL) was charged and cooled to 0 °C before the addition of *tert*-butylamine (14.4 mL, 137 mmol). At this temperature, aq. HCl (360 mL, 3 M in H_2O) was added dropwise over 1 h, and, once complete, the mixture was left to stir for a further 3 h. After this time, the organic layer was extracted with DCM. The organic solution was washed with brine, then dried with sodium sulfate, filtered, and carefully evaporated (150 mbar, bath at rt) to afford **212** (9.70 g, 50%) as a pale-yellow liquid.

FTIR: Could not be collected due to COVID-19 lockdown.

^{1}H NMR δ(400 MHz, $CDCl_3$): 1.41 ppm (s, 9H, alkyl CH_3 × 3).

^{13}C NMR δ(101 MHz, $CDCl_3$): 25.8, 72.8 ppm.

*Preparation of N-tert-butylbenzenesulfinimidoyl chloride **177***[112]

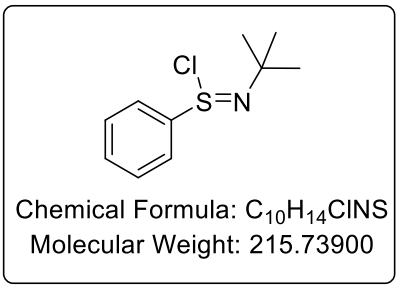

To a flame-dried round bottom flask equipped with a condenser containing *N*,*N*-dichloro-*tert*-butylamine **212** (0.50 g, 3.52 mmol), benzene (5.0 mL) was charged. S-phenylthioacetate (0.444 g, 2.92 mmol) was subsequently added and the resulting reaction mixture was left to stir for 3 h. After this time, the reaction flask was fitted into a flame-dried distillation kit and the volatiles were removed by distillation (100 °C), first at atmospheric pressure and then under reduced pressure (10 mmHg). Finally, the product was left under high vacuum (1.0 mmHg) to afford **177** (0.30 g, 47%) as a pale-orange semi-solid, which was stored at -18 °C under argon.

FTIR ($CHCl_3$): 2988, 1482, 1392 cm^{-1}.

1H NMR δ(400 MHz, $CDCl_3$): 1.55 (s, 9H, alkyl $CH_3 \times 3$), 7.57 – 7.66 (m, 3H, ArH), 8.12 – 8.15 ppm (m, 2H, ArH).

^{13}C NMR δ(101 MHz, $CDCl_3$): 29.9, 64.2, 126.1, 129.2, 133.5, 142.8 ppm.

Attempted Preparation of 1-(4,4-dibromobut-3-en-1-yl)-6-methoxy-1,5-dimethyl-3-(phenylselanyl)-3,4-dihydronaphthalen-2(1H)-one ***178***

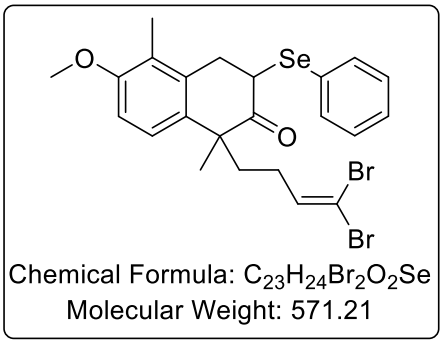

Chemical Formula: $C_{23}H_{24}Br_2O_2Se$
Molecular Weight: 571.21

Scheme 4.50

To a flame-dried round bottom flask, di-*iso*-propylamine (21 µL, 0.14 mmol) and THF (1.3 mL) were charged and cooled to -10 °C using an ice bath. At this temperature, ^{n}BuLi (2.5 M in hexanes, 61 µL, 0.35 mmol) was added dropwise *via* syringe and left to stir for 30 min. After this time, the reaction flask was cooled to -78 °C using a dry ice/acetone bath, then **169** (50 mg, 0.12 mmol) dissolved in THF (0.1 mL) was added, and the mixture was left to stir for 2 h. After this time, PhSeBr (37 mg, 0.16 mmol) was quickly added, and the resulting mixture was warmed to room temperature and left to stir for 16 h. After this time, the solution was quenched with saturated ammonium chloride and diluted with Et_2O. The organic solution was washed with brine, then dried with sodium sulfate, filtered, and evaporated. The crude mixture was purified by column chromatography (eluent: 0-33% Et_2O in petrol), unfortunately, affording none of the desired product **178**.

*Preparation of 6-methoxy-1,5-dimethyl-2-methylene-1-(pent-3-yn-1-yl)-1,2-dihydronaphthalene **96** from **168***[8,9]

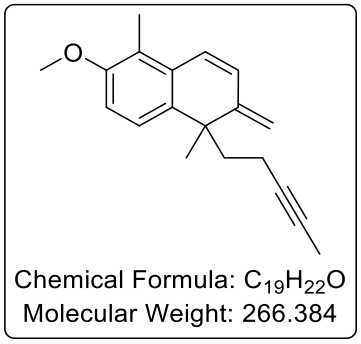

Scheme 4.51, Table 4.15, Entry 1

To a flame-dried round bottom flask containing $MePPh_3Br$ (230 mg, 0.64 mmol), THF (6.8 mL) was charged and cooled to 0 °C. At this temperature, KO^tBu (140 mg, 1.2 mmol) was added quickly and the reaction mixture was left to stir for 30 min. After this time, **168** (85 mg, 0.21 mmol) dissolved in THF (1.7 mL) was added dropwise *via* syringe and was left to stir for 2 h. After this time, the mixture was quenched with saturated ammonium chloride solution and extracted with Et_2O. The organic solution was then dried with sodium sulfate, filtered, and evaporated. The crude mixture was purified by silica chromatography (eluent: 0-33% Et_2O in petrol) to afford a 1:1 ratio of **179**:**180**, (45 mg, ~52%), which was used directly in the next step. To another flame-dried round bottom flask, the mixture dissolved in THF (8.2 mL) was charged and cooled to -78 °C using a dry ice/acetone bath. At this temperature, ^{n}BuLi (320 µL, 2.0 M in hexanes, 0.72 mmol) was added and the reaction mixture was left to stir for 30 min. Subsequently, MeI (58 µL, 0.92 mmol) was added to the solution, and, after 15 min, the reaction mixture was warmed to room temperature. The mixture was left to stir for a further 30 min before being quenched with saturated ammonium chloride solution and extracted with Et_2O. The organic solution was washed with brine, then dried with sodium sulfate, filtered, and evaporated. The crude mixture was purified by silica chromatography (eluent: 0-33% Et_2O in petrol) to afford **96** (20 mg, 37% over 2 steps) as a pale-yellow oil.

Scheme 4.51, Table 4.15, Entry 2

To a flame-dried round bottom flask containing $MePPh_3Br$ (1.9 g, 5.3 mmol), THF (33 mL) was charged and cooled to 0 °C. At this temperature, KO^{t}Bu (0.58 g, 5.3 mmol) was added quickly and the resulting mixture was left to stir for 30 min. After this time, **168** (0.71 g, 1.7 mmol) dissolved in THF (21 mL) was added dropwise *via* syringe and was left to stir for 1 h. To the flask, a further quanity of KO^{t}Bu (0.58 g, 5.3 mmol) was added and the resulting mixture was left to stir for a further 30 min. After this time, the mixture was quenched with saturated ammonium chloride solution and extracted with Et_2O. The organic solution was then dried with sodium sulfate, filtered, and evaporated. The crude mixture was purified by silica chromatography (eluent: 0-33% Et_2O in petrol) to afford a 19:1 ratio of **167**:**179**, (0.30 g, ~70%), which was used directly in the next step. To another flame-dried round bottom flask, the **167**/**179** mixture (0.30 g, ~1.19 mmol) dissolved in THF (40 mL) was charged and cooled to -78 °C using a dry ice/acetone bath. At this temperature, ^{n}BuLi (2.2 M in hexanes, 1.1 mL, 2.4 mmol) was added and the solution was left to stir for 30 min. Subsequently, MeI (0.30 mL, 4.8 mmol) was added, and, after 15 min, the reaction mixture was warmed to room temperature. The mixture was left to stir for 30 min before being quenched with saturated ammonium chloride solution and extracted with Et_2O. The organic solution was washed with brine, then dried with sodium sulfate, filtered, and evaporated. The crude mixture was purified by silica chromatography (eluent: 0-33% Et_2O in petrol) to afford **96** (0.38 g, 71% over 2 steps) as a pale-yellow oil.

FTIR ($CHCl_3$): 1570, 1595, 2918 cm^{-1}.

^{1}H NMR δ(400 MHz, $CDCl_3$): 1.41 (s, 3H, alkyl CH_3), 1.59 – 1.73 (m, 4H, alkynyl CH_3, diastereotopic alkyl CH_2), 1.85 – 1.94 (m, 2H, alkyl CH_2), 2.06 – 2.17 (m, 1H, diastereotopic alkyl CH_2), 2.23 (s, 3H, $ArCH_3$), 3.80 (s, 3H, $ArOCH_3$), 5.15 (s, 1H, terminal olefinic CH), 5.16 (s, 1H, terminal olefinic CH), 6.34 (d, J = 10.0 Hz, 1H, olefinic CH), 6.62 (d, J = 10.0 Hz, 1H, olefinic CH), 6.73 (d, J = 8.6 Hz, 1H, ArH), 7.16 ppm (d, J = 8.6 Hz, 1H, ArH).

^{13}C NMR δ(101 MHz, $CDCl_3$): 3.6, 10.8, 14.7, 32.5, 42.3, 45.9, 55.8, 75.1, 79.8, 109.6, 113.7, 122.2, 122.6, 123.5, 130.0, 131.9, 134.8, 149.9, 156.0 ppm.

Preparation of (5aS,11bS)-9-methoxy-3,8,11b-trimethyl-1,6,7,11b-tetrahydro-2H-pentaleno[1,6a-a]naphthalen-4(5H)-one ***97***[10]

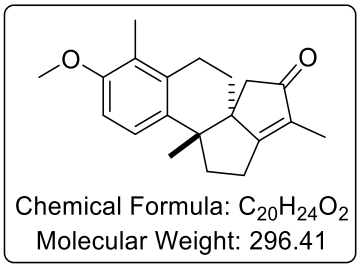

Scheme 4.53, Table 4.16

The following experiments were performed using *General Procedure N*. Results are reported as: (a) mass of **95**, (b) volume of 1,2-DCE, (c) mass of $CO_2(CO)_8$, (d) volume of DodSMe, and (e) isolated yield of **97**.

Entry 1: (a) 0.13 g, 0.48 mmol, (b) 5.0 mL, (c) 0.37 g, 0.53 mmol, (d) 0.45 mL, 1.7 mmol, and (e) 77%, 0.11 g.

Entry 2: (a) 0.43 g, 1.6 mmol, (b) 16 mL, (c) 0.60 g, 1.8 mmol, (d) 1.5 mL, 5.6 mmol, and (e) 76%, 0.36 g.

Melting point: 150–152 °C.

FTIR (neat): 1662, 1697, 2945 cm^{-1}.

^{1}H NMR δ(400 MHz, $CDCl_3$): 1.14 (s, 3H, alkyl CH_3), 1.44 (ddd, ^2J = 13.5 Hz, J = 5.1 Hz, J = 2.0 Hz, 1H, diastereotopic alkyl CH_2), 1.74 (s, 3H, vinylic CH_3), 1.96 – 2.09 (m, 2H, alkyl CH_2), 2.13 (s, 3H, $ArCH_3$), 2.26 – 2.43 (m, 3H, alkyl protons), 2.52 – 2.75 (m, 3H, alkyl protons containing alkyl $C(O)CH_2$), 2.86 (ddd, ^2J = 13.5 Hz, J = 5.1 Hz, J = 2.0 Hz, 1H, diastereotopic alkyl CH_2), 3.81 (s, 3H, OCH_3), 6.76 (d, J = 8.6 Hz, 1H, ArH), 7.17 ppm (d. J = 8.6 Hz, 1H, ArH).

^{13}C NMR δ(101 MHz, $CDCl_3$): 8.6, 11.5, 23.6, 23.7, 25.6, 31.9, 42.9, 43.3, 43.6, 53.9, 55.8, 108.8, 124.2, 124.8, 132.3, 134.4, 135.9, 155.8, 186.9, 211.1 ppm.

Preparation of 1,2-dihydro-6-methoxy-1,5-dimethyl-2-methylen-1-(pent-3-ynyl)naphthalene dicobalt hexacarbonyl ***182***[9]

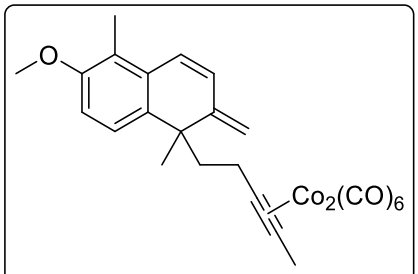

Chemical Formula: $C_{25}H_{22}Co_2O_7$
Molecular Weight: 552.30

Scheme 4.55

To a flame-dried round bottom flask, **96** (40 mg, 0.15 mmol) dissolved in petrol (1.7 mL) was added. Subsequently, $Co_2(CO)_8$ (54 mg, 0.16 mmol) was added quickly and the resulting mixture was left to stir for 1 h. After this time, the solvent was evaporated and the crude mixture was purified by silica chromatography (eluent: petrol) to afford **182** (80 mg, 97%) as a dark red oil.

FTIR: Could not be collected due to COVID-19 lockdown.

^{1}H NMR δ(400 MHz, $CDCl_3$): 1.45 (s, 3H, alkyl CH_3), 2.02 – 2.11 (m, 1H, diastereotopic alkyl CH_2), 2.18 – 2.35 (m, 5H, $ArCH_3$, alkyl CH_2), 2.54 – 2.62 (m, 4H, alkynyl CH_3, diastereotopic alkyl CH_2), 3.81 (s, 3H, $ArOCH_3$), 5.18 (s, 1H, terminal olefinic CH), 5.22 (s, 1H, terminal olefinic CH), 6.34 (d, J = 10.0 Hz, 1H, olefinic CH), 6.68 (d, J = 10.0 Hz, 1H, olefinic CH), 6.75 (d, J = 8.6 Hz, 1H, ArH), 7.20 ppm (d, J = 8.6 Hz, 1H, ArH).

^{13}C NMR δ(101 MHz, $CDCl_3$): 10.9, 20.4, 28.6, 34.4, 42.4, 46.9, 55.8, 100.9, 109.8, 113.5, 122.3, 122.6, 123.4, 129.9, 131.8, 134.9, 150.2, 156.0, 200.6 ppm. To note, missing 1 alkyne peak due to high dilution of sample.

Preparation of (5aR,11bR)-9-methoxy-3,8,11b-trimethyl-1,11b-dihydro-2H-pentaleno[1,6a-a]naphthalen-4(5H)-one ***98***[8,9]

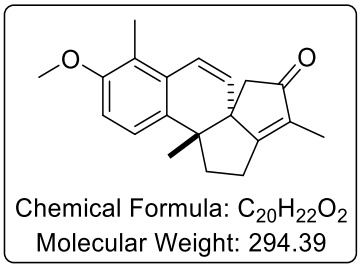

Chemical Formula: $C_{20}H_{22}O_2$
Molecular Weight: 294.39

Scheme 4.56, Table 4.17

The following experiments were performed using *General Procedure O*. Results are reported as: (a) apparatus used, (b) mass of **182**, (c) volume of solvent, (d) volume of DodSMe, (e) temperature, (f) overall time, (g) amounts of additional $Co_2(CO)_8$ and DodSMe, added at the specified reaction time(s), and (h) isolated yield of **98**.

Entry 1: (a) flask with condenser, (b) 100 mg, 0.18 mmol, (c) 1,2-DCE, 1.8 mL, (d) 170 µL, 0.63 mmol, (e) reflux, (f) 60 h, (g) n/a, and (h) 32%, 17 mg.

Entry 2: (a) flask with condenser, (b) 71 mg, 0.13 mmol, (c) 1,2-DCE, 1.3 mL, (d) 120 µL, 0.45 mmol, (e) reflux, (f) 70 h, (g) $Co_2(CO)_8$ (44 mg, 0.13 mmol) and DodSMe (34 µL, 0.13 mmol) at 16 h and 40 h, and (h) 39%, 15 mg.

Entry 3: (a) microwave vial, (b) 70 mg, 0.13 mmol, (c) 1,2-DCE, 1.3 mL, (d) 120 µL, 0.45 mmol, (e) 100 °C, (f) 24 h, (g) n/a, and (h) 27%, 10 mg.

Entry 4: (a) microwave vial, (b) 36 mg, 0.06 mmol, (c) 1,2-DCE, 0.7 mL, (d) 60 µL, 0.23 mmol, (e) 100 °C, (f) 70 h, (g) $Co_2(CO)_8$ (22 mg, 0.06 mmol) and DodSMe (17 µL, 0.06 mmol) at 16 h and 40 h, and (h) 16%, 3.0 mg.

Entry 5: (a) flask with condenser, (b) 30 mg, 0.05 mmol, (c) 1,2-DCE, 0.5 mL, (d) 30 µL, 0.12 mmol, (e) reflux, (f) 24 h, (g) $Co_2(CO)_8$ (17 mg, 0.05 mmol) and DodSMe (13 µL, 0.05 mmol) at 16 h, and (h) 38%, 6.0 mg.

Entry 6: (a) flask with condenser, (b) 30 mg, 0.05 mmol, (c) PhMe, 0.5 mL, (d) 30 µL, 0.12 mmol, (e) reflux, (f) 10 h, (g) $Co_2(CO)_8$ (17 mg, 0.05 mmol) and DodSMe (13 µL, 0.05 mmol) at 5 h, and (h) 38%, 6.0 mg.

Entry 7: (a) microwave vial, (b) 30 mg, 0.05 mmol, (c) PhMe, 0.5 mL, (d) 30 µL, 0.12 mmol, (e) reflux, (f) 10 h, (g) $Co_2(CO)_8$ (17 mg, 0.05 mmol) and DodSMe (13 µL, 0.05 mmol) at 5 h, and (h) 31%, 5.0 mg.

Scheme 4.57, Table 4.18

The following experiments were performed using *General Procedure P*. Results are reported as: (a) apparatus used, (b) mass of **96**, (c) volume of solvent, (d) mass of $Co_2(CO)_8$, (e) volume of DodSMe, (f) temperature, (g) overall time, (h) amounts of additional $Co_2(CO)_8$ and DodSMe, added at the specified reaction time(s), and (i) isolated yield of **98**.

Entry 1: (a) flask with condenser, (b) 20 mg, 0.08 mmol, (c) PhMe, 0.8 mL, (d) 28 mg, 0.08 mmol, (e) 70 µL, 0.26 mmol, (f) reflux, (g) 10 h, (h) $Co_2(CO)_8$ (17 mg, 0.05 mmol) and DodSMe (13 µL, 0.05 mmol) at 4 h, and (i) 45%, 10 mg.

Entry 2: (a) microwave vial, (b) 20 mg, 0.08 mmol, (c) PhMe, 0.8 mL, (d) 28 mg, 0.08 mmol, (e) 70 µL, 0.26 mmol, (f) 130 °C, (g) 8 h, (h) $Co_2(CO)_8$ (17 mg, 0.05 mmol) and DodSMe (13 µL, 0.05 mmol) at 4 h, and (i) 50%, 12 mg.

Entry 3: (a) microwave vial, (b) 20 mg, 0.08 mmol, (c) xylenes, 0.8 mL, (d) 28 mg, 0.08 mmol, (e) 70 µL, 0.26 mmol, (f) 130 °C, (g) 6 h, (h) $Co_2(CO)_8$ (17 mg, 0.05 mmol) and DodSMe (13 µL, 0.05 mmol) at 3 h, and (i) 38%, 6.0 mg.

Scheme 4.58, Table 4.19

The following experiments were performed using *General Procedure P*. Results are reported as: (a) apparatus used, (b) mass of **96**, (c) volume of solvent, (d) mass of $Co_2(CO)_8$, (e) volume of DodSMe, (f) temperature, (g) overall time, (h) amounts of additional $Co_2(CO)_8$ and DodSMe, added at the specified reaction time(s), and (i) isolated yield of **98**.

Entry 1: (a) microwave vial, (b) 20 mg, 0.08 mmol, (c) PhMe, 0.8 mL, (d) 56 mg, 0.17 mmol, (e) 70 µL, 0.26 mmol, (f) 130 °C, (g) 8 h, (h) n/a, and (i) 36%, 10 mg.

Entry 2: (a) microwave vial, (b) 20 mg, 0.08 mmol, (c) PhMe, 0.8 mL, (d) 57 mg, 0.08 mmol, (e) 120 µL, 0.45 mmol, (f) 130 °C, (g) 8 h, (h) n/a, and (i) 23%, 5.2 mg.

Melting point: 136–138 °C.

FTIR: Could not be collected due to COVID-19 lockdown.

^{1}H NMR δ(400 MHz, $CDCl_3$): 1.22 (s, 3H, alkyl CH_3), 1.71 – 1.80 (m, 4H, vinyl CH_3, diastereotopic alkyl CH_2), 2.10 (d, ^{2}J = 18.3 Hz, 1H, diastereotopic $C(O)CH_2$), 2.21 – 2.30 (m, 4H, $ArCH_3$, diastereotopic alkyl CH_2), 2.44 – 2.60 (m, 3H, alkyl CH_2, diastereotopic $C(O)CH_2$), 3.83 (s, 3H, $ArOCH_3$), 6.57 (d, *J* = 9.9 Hz, 1H, olefinic CH), 6.76 (d, *J* = 8.7 Hz, 1H, ArH), 6.80 (d, *J* = 9.9 Hz, 1H, olefinic CH) 7.20 ppm (d, *J* = 8.7 Hz, 1H, ArH).

^{13}C NMR δ(101 MHz, $CDCl_3$): 8.8, 10.9, 19.9, 24.8, 42.8, 43.2, 44.3, 55.8, 57.2, 109.2, 122.8, 123.2, 123.7, 130.4, 132.8, 133.2, 133.7, 156.5, 186.5, 210.5 ppm.

See the Appendix section for X-ray crystallography data for this compound (page 366).

7.6 Synthetic Substrates and Intermediates for Chapter 5

*Attempted Preparation of 7-bromo-9-methoxy-3,8,11b-trimethyl-1,6,7,11b-tetrahydro-2H-pentaleno[1,6a-a]naphthalen-4(5H)-one **183***

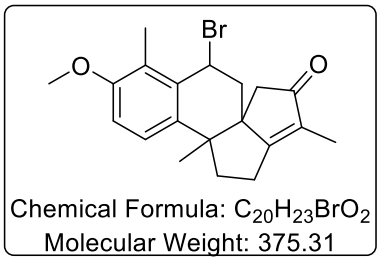

Scheme 5.3, Table 5.1

The following experiments were performed using *General Procedure Q*. Results are reported as: (a) mass of **97**, (b) volume of CCl_4, (c) mass of NBS, (d) mass of dibenzoyl peroxide, (e) time, and (f) outcome.

Entry 1: (a) 10 mg, 0.03 mmol, (b) 200 µL, (c) 6.1 mg, 0.03 mmol (d) 1.7 mg, 7.0 µmol, (e) 5 h, and (f) undetermined mixture of **183**, **97** and **98** by ^{1}H NMR analysis.

Entry 2: (a) 10 mg, 0.03 mmol, (b) 200 µL, (c) 6.1 mg, 0.03 mmol (d) 1.7 mg, 7.0 µmol, (e) 16 h, and (f) undetermined mixture of **183**, **97** and **98** by ^{1}H NMR analysis.

Entry 3: (a) 10 mg, 0.03 mmol, (b) 200 µL, (c) 6.1 mg, 0.03 mmol (d) 3.4 mg, 14 µmol, (e) 5 h, and (f) undetermined mixture of **183**, **97** and **98** by ^{1}H NMR analysis.

Entry 4: (a) 10 mg, 0.03 mmol, (b) 200 µL, (c) 12 mg, 0.06 mmol (d) 1.7 mg, 7.0 µmol, (e) 5 h, and (f) undetermined mixture of **183**, **97** and **98** by ^{1}H NMR analysis.

*Indicative data for **183**:*

^{1}H NMR δ(400 MHz, $CDCl_3$): 4.90 ppm (t, *J* = 7.5 Hz, 1H) indicates BrC**H**CH_2 in **183**.

LCMS *m*/*z* (ES-APCI): Calc. for $C_{20}H_{34}{}^{79}BrO_2$ (M^++H): 375.09. Found: 375.25.

Preparation of (5aR,11bR)-9-methoxy-3,8,11b-trimethyl-1,11b-dihydro-2H-pentaleno[1,6a-a]naphthalen-4(5H)-one ***98***[8,9]

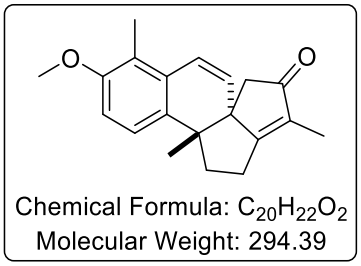

Chemical Formula: $C_{20}H_{22}O_2$
Molecular Weight: 294.39

Scheme 5.4

To a flame-dried round bottom flask equipped with a condenser, **97** (20 mg, 0.07 mmol) dissolved in the CCl_4 (400 µL) was charged. To the resulting mixture, NBS (12 mg, 0.07 mmol) and dibenzoyl peroxide (3.5 mg, 25% in H_2O, 0.01 mmol) were added and heated to reflux using an oil bath for 24 h. After this time, the reaction mixture was diluted with DCM and passed through a small silica plug to remove the solids. The solvent was removed and the crude mixture used directly in the next step. The crude mixture was dissolved in MeCN (1 mL), and DBU (25 µL, 0.14 mmol) was subsequently added. The reaction mixture was left to stir for 1 h, before being diluted in DCM and passed through a small silica plug to remove the solids. The solvent was removed and the crude mixture was analysed by ^{1}H NMR, which showed traces of **98**.

*Attempted Preparation of 9-methoxy-3,8,11b-trimethyl-1,11b-dihydro-2H-pentaleno[1,6a-a]naphthalene-4,7(5H,6H)-dione **99***

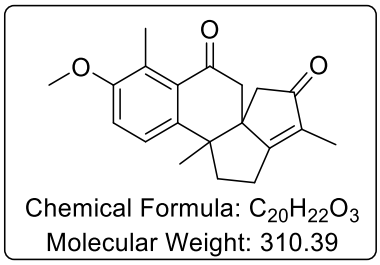

Scheme 5.6, Table 5.2

The following experiments were performed using *General Procedure R*. Results are reported as: (a) mass of **97**, (b) mass of Oxone®, (c) volume of $MeNO_2$, (d) mass of KBr, (e) temperature, (f) time, and (g) conversion to **184** determined by ^{1}H NMR analysis, comparing the peak at 7.17 ppm for **97** with that at 7.36 ppm for **184** (*see page 320 for indicative data for **184***).

Entry 1: (a) 10 mg, 0.03 mmol, (b) 16 mg, 0.10 mmol, (c) 200 µL, (d) 2.0 mg, 0.02 mmol (e) 50 °C, (f) 24 h, and (g) 40% conversion to **184**.

Entry 2: (a) 10 mg, 0.03 mmol, (b) 16 mg, 0.10 mmol, (c) 200 µL, (d) 9.5 mg, 0.08 mmol (e) 50 °C, (f) 24 h, and (g) decomposition.

Entry 3: (a) 10 mg, 0.03 mmol, (b) 16 mg, 0.10 mmol, (c) 200 µL, (d) 4.8 mg, 0.04 mmol (e) 50 °C, (f) 70 h, and (g) decomposition.

Scheme 5.7

To a flame-dried microwave vial opened to air, **97** (10 mg, 0.03 mmol), CuCl (0.3 mg, 3.0 µmol), TBHP (20 µL, 5-6 M, 0.10 mmol) and ^{t}BuOH (340 µL) were added. The resulting mixture was heated to 50 °C using an oil bath for 16 h. After this time, the reaction mixture was diluted with DCM and passed through a small silica plug to remove the solids. The solvent was removed, and the crude mixture was analysed by NMR. Unfortunately, the

desired product **99** was not identified, with the ^{1}H NMR spectrum indicating the formation of **185** instead (δ10.36 ppm, indicative of a formyl functional group).

10-bromo-9-methoxy-3,8,11b-trimethyl-1,6,7,11b-tetrahydro-2H-pentaleno[1,6a-a]naphthalen-4(5H)-one ***184***

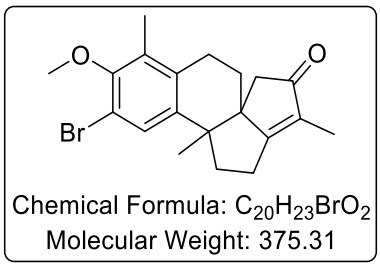

Indicative data for ***184****:*

^{1}H NMR δ(400 MHz, CDCl$_3$): 7.36 ppm (s, 1H) indicates ArH in **184**.

LCMS *m*/*z* (ES-APCI): Calc. for $C_{20}H_{24}{}^{79}BrO_2$ (M^++H): 375.09. Found: 375.27.

9-methoxy-3,11b-dimethyl-4-oxo-1,4,5,6,7,11b-hexahydro-2H-pentaleno[1,6a-a]naphthalene-8-carbaldehyde ***185***

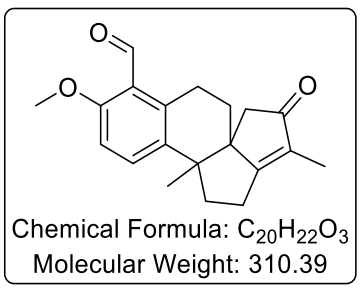

Indicative data for ***185****:*

^{1}H NMR δ(400 MHz, CDCl$_3$): 10.36 ppm (s, 1H) indicates formyl CH in **185**.

LCMS *m*/*z* (ES-APCI): Calc. for $C_{20}H_{23}O_3$ (M^++H): 311.39. Found: 311.34.

Attempted Preparation of (5aS,11bR)-5-(3-hydroxy-3-methylbutan-2-yl)-9-methoxy-3,8,11b-trimethyl-1,6,7,11b-tetrahydro-2H-pentaleno[1,6a-a]naphthalen-4(5H)-one ***187***

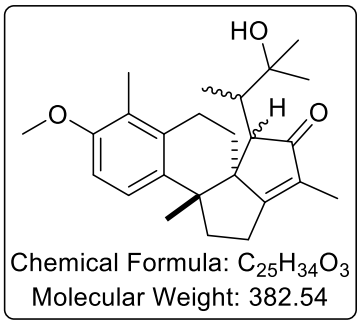

Scheme 5.9

To a flame-dried round bottom flask, LiCl (14 mg, 0.32 mmol) and di-*iso*-propylamine (46 µL, 0.32 mmol) dissolved in THF (1.0 mL) was charged, and subsequently cooled to 0 °C using an ice bath. At this temperature, ^{n}BuLi (130 µL, 2.5 M in hexanes, 0.32 mmol) was added dropwise *via* syringe, and left to stir for 20 min. After this time, the resulting mixture was cooled to -78 °C using a dry ice bath. At this temperature, **97** (45 mg, 0.16 mmol) dissolved in THF (0.10 mL) was added dropwise *via* syringe and left to stir for 30 min. Following this, the epoxide **186** (22 µL, 0.21 mmol) was added dropwise *via* syringe and left to stir for 1 h before being allowed to warm to room temperature overnight. The reaction mixture was quenched with saturated ammonium chloride solution and extracted with Et_2O. The organic solution was washed with brine, then dried with sodium sulfate, filtered, and evaporated. The crude mixture was analysed by NMR; unfortunately, the desired product **187** was not identified, with the spectrum indicating only starting material.

*Attempted Preparation of (5aS,11bR)-5-(3-hydroxy-3-methylbutan-2-yl)-9-methoxy-3,8,11b-trimethyl-1,11b-dihydro-2H-pentaleno[1,6a-a]naphthalen-4(5H)-one, agariblazeispirol C, **1***

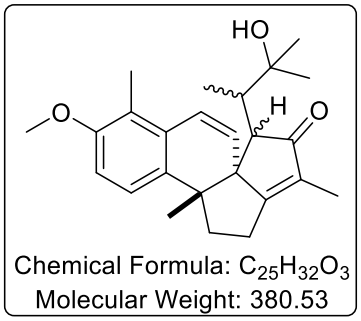

Chemical Formula: $C_{25}H_{32}O_3$
Molecular Weight: 380.53

Scheme 5.10

To a flame-dried round bottom flask, LiCl (14 mg, 0.32 mmol) and di-*iso*-propylamine (46 µL, 0.32 mmol) dissolved in THF (1.0 mL) was charged, and subsequently cooled to 0 °C using an ice bath. At this temperature, ^{n}BuLi (130 µL, 2.5 M in hexanes, 0.32 mmol) was added dropwise *via* syringe, and left to stir for 20 min. After this time, the resulting mixture was cooled to -78 °C using a dry ice bath. At this temperature, **98** (47 mg, 0.16 mmol) dissolved in THF (0.10 mL) was added dropwise *via* syringe and left to stir for 30 min. Following this, the epoxide **186** (22 µL, 0.21 mmol) was added dropwise *via* syringe and left to stir for 1 h before being allowed to warm to room temperature overnight. The reaction mixture was quenched with saturated ammonium chloride solution and extracted with Et_2O. The organic solution was washed with brine, then dried with sodium sulfate, filtered, and evaporated. The crude mixture was analysed by NMR; unfortunately, the desired product **1** was not identified, with the spectrum only returning starting material.

Preparation of (5aS,11bS)-9-methoxy-3,8,11b-trimethyl-1,6,7,11b-tetrahydro-2H-pentaleno[1,6a-a]naphthalen-4(5H)-one-5-d ***d-97***

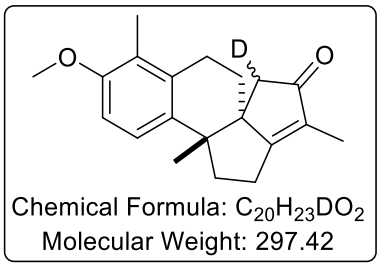

Scheme 5.11

To a flame-dried round bottom flask, LiCl (7.2 mg, 0.17 mmol) and di-*iso*-propylamine (24 µL, 0.17 mmol) dissolved in THF (1.0 mL) was charged, and subsequently cooled to 0 °C using an ice bath. At this temperature, ^{n}BuLi (70 µL, 2.5 M in hexanes, 0.17 mmol) was added dropwise *via* syringe, and left to stir for 30 min. After this time, the resulting mixture was cooled to -78 °C using a dry ice bath. At this temperature, **97** (25 mg, 0.08 mmol) dissolved in THF (0.1 mL) was added dropwise *via* syringe and left to stir for 30 min. Following this, D_2O (10 µL, 0.55 mmol) was added and the resulting solution was warmed to room temperature and left to stir for 2 h. The reaction mixture was quenched with saturated ammonium chloride solution and extracted with Et_2O. The organic solution was washed with brine, then dried with sodium sulfate, filtered, and evaporated. The crude mixture was analysed by NMR; unfortunately, the desired product **d-97** was not identified, with the spectrum only returning starting material.

Scheme 5.12

To a flame-dried round bottom flask, **97** (30 mg, 0.10 mmol) dissolved in DCM (1.2 mL) was charged, then subsequently Et_3N (70 µL, 0.51 mmol) was added. The reaction mixture was cooled to -5 °C using an ice bath, and TMSOTf (28 µL, 0.15 mmol) was added dropwise *via* syringe. This was left to stir for 30 min at this temperature before being quenched with saturated sodium bicarbonate solution, and extracted with DCM. The organic solution was then dried with sodium sulfate, filtered, and evaporated. The crude silyl enol ether (**188**) was used immediately in the next step due to its instability. To another

flame-dried round bottom flask, silyl enol ether **188** (40 mg, 0.11 mmol) dissolved in THF (0.60 mL) was charged, and subsequently cooled to -10 °C using an ice/salt bath. At this temperature, MeLi (60 µL, 1.6 M in Et_2O, 0.10 mmol) was added dropwise *via* syringe, and left to stir for 20 min. After this time, the resulting mixture was cooled to -78 °C using a dry ice bath and left to stir for 1 h. Following this, D_2O (10 µL, 0.55 mmol) was added and the solution was warmed to room temperature and left to stir for a further 2 h. The reaction mixture was quenched with saturated sodium bicarbonate solution and extracted with Et_2O. The organic solution was washed with brine, then dried with sodium sulfate, filtered, and evaporated. The crude mixture was analysed by ^{1}H NMR, which indicated >98% deuterium incorporation at the desired position with a 7:3 diastereomeric ratio.

The deuterium incorporation was determined through analysis of the ^{1}H NMR spectrum:

^{1}H NMR δ(400 MHz, $CDCl_3$): deuterium incorporation at δ = 2.53 – 2.72 ppm (m, 2.01H, alkyl protons), indicated >98% D using δ = 6.72 – 6.74 ppm (m, 1H, ArH) as a reference. To note: the corresponding signal for the analogous non-deuterated material is δ 2.52 – 2.75 ppm (m, 3H, alkyl protons).

The 7:3 diasteriomeric ratio was calculated using the vinyl CH_3 peaks; δ = 1.74 ppm and δ = 1.64 ppm.

*Attempted Preparation of (5aS,11bR)-5-(3-hydroxy-3-methylbutan-2-yl)-9-methoxy-3,8,11b-trimethyl-1,6,7,11b-tetrahydro-2H-pentaleno[1,6a-a]naphthalen-4(5H)-one **187***

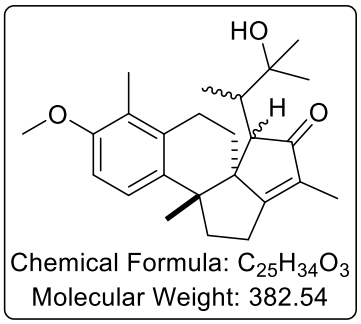

Scheme 5.13, Table 5.3, Entry 1

The following experiment was performed using *General Procedure S*. Results are reported as: (a) mass of core **97**, (b) volume of DCM, (c) volume of Et_3N, (d) volume of TMSOTf, (e) crude mass of silyl enol ether **188**, (f) volume of THF, (g) volume of MeLi, (h) volume of additive, (i) volume of epoxide **186**, and (j) isolated yield of starting material **97**.

(a) 70 mg, 0.27 mmol, (b) 3.0 mL, (c) 190 µL, 1.3 mmol, (d) 80 µL, 0.40 mmol (e) 80 mg, 0.22 mmol, (f) 1.1 mL, (g) 130 µL, 0.20 mmol, (h) HMPA, 120 µL, 0.72 mmol, (i) 30 µL, 0.28 mmol, and (j) 86%, 60 mg.

Scheme 5.13, Table 5.3

The following experiments were performed using *General Procedure T*. Results are reported as: (a) mass of core **97**, (b) volume of DCM, (c) volume of Et_3N, (d) volume of TMSOTf, (e) crude mass of silyl enol ether **188**, (f) volume of THF, (g) volume of MeLi, (h) volume of additive, (i) volume of epoxide **186**, and (j) isolated yield of starting material **97**.

Entry 2: (a) 40 mg, 0.13 mmol, (b) 1.3 mL, (c) 90 µL, 0.65 mmol, (d) 36 µL, 0.20 mmol (e) 45 mg, 0.12 mmol, (f) 0.60 mL, (g) 69 µL, 1.6 M in Et_2O, 0.11 mmol, (h) BF_3•OEt_2, 20 µL, 0.16 mmol, (i) 17 µL, 0.16 mmol, and (j) 70%, 28 mg.

Entry 3: (a) 40 mg, 0.13 mmol, (b) 1.3 mL, (c) 90 µL, 0.65 mmol, (d) 36 µL, 0.20 mmol (e) 44 mg, 0.12 mmol, (f) 0.60 mL, (g) 69 µL, 1.6 M in Et_2O, 0.11 mmol, (h) $TiCl_4$, 18 µL, 0.16 mmol, (i) 17 µL, 0.16 mmol, and (j) 55%, 22 mg.

*Attempted Preparation of (5aS,11bR)-5-(3-hydroxy-3-methylbutan-2-yl)-9-methoxy-3,8,11b-trimethyl-1,11b-dihydro-2H-pentaleno[1,6a-a]naphthalen-4(5H)-one, agariblazeispirol C, **1***

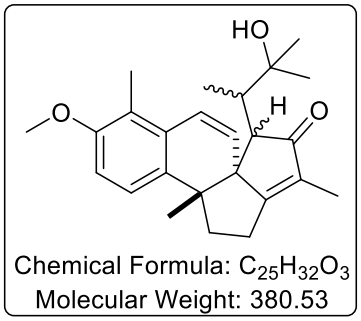

Chemical Formula: $C_{25}H_{32}O_3$
Molecular Weight: 380.53

Scheme 5.14

The following experiments were performed using *General Procedure S*. Results are reported as: (a) mass of core **98**, (b) volume of DCM, (c) volume of Et_3N, (d) volume of TMSOTf, (e) crude mass of silyl enol ether **189**, (f) volume of THF, (g) volume of MeLi, (h) volume of HMPA, (i) volume of epoxide **186**, and (j) outcome.

(a) 30 mg, 0.10 mmol, (b) 1.2 mL, (c) 70 µL, 0.51 mmol, (d) 28 µL, 0.15 mmol (e) 31 mg, 0.08 mmol, (f) 1.0 mL, (g) 58 µL, 1.6 M in Et_2O, 0.09 mmol, (h) 22 µL, 0.13 mmol, (i) 11 µL, 0.10 mmol, and (j) starting material observed by ^1H NMR analysis.

Scheme 5.15

To a flame-dried round bottom flask, **98** (30 mg, 0.10 mmol) dissolved in DCM (1.2 mL) was charged, then subsequently Et_3N (70 µL, 0.51 mmol) was added. The reaction mixture was cooled to -5 °C using an ice bath, and TMSOTf (28 µL, 0.15 mmol) was added dropwise *via* syringe. This was left to stir for 30 min at this temperature before being quenched with saturated sodium bicarbonate solution, and extracted with DCM. The organic solution was then dried with sodium sulfate, filtered, and evaporated. The crude silyl enol ether **189** was used immediately in the next step due to its instability. To another flame-dried round bottom flask, the specified silyl enol ether (30 mg, 0.08 mmol) dissolved in THF (1.0 mL) was charged, and subsequently cooled to -78 °C using a dry ice bath. At

this temperature, $TiCl_4$ (12 µL, 0.11 mmol) was added dropwise *via* syringe and left to stir for 1 h. Following this, epoxide **186** (11 µL, 0.11 mmol) was added dropwise *via* syringe and left to stir for 1 h before being allowed to warm to room temperature overnight. The reaction mixture was quenched with saturated sodium bicarbonate solution and extracted with Et_2O. The organic solution was washed with brine, then dried with sodium sulfate, filtered, and evaporated. The crude mixture was analysed by ^1H NMR, and unfortunately, the desired product **1** was not identified, with starting material **98** being the predominant compound within the mixture.

Attempted Preparation of (5aS,11bR)-9-methoxy-3,8,11b-trimethyl-5-(3-oxobutan-2-yl)-1,6,7,11b-tetrahydro-2H-pentaleno[1,6a-a]naphthalen-4(5H)-one ***192***

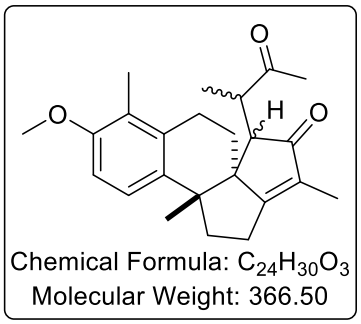

Scheme 5.17

The following experiments were performed using *General Procedure S*. Results are reported as: (a) mass of core **97**, (b) volume of DCM, (c) volume of Et_3N, (d) volume of TMSOTf, (e) crude mass of silyl enol ether **188**, (f) volume of THF, (g) volume of MeLi, (h) additive, (i) volume of chloroketone **191**, and (j) outcome.

(a) 30 mg, 0.10 mmol, (b) 1.2 mL, (c) 70 µL, 0.51 mmol, (d) 28 µL, 0.15 mmol (e) 15 mg, 0.04 mmol, (f) 0.40 mL, (g) 24 µL, 1.6 M in Et_2O, 0.04 mmol, (h) n/a, (i) 18 µL, 0.19 mmol, and (j) starting material observed by ^1H NMR analysis.

Preparation of methyl (S)-2-(((trifluoromethyl)sulfonyl)oxy)propanoate ***(S)-194***

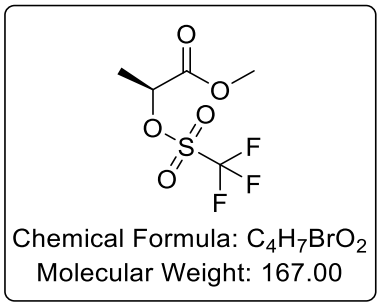

Scheme 5.18

To a flame-dried round bottom flask, **(*S*)-193** (0.40 mL, 4.2 mmol) dissolved in DCM (3.0 mL) and Et_3N (0.70 mL, 5.0 mmol) were added. The resulting mixture was cooled to -78 °C then Tf_2O (0.77 mL, 4.6 mmol) was added dropwise. After this addition, the solution was warmed to -10 °C and left at this temperature for 2 h. The reaction mixture was allowed to warm to room temperature before being quenched with saturated sodium bicarbonate solution, washed with 1 M HCl and brine. The organic layer was collected, dried with sodium sulfate, filtered and evaporated. The resulting crude mixture was purified by column chromatography (eluent: 0-33% Et_2O in petrol) to afford **(*S*)-194** (0.56 g, 80%) as a colourless oil.

FTIR ($CHCl_3$): 1414, 1759 cm^{-1}.

^{1}H NMR δ(400 MHz, $CDCl_3$): 1.71 (d, *J* = 7.0 Hz, 3H, alkyl CH_3), 3.86 (s, 3H, $C(O)CH_3$), 5.24 ppm (q, *J* = 7.0 Hz, 1H, OCH).

^{13}C NMR δ(101 MHz, $CDCl_3$): 18.2, 53.5, 80.0, 118.6 (q, $^1J_{C\text{-}F}$ = 319 Hz, CF_3) , 168.0 ppm.

^{19}F NMR δ(362 MHz, $CDCl_3$): -75.2 ppm.

HRMS: Could not be collected due to COVID-19 lockdown.

Attempted Preparation of methyl (2S)-2-((5aS,11bR)-9-methoxy-3,8,11b-trimethyl-4-oxo-1,4,5,6,7,11b-hexahydro-2H-pentaleno[1,6a-a]naphthalen-5-yl)propanoate ***195***

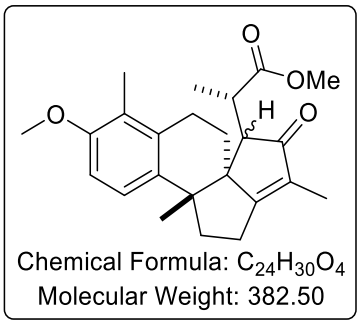

The following experiment was performed using *General Procedure S*. Results are reported as: (a) mass of core **97**, (b) volume of DCM, (c) volume of Et_3N, (d) volume of TMSOTf, (e) crude mass of silyl enol ether **188**, (f) volume of THF, (g) volume of MeLi, (h) additive, (i) volume of triflate ester **(*S*)-194**, and (j) outcome.

Scheme 5.19

(a) 30 mg, 0.10 mmol, (b) 1.2 mL, (c) 70 µL, 0.51 mmol, (d) 28 µL, 0.15 mmol (e) 30 mg, 0.08 mmol, (f) 0.80 mL, (g) 47 µL, 1.6 M in Et_2O, 0.08 mmol, (h) n/a, (i) 23 µL, 0.11 mmol, and (j) reaction decomposition by ^1H NMR analysis.

Preparation of (Z)-2-methylbut-2-en-1-ol ***200***[134]

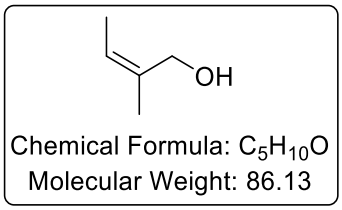

Scheme 5.21

To a flame-dried 3-neck round bottom flask, Et_2O (19 mL) was charged and cooled to 0 °C using an ice bath, then lithium aluminium hydride (2.5 g, 66 mmol) was added portion-wise. Methyl angelate **199** (2.5 g, 22 mmol) was dissolved in Et_2O (19 mL) and was then added dropwise *via* syringe pump. The mixture was allowed to stir at 0 °C for 20 min, then warmed to room temperature and left to stir for 16 h. After this, the slurry was cooled to 0 °C and quenched slowly with Na_2SO_4•$10H_2O$ and water, forming a white solid. This was filtered, and the crude mixture was extracted with Et_2O and washed with brine. The organic solution was dried with sodium sulfate, filtered, and evaporated (at low temperature) to afford **200** (1.8 g, 96%) as a colourless oil.

FTIR ($CHCl_3$): 1001, 1454, 2936, 3298 cm^{-1}.

^{1}H NMR δ(400 MHz, $CDCl_3$): 1.15 (t, *J* = 4.8 Hz, 1H, OH), 1.62 – 1.66 (m, 3H, vinyl CH_3), 1.78 – 1.80 (m, 3H, vinyl CH_3), 4.15 (d, *J* = 4.8 Hz, 2H, CH_2), 5.34 – 5.41 ppm (m, 1H, olefinic CH).

^{13}C NMR δ(101 MHz, $CDCl_3$): 13.2, 21.4, 61.5, 122.8, 135.1 ppm.

HRMS: Could not be collected due to COVID-19 lockdown.

*Preparation of (Z)-1-bromo-2-methylbut-2-ene **196***

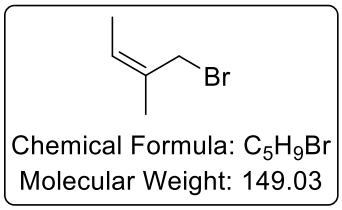

Scheme 5.21

To a flame-dried bottom flask, **200** (200 mg, 2.3 mmol) and Et_2O (2.0 mL) was charged and cooled to 0 °C using an ice bath. At this temperature, PBr_3 (0.10 mL, 1.2 mmol) was added dropwise *via* syringe, and the mixture was allowed to stir at this temperature for 2 h. After this, the reaction mixture was quenched slowly with saturated sodium bicarbonate solution, and was extracted with Et_2O, and washed with brine. The organic solution was dried with sodium sulfate, filtered and evaporated (at low temperature) to afford **196** (110 mg, 33%) as a colourless oil.

FTIR ($CHCl_3$): 1015, 1230, 1458, 1665, 2961 cm^{-1}.

^{1}H NMR δ(400 MHz, $CDCl_3$): 1.65 – 1.67 (m, 3H, vinyl CH_3), 1.81 – 1.84 (m, 3H, vinyl CH_3), 4.00 (s, 2H, CH_2Br), 5.47 ppm (qq, J = 6.9, ^4J = 1.4 Hz, 1H, olefinic CH).

^{13}C NMR δ(101 MHz, $CDCl_3$): 13.6, 21.9, 32.3, 126.0, 132.4 ppm.

HRMS: Could not be collected due to COVID-19 lockdown.

*Preparation of (5aS,11bR)-9-methoxy-3,8,11b-trimethyl-5-((Z)-2-methylbut-2-en-1-yl)-1,6,7,11b-tetrahydro-2H-pentaleno[1,6a-a]naphthalen-4(5H)-one **197***

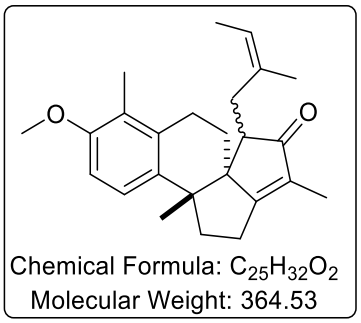

The following experiment was performed using *General Procedure S*. Results are reported as: (a) mass of core **97**, (b) volume of DCM, (c) volume of Et_3N, (d) volume of TMSOTf, (e) crude mass of silyl enol ether **188**, (f) volume of THF, (g) volume of MeLi, (h) additive, (i) volume of allyl bromide **196**, and (j) isolated yield of **197** over two steps.

Scheme 5.22

(a) 30 mg, 0.10 mmol, (b) 1.1 mL, (c) 70 µL, 0.51 mmol, (d) 28 µL, 0.15 mmol (e) 30 mg, 0.08 mmol, (f) 0.80 mL, (g) 47 µL, 1.6 M in Et_2O, 0.08 mmol, (h) n/a, (i) 24 mg in 0.10 mL THF, 0.11 mmol, and (j) 5.0 mg, 14%, 95:5 dr.

^{1}H NMR δ(400 MHz, $CDCl_3$): 1.11 – 1.13 (m, 3H, alkyl CH_3), 1.49 – 1.54 (m, 5H, vinyl CH_3, alkyl CH_2), 1.74 – 1.78 (m, 6H, 2 × vinyl CH_3), 2.04 – 2.15 (m, 4H, $ArCH_3$, diastereotopic alkyl CH_2), 2.19 – 2.33 (m, 4H, alkyl protons), 2.47 – 2.52 (m, 1H, diastereotopic alkyl CH_2), 2.56 – 2.62 (m, 1H, diastereotopic alkyl CH_2), 2.84 – 2.90 (m, 1H, diastereotopic alkyl CH_2), 3.00 – 3.11 (m, 1H, alkyl C(O)CH), 3.80 – 3.82 (m, 3H, $ArOCH_3$), 5.29 (q, J = 6.6 Hz, 0.95H, olefinic CH), 5.34 (q, J = 6.6 Hz, 0.05H, olefinic CH), 6.73 – 6.77 (m, 1H, ArH), 7.12 – 7.15 ppm (m, 1H, ArH).

^{13}C NMR δ(101 MHz, $CDCl_3$): 8.5, 11.5, 13.8, 23.6, 23.8, 25.8, 32.4, 36.6, 37.1, 43.6, 43.7, 50.8, 54.3, 55.7, 108.8, 121.7, 124.3, 124.8, 133.7, 133.8, 134.2, 135.8, 155.5, 188.6, 211.2 ppm.

HRMS *m*/*z* (ESI): Calc. for $C_{25}H_{33}O_3$ (M^++H): 365.2475. Found: 365.2475.

*Attempted Preparation of (5aS,11bR)-9-methoxy-3,8,11b-trimethyl-5-(3-oxobutan-2-yl)-1,11b-dihydro-2H-pentaleno[1,6a-a]naphthalen-4(5H)-one **202***

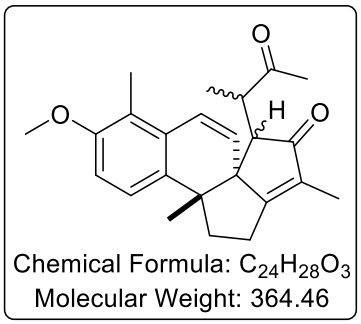

Scheme 5.23, Table 5.4

The following experiments were performed using *General Procedure S*. Results are reported as: (a) mass of core **98**, (b) volume of DCM, (c) volume of Et_3N, (d) volume of TMSOTf, (e) crude mass of silyl enol ether **189**, (f) volume of THF, (g) volume of MeLi, (h) volume of additive, (i) volume of bromoketone **201**, and (j) outcome.

Entry 1: (a) 30 mg, 0.10 mmol, (b) 1.1 mL, (c) 70 µL, 0.51 mmol, (d) 28 µL, 0.15 mmol (e) 38 mg, 0.10 mmol, (f) 1.0 mL, (g) 58 µL, 1.6 M in Et_2O, 0.09 mmol, (h) n/a, (i) 14 µL, 0.13 mmol, and (j) indication of **202** by ^{1}H NMR and LCMS; pure compound unobtainable following silica chromatography.

Entry 2: (a) 30 mg, 0.10 mmol, (b) 1.1 mL, (c) 70 µL, 0.51 mmol, (d) 28 µL, 0.15 mmol (e) 36 mg, 0.10 mmol, (f) 1.0 mL, (g) 58 µL, 1.6 M in Et_2O, 0.09 mmol, (h) HMPA, 23 µL, 0.13 mmol, (i) 14 µL, 0.13 mmol, and (j) indication of **202** by ^{1}H NMR and LCMS; pure compound unobtainable following silica chromatography.

FTIR ($CHCl_3$): 1260, 1655, 1703, 2963 cm^{-1}.

^{1}H NMR δ(400 MHz, $CDCl_3$): 1.04 (d, *J* = 6.9 Hz, 1H, alkyl CHC**H**$_3$), 1.17 – 1.22 (m, 5H, alkyl CH_3, alkyl CHC**H**$_3$), 1.68 – 1.83 (m, 4H, vinyl CH_3, diastereotopic alkyl CH_2), 1.89 – 2.18 (m, 5H, C(O)CH_3, alkyl protons), 2.25 – 2.27 (m, 3H, ArCH_3), 2.48 – 2.55 (m,

1H, diastereotopic alkyl CH_2), 2.79 – 2.92 (m, 1H, alkyl CH), 3.06 – 3.20 (m, 1H, alkyl CH), 3.82 – 3.86 (m, 3H, $ArOCH_3$), 5.63 – 5.66 (m, 1H, olefinic CH), 6.74 – 6.83 (m, olefinic CH, ArH), 7.13 – 7.21 ppm (m, 1H, ArH).

^{13}C NMR δ(101 MHz, $CDCl_3$): diagnostic peaks include 210.5, 210.6 (potential enone diastereomers), 211.4 ppm (ketone).

LCMS *m*/*z* (ES-APCI): Calc. for $C_{24}H_{29}O_3$ (M^++H): 365.46. Found: 365.50.

Preparation of methyl (S)-2-bromopropanoate ***(S)-204***

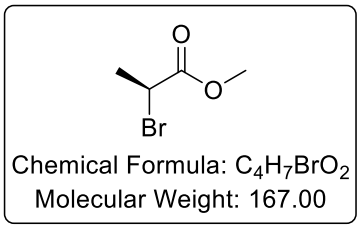

Scheme 5.24

To a flame-dried bottom flask, methyl (*R*)-2-hydroxypropanoate **(*R*)-203** (1.00 g, 9.61 mmol), CBr_4 (4.10 g, 12.5 mmol) and DCM (129 mL) were charged and cooled to 0 °C using an ice bath. At this temperature, PPh_3 (3.30 g, 14.4 mmol) was added quickly, and the mixture was allowed to warm slowly to room temperature overnight. After this, the reaction mixture was diluted with Et_2O to from a precipitate, where dilution was continued until no precipitate formed. Once stopped, the solids were then filtered, and the resulting solution was evaporated (at low temperature). The crude mixture was purified by silica chromatography (eluent: 0-33% Et_2O in petrol) to afford **(*S*)-204** (0.74 g, 46%) as a colourless oil.

FTIR: Could not be collected due to COVID-19 lockdown.

^{1}H NMR δ(400 MHz, $CDCl_3$): 1.83 (d, *J* = 7.0 Hz, 3H, alkyl CH_3), 3.79 (s, 3H, OCH_3), 4.38 ppm (q, *J* = 7.0 Hz, 1H, CHBr).

^{13}C NMR δ(101 MHz, $CDCl_3$): 21.8, 39.9, 53.1, 173.3 ppm.

HRMS: Could not be collected due to COVID-19 lockdown.

Preparation of (S)-3-bromobutan-2-one ***(S)-201***

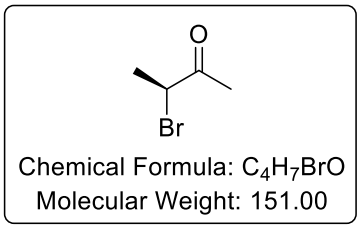

Scheme 5.25

To a flame-dried bottom flask, **(*S*)-204** (1.5 g, 9.0 mmol), *N*-methoxymethylamine hydrochloride salt (1.1 g, 11 mmol) and THF (88 mL) were charged and cooled to -5 °C using an ice bath. At this temperature, MeMgBr (18 mL, 2.5 M in Et_2O, 45 mmol) was added dropwise *via* syringe pump over 1 h. The mixture was left to stir at this temperature for 1 h before being allowed to warm slowly to room temperature overnight. After this, the reaction mixture was quenched with saturated ammonium chloride solution and extracted with Et_2O. The organic solution was washed with brine, then dried with sodium sulfate, filtered, and evaporated (at low temperature). The crude mixture was quickly purified by silica chromatography (eluent: 0-33% Et_2O in pentane) to afford **(*S*)-201** (0.22 g, 16%) as a volatile colourless liquid.

FTIR: Could not be collected due to COVID-19 lockdown.

1H NMR δ(400 MHz, $CDCl_3$): 1.75 (d, *J* = 6.9 Hz, 3H, alkyl CH_3), 2.38 (s, 3H, $C(O)CH_3$), 4.39 ppm (q, *J* = 6.9 Hz, 1H, CHBr).

^{13}C NMR δ(101 MHz, $CDCl_3$): 20.3, 26.1, 48.3, 202.3 ppm.

HRMS: Could not be collected due to COVID-19 lockdown.

Attempted Preparation of (5aS,11bR)-9-methoxy-3,8,11b-trimethyl-5-((S)-3-oxobutan-2-yl)-1,11b-dihydro-2H-pentaleno[1,6a-a]naphthalen-4(5H)-one ***202***

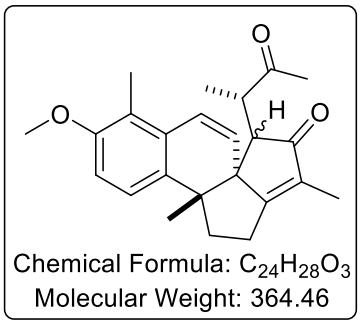

The following experiment was performed using *General Procedure S*. Results are reported as: (a) mass of core **98**, (b) volume of DCM, (c) volume of Et_3N, (d) volume of TMSOTf, (e) crude mass of silyl enol ether **189**, (f) volume of THF, (g) volume of MeLi, (h) volume of additive, (i) volume of bromoketone **(*S*)-204**, and (j) outcome.

Scheme 5.26

(a) 30 mg, 0.10 mmol, (b) 1.1 mL, (c) 70 µL, 0.51 mmol, (d) 28 µL, 0.15 mmol (e) 36 mg, 0.10 mmol, (f) 1.0 mL, (g) 58 µL, 1.6 M in Et_2O, 0.09 mmol, (h) HMPA, 23 µL, 0.13 mmol, (i) 14 µL, 0.13 mmol, and (j) indication of **202** by ^1H NMR and LCMS, where data was consistent with that detailed on *page 336*; pure compound unobtainable following silica chromatography.

Chapter 8

References

8. References

(1) Kawagisihi, H.; Katsumi, R.; Sazawa, T.; Mizuno, T.; Hagiwara, T.; Nakamura, T. *Phytochemistry* **1988**, *27*, 2777–2779.

(2) Mizuno, M.; Morimoto, M.; Minato, K.; Tsuchida, H. *Biosci. Biotechnol. Biochem.* **1998**, *62*, 434–437.

(3) Hirotani, M.; Sai, K.; Hirotani, S.; Yoshikawa, T. *Phytochemistry* **2002**, *59*, 571–577.

(4) Hirotani, M.; Masuda, M.; Sukemori, A.; Hirotani, S.; Sato, N.; Yoshikawa, T. *Tetrahedron* **2005**, *61*, 189–194.

(5) van Graas, G.; de Lange, F.; de Leeuw, J. W.; Schenck, P. A. *Nature* **1982**, *299*, 437–439.

(6) Hirotani, M.; Kaneko, A.; Asada, Y.; Yoshikawa, T. *Tetrahedron Lett.* **2000**, *41*, 6101–6104.

(7) Hirotani, M.; Hirotani, S.; Yoshikawa, T. *Tetrahedron Lett.* **2001**, *42*, 5261–5264.

(8) Brown, J. A. PhD Thesis, *University of Strathclyde*, **2007**.

(9) McPherson, A. R. PhD Thesis, *University of Strathclyde*, **2010**.

(10) Paterson, L. PhD Thesis, *University of Strathclyde*, **2011**.

(11) Forsyth, B. C. PhD Thesis, *University of Strathclyde*, **2013**.

(12) Giusti, L. 9 Month Report, *University of Strathclyde*, **2015**.

(13) Mizoroki, T.; Oestreich, M. *The Mizoroki–Heck Reaction*, 1st Ed.; John Wiley & Sons, Ltd: Chichester, UK, 2009.

(14) Negishi, E. *Handbook of Organopalladium Chemistry for Organic Synthesis*; 1st Ed.; John Wiley & Sons, Inc.: New York, USA, 2002.

(15) The Nobel Prize in Chemistry 2010 https://www.nobelprize.org/prizes/chemistry/2010/summary/ (accessed June 30, 2020).

(16) Heck, R. F. *J. Am. Chem. Soc.* **1968**, *90*, 5518–5526.

(17) Mizoroki, T.; Mori, K.; Ozaki, A. *Bull. Chem. Soc. Jpn.* **1971**, *44*, 581–581.

(18) Beletskaya, I. P.; Cheprakov, A. V. *Chem. Rev.* **2000**, *100*, 3009–3066.

(19) Gibson (née Thomas), S. E.; Middleton, R. J. *Contemp. Org. Synth.* **1996**, *3*, 447.

(20) Dounay, A. B.; Overman, L. E. *Chem. Rev.* **2003**, *103*, 2945–2963.

(21) Amatore, C.; Jutand, A. *J. Organomet. Chem.* **1999**, *576*, 254–278.

(22) Amatore, C.; Jutand, A. *Acc. Chem. Res.* **2000**, *33*, 314–321.

(23) Knowles, J. P.; Whiting, A. *Org. Biomol. Chem.* **2007**, *5*, 31–44.

(24) Harrington, P. J.; Hegedus, L. S. *J. Org. Chem.* **1984**, *49*, 2657–2662.

(25) Whitcombe, N. J.; Hii, K. K.; Gibson, S. E. *Tetrahedron* **2001**, *57*, 7449–7476.

(26) Hammett, L. P. *Physical Organic Chemistry: Reaction Rates, Equilibria, and Mechanisms*, 1st Ed.; McGraw-Hill: New York, 1970.

(27) Cabri, W.; Candiani, I.; DeBernardinis, S.; Francalanci, F.; Penco, S.; Santo, R. *J. Org. Chem.* **1991**, *56*, 5796–5800.

(28) Ozawa, F.; Kubo, A.; Hayashi, T. *J. Am. Chem. Soc.* **1991**, *113*, 1417–1419.

(29) Cabri, W.; Candiani, I.; Bedeschi, A.; Santi, R. *J. Org. Chem.* **1993**, *58*, 7421–7426.

(30) Littke, A. F.; Fu, G. C. *J. Am. Chem. Soc.* **2001**, *123*, 6989–7000.

(31) Mo, J.; Xu, L.; Xiao, J. *J. Am. Chem. Soc.* **2005**, *127*, 751–760.

(32) Oishi, T.; Mori, M.; Ban, Y. *Tetrahedron Lett.* **1971**, *12*, 1777–1780.

(33) Carpenter, N. E.; Kucera, D. J.; Overman, L. E. *J. Org. Chem.* **1989**, *54*, 5846–5848.

(34) Gibson (née Thomas), S. E.; Guillo, N.; Middleton, R. J.; Thuilliez, A.; Tozer, M. J. *J. Chem. Soc. Perkin Trans. 1* **1997**, 447–456.

(35) Burns, B.; Grigg, R.; Santhakumar, V.; Sridharan, V.; Stevenson, P.; Worakun, T. *Tetrahedron* **1992**, *48*, 7297–7320.

(36) Sato, Y.; Sodeoka, M.; Shibasaki, M. *J. Org. Chem.* **1989**, *54*, 4738–4739.

(37) Ashimori, A.; Matsuura, T.; Overman, L. E.; Poon, D. J. *J. Org. Chem.* **1993**, *58*, 6949–6951.

(38) McCartney, D.; Guiry, P. J. *Chem. Soc. Rev.* **2011**, *40*, 5122–5150.

(39) Ashimori, A.; Overman, L. E. *J. Org. Chem.* **1992**, *57*, 4571–4572.

(40) Overman, L. E.; Poon, D. J. *Angew. Chem. Int. Ed.* **1997**, *36*, 518–521.

(41) Albano, V. G.; Castellari, C.; Cucciolito, M. E.; Panunzi, A.; Vitagliano, A. *Organometallics* **1990**, *9*, 1269–1276.

(42) Thorn, D. L.; Hoffmann, R. *J. Am. Chem. Soc.* **1978**, *100*, 2079–2090.

(43) Samsel, E. G.; Norton, J. R. *J. Am. Chem. Soc.* **1984**, *106*, 5505–5512.

(44) Takemoto, T.; Sodeoka, M.; Sasai, H.; Shibasaki, M. *J. Am. Chem. Soc.* **1993**, *115*, 8477–8478.

(45) Shen, C.; Liu, R. R.; Fan, R. J.; Li, Y. L.; Xu, T. F.; Gao, J. R.; Jia, Y. X. *J. Am.*

Chem. Soc. **2015**, *137*, 4936–4939.

(46) Zhang, Z.-M.; Xu, B.; Wu, L.; Wu, Y.; Qian, Y.; Zhou, L.; Liu, Y.; Zhang, J. *Angew. Chem. Int. Ed.* **2019**, *58*, 14653–14659.

(47) Bai, X.; Wu, C.; Ge, S.; Lu, Y. *Angew. Chem. Int. Ed.* **2020**, *59*, 2764–2768.

(48) Maddaford, S. P.; Andersen, N. G.; Cristofoli, W. A.; Keay, B. A. *J. Am. Chem. Soc.* **1996**, *118*, 10766–10773.

(49) Dounay, A. B.; Humphreys, P. G.; Overman, L. E.; Wrobleski, A. D. *J. Am. Chem. Soc.* **2008**, *130*, 5368–5377.

(50) Del Bel, M.; Abela, A. R.; Ng, J. D.; Guerrero, C. A. *J. Am. Chem. Soc.* **2017**, *139*, 6819–6822.

(51) Ashimori, A.; Bachand, B.; Overman, L. E.; Poon, D. J. *J. Am. Chem. Soc.* **1998**, *120*, 6477–6487.

(52) Sun, J.; Jiang, H.; Rios Torres, R., *The Pauson-Khand Reaction*, 1st Ed.; John Wiley & Sons, Ltd: Chichester, UK, 2012.

(53) Blanco-Urgoiti, J.; Añorbe, L.; Pérez-Serrano, L.; Domínguez, G.; Pérez-Castells, J. *Chem. Soc. Rev.* **2004**, *33*, 32–42.

(54) Gibson, S. E.; Mainolfi, N. *Angew. Chem. Int. Ed.* **2005**, *44*, 3022–3037.

(55) Khand, I. U.; Knox, G. R.; Pauson, P. L.; Watts, W. E. *J. Chem. Soc. D Chem. Commun.* **1971**, *1*, 36.

(56) Khand, I. U.; Knox, G. R.; Pauson, P. L.; Watts, W. E.; Foreman, M. I. *J. Chem. Soc. Perkin Trans. 1* **1973**, 977.

(57) Magnus, P.; Principe, L. M. *Tetrahedron Lett.* **1985**, *26*, 4851–4854.

(58) Billington, D. C.; Malcolm Helps, I.; Pauson, P. L.; Thomson, W.; Willison, D. *J. Organomet. Chem.* **1988**, *354*, 233–242.

(59) D. C. Billington, P. Bladon, I. M. Helps, P. L. Pauson, W. Thomson, and D. Willison, *J. Chem. Res. (M)*, **1988**, 2601.

(60) Robert, F.; Milet, A.; Gimbert, Y.; Konya, D.; Greene, A. E. *J. Am. Chem. Soc.* **2001**, *123*, 5396–5400.

(61) Khand, I. U.; Knox, G. R.; Pauson, P. L.; Watts, W. E.; Foreman, M. I. *J. Chem. Soc. Perkin Trans. 1* **1973**, 977.

(62) Krafft, M. E. *J. Am. Chem. Soc.* **1988**, *110*, 968–970.

(63) De Bruin, T. J. M.; Milet, A.; Greene, A. E.; Gimbert, Y. *J. Org. Chem.* **2004**, *69*, 1075–1080.

(64) Khand, I. U.; Knox, G. R.; Pauson, P. L.; Watts, W. E. *J. Chem. Soc. Perkin Trans. 1* **1973**, *7*, 975.

(65) Pauson, P. L.; Khand, I. U. *Ann. N. Y. Acad. Sci.* **1977**, *295*, 2–14.

(66) Wender, P. A.; Deschamps, N. M.; Williams, T. J. *Angew. Chem. Int. Ed.* **2004**, *43*, 3076–3079.

(67) Schore, N. E.; Croudace, M. C. *J. Org. Chem.* **1981**, *46*, 5436–5438.

(68) Billington, D. C.; Willison, D. *Tetrahedron Lett.* **1984**, *25*, 4041–4044.

(69) Brown, S. W.; Pauson, P. L. *J. Chem. Soc. Perkin Trans. 1* **1990**, *4*, 1205.

(70) Simonian, S. O.; Smit, W. A.; Gybin, A. S.; Shashkov, A. S.; Mikaelian, G. S.; Tarasov, V. A.; Ibragimov, I. I.; Caple, R.; Froen, D. E. *Tetrahedron Lett.* **1986**, *27*, 1245–1248.

(71) Iqbal, M.; Vyse, N.; Dauvergne, J.; Evans, P. *Tetrahedron Lett.* **2002**, *43*, 7859–7862.

(72) Shambayani, S.; Crowe, W. E.; Schreiber, S. L. *Tetrahedron Lett.* **1990**, *31*, 5289–5292.

(73) Jeong, N.; Chung, Y. K.; Lee, B. Y.; Lee, S. H.; Yoo, S.-E. *Synlett* **1991**, *1991*, 204–206.

(74) Sugihara, T.; Yamada, M.; Ban, H.; Yamaguchi, M.; Kaneko, C. *Angew. Chem. Int. Ed.* **1997**, *36*, 2801–2804.

(75) Perez Del Valle, C.; Milet, A.; Gimbert, Y.; Greene, A. E. *Angew. Chem. Int. Ed.* **2005**, *44*, 5717–5719.

(76) Sugihara, T.; Yamada, M.; Yamaguchi, M.; Nishizawa, M. *Synlett* **1999**, *1999*, 771–773.

(77) Kerr, W. J.; Lindsay, D. M.; McLaughlin, M.; Pauson, P. L. *Chem. Commun.* **2000**, 16, 1467–1468.

(78) Brown, J. A; Irvine, S.; Kerr, W. J.; Pearson, C. M. *Org. Biomol. Chem.* **2005**, *3*, 2396–2398.

(79) Rautenstrauch, V.; Mégard, P.; Conesa, J.; Küster, W. *Angew. Chem. Int. Ed.* **1990**, *29*, 1413–1416.

(80) Gibson (née Thomas), S. E.; Stevenazzi, A. *Angew. Chem. Int. Ed.* **2003**, *42*, 1800–1810.

(81) Jeong, N.; Hwang, S. H.; Lee, Y.; Chung, Y. K. *J. Am. Chem. Soc.* **1994**, *116*, 3159–3160.

(82) Tang, Y.; Deng, L.; Zhang, Y.; Dong, G.; Chen, J.; Yang, Z. *Org. Lett.* **2005**, *7*, 593–595.

(83) Román, R.; Mateu, N.; López, I.; Medio-Simon, M.; Fustero, S.; Barrio, P. *Org. Lett.* **2019**, *21*, 2569–2573.

(84) Llobat, A.; Román, R.; Mateu, N.; Sedgwick, D. M.; Barrio, P.; Medio-Simón, M.; Fustero, S. *Org. Lett.* **2019**, *21*, 7294–7297.

(85) Shaw, P. PhD Thesis, *University of Strathclyde*, **2020**.

(86) Liu, D.-D.; Sun, T.-W.; Wang, K.-Y.; Lu, Y.; Zhang, S.-L.; Li, Y.-H.; Jiang, Y.-L.; Chen, J.-H.; Yang, Z. *J. Am. Chem. Soc.* **2017**, *139*, 5732–5735.

(87) Chang, Y.; Shi, L.; Huang, J.; Shi, L.; Zhang, Z.; Hao, H.-D.; Gong, J.; Yang, Z. *Org. Lett.* **2018**, *20*, 2876–2879.

(88) Ishizaki, M.; Iwahara, K.; Niimi, Y.; Satoh, H.; Hoshino, O. *Tetrahedron* **2001**, *57*, 2729–2738.

(89) Croatt, M. P.; Wender, P. A. *Eur. J. Org. Chem.* **2010**, *2010*, 19–32.

(90) Nuzillard, J.-M.; Boumendjel, A.; Massiot, G. *Tetrahedron Lett.* **1989**, *30*, 3779–3780.

(91) Ahmad, S. PhD Thesis, *University of Glasgow*, **2012**.

(92) Blanchette, M. A.; Choy, W.; Davis, J. T.; Essenfeld, A. P.; Masamune, S.; Roush, W. R.; Sakai, T. *Tetrahedron Lett.* **1984**, *25*, 2183–2186.

(93) Bennie, L. S.; Fraser, C. J.; Irvine, S.; Kerr, W. J.; Andersson, S.; Nilsson, G. N. *Chem. Commun.* **2011**, *47*, 11653.

(94) Kerr, W. J.; Mudd, R. J.; Brown, J. A. *Chem. Eur. J.* **2016**, *22*, 4738–4742.

(95) Dai, H.-X.; Yu, J.-Q. *J. Am. Chem. Soc.* **2012**, *134*, 134–137.

(96) Cochran, J. C.; Prindle, V.; Young, H. A.; Kumar, M. H.; Tom, S.; Petraco, N. D. K.; Mohoro, C.; Kelley, B. *Synth. React. Inorg. Met. Chem.* **2002**, *32*, 885–902.

(97) Firouzabadi, H.; Iranpoor, N.; Karimi, B. *Synlett* **1999**, *1999*, 321–323.

(98) Guan, Y.; Zheng, D.; Zhou, L.; Wang, H.; Yan, Z.; Wang, N.; Chang, H.; She, P.; Lei, P. *Bioorg. Med. Chem. Lett.* **2011**, *21*, 2921–2924.

(99) Yang, Z.-Y.; Liao, H.-Z.; Sheng, K.; Chen, Y.-F.; Yao, Z.-J. *Angew. Chem. Int. Ed.* **2012**, *51*, 6484–6487.

(100) Norton, D. M.; Mitchell, E. A.; Botros, N. R.; Jessop, P. G.; Baird, M. C. *J. Org. Chem.* **2009**, *74*, 6674–6680.

(101) Marcantoni, E.; Nobili, F.; Bartoli, G.; Bosco, M.; Sambri, L. *J. Org. Chem.* **1997**, *62*, 4183–4184.

(102) Dalpozzo, R.; De Nino, A.; Maiuolo, L.; Procopio, A.; Tagarelli, A.; Sindona, G.; Bartoli, G. *J. Org. Chem.* **2002**, *67*, 9093–9095.

(103) Sun, J.; Dong, Y.; Cao, L.; Wang, X.; Wang, S.; Hu, Y. *J. Org. Chem.* **2004**, *69*, 8932–8934.

(104) Cheung, C. W.; Ren, P.; Hu, X. *Org. Lett.* **2014**, *16*, 2566–2569.

(105) Maier, M. E.; Bayer, A. *Eur. J. Org. Chem.* **2006**, *17*, 4034–4043.

(106) Ohtsuki, K.; Matsuo, K.; Yoshikawa, T.; Moriya, C.; Tomita-Yokotani, K.;

Shishido, K.; Shindo, M. *Org. Lett.* **2008**, *10*, 1247–1250.

(107) Yang, L.-M.; Huang, L.-F.; Luh, T.-Y. *Org. Lett.* **2004**, *6*, 1461–1463.

(108) Makado, G.; Morimoto, T.; Sugimoto, Y.; Tsutsumi, K.; Kagawa, N.; Kakiuchi, K. *Adv. Synth. Catal.* **2010**, *352*, 299–304.

(109) Cini, E.; Airiau, E.; Girard, N.; Mann, A.; Salvadori, J.; Taddei, M. *Synlett* **2011**, *2*, 199–202.

(110) Gallant, P.; D'haenens, L.; Vandewalle, M. *Synth. Commun.* **1984**, *14*, 155–161.

(111) Hu, X. D.; Tu, Y. Q.; Zhang, E.; Gao, S.; Wang, S.; Wang, A.; Fan, C. A.; Wang, M. *Org. Lett.* **2006**, *8*, 1823–1825.

(112) Matsuo, J.; Iida, D.; Tatani, K.; Mukaiyama, T. *Bull. Chem. Soc. Jpn.* **2002**, *75*, 223–234.

(113) Chen, M.; Dong, G. *J. Am. Chem. Soc.* **2019**, *141*, 14889–14897.

(114) Williams, C. M.; Mander, L. N. *Tetrahedron* **2001**, *57*, 425–447.

(115) Bonvin, Y.; Callens, E.; Larrosa, I.; Henderson, D. A.; Oldham, J.; Burton, A. J.; Barrett, A. G. M. *Org. Lett.* **2005**, *7*, 4549–4552.

(116) Jin, C.; Zhang, L.; Su, W. *Synlett* **2011**, *2011*, 1435–1438.

(117) Moriyama, K.; Takemura, M.; Togo, H. *Org. Lett.* **2012**, *14*, 2414–2417.

(118) Cooper, J. C.; Luo, C.; Kameyama, R.; Van Humbeck, J. F. *J. Am. Chem. Soc.* **2018**, *140*, 1243–1246.

(119) Tanaka, H.; Oisaki, K.; Kanai, M. *Synlett* **2017**, *28*, 1576–1580.

(120) Kuwajima, I.; Nakamura, E. *Acc. Chem. Res.* **1985**, *18*, 181–187.

(121) Fotiadou, A. D.; Zografos, A. L. *Org. Lett.* **2011**, *13*, 4592–4595.

(122) Yuan, P.; Liu, X.; Yang, X.; Zhang, Y.; Chen, X. *J. Org. Chem.* **2017**, *82*, 3692–3701.

(123) Plietker, B.; Kazmaier, U. *Transition Metal Catalyzed Enantioselective Allylic Substitution in Organic Synthesis*, 1st Ed.; Topics in Organometallic Chemistry; Springer: Berlin, 2012.

(124) Clark, J. S.; Romiti, F.; Sieng, B.; Paterson, L. C.; Stewart, A.; Chaudhury, S.; Thomas, L. H. *Org. Lett.* **2015**, *17*, 4694–4697.

(125) Minami, I.; Takahashi, K.; Shimizu, I.; Kimura, T.; Tsuji, J. *Tetrahedron* **1986**, *42*, 2971–2977.

(126) Behenna, D. C.; Stoltz, B. M. *J. Am. Chem. Soc.* **2004**, *126*, 15044–15045.

(127) Nordmann, G.; Buchwald, S. L. *J. Am. Chem. Soc.* **2003**, *125*, 4978–4979.

(128) Stang, P. J.; Mangum, M. G.; Fox, D. P.; Haak, P. *J. Am. Chem. Soc.* **1974**, *96*,

4562–4569.

(129) Biswas, S.; Page, J. P.; Dewese, K. R.; RajanBabu, T. V. *J. Am. Chem. Soc.* **2015**, *137*, 14268–14271.

(130) Armarego, W. L. F.; Chai, C. L. L. In *Purification of Laboratory Chemicals*; Elsevier, 2003; pp 80–388.

(131) Kofron, W. G.; Baclawski, L. M. *J. Org. Chem.* **1976**, *41*, 1879–1880.

(132) Krasovskiy, A.; Knochel, P. *Synthesis* **2006**, 890–891.

(133) Barnes, R. A.; Sedlak, M. *J. Org. Chem.* **1962**, *27*, 4562–4566.

(134) Xu, Y.; Hong, Y. J.; Tantillo, D. J.; Brown, M. K. *Org. Lett.* **2017**, *19*, 3703–3706.

Chapter 9

Appendix

9. Appendix

9.1 List of Chiral Ligands

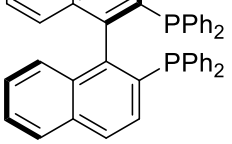

(*R*)-BINAP

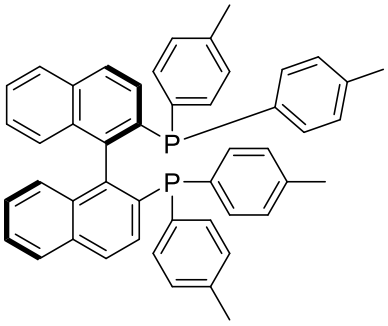

(*R*)-Tol-BINAP

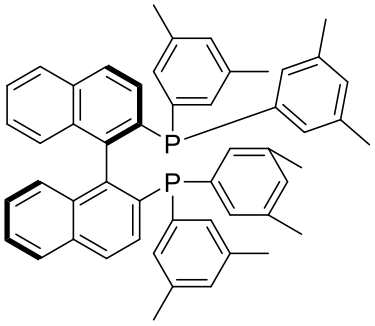

(*R*)-DM-BINAP

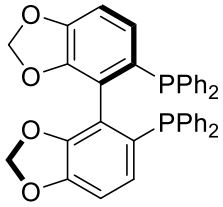

(*R*)-SEGPHOS

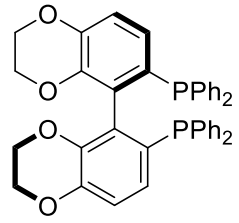

(*R*)-SYNPHOS

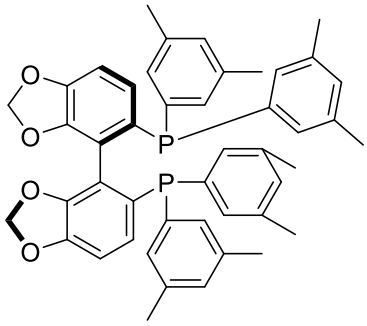

(*S*)-DM-SEGPHOS

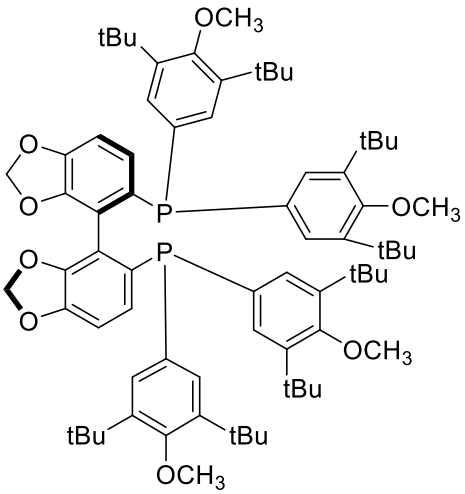

(*S*)-DTBM-SEGPHOS

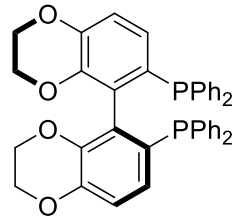

(*S*)-SYNPHOS

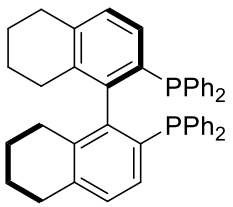

(*R*)-H_8-BINAP

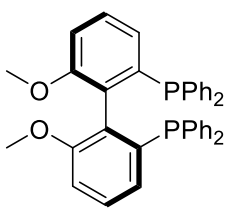

(*S*)-MeO-BIPHEP

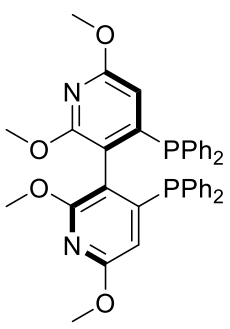

(*R*)-P-Phos

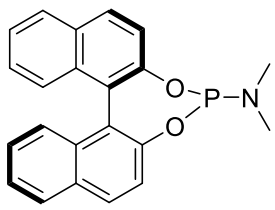

(*R*)-MonoPhos

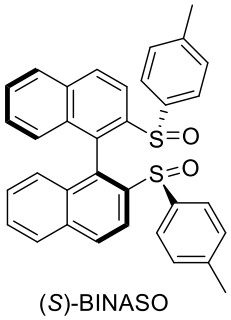

(*S*)-BINASO

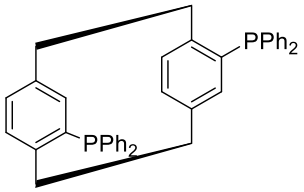

(*S*)-Phanephos

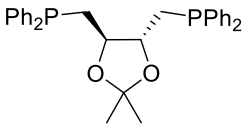

(-)-DIOP

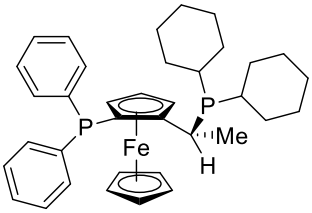

Josiphos
(SL-J001-1)

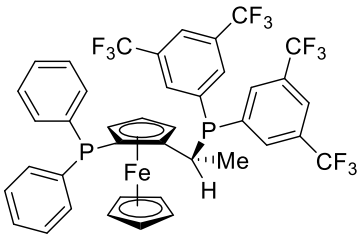

Walphos
(SL-W001-1)

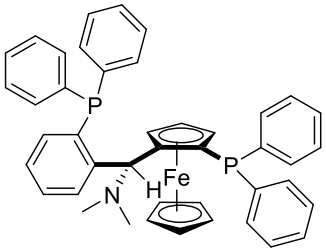

Taniaphos
(SL-T001-1)

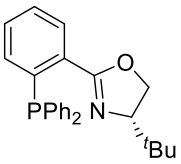

(S)-^{t}Bu-PHOX

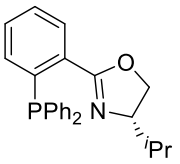

(S)-^{i}Pr-PHOX

9.2 NOSEY Data

9.2.1 ***(E)-129***

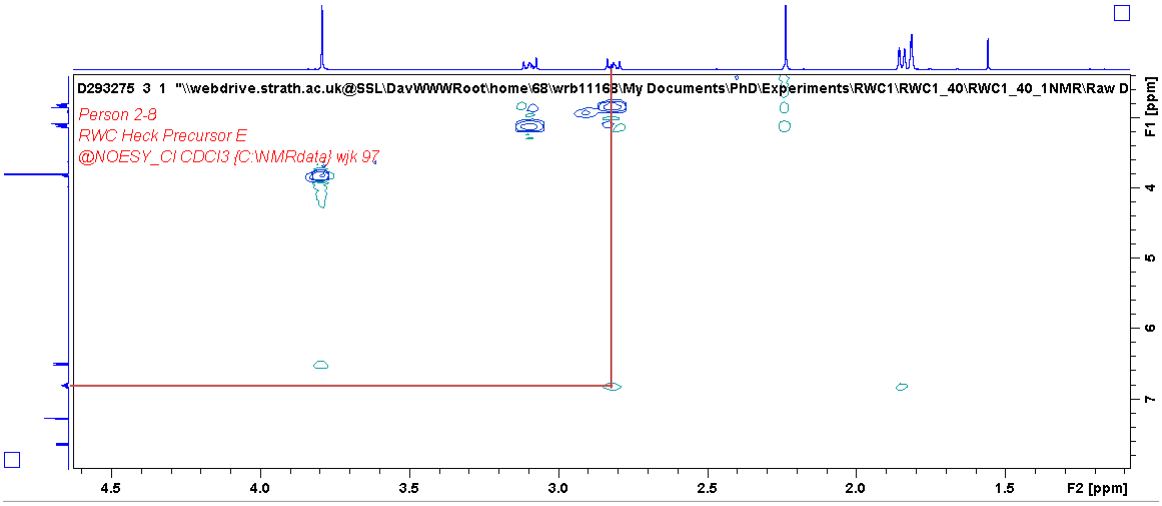

Cross-peak between 2.77 – 2.85 ppm (m, 2H, alkyl CH_2) (H_a) and 6.79 ppm (qq, J = 6.9, ^4J = 1.3 Hz, 1H, olefinic CH) (H_b) indicates (***E)*-129**.

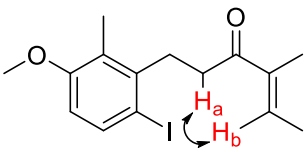

9.2.2 ***(E)-130***

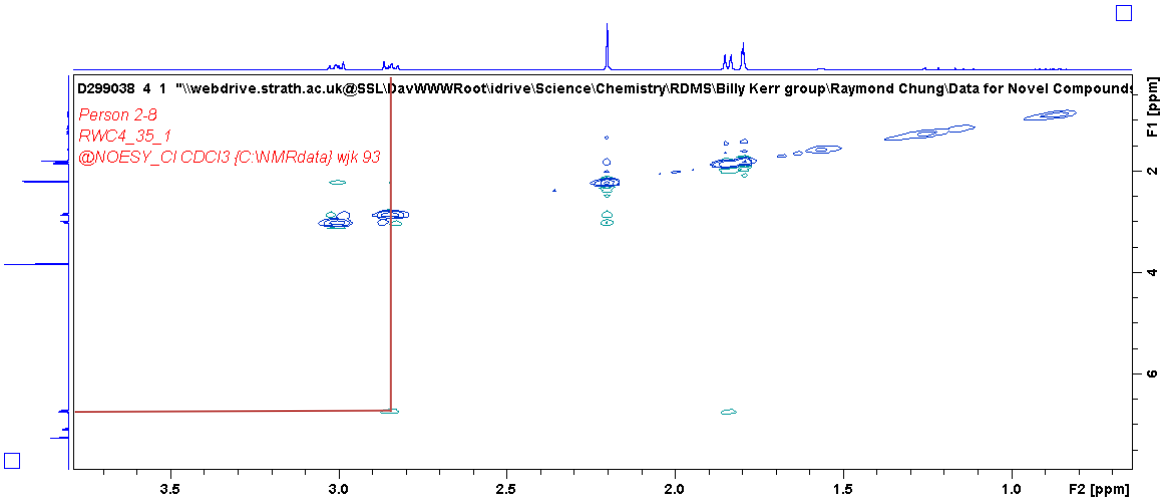

Cross-peak between 2.81 – 2.88 ppm (m, 2H, alkyl CH_2) (H_a) and 6.70 – 6.77 ppm (m, 2H, ArH, olefinic CH) (H_b) indicates (***E)*-130**.

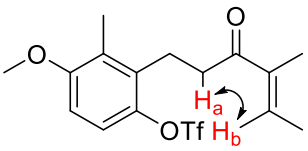

9.2.3 ***(Z)-129***

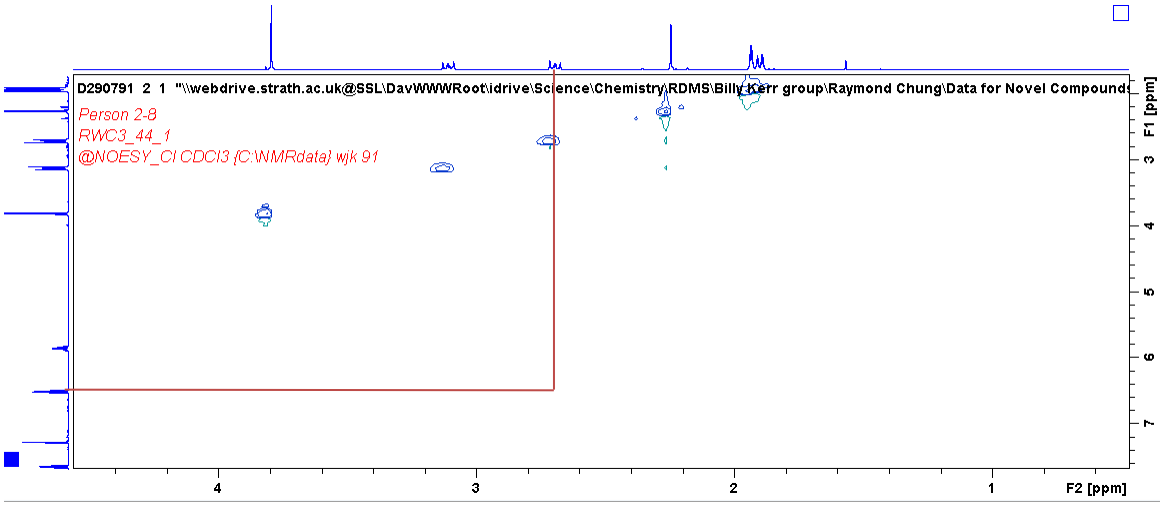

No Cross-peak between 2.67 – 2.74 ppm (m, 2H, alkyl CH_2) (H_a) and 5.83 ppm (qq, J = 6.9, ^4J = 1.3 Hz, 1H, olefinic CH) (H_b) indicates (***Z*)-129**.

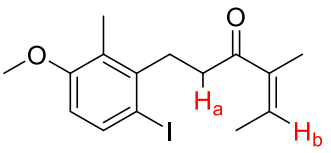

9.2.4 ***(Z)-130***

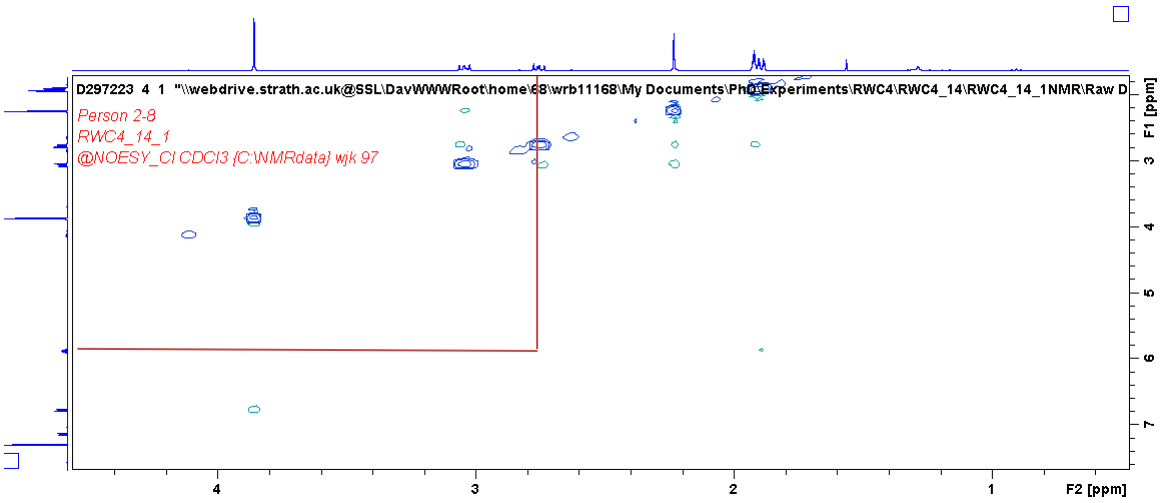

No Cross-peak between 2.68 – 2.76 ppm (m, 2H, alkyl CH_2) (H_a) and 5.80 – 5.88 ppm (m, 1H, olefinic CH) (H_b) indicates (***Z)*-130**.

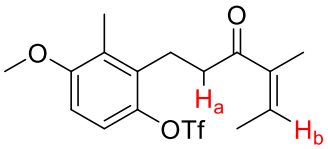

9.3 Crystal Structure Data for (*R*)-17

Table 1. Crystal data and structure refinement for jam_ray_july2018cu.

Identification code	jam_ray_july2018	
Empirical formula	C17 H22 O3	
Formula weight	274.34	
Temperature	123(2) K	
Wavelength	1.54184 Å	
Crystal system	Monoclinic	
Space group	P 2_1	
Unit cell dimensions	a = 7.5469(3) Å	α= 90°.
	b = 7.0088(3) Å	β= 103.672(4)°.
	c = 13.7869(6) Å	γ = 90°.
Volume	708.59(5) $Å^3$	
Z	2	
Density (calculated)	1.286 Mg/m^3	
Absorption coefficient	0.693 mm^{-1}	
F(000)	296	
Crystal size	0.5 x 0.4 x 0.04 mm^3	
Theta range for data collection	6.035 to 72.026°.	
Index ranges	-7<=h<=9, -8<=k<=8, -16<=l<=14	
Reflections collected	8175	
Independent reflections	2765 [R(int) = 0.0334]	
Completeness to theta = 70.000°	99.9 %	
Absorption correction	Semi-empirical from equivalents	
Max. and min. transmission	1.00000 and 0.17235	
Refinement method	Full-matrix least-squares on F^2	
Data / restraints / parameters	2765 / 1 / 184	
Goodness-of-fit on F^2	1.054	
Final R indices [I>2sigma(I)]	R1 = 0.0491, wR2 = 0.1313	
R indices (all data)	R1 = 0.0541, wR2 = 0.1362	
Absolute structure parameter	-0.11(14)	
Extinction coefficient	n/a	
Largest diff. peak and hole	0.302 and -0.214 $e.Å^{-3}$	

Table 2. Atomic coordinates (x 10^4) and equivalent isotropic displacement parameters ($Å^2$x 10^3) for jam_ray_july2018cu. U(eq) is defined as one third of the trace of the orthogonalized U^{ij} tensor.

	x	y	z	U(eq)
O(1)	8145(3)	8784(3)	6363(1)	33(1)
O(2)	8725(3)	8925(3)	783(2)	40(1)
O(3)	9355(3)	11204(3)	2004(2)	40(1)
C(1)	7481(3)	8735(4)	3276(2)	28(1)
C(2)	5965(3)	8794(4)	3687(2)	30(1)
C(3)	6132(3)	8781(5)	4706(2)	30(1)
C(4)	7862(4)	8735(4)	5347(2)	29(1)
C(5)	9430(3)	8674(4)	4962(2)	27(1)
C(6)	9230(3)	8644(4)	3930(2)	27(1)
C(7)	6588(4)	8765(6)	6771(2)	40(1)
C(8)	11285(4)	8634(5)	5677(2)	32(1)
C(9)	7154(4)	8743(5)	2142(2)	33(1)
C(10)	8946(4)	9236(5)	1825(2)	32(1)
C(11)	10533(4)	8079(5)	2422(2)	36(1)
C(12)	10921(3)	8595(5)	3522(2)	31(1)
C(13)	6474(6)	6757(6)	1743(3)	51(1)
C(14)	5774(5)	10302(7)	1721(3)	48(1)
C(15)	4349(6)	10147(11)	992(3)	77(2)
C(16)	8982(8)	10653(7)	329(3)	66(1)
C(17)	9297(6)	12127(6)	1097(3)	53(1)

Table 3. Bond lengths [Å] and angles [°] for jam_ray_july2018cu.

O(1)-C(4)	1.366(3)
O(1)-C(7)	1.418(3)
O(2)-C(16)	1.397(5)
O(2)-C(10)	1.424(4)
O(3)-C(17)	1.400(4)
O(3)-C(10)	1.422(4)
C(1)-C(2)	1.392(4)
C(1)-C(6)	1.413(4)
C(1)-C(9)	1.525(4)
C(2)-C(3)	1.380(4)
C(2)-H(2)	0.9500
C(3)-C(4)	1.393(4)
C(3)-H(3)	0.9500
C(4)-C(5)	1.408(4)
C(5)-C(6)	1.395(4)
C(5)-C(8)	1.510(3)
C(6)-C(12)	1.512(4)
C(7)-H(7A)	0.9800
C(7)-H(7B)	0.9800
C(7)-H(7C)	0.9800
C(8)-H(8A)	0.9800
C(8)-H(8B)	0.9800
C(8)-H(8C)	0.9800
C(9)-C(14)	1.527(5)
C(9)-C(13)	1.539(5)
C(9)-C(10)	1.554(4)
C(10)-C(11)	1.518(4)
C(11)-C(12)	1.519(4)
C(11)-H(11A)	0.9900
C(11)-H(11B)	0.9900
C(12)-H(12A)	0.9900
C(12)-H(12B)	0.9900
C(13)-H(13A)	0.9800
C(13)-H(13B)	0.9800
C(13)-H(13C)	0.9800
C(14)-C(15)	1.291(6)

C(14)-H(14)	0.9500
C(15)-H(15A)	0.9500
C(15)-H(15B)	0.9500
C(16)-C(17)	1.458(6)
C(16)-H(16A)	0.9900
C(16)-H(16B)	0.9900
C(17)-H(17A)	0.9900
C(17)-H(17B)	0.9900

C(4)-O(1)-C(7)	117.6(2)
C(16)-O(2)-C(10)	108.9(3)
C(17)-O(3)-C(10)	109.5(3)
C(2)-C(1)-C(6)	118.4(3)
C(2)-C(1)-C(9)	117.9(2)
C(6)-C(1)-C(9)	123.7(2)
C(3)-C(2)-C(1)	121.8(2)
C(3)-C(2)-H(2)	119.1
C(1)-C(2)-H(2)	119.1
C(2)-C(3)-C(4)	119.5(2)
C(2)-C(3)-H(3)	120.2
C(4)-C(3)-H(3)	120.2
O(1)-C(4)-C(3)	123.1(2)
O(1)-C(4)-C(5)	116.4(2)
C(3)-C(4)-C(5)	120.4(2)
C(6)-C(5)-C(4)	119.1(2)
C(6)-C(5)-C(8)	121.8(2)
C(4)-C(5)-C(8)	119.1(2)
C(5)-C(6)-C(1)	120.7(2)
C(5)-C(6)-C(12)	118.8(2)
C(1)-C(6)-C(12)	120.5(2)
O(1)-C(7)-H(7A)	109.5
O(1)-C(7)-H(7B)	109.5
H(7A)-C(7)-H(7B)	109.5
O(1)-C(7)-H(7C)	109.5
H(7A)-C(7)-H(7C)	109.5
H(7B)-C(7)-H(7C)	109.5
C(5)-C(8)-H(8A)	109.5
C(5)-C(8)-H(8B)	109.5

H(8A)-C(8)-H(8B)	109.5
C(5)-C(8)-H(8C)	109.5
H(8A)-C(8)-H(8C)	109.5
H(8B)-C(8)-H(8C)	109.5
C(1)-C(9)-C(14)	108.8(3)
C(1)-C(9)-C(13)	108.8(3)
C(14)-C(9)-C(13)	111.8(3)
C(1)-C(9)-C(10)	110.4(2)
C(14)-C(9)-C(10)	107.2(3)
C(13)-C(9)-C(10)	109.9(3)
O(3)-C(10)-O(2)	107.0(2)
O(3)-C(10)-C(11)	108.2(3)
O(2)-C(10)-C(11)	110.8(2)
O(3)-C(10)-C(9)	109.5(3)
O(2)-C(10)-C(9)	110.3(2)
C(11)-C(10)-C(9)	110.9(3)
C(10)-C(11)-C(12)	110.8(3)
C(10)-C(11)-H(11A)	109.5
C(12)-C(11)-H(11A)	109.5
C(10)-C(11)-H(11B)	109.5
C(12)-C(11)-H(11B)	109.5
H(11A)-C(11)-H(11B)	108.1
C(6)-C(12)-C(11)	113.3(2)
C(6)-C(12)-H(12A)	108.9
C(11)-C(12)-H(12A)	108.9
C(6)-C(12)-H(12B)	108.9
C(11)-C(12)-H(12B)	108.9
H(12A)-C(12)-H(12B)	107.7
C(9)-C(13)-H(13A)	109.5
C(9)-C(13)-H(13B)	109.5
H(13A)-C(13)-H(13B)	109.5
C(9)-C(13)-H(13C)	109.5
H(13A)-C(13)-H(13C)	109.5
H(13B)-C(13)-H(13C)	109.5
C(15)-C(14)-C(9)	127.1(5)
C(15)-C(14)-H(14)	116.4
C(9)-C(14)-H(14)	116.4
C(14)-C(15)-H(15A)	120.0

C(14)-C(15)-H(15B)	120.0
H(15A)-C(15)-H(15B)	120.0
O(2)-C(16)-C(17)	107.8(3)
O(2)-C(16)-H(16A)	110.2
C(17)-C(16)-H(16A)	110.2
O(2)-C(16)-H(16B)	110.2
C(17)-C(16)-H(16B)	110.2
H(16A)-C(16)-H(16B)	108.5
O(3)-C(17)-C(16)	106.7(3)
O(3)-C(17)-H(17A)	110.4
C(16)-C(17)-H(17A)	110.4
O(3)-C(17)-H(17B)	110.4
C(16)-C(17)-H(17B)	110.4
H(17A)-C(17)-H(17B)	108.6

Symmetry transformations used to generate equivalent atoms:

Table 4. Anisotropic displacement parameters ($Å^2 x\ 10^3$)for jam_ray_july2018cu. The anisotropic displacement factor exponent takes the form: $-2\pi^2[\ h^2 a^{*2} U^{11} + ... + 2\ h\ k\ a^*\ b^*\ U^{12}\ ]$

	U^{11}	U^{22}	U^{33}	U^{23}	U^{13}	U^{12}
O(1)	35(1)	38(1)	26(1)	2(1)	6(1)	0(1)
O(2)	50(1)	44(1)	27(1)	-6(1)	10(1)	-4(1)
O(3)	51(1)	36(1)	30(1)	-2(1)	6(1)	-6(1)
C(1)	28(1)	26(1)	29(1)	-1(1)	6(1)	0(1)
C(2)	27(1)	32(1)	30(1)	-2(1)	2(1)	-1(1)
C(3)	29(1)	30(1)	32(1)	-1(1)	8(1)	-1(1)
C(4)	33(1)	24(1)	28(1)	-1(1)	6(1)	-1(1)
C(5)	29(1)	22(1)	28(1)	0(1)	4(1)	0(1)
C(6)	28(1)	23(1)	29(1)	-2(1)	4(1)	-1(1)
C(7)	42(2)	48(2)	30(2)	2(2)	10(1)	-2(2)
C(8)	33(1)	30(1)	29(1)	-1(1)	0(1)	2(1)
C(9)	31(1)	39(2)	29(1)	-6(1)	5(1)	-4(1)
C(10)	35(1)	35(2)	26(1)	-5(1)	7(1)	-1(1)
C(11)	33(1)	40(2)	37(2)	-2(1)	11(1)	4(1)
C(12)	27(1)	32(1)	32(1)	0(1)	5(1)	1(1)
C(13)	61(2)	58(2)	37(2)	-18(2)	14(2)	-26(2)
C(14)	40(2)	70(2)	34(2)	11(2)	10(1)	13(2)
C(15)	49(2)	133(5)	46(2)	23(3)	6(2)	21(3)
C(16)	110(4)	56(3)	33(2)	4(2)	22(2)	-8(2)
C(17)	77(3)	42(2)	43(2)	3(2)	20(2)	-2(2)

Table 5. Hydrogen coordinates (x 10^4) and isotropic displacement parameters ($Å^2$x 10^3) for jam_ray_july2018cu.

	x	y	z	U(eq)
H(2)	4782	8845	3254	36
H(3)	5076	8802	4968	36
H(7A)	5847	7637	6531	59
H(7B)	5865	9920	6564	59
H(7C)	6976	8726	7502	59
H(8A)	11941	9815	5610	48
H(8B)	11979	7539	5524	48
H(8C)	11139	8522	6363	48
H(11A)	11632	8328	2167	44
H(11B)	10244	6703	2338	44
H(12A)	11787	7655	3907	37
H(12B)	11515	9863	3620	37
H(13A)	5293	6500	1896	77
H(13B)	7357	5787	2061	77
H(13C)	6338	6720	1018	77
H(14)	5986	11520	2029	57
H(15A)	4071	8962	657	92
H(15B)	3579	11219	791	92
H(16A)	7889	10966	-203	79
H(16B)	10043	10560	25	79
H(17A)	10463	12792	1121	64
H(17B)	8299	13078	956	64

Table 6. Torsion angles [°] for jam_ray_july2018cu.

C(6)-C(1)-C(2)-C(3)	0.5(5)
C(9)-C(1)-C(2)-C(3)	179.6(3)
C(1)-C(2)-C(3)-C(4)	1.0(5)
C(7)-O(1)-C(4)-C(3)	3.9(5)
C(7)-O(1)-C(4)-C(5)	-177.4(3)
C(2)-C(3)-C(4)-O(1)	177.7(3)
C(2)-C(3)-C(4)-C(5)	-0.9(5)
O(1)-C(4)-C(5)-C(6)	-179.3(3)
C(3)-C(4)-C(5)-C(6)	-0.6(5)
O(1)-C(4)-C(5)-C(8)	1.0(4)
C(3)-C(4)-C(5)-C(8)	179.8(3)
C(4)-C(5)-C(6)-C(1)	2.1(5)
C(8)-C(5)-C(6)-C(1)	-178.3(3)
C(4)-C(5)-C(6)-C(12)	179.5(2)
C(8)-C(5)-C(6)-C(12)	-0.8(5)
C(2)-C(1)-C(6)-C(5)	-2.1(5)
C(9)-C(1)-C(6)-C(5)	178.9(3)
C(2)-C(1)-C(6)-C(12)	-179.4(3)
C(9)-C(1)-C(6)-C(12)	1.5(5)
C(2)-C(1)-C(9)-C(14)	47.0(4)
C(6)-C(1)-C(9)-C(14)	-134.0(3)
C(2)-C(1)-C(9)-C(13)	-75.0(4)
C(6)-C(1)-C(9)-C(13)	104.0(4)
C(2)-C(1)-C(9)-C(10)	164.3(3)
C(6)-C(1)-C(9)-C(10)	-16.6(5)
C(17)-O(3)-C(10)-O(2)	3.1(4)
C(17)-O(3)-C(10)-C(11)	122.5(3)
C(17)-O(3)-C(10)-C(9)	-116.5(3)
C(16)-O(2)-C(10)-O(3)	-0.3(4)
C(16)-O(2)-C(10)-C(11)	-118.0(4)
C(16)-O(2)-C(10)-C(9)	118.8(4)
C(1)-C(9)-C(10)-O(3)	-72.4(3)
C(14)-C(9)-C(10)-O(3)	45.9(3)
C(13)-C(9)-C(10)-O(3)	167.6(3)
C(1)-C(9)-C(10)-O(2)	170.1(2)
C(14)-C(9)-C(10)-O(2)	-71.6(3)

C(13)-C(9)-C(10)-O(2)	50.1(3)
C(1)-C(9)-C(10)-C(11)	47.0(4)
C(14)-C(9)-C(10)-C(11)	165.3(3)
C(13)-C(9)-C(10)-C(11)	-73.0(3)
O(3)-C(10)-C(11)-C(12)	55.9(3)
O(2)-C(10)-C(11)-C(12)	172.9(3)
C(9)-C(10)-C(11)-C(12)	-64.3(3)
C(5)-C(6)-C(12)-C(11)	165.8(3)
C(1)-C(6)-C(12)-C(11)	-16.7(4)
C(10)-C(11)-C(12)-C(6)	47.6(4)
C(1)-C(9)-C(14)-C(15)	-132.2(4)
C(13)-C(9)-C(14)-C(15)	-11.9(5)
C(10)-C(9)-C(14)-C(15)	108.5(4)
C(10)-O(2)-C(16)-C(17)	-2.5(5)
C(10)-O(3)-C(17)-C(16)	-4.6(4)
O(2)-C(16)-C(17)-O(3)	4.4(5)

Symmetry transformations used to generate equivalent atoms:

9.4 Crystal Structure Data for 98

Table 1. Crystal data and structure refinement for kerr_ray_oct19a.

Identification code	kerr_ray_oct18a	
Empirical formula	C20 H22 O2	
Formula weight	294.37	
Temperature	123(2) K	
Wavelength	1.54184 Å	
Crystal system	Orthorhombic	
Space group	$P\ 2_1\ 2_1\ 2_1$	
Unit cell dimensions	a = 10.3895(3) Å	α= 90°.
	b = 10.6373(4) Å	β= 90°.
	c = 14.0367(4) Å	γ = 90°.
Volume	1551.28(9) $Å^3$	
Z	4	
Density (calculated)	1.260 Mg/m^3	
Absorption coefficient	0.624 mm^{-1}	
F(000)	632	
Crystal size	0.5 x 0.16 x 0.09 mm^3	
Theta range for data collection	5.217 to 73.223°.	
Index ranges	-12<=h<=9, -13<=k<=13, -17<=l<=15	
Reflections collected	8970	
Independent reflections	3069 [R(int) = 0.0355]	
Completeness to theta = 70.000°	99.9 %	
Absorption correction	Semi-empirical from equivalents	
Max. and min. transmission	1.00000 and 0.51163	
Refinement method	Full-matrix least-squares on F^2	
Data / restraints / parameters	3069 / 0 / 203	
Goodness-of-fit on F^2	1.058	
Final R indices [I>2sigma(I)]	R1 = 0.0443, wR2 = 0.1093	
R indices (all data)	R1 = 0.0529, wR2 = 0.1155	
Absolute structure parameter	-0.16(18)	
Extinction coefficient	n/a	
Largest diff. peak and hole	0.207 and -0.165 $e.Å^{-3}$	

Table 2. Atomic coordinates (x 10^4) and equivalent isotropic displacement parameters ($Å^2$x 10^3) for kerr_ray_oct19a. U(eq) is defined as one third of the trace of the orthogonalized U^{ij} tensor.

	x	y	z	U(eq)
O(1)	3804(2)	7460(2)	8789(2)	47(1)
O(2)	6090(2)	5862(2)	2237(1)	37(1)
C(1)	4609(3)	7629(3)	8176(2)	38(1)
C(2)	5886(3)	8208(3)	8312(2)	35(1)
C(3)	6503(3)	8177(3)	7484(2)	34(1)
C(4)	5810(3)	7490(3)	6691(2)	31(1)
C(5)	4444(3)	7336(3)	7117(2)	38(1)
C(6)	6321(3)	8769(4)	9234(2)	46(1)
C(7)	7676(3)	8829(4)	7111(2)	42(1)
C(8)	7518(3)	8745(3)	6021(2)	37(1)
C(9)	6080(3)	8361(3)	5821(2)	29(1)
C(10)	5218(3)	9522(3)	5862(2)	38(1)
C(11)	6389(3)	6207(3)	6531(2)	33(1)
C(12)	6590(3)	5727(3)	5671(2)	33(1)
C(13)	6311(3)	6417(3)	4792(2)	30(1)
C(14)	6009(3)	7703(3)	4858(2)	29(1)
C(15)	5758(3)	8362(3)	4032(2)	33(1)
C(16)	5785(3)	7782(3)	3151(2)	33(1)
C(17)	6065(3)	6507(3)	3085(2)	31(1)
C(18)	6321(3)	5803(3)	3905(2)	30(1)
C(19)	6608(3)	4413(3)	3821(2)	35(1)
C(20)	5858(3)	6562(3)	1392(2)	37(1)

Table 3. Bond lengths [Å] and angles [°] for kerr_ray_oct19a.

O(1)-C(1)	1.213(4)
O(2)-C(17)	1.375(3)
O(2)-C(20)	1.422(4)
C(1)-C(2)	1.475(4)
C(1)-C(5)	1.529(4)
C(2)-C(3)	1.328(4)
C(2)-C(6)	1.495(4)
C(3)-C(7)	1.497(4)
C(3)-C(4)	1.513(4)
C(4)-C(11)	1.508(4)
C(4)-C(5)	1.549(4)
C(4)-C(9)	1.559(4)
C(5)-H(5A)	0.9900
C(5)-H(5B)	0.9900
C(6)-H(6A)	0.9800
C(6)-H(6B)	0.9800
C(6)-H(6C)	0.9800
C(7)-C(8)	1.542(4)
C(7)-H(7A)	0.9900
C(7)-H(7B)	0.9900
C(8)-C(9)	1.574(4)
C(8)-H(8A)	0.9900
C(8)-H(8B)	0.9900
C(9)-C(14)	1.524(4)
C(9)-C(10)	1.526(4)
C(10)-H(10A)	0.9800
C(10)-H(10B)	0.9800
C(10)-H(10C)	0.9800
C(11)-C(12)	1.327(4)
C(11)-H(11)	0.9500
C(12)-C(13)	1.465(4)
C(12)-H(12)	0.9500
C(13)-C(14)	1.406(4)
C(13)-C(18)	1.406(4)
C(14)-C(15)	1.379(4)
C(15)-C(16)	1.383(4)

C(15)-H(15)	0.9500
C(16)-C(17)	1.390(4)
C(16)-H(16)	0.9500
C(17)-C(18)	1.398(4)
C(18)-C(19)	1.513(4)
C(19)-H(19A)	0.9800
C(19)-H(19B)	0.9800
C(19)-H(19C)	0.9800
C(20)-H(20A)	0.9800
C(20)-H(20B)	0.9800
C(20)-H(20C)	0.9800

C(17)-O(2)-C(20)	117.2(2)
O(1)-C(1)-C(2)	126.2(3)
O(1)-C(1)-C(5)	125.6(3)
C(2)-C(1)-C(5)	108.2(3)
C(3)-C(2)-C(1)	108.0(3)
C(3)-C(2)-C(6)	128.5(3)
C(1)-C(2)-C(6)	123.4(3)
C(2)-C(3)-C(7)	133.4(3)
C(2)-C(3)-C(4)	115.3(3)
C(7)-C(3)-C(4)	110.7(3)
C(11)-C(4)-C(3)	110.9(2)
C(11)-C(4)-C(5)	109.1(2)
C(3)-C(4)-C(5)	101.7(2)
C(11)-C(4)-C(9)	110.5(2)
C(3)-C(4)-C(9)	101.7(2)
C(5)-C(4)-C(9)	122.0(2)
C(1)-C(5)-C(4)	104.6(2)
C(1)-C(5)-H(5A)	110.8
C(4)-C(5)-H(5A)	110.8
C(1)-C(5)-H(5B)	110.8
C(4)-C(5)-H(5B)	110.8
H(5A)-C(5)-H(5B)	108.9
C(2)-C(6)-H(6A)	109.5
C(2)-C(6)-H(6B)	109.5
H(6A)-C(6)-H(6B)	109.5
C(2)-C(6)-H(6C)	109.5

H(6A)-C(6)-H(6C)	109.5
H(6B)-C(6)-H(6C)	109.5
C(3)-C(7)-C(8)	103.5(2)
C(3)-C(7)-H(7A)	111.1
C(8)-C(7)-H(7A)	111.1
C(3)-C(7)-H(7B)	111.1
C(8)-C(7)-H(7B)	111.1
H(7A)-C(7)-H(7B)	109.0
C(7)-C(8)-C(9)	107.0(2)
C(7)-C(8)-H(8A)	110.3
C(9)-C(8)-H(8A)	110.3
C(7)-C(8)-H(8B)	110.3
C(9)-C(8)-H(8B)	110.3
H(8A)-C(8)-H(8B)	108.6
C(14)-C(9)-C(10)	112.2(2)
C(14)-C(9)-C(4)	114.4(2)
C(10)-C(9)-C(4)	110.2(2)
C(14)-C(9)-C(8)	108.8(2)
C(10)-C(9)-C(8)	109.9(3)
C(4)-C(9)-C(8)	100.7(2)
C(9)-C(10)-H(10A)	109.5
C(9)-C(10)-H(10B)	109.5
H(10A)-C(10)-H(10B)	109.5
C(9)-C(10)-H(10C)	109.5
H(10A)-C(10)-H(10C)	109.5
H(10B)-C(10)-H(10C)	109.5
C(12)-C(11)-C(4)	123.1(3)
C(12)-C(11)-H(11)	118.4
C(4)-C(11)-H(11)	118.4
C(11)-C(12)-C(13)	122.8(3)
C(11)-C(12)-H(12)	118.6
C(13)-C(12)-H(12)	118.6
C(14)-C(13)-C(18)	120.8(3)
C(14)-C(13)-C(12)	118.4(2)
C(18)-C(13)-C(12)	120.8(3)
C(15)-C(14)-C(13)	118.8(2)
C(15)-C(14)-C(9)	121.4(2)
C(13)-C(14)-C(9)	119.6(2)

C(14)-C(15)-C(16)	121.4(3)
C(14)-C(15)-H(15)	119.3
C(16)-C(15)-H(15)	119.3
C(15)-C(16)-C(17)	119.9(3)
C(15)-C(16)-H(16)	120.0
C(17)-C(16)-H(16)	120.0
O(2)-C(17)-C(16)	123.3(3)
O(2)-C(17)-C(18)	116.2(3)
C(16)-C(17)-C(18)	120.5(3)
C(17)-C(18)-C(13)	118.6(3)
C(17)-C(18)-C(19)	119.8(2)
C(13)-C(18)-C(19)	121.6(3)
C(18)-C(19)-H(19A)	109.5
C(18)-C(19)-H(19B)	109.5
H(19A)-C(19)-H(19B)	109.5
C(18)-C(19)-H(19C)	109.5
H(19A)-C(19)-H(19C)	109.5
H(19B)-C(19)-H(19C)	109.5
O(2)-C(20)-H(20A)	109.5
O(2)-C(20)-H(20B)	109.5
H(20A)-C(20)-H(20B)	109.5
O(2)-C(20)-H(20C)	109.5
H(20A)-C(20)-H(20C)	109.5
H(20B)-C(20)-H(20C)	109.5

Symmetry transformations used to generate equivalent atoms:

Table 4. Anisotropic displacement parameters ($Å^2 x\ 10^3$)for kerr_ray_oct19a. The anisotropic displacement factor exponent takes the form: $-2\pi^2[\ h^2 a^{*2} U^{11} + ... + 2\ h\ k\ a^*\ b^*\ U^{12}\ ]$

	U^{11}	U^{22}	U^{33}	U^{23}	U^{13}	U^{12}
O(1)	49(1)	43(1)	48(1)	7(1)	19(1)	5(1)
O(2)	42(1)	38(1)	30(1)	-7(1)	-1(1)	2(1)
C(1)	39(2)	31(2)	45(2)	5(1)	8(1)	9(1)
C(2)	38(2)	36(2)	32(2)	3(1)	0(1)	8(1)
C(3)	32(1)	39(2)	32(2)	0(1)	-6(1)	7(1)
C(4)	28(1)	36(1)	30(1)	2(1)	-2(1)	2(1)
C(5)	33(2)	39(2)	41(2)	3(1)	2(1)	1(1)
C(6)	50(2)	56(2)	31(2)	0(2)	-1(1)	8(2)
C(7)	33(2)	60(2)	33(2)	-7(2)	-2(1)	-7(2)
C(8)	34(1)	46(2)	33(2)	-5(1)	1(1)	-8(1)
C(9)	31(1)	29(1)	28(1)	-1(1)	-2(1)	-1(1)
C(10)	49(2)	33(2)	31(2)	-2(1)	-5(1)	6(1)
C(11)	34(1)	34(2)	32(2)	8(1)	-3(1)	1(1)
C(12)	31(1)	31(1)	38(2)	0(1)	-2(1)	2(1)
C(13)	24(1)	33(1)	32(2)	-1(1)	-1(1)	0(1)
C(14)	25(1)	32(2)	29(2)	-2(1)	-1(1)	0(1)
C(15)	37(1)	27(1)	34(2)	-1(1)	-4(1)	2(1)
C(16)	34(1)	38(2)	28(2)	2(1)	-4(1)	3(1)
C(17)	25(1)	37(2)	33(2)	-5(1)	-1(1)	-2(1)
C(18)	24(1)	30(1)	35(2)	-3(1)	1(1)	-1(1)
C(19)	38(2)	34(2)	34(2)	-2(1)	2(1)	0(1)
C(20)	38(2)	45(2)	28(2)	-4(1)	1(1)	-1(1)

Table 5. Hydrogen coordinates (x 10^4) and isotropic displacement parameters ($Å^2$x 10^3) for kerr_ray_oct19a.

	x	y	z	U(eq)
H(5A)	3833	7930	6817	45
H(5B)	4124	6468	7025	45
H(6A)	7027	9360	9114	68
H(6B)	6620	8100	9660	68
H(6C)	5602	9216	9533	68
H(7A)	8470	8397	7322	50
H(7B)	7704	9715	7325	50
H(8A)	8113	8107	5755	45
H(8B)	7713	9567	5722	45
H(10A)	4353	9302	5640	56
H(10B)	5577	10181	5453	56
H(10C)	5172	9828	6520	56
H(11)	6622	5720	7071	40
H(12)	6929	4900	5624	40
H(15)	5562	9233	4070	39
H(16)	5613	8255	2591	40
H(19A)	7518	4263	3967	53
H(19B)	6425	4132	3170	53
H(19C)	6068	3945	4270	53
H(20A)	6478	7254	1349	56
H(20B)	4982	6904	1407	56
H(20C)	5954	6012	836	56

Table 6. Torsion angles [°] for kerr_ray_oct19a.

O(1)-C(1)-C(2)-C(3)	177.4(3)
C(5)-C(1)-C(2)-C(3)	-5.4(3)
O(1)-C(1)-C(2)-C(6)	-5.2(5)
C(5)-C(1)-C(2)-C(6)	172.0(3)
C(1)-C(2)-C(3)-C(7)	165.1(3)
C(6)-C(2)-C(3)-C(7)	-12.1(6)
C(1)-C(2)-C(3)-C(4)	-4.9(4)
C(6)-C(2)-C(3)-C(4)	177.9(3)
C(2)-C(3)-C(4)-C(11)	-103.2(3)
C(7)-C(3)-C(4)-C(11)	84.5(3)
C(2)-C(3)-C(4)-C(5)	12.7(4)
C(7)-C(3)-C(4)-C(5)	-159.6(3)
C(2)-C(3)-C(4)-C(9)	139.3(3)
C(7)-C(3)-C(4)-C(9)	-33.0(3)
O(1)-C(1)-C(5)-C(4)	-169.9(3)
C(2)-C(1)-C(5)-C(4)	12.8(3)
C(11)-C(4)-C(5)-C(1)	102.8(3)
C(3)-C(4)-C(5)-C(1)	-14.4(3)
C(9)-C(4)-C(5)-C(1)	-126.4(3)
C(2)-C(3)-C(7)-C(8)	-158.9(3)
C(4)-C(3)-C(7)-C(8)	11.5(3)
C(3)-C(7)-C(8)-C(9)	14.7(3)
C(11)-C(4)-C(9)-C(14)	37.9(3)
C(3)-C(4)-C(9)-C(14)	155.8(2)
C(5)-C(4)-C(9)-C(14)	-92.3(3)
C(11)-C(4)-C(9)-C(10)	165.4(2)
C(3)-C(4)-C(9)-C(10)	-76.8(3)
C(5)-C(4)-C(9)-C(10)	35.2(4)
C(11)-C(4)-C(9)-C(8)	-78.6(3)
C(3)-C(4)-C(9)-C(8)	39.3(3)
C(5)-C(4)-C(9)-C(8)	151.2(3)
C(7)-C(8)-C(9)-C(14)	-154.6(3)
C(7)-C(8)-C(9)-C(10)	82.2(3)
C(7)-C(8)-C(9)-C(4)	-34.1(3)
C(3)-C(4)-C(11)-C(12)	-138.4(3)
C(5)-C(4)-C(11)-C(12)	110.4(3)

C(9)-C(4)-C(11)-C(12)	-26.4(4)
C(4)-C(11)-C(12)-C(13)	2.3(4)
C(11)-C(12)-C(13)-C(14)	10.1(4)
C(11)-C(12)-C(13)-C(18)	-168.7(3)
C(18)-C(13)-C(14)-C(15)	-1.8(4)
C(12)-C(13)-C(14)-C(15)	179.4(3)
C(18)-C(13)-C(14)-C(9)	-176.5(2)
C(12)-C(13)-C(14)-C(9)	4.7(4)
C(10)-C(9)-C(14)-C(15)	29.7(4)
C(4)-C(9)-C(14)-C(15)	156.2(3)
C(8)-C(9)-C(14)-C(15)	-92.1(3)
C(10)-C(9)-C(14)-C(13)	-155.7(3)
C(4)-C(9)-C(14)-C(13)	-29.2(3)
C(8)-C(9)-C(14)-C(13)	82.5(3)
C(13)-C(14)-C(15)-C(16)	0.6(4)
C(9)-C(14)-C(15)-C(16)	175.3(3)
C(14)-C(15)-C(16)-C(17)	0.3(5)
C(20)-O(2)-C(17)-C(16)	2.2(4)
C(20)-O(2)-C(17)-C(18)	-178.8(2)
C(15)-C(16)-C(17)-O(2)	178.9(3)
C(15)-C(16)-C(17)-C(18)	0.0(4)
O(2)-C(17)-C(18)-C(13)	179.9(2)
C(16)-C(17)-C(18)-C(13)	-1.1(4)
O(2)-C(17)-C(18)-C(19)	0.2(4)
C(16)-C(17)-C(18)-C(19)	179.3(3)
C(14)-C(13)-C(18)-C(17)	2.0(4)
C(12)-C(13)-C(18)-C(17)	-179.2(2)
C(14)-C(13)-C(18)-C(19)	-178.3(3)
C(12)-C(13)-C(18)-C(19)	0.4(4)

Symmetry transformations used to generate equivalent atoms: